United States
Environmental Protection
Agency

January 2005
EPA/600/R-05/0054aA

Air Quality Criteria for Ozone and Related Photochemical Oxidants (First External Review Draft)

Volume I of III

EPA/600/R-05/004aA
January 2005

Air Quality Criteria for Ozone and Related Photochemical Oxidants

Volume I

National Center for Environmental Assessment-RTP Office
Office of Research and Development
U.S. Environmental Protection Agency
Research Triangle Park, NC

DISCLAIMER

This document is an external review draft for review purposes only and does not constitute U.S. Environmental Protection Agency policy. Mention of trade names or commercial products does not constitute endorsement or recommendation for use.

PREFACE

National Ambient Air Quality Standards (NAAQS) are promulgated by the United States Environmental Protection Agency (EPA) to meet requirements set forth in Sections 108 and 109 of the U.S. Clean Air Act (CAA). Sections 108 and 109 require the EPA Administrator (1) to list widespread air pollutants that reasonably may be expected to endanger public health or welfare; (2) to issue air quality criteria for them that assess the latest available scientific information on nature and effects of ambient exposure to them; (3) to set "primary" NAAQS to protect human health with adequate margin of safety and to set "secondary" NAAQS to protect against welfare effects (e.g., effects on vegetation, ecosystems, visibility, climate, manmade materials, etc); and (5) to periodically review and revise, as appropriate, the criteria and NAAQS for a given listed pollutant or class of pollutants.

In 1971, the U.S. Environmental Protection Agency (EPA) promulgated National Ambient Air Quality Standards (NAAQS) to protect the public health and welfare from adverse effects of photochemical oxidants. The EPA promulgates the NAAQS on the basis of scientific information contained in air quality criteria issued under Section 108 of the Clean Air Act. Following the review of criteria as contained in the EPA document, Air Quality Criteria for Ozone and other Photochemical Oxidants published in 1978, the chemical designation of the standards was changed from photochemical oxidants to ozone (O_3) in 1979 and a 1-hour O_3 NAAQS was set. The 1978 document focused primarily on the scientific air quality criteria for O_3 and, to a lesser extent, on those for other photochemical oxidants such as hydrogen peroxide and the peroxyacyl nitrates, as have subsequent revised versions of the ozone document.

To meet Clean Air Act requirements noted above for periodic review of criteria and NAAQS, the O_3 criteria document, *Air Quality Criteria for Ozone and Other Photochemical Oxidants*, was next revised and then released in August 1986; and a supplement, *Summary of Selected New Information on Effects of Ozone on Health and Vegetation*, was issued in January 1992. These documents were the basis for a March 1993 decision by EPA that revision of the existing 1-h NAAQS for O_3 was not appropriate at that time. That decision, however, did not take into account some of the newer scientific data that became available after completion of the 1986 criteria document. Such literature was assessed in the next periodic revision of the O_3 air quality criteria document, which was completed in 1996 and provided scientific bases supporting the setting by EPA in 1997 of an 8-h O_3 NAAQS that is currently in force together with the 1-h O_3 standard.

The purpose of this revised air quality criteria document for O_3 and related photochemical oxidants is to critically evaluate and assess the latest scientific information published since that assessed in the above 1996 Ozone Air Quality Criteria Document (O_3 AQCD), with the main focus being on pertinent new information useful in evaluating health and environmental effects data associated with ambient air O_3 exposures. However, some other scientific data are also presented and evaluated in order to provide a better understanding of the nature, sources, distribution, measurement, and concentrations of O_3 and related photochemical oxidants and their precursors in the environment. The document assesses pertinent literature available through 2004.

The present draft document (dated January 2005) is being released for public comment and review by the Clean Air Scientific Advisory Committee (CASAC) to obtain comments on the organization and structure of the document, the issues addressed, the approaches employed in assessing and interpreting the newly available information on O_3 exposures and effects, and the key findings and conclusions arrived at as a consequence of this assessment. Public comments and recommendations will be taken into account making any appropriate further revisions to this document for incorporation into a Second External Review Draft. That draft will be released for further public comment and CASAC review before last revisions are made in response and incorporated into a final version to be completed by early 2006. Evaluations contained in the present document will be drawn on to provide inputs to associated PM Staff Paper analyses prepared by EPA's Office of Air Quality Planning and Standards (OAQPS) to pose options for consideration by the EPA Administrator with regard to proposal and, ultimately, promulgation of decisions on potential retention or revision, as appropriate, of the current O_3 NAAQS.

Preparation of this document was coordinated by staff of EPA's National Center for Environmental Assessment in Research Triangle Park (NCEA-RTP). NCEA-RTP scientific staff, together with experts from other EPA/ORD laboratories and academia, contributed to writing of document chapters. Earlier drafts of document materials were reviewed by non-EPA experts in peer consultation workshops held by EPA. The document describes the nature, sources, distribution, measurement, and concentrations of O_3 in outdoor (ambient) and indoor environments. It also evaluates the latest data on human exposures to ambient O_3 and consequent health effects in exposed human populations, to support decision making regarding the primary, health-related O_3 NAAQS. The document also evaluates ambient O_3 environmental effects on vegetation and ecosystems, man-made materials, and surface level solar UV radiation flux and global climate change, to support decision making on secondary O_3 NAAQS.

NCEA acknowledges the valuable contributions provided by authors, contributors, and reviewers and the diligence of its staff and contractors in the preparation of this draft document.

Air Quality Criteria for Ozone and Related Photochemical Oxidants (First External Review Draft)

VOLUME I

Air Quality Criteria for Ozone and Related Photochemical Oxidants (First External Review Draft)

(cont'd)

VOLUME II

Air Quality Criteria for Ozone and Related Photochemical Oxidants (First External Review Draft)
(cont'd)

VOLUME III

Table of Contents

Page

Table of Contents
(cont'd)

Table of Contents
(cont'd)

Page

Table of Contents
(cont'd)

Table of Contents
(cont'd)

Page

List of Tables

List of Tables
(cont'd)

List of Tables
(cont'd)

List of Tables
(cont'd)

List of Figures

List of Figures
(cont'd)

List of Figures
(cont'd)

List of Figures
(cont'd)

List of Figures
(cont'd)

List of Figures
(cont'd)

List of Figures
(cont'd)

List of Figures
(cont'd)

List of Figures
(cont'd)

List of Figures
(cont'd)

List of Figures
(cont'd)

Authors, Contributors, and Reviewers

To be inserted in Second External Review draft.

U.S. Environmental Protection Agency Project Team for Development of Air Quality Criteria for Ozone and Related Photochemical Oxidants

To be inserted in Second External Review draft.

U.S. Environmental Protection Agency Science Advisory Board (SAB)
Staff Office Clean Air Scientific Advisory Committee (CASAC)
Ozone Review Panel

To be inserted in Second External Review draft.

Abbreviations and Acronyms

AC	air conditioning
AER	air exchange rate
AEROCE	Atmospheric/Ocean Ocean Chemistry Experiment
AGL	above ground level
AHC	anthropogenic hydrocarbons
AHCs	aromatic hydrocarbons
AirPEX	Air Pollution Exposure (model)
AirQUIS	Air Quality Information System (model)
AIRS	Aerometric Information Retrieval System
AP-CIMS	Atmospheric Pressure Chemical Ionization Mass Spectrometer
APEX	Air Pollutants Exposure Model
AQCD	Air Quality Criteria Document
AQS	Air Quality System
ATLAS	
A/V	surface-to-volume ratio
BC	black carbon
BEIS	Biogenic Emission Inventory System
BHC	biogenic hydrocarbons
BME	Bayesian Maxim Eutropy
C	carbon
CAA	Clean Air Act
CAAA	Clean Air Act Amendments of 1990
CADS	Cincinnati Activity Diary Study
RAMS	Regional Atmospheric Modeling System
CASAC	Clean Air Scientific Advisory Committee
CASTNet	Clean Air Status and Trends Network
CBL	convective boundary layer
CEPEX	Central Equatorial Pacific Experiment

CFD	computational fluid dynamics
CG	cloud to ground
CHAD	Consolidated Human Activities Database
CH_4	methane
CIMS	Chemical Ionization Mass Spectroscopy
CL	chemiluminescence
CLM	chemiluminescence method
CMAQ	Community Model for Air Quality
CMBO	chloromethylbutenone
CMSA	consolidated metropolitan statistical area
CN	condensation nuclei
CO	carbon monoxide
CO_2	carbon dioxide
COD	coefficient of divergence
CTM	Chemistry Transport Model
DA	dry airstream
DI	dry intrusion
DIAL	differential absorption lidar
DOAS	differential optical absorption spectroscopy/spectrometry
EDMAS	Exposure and Dose Modeling and Analysis System
EOF	empirical orthogonal function
EPA	U.S. Environmental Protection Agency
EPEM	Event Probability Exposure Model
EPRI	Electric Power Research Institute
ERAQS	Eastern Regional Air Quality Study
EVR	equivalent ventilation rate
FID	flame ionization detection
FR	Federal Register
FTIR	Fourier transform infrared absorption spectroscopy

GC	gas chromatography
GCE	Goddard Cumulus Ensemble
CG-FID	gas chromatography - flame ionization detection
GEOS-1 DAS	Goddard Earth Observing System Data Assimilation System
GEOS-CHEM	
H^+	hydrogen ion
HC	hydrocarbon
HCFC	hydrochlorofluorocarbon
H_2CO, HCHO	formaldehyde
HNO_2, HONO	nitrous acid
HNO_3	nitric acid
HO	hydroxyl
HO_2	hydroperoxyl; hydroperoxy
H_2O_2	hydrogen peroxide
HPLC	high-performance liquid chromatography
H_2SO_4	sulfuric acid
IBM	individual-based model
IC	intracloud
ID	identification (number)
ICEM	Indoor Chemistry and Exposure Model
I/O	indoor/outdoor
IPCC	Intergovernmental Panel on Climate Change
IPMMI	International Photolysis Frequency Measurement and Modeling Intercomparison
ISCCP	International Satellite Cloud Climatology Project
LFT	lower free troposphere
LIF	laser-induced fluorescence
LLJ	low level jet
LST	local standard time
LT	local time

LWC	liquid water content
MAQSIP	Multiscale Air Quality Simulation Platform
MBL	marine boundary layer
MBTH	3-methyl-2-benzothiazolone hydrazone
MCCP	Mountain Cloud Chemistry Program
MCM	master chemical mechanism
MENTOR	Modeling Environment for Total Risk Studies
MENTOR-OPERAS	Modeling Environment for Total Risk Studies — Ozone and Particles Exposure Risk Analysis System
MET	metabolic equivalent
MIESR	matrix isolation on ESR spectroscopy
MM5	Mesoscale Model, version 5
MoOx	molybdenum oxides
MOZAIC	Measurement of Ozone and Water Vapor by Airbus In-Service Aircraft
MPAN	peroxymethacryloyl nitrate; peroxy-methacrylic nitric anhydride
MS	mass spectrometry
MSA	Metropolitan Statistical Area
MS/MS	tandem mass spectrometry
N100	number of hours at an ozone concentration of $\geq$ 0.10 ppm
N_2O_5	dinitrogen pentoxide
NA, N/A	not available
NAAQS	National Ambient Air Quality Standards
NADP	National Atmospheric Deposition Program
NAMS	National Air Monitoring Station
NAPAP	National Acid Precipitation Assessment Program
NAPBN	National Air Pollution Background Network
NARE	North Atlantic Regional Experiment
NBS	National Bureau of Standards; now National Institute of Standards and Technology
NCAR	National Center for Atmospheric Research

NCEA-RTP	National Center for Environmental Assessment Division in Research Triangle Park, NC
NCLAN	National Crop Loss Assessment Network
ND	not detectable; not detected
NESCAUM	Northeast States for Coordinated Air Use Management
NDDN	National Dry Deposition Network
NEM	National Ambient Air Quality Standards Exposure Model
NF	national forest
NH_3	ammonia
NHAPS	National Human Activity Pattern Survey
NIST	National Institute of Standards and Technology
NM	national monument
NMHC	nonmethane hydrocarbon
NMOC	nonmethane organic compound
NMVOC	nonmethane volatile organic compound
NO	nitric oxide
NO_2	nitrogen dioxide
N_2O	nitrous oxide
NO_3^-	nitrate
NO_x	nitrogen oxides
NO_y	reactive nitrogen system components; sum of NO_x and NO_z; odd nitrogen species
NO_z	difference between NO_y and NO_x
NOAA	National Oceanic and Atmospheric Administration
NP	national park
NPAN	methacryloylperoxynitrate
NRC	National Research Council
NS	nonsignificant
NTRMs	NIST Traceable Reference Materials
$O(^1D)$	electronically excited oxygen atom

$O(^3P)$	ground-state oxygen atom
O_3	ozone
OAQPS	Office of Air Quality Planning and Standards
OBMs	observationally based methods
Obs.	observations
OH	hydroxyl; hydroxy
OPE	ozone production efficiency
O_x	odd oxygen species
P_{90}	values for the 90^{th} percentile
PAHs	polycyclic aromatic hydrocarbons
PAMS	Photochemical Aerometric Monitoring System
PAN	peroxyacetyl nitrate; peroxyacetic nitric anhydride
PANs	peroxyacyl nitrates
PAR	
p-ATP	*p*-acetamidophenol
PBL	planetary boundary layer
PBM	population-based model
PCA	principal component analysis
PEM	personal exposure monitor
pH	hydrogen ion concentration
PM	particulate matter
$PM_{2.5}$	fine particulate matter
pNEM	Probabilistic National Ambient Air Quality Standard Exposure Model
POC	particulate organic carbon
PPN	peroxypropionyl nitrate; peroxypropionic nitric anhydride
PPP	power plant plume
PRB	policy relevant background
PTR-MS	proton-transfer-reaction mass spectroscopy
PV	potential vorticity

r	linear regression correlation coefficient; Pearson correlation coefficient
R^2	multiple correlation coefficient
RACM	Regional Air Chemistry Mechanism
RADM	Regional Acid Deposition Model
RDBMS	Relational Database Management Systems
REHEX	Regional Human Exposure Model
RH	relative humidity
RMR	resting metabolic rate
RO_2	organic peroxyl; organic peroxy
RRMS	Relatively Remote Monitoring Sites
SAB	Science Advisory Board
SAI	Systems Applications International
SAPRC	Statewide Air Pollution Research Center, University of California, Riverside
SAROAD	Storage and Retrieval of Aerometric Data (U.S. Environmental Protection Agency centralized database; superseded by Aerometric Information Retrieval System [AIRS])
SHEDS	Simulation of Human Exposure and Dose System
SLAMS	State and Local Air Monitoring Station
SO_2	sulfur dioxide
SO_4^{2-}	sulfate
SOA	secondary organic aerosol
SOS	Southern Oxidant Study
SRM	standard reference material
STE	stratospheric-tropospheric exchange
STEP	Stratospheric-Tropospheric-Exchange Project
STPD	standard temperature and pressure, dry
STRF	Spatio-Temporal Random Field
SUM06	seasonal sum of all hourly average concentrations $\geq$ 0.06 ppm
SUM07	seasonal sum of all hourly average concentrations $\geq$ 0.07 ppm
SUM08	seasonal sum of all hourly average concentrations $\geq$ 0.08 ppm

SURE	Sulfate Regional Experiment Program
TAR	Third Assessment Report
TDLAS	tunable-diode laser absorption spectroscopy
Tg	teragram
TOMS	
TOPSE	Tropospheric Ozone Production About the Spring Equinox
TPLIF	two-photon laser-induced fluorescence
TRIM	Total Risk Integrated Methodology (model)
TTFMS	two-tone frequency-modulated spectroscopy
TVA	Tennessee Valley Authority
UAM	Urban Airshed Model
UTC	Coordinated Universal Time
UV	ultraviolet
UV-B	ultraviolet radiation of wavelengths 280 to 320 nm
UV-DIAL	Ultraviolet Differential Absorption Lidar
VOC	volatile organic compound
WFM	White Face Mountain
WMO/UNEP	World Meteorological Organization/United Nations Environment Program
W126	cumulative integrated exposure index with a sigmoidal weighting function

EXECUTIVE SUMMARY

To be prepared after CASAC review of this First External Review Draft and then inserted in Second External Review Draft to be released for further public comment and CASAC review.

1. INTRODUCTION

This is an update revision of the document, "*Air Quality Criteria for Ozone and Related Photochemical Oxidants*," published by the U.S. Environmental Protection Agency (EPA) in 1996 (U.S. Environmental Protection Agency, 1996). That 1996 Ozone Air Quality Criteria Document (O_3 AQCD) provided scientific bases for Congressionally-mandated periodic review by the EPA of the National Ambient Air Quality Standards for Ozone (O_3 NAAQS), which culminated in promulgation of new O_3 NAAQS by EPA in 1997.

The present document critically assesses the latest scientific information relative to determining the health and welfare effects associated with the presence of various concentrations of O_3 and related oxidants in ambient air. It builds upon the previous 1996 EPA O_3 AQCD, by focusing on evaluation and integration of information relevant to O_3 NAAQS criteria development that has become available since that covered by the 1996 criteria review; and it will provide scientific bases for the current periodic review of the O_3 NAAQS.

This introductory chapter of the revised O_3 AQCD presents: (a) background information on legislative requirements, the criteria and NAAQS review process, and the history of O_3 NAAQS reviews (including a chronology of changes in key elements of the O_3 standards); (b) an overview of the current O_3 criteria review process and projected schedule (including approaches and procedures used to prepare this document, as well as projected key milestones); and (c) an orientation to the general organizational structure and content of the document.

1.1 LEGAL AND HISTORICAL BACKGROUND

1.1.1 Legislative Requirements

Two sections of the Clean Air Act (CAA) govern the establishment, review, and revision of National Ambient Air Quality Standards (NAAQS). Section 108 (42 U.S.C. 7408) directs the Administrator of the U.S. Environmental Protection Agency (EPA) to identify ambient air pollutants that may be reasonably anticipated to endanger public health or welfare and to issue air quality criteria for them. These air quality criteria are to reflect the latest scientific information useful in indicating the kind and extent of all identifiable effects on public health or welfare that may be expected from the presence of a given pollutant in ambient air.

Section 109(a) of the CAA (42 U.S.C. 7409) directs the Administrator of EPA to propose and promulgate primary and secondary NAAQS for pollutants identified under Section 108. Section 109(b)(1) defines a primary standard as one that, in the judgment of the Administrator, is requisite to protect the public health (see inset below) based on the criteria and allowing for an adequate margin of safety. The secondary standard, as defined in Section 109(b)(2), must specify a level of air quality that, in the judgment of the Administrator, is requisite to protect the public welfare (see inset below) from any known or anticipated adverse effects associated with the presence of the pollutant in ambient air, based on the criteria.

PUBLIC HEALTH EFFECTS

- Effects on the health of the general population, or identifiable groups within the population, who are exposed to pollutants in ambient air
- Effects on mortality
- Effects on morbidity
- Effects on other health conditions including indicators of:
  - pre-morbid processes,
  - risk factors, and
  - disease

PUBLIC WELFARE EFFECTS

- Effects on personal comfort and well-being
- Effects on economic values
- Deterioration of property
- Hazards to transportation
- Effects on the environment, including:
  - animals
  - climate
  - crops
  - materials
  - soils
  - vegetation
  - visibility
  - water
  - weather
  - wildlife

Section 109(d) of the CAA (42 U.S.C. 7409) requires periodic review and, if appropriate, revision of existing criteria and standards. If, in the Administrator's judgment, the Agency's review and revision of criteria make appropriate the proposal of new or revised standards, such standards are to be revised and promulgated in accordance with Section 109(b). Alternatively, the Administrator may find that revision of the standards is inappropriate and conclude the review by leaving the existing standards unchanged. Section 109(d)(2) of the 1977 CAA Amendments also requires that an independent scientific review committee be established to advise the EPA Administrator on NAAQS matters, including the scientific soundness of criteria (scientific bases) supporting NAAQS decisions. This role is fulfilled by the Clean Air Scientific Advisory Committee (CASAC) of EPA's Science Advisory Board (SAB).

1.1.2 Criteria and NAAQS Review Process

Periodic reviews by EPA of criteria and NAAQS for a given criteria air pollutant progress through a number of steps, beginning with preparation by EPA's National Center for Environmental Assessment Division in Research Triangle Park, NC (NCEA-RTP) of an air quality criteria document (AQCD). The AQCD provides a critical assessment of the latest available scientific information upon which the NAAQS are to be based. Drawing upon the AQCD, staff of EPA's Office of Air Quality Planning and Standards (OAQPS) prepare a Staff Paper that evaluates policy implications of the key studies and scientific information contained in the AQCD and presents the conclusions and recommendations of the staff for standard-setting options for the EPA Administrator to consider. The Staff Paper is intended to help "bridge the gap" between the scientific assessment contained in the AQCD and the judgments required of the Administrator in determining whether it is appropriate to retain or to revise the NAAQS. Iterative drafts of both the AQCD and the Staff Paper (as well as other analyses, such as exposure and/or risk assessments, supporting the Staff Paper) are made available for public comment and CASAC review. The final versions of the AQCD and Staff Paper incorporate changes made in response to CASAC and public review. Based on the information in these documents, the Administrator proposes decisions on whether to retain or revise the NAAQS, taking into account public comments and CASAC advice and recommendations. The Administrator's proposed decisions are published in the *Federal Register*, with a preamble that presents the rationale for the decisions and solicits public comment. The Administrator makes a final decision after considering comments received on the proposed decisions. The Administrator's final decisions are promulgated in a *Federal Register* notice that addresses significant comments received on the proposal.

NAAQS decisions involve consideration of the four basic elements of a standard: *indicator*, *averaging time*, *form*, and *level*. The indicator defines the pollutant to be measured in the ambient air for the purpose of determining compliance with the standard. The averaging time defines the time period over which air quality measurements are to be obtained and averaged, considering evidence of effects associated with various time periods of exposure. The form of a standard defines the air quality statistic that is to be compared to the level of the standard (i.e., an ambient concentration of the indicator pollutant) in determining whether an area attains the standard. The form of the standard specifies the air quality measurements that are to be used for compliance purposes (e.g., the 98th percentile of an annual distribution of daily concentrations; the annual arithmetic average), the monitors from which the measurements are to be obtained (e.g., one or more population-oriented monitors in an area), and whether the statistic is to be averaged across multiple years. These basic elements of a standard are the primary focus of the staff conclusions and recommendations in the Staff Paper and in the subsequent rulemaking, building upon the policy-relevant scientific information assessed in the AQCD and on the policy analyses contained in the Staff Paper. These four elements taken together determine the degree of public health and welfare protection afforded by the NAAQS.

1.1.3 Regulatory Chronology[1]

On April 30, 1971, the EPA promulgated primary and secondary NAAQS for photochemical oxidants under Section 109 of the CAA (36 FR 8186). These were set at an hourly average of 0.08 ppm total photochemical oxidants, not to be exceeded more than 1 h per year. On April 20, 1977, the EPA announced (42 FR 20493) the first review and updating of the 1970 Air Quality Criteria Document for Photochemical Oxidants in accordance with Section 109(d) of the CAA. In preparing that AQCD, the EPA made two external review drafts of the document available for public comment, and these drafts were peer reviewed by the Subcommittee on Scientific Criteria for Photochemical Oxidants of EPA's Science Advisory Board (SAB). A final revised AQCD for ozone (O_3) and other photochemical oxidants was published on June 22, 1978.

Based on the 1978 revised AQCD and taking into account the advice and recommendations of the SAB Subcommittee and public comments, the EPA announced (44 FR 8202) a final decision to revise the NAAQS for photochemical oxidants on February 8, 1979. That final rulemaking revised the primary standard from 0.08 ppm to 0.12 ppm, set the secondary standard to be the same as the primary standard, changed the chemical designation of the standards from photochemical oxidants to O_3, and revised the definition of the point at which the standard is attained as indicated in Table 1-1.

[1]This following text is excerpted and adapted from the "Proposed Decision on the National Ambient Air Quality Standards for Ozone," 57 FR 35542, 35542-35557 (August, 10, 1992) and the "National Ambient Air Quality Standards for Ozone; Final Rule," 62 FR 38856, 83356-38896 (July 18, 1997).

Table 1-1. National Ambient Air Quality Standards (NAAQS) for Ozone

Date of Promulgation	Primary and Secondary NAAQS	Averaging Time
February 8, 1979	0.12 ppm[a] (235 μg/m^3)	1 h[b]
July 18, 1997	0.08 ppm[a] (157 μg/m^3)	8 h[c]

[a]1 ppm = 1962 μg/m^3, 1 μg/m^3 = 5.097 × 10^{-4} ppm @ 25 °C, 760 mm Hg.

[b]The standard is attained when the expected number of days per calendar year with a maximum hourly average concentration above 235 μg/m^3 (0.12 ppm) is equal to or less than one.

[c]Based on the 3-year average of the annual fourth-highest daily maximum 8-h average concentration measured at each monitor within an area.

Source: Federal Register (1979, 1997).

On March 17, 1982, in response to requirements of Section 109(d) of the CAA, the EPA announced (47 FR 11561) that it planned to revise the existing 1978 AQCD for O_3 and Other Photochemical Oxidants, and on August 22, 1983, it announced (48 FR 38009) that review of the primary and secondary NAAQS for O_3 had been initiated. The EPA provided a number of opportunities for expert review and public comment on revised chapters of the AQCD, including two public peer-review workshops in December 1982 and November 1983. Comments made at both workshops were considered by EPA in preparing the First External Review Draft that was made available (49 FR 29845) on July 24, 1984, for public review.

On February 13, 1985 (50 FR 6049) and then on April 2, 1986 (51 FR 11339), the EPA announced two public CASAC meetings, which were held on March 4-6, 1985 and April 21-22, 1986, respectively. At these meetings, the CASAC reviewed external review drafts of the revised AQCD for O_3 and Other Photochemical Oxidants. After these two reviews, the Chair summarized CASAC's consensus view in an October 1986 letter to the EPA Administrator, which stated that the document "represents a scientifically balanced and defensible summary of the extensive scientific literature." Taking into account public and CASAC comments on the two external review drafts, revisions were made by EPA and the final document was released by EPA in August 1986.

The first draft of the Staff Paper "Review of the National Ambient Air Quality Standards for Ozone: Assessment of Scientific and Technical Information" drew upon key findings and conclusions from the AQCD and was reviewed by CASAC at an April 21-22, 1986 public meeting. At that meeting, the CASAC recommended that new information on prolonged O_3 exposure effects be considered in a second draft of the Staff Paper. The CASAC reviewed the resulting second draft and also heard a presentation of new and emerging information on the health and welfare effects of O_3, at a public review meeting held on December 14-15, 1987. The CASAC concluded that sufficient new information existed to recommend incorporation of relevant new data into a supplement to the 1986 AQCD (O_3 Supplement) and in a third draft of the Staff Paper.

A draft O_3 Supplement, "Summary of Selected New Information on Effects of Ozone on Health and Vegetation: Draft Supplement to Air Quality Criteria for Ozone and Other Photochemical Oxidants," and the revised Staff Paper were made available to CASAC and to the public in November 1988. The O_3 Supplement assessed selected literature concerning exposure- and concentration-response relationships observed for health effects in humans and experimental animals and for vegetation effects that appeared in papers published or in-press from 1986 through early 1989. On December 14-15, 1988, CASAC held a public meeting to review these documents. The CASAC sent the EPA Administrator a letter, dated May 1, 1989, which stated that the draft O_3 Supplement, the 1986 AQCD, and the draft Staff Paper "provide an adequate scientific basis for the EPA to retain or revise the primary and secondary standards of ozone." The CASAC concluded (a) that it would be some time before sufficient new information on the health effects of multihour and chronic exposure to O_3 would be published in scientific journals to receive full peer review and, thus, be suitable for inclusion in a criteria document and (b) that such information could be considered in the next review of the O_3 NAAQS. A final version of the O_3 Supplement was published in 1992 (U.S. Environmental Protection Agency, 1992).

On October 22, 1991, the American Lung Association and other plaintiffs filed suit to compel the Agency to complete the review of the criteria and standards for O_3 in accordance with the CAA. The U.S. District Court for the Eastern District of New York subsequently issued an order requiring the EPA to announce its proposed decision on whether to revise the standards for O_3 by August 1, 1992, and to announce its final decision by March 1, 1993.

The proposed decision on O_3, appearing in the Federal Register on August 10, 1992 (57 FR 35542), indicated that revision of the existing 1-h NAAQS was not appropriate at this time. A public hearing on this decision took place in Washington, DC on September 1, 1992, and public comments were received through October 9, 1992. The final decision not to revise the

1-h NAAQS was published in the Federal Register on March 9, 1993 (58 FR 13008). However, that decision did not take into consideration a number of more recent studies on the health and welfare effects of O_3 that had been published since the last of the literature assessed in the O_3 Supplement (i.e., studies available through 1985 and into early 1986).

The Agency initiated consideration of such studies as part of the next congressionally-mandated periodic review of criteria and NAAQS for Ozone. The new studies were assessed in revised workshop draft O_3 AQCD chapters that were peer reviewed in July and September 1993, followed by public release of the First External Review Draft in February 1994 and CASAC review on July 20-21, 1994. Further drafts of the O_3 AQCD, revised in response to public comments and CASAC review, were reviewed by CASAC on March 21-25, 1995, and at a final CASAC review meeting on September 19-20, 1995. The scientific soundness of the revised O_3 AQCD was recognized by CASAC in a November 28, 1995 letter to the EPA Administrator; and the final AQCD for O_3 was published in July 1996.

The first draft of the associated Staff Paper, "Review of the National Ambient Air Quality Standards for Ozone: Assessment of Scientific and Technical Information," was also reviewed by CASAC at the March 21-22, 1995 public meeting. CASAC also reviewed subsequent drafts of the Staff Paper at public meetings on September 19-20, 1995 and March 21, 1996, with completion of CASAC review of the primary and secondary standard portions of the draft Staff Paper being communicated in letters to the EPA Administrator dated November 30, 1995 and April 4, 1996, respectively. The final O_3 Staff Paper was published in June 1996.

On December 13, 1996 EPA published its proposed decision to revise the O_3 NAAQS (61 FR 65716). EPA provided extensive opportunities for public comment on the proposed decision, including several public hearings and two national satellite telecasts. EPA's final decision to promulgate a new 8-h O_3 NAAQS (see Table 1-1) was published on July 18, 1997 (62 FR 38856).

Following promulgation of the new standards, numerous petitions for review of the standards were filed in the U.S. Court of Appeals for the District of Columbia Circuit (D.C. Circuit)[2]. On May 14, 1999, the Court remanded the O_3 NAAQS to EPA, finding that section 109 of the CAA, as interpreted by EPA, effected an unconstitutional delegation of legislative

---

[2]*American Trucking Associations* v. EPA, No. 97-1441

authority[3]. In addition, the Court directed that, in responding to the remand, EPA should consider the potential beneficial health effects of O_3 pollution in shielding the public from the effects of solar ultraviolet (UV) radiation. On January 27, 2000, EPA petitioned the U.S. Supreme Court for certiorari on the constitutional issue (and two other issues), but did not request review of the D.C. Circuit ruling regarding the potential beneficial health effects of O_3. On February 27, 2001 the U.S. Supreme Court unanimously reversed the judgment of the D.C. Circuit on the constitutional issue, holding that section 109 of the CAA does not delegate legislative power to the EPA in contravention of the Constitution, and remanded the case to the D.C. Circuit to consider challenges to the O_3 NAAQS that had not been addressed by that Court's earlier decisions[4]. On March 26, 2002, the D.C. Circuit issued its final decision, finding the 1997 O_3 NAAQS to be "neither arbitrary nor capricious," and denied the remaining petitions for review[5].

On November 14, 2001 EPA proposed to respond to the Court's remand to consider the potential beneficial health effects of O_3 pollution in shielding the public from the effects of solar UV radiation by leaving the 1997 8-h NAAQS unchanged. Following a review of information in the record and the substantive comments received on the proposed response, EPA issued a final response to the remand, reaffirming the 8 h O3 NAAQS (68 FR 614, January 6, 2003).

1.2 CURRENT OZONE CRITERIA AND NAAQS REVIEW

1.2.1 Key Milestones and Procedures for Document Preparation

It is important to note at the outset that development of the present document has and will continue to include substantial external expert review and opportunities for public input through (a) public workshops involving the general aerosol scientific community, (b) iterative reviews of successive drafts by CASAC, and (c) comments from the public on successive drafts. The extensive external input received through such reviews will help to ensure that the review of the

[3] *American Trucking Associations* v. EPA, 175 F.3d 1027 (D.C. Cir., 1999)

[4] *Whitman v. American Trucking Associations*, 531 U.S. 457 (2001)

[5] *American Trucking Associations v. EPA*, 283 F.3d 355, (D.C. Cir. 2002)

O_3 standards will be based on critical assessment in this document of the latest available pertinent science.

The procedures for developing this revised O_3 AQCD build on experience derived from the other recent criteria document preparation efforts, with key milestones for development of this O_3 AQCD being listed in Table 1-2. Briefly, the respective responsibilities for production of this O_3 AQCD and key milestones are as follows. An NCEA-RTP Ozone Team is responsible for the creation and implementation of a project plan for developing the O_3 AQCD, taking into account input from individuals in other EPA program and policy offices identified as part of the EPA Ozone Work Group. The resulting plan, i.e., the Project Work Plan for Revised Air Criteria for Ozone and Related Photochemical Oxidants (November 2002), was discussed with CASAC in January 2003. An ongoing literature search that was underway prior to initiation of work on this document has continued throughout its preparation to identify pertinent O_3 literature published since early 1996. Under the processes established in Sections 108 and 109 of the CAA, the EPA officially initiated the current criteria and NAAQS review by announcing the commencement of the review in the Federal Register (65 FR 57810, September, 2000) with a call for information. That Federal Register notice included (1) a request asking for recently available research information on O_3 that may not yet have been published and (2) a request for individuals with the appropriate type and level of expertise to contribute to the writing of O_3 AQCD materials to identify themselves. The specific authors of chapters or sections of the proposed document included both EPA and non-EPA scientific experts, who were selected on the basis of their expertise on the subject areas and their familiarity with the relevant literature. The project team defined critical issues and topics to be addressed by the authors and provided direction in order to emphasize evaluation of those studies most clearly identified as important for standard setting.

As with other NAAQS reviews, critical assessment of relevant scientific information is presented in this updated O_3 AQCD. The main focus of this document is the evaluation and interpretation of pertinent atmospheric science information, air quality data, human exposure information, and health and welfare effects information newly published since that assessed in the 1996 O_3 AQCD. Draft versions of AQCD chapter materials were evaluated via expert peer-consultation workshop discussions (see Table 1-2) that focused on the selection of pertinent studies to be included in the chapters, the potential need for additional information to be added to the chapters, and the quality of the characterization and interpretation of the literature. The

Table 1-2. Key Milestones for Development of Revised Ozone Air Quality Criteria Document[a]

Major Milestones	Target Dates
1. Literature Search	Ongoing
2. Federal Register Call for Information	September 2000
3. Draft Project Plan Available for Public Comment	Dec 2001 - March 2002
4. Revised Draft Project Plan Released for CASAC Review	December 2002
5. CASAC Review of Draft Project Work Plan	January 2003
6. Peer-Consultation Workshop on Draft Ecological Effects Materials	April 2003
7. Peer-Consultation Workshops on Draft Atmospheric Science/Exposure and Dosimetry/Health Chapters	July 2004
8. First External Review Draft of O_3 AQCD	January 2005
9. Public Comment Period (90 days)	Feb - April 2005
10. CASAC Public Review Meeting *(First External Review Draft)*	April/May 2005
11. Second External Review Draft of O_3 AQCD	Aug/Sept 2005
12. Public Comment Period (90 days)	Sept - Nov 2005
13. CASAC Public Review Meeting	December 2005
14. Final O_3 AQCD	February 2006

[a] Proposed schedule will be modified from time to time, as necessary, to reflect actual project requirements and progress.

authors of the draft chapters then revised them on the basis of the workshop and/or other expert review comments[6]. These and other integrative materials have been incorporated into this First External Review Draft of the O_3 AQCD (January 2005), which is being made available for public comment and for CASAC review (see Table 1-2).

Following the upcoming April/May 2005 CASAC meeting, EPA plans to incorporate revisions into the draft O_3 AQCD in response to comments from CASAC and the public and to make a Second External Review Draft available for further public comment and CASAC review according to the schedule projected in Table 1-2. More specifically, that Second External

[6]It should be noted that materials contributed by non-EPA authors have, at times, been modified by EPA Ozone Team staff in response to internal and/or external review comments, and that EPA is responsible for the ultimate content of this O_3 AQCD.

Review Draft is expected to be made available in August 2005 for public comment (90 days) and to be reviewed by CASAC at a public meeting in December 2005. The final O_3 AQCD is to be completed by February 28, 2006 and will be made publicly available electronically via an EPA website and will then be subsequently printed. Its availability will be announced in the Federal Register.

Once the CASAC has reviewed the First External Review Draft of the revised O_3 AQCD, thus providing a preliminary basis for review of the existing standards, the EPA's Office of Air Quality Planning and Standards (OAQPS) staff will prepare a draft O_3 Staff Paper drawing upon key information contained in the draft criteria document and presenting staff recommendations on whether to retain or, if appropriate, revise the O_3 NAAQS. After review of that draft Staff Paper by the public and by CASAC, EPA will take public and CASAC comments into account in producing a Second Draft Staff Paper. This Second Draft Staff Paper will be made available for further public comment and CASAC review before EPA produces a final Staff Paper by September 30, 2006.

1.3 ORGANIZATIONAL STRUCTURE OF THE DOCUMENT

1.3.1 General Document Format

The authors were provided with copies of the 1996 O_3 AQCD (U.S. Environmental Protection Agency, 1996) and were instructed to open each new section for the updated document with concise summarization of key findings and conclusions from the previous 1996 O_3 AQCD. After presentation of such background information, the remainder of each section typically attempts to provide an updated discussion of newer literature and resulting key conclusions. In some cases where no new information is available, the summary of key findings and conclusions from the previous criteria document must suffice as the basis for current key conclusions. Increased emphasis is placed in the main chapters of this revised O_3 AQCD on interpretative evaluation and integration of evidence pertaining to a given topic than has been typical of previous EPA air quality criteria documents, with more detailed descriptions of individual studies being provided in a series of accompanying annexes.

A list of references published since completion of the 1996 criteria document was made available to the authors. The references were selected from information data base searches conducted by EPA. Additional references have been added to the list (e.g., missed or recently published papers or "in press" publications) as work has proceeded in creating the draft document materials. As an aid in selecting pertinent new literature, the authors were also provided with a summary of issues that need to be addressed in the revised air quality criteria document for O_3. These issues were identified by authors and reviewers of the previous documents and continue to be expanded, as appropriate, based on public discussions, workshops, or other comments received by EPA.

1.3.2 Organization and Content of the Document

This revised AQCD for O_3 and Related Photochemical Oxidants critically assesses scientific information on the health and welfare effects associated with exposure to the concentrations of these pollutants in ambient air. The document does not provide a detailed literature review; but, rather, discusses cited references that reflect the current state of knowledge on the most relevant issues pertinent to the NAAQS for O_3. Although emphasis is placed on discussion of health and welfare effects information, other scientific data are presented and evaluated in order to provide a better understanding of the nature, sources, distribution, measurement, and concentrations of O_3 and related photochemical oxidants in ambient air, as well as the measurement of population exposure to these pollutants.

The main focus of the scientific information discussed in the text comes from literature published since completion of the 1996 O_3 AQCD (U.S. Environmental Protection Agency, 1996). Emphasis is placed on studies conducted at or near O_3 concentrations found in ambient air. Other studies are included if they contain unique data, such as the documentation of a previously unreported effect or of a mechanism for an observed effect; or if they were multiple-concentration studies designed to provide exposure-response relationships. Generally, this is not an issue for human clinical or epidemiology studies. However, for animal toxicology studies, consideration is given mainly to those studies conducted at less than 1 ppm O_3. Key information from studies assessed in the previous O_3 AQCD and whose data impacted the derivation of the current NAAQS are briefly summarized in the text, along with specific citations to the previous document. Prior studies are also discussed if they (1) are open to reinterpretation in light of newer data, or (2) are potentially useful in deriving revised standards for O_3. Generally, only information that has undergone scientific peer review and has been published (or accepted for publication) through 2004 is included in the draft document.

The document will consist of three volumes. The first volume will include an Executive Summary and Conclusions, as well as Chapters 1 through 3 and their accompanying annexes. This introductory chapter (Chapter 1) presents background information on the purpose of the document, legislative requirements, and the history of past O_3 NAAQS regulatory actions, as well as an overview of the organization and content of the document. Chapter 2 provides information on the physics and chemistry of O_3 and related photochemical oxidants in the atmosphere. Chapter 3 covers tropospheric O_3 environmental concentrations, patterns, and exposure estimates.

Health information pertinent to derivation of the primary O_3 NAAQS is then mainly covered in the next several chapters (Chapters 4 through 8) contained in Volume II. Chapter 4 discusses O_3 dosimetry aspects, and Chapters 5, 6, and 7 discuss animal toxicological studies, human health effects from controlled-exposure studies, and epidemiologic studies of ambient air exposure effects on human populations, respectively. Chapter 8 then provides an integrative and interpretive evaluation of key information relevant to O_3 exposure and health risks, of most pertinence to the review of primary O_3 NAAQS.

Volume III contains those chapters that assess welfare effects information pertinent to the review of secondary O_3 NAAQS. Chapter 9 deals with ecological and other environmental effects of O_3 and related photochemical oxidants. Chapter 10 assesses tropospheric O_3 involvement in climate change processes, including determination of solar UV flux in Earth's lower atmosphere. Lastly, Chapter 11 discusses O_3 effects on man-made materials as a third type of welfare effect of potential concern.

REFERENCES

Federal Register. (1979) National primary and secondary ambient air quality standards: revisions to the National Ambient Air Quality Standards for photochemical oxidants. F. R. (February 8) 44: 8202-8237.

Federal Register (1992) Proposed Decision on the National Ambient Air Quality Standards for Ozone, Preamble. Federal Register 57: 35542-35557.

Federal Register (1997) National Ambient Air Quality Standards for Ozone; Final Rule. 40 CFR 50; Federal Register 62: 38856-38896

U.S. Code (1999) Clean Air Act, title III-general, Section 302, definitions (h) effects on welfare. U.S.C. 42: § 7602.

U.S. Environmental Protection Agency. (1986) Air quality criteria for ozone and other photochemical oxidants. Research Triangle Park, NC: Office of Health and Environmental Assessment, Environmental Criteria and Assessment Office; EPA report nos. EPA-600/8-84-020aF-eF. Available from NTIS, Springfield, VA; PB87-142949.

U.S. Environmental Protection Agency. (1992) Summary of selected new information on effects of ozone on health and vegetation: supplement to 1986 air quality criteria for ozone and other photochemical oxidants. Research Triangle Park, NC: Office of Health and Environmental Assessment, Environmental Criteria and Assessment Office; EPA report no. EPA/600/8-88/105F. Available from NTIS, Springfield, VA; PB92-235670.

U.S. Environmental Protection Agency. (1996) Air quality criteria for ozone and related photochemical oxidants. Research Triangle Park, NC: Office of Research and Development; report nos. EPA/600/AP-93/004aF-cF. 3v. Available from: NTIS, Springfield, VA; PB96-185582, PB96-185590, and PB96-185608. Available online at: www.epa.gov/ncea/ozone.htm.

2. PHYSICS AND CHEMISTRY OF OZONE IN THE ATMOSPHERE

2.1 INTRODUCTION

Ozone (O_3) and other oxidants, such as peroxacyl nitrates and hydrogen peroxide (H_2O_2) form in polluted areas mainly by atmospheric reactions involving two classes of precursor pollutants, volatile organic compounds (VOCs) and nitrogen oxides (NO_x). Ozone is thus a secondary pollutant. The formation of O_3, other oxidants and oxidation products from these precursors is a complex, nonlinear function of many factors: the intensity and spectral distribution of sunlight; atmospheric mixing and processing on cloud and aerosol particles; the concentrations of the precursors in ambient air; and the rates of chemical reactions of the precursors. Information contained in this chapter and in greater detail in Annex AX2 describes these processes, numerical models that incorporate these processes to calculate O_3 concentrations, and techniques for measuring concentrations of ambient oxidants.

The atmosphere can be divided into several distinct vertical layers, based primarily on the major mechanisms by which they are heated and cooled. The lowest major layer is the troposphere, which extends from the earth's surface to about 8 km above polar regions and to about 16 km above tropical regions. The planetary boundary layer (PBL) is the lower sub-layer of the troposphere, extending from the surface to about 1 or 2 km and is most strongly affected by surface conditions. The stratosphere extends from the tropopause, or the top of the troposphere, to about 50 km in altitude (Annex AX2.2.1). The emphasis in this chapter is placed on chemical and physical processes occurring in the troposphere, in particular in the PBL.

2.2 CHEMICAL PROCESSES INVOLVED IN OZONE FORMATION AND DESTRUCTION

Ozone occurs not only in polluted urban atmospheres but also throughout the troposphere, even in remote areas of the globe. The same basic processes, involving sunlight driven reactions of NO_x and VOCs contribute to O_3 formation throughout the troposphere. These processes lead also to the formation of other photochemical products, such as peroxyacetyl nitrate (PAN), nitric acid (HNO_3), and sulfuric acid (H_2SO_4), and to other compounds, such as formaldehyde (HCHO) and other carbonyl compounds, such as aldehydes and ketones.

The photochemical formation of O_3 in the troposphere proceeds through the oxidation of nitric oxide (NO) to nitrogen dioxide (NO_2) by organic (RO_2) or hydro-peroxy (HO_2) radicals. The photolysis of NO_2 yields nitric oxide (NO) and a ground-state oxygen atom, $O(^3P)$, which then reacts with molecular oxygen to form O_3. The free radicals oxidizing NO to NO_2 are formed during the oxidation of VOCs (Annex AX2.2.2).

The term VOC refers to all carbon-containing gas-phase compounds in the atmosphere, both biogenic and anthropogenic in origin, excluding carbon monoxide (CO) and carbon dioxide (CO_2). Classes of compounds important for the photochemical formation of O_3 include alkanes, alkenes, aromatic hydrocarbons, carbonyl compounds (e.g., aldehydes and ketones), alcohols, organic peroxides, and halogenated organic compounds (e.g., alkyl halides). This array of compounds encompasses a wide range of chemical properties and lifetimes: isoprene has an atmospheric lifetime of approximately an hour, whereas methane has an atmospheric lifetime of about a decade.

In urban areas, compounds representing all classes of VOCs are important for O_3 formation. In nonurban vegetated areas, biogenic VOCs emitted from vegetation tend to be the most important. In the remote troposphere, CH_4 and CO are the main carbon-containing precursors to O_3 formation. CO also can play an important role in O_3 formation in urban areas. The oxidation of VOCs is initiated mainly by reaction with hydroxyl (OH) radicals. The primary source of OH radicals in the atmosphere is the reaction of electronically excited O atoms, $O(^1D)$, with water vapor. $O(^1D)$ is produced by the photolysis of O_3 in the Hartley bands. In polluted areas, the photolysis of aldehydes (e.g., HCHO), nitrous acid (HONO) and hydrogen peroxide (H_2O_2) can also be significant sources of OH or HO_2 radicals that can rapidly be converted to OH (Eisele et al., 1997). Ozone can oxidize alkenes; and at night, when they are most abundant, NO_3 radicals also oxidize alkenes. In coastal environments and other selected environments, atomic Cl and Br radicals can also initiate the oxidation of VOCs (Annex AX2.2.3).

There are a large number of oxidized nitrogen containing compounds in the atmosphere including NO, NO_2, NO_3, HNO_2, HNO_3, N_2O_5, HNO_4, PAN and its homologues, other organic nitrates and particulate nitrate. Collectively these species are referred to as NO_y. Oxidized nitrogen compounds are emitted to the atmosphere mainly as NO which rapidly interconverts with NO_2 and so NO and NO_2 are often "lumped" together into their own group or family, or NO_x. NO_x can be oxidized to reservoir and termination species (PAN and its homologues, organic nitrates, HNO_3, HNO_4 and particulate nitrate). These reservoir and termination species are referred to as NO_z. The major reactions involving inter-conversions of oxidized nitrogen species are discussed in Annex AX2.2.4.

The photochemical cycles by which the oxidation of hydrocarbons leads to O_3 production are best understood by considering the oxidation of methane, structurally the simplest VOC. The CH_4 oxidation cycle serves as a model for the chemistry of the relatively clean or unpolluted troposphere (although this is a simplification because vegetation releases large quantities of complex VOCs, such as isoprene, into the atmosphere). In the polluted atmosphere, the underlying chemical principles are the same, as discussed in Annex AX2.2.5. The conversion of NO to NO_2 occurring with the oxidation of VOCs is accompanied by the production of O_3 and the efficient regeneration of the OH radical, which in turn can react with other VOCs. A schematic overview showing the major processes involved in O_3 production and loss in the troposphere and stratosphere is given in Figure 2-1.

The oxidation of alkanes and alkenes in the atmosphere has been treated in depth in CD96 and is updated in Annexes AX2.2.6 and AX2.2.7. In contrast to simple hydrocarbons containing one or two carbon atoms, detailed kinetic information about the gas phase oxidation pathways of many anthropogenic hydrocarbons (e.g., aromatic compounds, such as benzene and toluene), biogenic hydrocarbons (e.g., isoprene, the monoterpenes), and their intermediate oxidation products (e.g., epoxides, nitrates, and carbonyl compounds) is lacking. Reaction with OH radicals represents the major loss process for alkanes. Reaction with chlorine atoms is an additional sink for alkanes. Stable products of alkane photooxidation are known to include carbonyl compounds, alkyl nitrates, and *d*-hydroxycarbonyls. Major uncertainties in the atmospheric chemistry of the alkanes concern the chemistry of alkyl nitrate formation; these uncertainties affect the amount of NO-to-NO_2 conversion occurring and, hence, the amounts of O_3 formed during photochemical degradation of the alkanes.

The reaction of OH radicals with aldehydes produced during the oxidation of alkanes forms acyl (R′CO) radicals, and acyl peroxy radicals ($R'C(O){-}O_2$) are formed by the further addition of O_2. As an example, the oxidation of ethane ($C_2H_5{-}H$) yields acetaldehyde ($CH_3{-}CHO$). The reaction of $CH_3{-}CHO$ with OH radicals yields acetyl radicals ($CH_3{-}CO$).

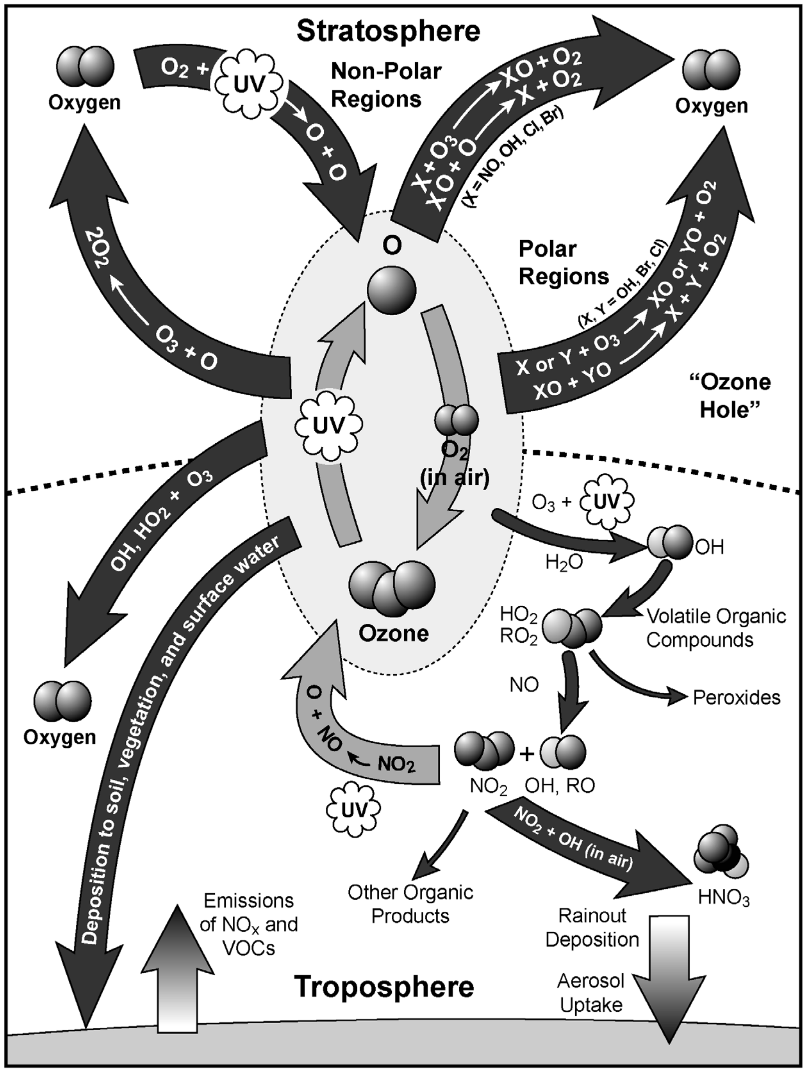

Figure 2-1. Schematic overview of O_3 photochemistry in the stratosphere and troposphere.

The acetyl radicals will then participate with O_2 in a termolecular recombination reaction to form acetyl peroxy radicals, which can then react with NO to form $CH_3 + CO_2$ (or they can react with NO_2 to form PAN). PAN acts as a temporary reservoir for NO_2. Upon the thermal decomposition of PAN, either locally or elsewhere, NO_2 is released to participate in the O_3 formation process again.

Alkenes react in ambient air with OH, NO_3 , and Cl radicals and with O_3. All of these reactions are important atmospheric transformation processes, and all proceed by initial addition to the $>C=C<$ bonds. Products of alkene photooxidation include carbonyl compounds, hydroxynitrates and nitratocarbonyls, and decomposition products from the energy-rich biradicals formed in alkene-O_3 reactions. Major uncertainties in the atmospheric chemistry of the alkenes concern the products and mechanisms of their reactions with O_3, especially the yields of free radicals that participate in O_3 formation. Examples of oxidation mechanisms of complex alkanes and alkenes can be found in comprehensive texts such as Seinfeld and Pandis (1998).

The oxidation of aromatic hydrocarbons constitutes an important component of the chemistry of O_3 formation in urban atmospheres (Annex AX2.2.8). Virtually all of the important aromatic hydrocarbon precursors emitted in urban atmospheres are lost through reaction with the hydroxyl radical. Loss rates for these compounds vary from slow (i.e., benzene) to moderate (e.g., toluene), to very rapid (e.g., xylene and trimethylbenzene isomers). These loss rates are very well understood at room temperature and atmospheric pressure and numerous experiments have been conducted that verify this. However, the mechanism for the reaction of OH with aromatic hydrocarbons is poorly understood as evident from the poor mass balance of the reaction products. The mechanism for the oxidation of toluene has been studied most thoroughly and there is general agreement on the initial steps in the mechanism. However, at present there is no promising approach for resolving the remaining issues concerning the later steps. The oxidation of aromatic hydrocarbons also leads to particle formation which could remove gas-phase constituents that participate in O_3 formation. The chemistry of secondary organic aerosol formation from gaseous precursors was summarized in the latest AQCD for particulate matter.

The reactions of oxygenated VOCs are also important components of O_3 formation (Annex AX2.2.9). They may be produced either by the oxidation of hydrocarbons or they may be present in ambient air as the result of direct emissions. For example, motor vehicles and some industrial processes emit formaldehyde and vegetation emits methanol.

As much as 30% of the carbon in hydrocarbons in many urban areas is in the form of aromatic compounds. Yet, mass balance analyses performed on irradiated smog chamber mixtures of aromatic hydrocarbons indicate that only about one-half of the carbon is in the form of compounds that can be identified. The situation is not much better for some smaller anthropogenic hydrocarbons. For example, only about 60% of the initial carbon can be accounted for in the OH initiated oxidation of 1,3-butadiene. About two-thirds of the initial carbon can be identified in product analyses of isoprene oxidation. Adequate analytical techniques needed to identify and quantify key intermediate species are not available for many compounds. In addition, methods to synthesize many of the suspected intermediate compounds are not available so that laboratory studies of their reaction kinetics cannot be performed. Similar considerations apply to the oxidation of biogenic hydrocarbons such as isoprene.

In addition to reactions occurring in the gas phase, reactions occurring on the surfaces of or within cloud droplets and airborne particles also occur. Their collective surface area is huge implying that collisions with gas phase species occur on very short time scales. In addition to hydrometeors (e.g., cloud and fog droplets and snow and ice crystals) there are also potential reactions involving atmospheric particles of varying composition (e.g., wet [deliquesced] inorganic particles, mineral dust, carbon chain agglomerates and organic carbon particles) to consider. Most of the well-established multiphase reactions tend to reduce the rate of O_3 formation in the polluted troposphere. Removal of HO_x and NO_x onto hydrated particles will reduce the production of O_3. The reactions of Br and Cl containing radicals deplete O_3 in selected environments such as the Arctic during spring, the tropical marine boundary layer and inland salt lakes. Direct reactions of O_3 and atmospheric particles appear to be too slow to reduce O_3 formation significantly at typical ambient PM levels. In addition, the oxidation of hydrocarbons by Cl radicals could lead to the rapid formation of peroxy radicals and higher rates of O_3 production in selected coastal environments. It should be stressed that knowledge of multiphase processes is still evolving and there are still many questions that remain to be answered as outlined in Annex AX2.2.10.

2.3 METEOROLOGICAL PROCESSES AFFECTING OZONE

Since CD96, substantial new information about transport processes has become available from numerical models, field experiments and satellite-based observations. Ozone is produced naturally by photochemical reactions in the stratosphere as shown in Figure 2-1. Some of this O_3 is transported downward into the troposphere throughout the year, with maximum contributions during late winter and early spring mainly in a process known as tropopause folding. Figure 2-2a shows a synoptic situation associated with a tropopause folding event. A vertical cross section taken through the atmosphere from a to a′ is shown in Figure 2-2b. In this figure the tropopause fold is shown folding downward above and slightly behind the surface cold front,

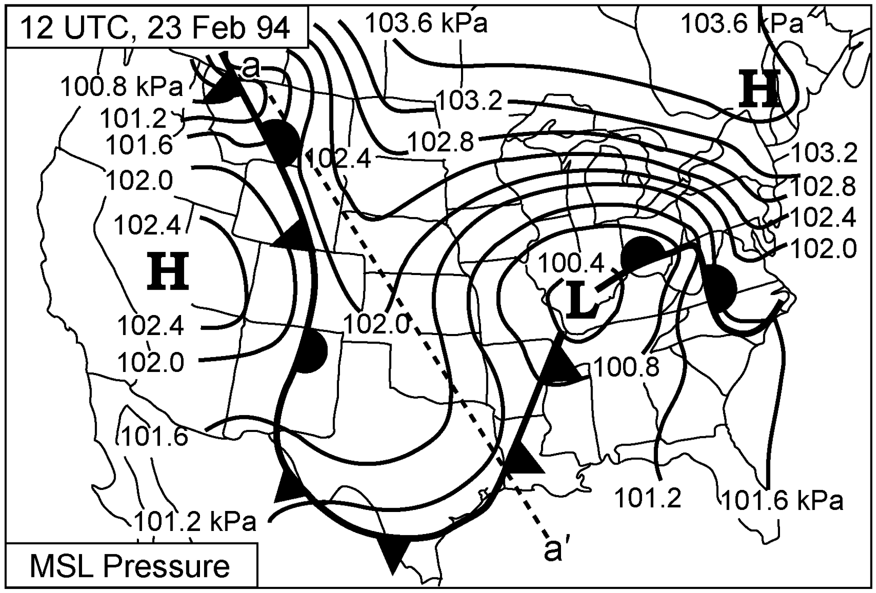

Figure 2-2a. Surface weather chart showing sea level (MSL) pressure (kPa), and surface fronts.

Source: Stull (2000).

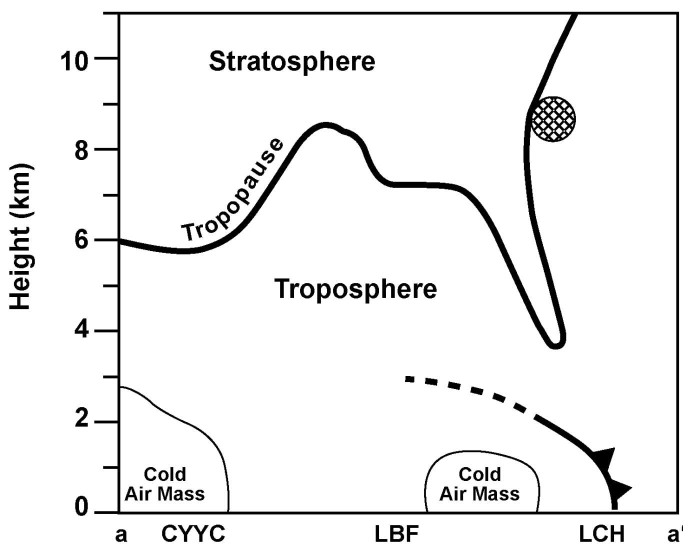

Figure 2-2b. Vertical cross section along dashed line (a-a′) from northwest to the southeast (CYYC = Calgary, Alberta; LBF = North Platte, NB; LCH = Lake Charles, LA). The approximate location of the jet stream core is indicated by the hatched area. The position of the surface front is indicated by the cold-frontal symbols and the frontal inversion top by the dashed line. Note: This is 12 h later than the situations shown in Figure 2-2a.

Source: Adapted from Stull (2000).

bringing stratospheric air with it. Although the tropopause is drawn with a solid line, it should not be taken to mean that it is a material surface, through which there is no exchange. Rather these folds should be though of as regions in which mixing of tropospheric and stratospheric air is occurring (Shapiro, 1980). This imported stratospheric air contributes to the natural background of O_3 in the troposphere especially in the free troposphere. It should be noted that there is considerable uncertainty in the magnitude and distribution of this potentially important source of tropospheric O_3. Stratospheric intrusions that reach the surface are rare. Much more common are intrusions which penetrate only to the middle and upper troposphere. However, O_3 transported to the upper and middle troposphere can still affect surface concentrations through various exchange mechanisms that mix air from the free troposphere with air in the planetary boundary layer. Substantial photochemical production of O_3 in the troposphere also begins in late winter and early spring, therefore it cannot be assumed that O_3 present at these times is only stratospheric in origin. The basic atmospheric dynamics and thermodynamics of stratospheric-tropospheric exchange are outlined in Annex AX2.3.1.

Our understanding of the meterological processes associated with summertime O_3 episodes remains basically the same as outlined in CD96. Major episodes of high O_3 concentrations in the eastern United States and in Europe are associated with slow moving, high pressure systems. High pressure systems during the warmer seasons are associated with the sinking of air, resulting in warm, generally cloudless skies, with light winds. The sinking of air results in the development of stable conditions near the surface which inhibit or reduce the vertical mixing of O_3 precursors. The combination of inhibited vertical mixing and light winds minimizes the dispersal of pollutants emitted in urban areas, allowing their concentrations to build up. Photochemical activity involving these precursors is enhanced because of higher temperatures and the availability of sunlight. In the eastern United States, high O_3 concentrations during a large scale episode can extend over hundreds of thousands square kilometers for several days. These conditions have been described in greater detail in CD96. The transport of pollutants downwind of major urban centers is characterized by the development of urban plumes. However, the presence of mountain barriers limits mixing as in Los Angeles and Mexico City and will result in even longer periods and a higher frequency of days with high O_3 concentrations. Ozone concentrations in southern urban areas, such as Houston, TX and Atlanta, GA tend to follow this pattern and they tend to decrease with increasing wind speed. In northern cities such as Chicago, IL; New York, NY; Boston, MA; and Portland, ME, the average O_3 concentrations over the metropolitan areas increase with wind speed indicating that transport of O_3 and its precursors from upwind areas is important (Husar and Renard, 1998; Schichtel and Husar, 2001).

Ozone and other secondary pollutants are determined by meteorological and chemical processes extending typically over spatial scales of several hundred kilometers (e.g., Civerolo et al., 2003; Rao et al., 2003). An analysis of the output of regional model studies conducted by Kasibhatla and Chameides (2000) suggests that O_3 can be transported over a few thousand kilometers in the upper boundary layer of the eastern half of the United States during specific O_3 episodes. Convection is capable of transporting O_3 and its precursors vertically through the troposphere as shown in Annex AX2.3.2. Nocturnal low level jets (LLJs) can also transport pollutants hundreds of kilometers (Annex AX2.3.3). Schematic diagrams showing the atmospheric conditions during the formation of low level jets and the regions in which they are most prevalent are given in Figures 2-3 and 2-4. They have also been observed off the coast of California. Turbulence associated with LLJs can bring these pollutants to the surface and result in secondary O_3 maxima in the early morning in many locations (Corsmeier et al., 1997).

Aircraft observations indicate that there can be substantial differences in mixing ratios of key species between the surface and the atmosphere above (Fehsenfeld et al., 1996; Berkowitz and Shaw, 1997). In particular, mixing ratios of O_3 can be higher in the lower free troposphere (aloft) than in the planetary boundary layer during multiday O_3 episodes (Taubmann et al., 2004). These conditions are illustrated schematically in Figure 2-5. Convective processes and small scale turbulence transport O_3 and other pollutants both upward and downward throughout the planetary boundary layer and the free troposphere. Ozone and its precursors can be transported vertically by convection into the upper part of the mixed layer on one day, then transported overnight as a layer of elevated mixing ratios and then entrained into a growing convective boundary layer downwind and brought back down to the surface. High concentrations of O_3 showing large diurnal variations at the surface in southern New England were associated with the presence of such layers (Berkowitz et al., 1998). Zhang et al. (1997) estimated that as much as 60% to 70% of O_3 observed at the surface during one case study in eastern Tennessee could have come from the upper boundary layer. Because of wind shear, winds several hundred meters above the ground can bring pollutants from the west, even though

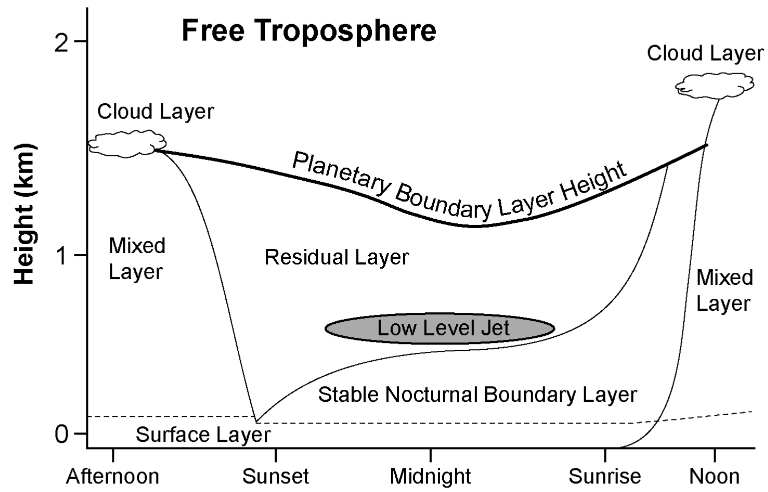

Figure 2-3. The diurnal evolution of the planetary boundary layer while high pressure prevails over land. Three major layers exist (not including the surface layer): a turbulent mixed layer; a less turbulent residual layer which contains former mixed layer air; and a nocturnal, stable boundary layer that is characterized by periods of sporadic turbulence.

Source: Adapted from Stull (1999) Figures 1.7 and 1.12.

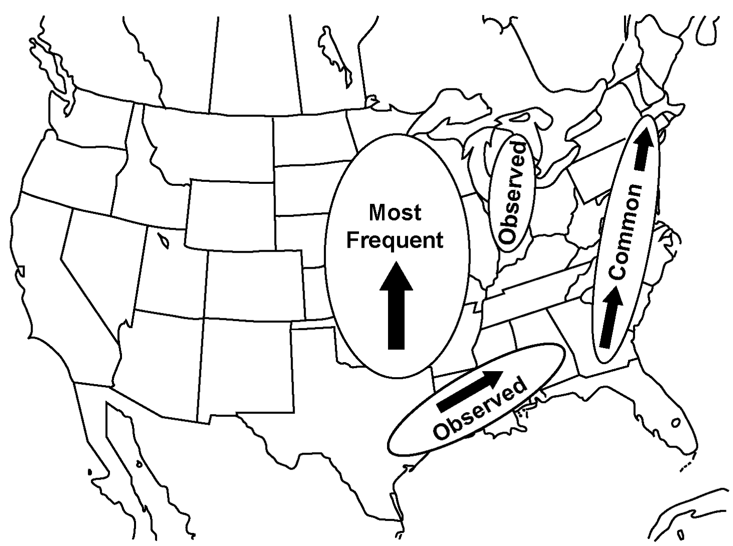

Figure 2-4. Locations of low level jet occurrences in decreasing order of prevalence (most frequent, common, observed). These locations are based on 2-years radiosonde data obtained over limited areas. With better data coverage, other low level jets may well be observed elsewhere in the United States.

Source: Bonner (1968).

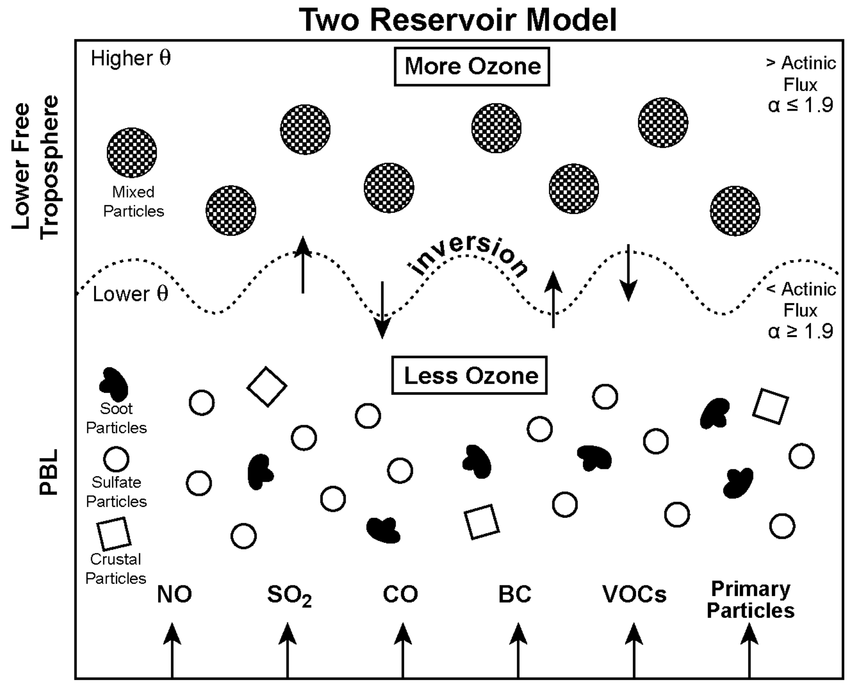

Figure 2-5. Conceptual two-reservoir model showing conditions in the PBL and in the lower free troposphere during a multiday O_3 episode. The dividing line, the depth of the mixed layer, is about km. Emissions occur in the PBL, where small, unmixed black carbon, sulfate, and crustal particles in the $PM_{2.5}$ size range are also shown. Ozone concentrations as well as potential temperature (θ) and actinic flux are lower in the PBL than in the lower free troposphere, while relative humidity and the Angstrom exponent for aerosol scattering (α) are higher. Larger, internally mixed sulfate and carbonaceous particles (still in the $PM_{2.5}$ size range) and more O_3 exist in the lower free troposphere.

Source: Taubman et al. (2004).

surface winds are from the southwest during periods of high O_3 in the eastern United States (Blumenthal et al., 1997). These considerations suggest that in many areas of the Unites States, O_3 formation involves processes occurring over hundreds if not thousands of square kilometers.

Although the vast majority of measurements are made near the Earth's surface, there is substantial photochemistry and transport of O_3 occurring above the boundary layer in the free troposphere. In the free troposphere, pollutants are chemically more stable and can be transported over much longer distances by westerly winds and O_3 is produced more efficiently than in the planetary boundary layer. Results from the Atmosphere/Ocean Ocean Chemistry Experiment (AEROCE) indicated that springtime maxima in surface O_3 over the western North Atlantic Ocean result from tropopause folding in close proximity to convective clouds (Annex AX2.3.4). The convection lifts O_3 and its precursors to the free troposphere where they mix with O_3 from the stratosphere and the mixture is transported eastward. Results from the North Atlantic Regional Experiment (Annex AX2.3.4) indicated that summertime air is transported along the East Coast northeastward and upward ahead of cold fronts. New England and the Maritime Provinces of Canada receive substantial amounts of O_3 and other pollutants through this mechanism. Pollutants transported in this way can then be entrained in stronger and more stable westerly winds aloft and can travel long distances across the North Atlantic Ocean. The pollutants can then be brought to the surface by subsidence in high pressure systems (typically behind the cold front in advance of the one mentioned above). Thus, pollutants from North America can be brought down either over the North Atlantic Ocean or in Europe. Pollutants can be transported across the North Pacific Ocean from Asia to North America in a similar way. Behind an advancing cold front, cold and dry stratospheric air is also being transported downward and southward. Stratospheric constituents and tropospheric constituents can then mix by small-scale turbulent exchange processes. The results of these studies suggest that the mechanisms involved in the long-range transport of O_3 and its precursors are closely tied to the processes involved in stratospheric-tropospheric exchange.

2.4 RELATIONS OF OZONE TO ITS PRECURSORS

The local rate of O_3 formation depends on atmospheric conditions such as the availability of solar ultraviolet radiation capable of initiating photolysis reactions, air temperatures and the concentrations of chemical precursors (Annex AX2.3.5). The dependence of daily 1-h maximum surface O_3 concentrations on daily maximum temperature is illustrated in Figure 2-6 for New York City. The notable trend is the apparent upper bound to O_3 concentrations as a function of temperature. However, this trend is absent in data from Phoenix, AZ (Figure 2-7). At any given temperature, there is a wide range of O_3 concentrations possible because other factors (e.g., cloudiness, mixing height, wind speed) can also influence O_3 production rates. It should be noted, however, that the data shown in Figures 2-6 and 2-7 were obtained during the

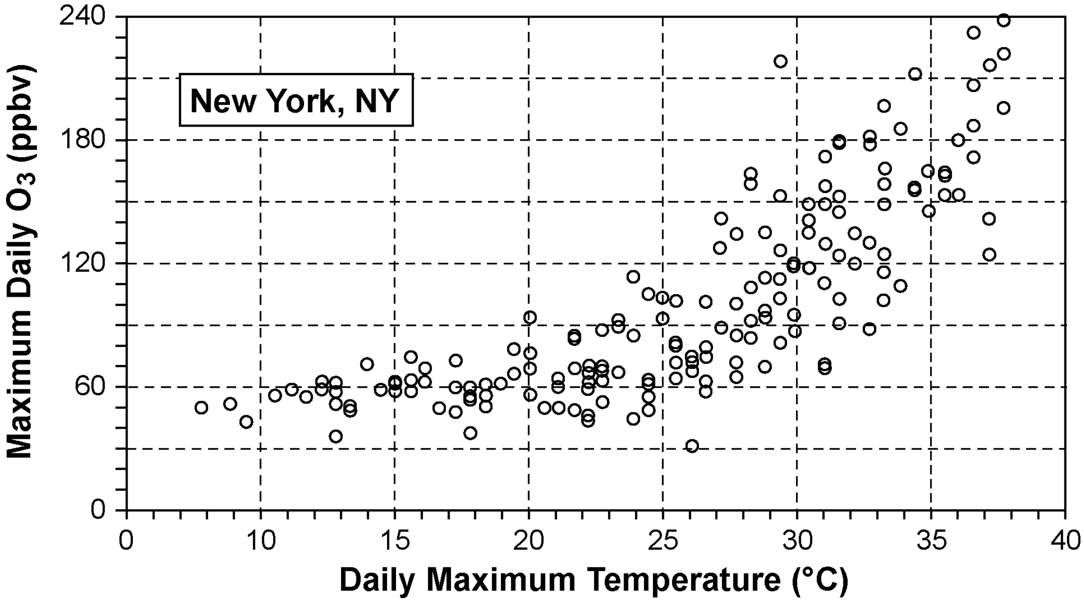

Figure 2-6. A scatter plot of daily 1-h maximum O_3 concentrations in New York, NY versus daily maximum temperature.

Source: U.S. Environmental Protection Agency (1996).

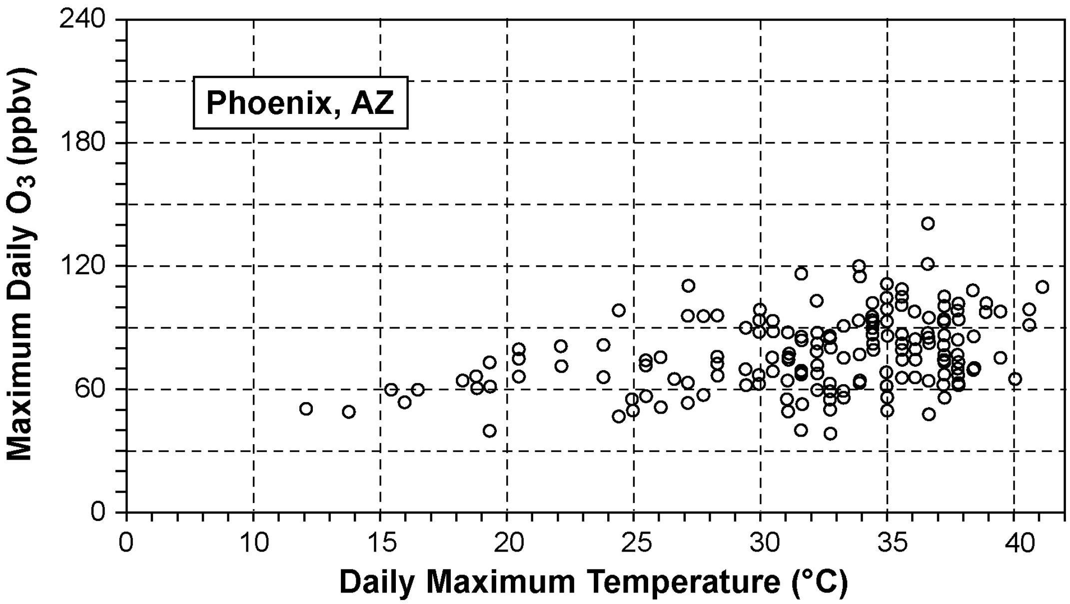

Figure 2-7. A scatter plot of daily 1-h maximum O_3 concentrations in Phoenix, AZ versus daily maximum temperature.

Source: U.S. Environmental Protection Agency (1996).

1980s and different relations might be obtained with current data. Relations of O_3 to precursor variables are seen to be location specific and relations observed in one area can not be readily extrapolated to another.

Rather than varying directly with emissions of its precursors, O_3 changes in a nonlinear fashion with the concentrations of its precursors (Annex AX2.4). At the low NO_x concentrations found in most environments, ranging from remote continental areas to rural and suburban areas downwind of urban centers (low - NO_x regime), the net production of O_3 increases with increasing NO_x. At the high NO_x concentrations found in downtown metropolitan areas, especially near busy streets and roadways, and in power plant plumes there is net destruction (titration) of O_3 by reaction with NO (high - NO_x regime). In between these two regimes there is a transition stage in which O_3 shows only a weak dependence on NO_x concentrations. In the high - NO_x regime, NO_2 scavenges OH radicals which would otherwise oxidize VOCs to produce peroxy radicals, which in turn would oxidize NO to NO_2. In this regime, O_3 production is limited by the availability of free radicals. The production of free radicals is in turn limited by the availability of solar UV radiation capable of photolyzing O_3 in the Hartley bands or aldehydes; and/ or by the abundance of VOCs whose oxidation would produce more radicals than they consume. In the low-NO_x regime, the oxidation of VOCs generates (or at least does not consume) free radicals, and O_3 production varies directly with NO_x. There are a number of ways to refer to the chemistry in these two chemical regimes. Sometimes the terms VOC-limited and NO_x-limited are used to describe these two regimes. However, there are difficulties with this usage because (1) VOC measurements are not as abundant as they are for nitrogen oxides, (2) rate coefficients for reaction of individual VOCs with free radicals vary over an extremely wide range, and (3) consideration is not given to CO nor to reactions that can produce free radicals without invoking VOCs. The terms NO_x-limited and NO_x-saturated (e.g., Jaegle et al., 2001) will be used wherever possible to more adequately describe these two regimes. However, the terminology used in original articles will also be used here.

The chemistry of OH radicals, which are responsible for initiating the oxidation of hydrocarbons, shows behavior similar to that for O_3 with respect to NO_x concentrations (Hameed et al., 1979; Pinto et al., 1993; Poppe et al., 1993; Zimmerman and Poppe, 1993). These considerations introduce a high degree of uncertainty into attempts to relate changes in O_3 concentrations to emissions of precursors. There are no definitive rules governing the levels of

NO_x at which the transition from NO_x-limited to NO_x-saturated conditions occurs. The transition between these two regimes is highly spatially and temporally dependent and depends also on the nature and abundance of the hydrocarbons that are present.

Trainer et al. (1993) and Olszyna et al. (1994) have shown that O_3 and NO_y are highly correlated in rural areas in the eastern United States. Trainer et al. (1993) also showed that O_3 levels correlate even better with NO_z than with NO_y, as may be expected because NO_z represents the amount of NO_x that has been oxidized, forming O_3 in the process. NO_z is equal to the difference between measured total reactive nitrogen, NO_y, and NO_x and represents the summed products of the oxidation of NO_x. NO_z is composed mainly of HNO_3, PAN and other organic nitrates, particulate nitrate, and HNO_4.

Trainer et al. (1993) also suggested that the slope of the regression line between O_3 and NO_z can be used to estimate the rate of O_3 production per NO_x oxidized (also known as the O_3 production efficiency, or OPE). Ryerson et al. (1998, 2001) used measured correlations between O_3 and NO_z to identify different rates of O_3 production in plumes from large point sources. A number of studies in the planetary boundary layer over the continental United States have found that the OPE ranges typically from one to nearly ten. However, it may be higher in the upper troposhere and in certain areas, such as the Houston-Galveston area. Observations indicate that the OPE depends mainly on the abundance of NO_x.

Various techniques have been proposed to use ambient NO_x and VOC measurements to derive information about the dependence of O_3 production on their concentrations. For example, it has been suggested that O_3 formation in individual urban areas could be understood in terms of measurements of ambient NO_x and VOC concentrations during the early morning (e.g., National Research Council, 1991). In this approach, the ratio of summed (unweighted) VOC to NO_x is used to determine whether conditions were NO_x-limited or VOC limited. This procedure is inadequate because it omits many factors that are important for O_3 production such as the impact of biogenic VOCs (which are typically not present in urban centers during early morning); important differences in the ability of individual VOCs to generate free radicals (rather than just total VOC) and other differences in O_3 forming potential for individual VOCs (Carter et al., 1995); and changes in the VOC to NO_x ratio due to photochemical reactions and deposition as air moves downwind from urban areas (Milford et al., 1994).

Photochemical production of O_3 generally occurs simultaneously with the production of various other species such as nitric acid (HNO_3), organic nitrates, and hydrogen peroxide. The relative rate of production of O_3 and other species varies depending on photochemical conditions, and can be used to provide information about O_3-precursor sensitivity. Sillman (1995) and Sillman and He (2002) identified several secondary reaction products that show different correlation patterns for NO_x-limited and NO_x-saturated conditions. The most important correlations are for O_3 versus NO_y, O_3 versus NO_z, O_3 versus HNO_3, and H_2O_2 versus HNO_3. The correlations between O_3 and NO_y, and O_3 and NO_z are especially important because measurements of NO_y and NO_x are more widely available than for VOCs. Measured O_3 versus NO_z (Figure 2-8) shows distinctly different patterns in different locations. In rural areas and in urban areas such as Nashville, TN, O_3 is highly correlated with NO_z. By contrast, in Los Angeles, CA, O_3 is not as highly correlated with NO_z, and the rate of increase of O_3 with NO_z is lower and the O_3 concentrations for a given NO_z value are generally lower. The different O_3 versus NO_z relations in Nashville, TN and Los Angeles, CA reflects the difference between NO_x-limited conditions in Nashville vs. an approach to NO_x- saturated conditions in Los Angeles.

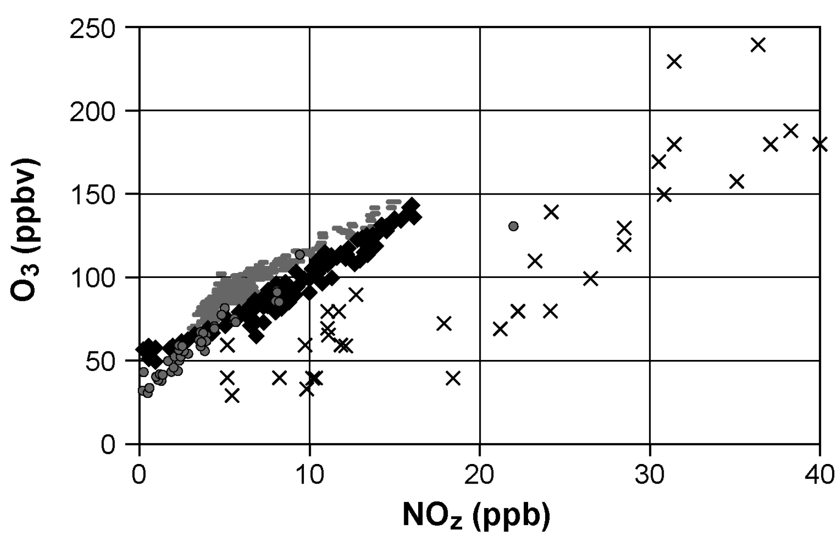

Figure 2-8. Measured values of O_3 and NO_z (NO_y – NO_x) during the afternoon at rural sites in the eastern United States (grey circles) and in urban areas and urban plumes associated with Nashville, TN (gray dashes); Paris, France (black diamonds); and Los, Angeles CA (Xs).

Sources: Trainer et al. (1993), Sillman et al. (1997, 1998), Sillman and He (2002).

The difference between NO_x-limited and NO_x-saturated regimes is also reflected in measurements of hydrogen peroxide (H_2O_2). Hydrogen peroxide production is highly sensitive to the abundance of free radicals and is thus favored in the NO_x-limited regime, typical of summer conditions. Differences between these two regimes are also related to the preferential formation of sulfate during summer and to the inhibition of sulfate and hydrogen peroxide formation during winter (Stein and Lamb, 2003). Measurements in the rural eastern United States (Jacob et al., 1995) Nashville, TN (Sillman et al., 1998), and Los Angeles, CA (Sakugawa and Kaplan, 1989), show large differences in H_2O_2 concentrations between likely NO_x-limited and radical-limited locations.

2.5 THE ROLE OF CHEMISTRY-TRANSPORT MODELS IN UNDERSTANDING ATMOSPHERIC OZONE

Chemistry-transport models (CTMs) are used to improve understanding of atmospheric chemical processes and to develop control strategies (Annex AX2.5). The main components of a CTM are summarized in Figure 2-9. Models such as the CMAQ (Community Model for Air Quality) system incorporate the processes shown in Figure 2-9 as numerical algorithms to predict time dependent concentration fields of a wide variety of gaseous and particulate phase pollutants. Also shown in Figure 2-9 is the meteorological model used to provide the inputs for calculating the transport of species in the CTM. The meteorological models such as the MM5 model, which supplies these inputs to the CTMs mentioned above, also provide daily weather forecasts. The domains of these models extend typically over areas of millions of square kilometers. Because these models are computationally intensive, it is often impractical to run them over larger domains without sacrificing some features. For these reasons, both the meteorological model and the CTM rely on boundary conditions that allow processes occurring outside the model domain to influence their predictions. The entire system of meteorological model emissions processors and output processors shown in Figure 2-9 constitutes the framework of EPA's Models-3.

Because of the large number of chemical species and reactions that are involved in considering the oxidation of realistic mixtures of anthropogenic and biogenic hydrocarbons, condensed mechanisms must be used in atmospheric models. These mechanisms are tested by

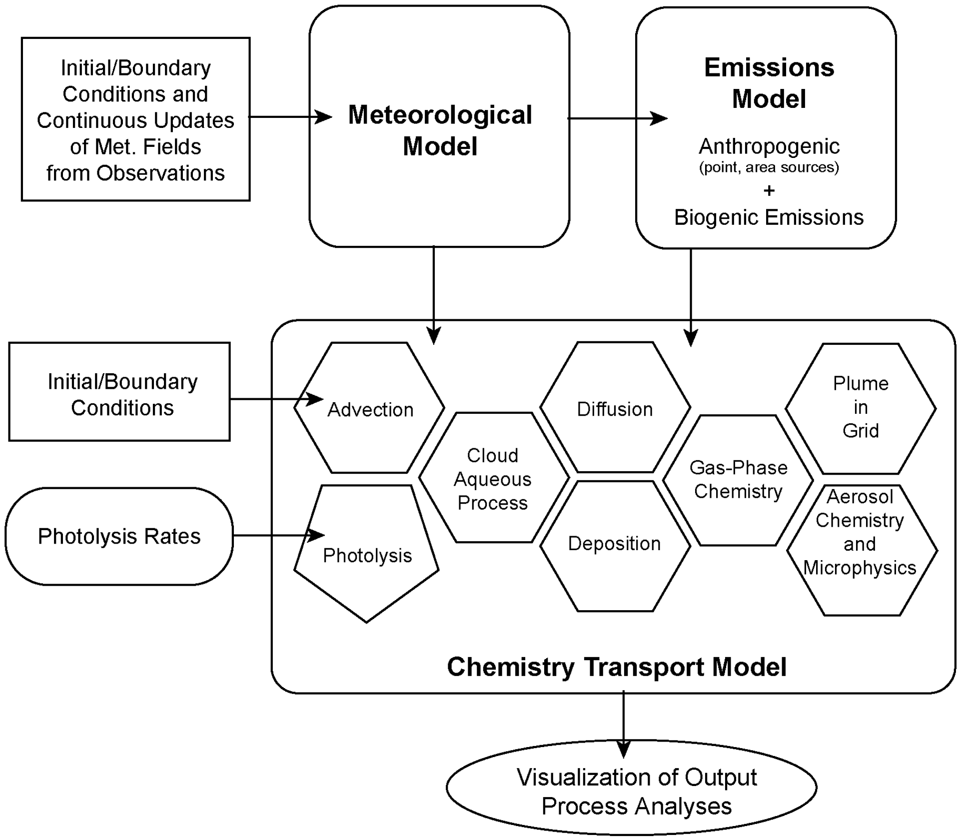

Figure 2-9. Main components of a comprehensive atmospheric chemistry modeling system, such as Models-3.

comparison with smog chamber data. However, the existing chemical mechanisms neglect many important processes such as the formation and subsequent reactions of long lived carbonyl compounds, the incorporation of the most recent information about intermediate compounds, and heterogeneous reactions involving cloud droplets and aerosol particles.

Emissions inventories are compiled for O_3 precursors (NO_x, VOCs, and CO). Recent estimates and more detailed discussions of the estimates are given in Annex AX2.5.2. Anthropogenic NO_x emissions are associated with combustion processes. Most emissions are in the form of NO, which is formed at high combustion temperatures from atmospheric nitrogen and oxygen and from fuel nitrogen. The two largest sources of NO_x are electric power generation plants and motor vehicles. Emissions of NO_x therefore are highest in areas having a high density of power plants and in urban regions having high traffic density. Natural NO_x sources include stratospheric intrusions, lightning, soils, and wildfires. Lightning, fertilized soils, and wildfires are the major natural sources of NO_x in the United States. Both nitrifying and denitrifying organisms in the soil can produce NO_x, mainly in the form of NO. Emission rates depend mainly on fertilization levels and soil temperature and moisture. Spatial and temporal variability in soil NO_x emissions leads to considerable uncertainty in emissions estimates. About 60% of lightning generated NO_x occurs in the southern United States and about 60% the total NO_x emitted by soils occurs in the central corn belt of the United States. The oxidation of NH_3 emitted mainly by livestock and soils, leads to the formation of a small amount of NO. Uncertainties in natural NO_x inventories are much larger than for anthropogenic NO_x emissions.

Hundreds of VOCs, containing mainly two to about twelve carbon atoms, are emitted by evaporation and combustion processes from a large number of anthropogenic sources. The two largest source categories in the U.S. EPA's emissions inventories are industrial processes and transportation. Emissions of VOCs from highway vehicles account for almost 75% of the transportation-related emissions.

The accuracy of VOC emission estimates is difficult to determine, both for stationary and mobile sources. Evaporative emissions, which depend on temperature and other environmental factors, compound the difficulties of assigning accurate emission factors. In assigning VOC emission estimates to the mobile source category, models are used that incorporate numerous input parameters (e.g., type of fuel used, type of emission controls, age of vehicle), each of which has some degree of uncertainty. Data for the ratio of CO to NO_x and NMOC to NO_x in traffic tunnels (e.g., Pierson et al., 1990) indicated that emissions of NMHCs and CO from motor vehicles have been underestimated by as much as a factor of two (based on the assumption that emissions of NO_x were reasonably well represented in the inventories). However, the results of more recent studies have been mixed, with many studies showing agreement to within ±50% (summarized in Air Quality Criteria for Carbon Monoxide [U.S. Environmental Protection Agency, 2000]). Remote sensing data (Stedman et al., 1991) indicate that about 50% of NMHC and CO emissions are produced by about 10% of the vehicles. These "super-emitters" are typically poorly maintained vehicles. Vehicles of any age engaged in off-cycle operations (e.g., rapid accelerations) emit much more than if operated in normal driving modes.

Vegetation emits significant quantities of VOCs such as terpenoid compounds (isoprene, -2-methyl-3-buten-2-ol, monoterpenes), compounds in the hexanal family, alkenes, aldehydes, organic acids, alcohols, ketones, and alkanes. The major species emitted by plants are isoprene (35%), 19 other terpenoid compounds and 17 non-terpenoid compounds including oxygenated compounds (40%) (Guenther et al., 2000). Coniferous forests represent the largest source on a nationwide basis, because of their extensive land coverage. Most biogenic emissions occur during the summer, because of their dependence on temperature and incident sunlight. Biogenic emissions are also higher in southern states than in northern states for these reasons and because of species variations. The uncertainty in natural emissions is about 50% for isoprene under midday summer conditions and could be as much as a factor of ten higher for some compounds (Guenther et al., 2000). Uncertainties in both biogenic and anthropogenic VOC emission inventories prevent determination of the relative contributions of these two categories at least in many urban areas. On the regional and global scales, emissions of VOCs from vegetation are much larger than those from anthropogenic sources.

The performance of CTMs must be evaluated by comparison with field data as part of a cycle of model improvements and subsequent evaluations. Discrepancies between model predictions and observations can be used to point out gaps in current understanding of atmospheric chemistry and to spur improvements in parameterizations of atmospheric chemical and physical processes. Model evaluation does not merely involve a straightforward comparison between model predictions and the concentration field of the pollutant of interest. Such comparisons may not be meaningful because it is difficult to determine if agreement between model predictions and observations truly represents an accurate treatment of physical and chemical processes in the CTM or the effects of compensating errors in complex model routines. Ideally, each of the model components (emissions inventories, chemical mechanism, meteorological driver) should be evaluated individually, however this is rarely done in practice. A comparison between free radical concentrations predicted by parameterized chemical mechanisms and observations, suggests that radical concentrations were overestimated by current chemical mechanisms for NO_x concentrations < ~5 ppb for that set of environmental conditions (Volz-Thomas et al., 2003).

In addition to comparisons between concentrations of calculated and measured species, comparisons of correlations between measured primary VOCs and NO_x and modeled VOCs and

NO_x are especially useful for evaluating results from chemistry-transport models. Likewise, comparisons of correlations between measured species and modeled species can be used to provide information about the chemical state of the atmosphere and to evaluate model representations (including O_3 production per NO_x, O_3-NO_x-VOC sensitivity, and the general accuracy of photochemical representations). A CTM that demonstrates the accuracy of both its computed VOC and NO_x in comparison with ambient measurements and the spatial and temporal relations among the critical secondary species associated with O_3 has a higher probability of representing O_3-precursor relations correctly than one that does not.

2.6 TECHNIQUES FOR MEASURING OZONE AND ITS PRECURSORS

Several techniques have been developed for sampling and measurement of O_3 in the ambient atmosphere at ground level. Although the chemiluminescence method (CLM) using ethylene is designated as the Federal Reference Method for measuring O_3, monitoring in the NAMS/SLAMS networks is conducted mainly with UV absorption spectrometry using commercial short path instruments. The primary reference standard instrument is a relatively long-path UV absorption spectrometer maintained under carefully controlled conditions at NIST (e.g., Fried and Hodgeson, 1982). Episodic measurements are made with a variety of other techniques based on the principles of chemiluminescence, electrochemistry, differential optical absorption spectroscopy (DOAS), and LIDAR.

In principle, each of these methods is subject to interference. Kleindienst et al. (1993) found that water vapor could cause a positive interference in the CLM with an average positive deviation of 3% ozone/% water vapor at 25 C. The UV absorption spectrometers are subject to positive interference by atmospheric constituents, such as certain aromatic aldehydes that absorb at the 253.7 nm Hg resonance line and are at least partially removed by the MnO_2 scrubber. Parrish and Fehsenfeld (2000) did not find any evidence for significant interference (> 1%) in flights through the Nashville urban plume. They also did not find any significant interference in extensive airborne and ground-based comparisons in the Houston, TX area. However, more extensive data in urban areas are lacking.

By far, most measurements of NO are made using the CLM, based on its reaction with O_3. Commercial instruments for measuring NO and NO_2 are constructed with an internal converter for reducing NO_2 to NO and then measuring NO by the CLM. In principle, this technique yields a measurement of NO_x with NO_2 found by difference between NO_x and NO. However, these converters also reduce NO_z compounds thereby introducing a positive interference in the measurement of NO_2. Other methods for measuring NO_2 are available, such as photolytic reduction followed by CLM, laser-induced fluorescence and DOAS. However, they require further development before they can be used for routine monitoring in the NAMS/SLAMS networks. More detailed descriptions of the issues and techniques discussed above and techniques for measuring HNO_3 and VOCs can be found in Annex AX2.6.

2.7 SUMMARY

Ozone (O_3) is formed by atmospheric reactions involving two classes of precursor compounds, volatile organic compounds (VOCs) and nitrogen oxides (NO_x). Ozone is thus a secondary pollutant. Ozone is ubiquitous throughout the atmosphere, it is present even in remote areas of the globe. The photochemical oxidation of almost all anthropogenic and biogenic VOCs is initiated by reaction with hydroxyl (OH) radicals. At night, when they are most abundant, NO_3 radicals also oxidize alkenes. In coastal and other select environments, Cl and Br radicals can also initiate the oxidation of VOCs.

In urban areas, basically all classes of VOCs (alkanes, alkenes, aromatic hydrocarbons, carbonyl compounds, etc.) and CO are important for ozone formation. Although knowledge of the oxidative mechanisms of VOCs has improved over the past several years, gaps in knowledge involving key classes, such as aromatic hydrocarbons, still remain. For example, only about half of the carbon initially present in aromatic hydrocarbons in smog chamber studies form compounds that can be identified.

In addition to gas phase reactions, reactions also occur on the surfaces of, or within cloud droplets and airborne particles. Most of the well-established multiphase reactions tend to reduce the rate of O_3 formation in polluted environments. Reactions of Cl and Br containing radicals deplete O_3 in selected environments such as the Arctic during spring, the tropical marine boundary layer and inland salt lakes. Direct reactions of O_3 and atmospheric particles appear to be too slow to reduce O_3 formation significantly at typical ambient PM levels.

Our basic understanding of the meteorological processes associated with summertime ozone episodes has not changed over the past several years. However, the realization that long-range transport processes are important for determining ozone concentrations at the surface is growing. In addition to synoptic scale flow fields, Nocturnal Low-Level Jets are capable of transporting pollutants hundreds of km from their sources in either the upper boundary layer or the lower free troposphere. Turbulence then brings ozone and other pollutants to the surface. On larger scales, important progress has been made in identifying the mechanisms of intercontinental transport of ozone and other pollutants.

Some ozone would be found near the earth's surface as the result of its downward transport from the stratosphere, even in the absence of photochemical reactions in the troposphere. Intrusions of stratospheric ozone that reach the surface are rare. Much more common are intrusions that penetrate to the middle and upper troposphere. However, O_3 transported to the middle and upper troposphere can still affect surface concentrations through various mechanisms that mix air between the planetary boundary layer and the free troposphere above.

The formation of ozone and associated compounds is a complex, nonlinear function of many factors including the intensity and spectral distribution of sunlight; atmospheric mixing and other atmospheric processes; and the concentrations of the precursors in ambient air. At the low NO_x concentrations found in most environments, ranging from remote continental areas to rural and suburban areas downwind of urban centers, the net production of O_3 increases with increasing NO_x. At the high concentrations found in downtown metropolitan areas, especially near busy streets and highways, and in power plant plumes there is net destruction of O_3 by reaction with NO. In between these two regimes there is a transition stage, in which O_3 production shows only a weak dependence on NO_x concentrations. The efficiency of ozone production per NO_x oxidized is generally highest in areas where NO_x concentrations are lowest and decrease with increasing NO_x concentration.

Chemistry transport models are used to improve understanding of atmospheric chemical and physical processes as well as to develop air pollution control strategies. The performance of these models must be evaluated by comparison with field data as part of a cycle of model improvements and subsequent evaluations. Discrepancies between model predictions and observations can be used to point out gaps in current understanding and thus to improve parameterizations of atmospheric chemical and physical processes. Model evaluation does not merely involve a straightforward comparison between model predictions and the concentration fields of a pollutant of interest (e.g., O_3). Such comparisons may not be meaningful because it is difficult to determine if agreement between measurements and model predictions truly represents an accurate treatment of physical and chemical processes in the model or the effects of compensating errors in model routines.

The main methods in use for routine monitoring of ambient ozone are based on chemiluminescence or UV absorption. Measurements at most ambient monitoring sites are based on UV absorption. Both of these methods are subject to interference by other atmospheric components. A few studies conducted in urban plumes have not found evidence for significant positive interference in the UV absorption technique. However, more extensive data are not available to completely resolve this issue in urban areas.

REFERENCES

Berkowitz, C. M.; Shaw, W. J. (1997) Airborne measurements of boundary layer chemistry during the Southern Oxidant Study: a case study. J. Geophys. Res. [Atmos.] 102: 12,795-12,804.

Berkowitz, C. M.; Fast, J. D.; Sprinston, S. R.; Larsen, R. J.; Spicer, C. W.; Doskey, P. V.; Hubbe, J. M.; Plastridge, R. (1998) Formation mechanisms and chemical characteristics of elevated photochemical layers over the northeast United States. J. Geophys. Res. [Atmos.] 103: 10,631-10,647.

Blumenthal, D. L.; Lurmann, F. W.; Kumar, N.; Dye, T. S.; Ray, S. E.; Korc, M. E.; Londergan, R.; Moore, G. (1997) Transport and mixing phenomena related to ozone exceedances in the northeast U.S. (analysis based on NARSTO-northeast data). Available: http://capita.wustl.edu/otag/reports/otagrept/otagrept.html (30 October 2003).

Bonner, W. D. (1968) Climatology of the low level jet. Mon. Weather Rev. 96: 833-850.

Carter, W. P. L. (1995) Computer modeling of environmental chamber studies of maximum incremental reactivities of volatile organic compounds. Atmos. Environ. 29: 2513.

Civerolo, K. L.; Mao, H. T.; Rao, S. T. (2003) The airshed for ozone and fine particulate pollution in the eastern United States. Pure Appl. Geophys. 160: 81-105.

Corsmeier, U.; Kalthhoff, N.; Kolle, O.; Motzian, M.; Fiedler, F. (1997) Ozone concentration jump in the stable nocturnal boundary layer during a LLJ-event. Atmos. Environ. 31: 1977-1989.

Eisele, F. L.; Mount, G. H.; Tanner, D.; Jefferson, A.; Shetter, R.; Harder, J. W.; Williams, E. J. (1997) Understanding the production and interconversion of the hydroxyl radical during the tropospheric OH photochemistry experiment. J. Geophys. Res. 102: 6457-6465.

Fehsenfeld, F. C.; Trainer, M.; Parrish, D. D.; Volz-Thomas, A.; Penkett, S. (1996) North Atlantic Regional Experiment (NARE) 1993 summer intensive: foreword. J. Geophys. Res. [Atmos.] 101: 28,869-28,875.

Fried, A.; Hodgeson, J. (1982) Laser photoacoustic detection of nitrogen dioxide in the gas-phase titration of nitric oxide with ozone. Anal. Chem. 54: 278-282.

Guenther, A.; Geron, C.; Pierce, T.; Lamb, B.; Harley, P.; Fall, R. (2000) Natural emissions of non-methane volatile organic compounds, carbon monoxide, and oxides of nitrogen from North America. Atmos. Environ. 34: 2205-2230.

Hameed, S.; Pinto, J. P.; Stewart, R. W. (1979) Sensitivity of the predicted CO-OH-CH_4 perturbation to tropospheric NO_x concentrations. J. Geophys. Res. C: Oceans Atmos. 84: 763-768.

Husar, R. B.; Renard, W. P. (1998) Ozone as a function of local wind speed and direction: Evidence of local and regional transport. Presented at: 91st annual meeting and exhibition of the Air & Waste Management Association; June; San Diego, CA. Pittsburgh, PA: Air & Waste Management Association; online paper no. 98-A922. Available: http://capita.wustl.edu/capita/CapitaReports/REPORTS1.HTML (13 November 2003).

Jacob, D. J.; Horowitz, L. W.; Munger, J. W.; Heikes, B. G.; Dickerson, R. R.; Artz, R. S.; Keene, W. C. (1995) Seasonal transition from NO_x- to hydrocarbon-limited conditions for ozone production over the eastern United States in September. J. Geophys. Res. 100: 9315-9324.

Kasibhatla, P.; Chameides, W. L. (2000) Seasonal modeling of regional ozone pollution in the eastern United States. Geophys. Res. Lett. 27: 1415-1418.

Kleindienst, T. E.; Hudgens, E. E.; Smith, D. F.; McElroy, F. F.; Bufalini, J. J. (1993) Comparison of chemiluminescence and ultraviolet ozone monitor responses in the presence of humidity and photochemical pollutants. Air Waste 43: 213-222.

Milford, J. B.; Gao, D.; Sillman, S.; Blossey, P.; Russell, A. G. (1994) Total reactive nitrogen (NO_y) as an indicator of the sensitivity of ozone to reductions in hydrocarbon and NO_x emissions. J. Geophys. Res. 99: 3533-3542.

National Research Council. (1991) Rethinking the ozone problem in urban and regional air pollution. Washington, DC: National Academy Press. Available: http://www.nap.edu/books/0309046319/html/ [26 March, 2004].

Olszyna, K. J.; Bailey, E. M.; Simonaitis, R.; Meagher, J. F. (1994) O_3 and NO_y relationships at a rural site. J. Geophys. Res. [Atmos.] 99: 14,557-14,563.

Parrish, D. D.; Fehsenfeld, F. C. (2000) Methods for gas-phase measurements of ozone, ozone precursors and aerosol precursors. Atmos. Environ. 34: 1921-1957.

Pierson, W. R.; Gertler, A. W.; Bradow, R. L. (1990) Comparison of the SCAQS tunnel study with historical data. Presented at: 83rd annual meeting & exhibition of the Air and Waste Management Association; June; Pittsburgh, PA. Pittsburgh, PA: Air and Waste Management Association; paper no. 90-175.3.

Pinto, J. P.; Bruhl, C.; Thompson, A. M. (1993) The current and future environmental role of atmospheric methane. In: Khalil, M. A. K., ed. Atmospheric methane sources, sinks, and role in global change, p. 514-531. (NATO ASI Series, v. 113).

Poppe, D.; Wallasch, M.; Zimmermann, J. (1993) The dependence of the concentration of OH on its precursors under moderately polluted conditions: a model study. J. Atmos. Chem. 16: 61-78.

Rao, S. T.; Ku, J.-Y.; Berman, S.; Zhang, K.; Mao, H. (2003) Summertime characteristics of the atmospheric boundary layer and relationships to ozone levels over the eastern United States. Pure Appl. Geophys. 160: 21-55.

Ryerson, T. B.; Buhr, M. P.; Frost, G. J.; Goldan, P. D.; Holloway, J. S.; Hübler, G.; Jobson, B. T.; Kuster, W. C.; McKeen, S. A.; Parrish, D. D.; Roberts, J. M.; Sueper, D. T.; Trainer, M.; Williams, J.; Fehsenfeld, F. C. (1998) Emissions lifetimes and ozone formation in power plant plumes. J. Geophys. Res. 103(D17): 22,569-22,583.

Ryerson, T. B.; Trainer, M.; Holloway, J. S.; Parrish, D. D.; Huey, L. G.; Sueper, D. T.; Frost, G. J.; Donnelly, S. G.; Schauffler, S.; Atlas, E. L.; Kuster, W. C.; Goldan, P. D.; Hübler, G.; Meagher, J. F.; Fehsenfeld, F. C. (2001) Observations of ozone formation in power plant plumes and implications for ozone control strategies. Science (Washington, DC) 292: 719-723.

Sakugawa, H.; Kaplan, I. R. (1989) H_2O_2 and O_3 in the atmosphere of Los Angeles and its vicinity: factors controlling their formation and their role as oxidants of SO_2. J. Geophys. Res. [Atmos.] 94: 12,957-12,973.

Schichtel, B. A.; Husar, R. B. (2001) Eastern North American transport climatology during high- and low-ozone days. Atmos. Environ. 35: 1029-1038.

Seinfeld, J. H.; Pandis, S. N. (1998) Atmospheric chemistry and physics: from air pollution to climate change. New York, NY: John Wiley & Sons, Inc.

Shapiro, M. A. (1980) Turbulent mixing within tropopause folds as a mechanism for the exchange of chemical constituents between the stratosphere and troposphere. J. Atmos. Sci. 37: 994-1004.

Sillman, S. (1995) The use of NO_y, H_2O_2 and HNO_3 as indicators for ozone-NO_x-hydrocarbon sensitivity in urban locations. J. Geophys. Res. 100: 14,175-14,188.

Sillman, S.; He, D.-Y. (2002) Some theoretical results concerning O_3-NO_x-VOC chemistry and NO_x-VOC indicators. J. Geophys. Res. (Atmos.) 107: 10.1029/2001JD001123.

Sillman, S.; He, D.; Cardelino, C.; Imhoff, R. E. (1997) The use of photochemical indicators to evaluate ozone-NO_x-hydrocarbon sensitivity: case studies from Atlanta, New York, and Los Angeles. J. Air Waste Manage. Assoc. 47: 1030-1040.

Sillman, S.; He, D.; Pippin, M. R.; Daum, P. H.; Imre, D. G.; Kleinman, L. I.; Lee, J. H.; Weinstein-Lloyd, J. (1998) Model correlations for ozone, reactive nitrogen, and peroxides for Nashville in comparison with measurements: implications for O_3-NO_x-hydrocarbon chemistry. J. Geophys. Res. [Atmos.] 103: 22,629-22,644.

Stedman, D. H.; Bishop, G.; Peterson, J. E.; Guenther, P. L. (1991) On-road CO remote sensing in the Los Angeles Basin: final report. Sacramento, CA: California Air Resources Board, ARB Contract No. A932-189.

Stein, A. F.; Lamb, D. (2003) Empirical evidence for the low- and high-NO_x photochemical regimes of sulfate and nitrate formation. Atmos. Environ. 37: 3615-3625.

Stull, R. B. (1999) An introduction to boundary layer meteorology. Dordrecht, The Netherlands: Kluwer Academic Publishers; pp. 9-15, 500-505.

Stull, R. B. (2000) Meteorology for scientists and engineers: a technical companion book with Ahrens' Meteorology Today. 2nd ed. Pacific Grove, CA: Brooks/Cole.

Taubman, B. F.; Marufu, L. T.; Piety, C. A.; Doddridge, B. G.; Stehr, J. W.; Dickerson, R. R. (2004) Airborne characterization of the chemical, optical, and meteorological properties, and origins of a combined ozone-haze episode over the eastern United States. J. Atmos. Sci. 61: 1781-1793.

Trainer, M.; Parrish, D. D.; Buhr, M. P.; Norton, R. B.; Fehsenfeld, F. C.; Anlauf, K. G.; Bottenheim, J. W.; Tang, Y. Z.; Wiebe, H. A.; Roberts, J. M.; Tanner, R. L.; Newman, L.; Bowersox, V. C.; Meagher, J. F.; Olszyna, K. J.; Rodgers, M. O.; Wang, T.; Berresheim, H.; Demerjian, K. L.; Roychowdhury, U. K. (1993) Correlation of ozone with NO_y in photochemically aged air. J. Geophys. Res. [Atmos.] 98: 2917-2925.

U.S. Environmental Protection Agency. (1996) Air quality criteria for ozone and related photochemical oxidants. Research Triangle Park, NC: Office of Research and Development; report nos. EPA/600/AP-93/004aF-cF. 3v. Available from: NTIS, Springfield, VA; PB96-185582, PB96-185590, and PB96-185608. Available: http://cfpub2.epa.gov/ncea/.

U.S. Environmental Protection Agency. (2000) Air quality criteria for carbon monoxide. Research Triangle Park, NC: National Center for Environmental Assessment; report no. EPA/600/P-99/001F. Available: http://www.epa.gov/ncea/pdfs/coaqcd.pdf (7 May 2003).

Volz-Thomas, A.; Geiss, H.; Hofzumahaus, A.; Becker, K.-H. (2003) Introduction to special section: photochemistry experiment in BERLIOZ. J. Geophys. Res. [Atmos.] 108(D4): 10.1029/JD002029.

Zhang et al., 1997
Zimmermann, J.; Poppe, D. (1993) Nonlinear chemical couplings in the tropospheric NO_x–HO_x gas phase chemistry. J. Atmos. Chem. 17: 141-155.

ANNEX AX2. PHYSICS AND CHEMISTRY OF OZONE IN THE ATMOSPHERE

AX2.1 INTRODUCTION

This annex (Annex AX2) provides detailed supporting information for Chapter 2 on the physics and chemistry of ozone (O_3) in the atmosphere. The organization of the material in this annex follows that used in prior Air Quality Criteria Documents, i.e., material is presented in sections and subsections. This annex provides material supporting Chapter 2 of the current draft Air Quality Criteria Document for Ozone.

Section AX2.2 focuses on the chemistry of O_3 formation. A very brief overview of atmospheric structure is presented in Section AX2.2.1. An overview of O_3 chemistry is given in Section AX2.2.2. Information about reactive chemical species that initiate the oxidation of VOCs is given in Section AX2.2.3. The chemistry of nitrogen oxides is then discussed briefly in Section AX2.2.4. The oxidation of methane, the simplest hydrocarbon is outlined in Section AX2.2.5.

The photochemical cycles leading to O_3 production are best understood by considering the oxidation of methane, structurally the simplest VOC. The CH_4 oxidation cycle serves as a model which can be viewed as representing the chemistry of the relatively clean or unpolluted troposphere (although this is a simplification because vegetation releases large quantities of complex VOCs, such as isoprene, into the atmosphere). Although the chemistry of the VOCs emitted from anthropogenic and biogenic sources in polluted urban and rural areas is more complex, a knowledge of the CH_4 oxidation reactions aids in understanding the chemical processes occurring in the polluted atmosphere because the underlying chemical principles are the same. The oxidation of more complex hydrocarbons (alkanes, alkenes, and aromatic compounds) is discussed in Sections AX2.2.6, AX2.2.7, and AX2.2.8, respectively. The chemistry of oxygenated species is addressed in Section AX2.2.9. Greater emphasis is placed on the oxidation of aromatic hydrocarbons in this section because of the large amount of new information available since the last Air Quality Criteria for Ozone document (AQCD 96) was published (U.S. Environmental Protection Agency, 1996) and because of their importance in O_3 formation in polluted areas. Multiphase chemical processes influencing O_3 are discussed in

Section AX2.2.10. Meteorological processes that control the formation of O_3 and other oxidants and that govern their transport and dispersion, and the sensitivity of O_3 to atmospheric parameters are given in Section AX2.3. Greater emphasis is placed on those processes for which a large amount of new information has become available since AQCD 96. The role of stratospheric-tropospheric exchange in determining O_3 in the troposphere is presented in Section AX2.3.1. The importance of deep convection in redistributing O_3 and its precursors and other oxidants throughout the troposphere is given in Section AX2.3.2. The possible importance of nocturnal low level jets in transporting O_3 and other pollutants is presented in Section AX2.3.3. Information about the mechanisms responsible for the intercontinental transport of pollutants and for the interactions between stratospheric-tropospheric exchange and convection is given in Section AX2.3.4. Much of the material in this section is based on results of field programs examining atmospheric chemistry over the North Atlantic ocean. The sensitivity of O_3 to solar ultraviolet radiation and temperature is given in Section AX2.3.5. The relations of O_3 to its precursors and to other oxidants based on field and modeling studies are discussed in Section AX2.4. Methods used to calculate relations between O_3 its precursors and other oxidants are given in Section AX2.5. Chemistry-transport models are discussed in Section AX2.5.1. Emissions of O_3 precursors are presented in Section AX2.5.2. Issues related to the evaluation of chemistry-transport models and emissions inventories are presented in Section AX2.5.3. Measurement methods are summarized in Section AX2.6. Methods used to monitor ground-level O_3 are given in Section AX2.6.1, NO and NO_2 in Section AX2.6.2, HNO_3 in Section AX2.6.3 and some important VOCs in Section AX2.6.4.

AX2.2 TROPOSPHERIC OZONE CHEMISTRY

AX2.2.1 Atmospheric Structure

The atmosphere can be divided into several distinct vertical layers, based primarily on the major mechanism by which that portion of the atmosphere is heated or cooled. The lowest major layer is the troposphere, which extends from the earth's surface to about 8 km above polar regions and to about 16 km above tropical regions. The troposphere is heated by convective transport from the surface, and by the absorption of infrared radiation emitted by the surface, principally by water vapor and CO_2. The planetary boundary layer (PBL) is the sublayer of the troposphere that mixes with surface air on time scales of a few hours or less. It typically extends to 1-2 km altitude and is often capped by a temperature inversion. The sublayer of the troposphere above the PBL is called the free troposphere. Ventilation of the PBL with free tropospheric air takes place on a time scale of a week. Vertical mixing of the whole troposphere takes place on a time scale of a month or two. The stratosphere extends from the tropopause, or the top of the troposphere, to about 50 km in altitude. The upper stratosphere is heated by the absorption of solar ultraviolet radiation by O_3, while dissipation of wave energy transported upwards from the troposphere is a primary heating mechanism in the lower stratosphere. Heating of the stratosphere is balanced by radiative cooling due to infrared emissions to space by CO_2, H_2O, and O_3. As a result of heating of the upper stratosphere, temperatures increase with height, inhibiting vertical mixing. A schematic overview of the major chemical cycles involved in O_3 formation and destruction in the stratosphere and troposphere is shown in Figure AX2-1. The figure emphasizes gas phase processes, but the importance of multiphase processes is becoming apparent. The sequences of reactions shown in the lower right quadrant of the figure will be discussed in Section AX2.2. The reader is referred to any of the large number of texts on atmospheric chemistry, such as Wayne (2000) or Seinfeld and Pandis (1998), for an introduction to stratospheric photochemistry, including the impact of O_3-destroying compounds.

AX2.2.2 Overview of Ozone Chemistry

Ozone is found not only in polluted urban atmospheres but throughout the troposphere, including remote areas of the globe. Even without ground-level production, some O_3 would be found in the troposphere due to downward transport from the stratosphere. Tropospheric photochemistry leading to the formation of O_3 and other photochemical air pollutants is complex, involving thousands of chemical reactions and thousands of stable and reactive intermediate products. Other photochemical oxidants, such as peroxyacetyl nitrate (PAN), are among the reactive products. Ozone can be photolyzed in the presence of water to form hydroxyl radical (OH), which is responsible for the oxidation of NO_x and SO_x to form nitric (HNO_3) and sulfuric acid (H_2SO_4), respectively. Ozone participates directly in the oxidation of unsaturated hydrocarbons, via the ozonolysis mechanism, yielding secondary organic compounds that contribute to aerosol formation and mass, as well as formaldehyde (H_2CO) and other carbonyl compounds, such as aldehydes and ketones.

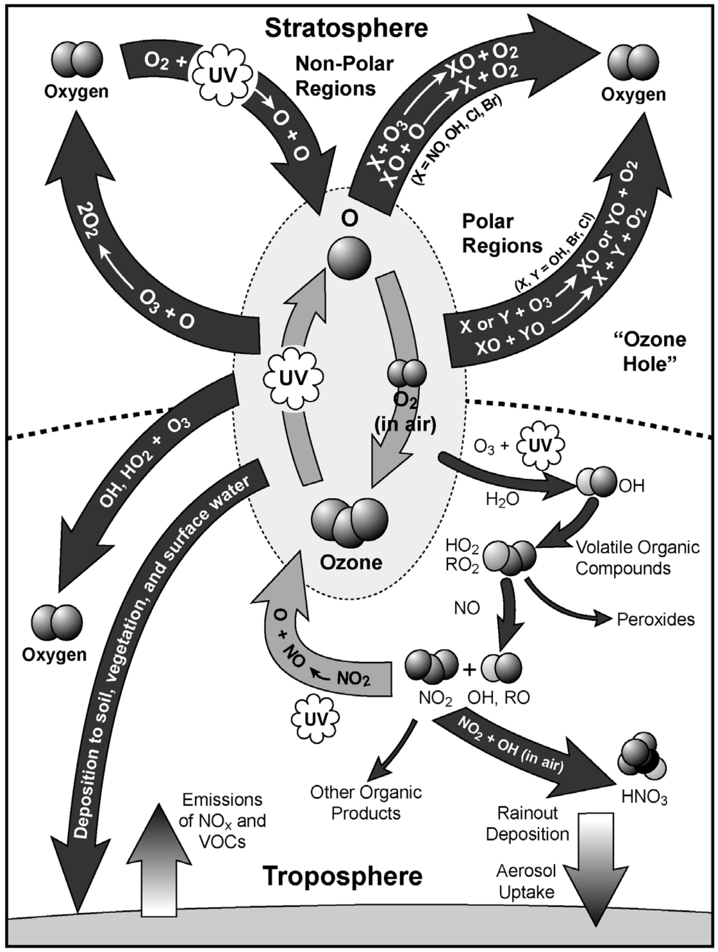

Figure AX2-1. Schematic overview of ozone photochemistry in the stratosphere and troposphere.

There is a rapid photochemical cycle in the troposphere that involves the photolysis of nitrogen dioxide (NO_2) by solar UV-A radiation to yield nitric oxide (NO) and a ground-state oxygen atom, $O(^3P)$,

$$NO_2 + h\nu \rightarrow NO + O(^3P), \qquad \text{(AX2-1)}$$

$O(^3P)$ then reacts with molecular oxygen to form O_3: A molecule from the surrounding air collides with the newly-formed O_3 molecule, removing excess energy to allow it to stabilize.

$$O(^3P) + O_2 + M \rightarrow O_3 + M, \text{ where M = an air molecule.} \qquad (AX2\text{-}2)$$

Reaction AX2-2 is the only significant reaction forming O_3 in the troposphere.

NO and O_3 react to reform NO_2:

$$NO + O_3 \rightarrow NO_2 + O_2. \qquad (AX2\text{-}3)$$

This reaction is responsible for O_3 decreases found near sources of NO (e.g., highways) especially at night. The oxidation of reactive VOCs leads to the formation of reactive radical species that allow the conversion of NO to NO_2 without the participation of O_3 (as in reaction AX2-3).

$$NO \xrightarrow{HO_2^\bullet,\ RO_2^\bullet} NO_2. \qquad (AX2\text{-}4)$$

O_3 can, therefore, accumulate as NO_2 photolyzes as in reaction AX2-1 followed by reaction AX2-2.

It is often convenient to speak about families of chemical species, that are defined in terms of members which interconvert rapidly among themselves on time scales that are shorter than that for formation or destruction of the family as a whole. For example, an 'odd oxygen' (O_x) family can be defined as $\sum (O(^3P) + O(^1D) + O_3 + NO_2)$ in much the same way as the NO_x ($NO + NO_2$) family is defined. We can then see that production of O_x occurs by the schematic reaction AX2-4, and that the sequence of reactions given by reactions AX2-1 through AX2-3 represents no net production of O_x. Definitions of species families and methods for constructing families are discussed in Jacobson (1999) and references therein. Other families that include nitrogen containing species, and will be referred to later in this chapter, are NO_z, which is the sum of the products of the oxidation of $NO_x = \sum (HNO_3 + PAN\ (CH_3CHO\text{-}OO\text{-}NO_2) + HNO_4 +$ other organic nitrates + particulate nitrate); and NO_y, which is the sum of NO_x and NO_z.

AX2.2.3 Initiation of the Oxidation of VOCs

The key reactive species in the troposphere is the OH radical. OH radicals are responsible for initiating the photochemical oxidation of CO and most anthropogenic and biogenic VOCs, including those responsible for depleting stratospheric O_3 (e.g., CH_3Br, hydroclorofluorocarbons), and those which contribute to the greenhouse effect (e.g., CH_4). Because of their role in removing so many potentially damaging species, OH radicals have sometimes been referred to as the atmosphere's detergent. In the presence of NO, reactions of OH with VOCs lead to the formation of O_3. In addition to OH radicals, there are several other atmospheric species such as OH, NO_3, Cl and Br radicals and O_3 that are capable of initiating VOC oxidation. Rate coefficients and estimated atmospheric lifetimes (the e-folding time) for reactions of a number of alkanes, alkenes and dienes involved in O_3 formation with these oxidants at concentrations characteristic of the relatively unpolluted planetary boundary layer are given in Table AX2-1. As can be seen from Table AX2-1, there is a wide range of lifetimes calculated for the different species. However, under certain conditions the relative importance of these oxidants can change from those shown in the table. For hydrocarbons whose atmospheric lifetime is much longer than a day, diurnally averaged concentrations of oxidant concentrations can be used, but for those whose lifetime is much shorter than a day it is more appropriate to use either daytime or night-time averages depending on when the oxidant is at highest concentrations. During these periods, these averages are of the order of twice the values used here.

The main source of OH radicals is the photolysis of O_3 by solar ultraviolet radiation at wavelengths < 340 nm (solar radiation at wavelengths < 320 nm is also referred to as UV-B) to generate electronically excited $O(^1D)$ atoms (Jet Propulsion Laboratory, 2003),

$$O_3 + h\nu \rightarrow O_2 + O(^1D). \qquad \text{(AX2-5)}$$

The $O(^1D)$ atoms can either be deactivated to the ground state $O(^3P)$ atom by collisions with N_2 and O_2, or they react with water vapor to form two OH radicals:

$$O(^1D) + H_2O \rightarrow 2(\bullet OH) \qquad \text{(AX2-6)}$$

Table AX2-1. Comparison of the Atmospheric Lifetimes (τ) of Low Molecular Weight Hydrocarbons Due to Reaction with OH, NO_3, Cl, Br and O_3

	k, cm^3 molecule^{-1} s^{-1}									
	OH		NO_3		Cl		Br		O_3	
Hydrocarbon	$k \times 10^{12}$	τ	$k \times 10^{12}$	τ	$k \times 10^{10}$	τ	$k \times 10^{12}$	τ	$k \times 10^{18}$	τ
Alkanes										
Ethane	0.24	48 d	< 1.0 x 10^{-5}	> 13 y	0.57	6.7 mo	3.1 × 10^{-7}	1.0 × 10^6 y[2]	< 0.01	> 3.2 y
Propane	1.1	11 d	0.00021	> 0.60	1.3	90 d	0	6.5 × 10^3 y[2]	< 0.01	> 3.2 y
2-Methylpropane	2.1	5.6 d	< 0.00007	> 18 y	1.3	90 d	< 1.0 ×	> 3.2 × 10^7 y[2]	< 0.01	> 3.2 y
n-Butane	2.3	5.2 d	0.000046	2.8 y	2.3	50 d	< 1.0 ×	> 3.2 × 10^7 y[2]	< 0.01	> 3.2 y
2-Methylbutane	4	2.9 d	0.00016	0.79 y	2	60 d	NA	NA	NA	NA
n-Pentane	3.8	3.0 d	0.000081	1.6 y	2.5	46 d	NA	NA	NA	NA
2,2-Dimethylbutane	2.7	4.3 d	NA	NA	NA	NA	NA	NA	NA	NA
2,3-Dimethylbutane	6.4	1.8d	0.00041	110 d	2	60 d	0.0064	50 y	NA	NA
2-Methylpentane	5.6	2.1 d	0.000017	7.5 y	2.5	47 d	NA	NA	NA	NA
3-Methylpentane	5.8	2.0 d	0.00002	6.3 y	2.5	46d	NA	NA	NA	NA
n-Hexane	5.2	2.2 d	0.00011	1.2 y	3.1	38 d	NA	NA	NA	NA
2,2,4-Trimethylpentane	3.8	3.0 d	0.000075	1.7 y	2.3	50 d	0.0068	47 y	NA	NA

Table AX2-1 (cont'd). Comparison of the Atmospheric Lifetimes (τ) of Low Molecular Weight Hydrocarbons Due to Reaction with OH, NO_3, Cl, Br and O_3

	k, cm^3 $molecule^{-1}$ s^{-1}									
	OH		**NO_3**		**Cl**		**Br**		**O_3**	
Hydrocarbon	$k \times 10^{12}$	τ	$k \times 10^{12}$	τ	$k \times 10^{10}$	τ	$k \times 10^{12}$	τ	$k \times 10^{18}$	τ
Alkenes										
Ethene	8.5	33 h	0	230 d	0.99	3.8 m	0.18	1.8 y	1.6	7.2 d
Propene	26	11 h	0.01	4.9 d	2.3	50 d	5.3	22 d	10	1.2 d
2-Methylpropene	51	5.4 h	0.34	3.3 h	0.42	9.0 m	NA	NA	11	1.1 d
1-Butene	31	9.0 h	0.013	3.6 d	1.4	65 d	3.4	34 d	9.6	1.2 d
trans-2-Butene	64	4.3 h	0.39	2.8 h	NA	NA	0.23	1.4 y	190	1.5 h
cis-2-Butene	56	5.0 h	0.35	3.2 h	NA	NA	6.3	18 d	125	2.3 h
1,3-Butadiene	67	4.1 h	0.1	11 h	4.2	28 d	57	2.0 d	6.3	1.8 d
Isoprene	100	2.8 h	0.68	1.6 h	5.1	23 d	74	1.6 d	13	21 h
2-Methyl-2-butene	87	3.2 h	9.4	0.12 h	NA	NA	19	6.1 d	400	0.69 h
1-Pentene	31	9.0 h	0.7	1.6 h	NA	NA	NA	NA	11	1.1 d
trans-2-Pentene	67	4.1 h	1.6	0.69 h	NA	NA	NA	NA	320	0.86 h
cis-2-Pentene	65	4.3 h	1.4	0.79 h	NA	NA	NA	NA	210	1.3 h
2,4,4-Trimethyl-1-pentene	65	4.3 h	0.51	2.2 h	NA	NA	NA	NA	NA	NA

Notes: NA = Reaction rate coefficient not available. Rate coefficients were calculated at 298k and 1 atmosphere. y = year. d = day.
OH = $1 \times 10^6/cm^3$; NO_3 = $2.5 \times 10^8/cm^3$; Cl = $1 \times 10^3/cm^3$; Br = $1 \times 10^5/cm^3$; O_3 = $1 \times 10^{12}/cm^3$. Value for BR calculated based on equilibrium with BrO = 1 ppt.
[1] Rate Coefficients were Obtained from the NIST Online Kinetics Database for Reactions of Alkanes and for all Cl and Br Reactions.
All Other Rate Coefficients were Obtained from the Evaluation
of Calvert et al. (2000).
[2] Lifetimes should be regarded as lower limits.

Sources: NIST online kinetics database (http://kinetics.nist.gov/index.php).

The $O(^3P)$ atoms formed directly in the photolysis of O_3 in the Huggins and Chappuis bands or formed from deactivation of $O(^1D)$ atoms reform O_3 through reaction AX2-2. Hydroxyl radicals produced by reactions AX2-5 and AX2-6 can react further with species such as carbon monoxide and with many hydrocarbons (for example, CH_4) to produce HO_2 radicals.

Measurements of OH radical concentrations in the troposphere (Poppe et al., 1995; Eisele et al., 1997; Brune et al., 1999; Martinez et al., 2003; Ren et al., 2003) show that, as expected, the OH radical concentrations are highly variable in space and time, with daytime maximum concentrations of $> 3 \times 10^6$ molecules /cm^3 in urban areas. A global, mass-weighted mean tropospheric OH radical concentration also can be derived from the estimated emissions and measured atmospheric concentrations of methylchloroform (CH_3CCl_3) and the rate constant for the reaction of the OH radical with CH_3CCl_3. Krol et al. (1998) derived a global average OH concentration of 1.07×10^6 molecules /cm^3 for 1993 along with an upward trend of about 0.5%/yr between 1978 and 1993. Using an integrated data set of observed O_3, H_2O, NO_y, CO, VOCs, temperature and cloud optical depth, Spivakovsky et al. (2000) calculated a global annual mean OH concentration of 1.16×10^6 molecules cm^{-3}, consistent to within less than 10% of the value obtained by Krol et al. (1998).

HO_2 radicals do not initiate the oxidation of hydrocarbons, but serve to recycle OH mainly by way of reaction with NO, ozone, and itself (the latter produces H_2O_2, which can photolyze to yield OH). The HO_2 radicals also react with organo-peroxy radicals produced during the oxidation of VOCs to form organo-peroxides (cf. Section AX2.2.5, reaction AX2-20, e.g.). Organo-peroxides may undergo wet or dry deposition (Wesely and Hicks, 2000), or degrade further by photolysis and reaction with OH (Jet Propulsion Laboratory, 2003).

At night, NO_3 assumes the role of primary oxidant (Wayne, 1991). Although it is generally less reactive than OH, its high abundance in the polluted atmosphere compensates for its lower reactivity. For several VOCs, however, including dimethylsulfide, isoprene, some terpenes (a-pinene, limonene, linalool) and some phenolic compounds (phenol, o-cresol), oxidation by NO_3 at night is competitive with oxidation by OH during the day, making it an important atmospheric removal mechanism for these compounds (Wayne, 1991) (see Table AX2-1). The role of NO_3 radicals in the chemistry of the remote marine boundary layer has been examined recently by Allen et al., (2000) and in the polluted continental boundary layer by Geyer and Platt (2002).

Cl atoms, derived from products of multiphase processes can initiate the oxidation of most of the same VOCs as OH radicals, however, the rate coefficients for the reactions of alkanes with Cl atoms are usually much higher. Cl will also oxidize alkenes and aromatic compounds, but with a significantly lower rate constant than for OH reactions. Following the initial reaction with Cl, the degradation of the hydrocarbon proceeds as with OH and NO_3, generating an enhanced supply of odd hydrogen radicals leading to O_3 production in the presence of sufficient NO_x. The corresponding reactions of Br with hydrocarbons proceed in a similar manner, but with rate coefficients that can be substantially lower or higher.

Chlorine and bromine radicals will also react directly with O_3 to form ClO and BrO radicals, providing a sink for odd oxygen if they do not react with NO to form NO_2 (e.g., Pszenny et al., 1993). As with other oxidants present in the atmosphere, Cl chemistry provides a modest net sink for O_3 when NO_x is less than 20 pptv, and is a net source at higher NO_x. Kasting and Singh (1986) estimated that as much as 25% of the loss of nonmethane hydrocarbons in the nonurban atmosphere can occur by reaction with Cl atoms, based on the production of Cl atoms from gas phase photochemical reactions involving chlorine containing molecules (HCl, CH_3Cl, $CHCl_3$, etc.). Elevated concentrations of atomic Cl and other halogen radicals can be found in polluted coastal cities where precursors are emitted directly from industrial sources and/or are produced via acid-catalyzed reactions involving sea-salt particles (Tanaka et al., 2000; Spicer et al., 2001).

Substantial chlorine-VOC chemistry has been observed in the cities of Houston and Beaumont/Port Arthur, Texas (Tanaka et al., 2000; Chang et al., 2002; Tanaka et al., 2003a). Industrial production activities in those areas frequently result in large releases of chlorine gas (Tanaka et al., 2000). Chloromethylbutenone (CMBO), the product of the oxidation of isoprene by atomic Cl and a unique marker for chlorine radical chemistry in the atmosphere (Nordmeyer et al., 1997), has been found at significant mixing ratios (up to 145 pptv) in ambient Houston air (Riemer and Apel, 2001). However, except for situations in which there are strong local sources such as these, the evidence for the importance of Cl as an oxidizing agent is mixed. Parrish et al. (1992, 1993) argued that ratios of selected hydrocarbons measured at Pt. Arena, CA were consistent with loss by reaction with OH radicals and that any deviations could be attributed to mixing processes. Finlayson-Pitts (1993), on the other hand had suggested that these deviations could have been the result of Cl reactions. McKeen et al. (1996) suggested that hydrocarbon ratios measured downwind of anthropogenic source regions affecting the western Pacific Basin are consistent with loss by reaction with OH radicals only. Rudolph et al. (1997), based on data for several pairs of hydrocarbons collected during a cruise in the western Mediterranean Sea, the eastern mid- and North Atlantic Ocean and the North Sea during April and May of 1991, also found that ratios of hydrocarbons to each other are consistent with their loss given mainly by reaction with OH radicals without substantial contributions from reactions with Cl. Their best estimate, for their sampling conditions was a ratio of Cl to OH of about 10^{-3}, implying a concentration of Cl of about $10^3/cm^3$ using the globally averaged OH concentration of about $10^6/cm^3$ given above. In contrast Wingenter et al. (1996) and Singh et al. (1996a) inferred significantly higher concentrations of atomic Cl (10^4 to 10^5 cm^{-3}) based on relative concentration changes in VOCs measured over the eastern North Atlantic and Pacific Oceans, respectively. Similar approaches employed over the high-latitude southern ocean yielded lower estimates of Cl concentrations (10^3 cm^{-3}; Wingenter et al., 1999). Taken at face value, these observations indicate substantial variability in Cl concentrations and uncertainty in "typical" values.

AX2.2.4 Chemistry of Nitrogen Oxides in the Troposphere

In the troposphere, NO, NO_2, and O_3 are interrelated by the following reactions:

$$NO + O_3 \rightarrow NO_2 + O_2 \qquad \text{(AX2-3)}$$

$$NO_2 + h\nu \rightarrow NO + O(^3P) \qquad \text{(AX2-1)}$$

$$O(^3P) + O_2 + M \rightarrow O_3 + M \qquad \text{(AX2-2)}$$

The reaction of NO_2 with O_3 leads to the formation of the nitrate (NO_3) radical,

$$NO_2 + O_3 \rightarrow NO_3^{\bullet} + O_2, \qquad \text{(AX2-7)}$$

which in the lower troposphere is nearly in equilibrium with dinitrogen pentoxide (N_2O_5):

$$NO_3^{\bullet} + NO_2 \xleftrightarrow{M} N_2\,O_5. \qquad \text{(AX2-8)}$$

However, because the NO_3 radical photolyzes rapidly (with a lifetime of ≈5 s for an overhead sun [Atkinson et al., 1992a]),

$$NO_3^{\bullet} + h\nu \rightarrow NO + O_2 \quad (10\%) \tag{Ax2-9a}$$

$$\rightarrow NO_2 + O(^3P) \quad (90\%) \tag{AX2-9b}$$

its concentration remains low during daylight hours, but can increase after sunset to nighttime concentrations of $< 5 \times 10^7$ to 1×10^{10} molecules cm^{-3} (< 2 to 430 ppt) over continental areas influenced by anthropogenic emissions of NO_x (Atkinson et al., 1986). This leads to an increase of N_2O_5 concentrations during the night by reaction (AX2-8).

The tropospheric chemical removal processes for NO_x involve the reaction of NO_2 with the OH radical and the hydrolysis of N_2O_5 in aqueous aerosol solutions to produce HNO_3.

$$\bullet OH + NO_2 \xrightarrow{M} HNO_3 \tag{AX2-10}$$

$$N_2O_5 \xrightarrow{H_2O(1)} HNO_3 \tag{AX2-11}$$

The gas-phase reaction of the OH radical with NO_2 initiates the major and ultimate removal process for NO_x in the troposphere. This reaction removes radicals (OH and NO_2) and competes with hydrocarbons for OH radicals in areas characterized by high NO_x concentrations, such as urban centers (see Section AX2.4). In addition to gas-phase nitric acid, Golden and Smith (2000) have concluded that, pernitrous acid (HOONO) is also produced by the reaction of NO_2 and OH radicals on the basis of theoretical studies. However, a recent assessment (Jet Propulsion Laboratory, 2003) has concluded that this channel represents a minor yield (approximately 15% at the surface). HOONO will thermally decompose or photolyze. Gas-phase HNO_3 formed from reaction AX2-10 undergoes wet and dry deposition to the surface and uptake by ambient aerosol particles. The tropospheric lifetime of NO_x due to reaction AX2-10 ranges from a few hours to a few days. Geyer and Platt (2002) concluded that reaction AX2-11 constituted about 10% of the removal of NO_x at a site near Berlin, Germany during spring and summer. However, during winter the relative importance of reaction AX2-11 could be much higher because of the much lower concentration of OH radicals and the enhanced stability of N_2O_5 due to lower temperatures and intensity of sunlight. Note that reaction AX2-11 surely proceeds as a heterogeneous reaction.

OH radicals also can react with NO to produce nitrous acid (HNO_2):

$$\bullet OH + NO \xrightarrow{M} HNO_2. \qquad (AX2\text{-}12)$$

In the daytime, HNO_2 is rapidly photolyzed back to the original reactants:

$$HNO_2 + h\nu \rightarrow \bullet OH + NO. \qquad (AX2\text{-}13)$$

At night, HNO_2 can be formed by heterogeneous reactions of NO_2 in aerosols or at the earth's surface (Lammel and Cape, 1996; Jacob, 2000; Sakamaki et al., 1983; Pitts et al., 1984a; Svensson et al., 1987; Jenkin et al., 1988; Lammel and Perner, 1988; Notholt et al., 1992a,b). This results in accumulation of HNO_2 during nighttime. Modeling studies suggest that photolysis of this HNO_2 following sunrise, could provide an important early-morning source of OH radicals to drive ozone formation (Harris et al., 1982).

Another important process controlling NO_x concentrations is the formation of organic nitrates. Oxidation of VOCs produces organic peroxy radicals (RO_2), as discussed in the hydrocarbon chemistry subsections to follow. Reaction of these RO_2 radicals with NO and NO_2 produces organic nitrates ($RONO_2$) and peroxynitrates (RO_2NO_2):

$$RO_2^{\bullet} + NO \xrightarrow{M} RONO_2 \qquad (AX2\text{-}14)$$

$$RO_2^{\bullet} + NO_2 \xrightarrow{M} RO_2NO_2 \qquad (AX2\text{-}15)$$

Reaction (AX2-14) is a minor branch for the reaction of RO_2 with NO (the major branch produces RO and NO_2, as discussed in the next section). The organic nitrate yield increases with carbon number (Atkinson, 2000).

The organic nitrates may react further, depending on the functionality of the R group, but they will typically not return NO_x and can therefore be viewed as a permanent sink for NO_x. This sink is usually small compared to HNO_3 formation, but the formation of isoprene nitrates may be a significant sink for NO_x in the United States in summer (Liang et al., 1998).

The peroxynitrates produced by (AX2-15) are thermally unstable and most have very short lifetimes (less than a few minutes) against thermal decomposition to the original reactants. They are thus not effective sinks of NO_x. Important exceptions are the peroxyacylnitrates (PANs) arising from the peroxyacyl radicals RC(O)OO produced by oxidation and photolysis of carbonyl compounds. PANs have lifetimes ranging from ~1 hour at room temperature to several weeks at 250K. They can thus provide an effective sink of NO_x at cold temperatures, but also a reservoir allowing eventual release of NO_x as air masses warm, in particular by subsidence. By far the most important of these PANs compounds is peroxyacetylnitrate (PAN), with formula $CH_3C(O)OONO_2$. PAN is a significant product in the oxidation of most VOCs. It is now well established that PAN decomposition provides a major source of NOx in the remote troposphere (Staudt et al., 2003). PAN decomposition in subsiding Asian air masses over the eastern Pacific could make an important contribution to O_3 enhancement in the U.S. from Asian pollution (Hudman et al., 2004).

AX2.2.5 The Methane Oxidation Cycle

The photochemical cycles leading to O_3 production are best understood by considering the oxidation of methane, structurally the simplest VOC. The CH_4 oxidation cycle serves as a model which describes the chemistry of the relatively clean or unpolluted troposphere (although this is a simplification because vegetation releases large quantities of complex VOCs into the atmosphere). Although the chemistry of the VOCs emitted from anthropogenic and biogenic sources in polluted urban and rural areas is more complex, a knowledge of the CH_4 oxidation reactions aids in understanding the chemical processes occurring in the polluted atmosphere because the underlying chemical principles are the same.

Methane is emitted into the atmosphere as the result of anaerobic microbial activity in wetlands, rice paddies, the guts of ruminants, landfills, and from mining and combustion of fossil fuels (Intergovernmental Panel on Climate Change, 2001). The major tropospheric removal process for CH_4 is by reaction with the OH radical,

$$\bullet OH + CH_4 \rightarrow H_2O + \dot{C}H_3. \qquad \text{(AX2-16)}$$

In the troposphere, the methyl radical reacts solely with O_2 to yield the methyl peroxy ($CH_3O_2\bullet$ radical (Atkinson et al., 1992a):

$$\dot{C}H_3 + O_2 \xrightarrow{M} CH_3O_2^{\bullet}. \qquad \text{(AX2-17)}$$

In the troposphere, the methyl peroxy radical can react with NO, NO_2, HO_2 radicals, and other organic peroxy (RO_2) radicals, with the reactions with NO and HO_2 radicals being the most important (see, for example, World Meteorological Organization, 1990). The reaction with NO leads to the formation of the methoxy ($CH_3\dot{O}$) radical,

$$CH_3O_2^{\bullet} + NO \rightarrow CH_3\dot{O} + NO_2. \qquad \text{(AX2-18)}$$

The reaction with the HO_2 radical leads to the formation of methyl hydroperoxide (CH_3OOH),

$$CH_3O_2^{\bullet} + HO_2^{\bullet} \rightarrow CH_3OOH + O_2, \qquad \text{(AX2-19)}$$

which can photolyze or react with the OH radical (Atkinson et al., 1992a):

$$CH_3OOH + h\nu \rightarrow CH_3\dot{O} + \bullet OH. \qquad \text{(AX2-20)}$$

$$\bullet OH + CH_3OOH \rightarrow H_2O + CH_3O_2^{\bullet} \qquad \text{(AX2-21a)}$$

or

$$\begin{aligned} &\rightarrow H_2O + CH_2OOH \qquad \text{fast decomposition} \\ &\dot{C}H_2OOH + M \rightarrow H_2CO + \bullet OH \end{aligned} \qquad \text{(AX2-21b)}$$

Methyl hydroperoxide is much less soluble than hydrogen peroxide (H_2O_2) and so wet deposition after incorporation into cloud droplets is much less important as a removal process than it is for H_2O_2. CH_3OOH can also be removed by dry deposition to the surface and it can also be transported by conversion to the upper troposphere. The lifetime of CH_3OOH in the troposphere due to photolysis and reaction with the OH radical is estimated to be ≈2 days. Methyl hydroperoxide is then a temporary sink of radicals, with its wet or dry deposition representing a loss process for tropospheric radicals.

The only important reaction for the methoxy radical ($CH_3\dot{O}$) is

$$CH_3\dot{O} + O_2 \rightarrow H_2CO + HO_2{\bullet}. \qquad \text{(AX2-22)}$$

$$HO_2{\bullet} + NO \rightarrow {\bullet}OH + NO_2 \qquad \text{(AX2-23)}$$

The HO_2 radicals produced in (AX2-22) can react with NO, O_3, or other HO_2 radicals according to,

$$HO_2{\bullet} + O_3 \rightarrow {\bullet}OH + 2O_2 \qquad \text{(AX2-24)}$$

$$HO_2{\bullet} + HO_2{\bullet} \rightarrow H_2O_2 + O_2. \qquad \text{(AX2-25)}$$

Formaldehyde (H_2CO) produced in reaction AX2-22 can be photolyzed:

$$H_2CO + h\nu \rightarrow H_2 + CO \quad (55\%) \qquad \text{(AX2-26a)}$$

$$\rightarrow {\bullet}H + H\dot{C}O \quad (45\%) \qquad \text{(AX2-26b)}$$

Formaldehyde also reacts with the OH radical,

$${\bullet}OH + H_2CO \rightarrow H_2O + H\dot{C}O. \qquad \text{(AX2-27)}$$

The H atom and $\dot{H}CO$ (formyl) radical produced in these reactions react solely with O_2 to form the HO_2 radical:

$$\bullet H + O_2 + M \rightarrow HO_2^{\bullet} + M \quad \text{(AX2-28)}$$

$$H\dot{C}O + O_2 \rightarrow HO_2^{\bullet} + CO. \quad \text{(AX2-29)}$$

The lifetimes of H_2CO due to photolysis and reaction with OH radicals are ≈4 h and 1.5 days, respectively, leading to an overall lifetime of slightly less than 4 hours for H_2CO for overhead sun conditions (Rogers, 1990).

The final step in the oxidation of CH_4 involves the oxidation of CO by reaction with the OH radical to form CO_2:

$$CO + \bullet OH \rightarrow CO_2 + \bullet H \quad \text{(AX2-30)}$$

$$H\dot{C}O + O_2 \rightarrow HO_2^{\bullet} + CO. \quad \text{(AX2-29)}$$

The lifetime of CO in the lower troposphere is ≈2 months at mid-latitudes.

NO and HO_2 radicals compete for reaction with CH_3O_2 and HO_2 radicals, and the reaction route depends on the rate constants for these two reactions and the tropospheric concentrations of HO_2 and NO. The rate constants for the reaction of the $CH_3O_2^{\cdot}$ radicals with NO (reaction AX2-18) and HO_2 radicals (reaction AX2-19) are of comparable magnitude (e.g., Jet Propulsion Laboratory, 2003). Based on expected HO_2 radical concentrations in the troposphere, Logan et al. (1981) calculated that the reaction of the $CH_3O_2^{\cdot}$ radical with NO dominates for NO mixing ratios of > 30 ppt. For NO mixing ratios < 30 ppt, the reaction of the CH_3O_2 radical with HO_2 dominates. The overall effects of methane oxidation on O_3 formation for the case when NO > 30 ppt can be written as:

$$CH_4 + \bullet OH + O_2 \rightarrow CH_3O_2^\bullet + H_2O \qquad \text{(AX2-16, AX2-17)}$$

$$CH_3O_2^\bullet + NO \rightarrow CH_3O\bullet + NO_2 \qquad \text{(AX2-18)}$$

$$CH_3O\bullet + O_2 \rightarrow H_2CO + HO_2^\bullet \qquad \text{(AX2-22)}$$

$$HO_2^\bullet + NO \rightarrow \bullet OH + NO_2 \qquad \text{(AX2-23)}$$

$$2(NO_2 + h\nu \rightarrow NO + O(^3P)) \qquad \text{(AX2-1)}$$

$$2(O(^3P) + O_2 + M \rightarrow O_3 + M) \qquad \text{(AX2-2)}$$

$$\text{Net:} \quad CH_4 + 4O_2 + 2h\nu \rightarrow H_2CO + 2O_3 + H_2O \qquad \text{(AX2-31)}$$

Further O_3 formation occurs, based on the subsequent reactions of H_2CO, e.g.,

$$H_2CO + h\nu + 2O_2 \rightarrow 2HO_2^\bullet + CO \qquad \text{(AX2-26b; AX2-28; AX2-29)}$$

$$2(HO_2^\bullet + NO \rightarrow \bullet OH + NO_2) \qquad \text{(AX2-23)}$$

$$2(NO_2 + h\nu \rightarrow NO + O(^3P)) \qquad \text{(AX2-1)}$$

$$2(O(^3P) + O_2 + M \rightarrow O_3 + M) \qquad \text{(AX2-2)}$$

$$\text{Net:} \quad H_2CO + 4O_2 + h\nu \rightarrow CO + 2O_3 + 2\bullet OH. \qquad \text{(AX2-32)}$$

Reactions in the above sequence lead to the production of two OH radicals which can further react with atmospheric constituents (e.g., Crutzen, 1973). There is also a less important pathway:

$$H_2CO + h\nu \rightarrow H_2 + CO \quad \text{(AX2-26a)}$$

$$CO + \bullet OH \rightarrow CO_2 + \bullet H \quad \text{(AX2-30)}$$

$$\bullet H + O_2 + M \rightarrow HO_2^{\bullet} + M \quad \text{(AX2-28)}$$

$$HO_2^{\bullet} + NO \rightarrow \bullet OH + NO_2 \quad \text{(AX2-23)}$$

$$NO_2 + h\nu \rightarrow NO + O(^3P) \quad \text{(AX2-1)}$$

$$O(^3P) + O_2 + M \rightarrow O_3 + M \quad \text{(AX2-2)}$$

$$\text{Net:} \quad H_2CO + 2O_2 + h\nu \rightarrow CO_2 + O_3 + H_2 \quad \text{(AX2-33)}$$

These reaction sequences are important for tropospheric chemistry because formaldehyde is an intermediate product of the oxidation of most VOCs. The reaction of O_3 and HO_2 radicals leads to the net destruction of tropospheric O_3:

$$HO_2^{\bullet} + O_3 \rightarrow \bullet OH + 2O_2 \quad \text{(AX2-24)}$$

Using the rate constants reported for reactions AX2-23 and AX2-24 (Atkinson et al., 1992a) and the background tropospheric O_3 mixing ratios given above, the reaction of HO_2 radicals with NO dominates over reaction with O_3 for NO mixing ratios > 10 ppt. The rate constant for reaction AX2-25 is such that an NO mixing ratio of this magnitude also means that the HO_2 radical reaction with NO will be favored over the self-reaction of HO_2 radicals.

Consequently, there are two regimes in the "relatively clean" troposphere, depending on the local NO concentration: (1) a "very low-NO_x" regime in which HO_2 and CH_3O_2 radicals combine (reaction AX2-19), and HO_2 radicals undergo self-reaction (to form H_2O_2) and react with O_3 (reactions AX2-25 and AX2-24), leading to net destruction of O_3 and inefficient OH radical regeneration (see also Ehhalt et al., 1991; Ayers et al., 1992); and (2) a "low-NO_x" regime (by comparison with much higher NO_x concentrations found in polluted areas) in which HO_2 and CH_3O_2 radicals react with NO to convert NO to NO_2, regenerate the OH radical, and, through the photolysis of NO_2, produce O_3. In the "low NO_x" regime there still may be significant competition from peroxy-peroxy reactions, depending on the local NO concentration.

Nitric oxide mixing ratios are sufficiently low in the remote marine boundary layer relatively unaffected by transport of NO_x from polluted continental areas (< 15 ppt) that oxidation of CH_4 will lead to net destruction of O_3, as discussed by Carroll et al. (1990) and Ayers et al. (1992). In continental and marine areas affected by transport of NO_x from combustion sources, NO mixing ratios are high enough (of the order of ~one to a few hundred ppt) for the oxidation of CH_4, nonmethane hydrocarbons (NMHCs) and CO to lead to net O_3 formation (e.g., Carroll et al., 1990; Dickerson et al., 1995). Generally, NO mixing ratios increase with altitude and can be of the order of fifty to a few hundred ppt, in the upper troposphere depending on location. The oxidation of peroxides, carbon monoxide and acetone transported upward by convection, in the presence of this NO, can lead to local O_3 formation (e.g., Singh et al., 1995; McKeen et al., 1997; Wennberg et al., 1998; Brühl et al., 2000).

AX2.2.6 The Atmospheric Chemistry of Alkanes

The same basic processes by which CH_4 is oxidized occur in the oxidation of other, even more reactive and more complex VOCs. As in the CH_4 oxidation cycle, the conversion of NO to NO_2 during the oxidation of VOCs results in the production of O_3 and the efficient regeneration of the OH radical, which in turn can react with other VOCs (Figure AX2-2). The chemistry of the major classes of VOCs important for O_3 formation such as alkanes, alkenes (including alkenes from biogenic sources), and aromatic hydrocarbons will be summarized in turn.

Reaction with OH radicals represents the main loss process for alkanes and as also mentioned earlier, reaction with nitrate and chlorine radicals are additional sinks for alkanes. For alkanes having carbon-chain lengths of four or less, the chemistry is well understood and the reaction rates are slow in comparison to alkenes and other VOCs of similar structure and molecular weight. See Table AX2-1 for a comparison of reaction rate constants for several small alkanes and their alkene and diene homologues. For alkanes larger than C5, the situation is more complex because the products generated during the degradation of these compounds are usually not well characterized. Branched alkanes have rates of reaction that are highly dependent on carbon backbone structure. Stable products of alkane photooxidation are known to include carbonyl compounds, alkyl nitrates, and hydroxycarbonyls.

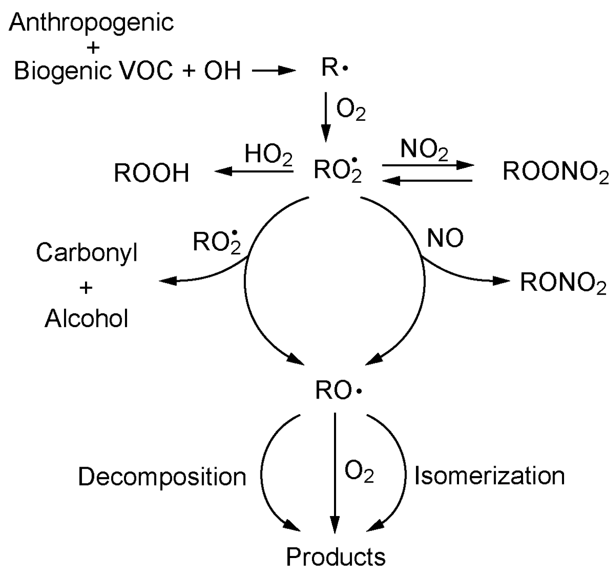

Figure AX2-2. General chemical mechanism for the oxidative degradation of VOCs.

Source: Atkinson (2000).

Alkyl nitrates form primarily as an alternate product of reaction AX2-34 (below). Several modeling studies have predicted that large fractions of NO_y exist as alkyl and hydroxy alkyl nitrates (Calvert and Madronich, 1987; Atherton and Penner, 1988; Trainer et al., 1991). In NO_x- and VOC-rich urban atmospheres, 100 different alkyl and 74 different hydroxy alkyl nitrate compounds have been predicted and identified (Calvert and Madronich, 1987; Schneider and Ballschmiter, 1999; Schneider et al., 1998). Uncertainties in the atmospheric chemistry of the alkanes include the branching ratio of reaction AX2-34, i.e., the extent to which alkyl nitrates form versus RO and NO_2. These uncertainties affect modeling predictions of NO_x concentrations, NO-to-NO_2 conversion and O_3 formation during photochemical degradation of the VOCs. Discrepancies between observations and theory have been found in aircraft measurements of NO_y (Singh et al., 1996b). Recent field studies conducted by Day et al. (2003) have shown that large fractions of organic nitrates, which may be associated with isoprene oxidation products, are present in urban and rural atmosphere that have not been previously measured and considered in NO_y calculations to date.

Alcohols and ethers in ambient air react almost exclusively with the OH radical, with the reaction proceeding primarily via H-atom abstraction from the C – H bonds adjacent to the oxygen-containing function group in these compounds (Atkinson and Arey, 2003).

The following list of general reactions, analogous to those described for methane, summarizes the role of alkane oxidation in tropospheric O_3 formation.

$$\bullet OH + RH \rightarrow H_2O + \bullet R \quad (AX2\text{-}34)$$

$$\bullet R + O_2 + M \rightarrow RO_2^\bullet + M \quad (AX2\text{-}35)$$

$$RO_2^\bullet + NO \rightarrow RO\bullet + NO_2 \quad (AX2\text{-}36)$$

$$HO_2^\bullet + NO \rightarrow \bullet OH + NO_2 \quad (AX2\text{-}23)$$

$$RO\bullet + O_2 \rightarrow R'CHO + HO_2^\bullet \quad (AX2\text{-}37)$$

$$2(NO_2 + h\nu \rightarrow NO + O) \quad (AX2\text{-}1)$$

$$2(O + O_2 + M \rightarrow O_3 + M) \quad (AX2\text{-}2)$$

$$\text{Net:} \quad RH + 4O_2 + 2h\nu \rightarrow R'CHO + 2O_3 + H_2O \quad (AX2\text{-}38)$$

The oxidation of alkanes can also be initiated by other oxidizing agents such as NO_3 and Cl radicals. In this case, there is net production of an OH radical which can re-initiate the oxidation sequence. The reaction of OH radicals with aldehydes forms acyl (R′CO) radicals, and acyl peroxy radicals (R′C(O)O_2) are formed by the addition of O_2. As an example, the oxidation of ethane (C_2H_5–H) yields acetaldehyde (CH_3–CHO). Acetyl (CH_3–CO) and acetylperoxy (CH_3–C(O)O_2) radicals can then be formed. Acetylperoxy radicals can combine with NO_2 to form peroxyacetyl nitrate (PAN) via:

$$CH_3C(O)O_2^\bullet + NO_2 + M \Leftrightarrow CH_3C(O)O_2NO_2 + M \quad (AX2\text{-}39)$$

PAN can act as a temporary reservoir for NO_2. Upon the decomposition of PAN, either locally or elsewhere, NO_2 is released to participate in the O_3 formation process again. During the oxidation of propane, the relatively long-lived intermediate acetone ($CH_3 - C(O)\ CH_3$) is formed, as shown in Figure AX2-3. The photolysis of acetone can be an important source of OH radicals, especially in the upper troposphere (e.g., Singh et al., 1995). Examples of oxidation mechanisms of more complex alkanes and other classes of hydrocarbons can be found in comprehensive texts such as Seinfeld and Pandis (1998).

AX2.2.7 The Atmospheric Chemistry of Alkenes

As shown in Figure AX2-3, the presence of a double carbon-carbon bond, i.e., $> C = C <$, in a VOC can greatly increase the range of potential reaction intermediates and products, complicating the prediction of O_3 production. The alkenes emitted from anthropogenic sources are mainly ethene, propene, and the butenes, with lesser amounts of the $\geq C_5$ alkenes. The major biogenic alkenes emitted from vegetation are isoprene (2-methyl-1,3-butadiene) and $C_{10}H_{16}$ monoterpenes (Atkinson and Arey, 2003), and their tropospheric chemistry is currently the focus of much attention (Zhang et al., 2002; Sauer et al., 1999; Geiger et al., 2003; Sprengnether et al., 2002; Witter et al., 2002; Bonn and Moortgat, 2003; Berndt et al., 2003; Fick et al., 2003; Kavouras et al., 1999; Atkinson and Arey, 2003).

Alkenes react in ambient air with OH and NO_3 radicals and with O_3. The mechanisms involved in their oxidation have been discussed in detail by Calvert et al. (2000). All three processes are important atmospheric transformation processes, and all proceed by initial addition to the $> C = C <$ bonds or, to a much lesser extent, by H atom extraction. Products of alkene photooxidation include carbonyl compounds, hydroxy alkyl nitrates and nitratocarbonyls, and decomposition products from the high energy biradicals formed in alkene-O_3 reactions. Table AX2-2 provides estimated atmospheric lifetimes for biogenic alkenes with respect to oxidation by OH, NO_3 and O_3. The structures of most of the compounds gives in Table AX2-2 are shown in Figure AX2-4.

Uncertainties in the atmospheric chemistry of the alkenes concern the products and mechanisms of their reactions with O_3, especially the yields of OH radicals, H_2O_2, and secondary organic aerosol in both outdoor and indoor environments. However, many product analyses of important biogenic and anthropogenic alkenes in recent years have aided in the narrowing of these uncertainties. The reader is referred to extensive reviews by Calvert et al.(2000) and Atkinson and Arey (2003) for detailed discussions of these products and mechanisms.

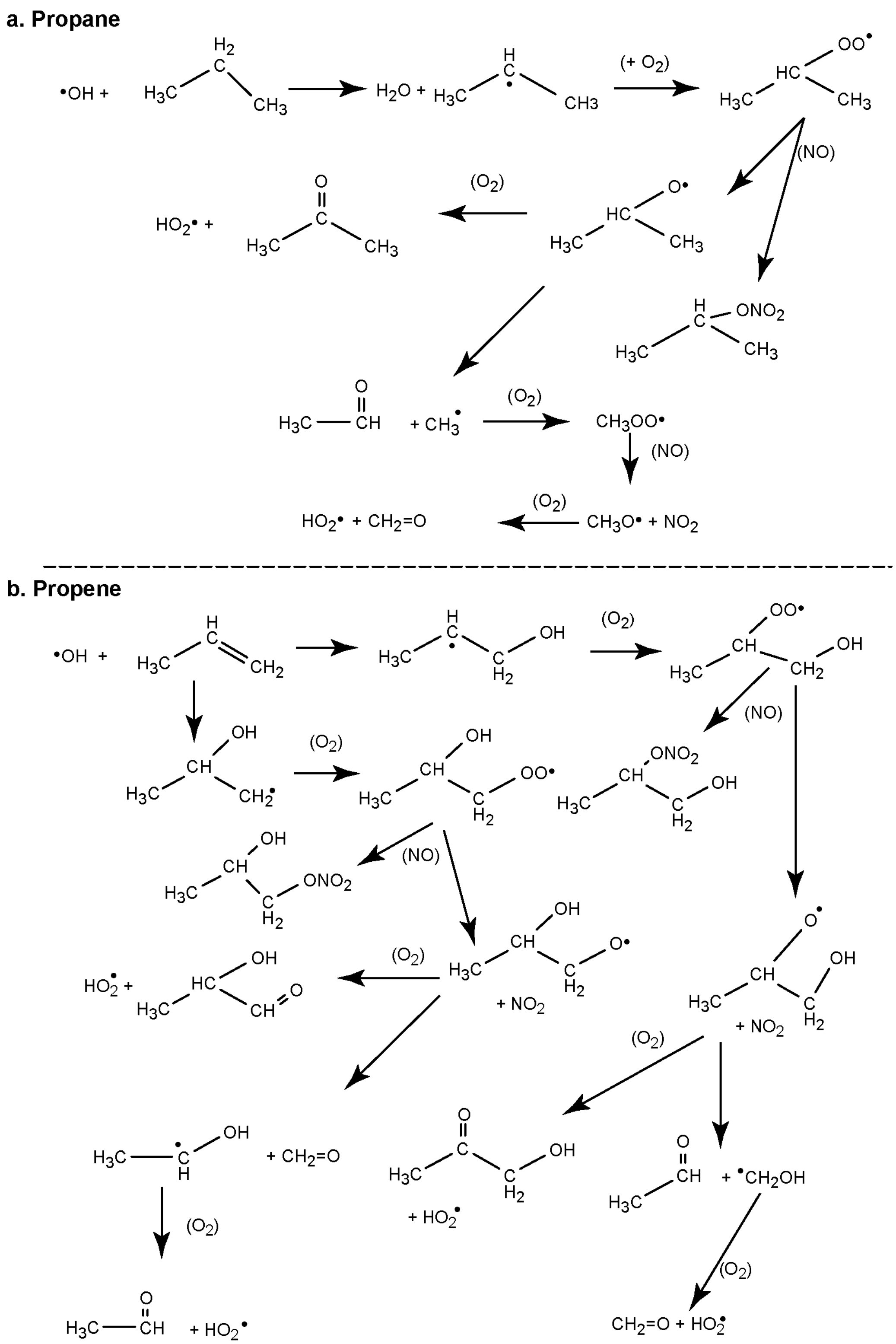

Figure AX2-3. Hydroxyl radical initiated oxidation of a) propane and b) propene.

Source: Calvert et al. (2000).

Table AX2-2. Calculated Atmospheric Lifetimes of Biogenic Volatile Organic Compounds (adapted from Atkinson and Arey, 2003) [a]

	Lifetime for Reaction with		
Biogenic VOC	**OH [b]**	**O_3 [c]**	**NO_3 [d]**
Isoprene	1.4 h	0.92 d	1.6 h
Monoterpenes			
Camphene	2.6 h	13 d	1.7 h
2-Carene	1.7 h	1.2 h	4 min
3-Carene	16 h	8.0 h	7 min
Limonene	49 min	1.4 h	5 min
Myrcene	39 min	35 min	6 min
cis-/*trans*-Ocimene	33 min	31 min	3 min
α-Phellandrene	27 min	5.6 min	0.9 min
β-Phellandrene	50 min	5.9 h	8 min
α-Pinene	2.6 h	3.2 h	11 min
β-Pinene	1.8 h	0.77 d	27 min
Sabinene	1.2 h	3.4 h	7 min
α-Terpinene	23 min	0.7 min	0.5 min
γ-Terpinene	47 min	2.0 h	2 min
Terpinolene	37 min	9.1 min	0.7 min
Sesquiterpenes			
β-Caryophyllene	42 min	1.4 min	3 min
α-Cedrene	2.1 h	9.8 h	8 min
α-Copaene	1.5 h	1.8 h	4 min
α-Humulene	28 min	1.4 min	2 min
Longifolene	2.9 h	> 23 d	1.6 h
Oxygenates			
Acetone [e]	61 d [f]	> 3.2 y [g]	> 8 y [f]
Camphor	2.5 d [h]	> 165 d [h]	> 300 d [h]
1,8-Cineole	1.0 d [i]	> 77 d [j]	1.5 y [i]
cis-3-Hexen-1-ol	1.3 h [k]	4.3 h [k]	4.1 h [k]
cis-3-Hexenyl acetate	18 h [k]	5.1 h [k]	4.S h [k]
Linalool	52 min [k]	39 min [k]	6 min [k]

Table AX-2 (cont'd). Calculated Atmospheric Lifetimes of Biogenic Volatile Organic Compounds (adapted from Atkinson and Arey, 2003)[a]

	Lifetime for Reaction with		
Biogenic VOC	**OH [b]**	**O_3 [c]**	**NO_3 [d]**
Oxygenates (cont'd)			
Methanol	12 d [f]	> 3.2 y [g]	2.0 y [f]
2-Methyl-3-buten-2-ol	2.4 h[l]	1.2 d [m]	7.7 d [n]
6-Methyl-5-hepten-2-one	53 min [o]	0.7 h [o]	9 min [o]

[a] Rate coefficients rom Calvert et al. (2000) unless noted otherwise.
[b] Assumed OH radical concentration: 1.0×10^6 molecule cm^{-3}.
[c] Assumed O_3 concentration: 1×10^{12} molecule cm^{-3}, 24-h average.
[d] Assumed NO_3 radical concentration: 2.5×10^8 molecule cm^{-3}, 12-h nighttime average.
[e] Photolysis will also occur with a calculated photolysis lifetime of ~60 day for the lower troposphere, July, 40 °N (Meyrahn et al., 1986).
[f] Atkinson et al. (1999).
[g] Estimated.
[h] Reissell et al. (2001).
[i] Corchnoy and Atkinson (1990).
[j] Atkinson et al. (1990).
[k] Atkinson et al. (1995).
[l] Papagni et al. (2001).
[m] Grosjean and Grosjean (1994).
[n] Rudich et al. (1996).
[o] Smith et al. (1996).

Oxidation by OH

As noted above, the OH radical reactions with the alkenes proceed mainly by OH radical addition to the > C = C < bonds. As shown in Figure AX2-3, for example, the OH radical reaction with propene leads to the formation of two OH-containing radicals. The subsequent reactions of these radicals are similar to those of the alkyl radicals formed by H-atom abstraction from the alkanes. Under high NO conditions, CH_3CHCH_2OH continues to react — producing several smaller, "second generation," reactive VOCs.

For the simple $\leq C_4$ alkenes, the intermediate OH-containing radicals appear to undergo mainly decomposition at room temperature and atmospheric pressure. Hence, for propene, the "first-generation" products of the OH radical reaction in the presence of NO are HCHO and CH_3CHO, irrespective of which OH-containing radical is formed.

For the more complex alkenes of biogenic origin, multiple products may be possible from the initial oxidation step. Each product will further react, following a distinct degradation pathway. Formaldehyde (HCHO), methacrolein ($CH_2 = C(CH_3)$-CHO) and methyl vinyl ketone (CH_3-C(O)-CH=CH_2 have been identified as the major products of the OH-isoprene reaction. These products also react with OH radicals and undergo photolysis. Yields of these products(and others) are sensitive to the concentration of NO_x used in laboratory experiments. For NO_x ~100 ppt, methacrolein, methyl vinyl ketone and formaldehyde are formed with yields of roughly 20%, 16%, and 33% and yields of other carbonyl compounds are about 17%, based on the results of Ruppert and Becker (2000) and references therein. Ruppert and Becker also observed much lower yields of C5-unsaturated diols (2 to 5%), methanol and methyl hydroperoxide indicating the presence of peroxy radical interactions. For NO_x ~1 ppb, the yields of methacrolein are similar to those for NO_x ~100 ppb, but the yields of methyl vinyl ketone (~33%), formaldehyde (~60%) are much higher and the diols, methanol and methyl hydroperoxide were not observed. Orlando et al. (1999) found that the major products of the oxidation of methacrolein were CO, CO_2, hydroxyacetone, formaldehyde and methacryloylperoxynitrate (MPAN) in their experiment. Horowitz et al. (1998) suggested that isoprene may be the principal precursor of PAN over the United States in summer. Hydroperoxy and organic peroxy radicals formed during the oxidation of isoprene and its products can oxidize NO to NO_2, initiating photochemical O_3 formation. It should be noted that only about two-thirds of the carbon in isoprene can be accounted for on a carbon atom basis for $NO_x \geq 1$ ppb. The values are much lower for lower NO_x concentrations. The situation is much better for methacrolein. Observed products can account for more than 90% of the reacted carbon.

The rates of formation of condensible, oxidation products of biogenic compounds that may contribute to secondary organic aerosol formation is an important matter for the prediction of ambient aerosol concentrations. Isoprene photooxidation has been shown to make a very small contribution to secondary organic aerosol formation under atmospheric conditions (Pandis et al., 1991; Zhang et al., 1992). Claeys et al. (2004) found that 2-methyltetrols are formed from the oxidation of isoprene in yields of about 0.2% on a molar basis, or 0.4% on a mass basis. These are semi-volatile compounds that can condense on existing particles. On the other hand, pinene oxidation leads to substantial organic aerosol formation.

Oxidation by Nitrate Radical

NO_3 radical reacts with alkenes mainly by addition to the double bond to form a b-nitrooxyalkyl radical.(Atkinson 1991, 1994, 1997). The abstraction pathway may account for up to 20% of the reaction. For propene, the initial reaction is followed by a series of reactions

$$\begin{aligned} NO_3^{\bullet} + CH_3CH{=}CH_2 &\rightarrow CH_3\dot{C}HCH_2ONO_2 \\ &\rightarrow CH_3CH(ONO_2)\dot{C}H_2 \end{aligned} \tag{AX2-40}$$

that (Atkinson, 1991) to lead to the formation of, among others, carbonyls and nitrato-carbonyls including formaldehyde (HCHO), acetaldehyde (CH_3CHO), 2-nitratopropanal ($CH_3CH(ONO_2)CHO$), and 1-nitratopropanone ($CH_3C(O)CH_2ONO_2$). By analogy to OH, conjugated dienes like butadiene and isoprene will react with NO_3 to form d-nitrooxyalkyl radicals. (Atkinson, 2000). If NO_3 is available for reaction in the atmosphere, then NO concentrations will be low, owing to the rapid reaction between NO_3 and NO. Consequently, nitrooxyalkyl peroxy radicals are expected to react primarily with NO_2, yielding thermally unstable peroxy nitrates, NO_3, HO_2, and organoperoxy radicals (Atkinson, 2000).

Several studies have undertaken the quantification of the products of NO_3^- initiated degradation of several of the important biogenic alkenes in O_3 and secondary organic aerosol formation, including isoprene, a- and b-pinene, 3-carene, limonene, linalool, and 2-methyl-3-buten-2-ol. See Figure AX2-4 for the chemical structures of these and other biogenic compounds. The results of these studies have been tabulated by Atkinson and Arey (2003).

Oxidation by Ozone

Unlike other organic compounds in the atmosphere, alkenes react at significant rates with O_3. Ozone initiates the oxidation of alkenes by addition across carbon-carbon double bonds, at rates that are competitive with reaction with OH (see Table AX2-1). The addition of O_3 across the double bond yields an unstable ozonide, a 5-member ring including a single carbon-carbon bond linked to the three oxygen atoms, each singly bound. The ozonide rearranges spontaneously and

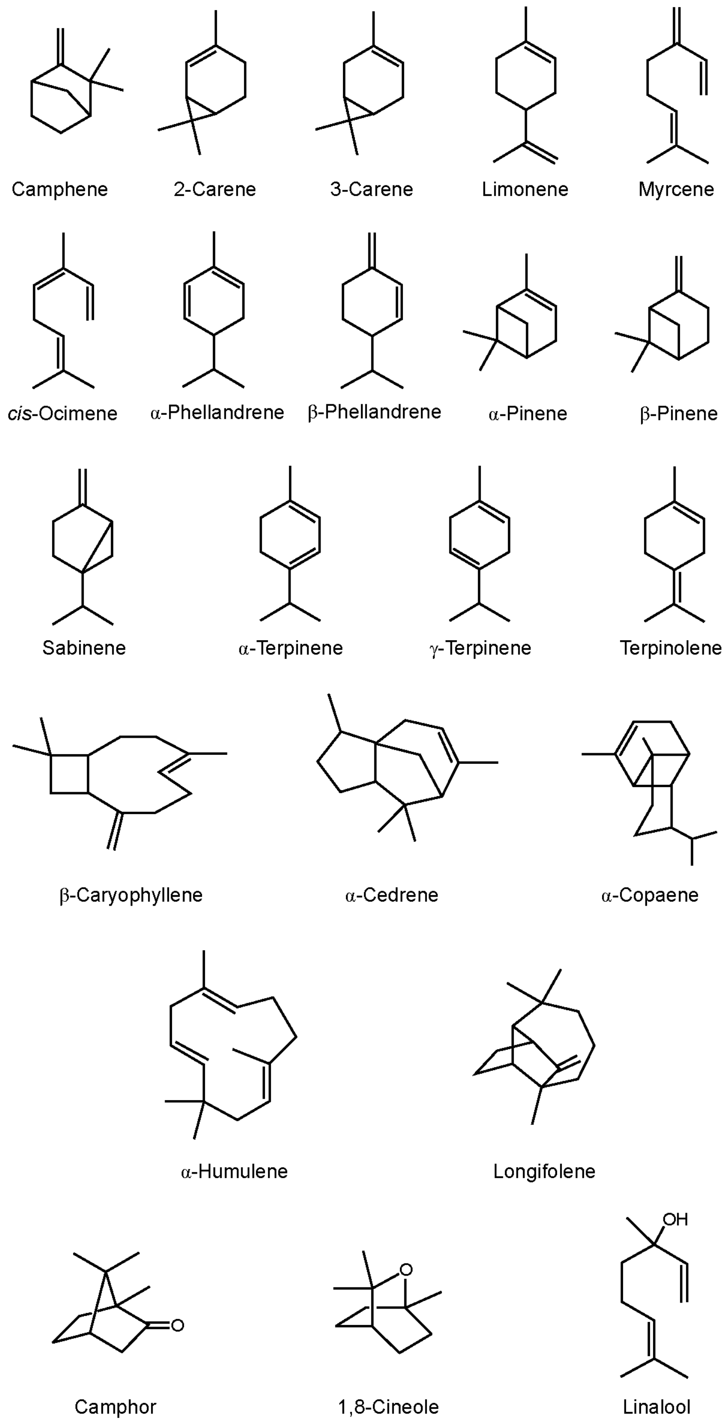

Figure AX2-4. Structures of a selected number of terpene and sesquiterpene compounds.

Source: Atkinson and Arey (2003).

then fragments to form an aldehyde or ketone, depending on the original position of the double bond, and a high energy Criegee biradical. Collisional energy transfer may stabilize the radical, preventing it from decomposing. Low pressure studies of the decomposition of the Criegee biradical have shown high yields of the OH radical. At atmospheric pressures, the rates of OH production have not been reliably established, due to complications arising from subsequent reactions of the OH produced with the ozonide fragments (Calvert et al., 2000).

The ozonolysis of larger biogenic alkenes yields high molecular weight oxidation products with sufficiently low vapor pressures to allow condensation into the particle phase. Many oxidation products of larger biogenic alkenes have been identified in ambient aerosol, eliminating their further participation in O_3 production. Figure AX2-5 shows the chemical structures of the oxidation products of a-pinene and illustrates the complexity of the products. Carbonyl containing compounds are especially prevalent. A summary of the results of product yield studies for several biogenic alkenes can be found in Atkinson and Arey (2003).

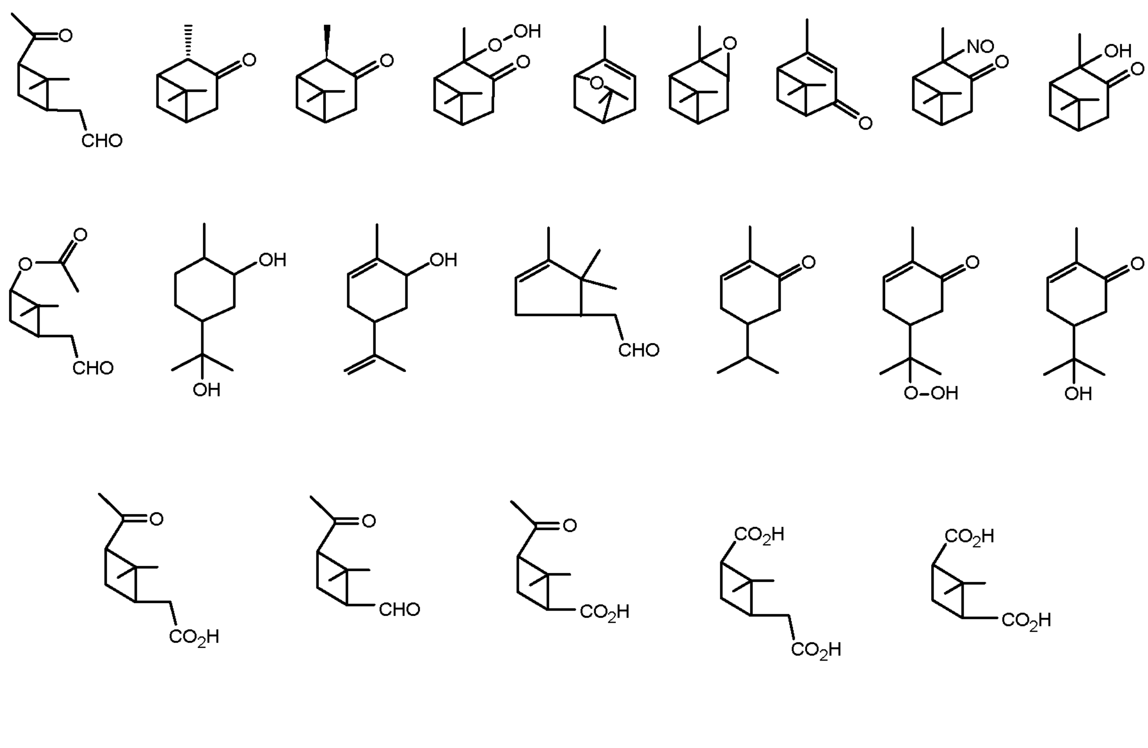

Figure AX2-5. Products from the reaction of terpenes with ozone.

Source: Atkinson and Arey (2003).

NO_2 also participates to a very small degree in the oxidation of alkenes by addition to double bonds in a manner similar to O_3. Rate constants for reactions of this type range from 10^{-18} to 10^{-24} for dienes and monoalkenes (King et al., 2002). It should also be noted that O_3 reacts with terpenoid compounds released from household products such as air fresheners and cleaning agents in indoor air to produce ultrafine particles (Wainman et al., 2000; Sarwar et al., 2002).

AX2.2.8 The Atmospheric Chemistry of Aromatic Hydrocarbons

Aromatic hydrocarbons represent a major class of compounds found in gasoline and other liquid fuels. Upon vaporization, most of these compounds react rapidly in the atmosphere (Davis et al., 1975) and following a series of complex processes, involving molecular oxygen and oxides of nitrogen, produce O_3. The reaction of OH radicals with aromatic hydrocarbons serves as their major atmospheric loss process. Atmospheric losses of alkyl aromatic compounds by O_3 and nitrate radicals have been found to be minor processes for most monocyclic aromatic hydrocarbons. (However, the reaction with of the nitrate radical with substituted hydroxybenzenes, such as phenol or o-,m-,p-cresol, can be an important atmospheric loss process for these compounds.) Much of the early work in this field focused on the temperature dependence of the OH reactions (Perry et al., 1977; Tully et al., 1981) using absolute rate techniques. Typically two temperature regions were observed for a large number of aromatic compounds and the complex temperature profile suggested that two mechanisms were operative. In the high temperature region, hydrogen (H)-atom abstraction from the aromatic ring dominates, and in the temperature regime less than 320K, OH addition to the aromatic ring is the dominant process. Thus, at normal temperatures and pressures in the lower troposphere, ring addition is the most important reactive process followed by H-atom abstraction from any alkyl substituents. The kinetics of monocyclic aromatic compounds are generally well understood and there is generally broad consensus regarding the atmospheric lifetimes for these compounds. By contrast, there is generally a wide range of experimental results from product studies of these reactions. This leads to a major problem in model development due to a general lack of understanding of the product identities and yields for even the simplest aromatic compounds, which is due to the complex reaction paths following initial reaction with OH, primarily by the addition pathway.

In the past three years, two comprehensive reviews have been written which provide a detailed understanding of the current state-of-science of aromatic hydrocarbons. Atkinson (2000) reviewed the atmospheric chemistry of volatile organic compounds, of which aromatic hydrocarbons are included in one section of the review. More recently Calvert et al. (2002) conducted a highly comprehensive examination of the reaction rates, chemical mechanisms, aerosol formation, and contributions to O_3 formation for monocyclic and polycyclic aromatic hydrocarbons.

AX2.2.8.1 Chemical Kinetics and Atmospheric Lifetimes of Aromatic Hydrocarbons

Rate constants for the reaction of species in the atmosphere with aromatic hydrocarbons vary widely depending on the number of aromatic rings and substituent groups. Reactions of O_3 with aromatic hydrocarbons (AHCs) are generally slow except for monocyclic aromatic hydrocarbons having unsaturated substituent groups. For example, indene and styrene have atmospheric lifetimes of 3.3 h and 23 h with respect to reaction with O_3, which are much longer than that due to reactive loss with either OH or NO_3. Thus, the atmospheric lifetimes and reaction products of O_3 and aromatic hydrocarbons will be ignored in this discussion. In addition to chemical reaction, some organic compounds photolyze in the lower atmosphere. Virtually all aromatic precursors are not subject to photolysis, although many of the ring fragmentation products having multiple carbonyl groups can photolyze in the troposphere.

The reaction rates and atmospheric lifetimes of monocyclic aromatic compounds due to reaction with OH radicals are generally dependent on the number and types of substituent groups associated with the ring. These reaction rates have been found to be highly temperature and pressure dependent. The temperature regimes are governed by the processes involved and show a quite complex appearance. At room temperature (~300 K), both addition to the aromatic ring and H-atom abstraction occur with the addition reaction being dominant. For the two smallest monocyclic aromatic hydrocarbons, the initial addition adduct is not completely stabilized at total pressures below 100 torr.

Numerous studies have been conducted to measure the OH + benzene rate constant over a wide range of temperatures and pressures. An analysis of absolute rate data taken at approximately 100 torr argon and not at the high pressure limit yielded a value of 1.2×10^{-12} cm^3 $molec^{-1}$ s^{-1}. Atkinson (1989) recommended a value of 1.4×10^{-12} $cm^3 molec^{-1}$ s^{-1} at room temperature and atmospheric pressure. This recommendation has been refined only slightly and is reflected in the recent value recommended by Calvert et al. (2002) which is given as 1.39×10^{-12} cm^3 molec^{-1}s^{-1}. This recommended value for the reaction of OH + benzene together with values for other monocyclic aromatic hydrocarbons is given in Table AX2-3.

In general, it is observed that the OH rate constants with monocyclic alkyl aromatic hydrocarbons are strongly influenced by the number of substituent groups found on the aromatic ring. (That is, the identity of the alkyl substituent groups has little influence on the overall reactions rate constant.) Single substituent single-ring aromatic compounds which include toluene, ethyl benzene, n-propylbenzene, isopropylbenzene, and t-butylbenzene have average OH reaction rate constants ranging from 4.5 to 7.0×10^{-12} cm^3 molec^{-1} s^{-1} at room temperature and atmospheric pressure. These rate constants lead to atmospheric lifetimes (see below) that are still greater than 1 day. Rate constants for monocyclic aromatic compounds with greater than 10 carbon atoms or more are generally not available.

The dominant monocyclic aromatic compounds with two substituents are m-,o-,p-xylene. Their recommended OH rate constants range from 1.4 to 2.4×10^{-11} cm^3 molec^{-1} s^{-1}. Similarly, the three isomers of ethyltoluene have recommended OH rate constants ranging from 1.2 to1.9 $\times 10^{-11}$ cm^3 molec^{-1} s^{-1}. The only other two substituent single-ring aromatic compound for which the OH rate constant has been measured is p-cymene (para-isopropyltoluene), giving a value of 1.5×10^{-11} cm^3 molec^{-1} s^{-1}.

OH rate constants for the C_9 trimethyl substituted aromatic hydrocarbons (1,2,3-; 1,2,4-; 1,3,5-trimethylbenzene) are higher by a factor of approximately 2.6 over the di-substituted compounds. Rate constants for the three isomers range from 3.3 to 5.7×10^{-11} cm^3 molec^{-1} s^{-1}. While concentrations for numerous other trisubstituted benzene compounds have been reported (e.g., 1,2-dimethyl-4-ethylbenzene), OH rate constants for trimethylbenzene isomers are the only trisubstituted aromatic compounds that have been reported.

Aromatic hydrocarbons having substituent groups with unsaturated carbon groups have much higher OH rate constants than their saturated analogues. The smallest compound in this group is the C_8 AHC, styrene. This compound reacts rapidly with OH and has a recommended rate constant of 5.8×10^{-11} cm^3 molec^{-1} s^{-1}. (Calvert, 2002). Other methyl substituted styrene-type compounds (e.g., α-methylstyrene) have OH rate constants within a factor of two of that with styrene. However, for unsaturated monocyclic aromatic hydrocarbons other processes

Table AX2-3. Hydroxyl Rate Constants and Atmospheric Lifetimes of Mono- and Di-cyclic Aromatic Hydrocarbons (adapted from Atkinson 2000)

Compound	OH Rate Constant ($\times 10^{12}$)	τ_{OH} (as indicated)
Benzene	1.4	8.3 d*
Toluene	5.6	2.1 d
Ethylbenzene	7	1.7 d
n-Propylbenzene	5.8	2.0 d
Isopropylbenzene	6.3	1.8 d
t-Butylbenzene	4.5	2.6 d
o-Xylene	14	20 h
m-Xylene	23	12 h
p-Xylene	14	19 h
o-Ethyltoluene	12	23 h
m-Ethyltoluene	19	15 h
p-Ethyltoluene	12	24 h
p-Cymene	14	19 h
1,2,3-Trimethylbenzene	33	8.4 h
1,2,4-Trimethylbenzene	33	8.6 h
1,3,5-Trimethylbenzene	57	4.8 h
Indan	19	15 h
Styrene[3]	58	4.8 h
α-Methylstyrene	51	5.4 h
Napthalene	23	12 h
1-Methylnapthalene	53	4.8 h
2-Methylnapthalene	52	8.8 h

[1] Rate coefficients given as cm^3/molec-sec.
[2] Lifetime for zero and single alkyl substituted aromatic based on OH concentration of 1×10^6 molec cm^{-3}.
[3] Lifetime for reaction of styrene with NO_3 is estimated to be 44 min based on a nighttime NO_3 concentration of 2.5×10^8 molec cm^{-3} and a rate coefficient of 1.5×10^{-12} cm^3/molec-sec.

including atmospheric removal by NO_3 radicals can also be an important process, particularly at night when photolysis does not substantially reduce the NO_3 radical concentration (see below).

Polycyclic aromatic hydrocarbons are found to a much lesser degree in the atmosphere than are the monocyclic aromatic hydrocarbons. For example, measurements made in Boston during 1995 (Fujita et al., 1995) showed that a single PAH (napthalene) was detected in the ambient morning air at levels of approximately 1% (C/C) of the total monocyclic aromatic hydrocarbons. 1-methyl and 2-methylnaphthalene have sufficient volatility to be present in the gas phase. Other higher molecular weight PAHs ($\leq$ 3 aromatic rings), if present, are expected to exist in the gas phase at much lower concentrations than napthalene and are not considered here. OH rate constants for napthalene and the two methyl substituted napthalene compounds the two have been reviewed by Calvert et al. (2002). The values recommended (or listed) by Calvert et al. (2002) are given in Table AX2-3. As seen in the monocyclic aromatic hydrocarbons, the substitution of methyl groups on the aromatic ring increases the OH rate constant, in this case by a factor of 2.3.

Some data is available for the reaction of OH with aromatic oxidation products. (In this context, aromatic oxidation products refer to those products which retain the aromatic ring structure.) These include the aromatic carbonyl compound, benzaldehyde, 2,4-; 2,5-; and 3,4-dimethyl-benzaldehyde, and t-cinnamaldehyde. Room temperature rate constants for these compounds range from 1.3×10^{-11} cm^3 $molec^{-1}$ s^{-1} (benzaldehyde) to 4.8×10^{-11} cm^3 $molec^{-1}$ s^{-1} (t-cinnamaldehyde). While the yields for these compounds are typically between 2 to 6%, they can contribute to the aromatic reactivity for aldehydes having high precursor concentration (e.g., toluene, 1,2,4-trimethylbenzene). OH also reacts rapidly with phenolic compounds. OH reaction rates with phenols and o-, m-, and p-cresol are typically rapid (2.7 to 6.8×10^{-11} cm^3 $molec^{-1}$ s^{-1}) at room temperature. Five dimethylphenols and two trimethylphenols have OH reaction rates ranging between 6.6×10^{-11} and 1.25×10^{-10} cm^3 $molec^{-1}$ s^{-1}. Finally, unlike the aromatic aldehydes and phenols, reaction rates for OH + nitrobenzene and OH + m-nitrotoluene are much lower than the parent molecules, given their electron withdrawing behavior from the aromatic ring. The room temperature rate constants are 1.4×10^{-13} and 1.2×10^{-12}, respectively.

The NO_3 radical is also known to react with selected AHCs and aromatic photooxidation products. Reaction can either occur by hydrogen atom abstraction or addition to the aromatic ring. However, these reactions are typically slow for alkyl aromatic hydrocarbons and the atmospheric removal due to this process is considered negligible. For AHCs having substituent groups with double bonds (e.g., styrene, α-methylstyrene), the reaction is much more rapid, due to the addition of NO_3 to the double bond. For these compounds, NO_3 rate constants are on the order of 10^{-12} cm^3 molec^{-1} s^{-1}. This leads to atmospheric lifetimes on the order of about 1 h for typical night time atmospheric NO_3 levels of 2.5×10^8 molec cm^{-3} (Atkinson, 2000).

The most important reactions of NO_3 with AHCs are those which involve phenol and methyl, dimethyl, and trimethyl analogs. These reactions can be of importance due to the high yields of phenol for the atmospheric benzene oxidation and o-,m-,p-cresol from toluene oxidation. The NO_3 + phenol rate has been given as 3.8×10^{-12} cm^3 molec^{-1} s^{-1}. Similarly, the cresol isomers each has an extremely rapid reaction rate with NO_3 ranging from 1.1 to 1.4×10^{-11} cm^3 molec^{-1} s^{-1}. As a result, these compounds, particularly the cresol isomers, can show rapid nighttime losses due to reaction with NO_3 with nighttime lifetimes on the order of a few minutes. There is little data for the reaction of NO_3 with dimethylphenols or trimethylphenols which have been found as products of the reaction of OH + m-, p-xylene and OH + 1,2,4-; 1,3,5-trimethylbenzene.

AX2.2.8.2 Reaction Products and Mechanisms of Aromatic Hydrocarbon Oxidation

An understanding of the mechanism of the oxidation of AHCs is important l if O_3 is to be accurately predicted in urban atmospheres through modeling studies. As noted above, most monocyclic aromatic hydrocarbons are removed from the atmosphere through reaction with OH. Thus, product studies of the OH + AHC should provide the greatest information regarding the AHC oxidation products. However, the effort to study these reactions has been intractable over the past two decades due to a number of difficulties inherent in the OH-aromatic reaction system. There are several reasons for the slow progress in understanding these mechanisms. (1) Product yields for OH-aromatic systems are poorly understood; for the most studied system, OH-toluene, approximately 50% of the reaction products have been identified under conditions where NO_2 reactions do not dominate the removal of the OH-aromatic adduct. (2) As noted, the reaction mechanism can change as the ratio of NO_2 to O_2 changes in the system (Atkinson and Aschmann, 1994). Thus, reaction product distributions that may be measured in the laboratory at high NO_2 (or NO_x) concentrations may not be applicable to atmospheric conditions. This also limits the usefulness of models to predict O_3 formation to the extent that secondary aromatic reactions are not completely parameterized in the system. (3) Aromatic reactions produce highly polar compounds for which there are few calibration standards available. In most cases, surrogate compounds have to be used in GC/MS calibrations. Moreover, it is not at all clear whether the present sampling techniques or analytical instruments are appropriate to measure the highly polar products produced in these systems. (4) Finally for benzene and toluene in particular, reaction rates of the products are substantially faster than that of the parent compounds. Thus, it is difficult to measure yields accurately without substantial interferences due to secondary reactions. Even given these difficulties, over the past decade a body of knowledge has been developed whereby the initial steps in the OH-initiated photooxidation have been established and a wide range of primary products from each of the major reaction systems have been catalogued.

Benzene is one of the most important aromatic hydrocarbons released into the atmosphere and is a recognized carcinogen. However, its reaction with OH is extremely slow and its contribution to urban O_3 formation is generally recognized to be negligible (Carter, 1994). As a result, relatively few studies have been conducted on the OH reaction mechanism of benzene. Major products of the oxidation of benzene have been found to be phenol and glyoxal (Berndt et al., 1999; Tuazon et al., 1986).

Most of the product analysis and mechanistic work on alkyl aromatic compounds in the gas phase has focused on examining OH reactions with toluene. The primary reaction of OH with toluene follows either of two paths, the first being an abstraction reaction from the methyl group and the second being addition to the ring. It has previously been found that H-atom abstraction from the aromatic ring is of minor importance (Tully et al., 1981). A number of studies have examined yields of the benzyl radical formed following OH abstraction from the methyl group. This radical forms the benzyl peroxy radical, which reacts with nitric oxide (NO) leading to the stable products benzaldehyde, with an average yield of 0.06, and benzyl nitrate, with an average yield less than 0.01 (Calvert et al., 2002). Thus, the overall yield for the abstraction channel is less than approximately 7%.

It is now generally recognized that addition of OH to the aromatic ring is the major process removing toluene from the atmosphere and appears to account for more than 90% of the reaction yield for OH + toluene. The addition of OH to the ring leads to an intermediate OH-toluene adduct that can be stabilized or can redissociate to the reactant compounds. For toluene, OH addition can occur at any of the three possible positions on the ring (ortho, meta, or para) to form the adduct. Addition of OH to the toluene has been shown to occur predominately at the ortho position (yield of 0.81) with lesser amounts at the meta (0.05) and para (0.14) positions (Kenley et al., 1981). The initial steps for both the abstraction and addition pathways in toluene have been shown in Figure AX2-6; only the path to form the ortho-adduct is shown, viz. reaction (2).

The OH-toluene adduct formed is an energy-rich intermediate that must be stabilized by third bodies in the system to undergo further reaction. Stabilization has been found to occur at pressures above 100 Torr for most third bodies (Perry et al., 1977; Tully et al., 1981). Therefore, at atmospheric pressure, the adduct will not substantially decompose back to its reactants as indicated by reaction (−2). The stabilized adduct (I) is removed by one of three processes: H-atom abstraction by O_2 to give a cresol, as in reaction (5); an addition reaction with O_2, as in reaction (6); or reaction with NO_2 to give m-nitrotoluene as in reaction (7).

The simplest fate for the adduct (I) is reaction with O_2 to form o-cresol. Data from a number of studies (e.g., Kenley et al., 1981; Atkinson et al., 1980; Smith et al., 1998; Klotz et al., 1998; summarized by Calvert et al., 2002) over a wide range of NO_2 concentrations (generally above 1 ppmv) show an average yield of approximately 0.15 for o-cresol. Most of the measurements suggest the o-cresol yield is independent of total pressure, identity of the third body, and NO_2 concentration (Atkinson and Aschmann, 1994; Moschonas et al., 1999), but the data tend to be scattered. This finding suggests that the addition of NO_2 to the hydroxy methylcyclo-hexadienyl radical does not contribute to the formation of phenolic-type compounds. Fewer studies have been conducted for m- and p-cresol yields, but the results of two studies indicate the yield is approximately 0.05 (Atkinson et al., 1980; Gery et al., 1985; Smith et al., 1998). The data suggests good agreement between the relative yields of the cresols from the product studies at atmospheric pressure and studies at reduced pressures. Thus, H-atom abstraction from adducts formed at all positions appears to represent approximately 20% of the total yield for toluene.

The OH-toluene adduct also reacts with O_2 to form a cyclohexadienyl peroxy radical (III), shown as a product of reaction (6) after rearrangement. This radical can undergo a number of possible processes. Most of these processes lead to ring fragmentation products, many of which have been seen in several studies (Dumdei and O'Brien, 1984; Shepson et al., 1984). Ring-fragmentation products are frequently characterized by multiple double bonds and/or multiple

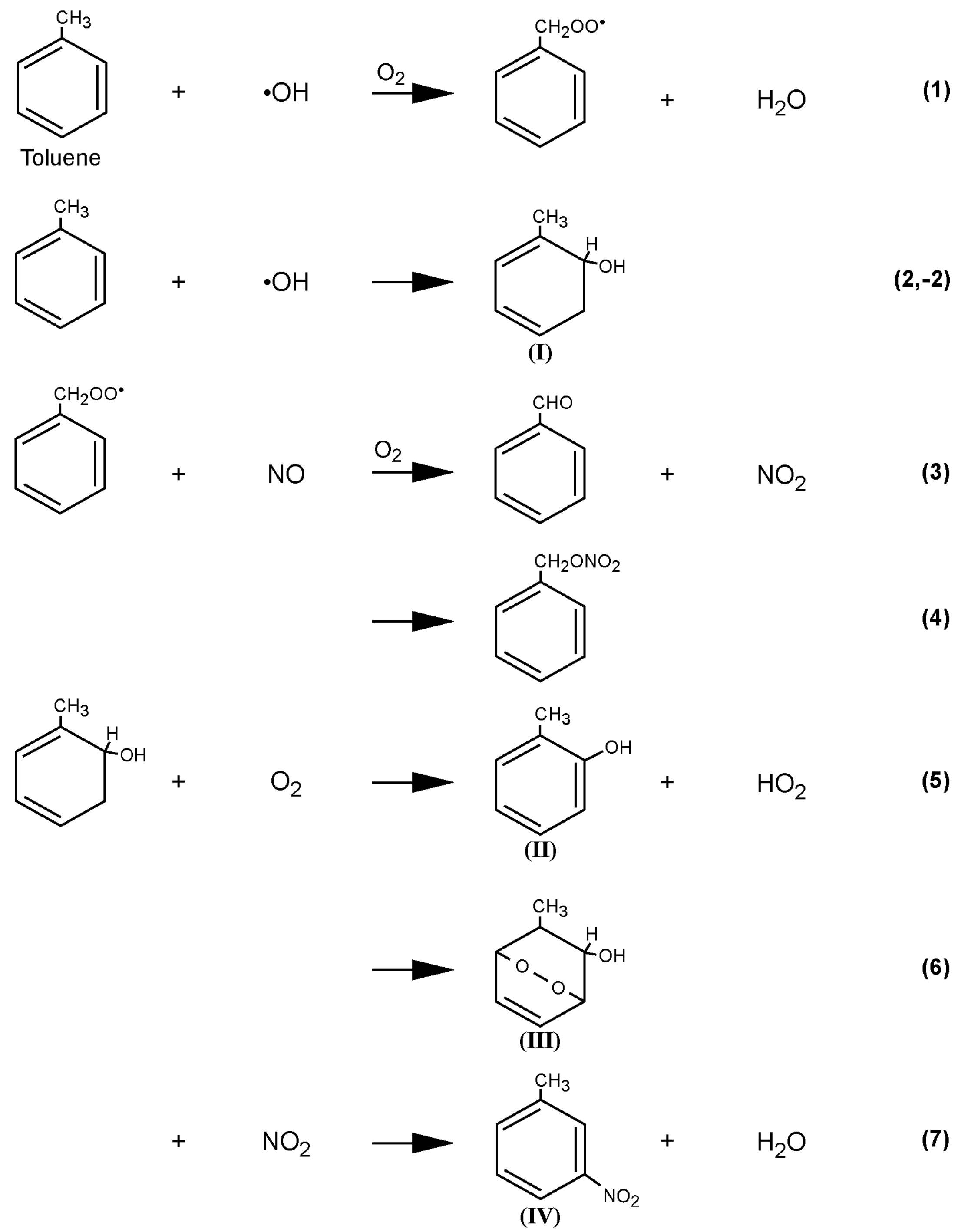

Figure AX2-6. Initial steps in the photooxidation mechanism of toluene initiated by its reaction with OH radicals.

functional groups. As such, these products are highly reactive and extremely difficult to detect and quantify.

Klotz et al. (1997; 1998) have suggested that the intermediate could also follow through a mechanism where toluene oxide/oxepin could be formed following the addition of O_2 to the OH-aromatic adduct. Recent experiments suggest that the formation of o-cresol through the photolysis of toluene oxide/oxepin is only a minor contributor to the overall o-cresol which has been measure (Klotz et al., 1998). This result contrasts to the high yield observed for the formation of phenol from the photolysis of benzene oxide/oxepin (Klotz et al., 1997). Recently, Berndt et al. (1999) used a flow tube to test the hypothetical formation of benzene oxide/oxepin from the OH + benzene reaction at pressures below 100 torr. They saw very little evidence for its formation.

A few studies have been conducted to identify fragmentation products using a variety of instruments. Several approaches have been used that employ structural methods, particularly mass spectrometry (MS), to identify individual products formed during the photooxidation. In one approach (Dumdei and O'Brien, 1984), the walls of the reaction chamber were extracted following an extended irradiation. In this study, the analysis was conducted by tandem mass spectrometry (MS/MS), which allowed products to be separated without the use of a chromatographic stationary phase. The investigators reported 27 photooxidation products from toluene, with 15 reportedly from ring fragmentation processes. However, the study was purely qualitative and product yields could not be obtained. No distinction could be made between primary and secondary products from the reaction because extended irradiations and species in various isotopic forms could not be differentiated. More refined approaches using atmospheric pressure ionization-tandem mass spectrometry has been used to study toluene (Dumdei et al., 1988) and m- and p-xylene (Kwok et al., 1997) photooxidation.

In another study, Shepson et al. (1984) demonstrated that a number of these fragmentation products could be analyzed by gas chromatography. Fragmentation products detected by the both investigations (Dumdei and O'Brien, 1984; Shepson et al., 1984) included glyoxal, methyl glyoxal, butenedial, 4-oxo-2-pentenal, hydroxybutenedial, 1-pentene-3,4-dione, 1-butene-3,4-dione, and methyl vinyl ketone. Additional evidence (Shepson et al., 1984) for fragmentation processes came from the detection of 2-methylfuran and furfural. These compounds, although cyclic in structure, result from a bridged oxygen intermediate. Yields of the detected fragmentation products were subsequently measured in a number of studies (e.g., Bandow et al., 1985a,b; Tuazon et al., 1986; Smith et al., 1998), were typically under 15% on a reacted carbon basis.

An additional possible pathway for reaction of the OH-toluene adduct is by reaction with NO_2 to give isomers of nitrotoluene. A yield of approximately 0.015 at NO_2 concentrations of about 1 ppmv has been measured (Atkinson et al., 1991). Although this yield itself is fairly minor, the investigators reported a positive intercept in plotting the nitrotoluene concentration against the NO_2 concentration; however, the data were considerably scattered. The positive intercept has been interpreted as suggesting that the OH-toluene adduct does not add O_2. This finding would require, therefore, another mechanism than that described above to be responsible for the fragmentation products.

The results of this study can be compared to experiments which directly examined the OH radical loss in reactions of OH with toluene and other aromatic compounds. Knipsel and co-workers (Knispel et al., 1990) have found a double exponential decay for toluene loss in the presence of added O_2, a rapid decay reflective of the initial adduct formation and a slower decay reflecting loss of the adduct by O_2 or other scavengers. From the decay data in the presence of O_2, they determine a loss rate for the OH-toluene of 5.4×10^{-16} cm^3 $molec^{-1}$ s^{-1}. Use of this rate constant suggests that the loss rate of 2500 s^{-1} for the adduct in the presence of air at atmospheric pressure. This loss rate compares to a loss due to NO_2 (with a nominal atmospheric concentration of 0.1 ppmv) of about 100 s^{-1}. This finding suggests that removal of the OH-toluene adduct by O_2 is a far more important loss process than removal by NO_2 under atmospheric conditions which is in contrast other findings (Atkinson et al., 1991). This finding was confirmed by the recent experiments from Moschonas et al. (1999).

Therefore, studies on the disposition of toluene following OH reaction can be summarized as follows. It is generally accepted that H-atom abstraction from the methyl group by OH is a relatively minor process accounting for a 6 to 7% yield in the OH reaction with toluene. Addition of OH to toluene to form an intermediate OH-toluene adduct is the predominant process. At atmospheric pressure, ring-retaining products such as the cresol and nitrotoluenes account for another 20% of the primary reaction products (Smith et al., 1999). The remaining 70 to 75% of the products are expected to be ring fragmentation products in the gas phase, having an uncertain mechanism for formation. Many of these fragmentation products have been detected, but appear to form at low yields, and relatively little quantitative information on their formation yields exists. As noted earlier, some of these products contain multiple double bonds, which are likely to be highly reactive with OH or photolyze which enhances the reactivity of systems containing aromatics. Mechanisms that cannot adequately reflect the formation of fragmentation products are likely to show depressed reactivity for the oxidation of toluene and other aromatic compounds.

The number of studies of the multiple-substituted alkyl aromatics, such as the xylenes or the trimethylbenzenes, is considerably smaller than for toluene. Kinetic studies have focused on the OH rate constants for these compounds. For the xylenes, this rate constant is typically a factor of 2 to 5 greater than that for OH + toluene. Thus, the OH reactivity of the fragmentation products is similar to that of the parent compounds, potentially making the study of the primary products of the xylenes less prone to uncertainties from secondary reactions of the primary products than is the case for toluene.

Products from the OH reaction with the three xylenes have been studied most comprehensively in a smog chamber using long-path FTIR (Bandow and Washida, 1985a) and gas chromatography (Shepson et al., 1984; Atkinson and Aschmann, 1994; Smith et al., 1999). Ring-fragmentation yields of 41, 55, and 36% were estimated for o-, m-, and p-xylene, respectively, based on the dicarbonyl compounds, glyoxal, methyl glyoxal, biacetyl, and 3-hexene-2,5-dione detected during the photooxidation. These values could be lower limits, given that Shepson et al. (1984) report additional fragmentation products from o-xylene, including 1-pentene-4,5-dione, butenedial, 4-oxo-pentenal, furan, and 2-methylfuran. In the earlier studies, aromatic concentrations were in the range of 5 to 10 ppmv with NO_x at 2 to 5 ppmv. At atmospheric ratios of NO_2 and O_2, the observed yields could be different. Smith et al. (1999) examined most of the ring retaining products in the OH + m-xylene and OH + p-xylene systems. In each case, tolualdehyde isomers, dimethylphenol isomers, and nitro xylene isomers specific for each system were detected. The total ring retaining yield for OH + m-xylene was 16.3%; the yield for OH + p-xylene it was 24.5%. A mass balance approach suggests that respective ring-fragmentation yields of 84% and 76%, respectively. Kwok et al. (1997) also measured products from the OH + m- and p-xylene systems using atmospheric pressure ionization-tandem mass spectrometry. Complementary ring-fragmentation products to glyoxal, methylglyoxal, and biacetyl were detected from the parent ion peaks, although the technique did not permit the determination of reaction yields.

Smith et al. (1999) also studied ring fragmentation products from the reaction of OH with 1,2,4- and 1,3,5-trimethylbenzene. Ring-retaining products from the reaction with 1,2,4-trimethylbenzene gave three isomers each of dimethylbenzaldehyde and trimethylphenol as expected by analogy with toluene. However, the ring-retaining products only accounted for 5.8% of the reacted carbon. Seven additional ring-fragmentation products were also detected from the reaction, although the overall carbon yield was 47%. For 1,3,5-trimethylbenzene, its reaction with OH leads to only two ring-retaining products, 3,5-dimethyl-benzaldehyde and 2,4,6-trimethylphenol, given its molecular symmetry. Only a single fragmentation product was detected, methyl glyoxal, at a molar yield of 90%. The overall carbon yield in this case was 61%. The formation of relatively low yields of aromatic aldehydes and methylphenols suggests that NO_x removal by these compound in these reaction systems will be minimized (see below).

In recent years, computational chemistry studies have been applied to reaction dynamics of the OH-aromatic reaction systems. Bartolotti and Edney (1995) used density functional-based quantum mechanical calculations to help identify intermediates of the OH-toluene adduct. These calculations were consistent with the main addition of OH to the ortho position of toluene followed by addition of O_2 to the meta position of the adduct. The reaction energies suggested the formation of a carbonyl epoxide which was subsequently detected in aromatic oxidation systems by Yu and Jeffries, (1997). Andino et al. (1996) conducted ab initio calculations using density functional theory with semiempirical intermediate geometries to examine the energies of aromatic intermediates and determine favored product pathways. The study was designed to provide some insight into the fragmentation mechanism, although only a group additivity approach to calculate ΔH_{rxn} was used to investigate favored reaction pathways. However, the similarity in energies of the peroxy radicals formed from the O_2 reaction with the OH-aromatic adduct were very similar in magnitude making it difficult to differentiate among structures.

A detailed analysis of toluene oxidation using smog chamber experiments and chemical models (Wagner et al., 2003) shows that there are still large uncertainties in the effects of toluene on O_3 formation. A similar situation is likely to be found for other aromatic hydrocarbons.

AX2.2.8.3 The Formation of Secondary Organic Aerosol as a Sink for Ozone Precursors

Aromatic hydrocarbons are known to generate secondary organic aerosol (SOA) following their reaction with OH or other reactive oxidants. Secondary organic aerosol refers to the formation of fine particulate matter either through nucleation processes or through condensation onto existing particles. Over the last 12 years numerous experiments have been conducted in environmental chambers to determine the yield of secondary organic aerosol as a function of the reacted aromatic hydrocarbon. A review of the results of these studies can be found in the latest Air Quality for Particulate Matter Document (U.S. Environmental Protection Agency, 2003).

The extent to which aromatic reaction products are removed from the gas phase and become incorporated in the particle phase will influence the extent to which oxygenated organic compounds will not be available for participation in the aromatic mechanisms that lead to O_3 formation. However, this may be overstated to some degree for products of aromatic precursors. First, at atmospheric loading levels of organic particulate matter, the SOA yields of the major aromatic hydrocarbons are in the low percent range. Second, the aromatic products that are likely to condense on particles are likely to be highly oxygenated and have OH reaction rates that make them largely unreactive. Thus, while there may be some reduction of O_3 formation, it is not expected to be large.

AX2.2.9 Importance of Oxygenated VOCs

The role of oxygenated VOCs in driving O_3 production has generated increasing interest over the past decade. These VOCs include carbonyls, peroxides, alcohols, and organic acids. They are produced in the atmosphere by oxidation of hydrocarbons, as discussed above, but are also directly emitted to the atmosphere, in particular by vegetation (Guenther et al., 2000). In rural and remote atmospheres, oxygenated VOCs often dominate over nonmethane hydrocarbons in terms of total organic carbon mass and reactivity (Singh et al., 2004). The most abundant by mass of these oxygenated VOCs is usually methanol, which is emitted by vegetation and is present in U.S. surface air at concentrations of typically 1-10 ppbv (Heikes et al., 2002).

Most oxygenated VOCs react with OH to drive ozone production in a manner similar to the hydrocarbon chemistry discussed in the previous sections. In addition, carbonyl compounds (aldehydes and ketones) photolyze to produce peroxy radicals that can accelerate ozone production, thus acting as a chemical amplifier (Jaeglé et al., 2001). Photolysis of formaldehyde by (A.26b) was discussed in section AX2.2.5. Also of particular importance is the photolysis of acetone (Blitz et al., 2004):

$$(CH_3)_2C(O) + h\nu \xrightarrow{2O_2} CH_3C(O)O_2^{\bullet} \qquad \text{(AX2-41)}$$

producing organic peroxy radicals that subsequently react with NO to produce O_3. The peroxyacetyl radical $CH_3C(O)OO$ can also react with NO_2 to produce PAN, as discussed in Section AX2.2.4. Photolysis of acetone are a minor but important source of HO_2 radicals in the upper troposphere (Arnold et al., 2004).

AX2.2.10 Influence of Multiphase Chemical Processes

In addition to reactions occurring in the gas phase, reactions occurring on the surfaces of or within cloud droplets and airborne particles also occur. Their collective surface area is huge, implying that collisions with gas phase species occur on very short time scales. The integrated aerosol surface area ranges from 4.2×10^{-7} cm^2/cm^3 for clean continental conditions to 1.1×10^{-5} cm^2/cm^3 for urban average conditions (Whitby, 1978). There have been substantial improvements in air quality especially in urban areas since the time these measurements were made and so the U.S. urban values should be scaled downward by roughly a factor of two to four. The resulting surface area is still substantial and the inferred collision time scale of a gaseous molecule with a particle ranges from a few seconds or less to a few minutes. These inferred time scales imply that heterogenous reactions will generally be much less important than gas phase reactions for determining radical concentrations especially when reaction probabilities much less then unity are considered. A large body of research has accumulated recently regarding chemical processes in cloud droplets, snow and ice crystals, wet (deliquesced) inorganic particles, mineral dust, carbon chain agglomerates and organic carbon-coated particles.

Jacob's (2000) comprehensive review of the potential influences of clouds and aerosols on tropospheric O_3 cycling provides the starting point for this section. Updates to that review will also be provided. Jacob's review evaluates the literature available through late 1999, discusses major areas of uncertainty, recommends experiments to reduce uncertainties, and (based on then current information) recommends specific multiphase pathways that should be considered in models of O_3 cycling. In regard to the latter, Jacob's recommendations should be viewed as conservative. Specifically, only reasonably well-constrained pathways supported by strong observational evidence are recommended for inclusion in models. Several poorly resolved and/or controversial pathways that may be significant in the ambient troposphere lack sufficient constraints for reliable modeling. Some of these areas are discussed in more detail below. It should be noted at the outset that many of the studies described in this section involve either aerosols that are not found commonly throughout the United States (e.g., marine aerosol) or correspond to unaged particles (e.g., soot, mineral dust). In many areas of the United States, particles accrete a layer of hydrated H_2SO_4 which will affect the nature of the multiphase processes occurring on particle surfaces.

Major conclusions from this review are summarized as follows (comments are given in parentheses):

HO_x Chemistry

(1) Catalytic O_3 loss via reaction of $O_2^- + O_{3(aq)}$ in clouds appears to be inefficient.

(2) Aqueous-phase loss of HCHO in clouds appears to be negligible (see also [Lelieveld and Crutzen 1990]).

(3) Scavenging of HO_2 by cloud droplets is significant and can be acceptably parameterized with a reaction probability of $\gamma_{HO_2} = 0.2$, range 0.1 to 1, for $HO_2 \rightarrow 0.5\ H_2O_2$. However, this approach may overestimate HO_2 uptake because the influence of $HO_{2(aq)}$ on the magnitude (and direction) of the flux is ignored.

(4) The uptake of alkyl peroxy radicals by aerosols is probably negligible.

(5) Hydrolysis of $CH_3C(O)OO$ in aqueous aerosols may be important at night in the presence of high PAN and aerosol surface area; $\gamma_{CH_3C(O)OO} = 4 \times 10^{-3}$ is recommended.

NO_x Chemistry

(6) Hydrolysis of N_2O_5 to HNO_3 in aqueous aerosols is important (Section AX2.2.4) (and can be parameterized with $\gamma_{HNO_3} = 0.01$ to 0.1, Schutze and Herrmann, 2002; Hallquist et al., 2003).

(7) Although the mechanism is uncertain, heterogeneous conversion of NO_2 to HONO on aerosol surfaces should be considered with $\gamma_{NO_2} = 10^{-4}$ (range 10^{-6} to 10^{-3}) for $NO_2 \rightarrow 0.5\ HONO + 0.5\ HNO_3$. (This reaction also occurs on snow, Crawford et al., 2001). Wet and dry deposition sinks for HONO should also be considered although scavenging by aerosols appears to be negligible.

(8) There is no evidence for significant multiphase chemistry involving PAN

(9) There is no evidence for significant conversion of HNO_3 to NO_x in aerosols.

Heterogeneous ozone loss

(10) There is no evidence for significant loss of O_3 to aerosol surfaces (except during dust storms observed in East Asia, e.g., Zhang and Carmichael, 1999).

Halogen radical chemistry

(11) There is little justification for considering BrO_x and ClO_x chemistry (except perhaps in limited areas of the United States and nearby coastal areas).

Most of the above conclusions remain valid but, as detailed below, some should be qualified based on recently published findings and on reevaluation of results form earlier investigations.

AX2.2.10.1 HO_x and Aerosols

Field measurements of HO_x reviewed by Jacob (2000) correspond to regions with relatively low aerosol concentrations (e.g., Mauna Loa [Cantrell et al., 1996]; rural Ontario [Plummer et al., 1996]; and the upper troposphere [Jaeglé et al., 1999]). In all cases, however, significant uptake of HO_2 or HO_2 + RO_2 radicals by aerosols was inferred based on imbalances between measured concentrations of peroxy radicals and photochemical models of gas-phase chemistry. Laboratory studies using artificial aerosols (both deliquesced and solid) confirm uptake but the actual mechanism remains unclear. Several investigations report significant HO_x and H_2O_2 production in cloud water (e.g., Anastasio et al., 1994). However the potential importance of this source is considered unlikely because measurements in continental air show no evidence of missing sources for HO_x or H_2O_2. No investigations involving the potential influences of marine aerosols as sources or sinks for HO_x were considered in the above analysis.

Relative to conservative seawater tracers such as Mg^{2+} and Na^+, organic C associated with sea-salt aerosols is typically enriched by 2 to 3 orders of magnitude in both polluted (e.g., Hoffman and Duce, 1976, 1977; Turekian et al., 2003) and remote regions (Chesselet et al., 1981). This organic C originates from three major sources: 1) organic surfactants concentrated from bulk seawater on walls of subsurface bubbles (Tseng et al., 1992), 2) the surface microlayer of the ocean (Gershey, 1983), and 3) condensation of organic gases (Pun et al., 2000).

Coagulation of chemically distinct aerosols (e.g., via cloud processing) may also contribute under some conditions.

Resolving chemical processes involving particles in the marine boundary layer (MBL) is constrained by the relative scarcity of measurements of particulate organic carbon (POC) (Penner, 1995) and its molecular composition (Saxena et al., 1995). In MBL regions impacted by direct continental outflow, POC may constitute more that half of the total dry aerosol mass (Hegg et al., 1997). Carbon isotopic compositions in the polluted North Atlantic MBL indicate that, on average, 35% to 40% of POC originates from primary (direct injection) and secondary (condensation of gases) marine sources (Turekian et al., 2003).

The photolysis of dissolved organic compounds is a major source for OH, H_2O_2, and C-centered radicals in both the surface ocean (e.g., Blough and Zepp, 1995; Blough, 1997; Mopper and Kieber, 2000) and in marine aerosols (e.g., McDow et al., 1996). Relative to the surface ocean, however, production rates in the aerosol are substantially greater per unit volume because organic matter is highly enriched (Turekian et al., 2003) and aerosol pH is much lower (Keene et al., 2002a). Lower pHs increase rates of many reactions including acid-catalyzed pathways such as the breakdown of the $HOCl^-$ radical (King et al., 1995), the formation of H_2O_2 from the photolysis of phenolic compounds (Anastasio et al., 1997), and the photolysis of organic acids.

To provide a semi-quantitative context for the potential magnitude of this source, we assume a midday OH production rate in surface seawater of 10^{-11} M sec^{-1} (Zhou and Mopper, 1990) and a dissolved organic carbon enrichment of 2 to 3 orders of magnitude in sea-salt aerosols. This yields an estimated OH production rate in fresh (alkaline) sea-salt aerosols of 10^{-9} to 10^{-8} M sec^{-1}. As discussed above, rapid (seconds to minutes) acidification of the aerosol should substantially enhance these production rates. Consequently, the midday OH production rates from marine-derived organic matter in acidified sea-salt aerosols may rival or perhaps exceed midday OH scavenging rates from the gas phase (approximately 10^{-7} M sec^{-1}; [Chameides and Stelson, 1992]). Scavenging is the only significant source for OH in acidified sea-salt aerosols considered by many current models.

Limited experimental evidence indicates that these pathways are important sources of HO_x and RO_x in marine air and possibly in coastal cities. For example, the absorption of solar energy by organic species dissolved in cloud water (e.g., Faust et al., 1993; Anastasio et al., 1997) and in deliquesced sea-salt aerosols (Anastasio et al., 1999) produces OH, HO_2, and H_2O_2. In addition, Fe(III) complexation by oxalate and similar ligands to metal such as iron can greatly enhance radical production through ligand to metal charge transfer reactions (Faust, 1994; Hoigné et al., 1994). Oxalate and other dicarboxylic anions are ubiquitous components of MBL aerosols in both polluted (e.g., Turekian et al., 2003) and remote regions (Kawamura et al., 1996).

Substantial evidence exists for washout of peroxy radicals. Near solar noon, mixing ratios of total HO_x plus RO_x radicals generally fall in the 50 ppt range, but during periods of rain these values dropped to below the detection limit of 3 to 5 ppt (Andrés-Hernández et al., 2001; Burkert et al., 2001a; Burkert et al., 2001b; Burkert et al., 2003). Such low concentrations cannot be explained by loss of actinic radiation, because nighttime radical mixing ratios were higher.

Burkert et al. (2003) investigated the diurnal behavior of the trace gases and peroxy radicals in the clean and polluted MBL by comparing observations to a time dependant, zero-dimensional chemical model. They identified significant differences between the diurnal behavior of RO_2^* derived from the model and that observed possibly attributable to multiphase chemistry. The measured HCHO concentrations differed from the model results and were best explained by reactions involving low levels of Cl.

Finally, photolytic NO_3^- reduction is important in the surface ocean (Zafiriou and True, 1979) and could contribute to OH production in sea-salt aerosols. Because of the pH-dependence of HNO_3 phase partitioning, most total nitrate (HNO_3 + particulate NO_3^-) in marine air is associated with sea salt (e.g., Huebert et al., 1996; Erickson et al., 1999). At high mM concentrations of NO_3^- in sea-salt aerosols under moderately polluted conditions (e.g., Keene et al., 2002) and with quantum yields for OH production of approximately 1% (Jankowski et al., 2000), this pathway would be similar in magnitude to that associated with scavenging from the gas phase and with photolysis of dissolved organics. Experimental manipulations of marine aerosols sampled under relatively clean conditions on the California coast confirms that this pathway is a major source for OH in sea-salt solutions (Anastasio et al., 1999).

Although largely unexplored, the potential influences of these poorly characterized radical sources on O_3 cycling in marine air are probably significant. At minimum, the substantial inferred concentrations of HO_2 in aerosol solutions would diminish and perhaps reverse HO_2 scavenging by marine aerosols and thereby increase O_3 production relative to models based on Jacob's (2000) recommended reaction probability.

AX2.2.10.2 NO_x Chemistry

Jacob (2000) recommended as a best estimate, $\gamma_{N_2O_5} = 0.1$ for the reaction probability of N_2O_5 on aqueous aerosol surfaces with conversion to HNO_3. Recent laboratory studies on sulfate and organic aerosols indicates that this reaction probability should be revised downward, to a range 0.01-0.05 (Kane et al., 2001; Hallquist et al., 2003; Thornton et al., 2003). Tie et al. (2003) found that a value of 0.04 in their global model gave the best simulation of observed NO_x concentrations over the Arctic in winter. A decrease in N_2O_5 slows down the removal of NO_x and thus increases O_3 production. Based on the consistency between measurements of NO_y partitioning and gas-phase models, Jacob (2000) considers it unlikely that significant HNO_3 is recycled to NO_x in the lower troposphere. However, only one of the reviewed studies (Schultz et al., 2000) was conducted in the marine troposphere and none were conducted in the MBL. An investigation over the equatorial Pacific reported discrepancies between observations and theory (Singh et al., 1996b) that might be explained by HNO_3 recycling. It is important to recognize that both Schultz et al. (2000) and Singh et al. (1996b) involved aircraft sampling which, in the MBL, significantly under represents sea-salt aerosols and thus most total NO_3 ($HNO_3 + NO_3^-$) and large fractions of NO_y in marine air (e.g., Huebert et al., 1996). Consequently, some caution is warranted when interpreting constituent ratios and NO_y budgets based on such data.

Recent work in the Arctic has quantified significant photochemical recycling of NO_3^- to NO_x and perturbations of OH chemistry in snow (Honrath et al., 2000; Dibb et al., 2002; Domine and Shepson, 2002), which suggests the possibility of similar multiphase pathways occurring in aerosols. As mentioned above, recent evidence also indicates that NO_3^- is photolytically reduced to NO_2^- (Zafariou and True, 1979) in acidic sea-salt solutions (Anastasio et al., 1999). Further photolytic reduction of NO_2^- to NO (Zafariou and True, 1979) could provide a possible mechanism for HNO_3 recycling. Early experiments reported production of NO_x during the irradiation of artificial seawater concentrates containing NO_3^- (Petriconi and Papee, 1972). Based on the above, we believe that HNO_3 recycling in sea-salt aerosols is potentially important and warrants further investigation. Other possible recycling pathways involving highly acidic aerosol solutions and soot are reviewed by Jacob (2000).

Ammann et al. (1998) reported the efficient conversion of NO_2 to HONO on fresh soot particles in the presence of water. They suggest that interaction between NO_2 and soot particles may account for high mixing ratios of HONO observed in urban environments. Conversion of NO_2 to HONO and subsequent photolysis to NO + OH would constitute an NO_x-catalyzed O_3 sink involving snow. High concentrations of HONO can lead to the rapid growth in OH concentrations shortly after sunrise, giving a "jump start" to photochemical smog formation. Prolonged exposure to ambient oxidizing agents appears to deactivate this process. Broske et al. (2003) studied the interaction of NO_2 on secondary organic aerosols and concluded that the uptake coefficients were too low for this reaction to be an important source of HONO in the troposphere.

Choi and Leu (1998) evaluated the interactions of nitric acid on a model black carbon soot (FW2), graphite, hexane and kerosene soot. They found that HNO_3 decomposed to NO_2 and H_2O at higher nitric acid surface coverages, i.e., $P(HNO_3) >= 10^{-4}$ Torr. None of the soot models used were reactive at low nitric acid coverages, at $P(HNO_3) = 5 \times 10^{-7}$ Torr or at lower temperatures (220K). They conclude that it is unlikely that aircraft soot in the upper troposphere/lower stratosphere reduces HNO_3.

Heterogeneous production on soot at night is believed to be the mechanism by which HONO accumulates to provide an early morning source of HO_x in high NO_x environments (Harrison et al., 1996; Jacob, 2000). HONO has been frequently observed to accumulate to levels of several ppb over night, and has been attributed to soot chemistry (Harris et al., 1982; Calvert et al., 1994; Jacob, 2000).

Longfellow et al. (1999) observed the formation of HONO when methane, propane, hexane and kerosene soots were exposed to NO_2. They estimate that this reaction may account for some part of the unexplained high levels of HONO observed in urban areas. They comment that without details about the surface area, porosity and amount of soot available for this reaction, reactive uptake values cannot reliably be estimated. They comment that soot and NO_2 are produced in close proximity during combustion, and that large quantities of HONO have been observed in aircraft plumes.

Saathoff et al. (2001) studied the heterogeneous loss of NO_2, HNO_3, NO_3/N_2O_5, HO_2/HO_2NO_2 on soot aerosol using a large aerosol chamber. Reaction periods of up to several days were monitored and results used to fit a detailed model. They derived reaction probabilities at 294 K and 50% RH for NO_2, NO_3, HO_2 and HO_2NO_2 deposition to soot, HNO_3 reduction to NO_2, and N_2O_5 hydrolysis. When these probabilities were included in photochemical box model calculations of a 4-day smog event, the only noteworthy influence of soot was a 10% reduction in the 2nd day O_3 maximum, for a soot loading of 20 µg m^{-3}, i.e., a factor of 2 to 10 times observed black carbon loadings seen during extreme U.S. urban pollution events, although such concentrations are observed routinely in the developing world.

Muñoz and Rossi (2002) conducted Knudsen cell studies of HNO_3 uptake on black and grey decane soot produced in lean and rich flames, respectively. They observed HONO as the main species released following nitric acid uptake on grey soot, and NO and traces of NO_2 from black soot. They conclude that these reactions would only have relevance in special situations in urban settings where soot and HNO_3 are present in high concentrations simultaneously.

AX2.2.10.3 Halogen Radical Chemistry

Barrie et al. (1988) first suggested that halogen chemistry on snow surfaces in the Arctic could lead to BrOx formation and subsequent O_3 destruction. More recent work suggests that halogen radical reactions may influence O_3 chemistry in mid latitudes as well.

The weight of available evidence supports the hypothesis that halogen radical chemistry significantly influences O_3 cycling over much of the marine boundary layer at lower latitudes and in at least some other regions of the troposphere. However, proposed chemical mechanisms are associated with substantial uncertainties and, based on available information, it appears unlikely that a simple parameterization (analogous to those recommended by Jacob (2000) for other multiphase transformations) would adequately capture major features of the underlying transformations.

Most of the Cl and Br in the marine boundary layer are produced in association with sea-salt aerosols by wind stress at the ocean surface (e.g., Gong et al., 1997). Fresh aerosols rapidly dehydrate towards equilibrium with ambient water vapor and undergo other chemical processes involving the scavenging of reactive gases, aqueous-phase transformations, and volatilization of products. Many of these processes are strongly pH-dependent (Keene et al., 1998). Throughout most of the marine boundary layer, sea-salt alkalinity is tritrated rapidly (seconds to minutes) by ambient acids (Chameides and Stelson, 1992; Erickson et al., 1999) and, under a given set of conditions, the pHs of the super-µm, sea-salt size fractions are buffered to similar values via HCl phase partitioning (Keene and Savoie, 1998; 1999; Keene et al., 2002).

Model calculations based on the autocatalytic halogen activation mechanism (Vogt et al., 1996; Keene et al., 1998; Sander et al., 1999; von Glasow et al., 2002a,b; Pszenny et al., 2003; Sander et al., 2003) predict that most particulate Br- associated with acidified sea-salt aerosol would react to form Br_2 and BrCl, which subsequently volatilize and photolyze in sunlight to produce atomic Br and Cl. Most Br atoms recycle in the gas phase via

$$\bullet Br + O_3 \rightarrow BrO\bullet + O_2 \qquad \text{(AX2-42)}$$

$$BrO\bullet + HO_2\bullet \rightarrow HOBr + O_2 \qquad \text{(AX2-43)}$$

$$HOBr + h\nu \rightarrow \bullet OH + \bullet Br \qquad \text{(AX2-44)}$$

and thereby catalytically destroy O_3, analogous to Br cycling in the stratosphere (e.g., Mozurkewitch, 1995; Sander and Crutzen, 1996). Side reactions with HCHO and other compounds produce HBr, which is either scavenged and recycled through the aerosol or lost to the surface via wet and dry deposition (Dickerson et al., 1999).

Cl-radical chemistry influences O_3 in two ways (e.g., Pszenny et al., 1993). Some atomic Cl in marine air reacts directly with O_3 initiating a catalytic sequence analogous to that of Br (AX2-42 through AX2-44 above). However, most atomic Cl in the MBL reacts with hydrocarbons (which, relative to the stratosphere, are present at high concentrations) via hydrogen extraction to form HCl vapor. The enhanced supply of odd hydrogen radicals from hydrocarbon oxidation leads to O_3 production in the presence of sufficient NO_x. Thus, Cl chemistry represents a modest net sink for O_3 when NO_x is less than 20 pptv and a net source at higher NO_x. Although available evidence suggest that significant Cl-radical chemistry occurs in clean marine air, its net influence on O_3 appears to be small relative to that of Br and I.

In addition to Br and Cl, several lines of recent evidence suggests that an autocatalytic cycle also sustains I-radical chemistry leading to significant net O_3 destruction in marine air (Vogt et al., 1996, 1999; von Glasow et al., 2002a). The cycle is initiated by photolysis of organoiodine compounds emitted from the ocean surface to generate atomic I (Carpenter et al., 1999). Iodine atoms react almost exclusively with O_3 to form IO. Most IO photodissociates in sunlight to generate I and atomic O, which rapidly recombines with O_2 to form O_3. Consequently, this cycle has no net effect on O_3 (Stutz et al., 1999). However, alternative reaction pathways analogous to reactions AX2-42 through AX2-44 above lead to catalytic O_3 destruction. Model calculations suggest that HOI recycles via acid-catalyzed aerosol scavenging to form ICl and IBr, which subsequently volatilize and photolyze to form halogen atoms. The net effect of this multiphase pathway is to increase concentrations of volatile reactive I. The self reaction of IO to form I and OIO may further enhance O_3 destruction (Cox et al., 1999; Ashworth et al., 2002). IO also reacts with NO_2 to form INO_3, which can be scavenged by aqueous aerosols. This pathway has been suggested as a potentially important sink for NO_x in the remote MBL and would, thus, contribute indirectly to net O_3 destruction (McFiggans et al., 2000).

Various lines of observational evidence support aspects of the above scenarios. Most measurements of particulate Br in marine air reveal large depletions relative to conservative sea-salt tracers (e.g., Sander et al., 2003) and, because HBr is highly soluble in acidic solution, these deficits cannot be explained by simple acid-displacement reactions (e.g., Ayers et al., 1999). Observed Br depletions are generally consistent with predictions based on the halogen activation mechanism. In contrast, available, albeit limited, data indicate that I is highly enriched in marine aerosols relative to bulk seawater (e.g., Sturges and Barrie, 1988), which indicates active multiphase iodine chemistry.

Direct measurements of BrO in marine air by differential optical absorption spectroscopy (DOAS) reveal mixing ratios that are near or below analytical detection limits of about 1 to 3 ppt (Hönninger, 1999; Pszenny et al., 2003; Leser et al., 2003) but within the range of model predictions. Column-integrated DOAS observations from space reveal substantial mixing ratios of tropospheric BrO (e.g., Wagner and Platt, 1998). Although the relative amounts in the MBL cannot be resolved, these data strongly suggest active destruction of tropospheric O_3 via the reaction sequence of AX2-42 through AX2-44. Similarly, measurements of IO (McFiggans et al., 2000) and OIO (Allan et al., 2001) indicate active O_3 destruction by an analogous pathway involving atomic I. In addition, anticorrelations on diurnal time scales between total volatile inorganic Br and particulate Br and between volatile inorganic I and particulate I have been reported (e.g., Rancher and Kritz, 1980; Pszenny et al., 2003). Although the lack of speciation precludes unambiguous interpretation, these relationships are also consistent with predictions based on the halogen activation mechanism.

Large diurnal variabilities in O_3 measured over the remote subtropical Atlantic and Indian Oceans (Dickerson et al., 1999; Burkert et al., 2003) and early morning depletions of O_3 observed in the remote temperate MBL (Galbally et al., 2000) indicate that only about half of the inferred O_3 destruction in the MBL can be explained by conventional HO_x/NO_x chemistry. Model calculations suggest that Br- and I-radical chemistry could account for a 'missing' O_3 sink of this magnitude (Dickerson et al., 1999; Stutz et al., 1999; McFiggans et al., 2000; von Glasow et al., 2002b). In addition to the pathway for O_3 destruction given by R AX2-39 to R AX2-41, in areas with high concentrations of halogen radicals the following generic loss pathways for O_3 can occur in the Arctic at the onset of spring and also over salt flats near the Dead Sea (Hebestreit et al., 1999) and the Great Salt Lake (Stutz et al., 2002) analogous to their occurrence in the lower stratosphere (Yung et al., 1980).

$$\bullet X + O_3 \rightarrow XO\bullet + O_2 \quad (X = Br, Cl, I) \qquad (AX2\text{-}45)$$

$$\bullet Y + O_3 \rightarrow YO\bullet + O_2 \quad (Y = Br, Cl, I) \qquad (AX2\text{-}46)$$

$$\underline{XO\bullet + YO\bullet \rightarrow \bullet X + \bullet Y + O_2} \qquad (AX2\text{-}47)$$

$$\text{Net:} \quad 2O_3 \rightarrow 3O_2 \qquad (AX2\text{-}48)$$

Note that the self reaction of ClO radicals is likely to be negligible in the troposphere. There are three major reaction pathways involved in reaction AX2-47. Short-lived radical species are produced. These radicals rapidly react to yield monoatomic halogen radicals. In contrast to the situation in marine air, where DOAS measurements indicate BrO concentrations of 1 to 3 ppt, Stutz et al. (2002) found peak BrO concentrations of about 6 ppt and peak ClO concentrations of about 15 ppt. They also derived a correlation coefficient of -0.92 between BrO and O_3 but much smaller values of r between ClO and O_3. Stutz et al. attributed the source of the reactive halogens to concentrated high molality solutions or crystalline salt around salt lakes, conditions that do not otherwise occur in more dilute or ocean salt water. They also suggest that halogens may be released from saline soils. The inferred atmospheric concentrations of Cl are about

10^5 / cm^3, or about a factor of 100 higher than found in the marine boundary layer by Rudolph et al. (1997) indicating that, under these conditions, the Cl initiated oxidation of hydrocarbons could be substantial.

Most of the well-established multiphase reactions tend to reduce the rate of O_3 formation in the polluted troposphere. Direct reactions of O_3 and atmospheric particles appears to be too slow to reduce smog significantly. Removal of HO_2 onto hydrated particles will decrease the production of O_3 by the reaction of HO_2 with NO. The uptake of NO_2 and HNO_3 will also result in the production of less O_3. Conditions leading to high concentrations of Br, Cl, and I radicals can lead to O_3 loss. The oxidation of hydrocarbons (especially alkanes) by Cl radicals, in contrast, may lead to the rapid formation of peroxy radicals and faster smog production in coastal environments where conditions are favorable for the release of gaseous Cl from the marine aerosol. There is still considerable uncertainty regarding the role of multiphase processes in tropospheric photochemistry and so results should be viewed with caution and an appreciation of their potential limitations.

AX2.2.10.4 Reactions on the Surfaces of Crustal Particles

Field studies have shown that O_3 levels are reduced in plumes containing high particle concentrations (e.g., DeReus et al.; 2000; Berkowitz et al., 2001; Gaffney et al., 2002). Laboratory studies of the uptake of O_3 on un-treated mineral surfaces (Hanisch and Crowley, 2002; Michel et al., 2002,2003) have shown that O_3 is lost by reaction on these surfaces and this loss is catalytic. Values of γ of $1.2 \pm 0.4 \times 10^{-4}$ were found for reactive uptake on α-Al2O_3 and $5 \pm 1 \times 10^{-5}$ for reactive uptake on SiO2 surfaces. Usher et al. (2003) found mixed behavior for O_3 uptake on coated surfaces with respect to untreated surfaces. They found that γ drops from $1.2 \pm 0.4 \times 10^{-4}$ to $3.4 \pm 0.6 \times 10^{-5}$ when α-Al2O_3 surfaces are coated with NO_3 derived from HNO_3, whereas they found that γ increases to $1.6 \pm 0.2 \times 10^{-4}$ after these surfaces have been pre-treated with SO_2. Usher et al. also pre-treated surfaces of SiO_2 with either a C8-alkene or a C8-alkane terminated organotrichlorosilane. They found that γ increased to $7 \pm 2 \times 10^{-5}$ in the case of treatment with the alkene, but that it decreased to $3 \pm 1 \times 10^{-5}$ for treatment with the alkane. Usher et al. (2003) suggested, on the basis of these results that mineral dust particles coated with nitrates or alkanes will affect O_3 less than dust particles that have accumulated coatings of sulfite or alkenes. These studies indicate the importance of aging of airborne particles on their ability to take up atmospheric gases. Reactions such as these may also be responsible for O_3 depletions observed in dust clouds transiting the Pacific Ocean.

Underwood et al. (2001) studied the uptake of NO_2 and HNO_3 on the surfaces of dry mineral oxides (containing Al, Ca, Fe, Mg, Si and Ti) and naturally occurring mineral dust. A wide range of values of $\gamma(NO_2)$ were found, ranging from $< 4 \times 10^{-10}$ for SiO_2 to 2×10^{-5} for CaO, with most other values $\sim 10^{-6}$. Values of γ for Chinese loess and Saharan dust were also of the order of 10^{-6}. They found that as the reaction of NO_2 proceeds on the surfaces that reduction to NO occurs. They recommended a value of γ for HNO_3 of about 1×10^{-3}. Not surprisingly, the values of γ increased from those given above if the surfaces were wetted. Underwood et al. (2001) also suggested that the uptake of NO_2 was likely to be only of marginal importance but that uptake of HNO_3 could be of significance for photochemical oxidant cycles.

Li et al. (2001) examined the uptake of acetaldehyde, acetone and propionaldehyde on the same mineral oxide surfaces listed above. They found that these compounds weakly and reversibly adsorb on SiO_2 surfaces. However, on the other oxide surfaces, they irreversibly adsorb and can form larger compounds. They found values of γ ranging from 10^{-6} to 10^{-4}. These reactions may reduce O_3 production efficiency in areas of high mineral dust concentration such as the American Southwest or in eastern Asia as noted earlier.

AX2.2.10.5 Reactions on the Surfaces of Aqueous H_2SO_4 solutions

The most recent evaluation of Photochemical and Chemical Data by the Jet Propulsion Laboratory (Jet Propulsion Laboratory, 2003) includes recommendations for uptake coefficients of various substances on a variety of surfaces including aqueous H_2SO_4 solutions. Although much of the data evaluated have been obtained mainly for stratospheric applications, there are studies in which the range of environmental parameters is compatible with those found in the troposphere. In particular, the uptake of N_2O_5 on the surface of aqueous H_2SO_4 solutions has been examined over a wide range of values. Typical values of γ are of the order of 0.1 (e.g., Jet Propulsion Laboratory, 2003). Values of γ for NO_2 are much lower (5×10^{-7} to within a factor of three) and thus the uptake of NO_2 on the surface of aqueous H_2SO_4 solutions is unlikely to be of importance for oxidant cycles. The available data indicate that uptake of OH and HO_2 radicals could be significant under ambient conditions with values of γ of the order of 0.1 or higher for OH, and perhaps similar values for HO_2.

AX2.3 PHYSICAL PROCESSES INFLUENCING THE ABUNDANCE OF OZONE

The abundance and distribution of O_3 in the atmosphere is determined by complex interactions between meteorology and chemistry. This section will address these interactions, based mainly on the results of field observations. The importance of a number of transport mechanisms, whose understanding has undergone significant advances since the last AQCD for O_3, will be discussed in this section.

Major episodes of high O_3 concentrations in the eastern United States and in Europe are associated with slow moving, high pressure systems. High pressure systems during the warmer seasons are associated with the sinking of air, resulting in warm, generally cloudless conditions, with light winds. The sinking of air results in the development of stable conditions near the surface which inhibit or reduce the vertical mixing of O_3 precursors. The combination of inhibited vertical mixing and light winds minimizes the dispersal of pollutants emitted in urban areas, allowing their concentrations to build up. Photochemical activity involving these precursors is enhanced because of higher temperatures and the availability of sunlight. In the eastern United States, high O_3 concentrations during a large scale episode can extend over a hundred thousand square kilometers for several days. These conditions have been described in greater detail in AQCD 96. The transport of pollutants downwind of major urban centers is characterized by the development of urban plumes. However, the presence of mountain barriers can limit mixing as in Los Angeles and Mexico City and will result in even longer periods and a higher frequency of days with high O_3 concentrations. Ozone concentrations in southern urban areas, such as Houston, TX and Atlanta, GA tend to follow this pattern and they tend to decrease with increasing wind speed. In northern cities, like Chicago, IL; New York, NY; and Boston, MA the average O_3 concentrations over the metropolitan areas increase with wind speed indicating that transport of O_3 and its precursors from upwind areas is important (Husar and Renard, 1998; Schichtel and Husar, 2001).

Aircraft observations indicate that there can be substantial differences in mixing ratios of key species between the surface and the atmosphere above (Fehsenfeld et al., 1996a; Berkowitz and Shaw, 1997). Convective processes and small scale turbulence transport O_3 and other pollutants both upward and downward throughout the planetary boundary layer and the free troposphere. Ozone and its precursors were found to be transported vertically by convection into the upper part of the mixed layer on one day, then transported overnight as a layer of elevated mixing ratios and then entrained into a growing convective boundary layer downwind and brought back down to the surface. High concentrations of O_3 showing large diurnal variations at the surface in southern New England were associated with the presence of such layers (Berkowitz et al., 1998). Zhang et al. (1997) estimated that as much as 60% to 70% of O_3 observed at the surface during one case study in eastern Tennessee could have come from the upper boundary layer. Because of wind shear, winds several hundred meters above the ground can bring pollutants from the west, even though surface winds are from the southwest during periods of high O_3 in the eastern United States (Blumenthal et al., 1997). Low level nocturnal jets can also transport pollutants hundreds of kilometers. Turbulence associated with them can bring these pollutants to the surface and in many locations result in secondary O_3 maxima in the early morning (Corsmeier et al., 1997). Based on analysis of the output of model studies conducted by Kasibhatla and Chameides (2000), Hanna et al. (2001) concluded that O_3 can be transported over thousands of kilometers in the upper boundary layer of the eastern half of the United States during specific O_3 episodes.

Stratospheric-tropospheric exchange (STE) will be discussed in Section AX2.3.1. The vertical redistribution of O_3 and other pollutants by deep, or penetrating convection is discussed in Section AX2.3.2. The potential importance of transport of O_3 and precursors by low level jets is the topic of Section AX2.3.3. Issues related to the transport of O_3 from North America are presented in Section AX2.3.4. Relations of O_3 to solar ultraviolet radiation and temperature will then be discussed in Section AX2.3.5.

AX2.3.1 Stratospheric-Tropospheric Ozone Exchange (STE)

In the stratosphere, O_3 formation is initiated by the photodissociation of molecular oxygen (O_2) by solar ultraviolet radiation at wavelengths less than 242 nm. Almost all of this radiation is absorbed in the stratosphere (except for regions near the tropical tropopause), preventing this mechanism from occurring in the troposphere. Some of the O_3 in the stratosphere is transported downward into the troposphere. The potential importance of this source of tropospheric O_3 has been recognized since the early work of Regener (1941), as cited by Junge (1963). Stratospheric-tropospheric exchange (STE) of O_3 and stratospheric radionuclides produced by the nuclear weapons tests of the 1960s is at a maximum during late winter and early spring (e.g., Ludwig et al., 1977 and references therein). Since AQCD 96 on O_3 substantial new information from numerical models, field experiments and satellite-based observations has become available. The following sections outline the basic atmospheric dynamics and thermodynamics of stratosphere/troposphere exchange and review these new developments.

There are several important mechanisms for injecting stratospheric O_3 into the troposphere, they include tropopause folds (Reed, 1955; Danielsen, 1968), cut-off lows (Price and Vaughan, 1993), clear air turbulence, mesoscale convective complexes and thunderstorms, breaking gravity waves (Poulida et al., 1996; Langford and Reid, 1998; Stohl et al., 2003) and streamers. Streamers are dry, stratospheric intrusions visible in satellite water vapor imagery that are sheared into long filamentary structures that often roll into vortices and exhibit visible evidence of the irreversible mixing of moist subtropical tropospheric and dry polar stratospheric air (Appenzeller et al., 1996; Wimmers et al., 2003). They are often present at a scale that eludes capture in large scale dynamical models of the atmosphere that cannot resolve features less than 1 degree (~100km). Empirical evidence for stratospheric intrusions comes from observations of indicators of stratospheric air in the troposphere. These indicators include high potential vorticity, low water vapor mixing ratios, high potential temperature, enhancements in the ratio of ^{7}Be to ^{10}Be in tropospheric aerosols, as well as enhancements in O_3 mixing ratios and total column amounts. These quantities can be observed with in situ aircraft and balloons, as well as remotely sensed from aircraft and ground-based lidars and both geostationary and polar (low earth orbiting) space platforms.

The exchange of O_3 between the stratosphere and the troposphere in middle latitudes occurs to a major extent by tropopause folding events (Reiter, 1963; Reiter and Mahlman, 1965; Danielsen, 1968; Reiter, 1975; Danielsen and Mohnen, 1977; Danielsen, 1980). The term, tropopause folding is used to describe a process in which the tropopause intrudes deeply into the troposphere along a sloping frontal zone bringing air from the lower stratosphere with it. Tropopause folds occur with the formation of upper level fronts associated with transverse circulations that develop around the core of the polar jet stream. South of the jet stream core, the tropopause is higher than to the north of it. The tropopause can be imagined as wrapping around the jet stream core and folding beneath it and extending into the troposphere (cf. Figure AX2-7a). Although drawn as a heavy solid line, the tropopause should not be imagined as a material surface, through which there is no exchange. Significant intrusions of stratospheric air

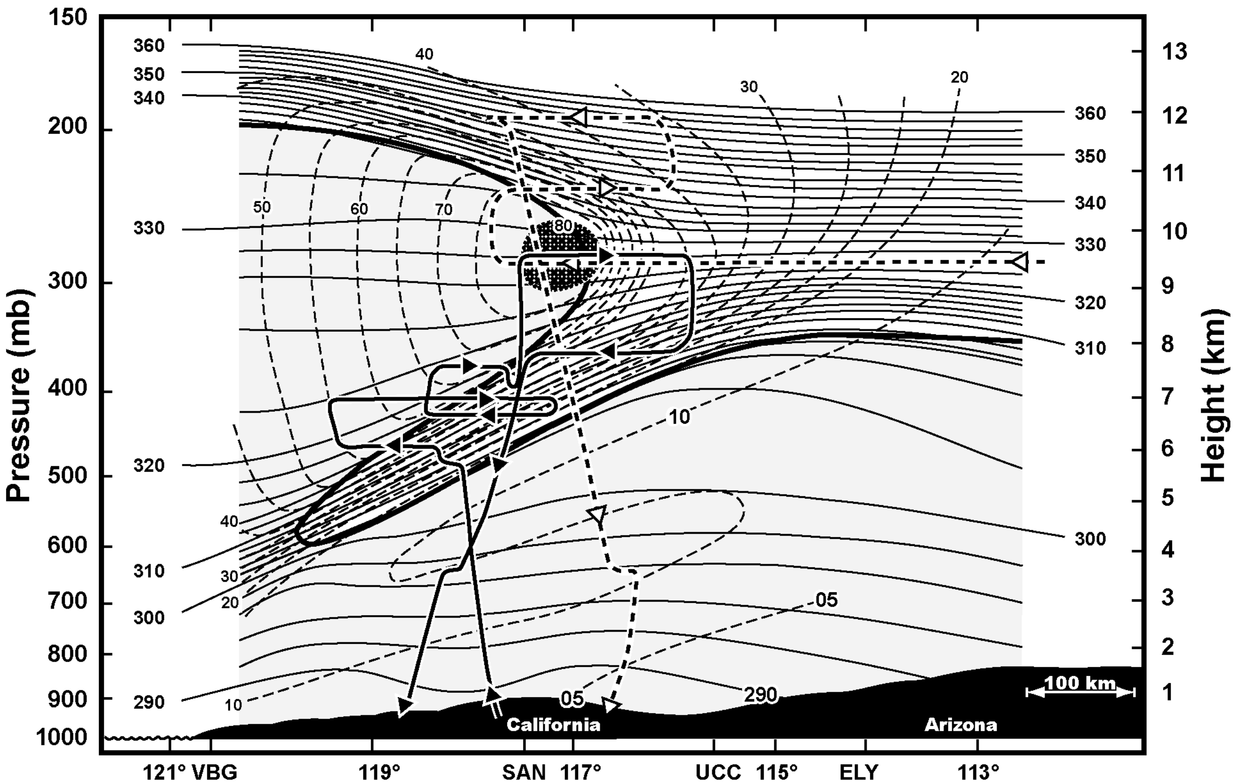

Figure AX2-7a. Cross section through a tropopause folding event on March 13, 1978 at 0000 GMT. Potential temperatures (K) are represented by thin solid lines. Wind speeds (m s^{-1}) are given by thin dashed lines. The hatched area near the center of the figure indicates the location of the jet stream core. The tropopause defined by a potential vorticity of 100 × 10^{-7} K mb^{-1} s^{-1} is shown as the heavy solid line. The two Sabreliner flight tracks through this cross section are shown as a heavy solid line with filled arrows and heavy dashed line with open arrows. Longitude is shown along the x-axis . Upper air soundings were taken at Vandenburg AFB, CA (VBG); San Diego, CA (SAN); Winnemucca, NV (UCC); and Ely, NV (ELY).

Source: Adapted from Shapiro (1980).

occur in "ribbons" ~200 to 1000 km in length, 100 to 300 km wide and about 1 to 4 km thick (Hoskins, 1972; Wimmers et al., 2003). These events occur throughout the year and their location follows the seasonal displacement of the polar jet stream.

The seasonal cycle of O_3 exchange from the stratosphere into the troposphere is not caused by a peak in the seasonal cycle of upper tropospheric cyclone activity. Instead, it is related to the large scale pattern of tracer transport in the stratosphere. During winter in the Northern Hemisphere, there is a maximum in the poleward, downward transport of mass, which moves O_3 from the tropical upper stratosphere to the lower stratosphere of the polar and mid-latitudes This global scale pattern is controlled by the upward propagation of large-scale and small-scale waves generated in the troposphere. As the energy from these disturbances dissipates, it drives this stratosphere circulation. As a result of this process, there is a springtime maximum in the total column abundance of O_3 over the poles. The concentrations of O_3 (and other trace substances) build up in the lower stratosphere until their downward fluxes into the lower stratosphere are matched by increased fluxes into the troposphere. Thus, there would be a springtime maximum in the flux of O_3 into the troposphere even if the flux of stratospheric air through the tropopause by tropopause folding remained constant throughout the year (Holton et al., 1995). Indeed, cyclonic activity in the upper troposphere is active throughout the entire year in transporting air from the lower stratosphere into the troposphere (Mahlman, 1997; and references therein). Oltmans et al. (1996) and Moody et al. (1996) provide evidence that stratospheric intrusions contribute to the O_3 abundance in the upper troposphere over the North Atlantic even during the summer.

There are a number of techniques that have been used to quantify the amount of O_3 in the free troposphere or even the amount of O_3 reaching the surface that can be attributed to downward transport from the stratosphere. Earlier work, cited in AQCD 96 relied mainly on the use of ^7Be as a tracer of stratospheric air. However, its use is ambiguous because it is also formed in the upper troposphere. Complications also arise because its production rate is also sensitive to solar activity (Lean, 2000). The ratio of ^7Be to ^{10}Be provides a much more sensitive tracer of stratospheric air than the use of ^7Be alone (Jordan et al., 2003 and references therein). More recent work than cited in AQCD 96 has focused on the use of potential vorticity (PV) as a tracer of stratospheric air. Potential vorticity is a *dynamical tracer* used in meteorology. Generally, PV is calculated from wind and temperature observations and represents the rotational tendency of a column of air weighted by the static stability, which is just the distance between isentropic surfaces. This quantity is a maximum in the lower stratosphere where static stability is great and along the jet stream where wind shear imparts significant rotation to air parcels. As air moves from the stratosphere to the troposphere, PV is conserved, and therefore it *traces* the motion of O_3. The static stability is lower in the troposphere, so to preserve PV, fluid rotation will increase. This is why STE is associated with cyclogenesis, or the formation of storms along the polar jet stream. Dynamical models clearly capture this correspondence between the location of storm tracks and preferred regions for STE. However, because PV is destroyed at a faster rate with increasing depth, it is not useful as a tracer of stratospheric air reaching the surface. Appenzeller et al. (1996) found that maps of PV coupled with satellite images of humidity can provide indications of the intrusion of stratospheric air into the troposphere, however, they had no measurements of O_3. Even if measurements of O_3 were available, the extrapolation of any relations to other events would still be problematic as Olsen et al. (2002) have noted that there are seasonal and geographic variations in the relation between O_3 and PV. Recent flights of the NCAR C130 during the TOPSE campaign measured in situ O_3, and curtains of O_3 above and below the aircraft observed with a lidar and clearly showed a correspondence between high PV and stratospheric levels of O_3 and satellite depictions of dry air indicating the presence of tropopause folding (Wimmers and Moody, 2004a,b).

Detailed cross sections through a tropopause folding event showing atmospheric structure, O_3 mixing ratios and condensation nuclei (CN) counts are given in Figures AX2-7a, AX2-7b, and AX2-7c (Shapiro, 1980). Flight tracks of an NCAR Sabreliner obtaining data through the tropopause fold are also shown. The core of the jet stream is indicated by the hatched area near the center of Figure AX2-7a. As can be seen from Figure AX2-7 a and b, there is a strong relation between the folding of the tropopause, indicated by the heavy solid line and O_3. CN counts during the portions of the flights in the lower troposphere were tropospheric were typically of the order of several $\times 10^{3}$ cm^{-3} and 100 or less in the stratospheric portion. However, it is clear that CN counts in the fold are much higher than in the stratosphere proper, suggesting that there was active mixing between tropospheric and stratospheric air in the fold. Likewise, it can also be seen form Figure AX2-7b that O_3 is being mixed outside the fold into the middle and upper troposphere. The two data sets shown in Figures AX2-7b and 7c indicate that small scale turbulent processes were occurring to mediate this exchange and that the folds are mixing regions whose chemical characteristics lie between those of the stratosphere and the troposphere (Shapiro, 1980). Chemical interactions between stratospheric and tropospheric constituents are also possible within tropopause folds. These considerations also imply that in the absence of turbulent mixing, tropopause folding can be a reversible process.

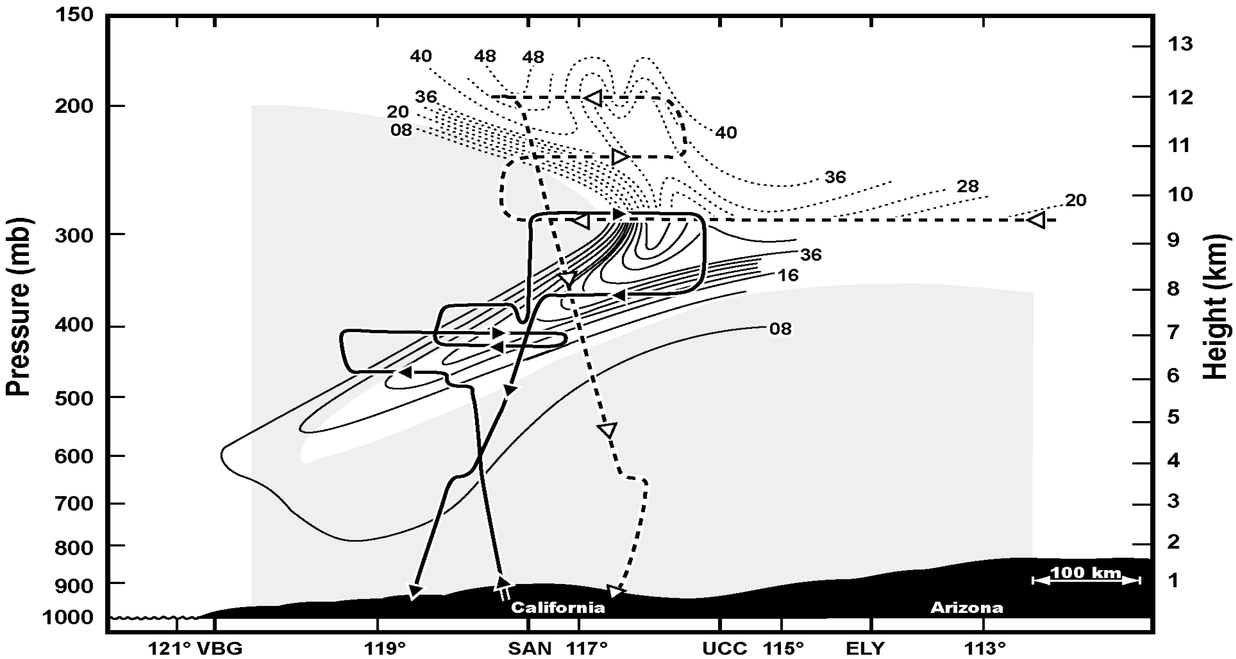

Figure AX2-7b. Ozone mixing ratios pphm (parts per hundred million) corresponding to Figure AX2-7A. The two Sabreliner flight tracks through this cross section are shown as a heavy solid line with filled arrows and a heavy dashed line with open arrows. Longitude is shown along the x-axis. Upper air soundings were taken at Vandenburg AFB, CA (VBG); San Diego, CA (SAN); Winnemucca, NV (UCC); and Ely, NV (ELY).

Source: Adapted from Shapiro (1980).

Several recent papers have attempted to demonstrate that the atmosphere is a fluid composed of relatively distinct airstreams with characteristic three-dimensional motions and corresponding trace gas signatures. Based on aircraft observations, satellite imagery, and back trajectories, it has been shown that dry airstreams, or dry intrusions (DA or DI) always advect stratospheric O_3 into the middle and upper troposphere (Cooper et al, 2001; Cooper et al., 2002a), however the seasonal cycle of O_3 in the lowermost stratosphere allows greater quantities of O_3 to enter the troposphere during spring (Cooper et al., 2002b). Other work has focused on the signatures of PV to show specific instances of STE (Olsen and Stanford, 2001). This correlation between TOMS gradients and PV was also used to derive the annual mass flux of O_3 from STE and generated an estimate somewhat higher (500 Tg/yr over the Northern

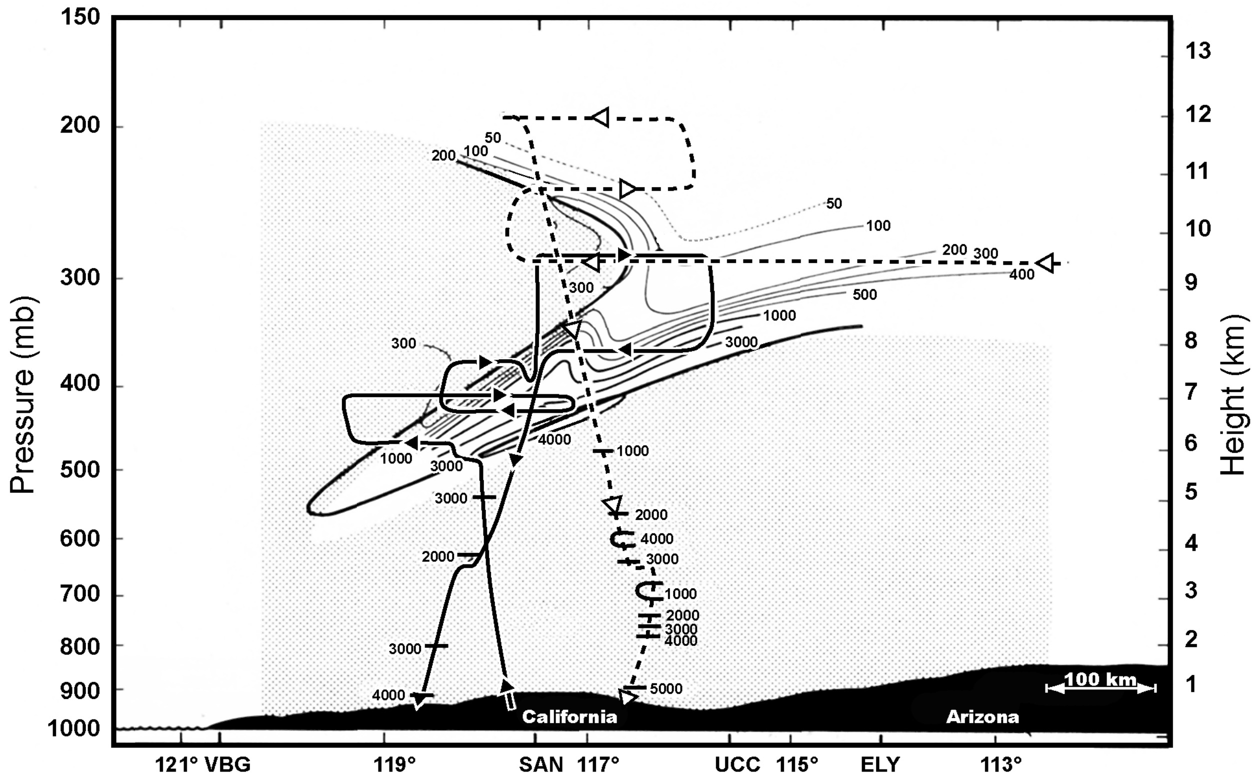

Figure AX2-7c. Condensation nuclei concentrations (particles cm^{-3}) corresponding to Figure AX2-7a. The two flight Sabreliner flight tracks through this cross section are shown as a heavy solid line with filled arrows and a heavy dashed line with open arrows. Longitude is shown along the x-axis. Upper air soundings were taken at Vandenburg AFB, CA (VBG); San Diego, CA (SAN); Winnemucca, NV (UCC); and Ely, NV (ELY).

Source: Adapted from Shapiro (1980).

Hemisphere) than the estimates of most general circulation models. The IPCC has reported a large range of model estimates of STE, expressed as the net global flux of O_3 in Tg/yr, from a low of 390 to a high of 1440 (reproduced as Table AX2-3C-1). A few other estimates have been made based on chemical observations in the lower stratosphere, or combined chemistry and dynamics (450 Tg/yr Murphy and Fahey, 1994; 510 Tg/yr extratropics only, Gettleman et al., 1997; and 500 Tg/yr midlatitude NH only (30 to 60N) (Olsen et al., 2002). These values illustrate the large degree of uncertainty that remains in quantifying this important source of O_3.

Based on the concept of tracing airstream motion, a number of Lagrangian model studies have resulted in climatologies that have addressed the spatial and temporal variability in stratosphere to troposphere transport (Stohl, 2001; Wernli and Borqui, 2002; Seo and Bowman, 2002; James et al., 2003a,b; Sprenger and Wernli, 2003; Sprenger et al., 2003). Both Stohl (2001) and Sprenger et al. (2003) produced one year climatologies of tropopause folds based on a 1° by 1° gridded meteorological data set. They each found the probability of deep folds (penetrating to the 800 hPa level) was a maximum during winter (December through February). The highest frequency of folding extended from Labrador down the east coast of North America. However, these deep folds occurred less than 1% of the six hour intervals for which meteorological data is assimilated for grid points in the United States. They observed a higher frequency of more shallow folds (penetrating to the upper troposphere) and medium folds (penetrating to levels between 500 and 600 hPa) of about 10% and 1 to 2% respectively. These events occur preferentially across the subtropics and the southern United States. At higher latitudes other mechanisms such as the erosion of cut-off lows and the breakup of stratospheric streamers are likely to play an important role in STE. Stohl (2001) also described the region of strong stirring in the upper extratropical troposphere related to the mid-latitude storm tracks. Stohl (2001) demonstrated that airstreams with strong vertical motion are all highly incoherent, they stir their air parcels into a new environment, producing filamentary tracer structures and paving the way for subsequent mixing. A 15-year climatology by Sprenger and Wernli (2003) shows the consistent pattern of STE occurring over the primary storm tracks in the Pacific and Atlantic along the Asian and North American coasts. This climatology, and the one of James et al. (2003a,b) both found that recent stratospheric air associated with deep intrusions are relatively infrequent occurrences in these models. Thus, stratospheric intrusions are most likely to directly affect the middle and upper troposhere and not the planetary boundary layer. However, this O_3 can still exchange with the planetary boundary layer through convection as described later in this sub-section and in Section AX2.3.2, AX2.3.3 and AX2.3.4.

Interannual variations in STE are related to anomalies in large-scale circulation such as the North Atlantic Oscillation which causes changes in storm track positions and intensities, and the El Niño-Southern Oscillation, which results in anomalous strong convection over the eastern Pacific (James et al., 2003a,b). It should also be remembered that the downward flux of O_3 into the troposphere is related to the depletion of O_3 within the wintertime stratospheric polar vortices. The magnitude of this depletion and the transport of ozone depleted air to mid-latitudes in the stratosphere (Mahlman et al., 1994; Hadjinicolaou and Pyle, 2004) shows significant interannual variability which may also be reflected in the downward flux of O_3 into the troposphere. All of these studies, from the analysis of individual events to multiyear climatologies are based on the consideration of the three-dimensional motion of discrete airstreams in the atmosphere. However, there is a significant body of work that reports that airstreams are not entirely independent of each other (Cooper et al., 2004a,b). Midlatitude cyclones typically form in a sequential manner, some trailing in close proximity along a quasi-stationary frontal boundary, with each system influenced by remnants of other systems. For example, a rising stream of air ahead of a cold front (also known as a warm conveyor belt or WCB) on the back (western) side of a surface anticyclone may entrain air that has subsided anticyclonically into the surface high pressure system from the upper troposphere and the lower stratosphere (also known as a Dry Airstream or DA) that intruded into the mid-troposphere in a cyclone that is further downstream. Convective mixing of the boundary layer in the WCB will distribute this enhanced O_3 throughout the lower troposphere and down to the surface (Davies and Shuepbach, 1994; Cooper and Moody, 2000). The net effect is that the DA of one cyclone may feed into the WCB of the system immediately upwind. Similarly, the lofting of warm moist air in the WCB may inject surface emissions into the upper troposphere adjacent to the western side of the subsiding Dry Airstream of the storm system immediately downwind, with subsequent interleaving of these two airstreams (Prados et al., 1999; Parrish et al., 2000; Cooper et al., 2004a,b) as illustrated schematically in Figure AX2-8. The ultimate mixing of these airstreams, which inevitably occurs at a scale that is not resolved by current models confounds our ability to attribute trace gases to their sources.

These studies suggest that both downward transport from the stratosphere and upward transport from the atmospheric boundary layer act in concert with their relative roles determined by the balance between the amount of O_3 in the lower stratosphere and the availability of free radicals to initiate the photochemical processes forming O_3 in the boundary layer. Dickerson et al. (1995) pointed out that springtime maxima in O_3 observed in Bermuda correlate well with maxima in carbon monoxide. Carbon monoxide, O_3 and its photochemical precursors may have been transported into the upper troposphere from the polluted continental boundary layer by deep convection. The photochemical processes involve the buildup of precursors during the

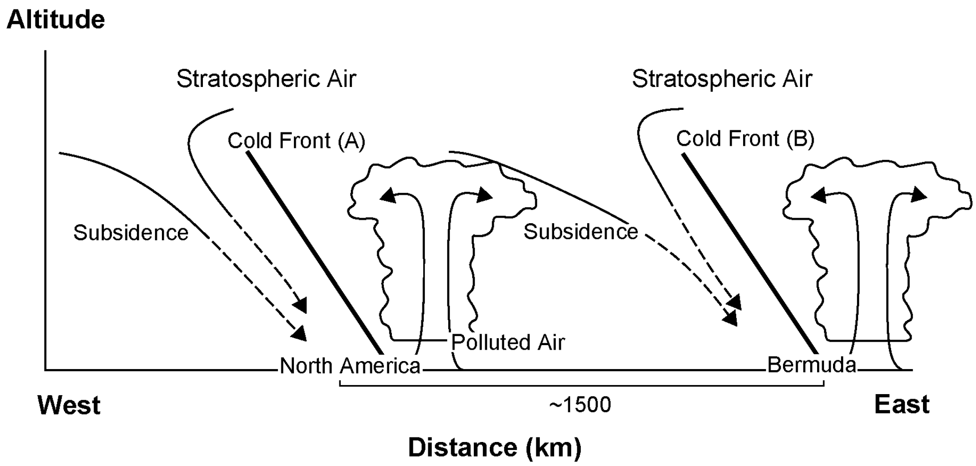

Figure AX2-8. Schematic diagram of a meteorological mechanism involved in high concentrations of ozone found in spring in the lower troposphere off the American east coast. Subsidence behind the first cold front meets convection ahead of a second cold front such that polluted air and ozone from the upper troposphere/lower stratosphere are transported in close proximity (or mixed) and advected over the north Atlantic Ocean. The vertical scale is about 10 km; the horizontal scale about 1500 km. (Note that not all cold fronts are associated with squall lines and that mixing occurs even in their absence.)

Source: Prados (2000).

winter at Northern mid- and high latitudes. Parrish et al. (1999) have noted that reactions occurring during the colder months may tend to titrate O_3. However, as NO_x and its reservoirs are transported sourthward they can initiate O_3 formation through reactions described in Section AX2.2 (see also Stroud et al., 2003).

AX2.3.2 Deep Convection in the Troposphere

Much of the upward motion in the troposphere is driven by convergence in the boundary layer and deep convection. Deep convection, as in developing thunderstorms can transport pollutants rapidly to the middle and upper troposphere (Dickerson et al., 1987). The outflow from these systems results in the formation of layers with distinctive chemical properties in the middle troposphere. In addition, layers are formed as the result of stratospheric intrusions.

Layers ranging in thickness typically from 0.3 to about 2 km in the middle troposphere (mean altitudes between 5 and 7 km) are ubiquitous and occupy up to 20% of the troposphere to 12 km (Newell et al., 1999). The origin of these layers can be judged by analysis of their chemical composition (typically by comparing ratios of H_2O, O_3 and CO to each other) or dynamical properties (such as potential vorticity). Thus, pollutants that have been transported into the middle and upper troposphere at one location can then be transported back down into the boundary layer somewhere else.

Crutzen and Gidel (1983), Gidel (1983), and Chatfield and Crutzen (1984) hypothesized that convective clouds played an important role in rapid atmospheric vertical transport of trace species and first tested simple parameterizations of convective transport in atmospheric chemical models. At nearly the same time, evidence was shown of venting of the boundary layer by shallow fair weather cumulus clouds (e.g., Greenhut et al., 1984; Greenhut, 1986). Field experiments were conducted in 1985, which resulted in verification of the hypothesis that deep convective clouds are instrumental in atmospheric transport of trace constituents (Dickerson et al., 1987; Luke et al., 1997). Once pollutants are lofted to the middle and upper troposphere, they typically have a much longer chemical lifetime and with the generally stronger winds at these altitudes they can be transported large distances from their source regions. Photochemical reactions occur during this long-range transport. Pickering et al. (1990) demonstrated that venting of boundary layer pollutants by convective clouds (both shallow and deep) causes enhanced O_3 production in the free troposphere. Therefore, convection aids in the transformation of local pollution into a contribution to global atmospheric pollution. Downdrafts within thunderstorms tend to bring air with less pollution from the middle troposphere into the boundary layer.

Field studies have established that downward transport of larger O_3 and NO_x mixing ratios from the free troposphere to the boundary layer is an important process over the remote oceans (e.g., Piotrowicz et al., 1991), as well as the upward transport of very low O_3 mixing ratios from the boundary layer to the upper troposphere (Kley et al., 1996). Global modeling by Lelieveld and Crutzen (1994) suggests that the downward mixing of O_3 into the boundary layer (where it is destroyed) is the dominant global effect of deep convection. Some indications of downward transport of O_3 from higher altitudes (possibly from the stratosphere) in the anvils of thunderstorms have been observed (Dickerson et al., 1987; Poulida et al., 1996; Suhre et al., 1997). Ozone is most effective as a greenhouse gas in the vicinity of the tropopause. Therefore, changes in the vertical profile of O_3 in the upper troposphere caused by deep convection have important radiative forcing implications for climate.

Other effects of deep convection include perturbations to photolysis rates, which include enhancement of these rates in the upper portion of the thunderstorm anvil. In addition, thunderstorms are effective in the production of NO by lightning and in wet scavenging of soluble species.

AX2.3.2.1 Observations of the Effects of Convective Transport

Some fraction of shallow fair weather cumulus clouds actively vent boundary layer pollutants to the free troposphere (Stull, 1985). The first airborne observations of this phenomenon were conducted by Greenhut et al. (1984) over a heavily urbanized area, measuring the in-cloud flux of O_3 in a relatively large cumulus cloud. An extension of this work was reported by Greenhut (1986) in which data from over 100 aircraft penetrations of isolated nonprecipitating cumulus clouds over rural and suburban areas were obtained. Ching and Alkezweeny (1986) reported tracer (SF_6) studies associated with nonprecipitating cumulus (fair weather cumulus and cumulus congestus). Their experiments showed that the active cumulus clouds transported mixed layer air upward into the overlying free troposphere and suggested that active cumuli can also induce rapid downward transport from the free troposphere into the mixed layer. A UV-DIAL (Ultraviolet Differential Absorption Lidar) provided space-height cross sections of aerosols and O_3 over North Carolina in a study of cumulus venting reported by Ching et al. (1988). Data collected on evening flights showed regions of cloud debris containing aerosol and O_3 in the lower free troposphere in excess of background, suggesting that significant vertical exchange had taken place during afternoon cumulus cloud activity. Efforts have also been made to estimate the vertical transport by ensembles of nonprecipitating cumulus clouds in regional chemical transport models (e.g., Vukovich and Ching, 1990).

The first unequivocal observations of deep convective transport of boundary layer pollutants to the upper troposphere were documented by Dickerson et al. (1987). Instrumentation aboard three research aircraft measured CO, O_3, NO, NO_x, NO_y, and hydrocarbons in the vicinity of an active mesoscale convective system near the Oklahoma/Arkansas border during the 1985 PRE-STORM experiment. Anvil penetrations about two hours after maturity found greatly enhanced mixing ratios of all of the aforementioned species compared with outside of the cloud. Among the species measured, CO is the best tracer of upward convective transport because it is produced primarily in the boundary layer and has an atmospheric lifetime much longer than the timescale of a thunderstorm. In the observed storm, CO measurements exceeded 160 ppbv as high as 11 km, compared with ~70 ppbv outside of the cloud (Figure AX2-9a). Cleaner middle tropospheric air appears to have descended in downdrafts forming a pool of lower mixing ratio CO beneath the cloud. Nonmethane hydrocarbons (NMHC) with moderate lifetimes can also serve as tracers of convective transport from the boundary layer. Ozone can also be an indicator of convective transport. In the polluted troposphere large O_3 values will indicate upward transport from the boundary layer, but in the clean atmosphere such values are indicative of downward transport from the uppermost troposphere or lowermost stratosphere. In this case measured O_3 in the upper rear portion of the anvil peaked at 98 ppbv, while boundary layer values were only ~65 ppbv (Figure AX2-9b). It is likely that some higher-O_3 stratospheric air mixed into the anvil.

The large amount of vertical trace gas transport noted by Dickerson et al. (1987) cannot, however, be extrapolated to all convective cells. Pickering et al. (1988) reported airborne measurements of trace gases taken in the vicinity of a line of towering cumulus and cumulonimbus clouds that also occurred during PRE-STORM. In this case trace gas mixing ratios in the tops of these clouds were near ambient levels. Meteorological analyses showed that these clouds were located above a cold front, which prevented entry of air from the boundary layer directly below or near the clouds. Instead, the air entering these clouds likely originated in the layer immediately above the boundary layer which was quite clean. Luke et al. (1992) summarized the air chemistry data from all 18 flights during PRE-STORM by categorizing each case according to synoptic flow patterns. Storms in the maritime tropical flow regime transported large amounts of CO, O_3, and NO_y into the upper troposphere with the midtroposphere remaining relatively clean. During frontal passages a combination of stratiform and convective clouds mixed pollutants more uniformly into the middle and upper levels; high mixing ratios of CO were found at all altitudes.

Prather and Jacob (1997) and Jaeglé et al. (1997) noted that in addition to the primary pollutants (e.g., NO_x, CO, VOCs), precursors of HO_x are also transported to the upper troposphere by deep convection. Precursors of most importance are water vapor, formaldehyde,

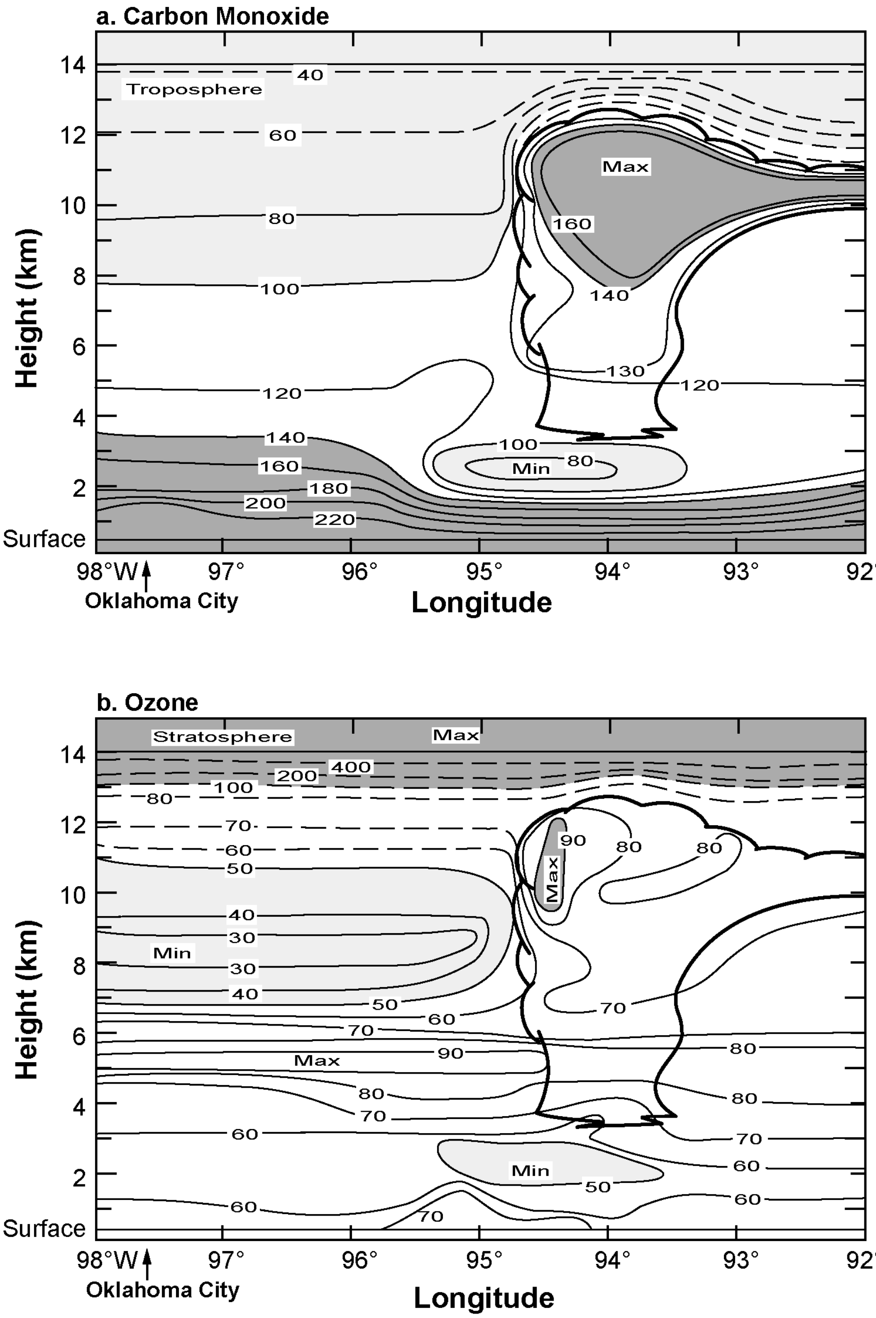

Figure AX2-9a,b. **(a) Contour plot of CO mixing ratios (ppbv) observed in and near the June 15, 1985, mesoscale convective complex in eastern Oklahoma. Heavy line shows the outline of the cumulonimbus cloud. Dark shading indicates high CO and light shading indicates low CO. Dashed contour lines are plotted according to climatology since no direct measurements were made in that area. (b) Same as (a) but for ozone (ppbv).**

Source: Dickerson et al. (1987).

hydrogen peroxide, methylhydroperoxide, and acetone. HO_x is critical for oxidizing NO to NO_2 in the O_3 production process.

Over remote marine areas the effects of deep convection on trace gas distributions differ from that over moderately polluted continental regions. Chemical measurements taken by the NASA ER-2 aircraft during the Stratosphere-Troposphere Exchange Project (STEP) off the northern coast of Australia show the influence of very deep convective events. Between 14.5 and 16.5 km on the February 2 to 3, 1987 flight, perturbations in the chemical profiles were noted that included pronounced maxima in CO, water vapor, and CCN and minima of NO_y, and O_3 (Pickering et al., 1993). Trajectory analysis showed that these air parcels likely were transported from convective cells 800 to 900 km upstream. Very low boundary layer mixing ratios of NO_y and O_3 in this remote region were apparently transported upward in the convection. A similar result was noted in CEPEX (Central Equatorial Pacific Experiment; Kley et al., 1996) where a series of ozonesonde ascents showed very low upper tropospheric O_3 following deep convection. It is likely that similar transport of low-O_3 tropical marine boundary layer air to the upper troposphere occurs in thunderstorms along the east coast of Florida. Convection over the Pacific will likely transport halogens to the upper troposphere where they may aid in the destruction of O_3. This low-O_3 convective outflow will likely descend in the subsidence region of the eastern Pacific, leading to some of the cleanest air that arrives at the west coast of the United States.

AX2.3.2.2 Modeling the Effects of Convection

The effects of deep convection may be simulated using cloud-resolving models, or in regional or global models in which the convection is parameterized. The Goddard Cumulus Ensemble (GCE) model (Tao and Simpson, 1993) has been used by Pickering et al. (1991; 1992a,b; 1993; 1996), Scala et al. (1990) and Stenchikov et al. (1996) in the analysis of convective transport of trace gases. The cloud model is nonhydrostatic and contains detailed representation of cloud microphysical processes. Two and three dimensional versions of the model have been applied in transport analyses. The initial conditions for the model are usually from a sounding of temperature, water vapor and winds representative of the region of storm development. Model-generated wind fields can be used to perform air parcel trajectory analyses and tracer advection calculations. Once transport calculations are performed for O_3 precursors, a

1-D photochemical model was employed to estimate O_3 production rates in the outflow air from the convection. These rates were then compared with those prior to convection to determine an enhancement factor due to convection.

Such methods were used by Pickering et al. (1992b) to examine transport of urban plumes by deep convection. Transport of the Oklahoma City plume by the 10 – 11 June 1985 PRE-STORM squall line was simulated with the 2-D GCE model. In this event forward trajectories from the boundary layer at the leading edge of the storm showed that almost 75% of the low level inflow was transported to altitudes exceeding 8 km. Over 35% of the air parcels reached altitudes over 12 km. Tracer transport calculations were performed for CO, NO_x, O_3, and hydrocarbons. The 3-D version of the GCE model has also been run for the 10 – 11 June 1985 PRE-STORM case. Free tropospheric O_3 production enhancement of a factor of 2.5 for Oklahoma rural air and ~4 for the Oklahoma City case were calculated.

Stenchikov et al. (1996) used the 2-D GCE model to simulate the North Dakota storm observed by Poulida et al. (1996). This storm showed the unusual feature of an anvil formed well within the stratosphere. The increase of CO and water vapor above the altitude of the preconvective tropopause was computed in the model. The total mass of CO across the model domain above this level increased by almost a factor of two during the convective event. VOCs injected into the lower stratosphere could enhance O_3 production there. Downward transport of O_3 from the stratosphere was noted in the simulation in the rear anvil.

Regional estimates of deep convective transport have been made through use of a traveling 1-D model, regional transport models driven by parameterized convective mass fluxes from mesoscale meteorological models, and a statistical-dynamical approach. Pickering et al. (1992c) developed a technique which uses a combination of deep convective cloud cover statistics from the International Satellite Cloud Climatology Project (ISCCP) and convective transport statistics from GCE model simulations of prototype storms to estimate the amount of CO vented from the planetary boundary layer (PBL) by deep convection. This statistical-dynamical approach was used by Thompson et al. (1994) to estimate the convective transport component of the boundary layer CO budget for the central United States (32.5° – 50° N, 90° – 105° W) for the month of June. They found that the net upward deep convective flux (~18×10^5 kg-CO/month) and the shallow convective flux (~16×10^5 kg-CO/month) to the free troposphere accounted for about 80% of the loss of CO from the PBL. These losses roughly balanced horizontal transport of CO

(~28 × 10^5 kg-CO/month), the oxidation of hydrocarbons (~8 × 10^5 kg-CO/month) and anthropogenic and biogenic emissions (~8 + ~1 × 10^5 kg-CO/month) into the PBL in the central United States. In this respect the central United States acts as a "chimney" for venting CO and other pollutants.

Regional chemical transport models have been used for applications such as simulations of photochemical O_3 production, acid deposition, and fine particulate matter. Walcek et al. (1990) included a parameterization of cloud-scale aqueous chemistry, scavenging, and vertical mixing in the chemistry model of Chang et al. (1987). The vertical distribution of cloud microphysical properties and the amount of subcloud-layer air lifted to each cloud layer are determined using a simple entrainment hypothesis (Walcek and Taylor, 1986). Vertically-integrated O_3 formation rates over the northeast U.S. were enhanced by ~50% when the in-cloud vertical motions were included in the model.

Wang et al. (1996) simulated the 10 – 11 June 1985 PRE-STORM squall line with the NCAR/Penn State Mesoscale Model (MM5; Grell et al., 1994; Dudhia et al., 1993). Convection was parameterized as a subgrid-scale process in MM5 using the Kain and Fritsch (1993) scheme. Mass fluxes and detrainment profiles from the convective parameterization were used along with the 3-D wind fields in CO tracer transport calculations for this convective event. The U.S. Environmental Protection Agency has developed a Community Multiscale Air Quality (CMAQ) modeling system that uses MM5 with the Kain-Fritsch convective scheme as the dynamical driver (Ching et al., 1998).

Convective transport in global chemistry and transport models is treated as a subgrid-scale process that is parameterized typically using cloud mass flux information from a general circulation model or global data assimilation system. While GCMs can provide data only for a "typical" year, data assimilation systems can provide "real" day-by-day meteorological conditions, such that CTM output can be compared directly with observations of trace gases. The NASA Goddard Earth Observing System Data Assimilation System (GEOS-1 DAS and successor systems; Schubert et al., 1993; Bloom et al., 1996) provides archived global data sets for the period 1980 to present, at 2° × 2.5° or better resolution with 20 layers or more in the vertical. Convection is parameterized with the Relaxed Arakawa-Schubert scheme (Moorthi and Suarez, 1992). Pickering et al. (1995) showed that the cloud mass fluxes from GEOS-1 DAS are reasonable for the 10 – 11 June 1985 PRE-STORM squall line based on comparisons with the

GCE model (cloud-resolving model) simulations of the same storm. In addition, the GEOS-1 DAS cloud mass fluxes compared favorably with the regional estimates of convective transport for the central U.S. presented by Thompson et al. (1994). However, Allen et al. (1997) have shown that the GEOS-1 DAS overestimates the amount and frequency of convection in the tropics and underestimates the convective activity over midlatitude marine storm tracks.

AX2.3.3 Nocturnal Low-Level Jets

Nocturnal low level jets (LLJ) are coincident with synoptic weather patterns involved with high O_3 episodes implying that they may play an important role in the formation of severe O_3 events (Rao and Zurbenko, 1994). LLJ can transport pollutants hundreds of kilometers from their sources. Figure AX2-10 shows the evolution of the planetary boundary layer (PBL) over land during periods when high-pressure weather patterns prevail (Stull, 1999). During synoptic weather patterns with stronger zonal flow, a schematic of the boundary layer could look quite different with generally more uniform mixing present. As can be seen from Figure AX2-10, the PBL can be divided into three sub-layers: a turbulent mixed layer (typically present during daylight hours), a less turbulent residual layer which occupies space that was formerly the mixed layer, and a nocturnal, stable boundary layer that has periods of sporadic turbulence (Stull, 1999). The LLJ forms in the residual layer. It is important to note, that during the nighttime, the PBL often comprises thin, stratified layers with different physical and chemical properties (Stull, 1988).

At night, during calm conditions, the planetary boundary layer is stably stratified and as a result verticle mixing is inhibited. On cloud-free evenings the LLJ begins to form shortly after sunset. The wedge of cool air in the stable nocturnal boundary layer decouples the surface layer from the residual layer and acts like a smooth surface allowing the air just above it (in the residual layer) to flow rapidly past the inversion mostly unencumbered by surface friction (Stull, 1999). As the sun rises, its energy returns to heat the land and the lower atmosphere begins to mix as the warm air rises. The jet diminishes as the nocturnal temperature inversion erodes and surface friction slows winds speeds. If stable synoptic conditions persist, the same conditions the next night could allow the low-level jet to reform with equal strength and similar consequences. LLJ formation results in vertical wind shear that induces mixing between the otherwise stratified layers.

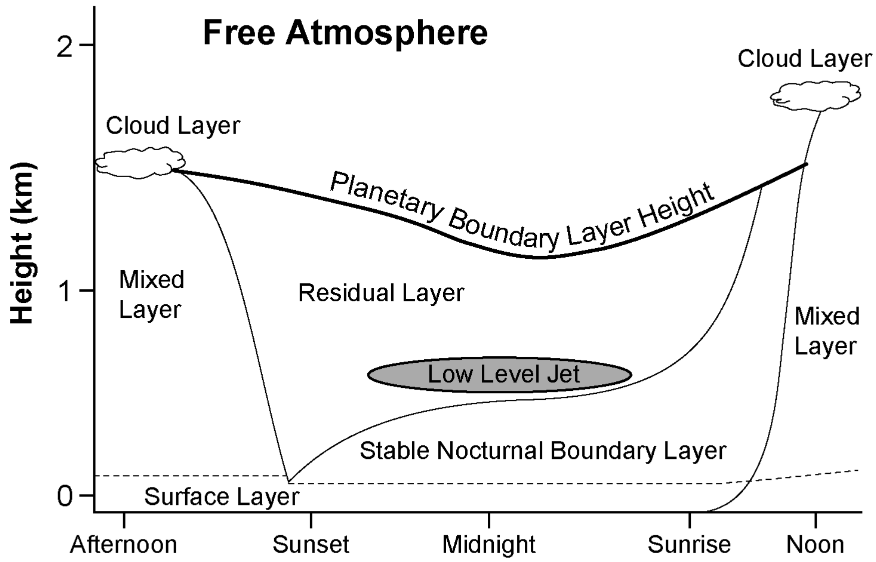

Figure AX2-10. The diurnal evolution of the planetary boundary layer while high pressure prevails over land. Three major layers exist (not including the surface layer): a turbulent mixed layer; a less turbulent residual layer which contains air formerly in the mixed layer; and a nocturnal, stable boundary layer which is characterized by periods of sporadic turbulence.

Source: Adapted from Stull (1999) Figures 1.7 and 1.12.

LLJs are often associated with mountain ranges. Mountains and pressure gradients on either side of a developing LLJ help concentrate the flow of air into a corridor or horizontal stream (Hobbs et al., 1996). Figure AX2-11 shows that LLJs commonly form east of the Rocky Mountains and east of the Appalachian Mountains (Bonner, 1968). There may be other locations in the U.S. where LLJs occur. The width of the jet can vary from location to location and from one weather pattern to another, but is typically less than several hundred km not greater than 1000 km long. In extreme cases, winds in a LLJ can exceed 60 ms^{-1} but average speeds are typically in the range of 10 to 20 ms^{-1}.

Nocturnal low-level jets are not unique to the United States; they have been detected in many other parts of the world (Corsmeier, 1997, Reitebuch, et al., 2000). Corsmeier et al. (1997) observed secondary maxima in surface O_3 at nighttime at a rural site in Germany, supporting the notion that downward transport from the residual layer was occurring. The

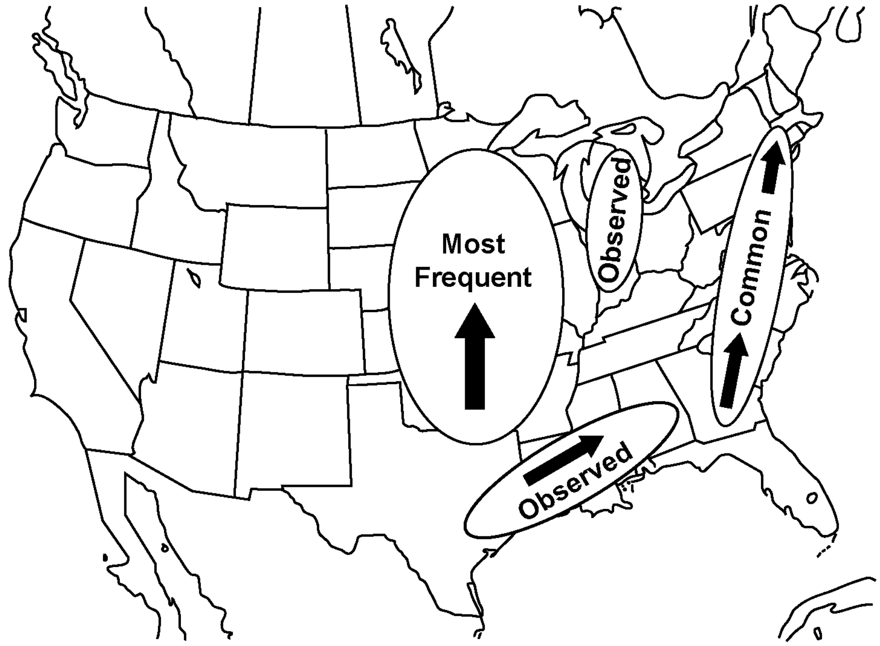

Figure AX2-11. Locations of low level jet occurrences in decreasing order of prevalence (most frequent, common, observed). These locations are based on 2-years radiosonde data obtained over limited areas. With better data coverage, other low level jets may well be observed elsewhere in the United States.

Source: Bonner (1968).

secondary maxima were, on average, 10% of the next day's O_3 maximum but at times could be as much as 80% of the maximum (Corsmeier et al., 1997). The secondary O_3 maxima were well correlated with an increase in wind speed and wind shear. The increased vertical shear over the very thin layer results in mechanical mixing that leads a downward flux of O_3 from the residual to the near surface layer (see Figures AX2-12 and AX2-13). Analysis of wind profiles from aerological stations in northeastern Germany revealed the spatial extent of that particular LLJ was up to 600 km in length and 200 km in width. The study concluded the importance of O_3 transport by low level jets was twofold: O_3 and other pollutants could be transported hundreds of kilometers at the jet core level during the night and then mixed to the ground far from their source region. Salmond and McKendry (2002) also observed secondary O_3 maxima (in the Lower Fraser Valley, British Columbia) associated with low level jets that occasionally

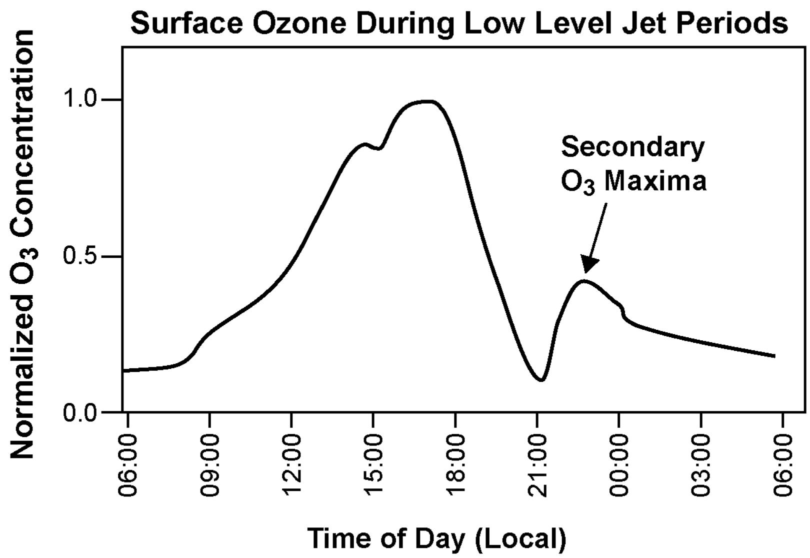

Figure AX2-12. Schematic diagram showing the diurnal behavior of ozone and the development of secondary ozone maxima resulting from downward transport from the residual layer when a low level jet is present.

Source: Adapted from Reitbuch et al. (2000); Corsmeier et al. (1997); and Salmond and McKendry (2002).

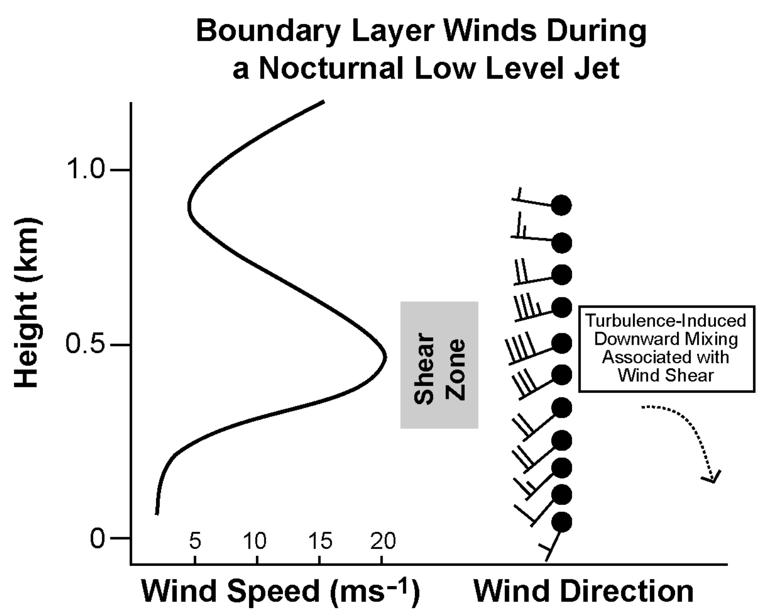

Figure AX2-13. The nocturnal low level jet occupies a thin slice of the atmosphere near the Earth's surface. Abrupt changes in wind speed and wind direction with height associated with the low level jet create conditions favorable for downward transport of air to the surface layer.

Source: Singh et al. (1997); Corsmeier et al. (1997).

exceeded half the previous day's maximum O_3 concentration. The largest increases in surface O_3 concentration occurred when boundary layer turbulence coincided with O_3 levels greater than 80 parts per billion were observed aloft. In addition, the study suggests horizontal transport efficiency during a low level jet event could be as much as six times greater than transport with light winds without an LLJ. Reitebuch et al. (2000) observed secondary O_3 maxima associated with low-level jet evolution in an urban area in Germany. The notion that O_3 was transported downward from the residual layer to the surface was supported by observed decreases in concentrations of NO, NO_2 and CO in the residual layer during secondary O_3 maxima. Unlike O_3 in the residual layer, concentrations of NO, NO_2, and CO should be lower than those found nearer the surface (Reitebuch et al., 2000; Seinfeld and Pandis, 1998). As in other studies, wind speed and directional shear were detected during these events. Calculations of the average wind speed and duration of the LLJ suggested that pollutants were transported several hundred kilometers. A study of the PBL and the vertical structure of O_3 observed at a costal site in Nova Scotia described how temperature and differences of surface roughness in a marine environment can induce LLJ formation and pollution transport (Gong et al., 2000). In this case, rather strong horizontal sea surface temperature gradients provided the necessary baroclinic forcing.

While the studies mentioned above have shed light on the possible role of the LLJ in the transport of O_3 and its precursors, quantitative statements about the significance of the LLJ in affecting local and regional O_3 budgets can not yet be made. This inability reflects the lack of available data for wind profiles in the planetary boundary layer in areas where LLJ are likely to occur and because of the inadequacy of numerical models in simulating their occurrence.

AX2.3.4 Intercontinental Transport of Ozone and Other Pollutants

AX2.3.4.1 The Atmosphere/Ocean Chemistry Experiment, AEROCE

The AEROCE experiment, initiated in the early 1990's set out to examine systematically the chemistry and meteorology leading to the trace gas and aerosol composition over the North Atlantic Ocean. One particular focus area was to determine the relative contribution of anthropogenic and natural processes to the O_3 budget and oxidizing capacity of the troposphere over the North Atlantic Ocean. Early results using isentropic back trajectories suggested that periodic pulses of O_3 mixing ratios up to 80 ppb were associated with large-scale subsidence from the mid-troposphere, favoring a natural source (Oltmans and Levy, 1992). Moody et al.

(1995) extended this work with a five-year seasonal climatology and found the highest concentrations of O_3 were always associated with synoptic scale post-frontal subsidence off the North American continent behind cold fronts, and this pattern was most pronounced in the April-May time frame. These post-frontal air masses had uniformly low humidity and high concentrations of ^{7}Be, a cosmogenic tracer produced in the upper troposphere and lower stratosphere. However, the pulsed occurrence of these postfrontal air masses also frequently delivered enhanced concentrations of species such as $SO_4^=$, NO_3^-, ^{210}Pb, etc. suggesting a component originating in North America. In a subsequent analysis of data from one year (1992) when CO observations were available, Dickerson et al. (1995) concluded that anthropogenic sources made a significant contribution to surface O_3, and using a simple mixing model they determined that 57% of the air had a continental boundary layer origin.

Based on these observations of the synoptically modulated concentrations, AEROCE conducted an aircraft and ozonesonde intensive in the spring of 1996. The intention was to adopt a meteorologically informed sampling strategy to clearly distinguish the characteristics of air masses ahead of and behind eastward progressing cold fronts. Sixteen research flights were conducted with the University of Wyoming King Air research aircraft. The goal was to differentiate the sources of enhanced O_3 mixing ratios observed on Bermuda after the passage of cold fronts, and to identify the major processes controlling the highly variable O_3 mixing ratios in the mid-to-upper troposphere over eastern North America and the North Atlantic Ocean during April and May. In addition to aircraft flights, near-daily ozonesondes were launched in a quasi-zonal transect from Purdue, Indiana, to Charlottesville, Virginia to Bermuda. An effort was made to time the release of ozonesondes to cleanly differentiate pre and post-frontal air masses.

In several aircraft flights, the presence at altitude of distinct layers of air with elevated concentrations of nonmethane hydrocarbons (NMHCs) attested to the dynamic vertical mixing associated with springtime frontal activity. Layers of mid-tropospheric air of high O_3 (140 ppb) and low background NMHC mixing ratios (1.44 ppbv ethane, 0.034 ppbv propene, 0.247 ppbv propane, and 0.034 ppbv isobutene, 0.041 ppbv n-butane, 0.063 ppbv benzene, 0.038 ppbv toluene) were indicative of descending, stratospherically influenced air on a flight to the east of Norfolk, VA on April 24 (alt 4600m). However layers of elevated NMHC concentrations (1.88 ppbv ethane, 0.092 ppbv propene, 0.398 ppbv propane, 0.063 ppbv isobutene, 0.075 ppbv n-butane, 0.106 ppbv benzene, 0.0102 ppbv toluene) occurred along with 60-70 ppbv of O_3 on a flight west of Bermuda April 28 (alt. 4100m), indicating air had been lofted from the continental boundary layer. Meteorological evidence, supported by ozonesonde observations and earlier King Air flights, indicated that stratosphere/troposphere exchange associated with an upstream frontal system had injected and advected dry, O_3-rich air into the mid-troposhere region over the continent. This subsiding air mass provided deep layers of enhanced O_3 in the offshore, postfrontal area. Convection from a developing (upwind) system lifted continental boundary layer air into the proximity of the dry, subsiding air layer (Prados, et al., 1999). This resulted in a mixture of high concentrations of anthropogenic pollutants along with naturally enhanced O_3. Ozone mixing ratios exceeded those attributable to boundary layer venting or in-transit photochemical production. These meteorological processes led to pollution and stratospherically enhanced O_3 co-occurring in post-frontal air masses over the North Atlantic Ocean. A similar event in February 1999 was observed by Parrish et al. (2000). It confirmed the occurrence of thin layers of anthropogenic and stratospheric air that subsequently mix. These results, along with recent modeling studies suggest that North American pollution clearly does contribute to the periodic influx of less-than-pristine air observed in the marine boundary layer over Bermuda (e.g., Li et al., 2002) and yet these incursions are not inconsistent with observing enhancements in O_3 due to stratospheric exchange.

The ozonesonde climatology of AEROCE clearly established that O_3 mixing ratios were always enhanced and increased with height in post-frontal air masses. Postfrontal O_3 in the lower troposphere over Bermuda originates in the postfrontal midtroposphere over the continent, supporting the hypothesis that naturally occurring stratospheric O_3 makes a contribution to air in the marine boundary layer (Cooper et al., 1998). A schematic of the meteorological processes responsible for the close proximity of natural and man-made O_3 can be seen in Figure AX2-8 from Prados (2000). Cold fronts over North America tend to be linked in wave-like patterns such that the subsidence behind one front may occur above with intrusions of convection ahead of the next cold front. Pollutants, including VOC and NOx, precursors to O_3, may be lofted into the mid-to-upper troposphere where they have the potential to mix with layers of air descending from O_3-rich but relatively unpolluted upper troposphere and lower stratosphere. Through this complex mechanism, both stratospheric and photochemically produced O_3 may be transported to the remote marine environment where they have large-scale impacts on the radiative and chemical properties of the atmosphere. Recent three-dimensional modeling studies of air mass motion over the Pacific provide further evidence that these complex mechanisms are indeed active (Cooper et al., 2004b).

AX2.3.4.2 The North Atlantic Regional Experiment, NARE

NARE was established by the International Global Atmospheric Chemistry Project to study the chemical processes occurring in the marine troposphere of the North Atlantic, the marine region expected to be the most impacted by industrial emissions from eastern North America and western Europe. Surface measurements from several surface sites were initiated in 1991, with major field intensives in summer 1993, spring 1996, early autumn 1997 and a few winter flights in 1999. In the summer of 1993, airborne and ground-based measurements of O_3 and O_3 precursors were made in the North Atlantic region by an international team of scientists to determine how the continents that rim the North Atlantic are affecting atmospheric composition on a hemispheric scale (Fehsenfeld et al., 1996a; Fehsenfeld et al., 1996b). The focus of NARE was to investigate the O_3 budget of the North Atlantic region. Previous observations indicated that the O_3 produced from anthropogenic sources is greater than that reaching the lower troposphere from the stratosphere and that O_3 derived from anthropogenic pollution has a hemisphere wide effect at northern mid latitudes. This study was performed to better quantify the contribution of continental sources to the O_3 levels over the North Atlantic.

Buhr et al. (1996) measured O_3, CO, NO, and NO_y as well as meteorological parameters aboard the NCAR King Air in August 1993 during 16 flights over and near the Gulf of Maine. They found that O_3 produced from anthropogenic precursors was dominant throughout the experimental region below 1500 m, in altitude.

The National Research Council of Canada Twin Otter aircraft was used to measure the O_3 and related compounds in the summertime atmosphere over southern Nova Scotia (Kleinman et al., 1996a; Kleinman et al., 1996b). Forty-eight flights were performed, primarily over the surface sampling site in Chebogue Point, Nova Scotia, or over the Atlantic Ocean. They found that a wide variety of air masses with varying chemical content impact Nova Scotia. The effect depends on flow conditions relative to the locations of upwind emission regions and the degree of photochemical processing associated with transport times ranging from about 1 – 5 d. Moist continental boundary layer air with high concentrations of O_3 and other anthropogenic pollutants was advected to Nova Scotia in relatively thin vertical layers, usually with a base altitude of several hundred meters. Dry air masses with high concentrations of O_3 often had mixed boundary layer and upper atmosphere source regions. When a moist and dry air mass with the same photochemical age and O_3 concentration were compared, the dry air mass had lower concentrations of NO_y and aerosol particles, which was interpreted as evidence for the selective removal of soluble constituents during vertical lifting.

Due to strong, low-level temperature inversions over the North Atlantic, near surface air is often unrepresentative of the eastward transport of the North American plume because of a decoupling from the air transported aloft (Kleinman et al., 1996a; Daum et al., 1996; Angervine et al., 1996). Pollution plumes were observed in distinct strata up to 1 km. Plume chemical compositions were consistent with the occurrence of considerable photochemical processing during transit from source regions over the eastern seaboard of the U.S. Ozone concentrations reached 150 ppbv, NO_x conversion to its oxidation products exceeded 85%, and high hydrogen peroxide concentrations were observed (median 3.6 ppbv, maximum 11 ppbv). CO and O_3 concentrations were well correlated ($R^2 = 0.64$) with a slope (0.26) similar to previous measurements in photochemically aged air (Parrish et al., 1998). Ozone depended nonlinearly on the NO_x oxidation product concentration, but there was a correlation ($r^2 = 0.73$) found between O_3 and the concentration of radical sink species as represented by the quantity $((NO_y - NO_x) + 2H_2O_2)$.

Banic et al. (1996) determined that the average mass of O_3 transported through an area 1 m in horizontal extent and 5 km in the vertical over the ocean near Nova Scotia to be 2.8 g s^{-1}, moving from west to east. Anthropogenic O_3 accounted for half of the transport below 1 km, 35 to 50% from 1 to 3 km, 25 to 50% from 3 to 4 km, and only 10% from 4 to 5 km. Merrill and Moody (1996) analyzed the meteorological conditions during the NARE intensive period (August 1 to September 13, 1993). They determined the ideal meteorological scenario for delivering pollution plumes from the U.S. East Coast urban areas over the Gulf of Maine to the Maritime Provinces of Canada to be warm sector flow ahead of an advancing cold front. In the winter phase of NARE, O_3 and CO were measured from the NOAA WP-3D Orion aircraft from St. John' s, Newfoundland, Canada, and Keflavik, Iceland, from February 2 to 25, 1999 (Parrish et al., 2000). In the lower troposphere over the western North Atlantic Ocean, the close proximity of air masses with contrasting source signatures was remarkable. High levels of anthropogenic pollution immediately adjacent to elevated O_3 of stratospheric origin were observed, similar to those reported by Prados et al., (1999). In air masses with differing amounts of anthropogenic pollution, O_3 was negatively correlated with CO, which indicates that emissions from surface anthropogenic sources had reduced O_3, in this wintertime period, even in air masses transported into the free troposphere.

The influence of the origin and evolution of airstreams on trace gas mixing ratios has been studied in great detail for NARE aircraft data. The typical mid-latitude cyclone is composed of four major component airstreams, the warm conveyor belt, the cold conveyor belt, the post cold-front airstream and the dry airstream (Cooper et al., 2001). The physical and chemical processing of trace species was characterized for each airstream, and a conceptual model of a mid-latitude cyclones was developed (Cooper et al., 2002a). This showed how airstreams within midlatitude cyclones drew and exported trace gases from the polluted continental boundary layer, and the stratospherically enhanced mid-troposphere. Using back trajectories, airstream composition was related to the origin and transport history of the associated air mass. The lowest O_3 values were associated with airstreams originating in Canada or the Atlantic Ocean marine boundary layer; the highest O_3 values were associated with airstreams of recent stratospheric origin. The highest NO_y values were seen in polluted outflow from New England in the lower troposphere. A steep and positive O_3/NO_y slope was found for all airstreams in the free troposphere regardless of air mass origin. Finally, the seasonal variation of photochemistry and meteorology and their impact on trace gas mixing ratios in the conceptual cyclone model was determined (Cooper et al., 2002b). Using a positive O_3/CO slope as an indicator of photochemical O_3 production, O_3 production during late summer-early autumn is associated with the lower troposphere post-cold-front airstream and all levels of the WCB, especially the lower troposphere. However, in the early spring, there is no significant photochemical O_3 production for airstreams at any level, and negative slopes in the dry air airstream indicate STE causes the O_3 increase in the mid- and upper troposphere.

Stohl et al. (2002) analyzed total odd nitrogen (NO_y) and CO data taken during NARE in spring 1996 and fall 1997. They studied the removal timescales of NO_y originating from surface emissions of NO_x and what fraction reached the free troposphere. NO_x limits O_3 production in the free troposphere and can be regenerated from NO_y after the primary NOx has been exhausted. It was determined that < 50% of the NO_y observed above 3 km came from anthropogenic surface emissions. The rest had to have been emitted in situ.

Several studies (e.g., Stohl and Trickl, 1999; Brunner et al., 1998; Schumann et al., 2000; Stohl et al., 2003; Traub et al., 2003) have identified plumes that have originated in North America over Europe and over the eastern Mediterranean basin (e.g., Roelofs et al., 2003; Traub et al., 2003). Modeling studies indicate that North American emissions contribute roughly 20% to European CO levels and 2 to 4 ppb to surface O_3, on average. Episodic events, such as forest fires in North America have also been found to result in elevated CO and O_3 levels and visible haze layers in Europe (Volz-Thomas, et al., 2003). The O_3 is either transported from North America or formed during transport across the North Atlantic Ocean, perhaps as the result of interactions between the photochemical degradation products of acetone with emissions of NO_x from aircraft (Bruhl et al., 2000; Arnold et al., 1997). In addition, North American and European pollution is exported to the Arctic. Eckhardt et al. (2003) show that this transport is related to the phase of the North Atlantic Oscillation which has a period of about 20 years.

AX2.3.5 The Relation of Ozone to Solar Ultraviolet Radiation, Aerosols, and Air Temperature

AX2.3.5.1 Solar Ultraviolet Radiation and Ozone

The effects of sunlight on photochemical oxidant formation, aside from the role of solar radiation in meteorological processes, are related to its intensity and its spectral distribution. Intensity varies diurnally, seasonally, and with latitude, but the effect of latitude is strong only in the winter. Ultraviolet radiation from the sun plays a key role in initiating the photochemical processes leading to O_3 formation and affects individual photolytic reaction steps. However, there is little empirical evidence in the literature, directly linking day-to-day variations in observed UV radiation levels with variations in O_3 levels.

In urban environments the rate of O_3 formation is sensitive to the rate of photolysis of several species including H_2CO, H_2O_2, O_3, and especially NO_2. Monte Carlo calculations suggest that model calculations of photochemical O_3 production are most sensitive to uncertainty in the photolysis rate coefficient for NO_2 (Thompson and Stewart, 1991; Baumann et al., 2000). The International Photolysis Frequency Measurement and Modeling Intercomparison (IPMMI) hosted recently by NCAR in Boulder, CO brought together more than 40 investigators from

8 institutions from around the world (Bais et al., 2003; Cantrell et al., 2003 and Shetter et al., 2003). They compared direct actinometric measurements, radiometric measurements, and numerical models of photolysis rate coefficients, focusing on O_3 to $O(^1D)$ and NO_2, referred to as $j(O_3)$ and $j(NO_2)$.

The combination of direct measurements and comparisons to model calculations indicated that for clear skies, zenith angles less than 70°, and low aerosol loadings, the absolute value of the $j(NO_2)$ at the Earth's surface is known to better than 10% with 95% confidence. The results suggest that the cross sections of Harder et al. (1997a) may yield more accurate values when used in model calculations of $j(NO_2)$. Many numerical models agreed among themselves and with direct measurements (actinometers) and semi-direct measurements (radiometers) when using ATLAS extraterrestrial flux from Groebner and Kerr (2001). The results of IPMMI indicate numerical models are capable of precise calculation of photolysis rates at the surface and that uncertainties in calculated chemical fields arise primarily from uncertainties in the variation of actinic flux with altitude in addition to the impact of clouds and aerosols on radiation.

AX2.3.5.2 Impact of Aerosols on Radiation and Photolysis Rates and Atmospheric Stability

Because aerosol particles influence the UV flux there is a physical link between particles and gases that depends on the concentration, distribution, and refractive index of the particles. Scattering of UV radiation by tropospheric aerosol particles can strongly impact photolysis rates and thus photochemical O_3 production or destruction. The effect shows high sensitivity to the properties of the aerosol. Particles in the boundary layer can accelerate photochemistry if the single scattering albedo is near unity, such as for sulfate and ammoniated sulfate aerosols, or inhibit O_3 production if the single scattering albedo is low, such as for mineral dust or soot (Dickerson et al., 1997; Jacobson, 1998; Liao et al., 1999; Castro et al., 2001; Park et al., 2001). Any aerosol layer in the free troposphere will reduce photolysis rates in the boundary layer.

The interaction of aerosols, photochemistry, and atmospheric thermodynamic processes can impact radiative transport, cloud microphysics, and atmospheric stability with respect to vertical mixing. Park et al. (2001) developed a single-column chemical transport model that simulates vertical transport by convection, turbulent mixing, photochemistry, and interactive calculations of radiative fluxes and photolysis rates. Results from simulations of an episode over the eastern United States showed strong sensitivity to convective mixing and aerosol optical depth. The aerosol optical properties observed during the episode produced a surface cooling of up to 120 W/m^2 and stabilized the atmosphere suppressing convection. This suggests two possible feedbacks mechanisms between aerosols and O_3–reduced vertical mixing would tend to increase the severity of O_3 episodes, while reduced surface temperatures would decrease it.

AX2.3.5.3 Temperature and Ozone

An association between surface O_3 concentrations and temperature has been demonstrated from measurements in outdoor smog chambers and from measurements in ambient air. Numerous ambient studies done over more than a decade have reported that successive occurrences or episodes of high temperatures characterize high O_3 years (Clark and Karl, 1982; Kelly et al., 1986). Figures AX2-14 and AX2-15 show the daily maximum O_3 concentrations versus maximum daily temperature for warm months (May to October), 1988 to 1990, for Atlanta and New York City, NY, and for Detroit, MI, and Phoenix, AZ, respectively. There appears to be an upper-bound on O_3 concentrations that increases with temperature. Likewise, Figure AX2-16 shows that a similar qualitative relationship exists between O_3 and temperature even at a number of nonurban locations.

The notable trend in these plots is the apparent upper-bound to O_3 concentrations as a function of temperature. It is clear that, at a given temperature, there is a wide range of possible O_3 concentrations because other factors (e.g., cloudiness, precipitation, wind speed) can reduce O_3 production rates. The upper edge of the curves may represent a practical upper bound on the maximum O_3 concentration achieved under the most favorable conditions. It can be seen that this quantity does increase with temperature, at least for temperatures greater than about 20 °C for all of the cities shown in Figures AX2-14 to AX2-16 except perhaps for Phoenix, AZ. Relationships between peak O_3 and temperature also have been recorded by Wunderli and Gehrig (1991) for three locations in Switzerland. At two sites near Zurich, peak O_3 increased 3 to 5 ppb/°C for diurnal average temperatures between 10 and 25 °C, and little change in peak O_3 occurred for temperatures below 10 °C. At the third site, a high-altitude location removed from anthropogenic influence, a much smaller variation of O_3 with temperature was observed.

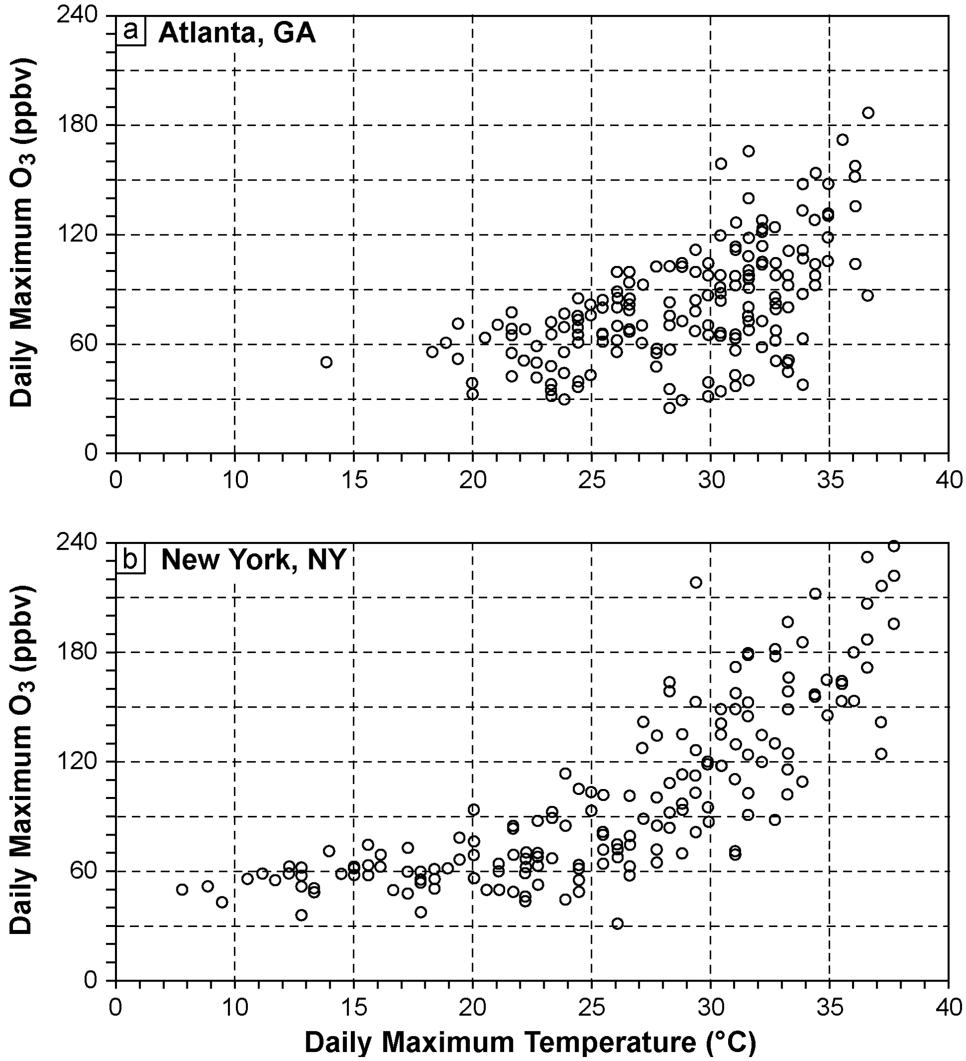

Figure AX2-14. A scatter plot of daily maximum ozone concentration in (a) Atlanta, GA and (b) New York NY, versus daily maximum temperature.

1 Some possible explanations for the correlation of O_3 with temperature include:

2 (1) Increased photolysis rates under meterological conditions associated with higher temperatures;

3 (2) Increased H_2O concentrations with higher temperatures as this will lead to greater OH production via R(2-6);

4 (3) Enhanced thermal decomposition of PAN and similar compounds to release NO_x at higher temperatures;

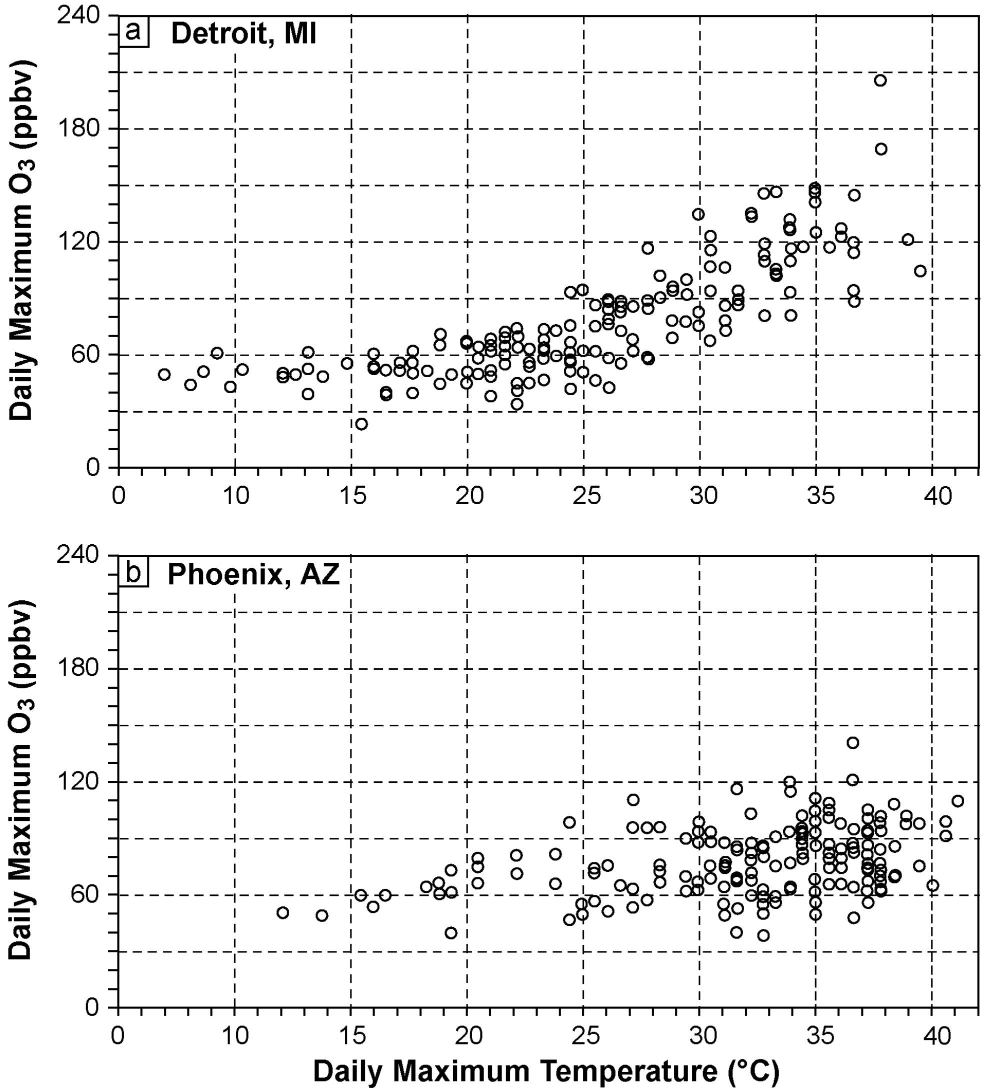

Figure AX2-15. A scatter plot of daily maximum ozone concentration in (a) Detroit, MI and (b) Phoenix, AZ versus daily maximum temperature.

(4) Increase of anthropogenic hydrocarbon (e.g., evaporative losses) emissions or NO_x, emissions with temperature or both;

(5) Increase of natural hydrocarbon emissions (e.g., isoprene) with temperature; and

(6) Relationships between high temperatures and stagnant circulation patterns.

(7) Advection of warm air enriched with O_3.

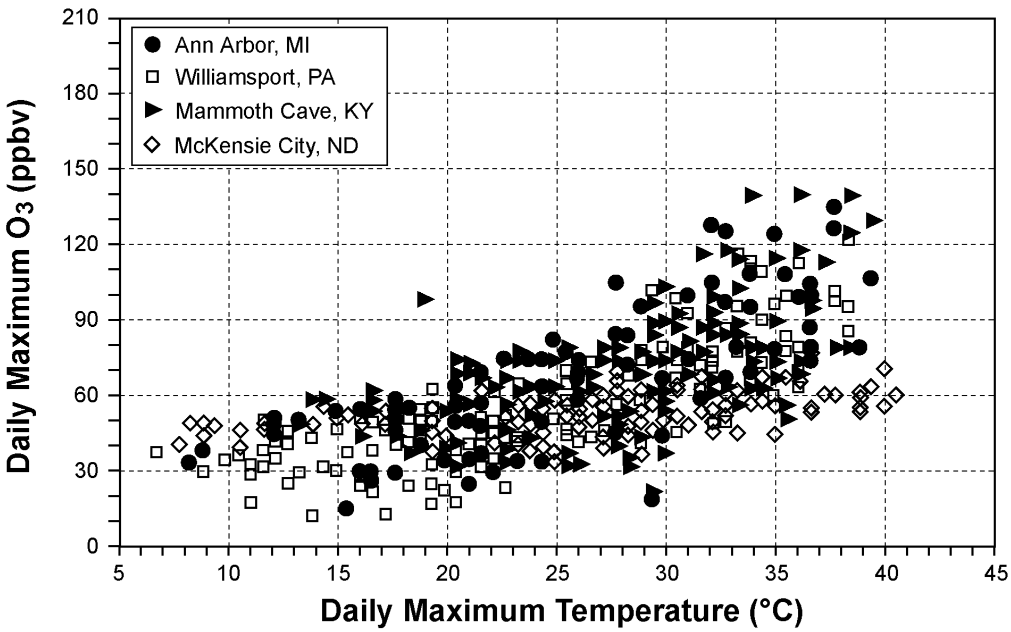

Figure AX2-16. A scatter plot of daily maximum ozone concentration versus daily maximum temperature for four nonurban sites. The relation with temperature is still apparent, although the slope is reduced from that of the urban areas.

Cardelino and Chameides (1990) and Sillman and Samson (1995) both identified the temperature-dependent thermal decomposition of PAN as the primary cause of the observed O_3-temperature relationship. When temperatures are low PAN is relatively stable. Formation of PAN represents a significant sink for NO_x (in low NO_x rural areas) and radicals (in high NO_x urban areas). This has the effect of slowing the rate of O_3 production. Sillman and Samson found that the impact of the PAN decomposition rate could explain roughly half of the observed correlation between O_3 and temperature. Jacob et al. (1993) found that warm events in summer in the United States were likely to occur during stagnant meteorological conditions, and the concurrence between warm temperatures and meteorological stagnation also explained roughly half of the observed O_3-temperature correlation. Other possible causes include higher solar radiation during summer, the strong correlation between biogenic emission of isoprene and temperature, and the somewhat weaker tendency for increased anthropogenic emissions coinciding with warmer temperatures.

However, it should also be noted that a high correlation of O_3 with temperature does not necessarily imply a causal relation. Extreme episodes of high temperatures (a heat wave) are often multi-day events- high O_3 episodes are also multi-day events, concentrations build, temperatures rise, but both are being influenced by larger-scale regional or synoptic meteorological conditions. It also seems apparent, that while there is a trend for higher O_3 associated with higher temperatures, there is also much greater variance in the range of O_3 mixing ratios at higher temperatures.

AX2.4 THE RELATION OF OZONE TO ITS PRECURSORS AND OTHER OXIDANTS

Ozone is unlike many other species whose rates of formation vary directly with the emissions of their precursors. Ozone changes in a nonlinear fashion with the concentrations of its precursors. At the low NO_x concentrations found in most environments, ranging from remote continental areas to rural and suburban areas downwind of urban centers the net production of O_3 increases with increasing NO_x. At the high NO_x concentrations found in downtown metropolitan areas, especially near busy streets and roadways, and in power plant plumes there is net destruction (titration) of O_3 by reaction with NO. In between these two regimes there is a transition stage in which O_3 shows only a weak dependence on NO_x concentrations. In the high NO_x regime, NO_2 scavenges OH radicals which would otherwise oxidize VOCs to produce peroxy radicals, which in turn would oxidize NO to NO_2. In the low NO_x regime, the oxidation of VOCs generates, or at least does not consume, free radicals and O_3 production varies directly with NO_x. Sometimes the terms VOC limited and NO_x limited are used to describe these two regimes. However, there are difficulties with this usage because (1) VOC measurements are not as abundant as they are for nitrogen oxides, (2) rate coefficients for reaction of individual VOCs with free radicals vary over an extremely wide range, and (3) consideration is not given to CO nor to reactions that can produce free radicals without invoking VOCs. The terms NO_x-limited and NO_x-saturated (e.g., Jaegle et al., 2001) will be used wherever possible to describe these two regimes more adequately. However, the terminology used in original articles will also be kept. The chemistry of OH radicals, which are responsible for initiating the oxidation of hydrocarbons, shows behavior similar to that for O_3 with respect to NO_x concentrations (Hameed et al., 1979;

Pinto et al., 1993; Poppe et al., 1993; Zimmerman and Poppe, 1993). These considerations introduce a high degree of uncertainty into attempts to relate changes in O_3 concentrations to emissions of precursors.

Various analytical techniques have been proposed that use ambient NO_x and VOC measurements to derive information about O_3 production and O_3-NO_x-VOC sensitivity. It has been suggested that O_3 formation in individual urban areas could be understood in terms of measurements of ambient NO_x and VOC concentrations during the early morning (e.g., National Research Council, 1991). In this approach, the ratio of summed (unweighted by chemical reactivity) VOC to NO_x is used to determine whether conditions were NO_x-sensitive or VOC sensitive. This procedure is inadequate because it omits many factors that are recognized as important for O_3 production: the impact of biogenic VOCs (which are not present in urban centers during early morning); important individual differences in the ability of VOCs to generate free radicals (rather than just total VOC) and other differences in O_3 forming potential for individual VOCs (Carter, 1995); the impact of multiday transport; and general changes in photochemistry as air moves downwind from urban areas (Milford et al., 1994).

Jacob et al. (1995) used a combination of field measurements and a chemistry-transport model (CTM) to show that the formation of O_3 changed from NO_x-limited to NO_x-saturated as the season changed from summer to fall at a monitoring site in Shenandoah National Park, VA. Photochemical production of O_3 generally occurs simultaneously with the production of various other species: nitric acid (HNO_3), organic nitrates, and hydrogen peroxide. The relative rate of production of O_3 and other species varies depending on photochemical conditions, and can be used to provide information about O_3-precursor sensitivity.

There are no hard and fast rules governing the levels of NO_x at which the transition from NO_x-limited to NO_x-saturated conditions occurs. The transition between these two regimes is highly spatially and temporally dependent. Similar responses to NO_x additions from commercial aircraft have also been found for the upper troposphere (Bruhl et al., 2000). Bruhl et al. (2000) found that the NO_x levels for O_3 production versus loss are highly sensitive to the radical sources included in model calculations. They found that the inclusion of only CH_4 and CO oxidation leads to a decrease in net O_3 production in the North Atlantic flight corridor due to NO emissions from aircraft. However, the inclusion of acetone photolysis was found to shift the maximum in

O_3 production to higher NO_x mixing ratios, thereby reducing or eliminating areas in which there is a decrease in O_3 production rates due to aircraft emissions.

Trainer et al. (1993) suggested that the slope of the regression line between O_3 and summed NO_x oxidation products (NO_z, equal to the difference between measured total reactive nitrogen, NO_y, and NO_x) can be used to estimate the rate of O_3 production per NO_x (also known as the O_3 production efficiency, or OPE). Ryerson et al. (1998, 2001) used measured correlations between O_3 and NO_z to identify different rates of O_3 production in plumes from large point sources.

Sillman (1995) and Sillman and He (2002) identified several secondary reaction products that show different correlation patterns for NO_x-limited conditions and NO_x-saturated conditions. The most important correlations are for O_3 versus NO_y, O_3 versus NO_z, O_3 versus HNO_3, and H_2O_2 versus HNO_3. The correlations between O_3 and NO_y, and O_3 and NO_z are especially important because measurements of NO_y and NO_x are widely available. Measured O_3 versus NO_z (Figure AX2-17) shows distinctly different patterns in different locations. In rural areas and in urban areas such as Nashville, TN, O_3 shows a strong correlation with NO_z and a relatively steep slope to the regression line. By contrast, in Los Angeles O_3 also increases with NO_z, but the rate of increase of O_3 with NO_z is lower and the O_3 concentrations for a given NO_z value are generally lower.

The difference between NO_x-limited and NO_x-saturated regimes is also reflected in measurements of hydrogen peroxide (H_2O_2). Hydrogen peroxide production is highly sensitive to the abundance of free radicals and is thus favored in the NO_x-limited regime, typical of summer conditions. Differences between these two regimes are also related to the preferential formation of sulfate during summer and to the inhibition of sulfate and hydrogen peroxide during winter (Stein and Lamb, 2003). Measurements in the rural eastern United States (Jacob et al., 1995) Nashville (Sillman et al., 1998), and Los Angeles (Sakugawa and Kaplan, 1989) show large differences in H_2O_2 concentrations between likely NO_x-limited and NO_x-saturated locations.

The discussion in Section AX2.4.1 centers mainly on the relations among O_3, NO_x and its oxidation products, represented as NO_z (NO_y – NO_x) and VOCs derived from the results of field studies. Most of these studies examined processes occurring in power plant and urban plumes.

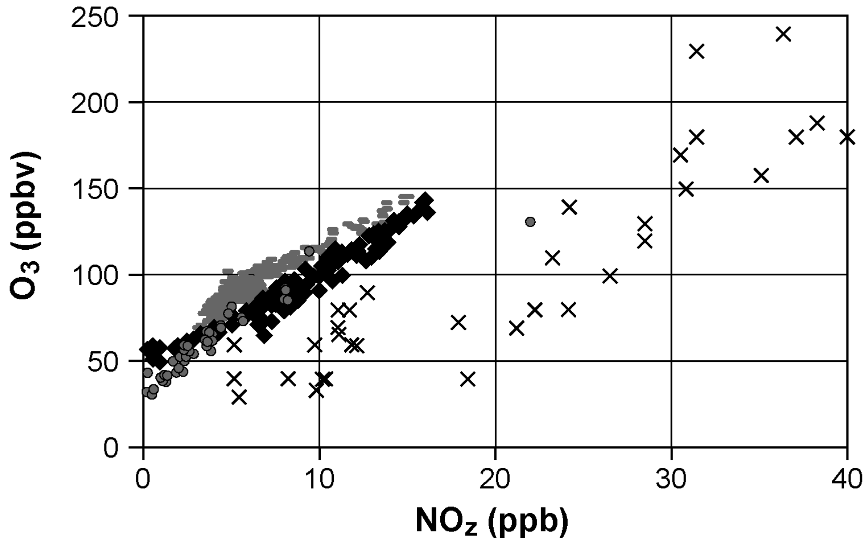

Figure AX2-17. Measured values of O_3 and NO_z (NO_y – NO_x) during the afternoon at rural sites in the eastern United States (grey circles) and in urban areas and urban plumes associated with Nashville, TN (gray dashes), Paris, FR (black diamonds) and Los Angeles, CA (X's).

Sources: Trainer et al. (1993), Sillman et al. (1997, 1998, 2003).

AX2.4.1 Summary of Results for the Relations Among Ozone, its Precursors and Other Oxidants from Recent Field Experiments

AX2.4.1.1 Results from the Southern Oxidant Study and Related Experiments

The Southern Oxidant Study (SOS) was initiated to describe the sources, variation, and distribution of O_3 and its precursors in the southeastern United States during the summer season (Hübler et al., 1998; Meagher et al., 1998; Goldan et al., 2000). Specific issues that were addressed included: (1) the role of biogenic VOC and NO_x emissions on local and regional O_3 production, (2) the effect of urban-rural exchange/interchange on local and regional O_3 production, (3) sub-grid-scale photochemical and meteorological processes, and (4) the provision of a high-quality chemical and meteorological data set to test and improve observation and emission-based air quality forecast models. Some of the more significant findings of the 1994 to 1995 studies include the following: (1) Ozone production in Nashville was found to be close to the transition between NO_x-limited and NO_x-saturated regimes. (2) The number of molecules of O_3 produced per molecule of NO_x oxidized in power plant plumes, or the ozone production efficiency (OPE) was found to be inversely proportional to the NO_x emission rate, with the plants having the highest NO_x emissions exhibiting the lowest OPE. (3) During stagnant conditions, winds at night dominated pollutant transport and represent the major mechanism for advecting urban pollutants to rural areas — specific findings follow.

As part of SOS, the Tennessee Valley Authority's instrumented helicopter conducted flights over Atlanta, Georgia to investigate the evolution of the urban O_3 plume (Imhoff et al., 1995). Ozone peak levels occurred at 20 – 40 km downwind of the city center. The OPE obtained from five afternoon flights ranged between 4 and 10 molecules of O_3 per molecule of NO_x.

Berkowitz and Shaw (1997) measured O_3 and its precursors at several altitudes over a surface site near Nashville during SOS to determine the effects of turbulent mixing on atmospheric chemistry. Early morning measurements of O_3 aloft revealed values near 70 ppb, while those measured at the surface were closer to 25 ppb. As the daytime mixed layer deepened, surface O_3 values steadily increased until they reached 70 ppb. The onset of turbulence increased isoprene mixing ratios aloft by several orders of magnitude and affected the slope of O_3 as a function of NO_y for each of the flight legs. Measurements from nonturbulent flight legs yielded slopes that were considerably steeper than those from measurements made in turbulence. This study shows that the concentration of O_3 precursors aloft is dependent on the occurrence of turbulence, and turbulent mixing could explain the evolution of O_3 concentrations at the surface. In general, conclusions regarding pollutant concentrations must account for both chemical and local dynamic processes.

Gillani et al. (1998) analyzed data from instrumented aircraft during SOS that flew through the plumes of three large, tall-stack, base-load, Tennessee Valley Authority (TVA) coal-fired power plants in northwestern Tennessee. They determined that plume chemical maturity and peak O_3 and NO_z production occurred within 30 to 40 km and 4 hours of summer daytime convective boundary layer (CBL) transport time for a coal-fired power plant in the Nashville, TN urban O_3 nonattainment area (Gallatin). For a rural coal-fired power plant in an isoprene-rich forested area about 100 km west of Nashville (Cumberland), plume chemical maturity and peak O_3 and NO_z production were realized within approximately 100 km and 6 hours of CBL transport time. Their findings included approximately 3 molecules of O_3 and more than 0.6 molecules of NO_z may be produced in large isolated rural power plant plumes (PPPs) per molecule of NO_x release; the corresponding peak yields of O_3 and NO_z may be significantly greater in urban PPPs. Both power plants can contribute as much as 50 ppb of excess O_3 to the Nashville area, raising the local levels to well above 100 ppb. Also using aircraft data collected during SOS, Ryerson et al. (1998) concluded that the lower and upper limits to O_3 production efficiency in the Cumberland and Paradise PPPs (located in rural Tennessee) were 1 and 2 molecules of O_3 produced per molecule of NO_x emitted. The estimated lower and upper limits to O_3 production efficiency in the Johnsonville PPP (also located in rural Tennessee) were higher, at 3 and 7.

The NOAA airborne O_3 lidar provided detailed, three-dimensional lower tropospheric O_3 distribution information during June and July 1995 in the Nashville area (Senff et al., 1998; Alvarez et al., 1998). The size and shape of power plant plumes as well as their impacts on O_3 concentration levels as the plume is advected downwind were studied. Specific examples include: the July 7 Cumberland plume that was symmetrical and confined to the boundary layer, and the July 19 Cumberland plume that was irregularly shaped with two cores, one above and the other within the boundary layer. The disparate plume characteristics on these two days were the result of distinctly different meteorological conditions. Ozone in the plume was destroyed at a rate of 5 to 8 ppbv h^{-1} due to NO_x titration close to the power plant, while farther downwind, O_3 was produced at rates between 1.5 and 4 ppbv h^{-1}. The lidar O_3 measurements compared reasonably well with *in situ* values, with the average magnitude of the offsets over all the flights at 4.3 ppbv (7%).

The highest O_3 concentrations observed during the 1995 SOS in middle Tennessee occurred during a period of strong, synoptic-scale stagnation from July 11 through July 15. This massive episode covered most of the eastern United States (e.g., Ryan et al., 1998). During this time, the effects of vertical wind profiles on the buildup and transport of O_3 were studied by Banta et al. (1998) using an airborne differential absorption lidar (DIAL) system. Vertical cross sections showed O_3 concentrations exceeding 120 ppb extending to nearly 2 km above ground level, but that O_3 moved little horizontally. Instead, it formed a dome of pollution over or near Nashville. Due to the stagnant daytime conditions (boundary layer winds ~1 to 3 m s^{-1}), nighttime transport of O_3 became disproportionately important. At night, in the layer between 100 and 2000 m AGL (which had been occupied by the daytime mixed layer), the winds could be accelerated to 5 to 10 m s^{-1} as a result of nocturnal decoupling from surface friction. Data from surface and other aircraft measurements taken during this period suggest that the background air and the edges of the urban plume were NO_x sensitive and the core of the urban plume was hydrocarbon sensitive (Valente et al., 1998). Also revealed was the fact that the surface monitoring network failed to document the maximum surface O_3 concentrations. Thus, monitoring networks, especially in medium-sized urban areas under slow transport conditions, may underestimate the magnitude and frequency of urban O_3 concentrations greater than 120 ppb.

Nunnermacker et al. (1998) used both aircraft and surface data from SOS to perform a detailed kinetic analysis of the chemical evolution of the Nashville urban plume. The analysis revealed OH concentrations around 1.2×10^7 cm^{-3} that consumed 50% of the NO_x within approximately 2 hours, at an OPE of 2.5 to 4 molecules for each molecule of NO_x. Anthropogenic hydrocarbons provided approximately 44% of the fuel for O_3 production by the urban plume.

Surface and aircraft observations of O_3 and O_3 precursors were compared during SOS to assess the degree to which mid-day surface measurements may be considered representative of the larger planetary boundary layer (PBL) (Luke et al., 1998). Overall agreement between surface and aircraft O_3 measurements was excellent in the well-developed mixed layer ($r^2 = 0.96$), especially in rural-regional background air and under stagnant conditions, where surface concentrations change only slowly. Vertical variations in trace gas concentrations were often minimal in the well-mixed PBL, and measurements at the surface always agreed well with aircraft observations up to the level of measurements (460 m above ground level). Under conditions of rapidly varying surface concentrations (e.g., during episodes of power plant plume fumigation and early morning boundary layer development), agreement between surface and aloft was dependent upon the spatial (aircraft) and temporal (ground) averaging intervals used in the comparison. Under these conditions, surface sites were representative of the PBL only to within a few kilometers horizontally.

On four days during SOS, air samples were taken in the plume of the Cumberland Power Plant in central Tennessee using an instrumented helicopter to investigate the evolution of photochemical smog (Luria et al., 1999, 2000). Twelve crosswind air-sampling traverses were made between 35 and 116 km from this Power Plant on 16 July 1995. Winds, from the west-northwest during the sampling period, directed the plume toward Nashville. Ten of the traverses were performed upwind of Nashville, where the plume was isolated, and two were made downwind of the city. The results indicated that even six hours after the plume left the stacks, excess O_3 production was limited to the edges of the plume. Excess O_3 production within the plume was found to vary from 20 ppb up to 55 ppb. It was determined that this variation corresponded to differences in ambient isoprene levels. Excess O_3 (up to 109 ppbv, 50 to 60 ppbv above background), was produced in the center of the plume when there was sufficient mixing upwind of Nashville. The power plant plume apparently mixed with the urban plume also, producing O_3 up to 120 ppbv 15 to 25 km downwind of Nashville.

Nunnermacker et al. (2000) used data from the DOE G-1 aircraft to characterize emissions from a small power plant plume (Gallatin) and a large power plant plume (Paradise) in the Nashville region. Observations made on July 3, 7, 15, 17, and 18, 1995, were compiled, and a kinetic analysis of the chemical evolution of the power plant plumes was performed. OPEs were found to be 3 in the Gallatin and 2 in the Paradise plumes. Lifetimes for NO_x (2.8 and 4.2 hours) and NO_y (7.0 and 7.7 hours) were determined in the Gallatin and Paradise plumes, respectively. These NO_x and NO_y lifetimes imply rapid loss of NO_z (assumed to be primarily HNO_3), with a lifetime determined to be 3.0 and 2.5 hours for the Gallatin and Paradise plumes, respectively.

AX2.4.1.2 Results from Studies on Biogenic and Anthropogenic Hydrocarbons and Ozone Production

Williams et al. (1997) made the first airborne measurements of peroxy-methacrylic nitric anhydride (MPAN), which is formed from isoprene-NO_x chemistry and is an indicator of recent O_3 production from isoprene and therefore biogenic hydrocarbons (BHC). They also measured peroxyacetic nitric anhydride (PAN), peroxypropionic nitric anhydride (PPN), and O_3 to estimate the contributions of anthropogenic hydrocarbons (AHC) and BHC to regional tropospheric O_3 production.

Airborne measurements of MPAN, PAN, PPN, and O_3 were made during the 1994 and 1995 Nashville intensive studies of SOS to determine the fraction of O_3 formed from anthropogenic NO_x and BHC (Roberts et al., 1998). It was found that PAN, a general product of hydrocarbon-NO_x photochemistry, could be well represented as a simple linear combination of contributions from BHC and AHC as indicated by MPAN and PPN, respectively. The PAN/MPAN ratios, characteristic of BHC-dominated chemistry, ranged from 6 to 10. The

PAN/PPN ratios, characteristic of AHC-dominated chemistry, ranged from 5.8 to 7.4. These ratios were used to estimate the contributions of AHC and BHC to regional tropospheric O_3 production. It was estimated that substantial O_3 (50 to 60 ppbv) was produced from BHC when high NO_x from power plants was present in areas of high BHC emission.

AX2.4.1.3 Results of Studies on Ozone Production in Mississippi and Alabama

Aircraft flights made in June 1990 characterized the variability of O_3 and reactive nitrogen in the lower atmosphere over Mississippi and Alabama. The variety and proximity of sources and the photochemical production and loss of O_3 were found to be contributing factors (Ridley et al., 1998). Urban, biomass burning, electrical power plant, and paper mill plumes were all encountered during these flights. Urban plumes from Mobile, AL had OPEs as high as 6 to 7 ppbv O_3 per ppbv of NO_x. Emissions measured from biomass burning had lower efficiencies of 2 to 4 ppbv O_3 per ppbv of NO_x, but the average rate of production of O_3 was as high as 58 ppbv hr^{-1} for one fire where the plume was prevented from vertical mixing. Near-source paper mill and power plant plumes showed O_3 titration, while far-field observations of power plant plumes showed net O_3 production. Early morning observations below a nocturnal inversion provided evidence for the nighttime oxidation of NO_x to reservoir species.

Aircraft measurements of O_3 and oxides of nitrogen were made downwind of Birmingham, AL to estimate the OPE in the urban plume (Trainer et al., 1995). NO_x emission rates were estimated at 0.6 x 10^{25} molecules s^{-1} with an uncertainty of a factor of 2. During the summertime it was determined that approximately 7 O_3 molecules could be formed for every molecule of NO_x emitted by the urban and proximately located power plant plumes. The regional O_3, the photochemical production of O_3 during the oxidation of the urban emissions, and wind speed and direction all combined to dictate the magnitude and location of the peak O_3 concentrations observed in the vicinity of the Birmingham metropolitan area.

Aircraft observations of rural U.S. coal-fired power plant plumes in the middle Mississippi and Tennessee Valleys were used to quantify the nonlinear dependence of tropospheric O_3 formation on plume NO_x concentration, determined by plant NO_x emission rate and atmospheric dispersion (Ryerson et al., 2001). The ambient availability of reactive VOC's, primarily biogenic isoprene, was also found to affect O_3 production rate and yield in these rural plumes. Plume O_3 production rates and yields as a function of NO_x and VOC concentrations differed by a factor of 2 or more. These large differences indicate that power plant NO_x emission rates and geographic locations play a large role in tropospheric O_3 production.

AX2.4.1.4 The Nocturnal Urban Plume Over Portland, Oregon

Aircraft observations of aerosol surface area, O_3, NO_y and moisture were made at night in the Portland, Oregon urban plume (Berkowitz et al., 2001). Shortly after sunset, O_3, relative humidity, NO_y and aerosol number density were all positively correlated. However, just before dawn, O_3 mixing ratios were highly anti-correlated with aerosol number density, NO_y and relative humidity. Back-trajectories showed that both samples came from a common source to the northwest of Portland. The pre-dawn parcels passed directly over Portland, while the other parcels passed to the west of Portland. Several hypotheses were put forward to explain the loss of O_3 in the parcels that passed over Portland, including homogeneous gas-phase mechanisms and a heterogeneous mechanism on the aerosol particle surface.

AX2.4.1.5 Effects of VOC's in Houston on Ozone Production

Aircraft Observations of O_3 and O_3 precursors over Houston, TX, Nashville, TN; New York, NY; Phoenix, AZ, and Philadelphia, PA showed that despite similar NO_x concentrations, high concentrations of VOC's in the lower atmosphere over Houston led to calculated O_3 production rates that were 2 to 5 times higher than in the other 4 cities (Kleinman et al., 2002). Concentrations of VOC's and O_3 production rates are highest in the Ship Channel region of Houston, where one of the largest petrochemical complexes in the world is located. As a result, Houston lays claim to the highest recorded hourly average O_3 concentrations in the United States within the last 5 years (in excess of 250 ppb).

AX2.4.1.6 Chemical and Meteorological Influences on the Phoenix Urban Ozone Plume

The interaction of chemistry and meteorology for western cities can contrast sharply with that of eastern cities. A 4-week field campaign in May and June of 1998 in the Phoenix area comprised meteorological and chemical measurements (Fast et al., 2000). Data from models and observations revealed that heating of the higher terrain north and east of Phoenix produced regular, thermally driven circulations during the afternoon from the south and southwest through most of the boundary layer, advecting the urban O_3 plume to the northeast. Deep mixed layers and moderate winds aloft ventilated the Phoenix area during the study period so that multi-day buildups of locally produced O_3 did not appear to contribute significantly to O_3 levels. Sensitivity simulations estimated that 20% to 40% of the afternoon surface O_3 mixing ratios (corresponding to 15 to 35 ppb) was due to the entrainment of O_3 reservoirs into the growing convective boundary layer. The model results also indicated that O_3 production in this arid region is NO_x-saturated, unlike most eastern U.S. sites.

AX2.4.1.7 Transport of Ozone and Precursors on the Regional Scale

Instrumented aircraft flights by the University of Maryland in a Cessna 172 and Sonoma Technology, Inc. in a Piper Aztec measured the vertical profiles of trace gases and meteorological parameters in Virginia, Maryland, and Pennsylvania on July 12 – 15, 1995 during a severe O_3 episode in the mid-Atlantic region (Ryan et al., 1998). Ozone measured upwind of the urban centers reached 80 to 110 ppbv. Layers of high O_3 aloft were associated with local concentration maxima of SO_2 and NO_y, but not CO or NO_x. This, together with a back trajectory analysis, implicated coal-fired power plants in the industrialized Midwest as the source of the photochemically aged air in the upwind boundary of the urban centers. When the PBL over the Baltimore-Washington area deepened, the O_3 and O_3 precursors that had been transported from the west and northwest mixed with the local emissions and O_3 in excess of 125 ppbv was measured at the surface.

During the blackout of August 14, 2003 Marufu et al. (2004) measured profiles of ozone, SO_2 and CO over areas in western Pennsylvania, Maryland and Virginia. They found notable decreases in O_3, SO_2, and NO_x, over areas affected by the blackout but not over those that were not affected. They also found that CO concentrations aloft were comparable over areas affected and not affected by the blackout. They attributed the differences in concentrations between what was observed and what was expected to the reduction in emissions from power plants mainly in the Ohio Valley. They also reasoned that the CO concentrations were relatively unaffected because they arise from traffic emissions, which may have been largely unaffected by the blackout. However, the blackout also disrupted many industries, small scale emission sources, and rail and air transportation.

The Department of Energy G-1 aircraft flew in the New York City metropolitan area in the summer of 1996 as part of the North American Research Strategy for Tropospheric

Ozone-Northeast effort to ascertain the causes leading to high O_3 levels in the northeastern United States (Kleinman et al., 2000). Ozone, O_3 precursors, and other photochemically active trace gases were measured upwind and downwind of New York City to characterize the O_3 formation process and its dependence on NO_x and VOCs. During two flights, the wind was south southwesterly and O_3 levels reached 110 ppb. On two other flights, the wind was from the north-northwest and O_3 levels were not as high. When the G-1 observed O_3 around 110 ppb, the NO_x/NO_y ratio measured at the surface was between 0.20 and 0.30, indicating an aged plume.

AX2.4.1.8 Model Calculations and Aircraft Observations of Ozone Over Philadelphia

Regional-scale transport and local O_3 production over Philadelphia was estimated using a new meteorological-chemical model (Fast et al., 2002). Surface and airborne meteorological and chemical measurements made during a 30-day period in July and August of 1999 as part of the Northeast Oxidant and Particulate Study were used to evaluate the model performance. Both research aircraft and ozonesondes, during the morning between 0900 and 1100 LST, measured layers of O_3 above the convective boundary layer. The model accounted for these layers through upwind vertical mixing the previous day, subsequent horizontal transport aloft, and NO titration of O_3 within the stable boundary layer at night. Entrainment of the O_3 aloft into the growing convective boundary contributed to surface O_3 concentrations. During the study period, most of the O_3 appeared to result from local emissions in the vicinity of Philadelphia and the Chesapeake Bay area, but during high O_3 episodes, up to 30 to 40% of the O_3 was due to regional transport from upwind sources.

AX2.4.1.9 The Two-Reservoir System

Studies described above and aircraft observations made in August 2002 over the mid-Atlantic region show that a two-reservoir system illustrated schematically in Figure AX2-18 may realistically represent both the dynamics and photochemistry of severe, multi-day haze and O_3 episodes over the eastern United States (Taubman et al., 2004). The first reservoir is the PBL, where most precursor species are injected, and the second is the lower free troposphere (LFT), where photochemical processes are accelerated and removal via deposition is rare. Bubbles of air lifted from urban and industrial sources were rich in CO and SO_2, but not O_3, and contained greater numbers of externally mixed primary sulfate and black carbon (BC) particles.

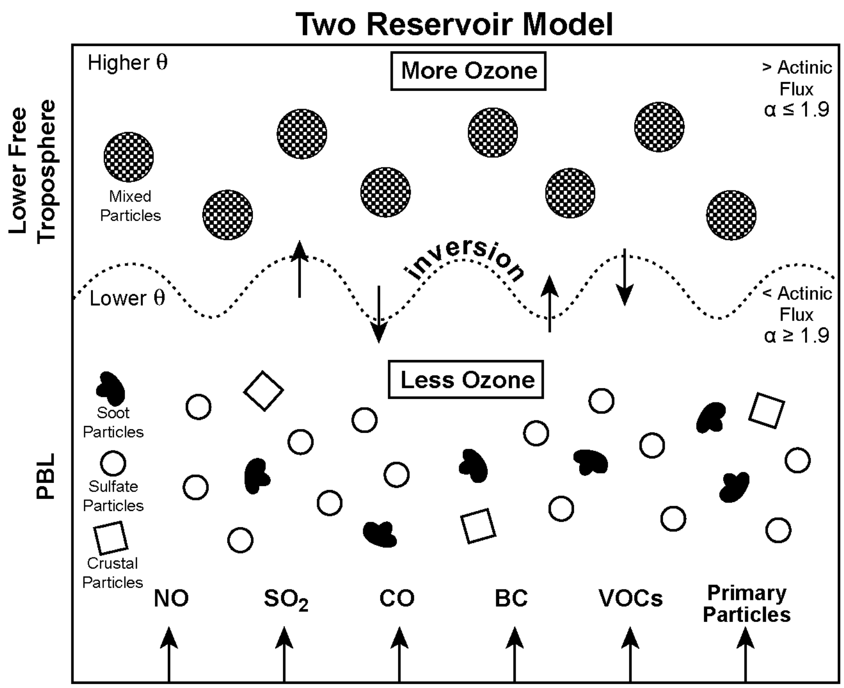

Figure AX2-18. Conceptual two-reservoir model showing conditions in the PBL and in the lower free troposphere during a multi-day ozone episode. The dividing line, the depth of the mixed layer, is about 1000 m. Emissions occur in the PBL, where small, unmixed black carbon, sulfate, and crustal particles in the $PM_{2.5}$ size range are also shown. Ozone concentrations as well as potential temperature (θ) and actinic flux are lower in the PBL than in the lower free troposphere, while RH is higher. Larger, mixed sulfate and carbonaceous particles (still in the $PM_{2.5}$ size range) and more ozone exist in the lower free troposphere.

Source: Taubman et al. (2004).

Correlations among O_3, air parcel altitude, particle size, and relative humidity suggest that greater O_3 concentrations and relatively larger particles are produced in the LFT and mix back down into the PBL. Backward trajectories indicated source regions in the Midwest and mid-Atlantic urban corridor, with southerly transport up the urban corridor augmented by the Appalachian lee trough and nocturnal low-level jet (LLJ). This concept of two-reservoirs may facilitate the numerical simulation of multiday events in the eastern United States. A relatively small number of vertical layers will be required if accurate representation of the sub-gridscale transport can be parameterized to represent the actual turbulent exchange of air between the PBL and lower free troposphere.

AX2.5 METHODS USED TO CALCULATE RELATIONS BETWEEN OZONE AND ITS PRECURSORS

Atmospheric chemistry and transport models are the major tools used to calculate the relations between O_3, its precursors, and other oxidation products. Other techniques, involving statistical relations between O_3 and other variables have also been used. Chemistry-transport models (CTM) are driven by emissions inventories for O_3 precursor compounds and by meterological fields. Emissions of precursor compounds can be divided into anthropogenic and natural source categories. Natural sources can be further divided into biotic (vegetation, microbes, animals) and abiotic (biomass burning, lightning) categories. However, the distinction between natural sources and anthropogenic sources is often difficult to make as human activities affect directly, or indirectly, emissions from what would have been considered natural sources during the pre-industrial era. Emissions from plants and animals used in agriculture are usually referred to as anthropogenic. Wildfire emissions may be considered natural, except that forest management practices may have led to the buildup of fuels on the forest floor, thereby altering the frequency and severity of forest fires. Needed meteorological quantities such as winds and temperatures are taken from operational analyses, reanalyses, or circulation models. In most cases, these are off-line analyses, i.e., they are not modified by radiatively active species such as O_3 and particles generated by the model.

A brief overview of atmospheric chemistry-transport models is given in Section AX2.5.1. A discussion of emissions inventories of precursors that are used by these models is given in Section AX2.5.2. Uncertainties in emissions estimates have also been discussed in Air Quality Criteria for Particulate Matter (U.S. Environmental Protection Agency, 2000). So-called ‘observationally based models’ which rely more heavily on observations of the concentrations of important species are discussed in Section AX2.5.3. Chemistry-transport model evaluation and an evaluation of the reliability of emissions inventories are presented in Section AX2.5.4.

AX2.5.1 Chemistry-Transport Models

Atmospheric chemistry-transport models (CTMs) are used to obtain better understanding of the processes controlling the formation, transport, and destruction of O_3 and other air pollutants; to understand the relations between O_3 concentrations and concentrations of its precursors such as NO_x and VOCs; and to understand relations among the concentration patterns of O_3 and other oxidants that may also exert health effects. Detailed examination of the concentrations of short-lived species in a CTM can provide important insights into how O_3 is formed under certain conditions and can suggest likely avenues for data analysis and future experiments and field campaigns. The dominant processes leading to the formation of O_3 in a particular time period (e.g., whether NO_x or VOCs were more important, the influence of meteorology, and the influence of emissions from a particular geographic region) and the transformation or formation of other pollutants that would not be possible in an experiment or even the most intensive field campaign could be examined using a CTM. As such, CTMs could play a major role in the interpretation of experimental results by allowing selected aspects of atmospheric chemistry to be examined on a scale not feasible in laboratory or in field experiments.

CTMs are also used for determining control strategies for O_3 precursors. However, this application has met with varying degrees of success because of the highly nonlinear relations between O_3 and emissions of its precursors. CTMs include mathematical descriptions of atmospheric transport, emissions, the transfer of solar radiation through the atmosphere, chemical reactions, and removal to the surface by turbulent motions and precipitation for chemical species of interest. Increasingly, the trend is for these processes to be broken down and handled by other models or sub-models, so a CTM will likely use emissions and meteorological data from at least two other models.

There are two major formulations of CTMs in current use. In the first approach, grid-based, or Eulerian, air quality models, the region to be modeled (the modeling domain) is subdivided into a three-dimensional array of grid cells. Spatial derivatives in the species continuity equations are cast in finite-difference form over this grid, and a system of equations for the concentrations of all the chemical species in the model are solved numerically at each grid point. The modeling domain may be limited to a particular airshed or provide global coverage and extend through several major atmospheric layers. Time dependent continuity (mass conservation) equations are solved for each species including terms for transport, chemical production and destruction, and emissions and deposition (if relevant), in each cell. Chemical processes are simulated with ordinary differential equations, and transport processes are simulated with partial differential equations. Because of a number of factors such as the different time scales inherent in different processes, the coupled, nonlinear nature of the chemical process terms, and computer storage limitations all of the terms in the equations cannot be solved simultaneously in three dimensions. Instead, a technique known as operator splitting, in which terms involving individual processes are solved sequentially, is used. In the second application of CTMs, trajectory or Lagrangian models, a large number of hypothetical air parcels are specified as following wind trajectories. In these models, the original system of partial differential equations is transformed into a system of ordinary differential equations.

A less common approach is to use a hybrid Lagrangian/Eulerian model, in which certain aspects of atmospheric chemistry and transport are treated with a Lagrangian approach and others are treaded in a Eulerian manner (e.g., Stein et al., 2000). Both modeling approaches have their advantages and disadvantages. The Eulerian approach is more general in that it includes processes that mix air parcels and allows integrations to be carried out for long periods during which individual air parcels lose their identity. There are, however, techniques for including the effects of mixing in Lagrangian models such as FLEXPART (e.g., Zanis et al., 2003), ATTILA (Reithmeir and Sausen, 2002), and CLaMS (McKenna et al., 2002).

Major modeling efforts within the U.S. Environmental Protection Agency center on the Models3/Community Modeling for Air Quality (CMAQ, Byun et al., 1998) and the Multi Scale Air Quality Simulation Platform (MAQSIP, Odman and Ingram, 1996) whose formulations are based on the regional acid deposition model (RADM, Chang et al., 1987). A number of other modeling platforms using the Lagrangian and Eulerian frameworks have been reviewed in AQCD 96. CTMs currently in use are summarized in the review by Russell and Dennis (2000). The domains of MAQSIP and CMAQ are flexible and can extend from several hundred km to the hemispherical scale. In addition, both of these classes of models allow the resolution of the calculations over specified areas to vary. CMAQ and MAQSIP are both driven by the MM5 mesoscale meteorological model (Seaman, 2000 and references therein), though both may be driven by other meteorological models (e.g., RAMS and Eta). Simulations of regional O_3 episodes have been performed with a horizontal resolution of 4 km. In principle, calculations over limited domains can be accomplished to even finer scales. However, simulations at these higher resolutions require better parameterizations of meteorological processes such as boundary layer fluxes, deep convection and clouds (Seaman, 2000), and knowledge of emissions. Resolution at finer scales will likely be necessary to resolve smaller-scale features such as the urban heat island; sea, bay, and land breezes; and the nocturnal low-level jet.

Currently, the most common approach to setting up the horizontal domain is to nest a finer grid within a larger domain of coarser resolution. However, a number of other strategies are currently being developed, such as the stretched grid (e.g., Fox-Rabinowitz et al., 2002) and the adaptive grid. In a stretched grid, the grid's resolution continuously varies throughout the domain, thereby eliminating any potential problems with the sudden change from one resolution to another at the boundary. One must be careful in using such a formulation, because certain parameterizations that are valid on a relatively coarse grid scale (such as convection, for example) are not valid or should not be present on finer scales. Adaptive grids are not set at the start of the simulation, but instead adapt to the needs of the simulation as it evolves (e.g., Hansen et al., 1994). They have the advantage that, if the algorithm is properly set up, the resolution is always sufficient to resolve the process at hand. However, they can be very slow if the situation to be modeled is complex. Additionally, if one uses adaptive grids for separate meteorological, emissions, and photochemical models, there is no reason a priori why the resolution of each grid should match; and the gains realized from increased resolution in one model will be wasted in the transition to another model. The use of finer and finer horizontal resolution in the photochemical model will necessitate finer-scale inventories of land use and better knowledge of the exact paths of roads, locations of factories, and, in general, better methods for locating sources. The present practice of locating a source in the middle of a county or distributing its emissions throughout a county if its location is unknown will likely not be adequate in the future.

The vertical resolution of these models continues to improve as more layers are added to capture atmospheric processes and structures. This trend will likely continue because a model with 25 vertical layers, for example, may have layers that are 500 m thick at the top of the planetary boundary layer. Though the boundary layer height is generally determined through other methods, the chemistry in the model is necessarily confined by such layering schemes. Because the height of the boundary layer is of critical importance in simulations of air quality, improved resolution of the boundary layer height would likely improve air quality simulations.

The difficulty of properly establishing the boundary layer height is most pronounced when considering tropopause folding events, which are important in determining the chemistry of the background atmosphere. In the vicinity of the tropopause, the vertical resolution of most any large scale model is quite unlikely to be able to capture such a feature. Additionally, any current model is likely to have trouble adequately resolving fine scale features such as the low level jet. Finally, models must be able to treat emissions, meteorology, and photochemistry differently in different areas. Emissions models are likely to need better resolution near the surface and possibly near any tall stacks. Photochemical models, on the other hand, may need better resolution away from the surface and be more interested in resolving the planetary boundary layer height, terrain differences, and other higher altitude features. Meteorological models share some of the concerns of photochemical models, but are less likely to need sufficient resolution to adequately treat a process such as dry deposition beneath a stable nocturnal boundary layer. Whether the increased computational power necessary for such increases in resolution will be ultimately justified by improved results in the meteorological and subsequent photochemical simulations remains to be seen.

CTMs require time dependent, three-dimensional wind fields for the time period of simulation. The winds may be either generated by a model using initial fields alone or four dimensional data assimilation can be used to improve the model's meteorological fields (i.e., model equations can be updated periodically [or "nudged'] to bring results into agreement with observations). Most modeling efforts have focused on simulations of several days duration (a typical time scale for individual O_3 episodes), but there have been several attempts at modeling longer periods. For example, Kasibhatla and Chameides (2000) simulated a four month period from May to September of 1995 using MAQSIP. The current trend appears to be toward simulating longer time periods. This will impose additional strains on computational resources, as most photochemical modeling until recently has been performed with an eye toward simulating only summertime episodes of peak O_3. With the shift toward modeling an entire year being driven by the desire to understand observations of periods of high wintertime PM (e.g., Blanchard et al., 2002), models will be further challenged to simulate air quality under conditions for which they may not have been used previously.

Chemical kinetics mechanisms (a set of chemical reactions) representing the important reactions that occur in the atmosphere are used in air quality models to estimate the net rate of formation of each pollutant simulated as a function of time. Chemical mechanisms that explicitly treat the chemical reactions of each individual reactive species are too lengthy and demanding of computer resources to be incorporated into three-dimensional atmospheric models. As an example, a master chemical mechanism includes approximately 10,500 reactions involving 3603 chemical species (Derwent et al., 2001 and references therein). Instead, "lumped" mechanisms, that group compounds of similar chemistry together, are used. The chemical mechanisms used in existing photochemical O_3 models contain significant uncertainties that may limit the accuracy of their predictions; the accuracy of each of these mechanisms is also limited by missing chemistry. Because of different approaches to the lumping of organic compounds into surrogate groups, chemical mechanisms, can produce somewhat different results under similar conditions. The CB-IV chemical mechanism (Gery et al., 1989), the RADM II mechanism (Stockwell et al., 1990), the SAPRC (e.g., Wang et al., 2000a; Wang et al., 2000b; Carter, 1990) and the RACM mechanisms can be used in CMAQ. Jimenez et al. (2003) provide brief descriptions of the features of the main mechanisms in use and they compared concentrations of several key species predicted by seven chemical mechanisms in a box model simulation over 24 h. The average deviation from the average of all mechanism predictions for O_3 and NO over the daylight period was less than 20%, and 10% for NO_2 for all mechanisms. However, much larger deviations were found for HNO_3, PAN, HO_2, H_2O_2, C_2H_4 and C_5H_8 (isoprene). An analysis for OH radicals was not presented. The large deviations shown for most species imply differences between the calculated lifetimes of atmospheric species and the assignment of model simulations to either NO_x limited or radical limited regimes between mechanisms. Gross and Stockwell (2003) found small differences between mechanisms for clean conditions with differences becoming more significant for polluted conditions, especially for NO_2 and organic peroxy radicals. They caution modelers to consider carefully the mechanisms they are using.

As CTMs incorporate more processes and knowledge of aerosol- and gas-phase chemistry improves, a "one atmosphere" approach is evolving. For example, CMAQ and PM-CAMx now incorporate some aerosol processes in its code PM-CAMx, and several attempts are currently underway to incorporate chemistry into meteorological models, usually MM5 (e.g., Grell et al., 2000; Liu et al., 2001; Lu et al., 1997 and Park et al., 2001) to examine feedbacks on meteorological processes. This coupling is necessary for cases such as the heavy aerosol loading found in forest fire plumes (Lu et al., 1997 and Park et al., 2001).

Spatial and temporal characterizations of anthropogenic and biogenic precursor emissions must be specified as inputs to a CTM. Emissions inventories have been compiled on grids of varying resolution for many hydrocarbons, aldehydes, ketones, CO, NH_3, and NO_x. Emissions inventories for many species require the application of some algorithm for calculating the dependence of emissions on physical variables such as temperature. For many species, information concerning the temporal variability of emissions is lacking, so long term (e.g., annual or O_3-season) averages are used in short term, episodic simulations. Annual emissions estimates are often modified by the emissions model to produce emissions more characteristic of the time of day and season. Significant errors in emissions can occur if an inappropriate time dependence or a default profile is used. Additional complexity arises in model calculations because different chemical mechanisms are based on different species, and inventories constructed for use with another mechanism must be adjusted to reflect these differences. This problem also complicates comparisons of the outputs of these models because one chemical mechanism will necessarily produce species that are different from those in another and neither output will necessarily agree with the measurements.

The effects of clouds on atmospheric chemistry are complex and introduce considerable uncertainty into CTM calculations. Thunderstorm clouds are optically very thick and have major effects on radiative fluxes and thus on photolysis rates. Madronich (1987) provided modeling estimates of the effects of clouds of various optical depths on photolysis rates. In the upper portion of a thunderstorm anvil, photolysis is likely to be enhanced (as much as a factor of 2 or more) due to multiple reflections off the ice crystals. In the lower portion of the cloud and beneath the cloud, photolysis is substantially decreased. Thunderstorm updrafts, which contain copious amounts of water, are regions where efficient scavenging of soluble species occurs (Balkanski et al., 1993). Direct field measurements of the amounts of specific trace gases scavenged in observed storms are sparse. Pickering et al. (2001) used a combination of model estimates of soluble species that did not include wet scavenging and observations of these species from the upper tropospheric outflow region of a major line of convection observed near Fiji. Over 90% of the nitric acid and hydrogen peroxide in the outflow air appeared to have been removed by the storm. Walcek et al. (1990) included a parameterization of cloud-scale aqueous chemistry, scavenging, and vertical mixing in the regional scale, chemistry-transport model of Chang et al. (1987). The vertical distribution of cloud microphysical properties and the amount of subcloud-layer air lifted to each cloud layer were determined using a simple entrainment hypothesis (Walcek and Taylor, 1986). Vertically-integrated O_3 formation rates over the northeastern United States were enhanced by ~50% when the in-cloud vertical motions were included in the model.

In addition to wet deposition, dry deposition (the removal of chemical species from the atmosphere by interaction with ground-level surfaces) is an important removal process for pollutants on both urban and regional scales and must be included in CTMs. The general approach used in most models is the three-resistance method, in which where dry deposition is parameterized with a deposition velocity, which is represented as $v_d = (r_a + r_b + r_c)^{-1}$ where r_a, r_b, and r_c represent the resistance due to atmospheric turbulence, transport in the fluid sublayer very near the elements of surface such as leaves or soil, and the resistance to uptake of the surface itself. This approach works for a range of substances although it is inappropriate for species with substantial emissions from the surface or for species whose deposition to the surface depends on its concentration at the surface itself. The approach is also modified somewhat for aerosols: the terms r_b and r_c are replaced with a surface deposition velocity to account for gravitational settling. In their review, Wesley and Hicks (2000) point out several shortcomings of current knowledge of dry deposition. Among those shortcomings are difficulties in representing dry deposition over varying terrain where horizontal advection plays a significant role in determining the magnitude of r_a and difficulties in adequately determining a deposition velocity for extremely stable conditions such as those occurring at night (e.g., Mahrt, 1998). Under the best of conditions, when a model is exercised over a relatively small area where dry deposition measurements have been made, models still commonly show uncertainties at least as large as ± 30% (e.g., Massman et al., 1994; Brook et al., 1996; Padro, 1996). Wesley and Hicks (2000) state that an important result of these comparisons is that the current level of sophistication of most dry deposition models is relatively low and relies heavily on empirical data. Still larger uncertainties exist when the surface features are not well known or when the surface comprises a patchwork of different surface types, as is common in the eastern United States.

The initial conditions, i.e., the concentration fields of all species computed by a model, and the boundary conditions, i.e., the concentrations of species along the horizontal and upper boundaries of the model domain throughout the simulation must be specified at the beginning of the simulation. It would be best to specify initial and boundary conditions according to observations. However, data for vertical profiles of most species of interest are sparse. Ozonesonde data have been used to specify O_3 fields, but the initial and boundary values of many other species are often set equal to zero because of a lack of observations. Further, ozonesondes are thought to be subject to errors in measurement and differences arising from improper corrections for pump efficiency and the solutions used (e.g., Hilsenrath et al., 1986; Johnson et al., 2002). The results of model simulations over larger, preferably global, domains can also be used. As may be expected, the influence of boundary conditions depends on the lifetime of the species under consideration and the time scales for transport from the boundaries to the interior of the model domain (Liu et al., 2001).

Each of the model components described above has an associated uncertainty, and the relative importance of these uncertainties varies with the modeling application. The largest errors in photochemical modeling are still thought to arise from the meteorological and emissions inputs to the model (Russell and Dennis, 2000). Within the model itself, horizontal advection algorithms are still thought to be significant source of uncertainty (e.g., Chock and Winkler, 1994) though more recently those errors are thought to have been reduced (e.g., Odman et al., 1996). There are also indications that problems with mass conservation continue to be present in photochemical and meteorological models (e.g., Odman and Russell, 1999); these can result in significant simulation errors. Uncertainties in meteorological variables and emissions can be large enough that they would lead one to make the wrong decision when considering control strategies (e.g., Russell and Dennis, 2000; Sillman et al., 1995). The effects of errors in initial conditions can be minimized by including several days "spin-up" time in a simulation to allow species to come to chemical equilibrium with each other before the simulation of the period of interest begins.

While the effects of poorly specified boundary conditions propagate through the model's domain, the effects of these errors remain undetermined. Many regional models specify constant O_3 profiles (e.g., 35 ppb) at their lateral and upper boundaries; ozonesonde data, however, indicate that the mixing ratio of O_3 increases vertically in the troposphere (to over 100 ppb at the tropopause) and into the stratosphere (e.g., Newchurch et al., 2003). The practice of using constant O_3 profiles strongly reduces the potential effects of vertical mixing of O_3 from above the planetary boundary layer (via mechanisms outlined in Section AX2.3) on surface O_3 levels. The use of an O_3 climatology (e.g., Fortuin and Kelder, 1998) might reduce the errors that would otherwise be incurred. Because many meteorological processes occur on spatial scales which are smaller than the grid spacing (either horizontally or vertically) and thus are not calculated explicitly, parameterizations of these processes must be used and these introduce additional uncertainty.

Uncertainty also arises in modeling the chemistry of O_3 formation because it is highly nonlinear with respect to NO_x concentrations. Thus, the volume of the grid cell into which emissions are injected is important because the nature of O_3 chemistry (i.e., O_3 production or titration) depends in a complicated way on the concentrations of the precursors and the OH radical. The use of ever-finer grid spacing allows regions of O_3 titration to be more clearly separated from regions of O_3 production. The use of grid spacing fine enough to resolve the chemistry in individual power-plant plumes is too demanding of computer resources for this to be attempted in most simulations. Instead, parameterizations of the effects of subgrid scale processes such as these must be developed; otherwise serious errors can result if emissions are allowed to mix through an excessively large grid volume before the chemistry step in a model calculation is performed. In light of the significant differences between atmospheric chemistry taking place inside and outside of a power plant plume (e.g., Ryerson et al., 1998 and Sillman, 2000), inclusion of a separate, meteorological module for treating large, tight plumes is necessary. Because the photochemistry of O_3 and many other atmospheric species is nonlinear, emissions correctly modeled in a tight plume may be incorrectly modeled in a more dilute plume. Fortunately, it appears that the chemical mechanism used to follow a plume's development need not be as detailed as that used to simulate the rest of the domain, as the inorganic reactions are the most important in the plume (e.g., Kumar and Russell, 1996). The need to include explicitly plume-in-grid chemistry disappears if one uses the adaptive grid approach mentioned previously, though such grids are more computationally intensive. The differences in simulations are significant because they can lead to significant differences in the calculated sensitivity of O_3 to its precursors (e.g., Sillman et al., 1995).

Because the chemical production and loss terms in the continuity equations for individual species are coupled, the chemical calculations must be performed iteratively until calculated concentrations converge to within some preset criterion. The number of iterations and the convergence criteria chosen also can introduce error.

The importance of global transport of O_3 and its contribution to regional O_3 levels in the United States is slowly becoming apparent. There are presently on the order of 20 three-dimensional global models that have been developed by various groups to address problems in tropospheric chemistry. These models resolve synoptic meteorology, O_3-NO_x-CO-hydrocarbon photochemistry, wet and dry deposition, and parameterize sub-grid scale vertical mixing such as convection. Global models have proven useful for testing and advancing scientific understanding beyond what is possible with observations alone. For example, they can calculate quantities of interest that we do not have the resources to measure directly, such as export of pollution from one continent to the global atmosphere or the response of the atmosphere to future perturbations to anthropogenic emissions.

The finest horizontal resolution at which global simulations are typically conducted is ~200 km^2 although rapid advances in computing power continuously change what calculations are feasible. The next generation of models will consist of simulations that link multiple horizontal resolutions from the global to the local scale. Finer resolution will only improve scientific understanding to the extent that the governing processes are more accurately described at that scale. Consequently there is a critical need for observations at the appropriate scales to evaluate the scientific understanding represented by the models.

Observations of specific chemical species have been useful for testing transport schemes. Radon-222 simulations in sixteen global models have been evaluated with observations to show that vertical mixing is captured to within the constraints offered by the mean observed concentrations (Jacob et al., 1997). Tracers such as cosmogenic ^{7}Be and terrigenic ^{210}Pb have been used to test and constrain model transport and wet deposition (e.g., Liu et al., 2001).

Other chemical species obtained from various platforms (surface measurements, aircraft, satellites) are useful for evaluating the simulation of chemical and dynamical processing in global models. For example, Emmons et al. (2000) compiled available measurements of 12 species relevant to O_3 photochemistry from a number of aircraft campaigns in different regions of the world and used this data composite to evaluate two global models. They concluded that one model (MOZART) suffered from weak convection and an underestimate of nitrogen oxide emissions from biomass burning, while another model (IMAGES) transported too much O_3 from the stratosphere to the troposphere (Emmons et al., 2000). The global coverage available from satellite observations offers new information for testing models. Recent efforts are using satellite observations to evaluate the emission inventories of O_3 precursors that are included in global models; such observations should help to constrain the highly uncertain natural emissions of isoprene and nitrogen oxides (e.g., Palmer et al., 2003; Martin et al., 2003).

A comparison of numerous global chemistry-transport models developed by groups around the world was included in Section 4.4 of the recent report of the Intergovernmental Panel on Climate Change (Prather and Ehhalt, 2001). In that report, monthly mean O_3 (O_3) and carbon monoxide (CO) simulated by the various models was evaluated with O_3 observations from global ozonesonde stations at 700, 500, and 300 hPa and with surface CO measurements from 17 selected NOAA/CMDL sites. The relevant figures (Figures AX2-4-10 and AX2-4-11) are reproduced here (as Figures AX2-19 for O_3 and AX2-20 for CO) along with the references in their Table AX2-10 (as Table AX2-4). Overall, the models capture the general features of the O_3 and CO seasonal cycles but meet with varying levels of success at matching the observed concentrations and the amplitude of the observed seasonal cycle. For O_3, the models show less disagreement in the lower troposphere than in the upper troposphere, reflecting the difficulty of representing the exchange between the stratosphere and troposphere and the loose constraints on the net O_3 flux that are provided by observations.

An evaluation of five global models with data from the Measurement of Ozone and Water Vapor by Airbus In-Service Aircraft (MOZAIC) project over New York City and Miami indicates that the models tend to underestimate the summer maximum in the middle and lower troposphere over northern mid-latitude cities such as New York City and to underestimate the variability over coastal cities such as Miami which are strongly influenced by both polluted continental and clean marine air masses (Law et al., 2000). Local maxima and minima are difficult to reproduce with global models because processes are averaged over an entire model grid cell. Much of the spatial and temporal variability in surface O_3 over the United States is modulated by synoptic meteorology (e.g., Logan, 1989; Eder et al., 1993; Vukovich, 1995, 1997; Cooper and Moody, 2000) which is resolved in the current generation of global models. For example, an empirical orthogonal function analysis on observed and simulated fields over

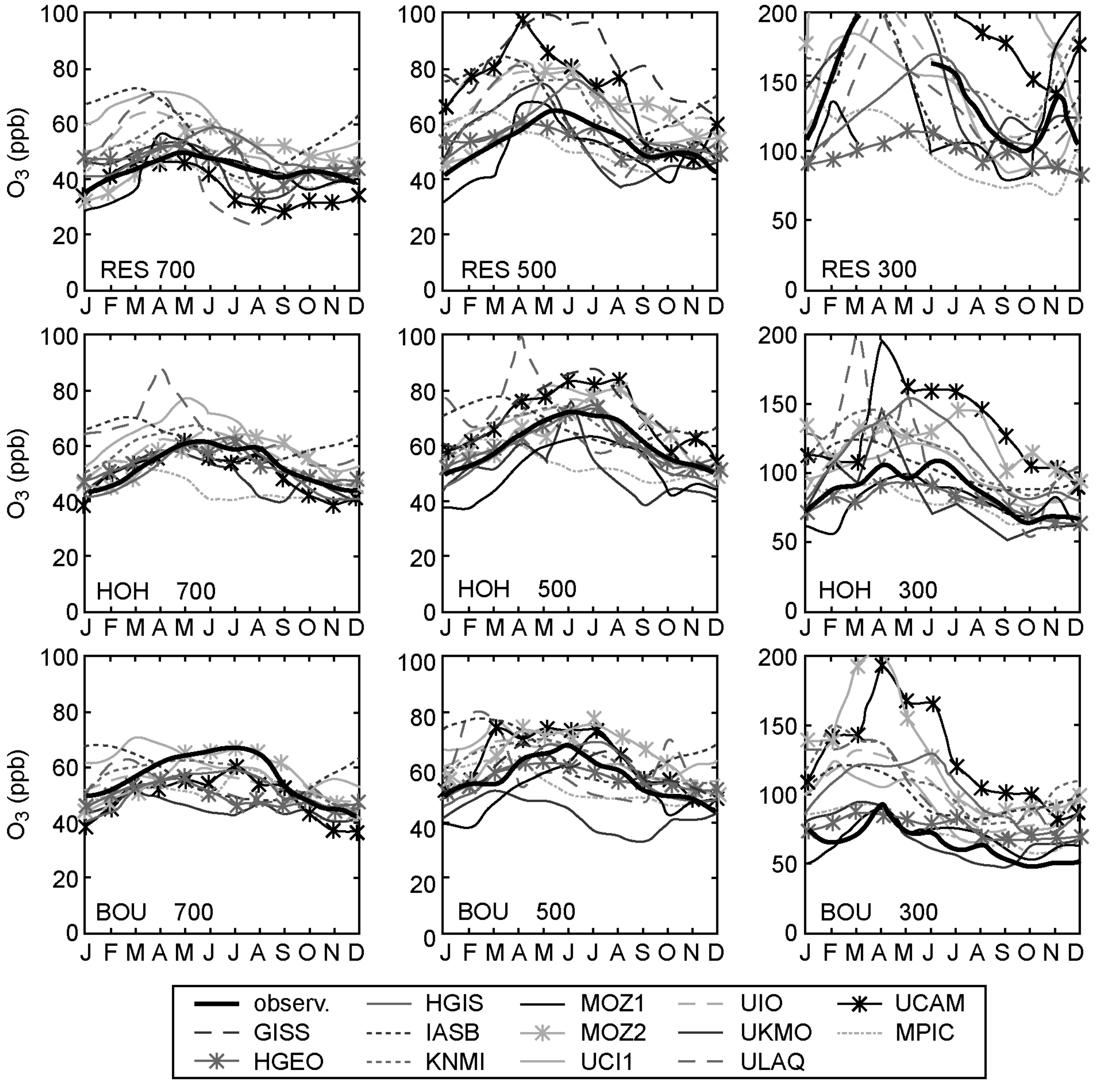

Figure AX2-19. Seasonal variability in ozone concentrations observed at a number of pressure surfaces at six ozonesonde sites and the predictions of 13 global scale chemistry-transport models.

Source: IPCC Third Assessment Report (2001).

the eastern United States in summer has shown that a 2° × 2.5° horizontal resolution global model (GEOS-CHEM) captures the synoptic-scale processes that control much of the observed variability (Fiore et al., 2003). Further evaluation of the same model showed that it can also

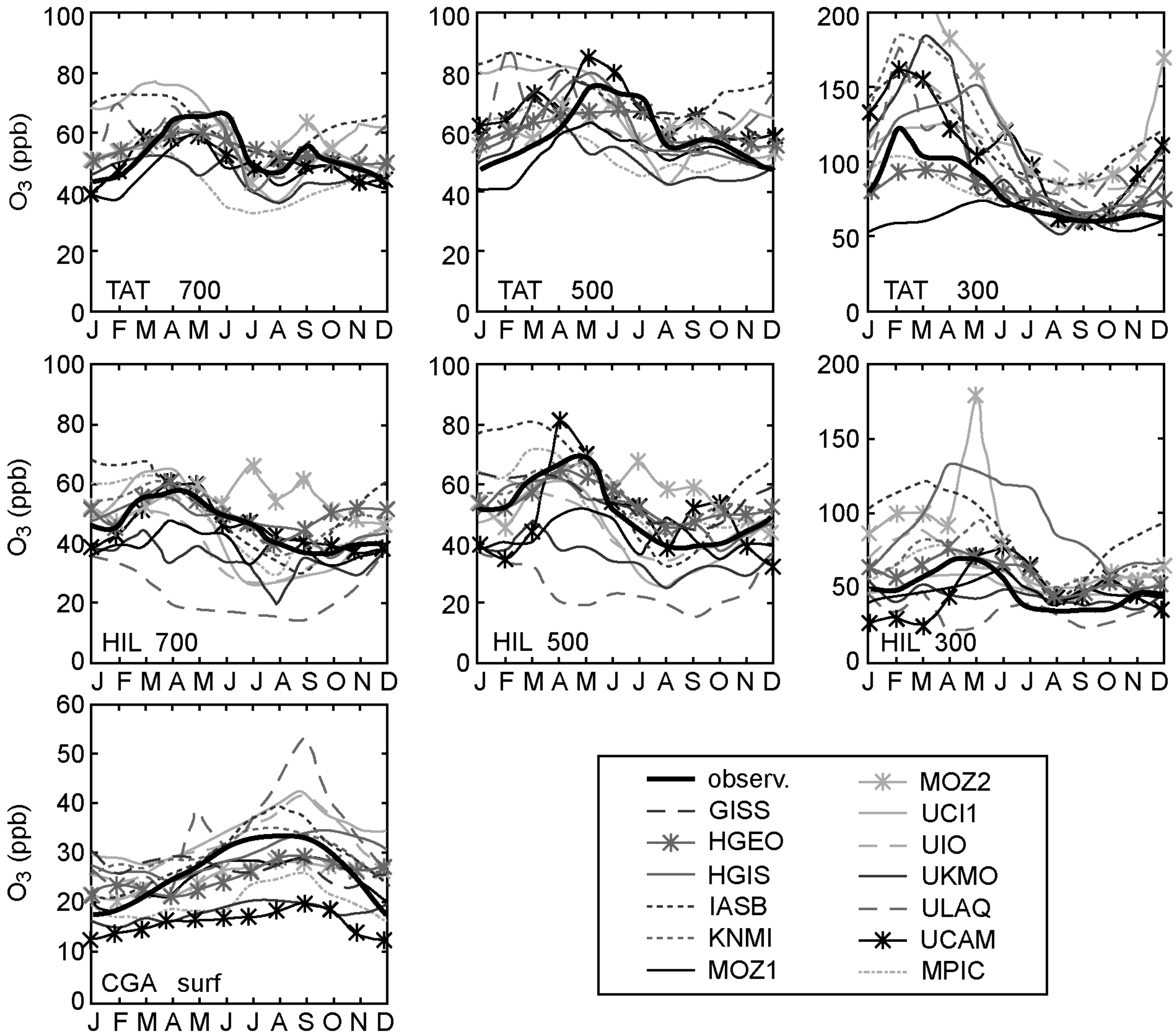

Figure AX2-20. Seasonal variability in ozone concentrations observed at a number of pressure surfaces at six ozonesonde sites and the predictions of 13 global scale chemistry-transport models.

Source: IPCC Third Assessment Report (2001).

capture many of the salient features of the observed distributions of O_3 as well as its precursors in surface air over the United States in summer, including formaldehyde concentrations and correlations between O_3 and the oxidation products of nitrogen oxides (O_3: NO_y-NO_x) , all of which indicate a reasonable photochemical simulation (Fiore et al., 2002).

Table AX2-4. Chemistry-Transport Models (CTM) Contributing to the Oxcomp Evaluation of Predicting Tropospheric O_3 and OH (Prather and Ehhalt, 2001)

CTM	Institute	Contributing Authors	References
GISS	GISS	Shindell/Grenfell	Hansen et al. (1997)
HGEO	Harvard U.	Bey/Jacob	Bey et al. (2001a)
HGIS	Harvard U.	Mickley/Jacob	Mickley et al. (1999)
IASB	IAS/Belg.	Müllller	Müller and Brasseur (1995, 1999)
KNMI	KNMI/Utrecht	van Weele	Jeuken et al. (1999), Houweling et al. (2000)
MOZ1	NCAR/CNRS	Hauglustaine/Brasseur	Brasseur et al. (1998), Hauglustaine et al. (1998)
MOZ2	NCAR	Horowitz/Brasseur	Brasseur et al. (1998), Hauglustaine et al.(1998)
MPIC	MPI/Chem	Kuhlmann/Lawrence	Crutzen et al. (1999), Lawrence et al. (1999)
UCI	UC Irvine	Wild	Hannegan et al. (1998), Wild and Prather (2000)
UIO	U. Oslo	Berntsen	Berntsen and Isaksen (1997), Fuglestvedt et al. (1999)
UIO2	U. Oslo	Sundet	Sundet (1997)
UKMO	UK Met Office	Stevenson	Collins et al. (1997), Johnson et al. (1999)
ULAQ	U. L. Aquila	Pitari	Pitari et al. (1997)
UCAM	U. Cambridge	Plantevin/Johnson (TOMCAT)	Law et al. (1998, 2000)

A significant amount of progress in evaluating the performance of three-dimensional global models with surface, aircraft, and satellite data has been made in recent years. Disagreement among model simulations mainly stems from differences in the driving meteorology and emissions. The largest discrepancies amongst models and between models and observations occur in the upper troposphere and likely reflect uncertainties in exchange between the stratosphere and troposphere and photochemical processes there; the models agree better with observations closer to the surface. Synoptic-scale meteorology is resolved in these models, enabling them to simulate much of the observed variability in pollutants in the lower troposphere.

AX2.5.2 Emissions of Ozone Precursors

Estimated annual emissions of nitrogen oxides, VOCs, CO, and NH_3 for 1999 (U.S. Environmental Protection Agency, 2001) are shown in Tables AX2-5, AX2-6, AX2-7, and AX2-8. Methods for estimating emissions of criteria pollutants, quality assurance procedures and examples of emissions calculated by using data are given in U.S. Environmental Protection Agency (1999).

Table AX2-5. Emissions of Nitrogen Oxides by Various Sources in the United States in 1999

Source	Emissions[1] (10^{12} g/y)	Notes
On-road vehicle exhaust	7.8	Gasoline (58%) and diesel (42%) vehicles.
Non-road vehicle exhaust	5	Diesel (49%) and gasoline (3%) vehicles; railroads (22%); marine vessels (18%); other sources (8%).
Fossil fuel combustion	9.1	Electric utilities (57%); industry (31%); commercial, institutional and residential combustion (12%).
Industrial Processes	0.76	Mineral products (43%); petrochemical products (17%); chemical mfg. (16%); metal processing (11%); misc. industries (12%).
Biomass burning	0.35	Residential wood burning (11%); open burning (8%); wildfires (81%).
Waste disposal	0.053	Non-biomass incineration.
Natural sources[2]	3.1	Lightning (50%); soils(50%).
Total	*26*	

[1]Emissions are expressed in terms of NO_2.
[2]Estimated on the basis of data given in Guenther et al. (2000).

Source: U.S. Environmental Protection Agency (2001).

Table AX2-6. Emissions of Volatile Organic Compounds by Various Sources in the United States in 1999

Source	Emissions (10^{12} g/y)	Notes
On-road vehicles	4.8	Exhaust and evaporative losses from gasoline (95%) and diesel (5%) vehicles.
Non-road vehicles	2.9	Exhaust and evaporative losses from gasoline (80%) and diesel (12%) vehicles; aircraft and other sources (8%).
Fossil fuel combustion	0.27	Electrical utilities; industrial, commercial, institutional, and residential sources.
Chemical industrial processes	0.36	Mfg. of organic chemicals, polymers and resins, and misc. products.
Petroleum industrial processes	0.39	Oil and gas production (64%); refining (36%).
Other industrial processes	0.48	Metal processing (15%); wood processing (32%); agricultural product processing (21%); misc. processes (18%).
Solvent volatilization	4.4	Surface coatings (44%); other industrial uses (20%); non-industrial uses (e.g., pesticide application, consumer solvents) (36%).
Storage and transport of volatile compounds	1.1	Evaporative losses from petroleum products and other organic compounds.
Biomass burning	1.2	Residential wood combustion (37%); open burning (22%); agricultural burning (22%); wildfires (19%).
Waste disposal	0.53	Residential burning (63%); waste water (23%); landfills (6%); non-biomass incineration (8%).
Biogenic sources[1]	4.4	Approximately 98% emitted by vegetation. (Isoprene [35%], monoterpenes [25%], and all other reactive and non-reactive compounds [40%]).
Total	*21*	

[1]Estimated on the basis of data given in Guenther et al. (2000).

Source: U.S. Environmental Protection Agency (2001).

Table AX2-7. Emissions of Ammonia by Various Sources in the United States in 1999

Source	Emissions (10^{12} g/y)	Notes
Exhaust from on-road and non-road engines and vehicles	0.25	Exhaust from on-road (96%) and non-road (4%) vehicles.
Fossil fuel combustion	0.044	Combustion by electric utilities, industry, commerce, institutions, residences.
Industry	0.18	Chemical manufacturing (67%); petroleum refining (9%); other industries (25%).
Agriculture	3.9	Livestock (82%); fertilizer application (18%).
Waste disposal and recycling	0.08	Wastewater treatment (99%).
Natural sources	0.032	Unmanaged soils; wild animals.
Total	*4.5*	

Source: U.S. Environmental Protection Agency (2001).

Emissions of nitrogen oxides associated with combustion arise from contributions from both fuel nitrogen and atmospheric nitrogen. Sawyer et al. (2000) have reviewed the factors associated with NO_x emissions by mobile sources. Estimates of NO_x emissions from mobile sources are generally regarded as fairly reliable although further work is needed to clarify this point (Sawyer et al., 2000). Both nitrifying and denitrifying bacteria in the soil can produce NO_x, mainly in the form of NO. Emission rates depend mainly on fertilization levels and soil temperature. About 60% of the total NO_x emitted by soils occurs in the central corn belt of the United States. The oxidation of NH_3, emitted mainly by livestock and soils, leads to the formation of NO. Estimates of emissions from natural sources are less certain than those from anthropogenic sources.

Natural sources of oxides of nitrogen include lightning, oceans, and soil. Of these, as reviewed in AQCD 96, only soil emissions appear to have the potential to impact surface O_3 over the U.S. On a global scale, the contribution of soil emissions to the oxidized nitrogen budget is on the order of 10% (van Aardenne et al., 2001; Finlayson-Pitts and Pitts, 2000; Seinfeld and Pandis, 1998), but attempts to quantify emissions of NO_x from fertilized fields show great variability. Soil NO emissions can be estimated from the fraction of the applied fertilizer

Table AX2-8. Emissions of Carbon Monoxide by Various Sources in the United States in 1999

Source	Emissions (10^{12} g/y)	Notes
On-road vehicle exhaust	50	Gasoline-fueled light-duty cars (54%) and trucks (32%), heavy-duty trucks (9%); diesel vehicles (5%); motorcycles (0.4%).
Non-road engines and vehicle exhaust	25	Gasoline-fueled (lawn and garden [44%], light commercial [17%], recreational [14%], logging [4%], industry and construction [6%, other [1%]); diesel-fueled (5%); aircraft (4%); other (5%).
Fossil fuel combustion	2	Electric utilities (22%); industry (58%); commercial, institutional and residential combustion (20%).
Industrial Processes	3.7	Metal processing (45%); chemical mfg. (29%); petrochemical production; (10%); mineral products (5%); wood products (10%); misc. industries (1%).
Biomass burning	16	Residential wood burning (21%); open burning (21%); agricultural burning (41%); wildfires (17%).
Waste disposal	0.42	Non-biomass incineration.
Other	0.19	Structural fires (45%); storage and transport (38%); misc. sources (17%).
Biogenic emssions[1]	4.7+	Primary emissions from vegetation and soils; secondary formation (?).
Total	*102+*	

[1]Estimated on the basis of data given in Guenther et al. (2000).

Source: U.S. Environmental Protection Agency (2001).

nitrogen emitted as NO_x, but the flux varies strongly with land use and temperature. The fraction nitrogen. Estimated globally averaged fractional applied nitrogen loss as NO varies from 0.3% (Skiba et al., 1997) to 2.5% (Yienger and Levy, 1995). Variability within biomes to which fertilizer is applied, such as shortgrass versus tallgrass prairie, accounts for a factor of three in uncertainty (Williams et al., 1992; Yienger and Levy, 1995; Davidson and Kingerlee, 1997).

The local contribution can be much greater than the global average, particularly in summer especially where corn is grown extensively. Williams et al. (1992) estimated that contributions from soils in Illinois contribute about 26% of the emissions from industrial and commercial processes in that State. In Iowa, Kansas, Minnesota, Nebraska, and South Dakota soil emissions may dominate. Conversion of ammonium to nitrate (nitrification) in aerobic soils appears to be the dominant pathway to NO. The mass and chemical form of nitrogen (reduced or oxidized) applied to soils, the vegetative cover, temperature, soil moisture, and agricultural practices such as tillage all influence the amount of fertilizer nitrogen released as NO.

As pointed out in the previous AQCD for O_3, emissions of NO from soils peak in summer when O_3 formation is at a maximum. A recent NRC report outlined the role of agricultural in emissions of air pollutants including NO and NH_3 (NRC, 2002). That report recommends immediate implementation of best management practices to control these emissions, and further research to quantify the magnitude of emissions and the impact of agriculture on air quality. Civerolo and Dickerson (1998) report that use of the no-till cultivation technique on a fertilized cornfield in Maryland reduced NO emissions by a factor of seven.

Annual global production of NO by lightning is the most uncertain source of reactive nitrogen. In the last decade literature values of the production rate range from 2 to 20 Tg-N per year. However, the most likely range is from 3 to 8 Tg-N per year, because the majority of the recent estimates fall in this range. The large uncertainty stems from several factors: (1) a large range of NO production rates per flash (as much as two orders of magnitude); (2) the open question of whether cloud-to-ground (CG) flashes and intracloud flashes (IC) produce substantially different amounts of NO; (3) the global flash rate; and (4) the ratio of the number of IC flashes to the number of CG flashes. Estimates of the amount of NO produced per flash have been made based on theoretical considerations (e.g., Price et al., 1997), laboratory experiments (e.g., Wang et al., 1998); field experiments (e.g., Stith et al., 1999; Huntrieser et al., 2002), and through a combination of cloud-resolving model simulations, observed lightning flash rates, and anvil measurements of NO (e.g., DeCaria et al., 2000). The latter method was also used by Pickering et al. (1998), who showed that only ~5% to 20% of the total NO production by lightning in a given storms exists in the boundary layer at the end of a thunderstorm. Therefore, the direct contribution to boundary layer O_3 production by lightning NO is thought to be small. However, lightning NO production can contribute substantially to O_3 production in the middle and upper troposphere. DeCaria et al. (2000) estimated that up to 7 ppbv of O_3 were produced in the upper troposphere in the first 24 hours following a Colorado thunderstorm due to the injection of lightning NO. A major uncertainty in mesoscale and global chemical transport models is the parameterization of lightning flash rates. Model variables such as cloud top height, convective precipitation rate, and upward cloud mass flux have been used to estimate flash rates. Allen and Pickering (2002) have evaluated these methods against observed flash rates from satellite, and examined the effects on O_3 production using each method.

Literally tens of thousands of organic compounds have been identified in plant tissues. However, most of these compounds either have sufficiently low volatility or are constrained so that they are not emitted in significant quantities. Less than 40 compounds have been identified by Guenther et al. (2000) as being emitted in large enough quantities to affect atmospheric composition. These compounds include terpenoid compounds (isoprene, 2-methyl-3-buten-2-ol, monoterpenes), compounds in the hexanal family, alkenes, aldehydes, organic acids, alcohols, ketones and alkanes. As can be seen from Table AX2-6, the major species emitted by plants are isoprene (35%), 19 other terpenoid compounds (25%) and 17 non-terpenoid compounds (40%) (Guenther et al., 2000). Of the latter, methanol contributes 12% of total emissions.

Because isoprene has been identified as the most abundant of biogenic VOCs (Guenther et al., 1995, 2000; Geron et al., 1994), it has been the focus of air quality model analyses in many published studies (Roselle, 1994; Sillman et al., 1995). The original Biogenic Emission Inventory System (BEIS) of Pierce et al. (1991) used a branch-level isoprene emission factor of 14.7 μg (g-foliar dry mass)$^{-1}$ h^{-1} for high isoprene emitting species (e.g., oaks, or North American *Quercus* species). When considering self-shading of foliage within branch enclosures, this is roughly equivalent to a leaf level emission rate of 20 to 30 μg-C (g-foliar dry mass)$^{-1}$ h^{-1} (Guenther at al, 1995). Geron et al (1994) reviewed studies between 1990 and 1994 and found that a much higher leaf-level rate of 70 μg-C (g-foliar dry mass)$^{-1}$ h^{-1} $\pm$ 50% was more realistic, and this rate was used in BEIS2 for high isoprene emitting tree species. BEIS3 (Guenther et al., 2000) applied similar emission factors at tree species levels (Geron et al 2000a, 2001) and more recent canopy environment models to estimate isoprene fluxes.

The results from several studies of isoprene emission measurements made at leaf, branch, tree, forest stand, and landscape levels have been used to test the accuracy of BEIS2 and BEIS3. These comparisons are documented in Geron et al. (1997) and Guenther et al. (2000). The results of these studies support the higher emission factors used in BEIS2 and BEIS3. Typically, leaf emission factors (normalized to standard conditions of PAR = 1000 μmol m^{-2} and leaf temperature of 30°C) measured at the top of tree canopies equal or exceed those used in BEIS2/3 while those in more shaded portions of the canopy tend to be lower than those assumed in the models, likely due to differences in developmental environments of leaves within the canopy (Monson et al., 1994; Sharkey et al., 1996; Harley et al., 1996; Geron et al., 2000b). Uncertainty in isoprene emissions due to variability in forest composition and leaf area remain in BVOC emission models and inventories. Seasonality and moisture stress also impact isoprene emission, but algorithms to simulate these effects are currently fairly crude (Guenther et al, 2000). The bulk of biogenic emissions occur during the summer, because of their dependence on temperature and incident sunlight. Biogenic emissions are also higher in southern states than in northern states for these reasons. The uncertainty associated with natural emissions ranges from about 50% for isoprene under midday summer conditions to about a factor of ten for other compounds (Guenther et al., 2000). In assessing the relative importance of these compounds, it should be borne in mind that the oxidation of many of the classes of compounds result in the formation of secondary organic aerosol and that many of the intermediate products may be sufficiently long lived to affect O_3 formation in areas far removed from where they were emitted. The oxidation of isoprene can also contribute about 10% of the source of CO (U.S. Environmental Protection Agency, 2000). Direct emissions of CO by vegetation is of much smaller importance. Soil microbes both emit and take up atmospheric CO, however, soil microbial activity appears to represent a net sink for CO.

Emissions from biomass burning depend strongly on the stage of combustion. Smoldering combustion, especially involving forest ecosystems favors the production of CH_4, NMHC and CO at the expense of CO_2, whereas active combustion produces more CO_2 relative to the other compounds mentioned above. Typical emissions ratios (defined as moles of compound per moles of emitted CO_2 expressed as a percentage) range from 6 to 14% for CO, 0.6 to 1.6% for CH_4, and 0.3 to 1.1% for NMHCs (Andreae, 1991). Most NMHC emissions are due to emissions of lighter compounds, containing 2 or 3 carbon atoms.

AX2.5.3 Observationally Based Models

As an alternative to chemistry-transport models, observationally-based methods (OBMs), which seek to infer O_3-precursor relations by relying more heavily on ambient measurements, can be used. Observationally-based methods are intuitively attractive because they provide an estimate of the O_3-precursor relationship based directly on observations of the precursors. These methods rely on observations as much as possible to avoid many of the uncertainties associated with chemistry/transport models (e.g., emission inventories and meteorological processes). However, these methods have large uncertainties with regards to photochemistry. As originally conceived, the observation-based approaches were intended to provide an alternative method for evaluating critical issues associated with urban O_3 formation. The proposed OBMs include calculations driven by ambient measurements (Chameides et al., 1992; Cardelino et al., 1995) and proposed "rules of thumb" that seek to show whether O_3 is primarily sensitive to NO_x or to VOC concentrations (Sillman, 1995; Chang et al., 1997; Tonnesen and Dennis, 2000a,b; Blanchard et al., 1999; Blanchard, 2000). These methods are controversial when used as “stand-alone” rules, because significant uncertainties and possible errors have been identified for all the methods (Chameides et al., 1988, Lu and Chang, 1998, Sillman and He, 2002; Blanchard and Stockenius, 2001). Methods such as these are most promising for use in combination with chemistry/transport models principally for evaluating the accuracy of model predictions.

Recent results (Tonnesen and Dennis, 2000a; Kleinman et al., 1997; 2000, 2001; Kleinman, 2000) suggest that ambient VOC and NO_x data can be used to identify the instantaneous production rate for O_3 and how the production rate varies with concentrations of NO_x and VOCs. The instantaneous production rate for O_3 is only one of the factors that affect the total O_3 concentration, because O_3 concentrations result from photochemistry and transport over time periods ranging from several hours to several days in regional pollution events. Ozone concentrations can be affected by distant emissions and by photochemical conditions at upwind locations, rather than instantaneous production at the site. Despite this limitation, significant information can be obtained by interpreting ambient NO_x and VOC measurements. Kleinman et al. (1997, 2000, 2001) and Tonnesen and Dennis (2000a) both derived simple expressions that relate the NO_x-VOC sensitivity of instantaneous O_3 production to ambient VOC and NO_x. These expressions usually involve summed VOC weighted by reactivity.

Cardelino et al. (1995, 2000) developed a method that seeks to identify O_3-NO_x-VOC sensitivity based on ambient NO_x and VOC data. Their method involves an area-wide sum of instantaneous production rates over an ensemble of measurement sites, which serve to represent the photochemical conditions associated with O_3 production in metropolitan areas. Their method, which relies on routine monitoring methods, is especially useful because it permits evaluation for a full season rather than just for individual episodes.

AX2.5.4 Chemistry-Transport Model Evaluation

The comparison of model predictions with ambient measurements represents a critical task for establishing the accuracy of photochemical models and evaluating their ability to serve as the basis for making effective control strategy decisions. The evaluation of a model's performance, or its adequacy to perform the tasks for which it was designed can only be conducted within the context of measurement errors and artifacts. Not only are there analytical problems, but there are also problems in assessing the representativeness of monitors at ground level for comparison with model values which represent typically an average over the volume of a grid box.

Chemistry/transport models for O_3 formation at the urban/regional scale have traditionally been evaluated based on their ability to correctly simulate O_3. A series of performance statistics that measure the success of individual model simulations to represent the observed distribution of ambient O_3, as represented by a network of surface measurements were recommended in U.S. Environmental Protection Agency (1991; see also Russell and Dennis, 2000). These statistics consist of the following:

- Unpaired peak O_3 within a metropolitan region (typically for a single day)
- Normalized bias equal to the summed difference between model and measured hourly concentrations divided by the sum of measured hourly concentrations.
- Normalized gross error, equal to the summed unsigned (absolute value) difference between model and measured hourly concentrations divided by the sum of measured hourly concentrations.

Normalized bias, D;

$$A_u = \frac{C_p(x,t)_{\max} - C_o(x',t')_{\max}}{C_o(x',t')_{\max}} \; * \; 100\%, \qquad \text{(AX2-49)}$$

Gross error, E_d (for hourly observed values of O_3 > 60 ppb)

$$D = \frac{1}{N}\sum_{i=1}^{N} \frac{\{C_p(x_i,t) - C_o(x_i,t)\}}{C_o(x_i,t)}, \quad t = 1, 24. \qquad \text{(AX2-50)}$$

Unpaired peak prediction accuracy, A_u

$$E_d = \frac{1}{N} \sum_{i=1}^{N} \frac{\left| C_p(x_i,t) - C_o(x_i,t) \right|}{C_o(x_i,t)}, \quad t = 1, 24. \qquad \text{(AX2-51)}$$

The following performance criteria for regulatory models were recommended in U.S. Environmental Protection Agency (1991): unpaired peak O_3 to within ± 15% or ± 20%; normalized bias within ± 5% to ± 15%; and normalized gross error less than 30% to 35%, but only when O_3 > 60 ppb. This can lead to difficulties in evaluating model performance since nighttime and diurnal cycles are ignored. A major problem with this method of model evaluation is that it does not provide any information about the accuracy of O_3-precursor relations predicted by the model. The process of O_3 formation is sufficiently complex that models can predict O_3 correctly without necessarily representing the O_3 formation process properly. If the O_3 formation process is incorrect, then the modeled source-receptor relations will also be incorrect.

Studies by Sillman et al. (1995, 2003), Reynolds et al. (1996) and Pierce et al. (1998) have identified instances in which different model scenarios can be created with very different O_3-precursor sensitivity, but without significant differences in the predicted O_3 fields. Figures AX2-21a,b provide an example. Referring to the O_3-NO_x-VOC isopleth plot (Figure AX2-22), it can be seen that similar O_3 concentrations can be found for photochemical conditions that have very different sensitivity to NO_x and VOCs.

Global-scale chemistry-transport models have generally been evaluated by comparison with measurements for a wide array of species, rather than just for O_3 (e.g., Wang et al., 1998; Emmons et al., 2000; Bey et al., 2001b; Hess, 2001; Fiore et al., 2002). These have included evaluation of major primary species (NO_x, CO, and selected VOCs) and an array of secondary species (HNO_3, PAN, H_2O_2) that are often formed concurrently with O_3. Models for urban/regional O_3 have also been evaluated against a broader ensemble of measurements in a few cases, often associated with measurement intensives (e.g., Jacobson et al., 1996, Lu et al., 1997; Sillman et al., 1998). The results of a comparison between observed and computed concentrations from Jacobson et al. (1996) for the Los Angeles Basin are shown in Figures AX2-23a,b.

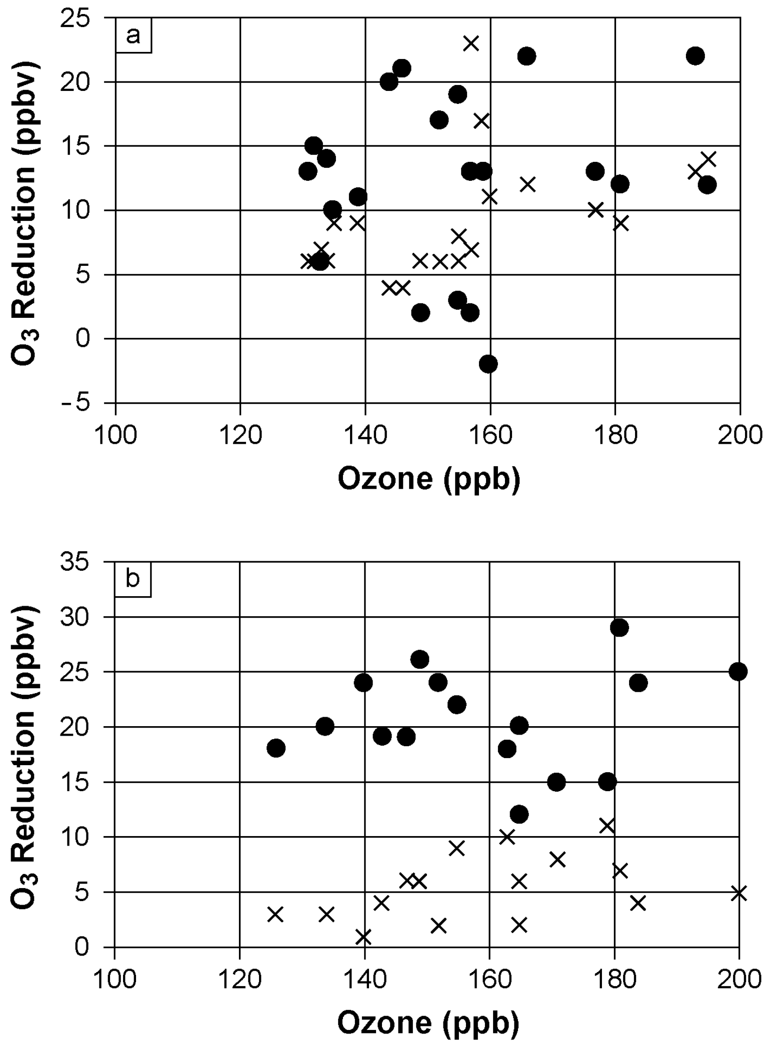

Figure AX2-21a,b. Impact of model uncertainty on control strategy predictions for ozone for two days (August 10[a] and 11[b], 1992) in Atlanta, GA. The figures show the predicted reduction in peak O_3 resulting from 35% reductions in anthropogenic VOC emissions (crosses) and from 35% reductions in NO_x (solid circles) in a series of model scenarios with varying base case emissions, wind fields, and mixed layer heights.

Source: Results are plotted from tabulated values published in Sillman et al. (1995, 1997).

The highest concentrations of primary species usually occur in close proximity to emission sources (typically in urban centers) and at times when dispersion rates are low. The diurnal cycle includes high concentrations at night, with maxima during the morning rush hour, and low concentrations during the afternoon (Figure AX2-23a). The afternoon minima are driven by the

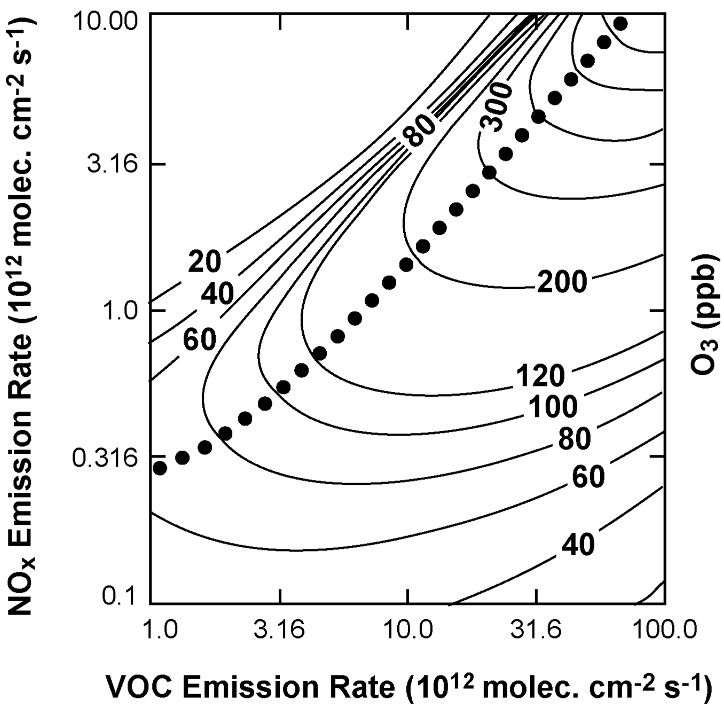

Figure AX2-22. Ozone isopleths (ppb) as a function of the average emission rate for NO_x and VOC (10^{12} molec. cm^{-2} s^{-1}) in zero dimensional box model calculations. The isopleths (solid lines) represent conditions during the afternoon following 3-day calculations with a constant emission rate, at the hour corresponding to maximum O_3. The ridge line (shown by solid circles) lies in the transition from NO_x-saturated to NO_x-limited conditions.

much greater rate of vertical mixing at that time. Primary species also show a seasonal maximum during winter, and are often high during fog episodes in winter when vertical mixing , is suppressed. By contrast, secondary species such as O_3 are typically highest during the afternoon (the time of greatest photochemical activity), on sunny days and during summer. During these conditions concentrations of primary species may be relatively low. Strong correlations between primary and secondary species are generally observed only in downwind rural areas where all anthropogenic species are high simultaneously. The difference in the diurnal cycles of primary species (CO, NO_x and ethane)and secondary species (O_3, PAN and HCHO) is evident in Figure AX2-23b.

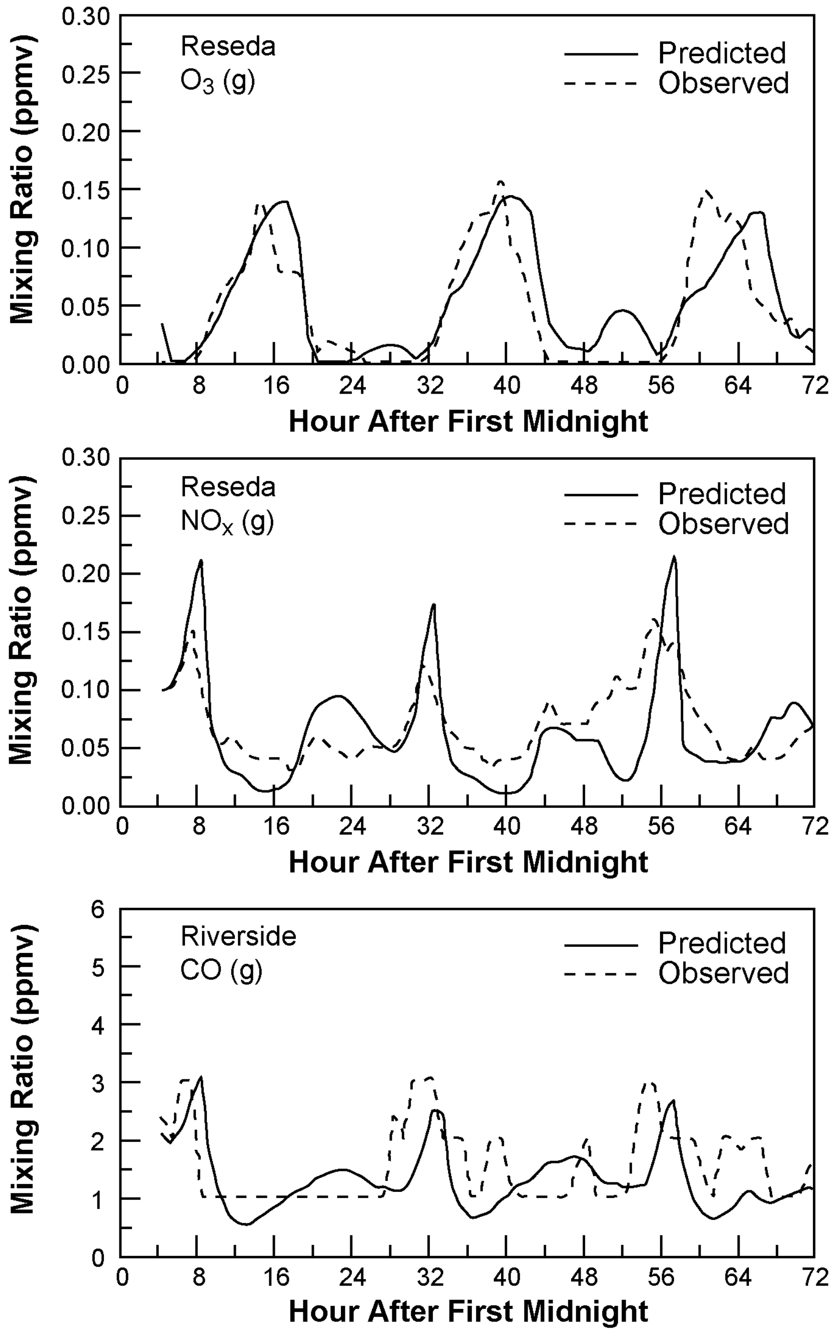

Figure AX2-23a. Time series for measured gas-phase species in comparison with results from a photochemical model. The dashed lines represent measurements, and solid lines represent model predictions (in parts per million, ppmv) for August 26 – 28, 1988 at sites in southern California. The horizontal axis represents hours past midnight, August 25. Results represent O_3 and NO_x at Reseda and CO at Riverside.

Source: Jacobson et al. (1996).

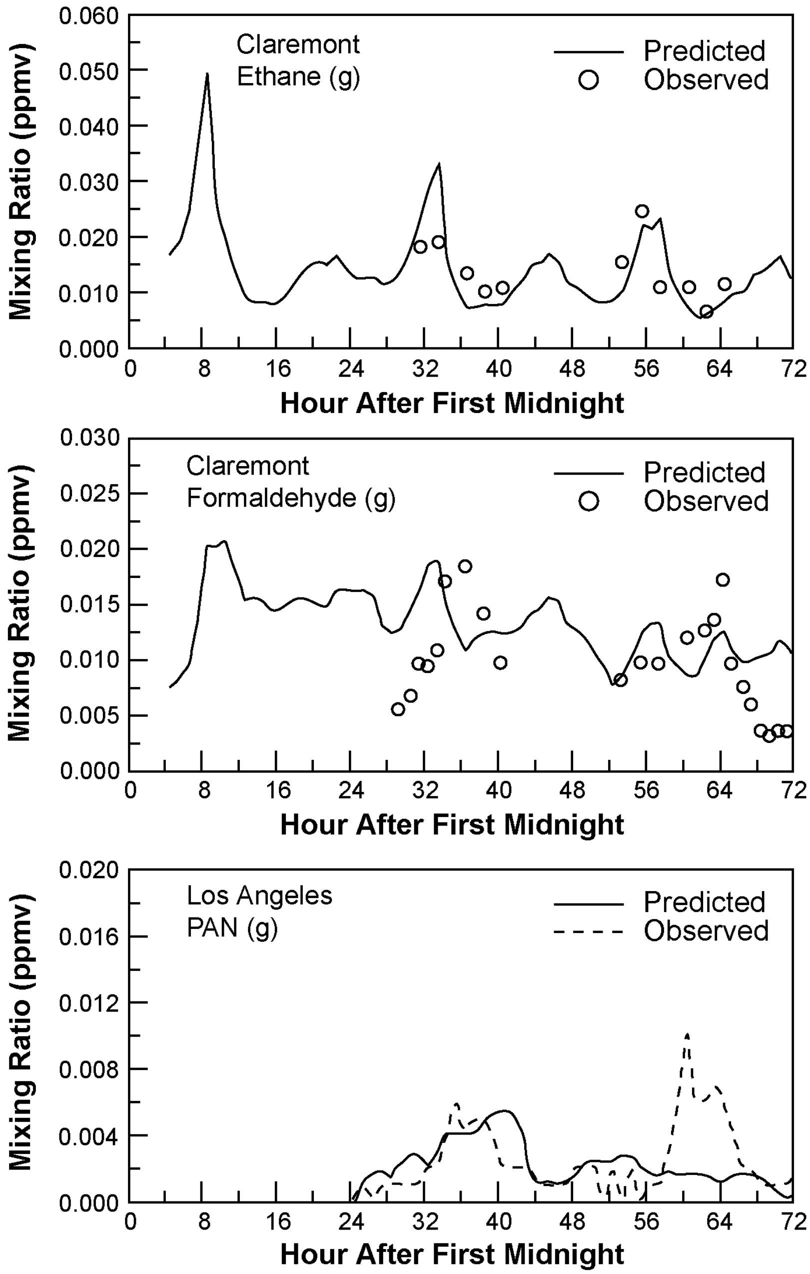

Figure AX2-23b. Time series for measured gas-phase species in comparison with results from a photochemical model. The circles represent measurements, and solid lines represent model predictions (in parts per million, ppmv) for August 26 – 28, 1988 at sites in southern California. The horizontal axis represents hours past midnight, August 25. Results represent ethane and formaldehyde at Claremont, and PAN at Los Angeles.

Source: Jacobson et al. (1996).

Models for urban/regional O_3 have been evaluated less extensively than global-scale models in part because the urban/regional context presents a number of difficult challenges. Global-scale models typically represent continental-scale events and can be evaluated effectively against a sparse network of measurements. By contrast, urban/regional models are critically dependent on the accuracy of local emission inventories and event-specific meteorology, and must be evaluated separately for each urban area that is represented.

The evaluation of urban/regional models is also limited by the availability of data. Measured NO_x and speciated VOC concentrations are widely available through the EPA PAMs network, but questions have been raised about the accuracy of those measurements and the data have not yet been analyzed thoroughly. Evaluation of urban/regional models versus measurements has generally relied on results from a limited number of field studies in the United States. Short term research-grade measurements for species relevant to O_3 formation, including VOCs, NO_x, PAN, nitric acid (HNO_3) and hydrogen peroxide (H_2O_2) are also widely available at rural and remote sites (e.g., Daum et al., 1990, 1996; Martin et al., 1997; Young et al., 1997; Thompson et al., 2000; Hoell et al., 1996, 1997; Fehsenfeld et al., 1996a; Emmons et al., 2000; Hess, 2001; Carroll et al., 2001). The equivalent measurements are available for some polluted rural sites in the eastern United States (e.g.) but only at a few urban locations (Meagher et al., 1998; Hübler et al., 1998; Kleinman et al., 2000, 2001; Fast et al., 2002; new SCAQS-need reference). Extensive measurements have also been made in Vancouver (Steyn et al., 1997) and in several European cities (Staffelbach et al., 1997; Prévôt et al., 1997, Dommen et al., 1999; Geyer et al., 2001; Thielman et al., 2001; Martilli et al., 2002; Vautard et al., 2002).

The results of straightforward comparisons between observed and predicted concentrations of O_3 can be misleading because of compensating errors, although this possibility is diminished when a number of species are compared. Ideally, each of the main modules of a chemistry-transport model system (for example, the meteorological model and the chemistry and radiative transfer routines) should be evaluated separately. However, this is rarely done in practice. To better indicate how well physical and chemical processes are being represented in the model, comparisons of relations between concentrations measured in the field and concentrations predicted by the model can be made. These comparisons could involve ratios and correlations between species. For example, correlation coefficients could be calculated between primary species as a means of evaluating the accuracy of emission inventories; or between secondary species as a means of evaluating the treatment of photochemistry in the model. In addition, spatial relations involving individual species (correlations, gradients) can also be used as a means of evaluating the accuracy of transport parameterizations. Sillman and He (2002) examined differences in correlation patterns between O_3 and NO_z in Los Angeles, CA, Nashville, TN and various sites in the rural United States. Model calculations (Figure AX2-24) show differences in correlation patterns associated with differences in the sensitivity of O_3 to NO_x and VOCs. Primarily NO_x-sensitive (NO_x-limited) areas in models show a strong correlation between O_3 and NO_z with a relatively steep slope, while primarily VOC-sensitive (NO_x-saturated) areas in models show lower O_3 for a given NO_z and a lower O_3-NO_z slope. They found that differences found in measured data ensembles were matched by predictions from chemical transport models. Measurements in rural areas in the eastern U.S. show differences in the pattern of correlations for O_3 versus NO_z between summer and autumn (Jacob et al., 1995; Hirsch et al., 1996), corresponding to the transition from NO_x-limited to NO_x-saturated patterns, a feature which is also matched by chemistry-transport models.

The difference in correlations between secondary species in NO_x-limited to NO_x-saturated environments can also be used to evaluate the accuracy of model predictions in individual applications. Figures AX2-25a and AX2-25b show results for two different model scenarios for Atlanta. As shown in the figures, the first model scenario predicts an urban plume with high NO_y and O_3 formation apparently suppressed by high NO_y. Measurements show much lower NO_y in the Atlanta plume. This error was especially significant because the model locations with high NO_y were not sensitive to NO_x, while locations with lower NO_y were primarily sensitive to NO_x. The second model scenario (with primarily NO_x-sensitive conditions) shows much better agreement with measured values. Figure AX2-26a,b shows model-measurement comparisons for secondary species in Nashville, showing better agreement with measured conditions. Greater confidence in the predictions made by chemistry-transport models will be gained by the application of techniques such as these on a more routine basis.

The ability of chemical mechanisms to calculate the concentrations of free radicals under atmospheric conditions was tested in the Berlin Ozone Experiment, BERLIOZ (Volz-Thomas et al., 2003) during July and early August at a site located about 50 km NW of Berlin. (This location was chosen as O_3 episodes in central Europe are often associated with SE winds.) Concentrations of major compounds such as O_3, hydrocarbons, etc., were fixed at observed

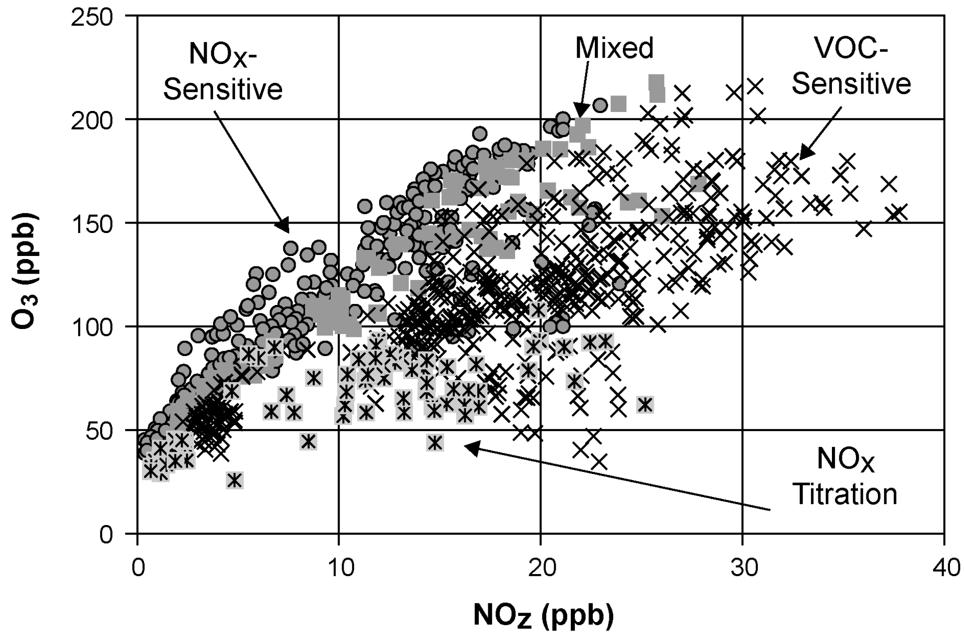

Figure AX2-24. Correlations for O_3 versus NO_z (NO_y – NO_x) in ppb from chemical transport models for the northeast corridor, Lake Michigan, Nashville, the San Joaquin Valley and Los Angeles. Each location is classified as NO_x-limited or NO_x-sensitive (circles), NO_x-saturated or VOC-sensitive (crosses), mixed or with near-zero sensitivity (squares), and dominated by NO_x titration (asterisks) based on the model response to reduced NO_x and VOC.

Source: Sillman and He (2002).

values. In this regard, the protocol used in this evaluation is an example of an observationally based method. Figure AX2-27 compares the concentrations of RO_2 (organic peroxy), HO_2 (hydroperoxy) and OH (hydroxyl) radicals predicted by RACM (regional air chemistry mechanism; Stockwell et al., 1997) and MCM (master chemical mechanism; Jenkin et al, 1997 with updates) with observations made by the laser induced fluorescence (LIF) technique and by matrix isolation ESR spectroscopy (MIESR). Also shown are the production rates of O_3 calculated using radical concentrations predicted by the mechanisms and those obtained by measurements, and measurements of NO_x concentrations. As can be seen, there is good agreement between measurements of organic peroxy, hydroperoxy and hydroxyl radicals with values predicted by both mechanisms at high concentrations of NO_x (> 10 ppb). However, at

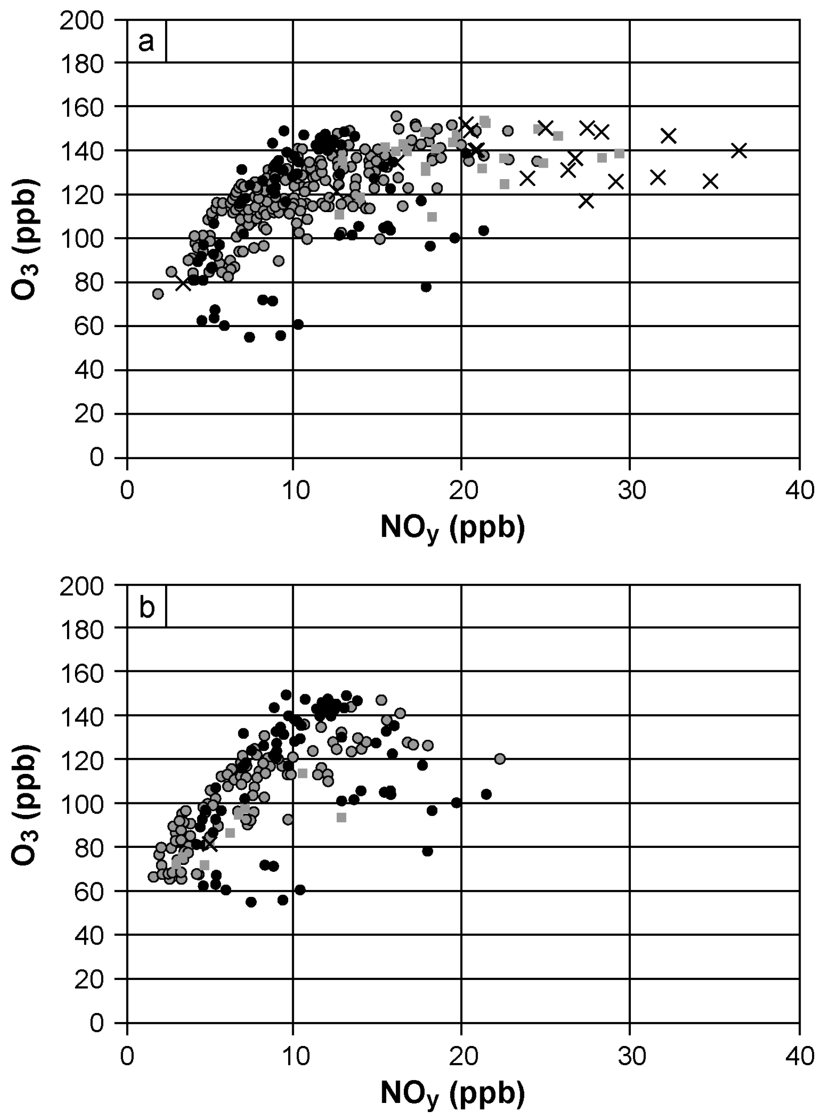

Figure AX2-25a,b. Evaluation of model versus measured O_3 versus NO_y for two model scenarios for Atlanta. The model values are classified as NO_x-limited (circles), NO_x-saturated (crosses), or mixed or with low sensitivity to NO_x (squares). Diamonds represent aircraft measurements.

Source: Sillman et al. (1997).

lower NO_x concentrations, both mechanisms substantially overestimate OH concentrations and moderately overestimate HO_2 concentrations. Agreement between models and measurements is generally better for organic peroxy radicals, although the MCM appears to overestimate their

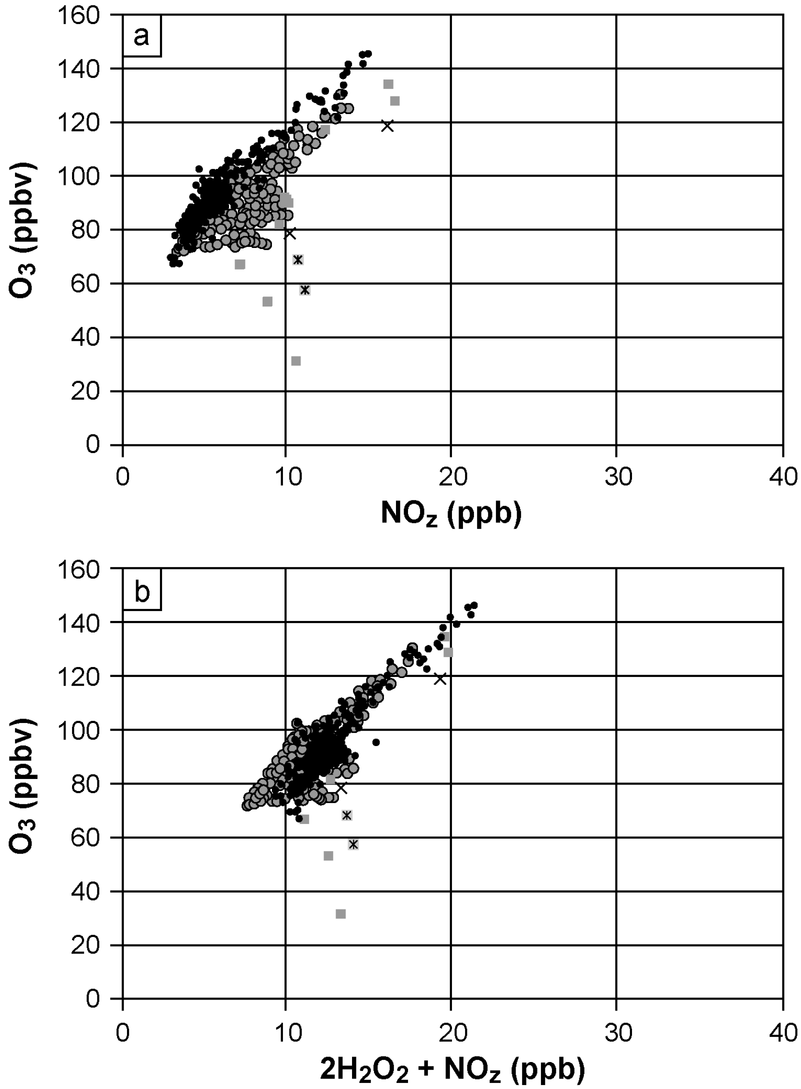

Figure AX2-26a,b. Evaluation of model versus: (a) measured O_3 versus NO_z and (b) O_3 versus the sum $2H_2O_2 + NO_z$ for Nashville, TN. The model values are classified as NO_x-limited (gray circles), NO_x-saturated (×s), mixed or with near-zero sensitivity (squares), or dominated by NO_x titration (filled circles). Diamonds represent aircraft measurements.

Source: Sillman et al. (1998).

concentrations somewhat. In general, the mechanisms reproduced the HO_2 to OH and RO_2 to OH ratios better than the individual measurements. The production of O_3 was found to increase linearly with NO (for NO < 0.3 ppb) and to decrease with NO (for NO > 0.5 ppb).

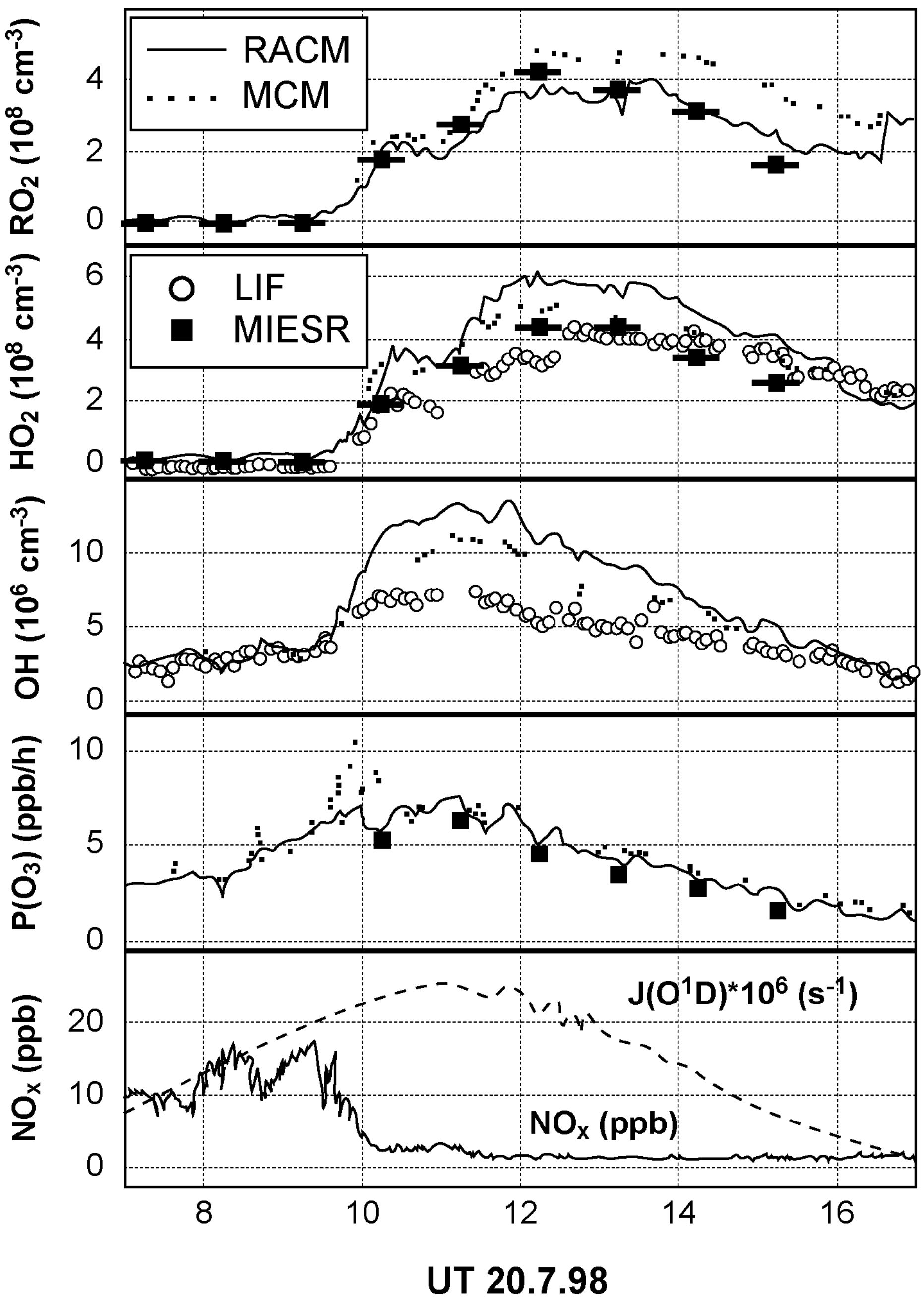

Figure AX2-27. Time series of concentrations of RO_2, HO_2, and OH radicals, local ozone photochemical production rate and concentrations of NO_x from measurements made during BERLIOZ. Also shown are comparisons with results of photochemical box model calculations using the RACM and MCM chemical mechanisms.

Source: Volz-Thomas et al. (2003).

OH and HO_2 concentrations measured during the $PM_{2.5}$ Technology Assessment and Characterization Study conducted at Queens College in New York City in the summer of 2001 were also compared with those predicted by RACM (Ren et al., 2003). The ratio of observed to predicted HO_2 concentrations over a diurnal cycle was 1.24 and the ratio of observed to predicted OH concentrations was about 1.10 during the day, but the mechanism significantly underestimated OH concentrations during the night.

AXA.5.4.1 Evaluation of Emissions Inventories

Comparisons of emissions model predictions with observations have been performed in a number of environments. A number of studies of ratios of concentrations of CO to NO_x and NMOC to NO_x during the early 1990s in tunnels and ambient air (summarized in Air Quality Criteria for Carbon Monoxide [U.S. Environmental Protection Agency, 2000]) indicated that emissions of CO and NMOC were systematically underestimated in emissions inventories. However, the results of more recent studies have been mixed in this regard, with many studies showing agreement to within ± 50% (U.S. Environmental Protection Agency, 2000). Improvements in many areas have resulted from the process of emissions model development, evaluation, and further refinement. It should be remembered that the conclusions from these reconciliation studies depend on the assumption that NO_x emissions are predicted correctly by emissions factor models. Road side remote sensing data indicate that over 50% of NMHC and CO emissions are produced by less than about 10% of the vehicles (Stedman et al., 1991). These “super-emitters” are typically poorly maintained vehicles. Vehicles of any age engaged in off-cycle operations (e.g., rapid accelerations) emit much more than if operated in normal driving modes. Bishop and Stedman (1996) found that the most important variables governing CO emissions are fleet age and owner maintenance.

Emissions inventories for North America can be evaluated with comparisons to measured long-term trends and or ratios of pollutants in ambient air. A decadal field study of ambient CO at a rural cite in the Eastern U.S. (Hallock-Waters et al., 1999) indicates a downward trend consistent with the downward trend in estimated emissions over the period 1988 to 1999 (U.S. Environmental Protection Agency, 1997), even when a global downward trend is accounted for. Measurements at two urban areas in the United States confirmed the decrease in CO emissions (Parrish et al., 2002). That study also indicated that the ratio of CO to NO_x emissions decreased by almost a factor of three over 12 yr (such a downward trend was noted in AQCD 96). Emissions estimates (U.S. Environmental Protection Agency, 1997) indicate a much smaller decrease in this ratio, suggesting that NO_x emissions from mobile sources may be underestimated and/or increasing. The authors conclude that O_3 photochemistry in U.S. urban areas may have become more NO_x-limited over the past decade.

Pokharel et al. (2002) employed remotely-sensed emissions from on-road vehicles and fuel use data to estimate emissions in Denver. Their calculations indicate a continual decrease in CO, HC, and NO emissions from mobile sources over the 6 yr study period. Inventories based on the ambient data were 30 to 70% lower for CO, 40% higher for HC, and 40 to 80% lower for NO than those predicted by the recent MOBILE6 model.

Stehr et al. (2000) reported simultaneous measurements of CO, SO_2 and NO_y at an East Coast site. By taking advantage of the nature of mobile sources (they emit NO_x and CO but little SO_2) and power plants (they emit NO_x and SO_2 but little CO), the authors evaluated emissions estimates for the eastern United States. Results indicated that coal combustion contributes 25 to 35% of the total NO_x emissions in agreement with emissions inventories (U.S. Environmental Protection Agency, 1997).

Parrish et al. (1998) and Parrish and Fehsenfeld (2000) proposed methods to derive emission rates by examining measured ambient ratios among individual VOC, NO_x and NO_y. There is typically a strong correlation among measured values for these species (e.g., Figure AX2-14) because emission sources are geographically collocated, even when individual sources are different. Correlations can be used to derive emissions ratios between species, including adjustments for the impact of photochemical aging. Investigations of this type include correlations between CO and NO_y (e.g., Parrish et al., 1991), between individual VOC species and NO_y (Goldan et al., 1995,1997, 2001; Harley et al., 1997) and between various individual VOC (Goldan et al., 1995, 1997; McKeen and Liu, 1993; McKeen et al., 1996). Buhr et al. (1992) derived emission estimates from principal component analysis (PCA) and other statistical methods. Many of these studies are summarized in Trainer et al. (2000), Parrish et al. (1998), and Parrish and Fehsenfeld (2000). Goldstein and Schade (2000) also used species correlations to identify the relative impacts of anthropogenic and biogenic emissions. Chang et al. (1996, 1997) and Mendoza-Dominguez and Russell (2000, 2001) used the more formal techniques of inverse modeling to derive emission rates, in conjunction with results from chemistry-transport models. Another concern regarding the use of emissions inventories is that emissions from all significant sources have been included. This may not always be the case. As an example, hydrocarbon seeps from off-shore oil fields may represent a significant source of reactive organic compounds in near by coastal areas (Quigley et al., 1999).

AX2.5.4.2 Availability and Accuracy of Ambient Measurements

The use of methods such as observationally based methods or source apportionment models, either as stand-alone methods or as a basis for evaluating chemistry/transport models, is often limited by the availability and accuracy of measurements. Measured speciated VOC and NO_x are widely available in the United States through the PAMS network. However, challenges have been raised about both the accuracy of the measurements and their applicability.

Parrish et al. (1998) and Parrish and Fehsenfeld (2000) developed a series of quality assurance tests for speciated VOC measurements. Essentially these tests used ratios among individual VOC with common emission sources to identify whether the variations in species ratios were consistent with the relative photochemical lifetimes of individual species. These tests were based on a number of assumptions: the ratio between ambient concentrations of long-lived species should show relatively little variation among measurements affected by a common emissions sources; and the ratio between ambient concentrations of long-lived and short-lived species should vary in a way that reflects photochemical aging at sites more different from source regions. Parrish et al. used these expectations to establish criteria for rejecting apparent errors in measurements. They found that the ratios among alkenes at many PAMS sites did not show variations that would be expected due to photochemical aging.

The PAMs network currently includes measured NO and NO_x. However, Cardelino and Chameides (2000) reported that measured NO during the afternoon was frequently at or below the detection limit of the instruments (1 ppb), even in large metropolitan regions (Washington, DC; Houston, TX; New York, NY). NO_x measurements are made with commercial chemilluminescent detectors with molybdenum converters. However these measurements typically include some organic nitrates in addition to NO_x, and cannot be interpreted as a “pure” NO_x measurement (see summary in Parrish and Fehsenfeld, 2000).

Total reactive nitrogen (NO_y) is included in the PAMS network only at a few sites. The possible expansion of PAMS to include more widespread NO_y measurements has been suggested

(McClenny, 2000). A major issue concerning measured NO_y is the possibility that HNO_3, a major component of NO_y, is sometimes lost in inlet tubes and not measured (Luke et al., 1998; Parrish and Fehsenfeld, 2000). This problem is especially critical if measured NO_y is used to identify NO_x-limited versus NO_x-saturated conditions. The correlation between O_3 and NO_y differs for NO_x-limited versus NO_x-saturated locations, but this difference is driven primarily by differences in the ratio of O_3 to HNO_3. If HNO_3 were omitted from the NO_y measurements, than the measurements would represent a biased estimate and their use would be problematic.

AX2.6 TECHNIQUES FOR MEASURING OZONE AND ITS PRECURSORS

AX2.6.1 Sampling and Analysis of Ozone

Numerous techniques have been developed for sampling and measurement of O_3 in the ambient atmosphere at ground level. As noted above, sparse surface networks tend to underestimate maximum O_3 concentrations. Today, monitoring is conducted almost exclusively with UV absorption spectrometry with commercial short path instruments, a method that has been thoroughly evaluated in clean air. The ultimate reference method is a relatively long-path UV absorption instrument maintained under carefully controlled conditions at NIST (e.g., Fried and Hodgeson, 1982). Episodic measurements are made with a variety of other techniques based on the principles of chemiluminescence, electrochemistry, DOAS, and LIDAR. The rationale, history, and calibration of O_3 measurements were summarized in AQCD 96, so this section will focus on the current state of ambient O_3 measurement, tests for artifacts, and on new developments.

Several reports in the reviewed scientific literature have investigated interferences in O_3 detection via UV radiation absorption. Kleindienst et al. (1993) investigated the effects of water vapor and VOC's on instruments based on both UV absorption and chemiluminescence. They concluded that water vapor had no significant impact on UV absorption-based instruments, but could cause a positive interference of up to 9% in chemiluminescence-based detectors at high humidities (dew point of 24 C). In smog chamber studies, aromatic compounds and their oxidation products were found to generate a positive but small interference in the UV absorption instruments. Kleindienst et al. concluded that "when the results are scaled back to ambient concentrations of toluene and NO_x, the effect appears to be very minor (ca. 3 percent under the study conditions)." More recently Narita et al. (1998) tested organic and inorganic compounds and found response to several, but not at levels likely to interfere with accurate determination of O_3 in an urban environment. The possibility for substantive interferences in O_3 detection exists, but such interferences have not been observed even in urban plumes. Ryerson et al. (1998) measured O_3 with UV absorption and chemiluminescence instruments operated off a common inlet on the NOAA WP-3 research aircraft. As reported by Parrish and Fehsenfeld (2000) "Through five field missions over four years, excellent correlations were found between the measurements of the two instruments, although the chemiluminescence instrument was systematically low (5%) throughout some flights. The data sets include many passes through the Nashville urban plume. There was never any indication (< 1%) that the UV instrument measured systematically higher in the urban plume."

Ozone can also be detected by differential optical absorption spectroscopy (DOAS) at a variety of wavelengths in the UV and visible parts of the spectrum. Prior comparisons of DOAS results to those from a UV absorption instrument showed good agreement, on the order of 10% (Stevens et al., 1993). Reisinger (2002) reported a positive interference due to an unidentified absorber in the 279 to 289 nm spectral region used by many commercial short-path DOAS systems for the measurement of O_3. Results of that study suggest that effluent from wood burning, used for domestic heating, may be responsible. Vandaele et al. (2002) reported good agreement with other methods in the detection of O_3 (and SO_2) over the course of several years in Brussels. While the DOAS method remains attractive due to its sensitivity and speed of response further intercomparisons and interference tests are recommended.

Electrochemical methods are commonly employed where sensor weight is a problem, such as in balloon borne sondes, and these techniques have been investigated for ambient monitoring. Recent developments include changes in the electrodes and electrolyte solution (Knake and Hauser, 2002) and selective removal of O_3 for a chemical zero (Penrose et al., 1995). Interferences from other oxidants such as NO_2 and HONO remain potential problems and further comparisons with UV absorption are necessary. Because of potential interferences from water vapor in some instruments, it is recommended (ASTM, 2003a,b) that calibrations and scrubber tests be conducted with air humidified to near ambient levels, rather than with dry compressed gas.

Change in the vibration frequency of a piezoelectric quartz crystal has been investigated as a means of detecting O_3. Ozone reacts with polybutadiene coated onto the surface of a crystal, and the resulting change in mass is detected as a frequency change (Black et al., 2000). While this sensor has advantages of reduced cost power consumption and weight, it is lacks the lifetime and absolute accuracy for ambient monitoring.

In summary, new techniques are being developed, but UV absorption remains the method of choice for ambient O_3 monitoring near the Earth's surface. These commercial UV absorption detectors are available at a moderate price. They show good absolute accuracy with only minor cross sensitivity in clean to moderately polluted environments; they are stable, reliable, and sensitive.

AX2.6.2 Sampling and Analysis of Nitrogen Oxides

The role of nitrogen oxides in tropospheric O_3 formation was reviewed thoroughly in the previous AQCD and will be only briefly summarized here. Reactive nitrogen is generally released as NO but quickly converted in ambient air to NO_2 and back again, thus these two species are often referred to together as NO_x (NO + NO_2). The photochemical interconversion of NO and NO_2 leads to O_3 formation. Because NO_2 is a health hazard at sufficiently high concentrations, it is itself a criteria pollutant. In EPA documents, emissions of NO_x are expressed in units of mass of NO_2 per unit time, i.e., the total mass of NO_x that would be emitted if all the NO were converted to NO_2. Ambient air monitors have been required to demonstrate compliance with the standard for NO_2 and thus have focused on measuring this gas or determining an upper limit for its concentration.

NO_x can be further oxidized to species including nitrous acid (HNO_2), nitric acid (HNO_3), aerosol nitrate (NO_3^-), and organo-nitrates such as alkyl nitrates ($RONO_2$) and peroxy acetyl nitrate, PAN, ($CH_3C(O)O_2NO_2$). The sum of these species (explicitly excluding N_2, N_2O, and reduced N such as NH_3 and HCN) is called NO_y. Nitrates play important roles in acid rain, and nutrient cycling including over nitrification of surface ecosystems and in the formation of fine particulate matter, but are generally inactive photochemically. Some studies refer specifically to the oxidized or processed NO_y species, NO_y-NO_x, as NO_z because this quantity is related to the degree of photochemical aging in the atmosphere. Several NO_z species such as PAN and HONO can be readily photolyzed or thermally dissociated to NO or NO_2 and thus act as reservoirs for

NO_x. This discussion focuses on current methods and on promising new technologies, but no attempt is made here to cover the extensive development of these methods or of methods such as wet chemical techniques, no longer in widespread use. More detailed discussions of the histories of these methods may be found elsewhere (U.S. Environmental Protection Agency, 1993, 1996).

AX2.6.2.1 Calibration Standards

Calibration gas standards of NO, in nitrogen (certified at concentrations of approximately 5 to 40 ppm) are obtainable from the Standard Reference Material (SRM) Program of the National Institute of Standards and Technology (NIST), formerly the National Bureau of Standards (NBS), in Gaithersburg, MD. These SRMs are supplied as compressed gas mixtures at about 135 bar (1900 psi) in high-pressure aluminum cylinders containing 800 L of gas at standard temperature and pressure, dry (STPD; National Bureau of Standards, 1975; Guenther et al., 1996). Each cylinder is supplied with a certificate stating concentration and uncertainty. The concentrations are certified to be accurate to ±1 percent relative to the stated values. Because of the resources required for their certification, SRMs are not intended for use as daily working standards, but rather as primary standards against which transfer standards can be calibrated.

Transfer stand-alone calibration gas standards of NO in N_2 (in the concentrations indicated above) are obtainable from specialty gas companies. Information as to whether a company supplies such mixtures is obtainable from the company, or from the SRM Program of NIST. These NIST Traceable Reference Materials (NTRMs) are purchased directly from industry and are supplied as compressed gas mixtures at approximately 135 bars (1,900 psi) in high-pressure aluminum cylinders containing 4,000 L of gas at STPD. Each cylinder is supplied with a certificate stating concentration and uncertainty. The concentrations are certified to be accurate to within ±1 percent of the stated values (Guenther et al., 1996). Additional details can be found in the previous AQCD for O_3 (U.S. Environmental Protection Agency, 1996).

AX2.6.2.2 Measurement of Nitric Oxide

Gas-Phase Chemiluminescence (CL) Methods

Nitric oxide, NO, can be measured reliably using the principle of gas-phase chemiluminescence induced by the reaction of NO with O_3 at low pressure. Modern commercial

NO_x analyzers have sufficient sensitivity and specificity for adequate measurement in urban and many rural locations (U.S. Environmental Protection Agency, 1996). The physics of the method, detection limits, interferences, and comparisons under field comparisons have been thoroughly reviewed in the previous AQCD. Research grade CL instruments have been compared under realistic field conditions to spectroscopic instruments, and the results indicate that both methods are reliable (at concentrations relevant to smog studies) to better than 15 percent with 95 percent confidence. Response times are on the order of 1 minute. For measurements meaningful for understanding O_3 formation, emissions modeling, and N deposition, special care must be taken to frequently zero and calibrate the instrument. A chemical zero, by reacting the NO up stream and out of view of the PMT, is preferred because it accounts for unsaturated hydrocarbon or other interferences. Calibration should be performed with NIST-traceable reference material of compressed NO in N_2. Standard additions of NO at the inlet will account for NO loss or conversion to NO_2 in the lines. In summary CL methods, when operated in an appropriate manner, can be suitable for measuring or monitoring NO (e.g., Crosley, 1996).

Spectroscopic Methods for Nitric Oxide

Nitric oxide has also been successfully measured in ambient air with direct spectroscopic methods; these include two-photon laser-induced fluorescence (TPLIF), tunable diode laser absorption spectroscopy (TDLAS), and two-tone frequency-modulated spectroscopy (TTFMS). These were reviewed thoroughly in the previous AQCD and will be only briefly summarized here. The spectroscopic methods demonstrate excellent sensitivity and selectivity for NO with detection limits on the order of 10 ppt for integration times of 1 min. Spectroscopic methods compare well with the CL method for NO in controlled laboratory air, ambient air, and heavily polluted air (e.g., Walega et al., 1984; Gregory et al., 1990; Kireev et al., 1999). These spectroscopic methods remain in the research arena due to their complexity, size, and cost, but are essential for demonstrating that CL methods are reliable for monitoring NO concentrations involved in O_3 formation — from 100s of ppb to around 20 ppt.

Atmospheric pressure laser ionization followed by mass spectroscopy has also been reported for detection of NO and NO_2. Garnica et al. (2000) describe a technique involving selective excitation at one wavelength followed by ionization at a second wavelength. They report good selectivity and detection limits well below 1 ppb. The practicality of the instrument for ambient monitoring has yet to be demonstrated.

AX2.6.2.3 Measurements of Nitrogen Dioxide

Gas-Phase Chemiluminescence Methods

Since the previous AQCD, photolytic reduction followed by CL has been improved and the method of laser-induced fluorescence has been developed. Ryerson et al. (2000) developed a photolytic converter based on a Hg lamp with increased radiant intensity in the region of peak NO_2 photolysis (350 to 400 nm) and producing conversion efficiencies of 70% or more in less than 1 s. Because the converter produces little radiation at wavelengths less than 350 nm, interferences from HNO_3 and PAN are minimal.

Alternative methods to photolytic reduction followed by CL are desirable to test the reliability of this widely used technique. In any detector based on conversion to another species interferences can be a problem. Several atmospheric species, PAN and HO_2NO_2 for example, dissociate to NO_2 at higher temperatures.

Laser induced fluorescence for NO_2 detection involves excitation of atmospheric NO_2 with laser light emitted at wavelengths too long to induce photolysis. The resulting excited molecules relax in a photoemissive mode and the fluorescing photons are counted. Because collisions would rapidly quench electronically excited NO_2, the reactions are conducted at low pressure (Cohen, 1999; Thornton et al., 2000; Day et al., 2002). For example Cleary et al. (2002) describe field tests of a system that uses continuous, supersonic expansion followed by excitation at 640 nm with a commercial cw external-cavity tunable diode laser. Sensitivity is adequate for measurements in most continental environments (145 ppt in 1 min) and no interferences have been identified.

Matsumi et al. (2001) describe a comparison of laser-induced fluorescence with a photofragmentation chemiluminescence instrument. The laser-induced fluorescence system involves excitation at 440 nm with a multiple laser system. They report sensitivity of 30 ppt in 10 s and good agreement between the two methods under laboratory conditions at mixing ratios up to 1.0 ppb. This high-sensitivity laser-induced fluorescence system has yet to undergo long-term field tests.

NO_2 can be detected by differential optical absorption spectroscopy (DOAS) in an open, long-path system (Kim and Kim, 2001). Vandaele et al. (2002) reported that the DOAS technique measured higher NO_2 concentrations than were reported by other techniques in a three-year study conducted in Brussels. Harder et al. (1997b) conducted an experiment in rural Colorado involving simultaneous measurements of NO_2 with DOAS and photolysis followed by chemiluminescence. The found differences of as much as 110% in clean air from the west, but for NO_2 mixing ratios in excess of 300 ppt, the two methods agreed to better than 10%. Stutz and Platt (1996) report less uncertainty.

AX2.6.2.4 Monitoring for NO_2 Compliance Versus Monitoring for Ozone Formation

Observations of NO_2 have been focused on demonstrating compliance with the NAAQS for NO_2. Today, few locations violate that standard, but NO_2 and related NO_y compounds remain among the most important atmospheric trace gases to measure and understand. Commercial instruments for NO/NO_x detection are generally constructed with an internal converter for reduction of NO_2 to NO, and generate a signal referred to as NO_x. These converters, generally constructed of molybdenum oxides (MoOx), reduce not only NO_2 but also most other NO_y species (Fehsenfeld et al., 1987; Crosley, 1996; Nunnermacker et al., 1998). Thus the NO_x signal is more accurately referred to as NO_y. Unfortunately with an internal converter, the instruments may not give a faithful indication of NO_y either — reactive species such as HNO_3 will adhere to the walls of the inlet system. Most recently, commercial vendors such as Thermo Environmental (Franklin, MA) have offered NO/NO_y detectors with external Mo converters. If such instruments are calibrated through the inlet with a reactive nitrogen species such as propyl nitrate, they should give accurate measurements of total NO_y, suitable for evaluation of photochemical models. States should be encouraged to make these NO_y measurements where ever possible.

AX2.6.3 Measurements of Nitric Acid Vapor, HNO_3

Accurate measurement of nitric acid vapor, HNO_3, has presented a long-standing analytical challenge to the atmospheric chemistry community. In this context, it is useful to consider the major factors that control HNO_3 partitioning between the gas and deliquesced-particulate phases in ambient air. In equation form,

$$HNO_{3g} \overset{K_H}{\Leftrightarrow} [HNO_{3aq}] \overset{K_a}{\Leftrightarrow} [H^+] + [NO_3^-] \quad \text{(AX2-52)}$$

where K_H is the Henry's Law constant in M atm-1 and Ka is the acid dissociation constant in M.

Thus, the primary controls on HNO_3 phase partitioning are its thermodynamic properties (K_H, K_a, and associated temperature corrections), aerosol liquid water content (LWC), solution pH, and kinetics. Aerosol LWC and pH are controlled by the relative mix of different acids and bases in the system, hygroscopic properties of condensed compounds, and meteorological conditions (RH, temperature, and pressure). It is evident from relationship XX that, in the presence of chemically distinct aerosols of varying acidities (e.g., super-µm predominantly sea salt and sub-µm predominantly S aerosol), HNO_3 will partition preferentially with the less-acidic particles, which is consistent with observations (e.g., Huebert et al., 1996; Keene and Savoie, 1998; Keene et al., 2002). Kinetics are controlled by atmospheric concentrations of HNO_3 vapor and particulate NO_3^- and the size distribution and corresponding atmospheric lifetimes of particles against deposition. Sub-µm-diameter aerosols typically equilibrate with the gas phase in seconds to minutes while super-um aerosols require hours to a day or more (e.g., Meng and Seinfeld, 1996; Erickson et al., 1999. Consequently, smaller aerosol size fractions are typically close to thermodynamic equilibrium with respect to HNO_3 whereas larger size fractions (for which atmospheric lifetimes against deposition range from hours to a few days) are often undersaturated (e.g., Erickson et al., 1999; Keene and Savioe, 1998).

Many sampling techniques for HNO_3 (e.g., standard filterpack and mist-chamber samplers) employ upstream prefilters to remove particulate species from sample air. However, when chemically distinct aerosols with different pHs (e.g., sea salt and S aerosols) mix together on a bulk filter, the acidity of the bulk mixture will be greater than that of the less acidic aerosols with which most NO_3^- is associated. This change in pH may cause the bulk mix to be supersaturated with respect to HNO_3 leading to volatilization and, thus, positive measurement bias in HNO_3 sampled downstream. Alternatively, when undersaturated super-um size fractions (e.g., sea salt) accumulate on a bulk filter and chemically interacts over time with HNO_3 in the sample air stream, scavenging may lead to negative bias in HNO_3 sampled downsteam. Because the magnitude of both effects will vary as functions of the overall composition and thermodynamic state of the multiphase system, the combined influence can cause net positive or net negative measurement bias in resulting data. Pressure drops across particle filters can also lead to artifact volatilization and associated positive bias in HNO_3 measured downstream.

Widely used methods for measuring HNO_3 include standard filterpacks configured with nylon or alkaline-impregnated filters (e.g., Goldan et al., 1983; Bardwell et al., 1990; respectively) and standard mist chambers (Talbot et al., 1990). Samples are typically analyzed by ion chromatography. Intercomparisons of these measurement techniques (e.g., Hering et al., 1988; Tanner et al., 1989; Talbot et al., 1990) report differences of a factor of two or more.

More recently, sensitive HNO_3 measurements based on the principle of Chemical Ionization Mass Spectroscopy (CIMS) have been reported (e.g., Huey et al., 1998; Mauldin et al., 1998; Furutani and Akimoto, 2002; Neuman et al., 2002). CIMS relies on selective formation of ions such as $SiF_5^-{\cdot}HNO_3$ or $HSO_4^-{\cdot}HNO_3$ followed by detection via mass spectroscopy. Two CIMS techniques and a filter pack technique were intercompared in Boulder, CO (Fehsenfeld et al., 1998). Results indicated excellent agreement (within 15%) between the two CIMS instruments and between the CIMS and filterpack methods under relatively clean conditions with HNO_3 mixing ratios between 50 and 400 pptv. In more polluted air, the filterpack technique generally yielded higher values than the CIMS suggesting that interactions between chemically distinct particles on bulk filters is a more important source of bias in polluted continental air. Differences were also greater at lower temperature when particulate NO_3^- corresponded to relatively greater fractions of total NO_3^-.

AX2.6.4 Sampling and Analysis of Volatile Organic Compounds

Hydrocarbons can be measured with gas chromatography followed by flame ionization detection (GC-FID). Detection by mass spectroscopy is sometimes used to confirm species identified by retention time (Westberg and Zimmerman, 1993; Dewulf and Van Langenhove, 1997). Preconcentration is typically required for less abundant species. Details are available in AQCD 96.

Because of their variety, nonmethane hydrocarbons pose special analytical problems, and several laboratory and field studies have recently addresses the uncertainty of VOC measurements. An intercomparison conducted with 16 components among 28 laboratories, showed agreement on the order of 10s of percents (Apel et al., 1994). In a more recent intercomparison (Apel et al., 1999) 36 investigators from around the world were asked to identify and quantify C_2 to C_{10} hydrocarbons (HCs) in a mixture in synthetic air. Calibration was based on gas standards of individual compounds, such as propane in air, and a 16-compound mixture of C_2 to C_{16} n-alkanes, all prepared by NIST and certified to ± 3 percent. The top-performing laboratories, including several in the United States, identified all the compounds correctly, and obtained agreement of generally better than 20 percent for the 60 compounds. Intercomparison of NMHCs in ambient air has only recently been reported by a European group of 12 – 14 laboratories (Slemr et al., 2002). Some compounds gave several groups difficulties, including isobutene, butadiene, methyl pentanes, and trimethyl benzenes. These intercomparisons illustrated the need for reliable, multicomponent calibration standards.

AX2.6.4.1 Polar Volatile Organic Compounds

Many of the more reactive oxygen- and nitrogen-containing organic compounds play a role in O_3 formation and are included among list of 189 hazardous air pollutants specified in the 1990 CAAA (U.S. Congress, 1990). These compounds are emitted directly from a variety of sources including biogenic processes, biomass burning, industry, vehicles, and consumer products. Some can also be formed in the atmosphere by photochemical oxidation of hydrocarbons. Although these compounds have been referred to collectively as PVOCs, their reactivity and water solubility, rather than just polarity, make sampling and measurement challenging. As indicated in the earlier AQCD, few ambient data exist for these species, but that database has grown. The previous AQCD discusses two analytical methods for PVOCs — cryogenic trapping techniques similar to those used for the nonpolar hydrocarbon species, and adsorbent material for sample preconcentration. Here we discuss recently developed methods.

Several techniques for sampling, preconcentrating and detecting oxygenated volatile organic compounds were inter-compared during the 1995 Southern Oxidants Study Nashville Intensive (Apel et al., 1998). Both chemical traps and derivatization followed by HPLC and pre-concentration and gas chromatography followed by mass spectrometric of flame ionization were investigated. Both laboratory and field tests were conducted for formaldehyde, acetaldehyde, acetone, and propanal. Substantial differences were observed indicating that reliable sampling and measurement of PVOCs remains an analytical challenge and high research priority.

Chemical ionization-mass spectroscopy, such as proton-transfer-reaction mass spectroscopy (PTR-MS) can also be used for fast-response measurement of volatile organic compounds including acetonitrile (CH_3CN), methanol (CH_3OH), acetone (CH_3COCH_3), acetaldehyde (CH_3CHO), benzene (C_6H_6) and toluene ($C_6H_5CH_3$) (e.g., Hansel et al., 1995a,b; Lindinger et al., 1998; Leibrock and Huey, 2000; Warneke et al., 2001). The method relies on gas phase proton transfer reactions between H_3O^+ primary ions and volatile trace gases with a proton affinity higher than that of water. Into a flow drift tube continuously flushed with ambient air, H_3O^+ ions (from a hollow cathode ion source) are injected. On collisions between H_3O^+ ions and organic molecules protons H^+ are transferred thus charging the reagent. Both primary and product ions are analyzed in a quadrupole mass spectrometer and detected by a secondary electron multiplier/pulse counting system. The instrument has been successfully employed in several field campaigns and compared to other techniques including gas chromatography and Atmospheric Pressure Chemical Ionization Mass Spectrometer (AP-CIMS) (Crutzen et al., 2000; Sprung et al., 2001). Sufficient sensitivity was observed for urban and rural measurements; no interferences were discovered, although care must be exercised to avoid sampling losses. Commercial instruments are becoming available, but their price still precludes wide spread monitoring.

REFERENCES

Allan, B. J.; McFiggans, G.; Plane, J. M. C. (2000) The nitrate radical in the remote marine boundary layer. J. Geophys. Res. [Atmos.] 105(D19): 24,191-24,204.

Allan, B. J.; Plane, J. M. C.; McFiggans, G. (2001) Observations of OIO in the remote marine boundary layer. Geophys. Res. Lett. 28: 1945-1948.

Allen, D. J.; Pickering, K. E. (2002) Evaluation of lightning flash rate parameterizations for use in a global chemical transport model. J. Geophys. Res. [Atmos.] 107(D23): 10.1029/2002JD002066.

Allen, D. J.; Pickering, K. E.; Molod, A. (1997) An evaluation of deep convective mixing in the Goddard Chemical Transport Model using ISCCP cloud parameters. J. Geophys. Res. [Atmos.] 102: 25,467-25,476.

Allen, D.; Pickering, K.; Stenchikov, G.; Thompson, A.; Kondo, Y. (2000) A three-dimensional total odd nitrogen (NO_y) simulation during SONEX using a stretched-grid chemical transport model. J. Geophys. Res. [Atmos.] 105: 3851-3876.

Altshuller, A. P. (1986) The role of nitrogen oxides in nonurban ozone formation in the planetary boundary layer over N America, W Europe and adjacent areas of ocean. Atmos. Environ. 20: 245-268.

Altshuller, A. P.; Lefohn, A. S. (1996) Background ozone in the planetary boundary layer over the United States. J. Air Waste Manage. Assoc. 46: 134-141.

Alvarez, II; Senff, C. J.; Hardesty, R. M.; Parrish, D. D.; Luke, W. T.; Watson, T. B.; Daum, P. H.; Gillani, N. (1998) Comparisons of airborne lidar measurements of ozone with airborne in situ measurements during the 1995 Southern Oxidants study. J. Geophys. Res. [Atmos.] 103: 31155-35171.

American Society for Testing and Materials (ASTM) International. (2003a) Standard test method for ozone in the atmosphere: continuous measurement by ethylene chemiluminescence. In: Annual Book of ASTM Standards 2003, v. 11.03: D 5149-02. West Conshohocken, PA: American Society for Testing and Materials; pp. 443-447.

American Society for Testing and Materials (ASTM) International. (2003b) Standard test methods for continuous measurement of ozone in ambient, workplace, and indoor atmospheres (ultraviolet absorption). In: Annual Book of ASTM Standards 2003, v. 11.03: D 5156-02. West Conshohocken, PA: American Society for Testing and Materials; pp. 448-454.

Ammann, M.; Kalberer, M.; Jost, D. T.; Tobler, L.; Rössler, E.; Piguet, D.; Gäggeler, H. W.; Baltensperger, U. (1998) Heterogeneous production of nitrous acid on soot in polluted air masses. Nature (London) 395: 157-160.

Anastasio, C.; Faust, B. C.; Allen, J. M. (1994) Aqueous phase photochemical formation of hydrogen peroxide in authentic cloud waters. J. Geophys. Res. [Atmos.] 99: 8231-8248.

Anastasio, C.; Faust, B. C.; Rao, C. J. (1997) Aromatic carbonyl compounds as aqueous-phase photochemical sources of hydrogen peroxide in acidic sulfate aerosols, fogs, and clouds. 1. Non-phenolic methoxybenzaldehydes and methoxyacetophenones with reductants (phenols). Environ. Sci. Technol. 31: 218-232.

Anastasio, C.; Newberg, J. T.; Williams, D. K.; Chu, G. B.; Mathew, B. M. (1999) Photoformation of hydroxyl radical in sea salt particles. EOS Trans. Am. Geophys. Union 80: F147.

Andino, J. M.; Smith, J. N.; Flagan, R. C.; Goddard, W. A., III; Seinfeld, J. H. (1996) Mechanism of the atmospheric photooxidation of aromatics: a theoretical study. J. Phys. Chem. 100: 10,967-10,980.

Andreae, M. O. (1991) Biomass burning: its history, use, and distribution and its impact on environmental quality and global climate. In: Levine, J. S., ed. Global biomass burning: atmospheric, climatic, and biospheric implications. Cambridge, MA: MIT Press; pp. 1-21.

Andrés Hernández, M. D.; Burkert, J.; Reichert, L.; Stöbener, D.; Meyer-Arnek, J.; Dickerson, R. R.; Doddridge, B. G.; Burrows, J. P. (2001) Marine boundary layer peroxy radical chemistry during the AEROSOLS99 campaign: measurements and analysis. J. Geophys. Res. (Atmos.) 106(D18): 20,833-20,846.

Andronache, C.; Chameides, W. L.; Rodgers, M. O.; Martinez, J. E.; Zimmerman, P.; Greenberg, J. (1994) Vertical distribution of isoprene in the lower boundary layer of the rural and urban southern United States. J. Geophys. Res. [Atmos.]) 99: 16,989-17,000.

Angevine, W. M.; Buhr, M. P.; Holloway, J. S.; Trainer, M.; Parrish, D. D.; MacPherson, J. I.; Kok, G. L.; Schillawski, R. D.; Bowlby, D. H. (1996) Local meteorological features affecting chemical measurements at a North Atlantic coastal site. J. Geophys. Res. (Atmos.) 101(D22): 28,935-28,946.

Apel, E. C.; Calvert, J. G.; Fehsenfeld, F. C. (1994) The nonmethane hydrocarbon intercomparison experiment (NOMHICE): tasks 1 and 2. J. Geophys. Res. [Atmos.] 99(D8): 16,651-16,664.

Apel, E. C.; Calvert, J. G.; Riemer, D.; Pos, W.; Zika, R.; Kleindienst, T. E.; Lonneman, W. A.; Fung, K.; Fujita, E.; Shepson, P. B.; Starn, T. K.; Roberts, P. T. (1998) Measurements comparison of oxygenated volatile organic compounds at a rural site during the 1995 SOS Nashville Intensive. J. Geophys. Res. (Atmos.) 103(D17): 22,295-22,316.

Apel, E. C.; Calvert, J. G.; Gilpin, T. M.; Fehsenfeld, F. C.; Parrish, D. D.; Lonneman, W. A. (1999) The Nonmethane Hydrocarbon Intercomparison Experiment (NOMHICE): task 3. J. Geophys. Res. [Atmos.] 104(D21): 26,069-26,086.

Appenzeller, C.; Davies, H. C. (1992) Structure of stratospheric intrusions into the troposphere. Nature 358: 570-572.

Appenzeller, C.; Davies, H. C.; Norton, W. A. (1996) Fragmentation of stratospheric intrusions. J. Geophys. Res. [Atmos.] 101: 1435-1456.

Arnold, F.; Bürger, V.; Droste-Fanke, B.; Grimm, F.; Krieger, A.; Schneider, J.; Stilp, T. (1997) Acetone in the upper troposphere and lower stratosphere: impact on trace gases and aerosols. Geophys. Res. Lett. 24: 3017-3020.

Arnold, S. R.; Chipperfield, M. P.; Blitz, M. A.; Heard, D. E.; Pilling, M. J. (2004) Photodissociation of acetone: atmospheric implications of temperature-dependent quantum yields. Geophys. Res. Lett. 31(L07110): 10.1029/2003GL019099.

Ashworth, S. H.; Allan, B. J.; Plane, J. M. C. (2002) High resolution spectroscopy of the OIO radical: implications for the ozone-depleting potential of iodine. Geophys. Res. Lett. 29: 65-1 - 65-4.

Atherton, C. S.; Penner, J. E. (1988) The transformation of nitrogen oxides in the polluted troposphere. Tellus B 40: 380-392.

Atkinson, R. (1989) Kinetics and mechanisms of the gas-phase reactions of the hydroxyl radical with organic compounds. Washington, DC: American Chemical Society. (J. Phys. Chem. Ref. Data Monograph no. 1).

Atkinson, R. (1990) Gas-phase tropospheric chemistry of organic compounds: a review. Atmos. Environ. Part A 24: 1-41.

Atkinson, R. (1991) Kinetics and mechanisms of the gas-phase reactions of the NO_x radical with organic compounds. J. Phys. Chem. Ref. Data 20: 459-507.

Atkinson, R. (1994) Gas-phase tropospheric chemistry of organic compounds. Washington, DC: American Chemical Society. (J. Phys. Chem. Ref. Data Monograph no. 2).

Atkinson, R. (1997) Atmospheric reactions of alkoxy and β-hydroxyalkoxy radicals. Int. J. Chem. Kinet. 29: 99-111.

Atkinson, R. (2000) Atmospheric chemistry of VOCs and NO_x. Atmos. Environ. 34: 2063-2101.

Atkinson, R.; Arey, J. (2003) Gas-phase tropospheric chemistry of biogenic volatile organic compounds: a review. Atmos. Environ.: 10.1016/S1352-2310(03)00391-1.

Atkinson, R.; Aschmann, S. M. (1994) Products of the gas-phase reactions of aromatic hydrocarbons: effect of NO_2 concentration. Int. J. Chem. Kinet. 26: 929-944.

Atkinson, R.; Carter, W. P. L.; Darnall, K. R.; Winer, A. M.; Pitts, J. N., Jr. (1980) A smog chamber and modeling study of the gas phase NO_x-air photooxidation of toluene and the cresols. Int. J. Chem. Kinet. 12: 779-836.

Atkinson, R.; Winer, A. M.; Pitts, J. N., Jr. (1986) Estimation of night-time N_2O_5 concentrations from ambient NO_2 and NO_3 radical concentrations and the role of N_2O_5 in night-time chemistry. Atmos. Environ. 20: 331-339.

Atkinson, R.; Aschmann, S. M.; Arey, J.; Carter, W. P. L. (1989) Formation of ring-retaining products from the OH radical-initiated reactions of benzene and toluene. Int. J. Chem. Kinet. 21: 801-827.

Atkinson, R.; Arey, J.; Zielinska, B.; Aschmann, S. M. (1990) Kinetics and nitro-products of the gas-phase OH and NO_3 radical-initiated reactions of naphthalene-d8, fluoranthene-d10 and pyrene. Int. J. Chem. Kinet. 22: 999-1014.

Atkinson, R.; Baulch, D. L.; Cox, R. A.; Hampson, R. F., Jr.; Kerr, J. A.; Troe, J. (1992a) Evaluated kinetic and photochemical data for atmospheric chemistry: supplement IV, IUPAC Subcommittee on Gas Kinetic Data Evaluation for Atmospheric Chemistry. J. Phys. Chem. Ref. Data 21: 1125-1568.

Atkinson, R.; Aschmann, S. M.; Arey, J.; Shorees, B. (1992b) Formation of OH radicals in the gas phase reactions of O_3 with a series of terpenes. J. Geophys. Res. [Atmos.] 97: 6065-6073.

Atkinson, R.; Kwok, E. S. C.; Arey, J.; Aschmann, S. M. (1995) Faraday Discuss. 100: 23.

Atkinson, R.; Baulch, D. L.; Cox, R. A.; Hampson, R. F., Jr.; Kerr, J. A.; Rossi, M. J.; Troe, J. (1999) Evaluated kinetic and photochemical data for atmospheric chemistry, organic species: supplement VII. J. Phys. Chem. Ref. Data 28: 191-393.

Ayers, G. P.; Penkett, S. A.; Gillett, R. W.; Bandy, B.; Galbally, I. E.; Meyer, C. P.; Elsworth, C. M.; Bentley, S. T.; Forgan, B. W. (1992) Evidence for photochemical control of ozone concentrations in unpolluted marine air. Nature (London) 360: 446-449.

Ayers, G. P.; Gillett, R. W.; McAiney, J. M.; Dick, A. L. (1999) Chloride and bromide loss from sea-salt particles in the southern ocean air. J. Atmos. Chem. 33: 299-319.
Bais, A. F.; Madronich, S.; Crawford, J.; Hall, S. R.; Mayer, B.; Van Weele, M.; Lenoble, J.; Calvert, J. G.; Cantrell, C. A.; Shetter, R. E.; Hofzumahaus, A.; Koepke, P.; Monks, P. S.; Frost, G.; McKenzie, R.; Krotkov, N.; Kylling, A.; Swartz, W. H.; Lloyd, S.; Pfister, G.; Martin, T. J.; Roeth, E.-P.; Griffioen, E.; Ruggaber, A.; Krol, M.; Kraus, A.; Edwards, G. D.; Mueller, M.; Lefer, B. L. (2003) International Photolysis Frequency Measurement and Model Intercomparison (IPMMI): Spectral actinic solar flux measurements and modeling. J. Geophys. Res. [Atmos.] 108(D16): 10.1029/2002JD002891.
Balkanski, Y. J.; Jacob, D. J.; Gardener, G. M.; Graustein, W. C.; Turekian, K. K. (1993) Transport and residence times of tropospheric aerosols inferred from a global three-dimensional simulation of ^{210}Pb. J. Geophys. Res. [Atmos.] 98: 20,573-20,586.
Bandow, H.; Washida, N. (1985a) Ring-cleavage reactions of aromatic hydrocarbons studied by FT-IR spectroscopy. II photooxidation of *o*-, *m*-, and *p*-xylenes in the NO_x-air system. Bull. Chem. Soc. Jpn. 58: 2541-2548.
Bandow, H.; Washida, N. (1985b) Ring-cleavage reactions of aromatic hydrocarbons studied by FT-IR spectroscopy. III photooxidation of 1,2,3-, 1,2,4-, and 1,3,5-trimethylbenzene in the NO_x-air system. Bull. Chem. Soc. Jpn. 58: 2549-2555.
Banic, C. M.; Leaitch, W. R.; Isaac, G. A.; Couture, M. D.; Kleinman, L. I.; Springston, S. R.; MacPherson, J. I. (1996) Transport of ozone and sulfur to the North Atlantic atmosphere during the North Atlantic Regional Experiment. J. Geophys. Res. [Atmos.] 101: 29,091-29,104.
Banta, R. M.; Senff, C. J.; White, A. B.; Trainer, M.; McNider, R. T.; Valente, R. J.; Mayor, S. D.; Alvarez, R. J.; Hardesty, R. M.; Parrish, D.; Fehsenfeld, F. C. (1998) Daytime buildup and nighttime transport of urban ozone in the boundary layer during a stagnation episode. J. Geophys. Res. [Atmos.] 103: 22,519-22,544.
Bardwell, C. A.; Maben, J. R.; Hurt, J. A.; Keene, W. C.; Galloway, J. N.; Boatman, J. F.; Wellman, D. (1990) A technique using high-flow, dichotomous filter packs for measuring major atmospheric chemical constituents. Glob. Biogeochem. Cycles 4: 151-163.
Barrie, L. A.; Bottenheim, J. W.; Crutzen, P. J.; Rasmussen, R. A. (1988) Ozone destruction at polar sunrise in the lower Arctic atmosphere. Nature 334: 138-141.
Bartolotti, L. J.; Edney, E. O. (1995) Density functional theory derived intermediates from the OH initiated atmospheric oxidation of toluene. Chem. Phys. Lett. 245: 119-122.
Baugues, K. (1986) A review of NMOC, NO_x and NMOC/NO_x ratios measured in 1984 and 1985. Research Triangle Park, NC: U.S. Environmental Protection Agency, Office of Air Quality Planning and Standards; report no. EPA-450/4-86-015. Available from: NTIS, Springfield, VA; PB87-166963/HSU.
Baumann, K.; Williams, E. J.; Angevine, W. M.; Roberts, J. M.; Norton, R. B.; Frost, G. J.; Fehsenfeld, F. C.; Springston, S. R.; Bertman, S. B.; Hartsell, B. (2000) Ozone production and transport near Nashville, Tennessee: results from the 1994 study at New Hendersonville. J. Geophys. Res. [Atmos.] 105(D7): 9137-9153.
Behnke, W.; George, C.; Sheer, V.; Zetzsch, C. (1997) Production and decay of $ClNO_2$ from the reaction of gaseous N_2O_5 with NaCl solution: bulk and aerosol experiments. J. Geophys. Res. 102: 3795-3804.
Bell, G. B. (1960) Meteorological conditions during oxidant episodes in coastal San Diego County in October and November, 1959. Sacramento, CA: State of California, Department of Public Health.
Benjamin, S. G.; Carlson, T. N. (1986) Some effects of surface heating and topography on the region severe storm environment. Part I: three dimensional simulations. Mon. Weather Rev. 114: 307-329.
Bergin, M. H.; Pandis, S. N.; Davidson, C. I.; Jaffrezo, J.-L.; Dibb, J. E.; Russell, A. G.; Kuhns, H. D. (1996) Modeling of the processing and removal of trace gas and aerosol species by Arctic radiation fogs and comparison with measurements. J. Geophys. Res. [Atmos.] 101: 14,465-14,478.
Berkowitz, C. M.; Shaw, W. J. (1997) Airborne measurements of boundary layer chemistry during the Southern Oxidant Study: a case study. J. Geophys. Res. [Atmos.] 102: 12,795-12,804.
Berkowitz, C. M.; Fast, J. D.; Sprinston, S. R.; Larsen, R. J.; Spicer, C. W.; Doskey, P. V.; Hubbe, J. M.; Plastridge, R. (1998) Formation mechanisms and chemical characteristics of elevated photochemical layers over the northeast United States. J. Geophys. Res. [Atmos.] 103: 10,631-10,647.
Berkowitz, C. M.; Fast, J. D.; Easter, R. C. (2000) Boundary layer vertical exchange processes and the mass budget of ozone: observations and model results. J. Geophys. Res. [Atmos.] 105: 14,789-14,805.
Berkowitz, C. M.; Zaveri, R. A.; Bian, X.; Zhong, S.; Disselkamp, R. S.; Laulainen, N. S.; Chapman, E. G. (2001) Aircraft observations of aerosols, O_3 and NO_y in a nighttime urban plume. Atmos. Environ. 35: 2395-2404.
Berndt, T.; Böge, O.; Herrmann, H. (1999) On the formation of benzene oxide/oxepin in the gas-phase reaction of OH radicals with benzene. Chem. Phys. Lett. 314: 435-442.

Berndt, T.; Böge, O.; Stratmann, F. (2003) Gas-phase ozonolysis of α-pinene: gaseous products and particle formation. Atmos. Environ. 37: 3933-3945.
Berntsen, T.; Isaksen, I. S. A. (1997) A global three-dimensional chemical transport model for the troposphere. 1. Model description and CO and ozone results. J. Geophys. Res. [Atmos.] 102: 21,239-21,280.
Bey, I.; Jacob, D. J.; Logan, J. A.; Yantosca, R. M. (2001a) Asian chemical outflow to the Pacific in spring: origins, pathways, and budgets. J. Geophys. Res. [Atmos.] 106: 23,097-23,113.
Bey, I.; Jacob, D. J.; Yantosca, R. M.; Logan, J. A.; Field, B.; Fiore, A. M.; Li, Q.; Liu, H.; Mickley, L. J.; Schultz, M. G. (2001b) Global modeling of tropospheric chemistry with assimilated meteorology: model description and evaluation. J. Geophys. Res. [Atmos.] 106: 23,073-23,095.
Bierbach, A.; Barnes, I.; Becker, K. H.; Wiesen, E. (1994) Atmospheric chemistry of unsaturated carbonyls: butenedial, 4-Oxo-2-Pentenal, 3-Hexene-2,5-Dione, Maleic Anhydride, 3H-Furan-2-one, and 5-Methyl-3H-Furan-2-one. Environ. Sci. Technol. 28: 715-729.
Bishop, G. A.; Stedman, D. H. (1990) On-road carbon monoxide emission measurement comparisons for the 1988-1989 Colorado oxy-fuels program. Environ. Sci. Technol. 24: 843-847.
Bishop, G. A.; Stedman, D. H. (1996) Measuring the emissions of passing cars. Acc. Chem. Res. 29: 489-495.
Black, D. R.; Harley, R. A.; Hering, S. V.; Stolzenburg, M. R. (2000) A new, portable, real-time monitor. Environ. Sci. Technol. 34: 3031-3040.
Blanchard, C. L. (2000) Ozone process insights from field experiments. Part III: extent of reaction and ozone formation. Atmos. Environ. 34: 2035-2043.
Blanchard, C. L.; Lurmann, F. W.; Roth, P. M.; Jeffries, H. E.; Korc, M. (1999) The use of ambient data to corroborate analyses of ozone control strategies. Atmos. Environ. 33: 369-381.
Blanchard, C. L.; Stoeckenius, T. (2001) Ozone response to precursor control: comparision of data analysis methods with the predictions of photochemical air quality simulation models. Atmos. Environ. 35: 1203-1215.
Blanchard, P.; Brook, J. R.; Brazil, P. (2002) Chemical characterization of the organic fraction of atmospheric aerosol at two sites in Ontario, Canada. J. Geophys. Res. [Atmos.] 107(D21): 10.1029/2001JD000627.
Bloom, S. C.; Takacs, L. L.; Da Silva, A. M.; Ledvina, D. (1996) Data assimilation using incremental analysis updates. Mon. Weather Rev. 124: 1256-1271.
Blough, N. V. (1997) Photochemistry in the sea-surface microlayer. In: Liss, P. S.; Duce, R. A., eds. The sea surface and global change. New York, NY: Cambridge University Press, pp. 383-424.
Blough, N. V.; Zepp. R. G. (1995) Reactive oxygen species in natural waters. In: Foote, C. S.; Valentine, A.; Greenberg, A.; Liebman, J. F., eds. Active Oxygen in Chemistry. New York, NY: Chapman and Hall, Ch.8, pp. 280-333.
Blumenthal, D. L.; Lurmann, F. W.; Kumar, N.; Dye, T. S.; Ray, S. E.; Korc, M. E.; Londergan, R.; Moore, G. (1997) Transport and mixing phenomena related to ozone exceedances in the northeast U.S. (analysis based on NARSTO-northeast data). Available: http://capita.wustl.edu/otag/reports/otagrept/otagrept.html (30 October 2003).
Bonn, B.; Moortgat, G. K. (2003) Sesquiterpene ozonolysis: origin of atmospheric new particle formation from biogenic hydrocarbons. Geophys. Res. Lett. 30: 10.1029/2003GL017000.
Bonner, W. D. (1968) Climatology of the low level jet. Mon. Weather Rev. 96: 833-850.
Bottenheim, J. W.; Barrie, L. A.; Atlas, E.; Heidt, L. E.; Niki, H.; Rasmussen, R. A.; Shepson, P. B. (1990) Depletion of lower tropospheric ozone during Arctic spring: The Polar Sunrise Experiment 1988. J. Geophys. Res. (Atmos.) 95: 18,555-18,568.
Brasseur, G. P.; Hauglustaine, D. A.; Walters, S.; Rasch, P. J.; Müller, J.-F.; Granier, C.; Tie, X. X. (1998) MOZART, a global transport model for ozone and related chemical tracers: 1. model description. J. Geophys. Res. [Atmos.] 103: 28,265-28,289.
Brook, J. R.; Sirois, A.; Clarke, J. F. (1996) Comparison of dry deposition velocities for SO_2, HNO_3, and SO_4^{2-} estimated with two inferential models. Water Air Soil Pollut. 87: 205-218.
Bröske, R.; Kleffmann, J.; Wiesen, P. (2003) Heterogeneous conversion of NO_2 on secondary organic aerosol surfaces: a possible source of nitrous acid (HONO) in the atmosphere? Atmos. Chem. Phys. 3: 469-474.
Browell, E. V.; Fenn, M. A.; Butler, C. F.; Grant, W. B.; Ismail, S.; Ferrare, R. A.; Kooi, S. A.; Brackett, V. G.; Clayton, M. B.; Avery, M. A.; Barrick, J. D. W.; Fuelberg, H. E.; Maloney, J. C.; Newell, R. E.; Zhu, Y.; Mahoney, M. J.; Anderson, B. E.; Blake, D. R.; Brune, W. H.; Heikes, B. G.; Sachse, G. W.; Singh, H. B.; Talbot, R. W. (2001) Large-scale air mass characteristics observed over the remote tropical Pacific Ocean during March-April 1999: results from PEM-Tropics B field experiment. J. Geophys. Res. [Atmos.] 106: 32,481-32,501.

Brueggemann, N.; Schnitzler, J.-P. (2002) Comparison of isoprene emission, intercellular isoprene concentration and photosynthetic performance with water-limited oak (*Quercus pubescens* Willd. and *Quercus robur* L.) saplings. Plant Biol. 4: 456-463.

Brühl, C.; Pöschl, U.; Crutzen, P. J.; Steil, B. (2000) Acetone and PAN in the upper troposphere: impact on ozone production from aircraft emissions. Atmos. Environ. 34: 3931-3938.

Brune, W. H. et al. (1999) OH and HO_2 chemistry in the North Atlantic free troposphere. Geophys. Res. Lett. 26: 3077-3080.

Brunner, D.; Staehelin, J.; Jeker, D. (1998) Large-scale nitrogen oxide plumes in the tropopause region and implications for ozone. Science (Washington, DC) 282: 1305-1309.

Buhr, M. P.; Trainer, M.; Parrish, D. D.; Sievers, R. E.; Fehsenfeld, F. C. (1992) Assessment of pollutant emission inventories by principal component analysis of ambient air measurements. Geophys. Res. Lett. 19: 1009-1012.

Buhr, M.; Parrish, D.; Elliot, J.; Holloway, J.; Carpenter, J.; Goldan, P.; Kuster, W.; Trainer, M.; Montzka, S.; McKeen, S.; Fehsenfeld, F. C. (1995) Evaluation of ozone precursor source types using principal component analysis of ambient air measurements in rural Alabama. J. Geophys. Res. [Atmos.] 100: 22,853-22,860.

Buhr, M.; Sueper, D.; Trainer, M.; Goldan, P.; Kuster, B.; Fehsenfeld, F. (1996) Trace gas and aerosol measurements using aircraft data from the North Atlantic Regional Experiment (NARE 1993). J. Geophys. Res. [Atmos.] 101: 29,013-29,027.

Burkert, J.; Behmann, T.; Andres-Hernández, M. D.; Stöbener, D.; Weißenmeyer, M.; Perner, D.; Burrows, J. P. (2001a) Measurements of peroxy radicals in a forested area of Portugal. Chemosphere Glob. Change Sci. 3: 327-338.

Burkert, J.; Andrés-Hernández, M. D.; Stöbener, D.; Burrows, J. P.; Weißenmeyer, M.; Kraus, A. (2001b) Peroxy radical and related trace gas measurements in the boundary layer above the Atlantic Ocean. J. Geophys. Res. (Atmos.) 106: 5457-5477.

Burkert, J.; Andrés-Hernández, M. D.; Reichert, L.; Meyer-Arnek, J.; Burrows, J. P.; Doddridge, B. G.; Dickerson, R. R.; Muehle, J.; Zhan, A.; Carsey, T. (2003) Trace gas and radical diurnal behavior in the marine boundary layer during INDOEX 1999. J. Geophys. Res. (Atmos.) 108(D8): 10.1029/2002JD002790.

Byun, D.; Young, J.; Gipson, G.; Schere, K.; Godowitch, J. (1998) Urban air quality simulation with community multi-scale air quality (CMAQ) modeling system. Research Triangle Park, NC: U.S. Environmental Protection Agency, National Exposure Research Laboratory; report no., EPA--600/A-98/115. Available from: NTIS, Springfield, VA; PB99-102246.

Calvert, J. G.; Madronich, S. (1987) Theoretical study of the initial products of the atmospheric oxidation of hydrocarbons. J. Geophys. Res. [Atmos.] 92: 2211-2220.

Calvert, J. G.; Heywood, J. B.; Sawyer, R. F.; Seinfeld, J. H. (1993) Achieving acceptable air quality: some reflections on controlling vehicle emissions. Science (Washington, DC) 261: 37-45.

Calvert, J. G.; Yarwood, G.; Dunker, A. M. (1994) An evaluation of the mechanism of nitrous acid formation in the urban atmosphere. Res. Chem. Intermed. 20: 463-502.

Calvert, J. G.; Atkinson, R.; Kerr, J. A.; Madronich, S.; Moortgat, G. K.; Wallington, T. J.; Yarwood, G. (2000) The mechanisms of atmospheric oxidation of the alkenes. New York, NY: Oxford University Press, Inc.

Calvert, J. G.; Atkinson, R.; Becker, K. H.; Kamens, R. M.; Seinfeld, J. H.; Wallington, T. J.; Yarwood, G. (2002) The mechanisms of atmospheric oxidation of aromatic hydrocarbons. New York, NY: Oxford University Press, Inc.

Cantrell, C. A.; Shetter, R. E.; Gilpin, T. M.; Calvert, J. G.; Eisele, F. L.; Tanner, D. J. (1996) Peroxy radical concentrations measured and calculated from trace gas measurements in the Mauna Loa Observatory Photochemistry Experiment 2. J. Geophys. Res. (Atmos.) 101: 14,653-14,664.

Cantrell, C. A.; Calvert, J. G.; Bais, A.; Shetter, R. E.; Lefer, B. L.; Edwards, G. D. (2003) Overview and conclusions of the International Photolysis Frequency Measurement and Modeling Intercomparison (IPMMI) study. J. Geophys. Res. (Atmos.) 108(D16): 10.1029/2002JD002962.

Cardelino, C. A.; Chameides, W. L. (1990) Natural hydrocarbons, urbanization, and urban ozone. J. Geophys. Res. [Atmos.] 95: 13,971-13,979.

Cardelino, C. A.; Chameides, W. L. (1995) An observation-based model for analyzing ozone precursor relationships in the urban atmosphere. J. Air Waste Manage. Assoc. 45: 161-180.

Cardelino, C. A.; Chameides, W. L. (2000) The application of data from photochemical assessment monitoring stations to the observation-based model. Atmos. Environ. 34: 2325-2332.

Carpenter, L. J.; Sturges, W. T. Liss, P. S.; Penkett, S. A.; Alicke, B.; Hebestreit, K.; Platt, U. (1999) Short-lived alkyl iodides and bromides at Mace Head, Ireland: links to biogenic sources and halogen oxide production. J. Geophys. Res. (Atmos.) 104: 1679-1689.

Carroll, M. A.; Hastie, D. R.; Ridley, B. A.; Rodgers, M. O.; Torres, A. L.; Davis, D. D.; Bradshaw, J. D.; Sandholm, S. T.; Schiff, H. I.; Karecki, D. R.; Harris, G. W.; Mackay, G. I.; Gregory, G. L.; Condon, E. P.; Trainer, M.; Hubler, G.; Montzka, D. D.; Madronich, S.; Albritton, D. L.; Singh, H. B.; Beck, S. M.; Shipham, M. C.; Bachmeier, A. S. (1990) Aircraft measurement of NO_x over the eastern Pacific and continental United States and implications for ozone production. J. Geophys. Res. [Atmos.] 95: 10,205-10,233.
Carroll, M. A.; Bertman, S. B.; Shepson, P. B. (2001) Overview of the program for research on oxidants, photochemistry, emissions and transport (PROPHET) summer 1998 measurements intensive. J. Geophys. Res. [Atmos.] 106: 24,275-24,288.
Carter, W. P. L. (1990) A detailed mechanism for the gas-phase atmospheric reactions of organic compounds. Atmos. Environ. Part A 24: 481-518.
Carter, W. P. L. (1994) Development of ozone reactivity scales for volatile organic compounds. J. Air Waste Manage. Assoc. 44: 881-899.
Carter, W. P. L. (1995) Computer modeling of environmental chamber studies of maximum incremental reactivities of volatile organic compounds. Atmos. Environ. 29: 2513.
Castro, T; Madronich, S; Rivale, S; Muhlia, A; Mar, B. (2001) The influence of aerosols on photochemical smog in Mexico City. Atmos. 35: 1765-1772..
Chameides, W. L.; Stelson, A. W. (1992) Aqueous-phase chemical processes in deliquescent sea-salt aerosols: A mechanism that couples the atmospheric cycles of S and sea salt. J. Geophys. Res. [Atmos.] 97(D18): 20,565-20,580.
Chameides, W. L.; Lindsay, R. W.; Richardson, J.; Kiang, C. S. (1988) The role of biogenic hydrocarbons in urban photochemical smog: Atlanta as a case study. Science (Washington, DC) 241: 1473-1475.
Chameides, W. L.; Fehsenfeld, F.; Rodgers, M. O.; Cardelino, C.; Martinez, J.; Parrish, D.; Lonneman, W.; Lawson, D. R.; Rasmussen, R. A.; Zimmerman, P.; Greenberg, J.; Middleton, P.; Wang, T. (1992) Ozone precursor relationships in the ambient atmosphere. J. Geophys. Res. [Atmos.] 97: 6037-6055.
Chang, J. S.; Brost, R. A.; Isaken, I. S. A.; Madronich, S.; Middleton, P.; Stockwell, W. R.; Walcek, C. J. (1987) A three-dimensional Eulerian acid deposition model: physical concepts and formulation. J. Geophys. Res. [Atmos.] 92: 14,681-14,700.
Chang, M. E.; Cardelino, C.; Hartley, D.; Chang, W. L. (1996) Inverse modeling of biogenic emissions. Geophys. Res. Lett. 23: 3007ff.
Chang, M. E.; Hartley, D. E.; Cardelino, C.; Hass-Laursen, D.; Chang, W. L. (1997) On using inverse methods for resolving emissions with large spatial inhomogeneities. J. Geophys. Res. (Atmos.) 102: 16,023-16,036.
Chang, T. Y.; Chock, D. P.; Nance, B. I.; Winkler, S. L. (1997) A photochemical extent parameter to aid ozone air quality management. Atmos. Environ. 31: 2787-2794.
Chang, S.; McDonand-Buller, E. C.; Kimura, Y.; Russell, M. M.; Tanaka, P. L.; Allen, D. T. (2002) Spatial and temporal impacts of chlorine chemistry on ozone formation in southeastern Texas. Austin, TX: The Texas Natural Resource Conservation Commission; Contract No. 9880077600-18. Available: ftp://ftp.tnrcc.state.tx.us/pub/OEPAA/TAD/Modeling/HGAQSE/Contract_Reports/Others/Impacts_Chlorine_on_Ozone_Formation.pdf (17 December 2003).
Chatfield, R. B.; Crutzen, P. J. (1984) Sulfur dioxide in remote oceanic air: cloud transport of reactive precursors. J. Geophys. Res. 89: 7111-7132.
Chen, L.-W. A.; Chow, J. C.; Doddridge, B. G.; Dickerson, R. R.; Ryan, W. F.; Mueller, P. K. (2003) Analysis of summertime $PM_{2.5}$ and haze episode in the mid-Atlantic region. J. Air Waste Manage. Assoc. 53: 946-956.
Cheng, M.-D.; Hopke, P. K.; Zeng, Y. (1993) A receptor-oriented methodology for determining source regions of particulate sulfate observed at Dorset, Ontario. J. Geophys. Res. [Atmos.] 98: 16,839-16,849.
Chesselet, R.; Fontugne, M.; Buat-Menard, P.; Ezat, U.; Lambert, C. E. (1981) The origin of particulate organic carbon in the marine atmosphere as indicated by its stable carbon isotopic composition. Geophys. Res. Lett. 8: 345-348.
Ching, J. K. S.; Alkezweeny, A. J. (1986) Tracer study of vertical exchange by cumulus clouds. J. Clim. Appl. Meteorol. 25: 1702-1711.
Ching, J. K. S.; Shipley, S. T.; Browell, E. V. (1988) Evidence for cloud venting of mixed layer ozone and aerosols. Atmos. Environ. 22: 225-242.
Ching, J. K. S.; Byun, D.; Young, J.; Binkowski, F. S.; Pleim, J.; Roselle, S.; Godowitch, J.; Benjey, W.; Gipson, G. (1998) Science features in Models-3 Community Multiscale Air Quality System. In: Preprints of the 10th Joint AMS/AWMA Conference on Applications of Air Pollution Meteorology; Phoenix, AZ. Pittsburgh, PA: Air & Waste Management Association.

Chock, D. P.; Winkler, S. L. (1994) A comparison of advection algorithms coupled with chemistry. Atmos. Environ. 28: 2659-2675.
Choi, W.; Leu, M.-T. (1998) Nitric acid uptake and decomposition on black carbon (soot) surfaces: its implications for the upper troposphere and lower stratosphere. J. Phys. Chem. A 102: 7618-7630.
Choi, Y. J.; Ehrman, S. H. (2004) Investigation of sources of volatile organic carbon in the Baltimore area using highly time-resolved measurements. Atmos. Environ. 38: 775-791.
Civerolo, K.; Dickerson, R. R. (1998) Nitric oxide soil emissions from tilled and untilled cornfields. Agric. For. Meteorol. 90: 307-311.
Civerolo, K. L.; Mao, H. T.; Rao, S. T. (2003) The airshed for ozone and fine particulate pollution in the eastern United States. Pure Appl. Geophys. 160: 81-105.
Claeys, M.; Wang, W.; Ion, A. C.; Kourtchev, I.; Gelencsér, A.; Maenhaut, W. (2004) Formation of secondary organic aerosols from isoprene and its gas-phase oxidation products through reaction with hydrogen peroxide. Atmos. Environ. 38: 4093-4098.
Clark, T. L.; Karl, T. R. (1982) Application of prognostic meteorological variables to forecasts of daily maximum one-hour ozone concentrations in the northeastern United States. J. Appl. Meteorol. 21: 1662-1671.
Cleary, P. A.; Wooldridge, P. J.; Cohen, R. C. (2002) Laser-induced fluorescence detection of atmospheric NO_2 with a commercial diode laser and a supersonic expansion. Appl. Optics 41: 6950-6956.
Cleveland, W. S.; Guarino, R.; Kleiner, B.; McRae, J. E.; Warner, J. L. (1976) The analysis of the ozone problem in the northeast United States. In: Specialty conference on: ozone/oxidants-interactions with the total environment; March; Dallas, TX. Pittsburgh, PA: Air Pollution Control Association; pp. 109-119.
Cleveland, W. S.; Kleiner, B.; McRae, J. E.; Warner, J. L. (1976) Photochemical air pollution: transport from New York City area into Connecticut and Massachusetts. Science (Washington, DC) 191: 179-181.
Cohen, R. C. (1999) Laser-induced fluorescence detection of atmospheric NO_2 at parts per trillion mixing ratios: implications for nitrogen oxide photochemistry in the stratosphere and troposphere. Abstr. Pap. Am. Chem. Soc. (Phys.) 218(Pt. 2): 262.
Collins, W. J.; Stevenson, D. S.; Johnson, C. E.; Derwent, R. G. (1997) Tropospheric ozone in a global-scale three-dimensional Lagrangian model and its response to NO_x emission controls. J. Atmos. Chem. 26: 223-274.
Comes, F. J.; Armerding, W.; Grigonis, R.; Herbert, A.; Spiekermann, M.; Walter, J. (1992) Tropospheric OH: local measurements and their interpretations. Ber. Bunsen-Ges. Phys. Chem. 96: 284-286.
Cooper, O. R.; Moody, J. L. (2000) Meteorological controls on ozone at an elevated eastern United States regional background monitoring site. J. Geophys. Res. [Atmos.] 105: 6855-6869.
Cooper, O. R.; Moody, J. L.; Davenport, J. C.; Oltmans, S. J.; Johnson, B. J.; Chen, X.; Shepson, P. B.; Merrill, J. T. (1998) Influence of springtime weather systems on vertical ozone distributions over three North American sites. J. Geophys. Res. [Atmos.] 103: 22,001-22,013.
Cooper, O. R.; Moody, J. L.; Parrish, D. D.; Trainer, M.; Ryerson, T. B.; Holloway, J. S.; Hübler, G.; Fehsenfeld, F. C.; Oltmans, S. J.; Evans, M. J. (2001) Trace gas signatures of the airstreams within North Atlantic cyclones: case studies from the North Atlantic Regional Experiment (NARE '97) aircraft intensive. J. Geophys. Res. [Atmos.] 106: 5437-5456.
Cooper, O. R.; Moody, J. L.; Parrish, D. D.; Trainer, M.; Ryerson, T. B.; Holloway, J. S.; Hübler, G.; Fehsenfeld, F. C.; Evans, M. J. (2002a) Trace gas composition of mid-latitude cyclones over the western North Atlantic Ocean: a conceptual model. J. Geophys. Res. [Atmos.] 107(D7): 10.1029/2000JD000901.
Cooper, O. R.; Moody, J. L.; Parrish, D. D.; Trainer, M.; Holloway, J. S.; Hübler, G.; Fehsenfeld, F. C.; Oltmans, S. J.; Evans, M. J. (2002b) Trace gas composition of mid-latitude cyclones over the western North Atlantic Ocean: a seasonal comparison of O_3 and CO. J. Geophys. Res. [Atmos.] 107(D7): 10.1029/2001JD000902.
Cooper, O.; Forster, C.; Parrish, D.; Dunlea, E.; Hübler, G.; Fehsenfeld, F.; Holloway, J.; Oltmans, S.; Johnson, B.; Wimmers, A.; Horowitz, L. (2004a) On the life cycle of a stratospheric intrusion and its dispersion into polluted warm conveyor belts. J. Geophys. Res. (Atmos.) 109(D23S09): 10.1029/2003JD004006.
Cooper, O. R.; Forster, C.; Parrish, D.; Trainer, M.; Dunlea, E.; Ryerson, T.; Hübler, G.; Fehsenfeld, F.; Nicks, D.; Holloway, J.; De Gouw, J.; Warneke, C.; Roberts, J. M.; Flocke, F.; Moody, J. (2004b) A case study of transpacific warm conveyor belt transport: the influence of merging airstreams on trace gas import to North America. J. Geophys. Res. (Atmos.) 109(D23S08): 10.1029/2003JD003624.
Corchnoy, S. B.; Atkinson, R. (1990) Kinetics of the gas-phase reactions of OH and NO_3 radicals with 2-Carene, 1,8-cineole, *p*-cymene, and terpinolene. Environ. Sci. Technol. 24: 1497-1502.
Cornell, S.; Rendell, A.; Jickells, T. (1995) Atmospheric inputs of dissolved organic nitrogen to the oceans. Nature 376: 243-246.

Cornell, S. E.; Jickells, T. D.; Thornton, C. A. (1998) Urea in rainwater and atmospheric aerosols. Atmos. Environ. 32: 1903-1910.
Cornell, S.; Mace, K.; Coeppicus, S.; Duce, R.; Huebert, B.; Jickells, T.; Zhuang, L. Z. (2001) Organic nitrogen in Hawaiian rain and aerosols. J. Geophys. Res. (Atmos.) 106: 7973-7983.
Corsmeier, U.; Kalthhoff, N.; Kolle, O.; Motzian, M.; Fiedler, F. (1997) Ozone concentration jump in the stable nocturnal boundary layer during a LLJ-event. Atmos. Environ. 31: 1977-1989.
Cowling, E. B.; Chameides, W. L.; Kiang, C. S.; Fehsenfeld, F. C.; Meagher, J. F. (2000) Introduction to special section: Southern Oxidant Study Nashville/Middle Tennessee Ozone Study, part 2. J. Geophys. Res. (Atmos.) 105: 9075-9077.
Cox, R. A.; Bloss, W. J.; Jones, R. L.; Rowley, D. M. (1999) OIO and the atmospheric cycle of iodine. Geophys. Res. Lett. 26: 1857-1860.
Crawford, J. H.; Davis, D. D.; Chen, G.; Buhr, M.; Oltmans, S.; Weller, R.; Mauldin, L.; Eisele, F.; Shetter, R.; Lefer, B.; Arimoto, R.; Hogan, A. (2001) Evidence for photochemical production of ozone at the South Pole surface. Geophys. Res. Lett. 28: 3641-3644.
Crosley, D. R. (1996) NO_y blue ribbon panel. J. Geophys. Res. [Atmos.] 101(D1): 2049-2052.
Crutzen, P. (1973) A discussion of the chemistry of some minor constituents in the stratosphere and troposphere. Pure Appl. Geophys. 106-108: 1385-1399.
Crutzen, P. J.; Gidel, L. T. (1983) A two-dimensional photochemical model of the atmosphere. 2. The tropospheric budgets of the anthropogenic chlorocarbons, CO, CH_4, CH_3Cl and the effect of various NO_x sources on tropospheric ozone. J. Geophys. Res. [Atmos.] 88: 6641-6661.
Crutzen, P. J.; Lawrence, M. G.; Pöschl, U. (1999) On the background photochemistry of tropospheric ozone. Tellus 51A-B: 123-146.
Crutzen, P. J.; Williams, J.; Pöschl, U.; Hoor, P.; Fischer, H.; Warneke, C.; Holzinger, R.; Hansel, A.; Lindinger, W.; Scheeren, B.; Lelieveld, J. (2000) High spatial and temporal resolution measurements of primary organics and their oxidation products over the tropical forest of Surinam. Atmos. Environ. 34: 1161-1165.
Cziczo, D. J.; Abbatt, J. P. D. (1999) Deliquescence, efflorescence, and supercooling of ammonium sulfate aerosols at low temperature: implications for cirrus cloud formation and aerosol phase in the atmosphere. J. Geophys. Res. [Atmos.] 104: 13,781-13,790.
Czoschke, N. M.; Jang, M.; Kamens, R. M. (2003) Effect of acidic seed on biogenic secondary organic aerosol growth. Atmos. Environ. 37: 4287-4299.
Danielsen, E. F. (1968) Stratospheric-tropospheric exchange based on radioactivity, ozone and potential vorticity. J. Atmos. Sci. 25: 502-518.
Danielsen, E. F. (1980) Stratospheric source for unexpectedly large values of ozone measured over the Pacific Ocean during Gametag, August 1977. J. Geophys. Res. C: Oceans Atmos. 85: 401-412.
Danielsen, E. F. (1993) In situ evidence of rapid, vertical, irreversible transport of lower tropospheric air into the lower tropical stratosphere by convective cloud turrets and by larger-scale upwelling in tropical cyclones. J. Geophys. Res. [Atmos.] 98(D5): 8665-8681.
Danielsen, E. F.; Mohnen, V. A. (1977) Project Dustorm report: ozone transport, in situ measurements, and meteorological analyses of tropopause folding. J. Geophys. Res. [Atmos.] 82: 5867-5877.
Danielsen, E. F., Hipskind, R. S.; Gaines, S. E.; Sachse, G. W.; Gregory, G. L.; Hill, G. F. (1987) Three-dimensional analysis of potential vorticity associated with tropopause folds and observed variations of ozone and carbon monoxide. J. Geophys. Res. [Atmos.] 92: 2103-2111.
Daum, P. H.; Kleinman, L. I.; Hills, A. J.; Lazrus, A. L.; Leslie, A. C. D.; Busness, K.; Boatman, J. (1990) Measurement and interpretation of concentrations of H_2O_2 and related species in the upper midwest during summer. J. Geophys. Res. [Atmos.] 95: 9857-9871.
Daum, P. H.; Kleinman, L. I.; Newman, L.; Luke, W. T.; Weinstein-Lloyd, J.; Berkowitz, C. M.; Busness, K. M. (1996) Chemical and physical properties of plumes of anthropogenic pollutants transported over the North Atlantic during the North Atlantic Regional Experiment. J. Geophys. Res. [Atmos.] 101: 29,029-29,042.
Davidson, E. A.; Kingerlee, W. (1997) A global inventory of nitric oxide emissions from soils. Nutr. Cycling Agroecosyst. 48: 37-50.
Davies, T. D.; Schuepbach, E. (1994) Episodes of high ozone concentrations at the earth's surface resulting from transport down from the upper troposphere/lower stratosphere: a review and case studies. Atmos. Environ. 28: 53-68.
Davis, D. D.; Bollinger, W.; Fischer, S. (1975) A kinetics study of the reaction of the OH free radical with aromatic compounds I. Absolute rate constants for reaction with benzene and toluene at 300°K. J. Phys. Chem. 79: 293-294.

Day, D. A.; Wooldridge, P. J.; Dillon, M. B.; Thornton, J. A.; Cohen, R. C. (2002) A thermal dissociation laser-induced fluorescence instrument for in situ detection of NO_2, peroxy nitrates, alkyl nitrates, and HNO_3. J. Geophys. Res. (Atmos.) 107(D5-D6): 10.1029/2001JD000779.
DeCaria, A. J.; Pickering, K. E.; Stenchikov, G. L.; Scala, J. R.; Stith, J. L.; Dye, J. E.; Ridley, B. A.; Laroche, P. (2000) A cloud-scale model study of lightning-generate NO_x in an individual thunderstorm during STERAO-A. J. Geophys. Res. [Atmos.] 105: 11601-11616.
DeMore, W. B.; Sander, S. P.; Golden, D. M.; Hampson, R. F.; Kurylo, M. J.; Howard, C. J.; Ravishankara, A. R.; Kolb, C. E.; Molina, M. J. (1992) Chemical kinetics and photochemical data for use in stratospheric modeling: evaluation number 10. Pasadena, CA: National Aeronautics and Space Administration, Jet Propulsion Laboratory; JPL publication no. 92-20.
Dennis, R. L.; Novak, J. H. (1992) EPA's third generation modeling system (Models-3): an overview. In: Berglund, R. L., ed. Tropospheric ozone and the environment II: effects, modeling and control [papers from an international specialty conference]; November; Atlanta, GA. Pittsburgh, PA: Air & Waste Management Association; pp. 137-147. (A&WMA transactions series no. 20).
De Reus, M.; Dentener, F.; Thomas, A.; Borrmann, S.; Strom, J.; Lelieveld, J. (2000) Airborne observations of dust aerosol over the North Atlantic Ocean during ACE 2: indications for heterogeneous ozone destruction. J. Geophys. Res. [Atmos.] 105: 15,263-15,275.
Derwent, R. G.; Jenkin, M. E. (1991) Hydrocarbons and the long-range transport of ozone and PAN across Europe. Atmos. Environ. Part A 25: 1661-1678.
Derwent, R. G.; Jenkin, M. E.; Saunders, S. M. (1996) Photochemical ozone creation potentials for a large number of reactive hydrocarbons under European conditions. Atmos. Environ. 30: 181-199.
Derwent, R. G.; Jenkin, M. E.; Saunders, S. M.; Pilling, M. J. (1998) Photochemical ozone creation potentials for organic compounds in northwest Europe calculated with a master chemical mechanism. Atmos. Environ. 32: 2429-2441.
Derwent, R. G.; Collins, W. J.; Johnson, C. E.; Stevenson, D. S. (2001) Transient behaviour of tropospheric ozone precursors in a global 3-D CTM and their indirect greenhouse effects. Climatic Change 49: 463-487.
Dewulf, J.; Van Langenhove, H. (1997) Analytical techniques for the determination and measurement data of 7 chlorinated C1- and C2-hydrocarbons and 6 monocyclic aromatic hydrocarbons in remote air masses: an overview. Atmos. Environ. 31: 3291-3307.
Dibb, J. E.; Arsenault, M.; Peterson, M. C. (2002) Fast nitrogen oxide photochemistry in Summit, Greenland snow. Atmos. Environ. 36: 2501-2511.
Dickerson, R. R.; Huffman, G. J.; Luke, W. T.; Nunnermacker, L. J.; Pickering, K. E.; Leslie, A. C. D.; Lindsey, C. G.; Slinn, W. G. N.; Kelly, T. J.; Daum, P. H.; Delany, A. C.; Greenberg, J. P.; Zimmerman, P. R.; Boatman, J. F.; Ray, J. D.; Stedman, D. H. (1987) Thunderstorms: an important mechanism in the transport of air pollutants. Science (Washington, DC) 235: 460-465.
Dickerson, R. R.; Doddridge, B. G.; Kelley, P.; Rhoads, K. P. (1995) Large-scale pollution of the atmosphere over the remote Atlantic Ocean: evidence from Bermuda. J. Geophys. Res. [Atmos.]100: 8945-8952.
Dickerson, R. R.; Kondragunta, S.; Stenchikov, G.; Civerolo, K. L.; Doddridge, B. G.; Holben, B. N. (1997) The impact of aerosols on solar ultraviolet radiation and photochemical smog. Science (Washington, DC) 278: 827-830.
Dickerson, R. R.; Rhoads, K. P.; Carsey, T. P.; Oltmans, S. J.; Burrows, J. P.; Crutzen, P. J. (1999) Ozone in the remote marine boundary layer: a possible role for halogens. J. Geophys. Res. [Atmos.] 104: 21,385-21,395.
Djurić, D.; Damiani, M. S., Jr. (1980) On the formation of the low-level jet over Texas. Mon. Weather Rev. Vol. 108: 1854-1865.
Dodge, M. C. (1977) Combined use of modeling techniques and smog chamber data to derive ozone-precursor relationships. In: Dimitriades, B., ed. International conference on photochemical oxidant pollution and its control - proceedings: volume II; September 1976; Raleigh, NC. Research Triangle Park, NC: U.S. Environmental Protection Agency, Environmental Sciences Research Laboratory; pp. 881-889; report no. EPA-600/3-77-001b. Available from: NTIS, Springfield, VA; PB-264233.
Dodge, M. C. (1977) Effect of selected parameters on predictions of a photochemical model. Research Triangle Park, NC: U.S. Environmental Protection Agency, Environmental Sciences Research Laboratory; EPA report no. EPA-600/3-77-048. Available from: NTIS, Springfield, VA; PB-269858.
Dominé, F.; Shepson, P. B. (2002) Air-snow interactions and atmospheric chemistry. Science (Washington, DC) 297: 1506-1510.
Dommen, J.; Prévôt, A. S. H.; Hering, A. M.; Staffelbach, T.; Kok, G. L.; Schilawsky, R. D. (1999) Photochemical production and aging of an urban air mass. J. Geophys. Res. (Atmos.) 104: 5493-5506.

Dudhia, J. (1993) A nonhydrostatic version of the Penn State-NCAR mesoscale model: validation tests and simulation of an Atlantic cyclone and cold front. Mon. Weather Rev. 121: 1493-1513.

Dumdei, B. E.; O'Brien, R. J. (1984) Toluene's degradation products under simulated atmospheric conditions. Nature (London) 311: 248-250.

Dumdei, B. E.; Kenny, D. V.; Shepson, P. B.; Kleindienst, T. E.; Nero, C. M.; Cupitt, L. T.; Claxton, L. D. (1988) MS/MS analysis of the products of toluene photooxidation and measurement of their mutagenic activity. Environ. Sci. Technol. 22: 1493-1498.

Eckhardt, S.; Stohl, A.; Beirle, S.; Spichtinger, N.; James, P.; Forster, C.; Junker, C.; Wagner, T.; Platt, U.; Jennings, S. G. (2003) The North Atlantic oscillation controls air pollution transport to the Arctic. Atmos. Chem. Phys. 3: 1769-1778.

Eder, B. K.; Davis, J. M.; Bloomfield, P. (1993) A characterization of the spatiotemporal variability of non-urban ozone concentrations over the Eastern United States. Atmos. Environ. 27A: 2645-2668.

Eder, B. K.; Davis, J. M.; Bloomfield, P. (1994) An automated classification scheme designed to better elucidate the dependence of ozone on meteorology. J. Appl. Meteorol. 33: 1182-1199.

Edney, E. O.; Driscoll, D. J.; Weathers, W. S.; Kleindienst, T. E.; Conver, T. S.; McIver, C. D.; Li, W. (2001) Formation of polyketones in irradiated toluene/propylene/NO_x/air mixtures. Aerosol Sci. Technol. 35: 998-1008.

Ehhalt, D. H.; Dorn, H.-P.; Poppe, D. (1991) The chemistry of the hydroxyl radical in the troposphere. In: Last, F. T.; Watling, R., eds. Acidic deposition: its nature and impacts. Proceedings of the international symposium; September 1990; Glasgow, United Kingdom. Proc. R. Soc. Edinburgh, Sect. B: Biol. Sci. 97: 17-34.

Eisele, F. L.; Mount, G. H.; Tanner, D.; Jefferson, A.; Shetter, R.; Harder, J. W.; Williams, E. J. (1997) Understanding the production and interconversion of the hydroxyl radical during the tropospheric OH photochemistry experiment. J. Geophys. Res. 102: 6457-6465.

Emmons, L. K.; Carroll, M. A.; Hauglustaine, D. A.; Brasseur, G. P.; Atherton, C.; Penner, J.; Sillman, S.; Levy, H., II; Rohrer, F.; Wauben, W. M. F.; van Velthoven, P. F. J.; Wang, Y.; Jacob, D.; Bakwin, P.; Dickerson, R.; Doddridge, B.; Gerbig, C.; Honrath, R.; Hübler, G.; Jaffe, D.; Kondo, Y.; Munger, J. W.; Torres, A.; Volz-Thomas, A. (1997) Climatologies of NO_x and NO_y: a comparison of data and models. Atmos. Environ. 31: 1837-1850.

Emmons, L. K.; Hauglustaine, D. A.; Müller, J.-F.; Carroll, M. A.; Brasseur, G. P.; Brunner, D.; Staehelin, J.; Thouret, V.; Marenco, A. (2000) Data composites of airborne observations of tropospheric ozone and its precursors. J. Geophys. Res. [Atmos.] 105: 20,497-20,538.

Erickson, D. J.; Seuzaret, C.; Keene, W. C.; Gong, S.-L. (1999) A general circulation model based calculation of HCl and $ClNO_2$ production from sea-salt dechlorination: reactive chlorine emissions inventory. J. Geophys. Res. [Atmos.] 104: 8347-8372.

Fast, J. D.; Zhong, S. Y. (1998) Meteorological factors associated with inhomogeneous ozone concentrations within the Mexico City basin. J. Geophys. Res. (Atmos.) 103: 18,927-18,946.

Fast, J. D.; Doran, J.; Shaw, W. J.; Coulter, R. L.; Martin, T. J. (2000) The evolution of the boundary layer and its effect on air chemistry in the Phoenix area. J. Geophys. Res. [Atmos.] 105: 22,833-22,848.

Fast, J. D.; Zaveri, R. A.; Bian, R. X.; Chapman, E. G.; Easter, R. C. (2002) Effect of regional-scale transport on oxidants in the vicinity of Philadelphia during the 1999 NE-OPS Field Campaign. J. Geophys. Res. [Atmos.] 107(D16): 10.1029/2001JD000980.

Faust, B. C.; Anastasio, C.; Allen, J. M.; Arakaki, T. (1993) Aqueous-phase photochemical formation of peroxides in authentic cloud and fog waters. Science 260: 73-75.

Faust, B. C. (1994) A review of the photochemical redox reactions of iron(III) species in atmospheric, oceanic, and surface waters: influences on geochemical cycles and oxidant formation. In: Helz, G. R.; Zepp, R. G.; Crosby, D. G., eds. Aquatic and Surface Photochemistry. Boca Raton, FL: Lewis Publishers; pp. 3-37.

Faust, B. C. (1994) Photochemistry of clouds, fogs, and aerosols. Environ. Sci. Technol. 28: 217A-222A.

Fehsenfeld, F. C.; Dickerson, R. R.; Hübler, G.; Luke, W. T.; Nunnermacker, L. J.; Williams, E. J.; Roberts, J. M.; Calvert, J. G.; Curran, C. M.; Delany, A. C.; Eubank, C. S.; Fahey, D. W.; Fried, A.; Gandrud, B. W.; Langford, A. O.; Murphy, P. C.; Norton, R. B.; Pickering, K. E.; Ridley, B. A. (1987) A ground-based intercomparison of NO, NO_x, and NO_y measurement techniques. J. Geophys. Res. [Atmos.] 92: 14,710-14,722.

Fehsenfeld, F.; Calvert, J.; Fall, R.; Goldan, P.; Guenther, A. B.; Hewitt, C. N.; Lamb, B.; Liu, S.; Trainer, M.; Westberg, H.; Zimmerman, P. (1992a) Emissions of volatile organic compounds from vegetation and the implications for atmospheric chemistry. Global Biogeochem. Cycles 6: 389-430.

Fehsenfeld, F. C.; Trainer, M.; Parrish, D. D.; Volz-Thomas, A.; Penkett, S. (1996a) North Atlantic Regional Experiment (NARE) 1993 summer intensive: foreword. J. Geophys. Res. [Atmos.] 101: 28,869-28,875.
Fehsenfeld, F. C.; Daum, P.; Leaitch, W. R.; Trainer, M.; Parrish, D. D.; Hübler, G. (1996b) Transport and processing of O_3 and O_3 precursors over the North Atlantic: an overview of the 1993 North Atlantic Regional Experiment (NARE) summer intensive. J. Geophys. Res. [Atmos.] 101(D22): 28877-28891.
Fehsenfeld, F. C.; Huey, L. G.; Sueper, D. T.; Norton, R. B.; Williams, E. J.; Eisele, F. L.; Mauldin, R. L., III; Tanner, D. J. (1998) Ground-based intercomparison of nitric acid measurement techniques. J. Geophys. Res. [Atmos.] 103(D3): 3343-3353.
Ferman, M. A.; Monson, P. R. (1978) Comparison of rural and urban air quality. Presented at: 71st annual meeting of the Air Pollution Control Association; June; Houston, TX. Pittsburgh, PA: Air Pollution Control Association; paper no. 78-10.4.
Fick, J.; Pommer, L.; Nilsson, C.; Andersson, B. (2003) Effect of OH radicals, relative humidity, and time on the composition of the products formed in the ozonolysis of α-pinene. Atmos. Environ. 37: 4087-4096.
Finlayson-Pitts, B. J. (1993) Comment on "Indications of photochemical histories of Pacific air masses from measurements of atmospheric trace species at Point Arena, California" by D. D. Parrish et al. J. Geophys. Res. [Atmos.] 98(D8): 14,991-14,993.
Finlayson-Pitts, B. J.; Pitts, J. N., Jr. (1993) Atmospheric chemistry of tropospheric ozone formation: scientific and regulatory implications. Air Waste 43: 1091-1100.
Finlayson-Pitts, B. J.; Pitts, J. N., Jr. (2000) Chemistry of the upper and lower atmosphere theory, experiments and applications. San Diego, CA: Academic Press.
Fiore, A. M.; Jacob, D. J.; Bey, I.; Yantosca, R. M.; Field, B. D.; Fusco, A. C.; Wilkinson, J. G. (2002) Background ozone over the United States in summer: origin, trend, and contribution to pollution episodes. J. Geophys. Res. (Atmos.) 107(D15): 10.1029/2001JD000982.
Fiore, A. M.; Jacob, D. J.; Mathur, R.; Martin, R. V. (2003) Application of empirical orthogonal functions to evaluate ozone simulations with regional and global models. J. Geophys. Res. [Atmos.]: in press.
Fiore, A.; Jacob, D. J.; Liu, H.; Yantosca, R. M.; Fairlie, T. D.; Li, Q. (2003) Variability in surface ozone background over the United States: implications for air quality policy. J. Geophys. Res. (Atmos.): submitted.
Fishman, J.; Wozniak, A. E.; Creilson, J. K. (2003) Global distribution of tropospheric ozone from satellite measurements using the empirically corrected tropospheric ozone residual technique: identification of the regional aspects of air pollution. Atmos. Chem. Phys. 3: 893-907.
Forstner, H. J. L.; Flagan, R. C.; Seinfeld, J. H. (1997) Secondary organic aerosol from the photooxidation of aromatic hydrocarbons: molecular composition. Environ. Sci. Technol. 31: 1345-1358.
Fortuin, J. P. F.; Kelder, H. (1998) An ozone climatology based on ozonesonde and satellite measurements. J. Geophys. Res. 103: 31,709-31,734.
Fox-Rabinovitz, M. S.; Takacs, L. L.; Govindaraju, R. C. (2002) A variable-resolution stretched-grid general circulation model and data assimilation system with multiple areas of interest: studying the anomalous regional climate events of 1998. J. Geophys. Res. [Atmos.] 107(D24): 10.1029/2002JD002177.
Fried, A.; Hodgeson, J. (1982) Laser photoacoustic detection of nitrogen dioxide in the gas-phase titration of nitric oxide with ozone. Anal. Chem. 54: 278-282.
Fuglestvedt, J. S.; Berntsen, T. K.; Isaksen, I. S. A.; Mao, H.; Liang, X.-Z.; Wang, W.-C. (1999) Climatic forcing of nitrogen oxides through changes in tropospheric ozone and methane; global 3D model studies. Atmos. Environ. 33: 961-978.
Fujita, E. M.; Croes, B. E.; Bennett, C. L.; Lawson, D. R.; Lurmann, F. W.; Main, H. H. (1992) Comparison of emission inventory and ambient concentration ratios of CO, NMOG, and NO_x in California's south coast air basin. J. Air Waste Manage. Assoc. 42: 264-276.
Fujita et al., 1995.
Furutani, H.; Akimoto, H. (2002) Development and characterization of a fast measurement system for gas-phase nitric acid with a chemical ionization mass spectrometer in the marine boundary layer. J. Geophys. Res. (Atmos.) 107(D1-D2): 10.1029/2000JD000269.
Fusco, A. C.; Logan, J. A. (2003) Analysis of 1970-1995 trends in tropospheric ozone at Northern Hemisphere midlatitudes with the GEOS-CHEM model. J. Geophys. Res. (Atmos.) 108: 10.1029/2002JD002742.
Gaffney, J. S.; Marley, N. A.; Drayton, P. J.; Doskey, P. V.; Kotamarthi, V. R.; Cunningham, M. M.; Baird, J. C.; Dintaman, J.; Hart, H. L. (2002) Field observations of regional and urban impacts on NO_2, ozone, UVB, and nitrate radical production rates in the Phoenix air basin. Atmos. Environ. 36: 825-833.
Galbally, I. E.; Bentley, S. T.; Meyer, C. P. (2000) Mid-latitude marine boundary-layer ozone destruction at visible sunrise observed at Cape Grim, Tasmania, 41°S. Geophys. Res. Lett. 27: 3841-3844.

Galloway, J. N.; Whelpdale, D. M. (1980) An atmospheric sulfur budget for eastern North America. Atmos. Environ. 14: 409-417.
Galmarini, S.; Duynkerke, P. G.; de Arellano, J. V. G. (1997) Evolution of nitrogen oxide chemistry in the nocturnal boundary layer. J. Appl. Meteorol. 36: 943-957.
Garnica, R. M.; Appel, M. F.; Eagan, L. (2000) A REMPI method for the ultrasensitive detection of NO and NO_2 using atmospheric pressure laser ionization mass spectrometry. Anal. Chem. 72: 5639-5646.
Gauss, M.; Myhre, G.; Pitari, G.; Prather, M. J.; Isaksen, I. S. A.; Berntsen, T. K.; Brasseur, G. P.; Dentener, F. J.; Derwent, R. G.; Hauglustaine, D. A.; Horowitz, L. W.; Jacob, D. J.; Johnson, M.; Law, K. S.; Mickley, L. J.; Müller, J.-F.; Plantevin, P. H.; Pyle, J. A.; Rogers, H. L.; Stevenson, D. S.; Sundet, J. K.; Van Weele, M.; Wild, O. (2003) Radiative forcing in the 21st century due to ozone changes in the troposphere and the lower stratosphere. J. Geophys. Res. (Atmos.) 108(D9): 10.1029/2002JD002624.
Geiger, H.; Barnes, I.; Bejan, I.; Benter, T.; Spittler, M. (2003) The tropospheric degradation of isoprene: an updated module for the regional atmospheric chemistry mechanism. Atmos. Environ. 37: 1503-1519.
Geron, C. D.; Guenther, A. B.; Pierce, T. E. (1994) An improved model for estimating emissions of volatile organic compounds from forests in the eastern United States. J. Geophys. Res. [Atmos.] 99: 12,773-12,791.
Geron, C. D.; Nie, D.; Arnts, R. R.; Sharkey, T. D.; Singsaas, E. L.; Vanderveer, P. J.; Guenther, A.; Sickles, J. E., II; Kleindienst, T. E. (1997) Biogenic isoprene emission: model evaluation in a southeastern United States bottomland deciduous forest. J. Geophys. Res. [Atmos.] 102(D15): 18,889-18,901.
Geron, C. ; Guenther, A.; Sharkey, T.; Arnts, R.R. (2000a) Temporal variability in basal isoprene emission factor. Tree Physiol. 20: 799-805.
Geron, C.; Rasmussen, R.; Arnts, R. R.; Guenther, A. (2000b) A review and synthesis of monoterpene speciation from forests in the United States. Atmos. Environ. 34: 1761-1781.
Geron, C. D.; Harley, P.; Guenther, A. (2001) Isoprene emission capacity for US tree species. Atmos. Environ. 35: 3341-3352.
Gershenzon, Y. M.; Grigorieva, V. M.; Ivanov, A. V.; Remorov, R. G. (1995) O_3 and OH sensitivity to heterogeneous sinks of HO_x and CH_3O_2 on aerosol particles. Faraday Discuss. 100: 83-100.
Gershenzon, M. Y.; Il'in, S.; Fedotov, N. G.; Gershenzon, Y. M.; Aparina, E. V.; Zelenov, V. V. (1999) The mechanism of reactive NO_3 uptake on dry NaX (X=Cl, Br). J. Atmos. Chem. 34: 119-135.
Gershey, R. M. (1983) Characterization of seawater organic matter carried by bubble-generated aerosols. Limnol. Oceanogr. 28: 309-319.
Gertler, A. W.; Sagebiel, J. C.; Dippel, W. A.; O'Connor, C. M. (1999) The impact of California phase 2 reformulated gasoline on real-world vehicle emissions. J. Air Waste Manage. Assoc. 49: 1339-1346.
Gery, M. W.; Fox, D. L.; Jeffries, H. E.; Stockburger, L.; Weathers, W. S. (1985) A continuous stirred tank reactor investigation of the gas-phase reaction of hydroxyl radicals and toluene. Int. J. Chem. Kinet. 17: 931-955.
Gery, M. W.; Whitten, G. Z.; Killus, J. P. (1988) Development and testing of the CMB-IV for urban and regional modeling. Research Triangle Park, NC: U.S. Environmental Protection Agency, Atmospheric Sciences Research Laboratory; report no. EPA-600/3-88-012. Available from: NTIS, Springfield, VA; PB88-180039.
Gery, M. W.; Whitten, G. Z.; Killus, J. P.; Dodge, M. C. (1989) A photochemical kinetics mechanism for urban and regional scale computer modeling. J. Geophys. Res. [Atmos.] 94: 12,925-12,956.
Gettelman, A.; Holton, J. R.; Rosenlof, K. H. (1997) Mass fluxes of O_3, CH_4, N_2O, and CF_2Cl_2 in the lower stratosphere calculated from observational data. J. Geophys. Res. 102(D15): 19,149-19,159.
Geyer, A.; Alicke, B.; Konrad, S.; Schmitz, T.; Stutz, J.; Platt, U. (2001) Chemistry and oxidation capacity of the nitrate radical in the continental boundary layer near Berlin. J. Geophys. Res. (Atmos.) 106: 8013-8025.
Geyer, A.; Platt, U. (2002) Temperature dependence of the NO_3 loss frequency: A new indicator for the contribution of NO_3 to the oxidation of monoterpenes and NO_x removal in the atmosphere. J. Geophys. Res. (Atmos.) 107(D20): 10.1029/2001JD001215.
Gidel, L. T. (1983) Cumulus cloud transport of transient tracers. J. Geophys. Res. [Atmos.] 88: 6587-6599.
Gillani, N. V.; Pleim, J. E. (1996) Sub-grid-scale features of anthropogenic emissions of NO_x and VOC in the context of regional Eulerian models. Atmos. Environ. 30: 2043-2059.
Gillani, N. V.; Meagher, J. F.; Valente, R. J.; Imhoff, R. E.; Tanner, R. L.; Luria, M. (1998) Relative production of ozone and nitrates in urban and rural power plant plumes. 1. Composite results based on data from 10 field measurement days. J. Geophys. Res. [Atmos.] 103: 22,593-22,615.
Gilpin, T.; Apel, E.; Fried, A.; et al. (1997) Intercomparison of six ambient (CH_2O) measurement techniques. J. Geophys. Res. (Atmos.) 102(D17): 21,161-21,188.
Goldan, P. D.; Kuster, W. C.; Albritton, D. L.; Fehsenfeld, F. C.; Connell, P. S.; Norton, R. B.; Huebert, B. J. (1983) Calibration and tests of the filter-collection method for measuring clean-air, ambient levels of nitric acid. Atmos. Environ. 17: 1355-1364.

Goldan, P. D.; Kuster, W. C.; Fehsenfeld, F. C. (1997) Non-methane hydrocarbon measurements during the tropospheric OH photochemistry experiment. J. Geophys. Res. (Atmos.) 102: 6315-6324.
Goldan, P. D.; Trainer, M.; Kuster, W. C.; Parrish, D. D.; Carpenter, J.; Roberts, J. M.; Yee, J. E.; Fehsenfeld, F. C. (1995) Measurements of hydrocarbons, oxygenated hydrocarbons, carbon monoxide, and nitrogen oxides in an urban basin in Colorado: implications for emission inventories. J. Geophys. Res. [Atmos.] 100: 22,771-22,783.
Goldan, P. D.; Parrish, D. D.; Kuster, W. C.; Trainer, M.; McKeen, S. A.; Holloway, J.; Jobson, B. T.; Sueper, D. T.; Fehsenfeld, F. C. (2000) Airborne measurements of isoprene, CO, and anthropogenic hydrocarbons and their implications. J. Geophys. Res. [Atmos.] 105: 9091-9105.
Golden, D. M.; Smith, G. P. (2000) Reaction of OH + NO2 + M: a new view. J. Phys. Chem. A 104: 3991-3997.
Goldstein, A. H.; Schade, G. W. (2000) Quantifying biogenic and anthropogenic contributions to acetone mixing ratiosin a rural environment. Atmos. Environ. 34: 4997-5006.
Gong, S. L.; Barrie, L. A.; Blanchet, J.-P. (1997) Modeling sea-salt aerosols in the environment: 1. model development. J. Geophys. Res. 102: 3805-3818.
Gong, W.; Mickle, R. E.; Bottenheim, F. F.; Beauchamp, S.; Waugh, D. (2000) Marine/coastal boundary layer and vertical structure of ozone observed at a coastal site in Nova Scotia during the 1996 NARSTO-CE field campaign. Atmos. Environ. 34: 4139-4154.
Gorzelska, K.; Galloway, J. N.; Watterson, K.; Keene, W. C. (1992) Water-soluble primary amine compounds in rural continental precipitation. Atmos. Environ. 26: 1005-1018.
Goult, J. (1938) Vents en alitude a Fort Lamy (Tach). Ann. Phys. (Paris, France) 5: 373-379.
Grassi, B.; Pitari, G.; Visconti, G. (1997) Results of a chemical-transport model with interactive aerosol microphysics. In: Bojkov, R.; Visconti, G. Proceedings of the XVIII Quadrennial Ozone Symposium; September, 1996; L'Aquila, Italy.
Greenhut, G. K. (1986) Transport of ozone between boundary layer and cloud layer by cumulus clouds. J. Geophys. Res. [Atmos.] 91: 8613-8622.
Greenhut, G. K.; Ching, J. K. S.; Pearson, R., Jr.; Repoff, T. P. (1984) Transport of ozone by turbulence and clouds in an urban boundary layer. J. Geophys. Res. [Atmos.] 89: 4757-4766.
Gregg, J. W.; Jones, C. G.; Dawson, T. E. (2003) Urbanization effects on tree growth in the vicinity of New York City [letter]. Nature 424: 183-187.
Gregory, G. L.; Hoell, J. M., Jr.; Torres, A. L.; Carroll, M. A.; Ridley, B. A.; Rodgers, M. O.; Bradshaw, J.; Sandholm, S.; Davis, D. D. (1990) An intercomparison of airborne nitric oxide measurements: a second opportunity. J. Geophys. Res. [Atmos.] 95: 10,129-10,138.
Grell, G. A.; Dudhia, J.; Stauffer, D. R. (1994) Description of the fifth-generation Penn State/NCAR mesoscale model (MM5). Boulder, CO: National Center for Atmospheric Research, Mesoscale and Microscale Meteorology Division; report no. NCAR/TN-398+STR. Available from: NTIS, Springfield, VA; PB95-206348.
Grell, G. A.; Emeis, S.; Stockwell, W. R.; Schoenemeyer, T.; Forkel, R.; Michalakes, J.; Knoche, R.; Seidl, W. (2000) Application of a multiscale, coupled MM5/chemistry model to the complex terrain of the VOTALP valley campaign. Atmos. Environ. 34: 1435-1453.
Gröbner, J.; Kerr, J. B. (2001) Ground-based determination of the spectral ultraviolet extraterrestrial solar irradiance: providing a link between space-based and ground-based solar UV measurements. J. Geophys. Res. (Atmos.) 106(D7): 7211-7217.
Grosjean, E.; Grosjean, D. (1994) Rate constants for the gas-phase reactions of ozone with unsaturated aliphatic alcohols. Int. J. Chem. Kinetics 26: 1185-1191.
Grosjean, D.; Williams, E. L., II; Grosjean, E.; Novakov, T. (1994) Evolved gas analysis of secondary organic aerosols. Aerosol Sci. Technol. 21: 306-324.
Gross, A.; Stockwell, W. R. (2003) Comparison of the EMEP, RADM2 and RACM Mechanisms. J. Atmos. Chem. 44: 151-170.
Guenther, A.; Hewitt, C. N.; Erickson, D.; Fall, R.; Geron, C.; Graedel, T.; Harley, P.; Klinger, L.; Lerdau, M.; McKay, W. A.; Pierce, T.; Scholes, B.; Steinbrecher, R.; Tallamraju, R.; Taylor, J.; Zimmerman, P. (1995) A global model of natural volatile organic compound emissions J. Geophys. Res. (Atmos.) 100(D5): 8873-8892.
Guenther, A.; Baugh, W.; Davis, K.; Hampton, G.; Harley, P.; Klinger, L.; Vierling, L.; Zimmerman, P.; Allwine, E.; Dilts, S.; Lamb, B.; Westberg, H.; Baldocchi, D.; Geron, C.; Pierce, T. (1996) Isoprene fluxes measured by enclosure, relaxed eddy accumulation, surface layer gradient, mixed layer gradient, and mixed layer mass balance techniques. J. Geophys. Res. (Atmos.) 101: 18,555-18,567.

Guenther, F. R.; Dorko, W. D.; Miller, W. R.; Rhoderick, G. C. (1996) The NIST traceable reference material program for gas standards. Washington, DC: U.S. Department of Commerce, National Institute of Standards and Technology; NIST special publication 260-126.

Guenther, A.; Geron, C.; Pierce, T.; Lamb, B.; Harley, P.; Fall, R. (2000) Natural emissions of non-methane volatile organic compounds, carbon monoxide, and oxides of nitrogen from North America. Atmos. Environ. 34: 2205-2230.

Hadjinicolaou, P.; Pyle, J. A. (2004) J. Atmos. Chem. 47: 25-43.

Hallock-Waters, K. A.; Doddridge, B. G.; Dickerson, R. R.; Spitzer, S.; Ray, J. D. (1999) Carbon monoxide in the U.S. mid-Atlantic troposphere: evidence for a decreasing trend. Geophys. Res. Lett. 26: 2861-2864.

Hallquist, M.; Stewart, D. J.; Stephenson, S. K.; Cox, R. A. (2003) Hydrolysis of N_2O_5 on sub-micron sulfate aerosols. Phys. Chem. Chem. Phys. 5: 3453-3463.

Hameed, S.; Pinto, J. P.; Stewart, R. W. (1979) Sensitivity of the predicted CO-OH-CH_4 perturbation to tropospheric NO_x concentrations. J. Geophys. Res. C: Oceans Atmos. 84: 763-768.

Hanisch, F.; Crowley, J. N. (2002) Ozone decomposition on Saharan dust: an experimental investigation. Atmos. Chem. Phys. Disc. 2: 1809-1845.

Hanna, A. F.; Mathur, R.; Pinto, J.; Jang, C. (2001) Seasonal modeling of the export of pollutants from North America using the Multi Scale Air Quality Simulation Pattern (MAQSIP). Presented at: Workshop on photooxidants, particles, and haze across the Arctic and North Atlantic: observations and models; June; New York, NY. Palisades, NY: Center for International Earth Science Information Network (CIESIN). Available: http://www.ciesin.org/pph/uploads/H_A_Seasonal_Modeling_PDF.pdf (29 December 2003).

Hannegan, B.; Olsen, S.; Prather, M.; Zhu, X.; Rind, D.; Lerner, J. (1998) The dry stratosphere: a limit on cometary water influx. Geophys. Res. Lett. 25: 1649-1652.

Hansel, A.; Jordan, A.; Taucher, J. (1995) Analysis of volatile organic compounds using proton-transfer-reaction-mass spectrometry (PTR-MS) in the ppb range. In: Becker, K. H.; Carr, W. E.; Kunhardt, E. E., eds. Proceedings of the XXII International conference on phenomena in ionized gases; July-August; Hoboken, NJ. Hoboken, NJ: Stevens Institute of Technology; pp. 181-182.

Hansel, A.; Jordan, A.; Holzinger, R.; Prazeller, P.; Vogel, W.; Lindinger, W. (1995) Proton transfer reaction mass spectrometry: on-line trace gas analysis at the ppb level. Int. J. Mass Spectrom. Ion Proc. 149/150: 609-619.

Hansen, K.; Draaijers, G. P. J.; Ivens, W. P. M. F.; Gundersen, P.; van Leeuwen, N. F. M. (1994) Concentration variations in rain and canopy throughfall collected sequentially during individual rain events. Atmos. Environ. 28: 3195-3205.

Hansen, J.; Sato, M.; Ruedy, R.; Lacis, A.; Asamoah, K.; Beckford, K.; Borenstein, S.; Brown, E.; Cairns, B.; Carlson, B.; Curran, B.; de Castro, S.; Druyan, L.; Etwarrow, P.; Ferede, T.; Fox, M.; Gaffen, D.; Glascoe, J.; Gordon, H.; Hollandsworth, S.; Jiang, X.; Johnson, C.; Lawrence, N.; Lean, J.; Lerner, J.; Lo, K.; Logan, J.; Luckett, A.; McCormick, M. P.; McPeters, R.; Miller, R.; Minnis, P.; Ramberran, I.; Russell, G.; Russell, P.; Stone, P.; Tegen, I.; Thomas, S.; Thomason, L.; Thompson, A.; et al. (1997) Forcings and chaos in interannual to decadal climate change. J. Geophys. Res. [Atmos.] 102: 25,679-25,720.

Hara, K.; Osada, K.; Hayashi, M.; Matsunaga, K.; Shibata, T.; Iwasaka, Y.; Furuya, K. (1999) Fractionation of inorganic nitrates in winter Arctic troposphere: coarse aerosol particles containing inorganic nitrates. J. Geophys. Res. (Atmos.) 104: 23,671-23,679.

Hard, T. M.; Mehrabzadeh, A. A.; Chan, C. Y.; O'Brien, R. J. (1992) FAGE measurements of tropospheric HO with measurements and model of interferences. J. Geophys. Res. [Atmos.] 97: 9795-9817.

Harder, J. W.; Brault, J. W.; Johnston, P. V.; Mount, G. H. (1997a) Temperature dependent NO_2 cross sections at high spectral resolution. J. Geophys. Res. [Atmos.] 102: 3861-3879.

Harder, J. W.; Williams, E. J.; Baumann, K.; Fehsenfeld, F. C. (1997b) Ground-based comparison of NO_2, H_2O, and O_3 measured by long-path and in situ techniques during the 1993 Tropospheric OH Photochemistry Experiment. J. Geophys. Res. 102: 6227-6243.

Harley, P.; Guenther, A.; Zimmerman, P. (1996) Effects of light, temperature and canopy position on net photosynthesis and isoprene emission from sweetgum (*Liquidambar styraciflua*) leaves. Tree Physiol. 16: 25-32.

Harris, G. W.; Carter, W. P. L.; Winer, A. M.; Pitts, J. N., Jr.; Platt, U.; Perner, D. (1982) Observations of nitrous acid in the Los Angeles atmosphere and implications for predictions of ozone-precursor relationships. Environ. Sci. Technol. 16: 414-419.

Harris, J. M.; Oltmans, S. J.; Bodeker, G. E.; Stolarski, R.; Evans, R. D.; Quincy, D. M. (2003) Long-term variations in total ozone derived from Dobson and satellite data. Atmos. Environ. 37: 3167-3175.

Harrison, R. M.; Peak, J. D.; Collins, G. M. (1996) Tropospheric cycle of nitrous acid. J. Geophys. Res. (Atmos.) 101: 14,429-14,439.

Hauglustaine, D. A.; Brasseur, G. P.; Walters, S.; Rasch, P. J.; Müller, J.-F.; Emmons, L. K.; Carroll, M. A. (1998) MOZART, a global chemical transport model for ozone and related chemical tracers 2. model results and evaluation. J. Geophys. Res. (Atmos.) 103: 28291-28335.
Hebestreit, K.; Stutz, J.; Rosen, D.; Matveiv, V.; Peleg, M.; Luria, M.; Platt, U. (1999) DOAS measurements of tropospheric bromine oxide in mid-latitudes. Science 283: 55-57.
Hegg, D. A.; Livingston, J.; Hobbs, P. V.; Novakov, T.; Russell, P. (1997) Chemical apportionment of aerosol column optical depth off the mid-Atlantic coast of the United States. J. Geophys. Res. (Atmos.) 102: 25,293-25,303.
Heikes, B. G.; Chang, W.; Pilson, M. E. Q.; Swift, E.; Singh, H. B.; Guenther, A.; Jacob, D. J.; Field, B. D.; Fall, R.; Riemer, D.; Brand, L. (2002) Atmospheric methanol budget and ocean implication. Glob. Biogeochem. Cycles 16: 10.1029/2002GB001895.
Henry, R. C.; Lewis, C. W.; Hopke, P. K.; Williamson, H. J. (1984) Review of receptor model fundamentals. Atmos. Environ. 18: 1507-1515.
Hering, S. V.; Lawson, D. R.; Allegrini, I.; Febo, A.; Perrino, C.; Possanzini, M.; Sickles, J. E., II; Anlauf, K. G.; Wiebe, A.; Appel, B. R.; John, W.; Ondo, J.; Wall, S.; Braman, R. S.; Sutton, R.; Cass, G. R.; Solomon, P. A.; Eatough, D. J.; Eatough, N. L.; Ellis, E. C.; Grosjean, D.; Hicks, B. B.; Womack, J. D.; Horrocks, J.; Knapp, K. T.; Ellestad, T. G.; Paur, R. J.; Mitchell, W. J.; Pleasant, M.; Peake, E.; MacLean, A.; Pierson, W. R.; Brachaczek, W.; Schiff, H. I.; Mackay, G. I.; Spicer, C. W.; (1988) The nitric acid shootout: field comparison of measurement methods. Atmos. Environ. 22: 1519-1539.
Herlihy, L. J.; Galloway, J. N.; Mills, A. L. (1987) Bacterial utilization of formic and acetic acid in rainwater. Atmos. Environ. 21: 2397-2402.
Hess, P. G. (2001) Model and measurement analysis of springtime transport and chemistry of the Pacific Basin. J. Geophys. Res. (Atmos.) 106: 12,689-12,717.
Hilsenrath, E.; Attmannspacher, W.; Bass, A.; Evans, W.; Hagemeyer, R.; Barnes, R. A.; Komhyr, W.; Mauersberger, K.; Mentall, J.; Proffitt, M.; Robbins, D.; Taylor, S.; Torres, A.; Weinstock, E. (1986) Results from the ballon ozonr intercomparison campaign (BOIC). J. Geophys. Res. 91: 13,137-13,152.
Hirsch, A. I.; Munger, J. W.; Jacob, D. J.; Horowitz, L. W.; Goldstein, A. H. (1996) Seasonal variation of the ozone production efficiency per unit NO_x at Harvard Forest, Massachusetts. J. Geophys. Res. [Atmos.] 101: 12,659-12,666.
Hobbs, P. V.; Locatelli, J. D.; Martin, J. E. (1996) A new conceptual model for cyclones generated in the lee of the Rocky Mountains. Bull. Am. Meteorol. Soc. 77: 1169-1178.
Hoell, J. M.; Davis, D. D.; Jacob, D. J.; Rodgers, M. O.; Newell, R. E.; Fuelberg, H. E.; McNeal, R. J.; Raper, J. L.; Bendura, R. J. (1996) Pacific exploratory mission in the tropical Pacific: PEM-Tropics A, August-September 1996. J. Geophys. Res. (Atmos.) 104: 5567-5583.
Hoell, J. M.; Davis, D. D.; Liu, S. C.; Newell, R. E.; Akimoto, H.; McNeal, R. J.; Bendura, R. J. (1997) The Pacific exploratory mission A west phase B: February-March, 1994. J. Geophys. Res. [Atmos.] 102(D23): 28223-28239.
Hoffman, E. J.; Duce, R. A. (1976) Factors influencing the organic carbon content of marine aerosols: a laboratory study. J. Geophys. Res. (Atmos.) 81: 3667-3670.
Hoffman, E. J.; Duce, R. A. (1977) Organic carbon in marine atmospheric particulate matter: concentration and particle size distribution. Geophys. Res. Lett. 4: 449-452.
Hoigné, J.; Zuo, Y.; Nowell, L. (1994) Photochemical reactions in atmospheric waters: role of dissolved iron species. In: Helz, G. R.; Zepp, R. G.; Crosby, D. C. Aquatic and Surface Photochemistry. Boca Raton, FL: Lewis Publishers.
Holton, J. R. (1967) The diurnal boundary layer wind oscillation above sloping terrain. Tellus 19: 199-205.
Holton, J. R.; Haynes, P. H.; McIntyre, M. E.; Douglass, A. R.; Rood, R. B.; Pfister, L. (1995) Stratosphere-troposphere exchange. Rev. Geophys. 33: 403-439.
Hönninger, G. (1999) Referenzspektren reaktiver halogenverbindungen fur DOAS-messungen. Heidelberg, Germany: Ruprecht Karls University.
Honrath, R. E.; Guo, S.; Peterson, M. C. (2000) Photochemical production of gas phase NO_x from ice crystal NO_3^-. J. Geophys. Res. (Atmos.) 105: 24,183-24,190.
Hopke, P. K. (1985) Receptor modeling in environmental chemistry. New York, NY: John Wiley & Sons.
Horowitz, L. W.; Liang, J.; Gardner, G. M.; Jacob, D. J . (1998) Export of reactive nitrogen from North America during summertime: sensitivity to hydrocarbon chemistry. J. Geophys. Res. 103(D11): 13451-13476.
Hoskins, B. J. (1972) Non-boussinesq effects and further development in a model of upper tropospheric frontogenesis. Q. J. Roy. Meteorol. Soc. 98: 532-541.

Houweling, S.; Dentener, F.; Lelieveld, J.; Walter, B.; Dlugokencky, E. (2000) The modeling of tropospheric methane: how well can point measurements be reproduced by a global model? J. Geophys. Res. (Atmos.) 105: 8981-9002.
Hübler, G.; Alvarez, R., II; Daum, P.; Dennis, R.; Gillani, N.; Kleinman, L.; Luke, W.; Meagher, J.; Rider, D.; Trainer, M.; Valente, R. (1998) An overview of the airborne activities during the Southern Oxidants Study (SOS) 1995 Nashville/Middle Tennessee ozone study. J. Geophys. Res. [Atmos.] 103: 22,245-22,259.
Hudman, R. C.; Jacob, D. J.; Cooper, O. C.; Evans, M. J.; Heald, C. L.; Park, R. J.; Fehsenfeld, F.; Flocke, F.; Holloway, J.; Hübler, G.; Kita, K.; Koike, M.; Kondo, Y.; Neuman, A.; Nowak, J.; Oltmans, S.; Parrish, D.; Roberts, J. M.; Ryerson, T. (2004) Ozone production in transpacific Asian pollution plumes and implications for ozone air quality in California. J. Geophys. Res. (Atmos.) 109(D23): 10.1029/2004JD004974.
Huebert, B. J.; Zhuang, L.; Howell, S.; Noone, K.; Noone, B. (1996) Sulfate, nitrate, methanesulfonate, chloride, ammonium, and sodium measurements from ship, island, and aircraft during the Atlantic Stratocumulus Transition Experiment/Marine Aerosol Gas Exchange. J. Geophys. Res. (Atmos.) 101: 4413-4423.
Huey, L. G.; Dunlea, E. J.; Lovejoy, E. R.; Hanson, D. R.; Norton, R. B.; Fehsenfeld, F. C.; Howard, C. J. (1998) Fast time response measurements of HNO_3 in air with a chemical ionization mass spectrometer. J. Geophys. Res. 103(D3): 3355-3360.
Hunsaker, C.; Graham, R.; Turner, R. S.; Ringold, P. L.; Holdren, G. R., Jr.; Strickland, T. C. (1993) A national critical loads framework for atmospheric deposition effects assessment: II. Defining assessment end points, indicators, and functional subregions. Environ. Manage. 17: 335-341.
Huntrieser, H.; Feigl, C.; Schlager, H.; Schröder, F.; Gerbig, C.; Van Velthoven, P.; Flatøy, F.; Théry, C.; Petzold, A.; Höller, H.; Schumann, U. (2002) Airborne measurements of NO_x, tracer species, and small particles during the European Lightning Nitrogen Oxides Experiment. J. Geophys. Res. 107(D11): 10.1029/2000JD000209.
Husain, L.; Coffey, P. E.; Meyers, R. E.; Cederwall, R. T. (1977) Ozone transport from stratosphere to troposphere. Geophys. Res. Lett. 4: 363-365.
Husar, R. B.; Renard, W. P. (1998) Ozone as a function of local wind speed and direction: Evidence of local and regional transport. Presented at: 91st annual meeting and exhibition of the Air & Waste Management Association; June; San Diego, CA. Pittsburgh, PA: Air & Waste Management Association; online paper no. 98-A922. Available: http://capita.wustl.edu/capita/CapitaReports/REPORTS1.HTML (13 November 2003).
Imhoff, R. E.; Valente, R.; Meagher, J. F.; Luria, M. (1995) The production of O_3 in an urban plume - airborne sampling of the Atlanta urban plume. Atmos. Environ. 29: 2349-2358.
Intergovernmental Panel on Climate Change (IPCC). (1995) Climate change 1994: radiative forcing of climate change and an evaluation of the IPCC IS92 emission scenarios. Cambridge, United Kingdom: University Press.
Intergovernmental Panel on Climate Change (IPCC). (1996) Climate change 1995: the science of climate change: contribution of working group I to the second assessment of the Intergovernmental Panel on Climate Change. Cambridge, United Kingdom: Cambridge University Press.
Intergovernmental Panel on Climate Change (IPCC). (2001) Climate change 2001: the scientific basis. Contribution of working group I to the third assessment report of the Intergovernmental Panel on Climate Change. Cambridge, United Kingdom: Cambridge University Press.
Jacob, D. J. (2000) Heterogeneous chemistry and tropospheric ozone. Atmos. Environ. 34: 2131-2159.
Jacob, D. J.; Logan, J. A.; Gardner, G. M.; Yevich, R. M.; Spivakovsky, C. M.; Wofsy, S. C.; Sillman, S.; Prather, M. J. (1993) Factors regulating ozone over the United States and its export to the global atmosphere. J. Geophys. Res. [Atmos.] 98: 14,817-14,826.
Jacob, D. J.; Horowitz, L. W.; Munger, J. W.; Heikes, B. G.; Dickerson, R. R.; Artz, R. S.; Keene, W. C. (1995) Seasonal transition from NO_x- to hydrocarbon-limited conditions for ozone production over the eastern United States in September. J. Geophys. Res. 100: 9315-9324.
Jacob, D. J.; Prather, M. J.; Rasch, P. J.; Shia, R.-L.; Balkanski, Y. J.; Beagley, S. R.; Bergman, D. J.; Blackshear, W. T.; Brown, M.; Chiba, M.; Chipperfield, M.; De Grandpré, J.; Dignon, J. E.; Feichter, J.; Genthon, C.; Grose, W.L.; Kasibhatla, P. S.; Köhler, I.; Kritz, M. A.; Law, K.; Penner, J. E.; Ramonet, M.; Reeves, C. E.; Rotman, D. A.; Stockwell, D. Z.; VanVelthoven, P. F. J.; Verver, G.; Wild, O.; Yang, H.; Zimmermann, P. (1997) Evaluation and intercomparison of global atmospheric transport models using 222Rn and other short-lived tracers. J. Geophys. Res. [Atmos.] 102: 5953-5970.
Jacobi, C.; Becker, C.; Kratzsch, T.; Siemer, A.; Roth, R. (1994) Experimental investigations of nocturnal low-level jets with some remarks on flight safety. Contrib. Atmos. Phys. 67: 71-82.
Jacobson, M. Z. (1997) Development and application of a new air pollution modeling system - Part III. aerosol-phase simulations. Atmos. Environ. 31: 587-608.

Jacobson, M. Z. (1998) Studying the effects of aerosols on vertical photolysis rate coefficient and temperature profiles over an urban airshed. J. Geophys. Res. [Atmos.] 103: 10,593-10,604.
Jacobson, M. Z. (1999) Isolating nitrated and aromatic aerosols and nitrated aromatic gases as sources of ultraviolet light absorption. J. Geophys. Res. (Atmos.) 104: 3527-3542.
Jacobson, M. Z.; Lu, R.; Turco, R. P.; Toon, O. P. (1996) Development and application of a new air pollution modeling system-Part I: gas-phase simulations. Atmos. Environ. 30: 1939-1963.
Jacobson, M. C.; Hansson, H.-C.; Noone, K. J.; Charlson, R. J. (2000) Organic atmospheric aerosols: review and state of the science. Rev. Geophys. 38: 267-294.
Jaeglé, L.; Jacob, D. J.; Wennberg, P. O.; Spivakovsky, C. M.; Hanisco, T. F.; Lanzendorf, E. J.; Hintsa, E. J.; Fahey, D. W.; Keim, E. R.; Proffitt, M. H.; Atlas, E. L.; Flocke, F.; Schauffler, S.; McElroy, C. T.; Midwinter, C.; Pfister, L.; Wilson, J. C. (1997) Observed OH and HO_2 in the upper troposphere suggests a major source from convective injection of peroxides. Geophys. Res. Lett. 24: 3181-3184.
Jaeglé, L.; Jacob, D. J.; Brune, W. H.; Faloona, I. C.; Tan, D.; Kondo, Y.; Sachse, G. W.; Anderson, B.; Gregory, G. L.; Vay, S.; Singh, H. B.; Blake, D. R.; Shetter, R. (1999) Ozone production in the upper troposphere and the influence of aircraft during SONEX: approach of NO_x-saturated conditions. Geophys. Res. Lett. 26: 3081-3084.
Jaeglé, L.; Jacob, D. J.; Brune, W. H.; Faloona, I.; Tan, D.; Heikes, B. G.; Kondo, Y.; Sachse, G. W.; Anderson, B.; Gregory, G. L.; Singh, H. B.; Pueschel, R.; Ferry, G.; Blake, D. R.; Shetter, R. E. (2000) Photochemistry of HO_x in the upper troposphere at northern midlatitudes. J. Geophys. Res. (Atmos.) 105(D3): 3877-3892.
Jaeglé, L.; Jacob, D. J.; Brune, W. H.; Wennberg, P. O. (2001) Chemistry of HO_x radicals in the upper troposphere. Atmos. Environ. 35: 469-489.
Jaffe, D.; Price, H.; Parrish, D.; Goldstein, A.; Harris, J. (2003) Increasing background ozone during spring on the west coast of North America. Geophys. Res. Lett. 30: 10,1029/2003GL017024.
Jaffe, D.; McKendry, I.; Anderson, T.; Price, H. (2003) Six 'new'episodes of trans-Pacific transport of air pollutants. Atmos. Environ. 37: 391-404.
James, P.; Stohl, A.; Forster, C.; Eckhardt, S.; Seibert, P.; Frank, A. (2003a) A 15-year climatology of stratosphere-troposphere exchange with a Lagrangian particle dispersion model: 1. Methodology and validation. J. Geophys. Res. 108(D12): 10.1029/2002JD002637.
James, P.; Stohl, A.; Forster, C.; Eckhardt, S.; Seibert, P.; Frank, A. (2003b) A 15-year climatology of stratosphere-troposphere exchange with a Lagrangian particle dispersion model. 2. Mean climate and seasonal variability. J. Geophys. Res. (Atmos.) 108(D12): 10.1029/2002JD002639.
Jang, M.; Kamens, R. M. (2001) Characterization of secondary aerosol from the photooxidation of toluene in the presence of NO_x and 1-propene. Environ. Sci. Technol. 35: 3626-3639.
Jankowski, J. J.; Kieber, D. J.; Mopper, K.; Neale, P. J. (2000) Development and intercalibration of ultraviolet solar actinometers. Photochem. Photobiol. 71: 431-440.
Jenkin, M. E.; Cox, R. A.; Williams, D. J. (1988) Laboratory studies of the kinetics of formation of nitrous acid from the thermal reaction of nitrogen dioxide and water vapour. Atmos. Environ. 22: 487-498.
Jenkin, M. E.; Saunders, S. M.; Pilling, M. J. (1997) The tropospheric degradation of volatile organic compounds: a protocol for mechanism development. Atmos. Environ. 31: 81-104.
Jet Propulsion Laboratory. (2003) Chemical kinetics and photochemical data for use in atmospheric studies. Pasadena, CA: California Institute of Technology; JPL publication no. 02-25. Available: http://jpldataeval.jpl.nasa.gov/pdf/JPL_02-25_1_intro_rev0.pdf (18 December 2003).
Jeuken, A. B. M.; Eskes, H. J.; Van Velthoven, P. F. J.; Kelder, H. M.; Hólm, E. V. (1999) Assimilation of total ozone satellite measurements in a three-dimensional tracer transport model. J. Geophys. Res. (Atmos.) 104: 5551-5563.
Jimenez, P.; Baldasano, J. M.; Dabdub, D. (2003) Comparison of photochemical mechanisms for air quality modeling. Atmos. Environ. 37: 4179-4194.
Johnson, W. B.; Viezee, W. (1981) Stratospheric ozone in the lower troposphere - I. presentation and interpretation of aircraft measurements. Atmos. Environ. 15: 1309-1323.
Johnson, C. E.; Collins, W. J.; Stevenson, D. S.; Derwent, R. G. (1999) The relative roles of climate and emissions changes on future oxidant concentrations. J. Geophys. Res. (Atmos.) 104: 18,631-18,645.
Johnson, B. J.; Oltmans, S. J.; Vömel, H.; Smit, H. G. J.; Deshler, T.; Kröger, C. (2002) Electrochemical concentration cell (ECC) ozonesonde pump efficiency measurements and tests on the sensitivity to ozone of buffered and unbuffered ECC sensor cathode solutions. J. Geophys. Res. 107(D19): 10.1029/2001JD000557.
Jordan, C. E.; Dibb, J. E.; Finkel, R. C. (2003) $^{10}Be/^{7}Be$ tracer of atmospheric transport and stratosphere-troposphere exchange. J. Geophys. Res. 108(D8): 10.1029/2002JD002395.
Junge, C. E. (1962) Global ozone budget and exchange between stratosphere and troposphere. Tellus 14: 363-377.

Junge, C. E. (1963) Air chemistry and radioactivity. New York, NY: Academic Press. (Van Mieghem, J.; Hales, A. L., eds. International geophysics series: v. 4).
Kain, J. S.; Fritsch, J. M. (1993) Convective parameterization in mesoscale models: the Kain-Fritsch scheme. In: Emanuel, K. A.; Raymond, D. J., eds. The Representation of Cumulus Convection in Numerical Models. Boston, MA: American Meteorological Society; pp. 165-170. (Meteorological Monographs, v. 24, no. 46).
Kane, M. M.; Rendell, A. R.; Jickells, T. D. (1994) Atmospheric scavenging processes over the North Sea. Atmos. Environ. 28: 2523-2530.
Kane, S. M.; Caloz, F.; Leu, M.-T. (2001) Heterogeneous uptake of gaseous N_2O_5 by $(NH_4)_2SO_4$ NH_4HSO_4, and H_2SO_4 aerosols. J. Phys. Chem. A 105: 6465-6470.
Karamchandani, P.; Santos, L.; Sykes, I.; Zhang, Y.; Tonne, C.; Seigneur, C. (2000) Development and evaluation of a state-of-the-science reactive plume model. Environ. Sci. Technol. 34: 870-880.
Karamchandani, P.; Seigneur, C.; Vijayaraghavan, K.; Wu, S.-Y. (2002) Development and application of a state-of-the-science plume-in-grid model. J. Geophys. Res. (Atmos.) 107: 10.1019/2002D002123.
Kasibhatla, P.; Chameides, W. L. (2000) Seasonal modeling of regional ozone pollution in the eastern United States. Geophys. Res. Lett. 27: 1415-1418.
Kasting, J. F.; Singh, H. B. (1986) Nonmethane hydrocarbons in the troposphere: impact on the odd hydrogen and odd nitrogen chemistry, J. Geophys. Res. 91: 13,239-13,256.
Kavouras, I. G.; Mihalopoulus, N.; Stephanou, E. G. (1999) Secondary organic aerosol formation vs primary organic aerosol emission: in situ evidence for the chemical coupling between monoterpene acidic photooxidation products and new particle formation over forests. Environ. Sci. Technol. 33: 1028-1037.
Kawamura, K.; Seméré, R.; Imai, Y.; Fuji, Y.; Hayashi, M. (1996) Water soluble dicarboxylic acids and related compounds in Antarctic aerosols. J. Geophys. Res. 101: 18,721-18,728.
Keene, W. C.; Savoie, D. L. (1998) The pH of deliquesced sea-salt aerosol in polluted marine air. Geophys. Res. Lett. 25: 2181-2194.
Keene, W. C.; Savoie, D. L. (1999) Correction to "The pH of deliquesced sea-salt aerosol in polluted marine air." Geophys. Res. Lett. 26: 1315-1316.
Keene, W. C.; Sander, R.; Pszenny, A. A. P.; Vogt, R.; Crutzen, P. J.; Galloway, J. N. (1998) Aerosol pH in the marine boundary layer: a review and model evaluation. J. Aerosol Sci. 29: 339-356.
Keene, W. C.; Pszenny, A. A. P.; Maben, J. R.; Sander, R. (2002) Variation of marine aerosol acidity with particle size. Geophys. Res. Lett. 29(7): 10.1029/2001GL013881.
Kelly, N. A.; Wolff, G. T.; Ferman, M. A. (1982) Background pollutant measurements in air masses affecting the eastern half of the United States - I. air masses arriving from the northwest. Atmos. Environ. 16: 1077-1088.
Kelly, N. A.; Ferman, M. A.; Wolff, G. T. (1986) The chemical and meteorological conditions associated with high and low ozone concentrations in southeastern Michigan and nearby areas of Ontario. J. Air Pollut. Control Assoc. 36: 150-158.
Kenley, R. A.; Davenport, J. E.; Hendry, D. G. (1981) Gas-phase hydroxyl radical reactions. Products and pathways for the reaction of OH with aromatic hydrocarbons. J. Phys. Chem. 85: 2740-2746.
Kim, B. M.; Henry, R. C. (2000) Application of SAFER model to the Los Angeles PM10 data. Atmos. Environ. 34: 1747-1759.
Kim, K.-H.; Kim, M.-Y. (2001) Comparison of an open path differential optical absorption spectroscopy system and a conventional in situ monitoring system on the basis of long-term measurements of SO_2, NO_2, and O_3. Atmos. Environ. 35: 4059-4072.
King, D. W.; Lounsbury, H. A.; Millero, F. J. (1995) Rates and mechanisms of Fe(II) oxidation at nonmolar total iron concentrations. Environ. Sci. Technol. 29: 818-824.
King, M. D.; Canosa-Mas, C. E.; Wayne, R. P. (2002) A structure activity relationship (SAR) for predicting rate constants for the reaction of nitrogen dioxide (NO_2) with alkenes. Phys. Chem. Chem. Phys. 4: 295-303.
Kireev, S. V.; Shnyrev, S. L.; Zhiganov, A. A. (1999) A laser fluorimeter for NO and NO_2 in atmosphere. Instrum. Exp. Tech. 42: 701-703.
Kleindienst, T. E.; Hudgens, E. E.; Smith, D. F.; McElroy, F. F.; Bufalini, J. J. (1993) Comparison of chemiluminescence and ultraviolet ozone monitor responses in the presence of humidity and photochemical pollutants. Air Waste 43: 213-222.
Kleindienst, T. E.; Smith, D. F.; Li, W.; Edney, E. O.; Driscoll, D. J.; Speer, R. E.; Weathers, W. S. (1999) Secondary organic aerosol formation from the oxidation of aromatic hydrocarbons in the presence of dry submicron ammonium sulfate aerosol. Atmos. Environ. 33: 3669-3681.
Kleinman, L. I. (2000) Ozone process insights from field experiments - part II: observation-based analysis for ozone production. Atmos. Environ. 34: 2023-2034.

Kleinman, L. I.; Daum, P. H.; Lee, Y.-N.; Springston, S. R.; Newman, L.; Leaitch, W. R.; Banic, C. M.; Isaac, G. A.; MacPherson, J. I. (1996a) Measurement of O_3 and related compounds over southern Nova Scotia. 1. Vertical distributions. J. Geophys. Res. [Atmos.] 101: 29,043-29,060.
Kleinman, L. I.; Daum, P. H.; Springston, S. R.; Leaitch, W. R.; Banic, C. M.; Isaac, G. A.; Jobson, T. B.; Niki, H. (1996b) Measurement of O_3 and related compounds over southern Nova Scotia. 2. Photochemical age and vertical transport. J. Geophys. Res. [Atmos.] 101: 29,061-29,074.
Kleinman, L. I.; Daum, P. H.; Lee, J. H.; Lee, Y.-N.; Nunnermacker, S. R.; Springston, L.; Newman, J.; Weinstein-Lloyd, J.; Sillman, S. (1997) Dependence of ozone production on NOand hydrocarbons in the troposphere. Geophys. Res. Lett. 24: 2299-2302.
Kleinman, L. I.; Daum, P. H.; Imre, D. G.; Lee, J. H.; Lee, Y.-N.; Nunnermacker, L. J.; Springston, S. R.; Weinstein-Lloyd, J.; Newman, L. (2000) Ozone production in the New York City urban plume. J. Geophys. Res. [Atmos.] 105: 14,495-14,511.
Kleinman, L. I.; Daum, P. H.; Lee, Y.-N.; Nunnermacker, L. J.; Springston, S. R.; Weinstein-Lloyd, J.; Rudolph, J. (2001) Sensitivity of ozone production rate to ozone precursors. Geophys. Res. Lett. 28: 2903-2906.
Kleinman, L. I.; Daum, P. H.; Imre, D.; Lee, Y.-N.; Nunnermacker, L. J.; Springston, S. R.; Weinstein-Lloyd, J.; Rudolph, J. (2002) Ozone production rate and hydrocarbon reactivity in 5 urban areas: a cause of high ozone concentration in Houston. Geophys. Res. Lett. 29: 10.1029/2001GL014569.
Kley, D.; Crutzen, P. J.; Smit, H. G. J.; Vomel, H.; Oltmans, S. J.; Grassl, H.; Ramanathan, V. (1996) Observations of near-zero ozone concentrations over the convective Pacific: effects on air chemistry. Science 274: 230-233.
Klotz, B.; Barnes, I.; Becker, K. H.; Golding, B. T. (1997) Atmospheric chemistry of benzene oxide/oxepin. J. Chem. Soc. Faraday Trans. 93: 1507-1516.
Klotz, B; Barnes, I.; Becker, K. H. (1998) New results on the atmospheric photooxidation of simple alkylbenzenes. Chem. Phys. 231: 289-301.
Knake, R.; Hauser, P. C. (2002) Sensitive electrochemical detection of ozone. Anal. Chim. Acta 459: 199-207.
Knispel, R.; Koch, R.; Siese, M.; Zetzsch, C. (1990) Adduct formation of OH radicals with benzene, toluene, and phenol and consecutive reactions of the adducts with NO_x and O_2. Ber. Bunsen-Ges. Phys. Chem. 94: 1375-1379.
Koch, T. G.; Banham, S. F.; Sodeau, J. R.; Horn, A. B.; McCoustra, M. R. S.; Chesters, M. A. (1997) Mechanisms for the heterogeneous hydrolysis of hydrogen chloride, chlorine nitrate and dinitrogen pentoxide on water-rich atmospheric particle surfaces. J. Geophys Res. (Atmos.) 102: 1513-1522.
Konrad, S.; Schmitz, T.; Buers, H.-J.; Houben, N.; Mannschreck, K.; Mihelcic, D.; Müsgen, P.; Pätz, H.-W.; Holland, F.; Hofzumahaus, A.; Schäfer, H.-J.; Schröder, S.; Volz-Thomas, A.; Bächmann, K.; Schlomski, S.; Moortgat, G.; Großmann, D. (2003) Hydrocarbon measurements at Pabstthum during the BERLIOZ campaign and modeling of free radicals. J. Geophys. Res. [Atmos.] 108(D4): 10.1029/2001JD000866.
Kotamarthi, V. R.; Gaffney, J. S.; Marley, N. A.; Doskey, P. V. (2001) Heterogeneous NO_x chemistry in the polluted PBL. Atmos. Environ. 35: 4489-4498.
Krol, M.; Van Leeuwen, P. J.; Lelieveld, J. (1998) Global OH trend inferred from methylchloroform measurements. J. Geophys. Res. [Atmos.] 103: 10,697-10,711.
Kumar, N.; Russell, A. G. (1996) Development of a computationally efficient, reactive subgrid-scale plume model and the impact in the northeastern United States using increasing levels of chemical detail. J. Geophys. Res. [Atmos.] 101: 16,737-16,744.
Kwok, E. S. C.; Aschmann, S. M.; Atkinson, R.; Arey, J. (1997) Products of the gas-phase reactions of *o*-, *m*- and *p*-xylene with the OH radical in the presence and absence of NO_x. J. Chem. Soc. Faraday Trans. 93: 2847-2854.
Lamb, B.; Gay, D.; Westberg, H.; Pierce, T. (1993) A biogenic hydrocarbon emission inventory for the U.S.A. using a simple forest canopy model. Atmos. Environ. Part A 27: 1673-1690.
Lammel, G.; Cape, J. N. (1996) Nitrous acid and nitrite in the atmosphere. Chem. Soc. Rev. 25: 361-369.
Lammel, G.; Perner, D. (1988) The atmospheric aerosol as a source of nitrous acid in the polluted atmosphere. J. Aerosol Sci. 19: 1199-1202.
Langford, A. O.; Reid, S. J. (1998) Dissipation and mixing of a small-scale stratospheric intrusion in the upper troposphere. J. Geophys. Res. 103(D23): 31,265-31,276.
Lantz, K. O.; Shetter, R. E.; Cantrell, C. A.; Flocke, S. J.; Calvert, J. G.; Madronich, S. (1996) Theoretical, actinometric, and radiometric determinations of the photolysis rate coefficient of NO2 during the Mauna Loa Observatory Photochemistry Experiment 2. J. Geophys. Res. (Atmos.) 101(D9): 14,613-14629.
Law, K. S.; Plantevin, P. H.; Shallcross, D. E.; Rogers, H. L.; Pyle, J. A.; Grouhel, C.; Thouret, V.; Marenco, A. (1998) Evaluation of modeled O_3 using measurement of ozone by airbus in-service aircraft (MOZAIC) data. J. Geophys. Res. (Atmos.) 103: 25,721-25,737.

Law, K. S.; Plantevin, P.-H.; Thouret, V.; Marenco, A.; Asman, W. A. H.; Lawrence, M.; Crutzen, P. J.; Muller, J. F.; Hauglustaine, D. A.; Kanakidou, M. (2000) Comparison between global chemistry transport model results and measurement of ozone and water vapor by airbus in-service aircraft (MOZAIC) data. J. Geophys. Res. (Atmos.) 105: 1503-1525.

Lawrence, M. G.; Crutzen, P. J.; Rasch, P. J.; Eaton, B. E.; Mahowald, N. M. (1999) A model for studies of tropospheric photochemistry: description, global distributions and evaluation. J. Geophys. Res. (Atmos.) 104: 26,245-26,277.

Lean, J. L. (2000) Short term, direct indices of solar variability. Space Science Reviews 94: 39-51.

Lefohn, A. S.; Oltmans, S. J.; Dann, T.; Singh, H. B. (2001) Present-day variability of background ozone in the lower troposphere. J. Geophys. Res. [Atmos.] 106: 9945-9958.

Leibrock, E.; Huey, L. G. (2000) Ion chemistry for the detection of isoprene and other volatile organic compounds in ambient air. Geophys. Res. Lett. 27: 1719-1722.

Lelieveld, J.; Crutzen, P. J. (1990) Influences of cloud photochemical processes on tropospheric ozone. Nature (London) 343: 227-233.

Lelieveld, J.; Crutzen, P. J. (1994) Role of deep cloud convection in the ozone budget of the troposphere. Science 264: 1759-1761.

Lelieveld, J.; Dentener, F. J. (2000) What controls tropospheric ozone? J. Geophys. Res. [Atmos.] 105: 3531-3551.

Leser, H.; Hönninger, G.; Platt, U. (2003) MAX-DOAS measurements of BrO and NO_2 in the marine boundary layer. Geophys. Res. Lett. 30: 10.1029/2002GL015811.

Leu, M.-T. (2003) Laboratory studies of interaction between trace gases and sulphuric acid or sulphate aerosols using flow-tube reactors. Int. Rev. Phys. Chem. 22: 341-376.

Li, Q.; Jacob, D. J.; Logan, J. A.; Bey, I.; Yantosca, R. M.; Liu, H.; Martin, R. V.; Fiore, A. M.; Field, B. D.; Duncan, B. N. (2001) A tropospheric ozone maximum over the Middle East. Geophys. Res. Lett. 28: 3235-3238.

Li, Q.; Jacob, D. J.; Fairlie, T. D.; Liu, H.; Martin, R. V.; Yantosca, R. M. (2002) Stratospheric versus pollution influences on ozone at Bermuda: reconciling past analyses. J. Geophys. Res. 107(D22): 10.1029/2002JD002138.

Liang, J.; Horowitz, L. W.; jacob, D. J.; Wang, Y.; Fiore, A. M.; Logan, J. A.; Gardner, G. M.; Munger, J. W. (1998) Seasonal variations of reactive nitrogen species and ozone over the United States, and export fluxes to the global atmosphere. J. Geophys. Res. (Atmos.) 103: 13,435-13,450.

Liao, H.; Yung, Y. L.; Seinfeld, J. H. (1999) Effects of aerosols on tropospheric photolysis rates in clear and cloudy atmospheres. J. Geophys. Res. (Atmos.) 104: 23,697-23,707.

Lillis, D.; Cruz, C. N.; Collett, J.; Richards, L. W.; Pandis, S. N. (1999) Production and removal of aerosol in a polluted fog layer: model evaluation and fog effect on PM. Atmos. Environ. 33: 4797-4816.

Lin, C.; Milford, J. B. (1994) Decay-adjusted chemical mass balance receptor modeling for volatile organic compounds. Atmos. Environ. 28: 3261-3276.

Lin, X.; Trainer, M.; Liu, S. C. (1988) On the nonlinearity of the tropospheric ozone production. J. Geophys. Res. [Atmos.] 93: 15,879-15,888.

Lindinger, W.; Hansel, A.; Jordan, A. (1998) Proton-transfer-reaction mass spectrometry (PTR-MS): on-line monitoring of volatile organic compounds at pptv levels. Chem. Soc. Rev. 27: 347-354.

Liu, M.-K.; Seinfeld, J. H. (1975) On the validity of grid and trajectory models of urban air pollution. Atmos. Environ. 9: 555-574.

Liu, S. C.; Trainer, M.; Fehsenfeld, F. C.; Parrish, D. D.; Williams, E. J.; Fahey, D. W.; Hübler, G.; Murphy, P. C. (1987) Ozone production in the rural troposphere and the implications for regional and global ozone distributions. J. Geophys. Res. [Atmos.] 92: 4191-4207.

Liu, X. H.; Hegg, D. A.; Stoelinga, M. T. (2001) Numerical simulation of new particle formation over the northwest Atlantic using the MM5 mesoscale model coupled with sulfur chemistry. J. Geophys. Res. [Atmos.] 106: 9697-9715.

Liu, H.; Jacob, D. J.; Bey, I.; Yantosca, R. M. (2001) Constraints from ^{210}Pb and ^{7}Be on wet deposition and transport in a global three-dimensional chemical tracer model driven by assimilated meteorological fields. J. Geophys. Res. [Atmos.] 106: 12,109-12,128.

Logan, J. A. (1989) Ozone in rural areas of the United States. J. Geophys. Res. [Atmos.] 94: 8511-8532.

Logan, J. A.; Prather, M. J.; Wofsy, S. C.; McElroy, M. B. (1981) Tropospheric chemistry: a global perspective. J. Geophys. Res. C: Oceans Atmos. 86: 7210-7254.

Logan, J. A. (1994) Trends in the vertical distribution of ozone: an analysis of ozonesonde data. J. Geophys. Res. (Atmos.) 99: 25,553-25,585.

Longfellow, C. A.; Ravishankara, A. R.; Hanson, D. R. (1999) Reactive uptake on hydrocarbon soot: focus on NO_2. J. Geophys. Res. (Atmos.) 104: 13,833-13,840.
Lonneman, W. A.; Seila, R. L. (1993) Hydrocarbon compositions in Los Angeles and New York 20 years later. Presented at: International symposium on measurement of toxic and related air pollutants. Pittsburgh, PA: Air & Waste Management Association.
Lu, C.-H.; Chang, J. S. (1998) On the indicator-based approach to assess ozone sensitivities and emissions features. J. Geophys. Res. (Atmos.) 103: 3453-3462.
Lu, R.; Turco, R. P.; Jacobson, M. Z. (1997) An integrated air pollution modeling system for urban and regional scales: 1. Structure and performance. J. Geophys. Res. [Atmos.] 102: 6063-6079.
Ludwig, F. L.; Reiter, E.; Shelar, E.; Johnson, W. B. (1977) The relation of oxidant levels to precursor emissions and meteorological features: v. 1, analysis and findings. Research Triangle Park, NC: U.S. Environmental Protection Agency, Office of Air Quality Planning and Standards; report no. EPA-450/3-77-022a. Available from: NTIS, Springfield, VA; PB-275 001.
Luke, W. T. (1997) Evaluation of a commercial pulsed fluorescence detector for the measurement of low-level SO_2 concentrations during the Gas-Phase Sulfur Intercomparison Experiment. J. Geophys. Res. (Atmos.) 102: 16,255-16,265.
Luke, W. T.; Dickerson, R. R.; Ryan, W. F.; Pickering, K. E.; Nunnermacker, L. J. (1992) Tropospheric chemistry over the lower Great Plains of the United States. 2. Trace gas profiles and distributions. J. Geophys. Res. 97(D18): 20647-20670.
Luke, W. T.; Watson, T. B.; Olszyna, K. J.; Gunter, R. L.; McMillen, R. T.; Wellman, D. L.; Wilkison, S. W. (1998) A comparison of airborne and surface trace gas measurements during the Southern Oxidants Study (SOS). J. Geophys. Res. [Atmos.] 103: 22,317-22,337.
Luria, M.; Valente, R. J.; Tanner, R. L.; Gillani, N. V.; Imhoff, R. E.; Mueller, S. F.; Olszyna, K. J.; meagher, J. F. (1999) The evolution of photochemical smog in a power plant plume. Atmos. Environ. 33: 3023-3036.
Luria, M.; Tanner, R. L.; Imhoff, R. E.; Valente, R. J.; Bailey, E. M.; Mueller, S. F. (2000) Influence of natural hydrocarbons on ozone formation in an isolated power plant plume. J. Geophys. Res. [Atmos.] 105: 9177-9188.
Madronich, S. (1987) Photodissociation in the atmosphere. 1. Actinic flux and the effects of ground reflections and clouds. J. Geophys. Res. [Atmos.] 92: 9740-9752.
Madronich, S.; McKenzie, R. L.; Caldwell, M. M.; Bjorn, L. O. (1995) Changes in ultraviolet radiation reaching the Earth's surface. Ambio 24: 143-152.
Mahlman, J. D. (1997) Dynamics of transport processes in the upper troposphere. Science 276: 1079-1083.
Mahlman, J. D.; Pinto, J. P.; Umscheid, L. J. (1994) Transport, radiative, and dynamical effects of the Antarctic ozone hole: a GFDL ``SKYHI" model experiment. J. Atmos. Sci. 51: 489-508.
Mahrt, L. (1998) Stratified atmospheric boundary layers and breakdown of models. Theor. Comput. Fluid Dyn. 11: 263-279.
Martilli, A.; Neftel, A.; Favaro, G.; Kirchner, F.; Sillman, S.; Clappier, A. (2002) Simulation of the ozone formation in the northern part of the Po Valley. J. Geophys. Res. (Atmos.) 107(D22): 10.1029/2001JD000534.
Martin, D.; Tsivou, M.; Bonsang, B.; Abonnel, C.; Carsey, T.; Springer-Young, M.; Pszenny, A.; Suhre, K. (1997) Hydrogen peroxide in the marine atmospheric boundary layer during the Atlantic Stratocumulus Transition Experiment/Marine Aerosol and Gas Exchange experiment in the eastern subtropical North Atlantic. J. Geophys. Res. (Atmos.) 102: 6003-6015.
Martin, R. V.; Jacob, D. J.; Chance, K. V.; Kurosu, T. P.; Palmer, P. I.; Evans, M. J. (2003) Global inventory of nitrogen oxide emissions constrained by space-based observations of NO2 columns. J. Geophys. Res. 108(D17): 10.1029/2003JD003453.
Martinez, M.; Harder, H.; Kovacs, T. A.; Simpas, J. B.; Bassis, J.; Lesher, R.; Brune, W. H.; Frost, G. J.; Williams, E. J.; Stroud, C. A.; Jobson, B. T.; Roberts, J. M.; Hall, S. R.; Shetter, R. E.; Wert, B.; Fried, A.; Alicke, B.; Stutz, J.; Young, V. L.; White, A. B.; Zamora, R. J. (2003) OH and HO2 concentrations, sources, and loss rates during the Southern Oxidants study in Nashville, Tennessee, summer 1999. J. Geophys. Res. (Atmos.) 108(D19): 10.1029/2003JD003551.
Marufu, L. T.; Taubman, B. F.; Bloomer, B.; Piety, C. A.; Doddridge, B. G.; Stehr, J. W.; Dickerson, R. R. (2004) The 2003 North American electrical blackout: an accidental experiment in atmospheric chemistry. Geophys. Res. Lett. 31(L13106): 10.1029/2004GL019771.
Massman, W. J.; Pederson, J.; Delany, A.; Grantz, D.; Denhartog, G.; Neumann, H. H.; Oncley, S. P.; Pearson, R.; Shaw, R. H. (1994) An evaluation of the regional acid deposition model surface module for ozone uptake at 3 sites in the San-Joaquin valley of California. J. Geophys. Res. [Atmos.] 99: 8281-8294.

Matsumi, Y.; Murakami, S.-I.; Kono, M. (2001) High-sensitivity instrument for measuring atmospheric NO_2. Anal. Chem. 73: 5485-5493.
Mauldin, R. L., III; Tanner, D. J.; Eisele, F. L. (1998) A new chemical ionization mass spectrometer technique for the fast measurement of gas phase nitric acid in the atmosphere. J. Geophys. Res. 103(D3): 3361-3367.
McClenny, W. A., ed. (2000) Recommended methods for ambient air monitoring of NO, NO_2, NO_y, and individual NO_z species. Research Triangle Park, NC: U.S. Environmental Protection Agency, National Exposure Research Laboratory; report no. GPRA APM #442.
McDow, S. R.; Jang, M.; Hong, Y.; Kamens, R. M. (1996) An approach to studying the effect of organic composition on atmospheric aerosol photochemistry. J. Geophys. Res. (Atmos.) 101(D14): 19,593-19,600.
McFiggans, G.; Allan, B.; Coe, H.; Plane, H. M. C.; Carpenter, L. J.; O'Dowd, C. (2000) A modeling study of iodine chemistry in the marine boundary layer. J. Geophys. Res. (Atmos.) 105: 14,371-14,385.
McFiggans, G.; Cox, R. A.; Mössinger, J. C.; Allan, B. J.; Plane, J. M. C. (2002) Active chlorine release from marine aerosols: roles for reactive iodine and nitrogen species. J. Geophys. Res. 17(D15): 10.1029/2001JD000383.
McKeen, S. A.; Liu, S. C. (1993) Hydrocarbon ratios and photochemical history of air masses. Geophys. Res. Lett. 20: 2363-2366.
McKeen, S. A.; Liu, S. C. (1997) Hydrocarbon ratios and the photochemical history of air masses. Geophys. Res. Lett. 20: 2363-2366.
McKeen, S. A.; Liu, S. C.; Hsie, E.-Y.; Lin, X.; Bradshaw, J. D.; Smyth, S.; Gregory, G. L.; Blake, D. R. (1996) Hydrocarbon ratios during PEM-WEST A: a model perspective. J. Geophys. Res. (Atmos.) 101(D1): 2087-2109.
McKeen, S. A.; Mount, G.; Eisele, F.; Williams, E.; Harder, J.; Goldan, P.; Kuster, W.; Liu, S. C.; Baumann, K.; Tanner, D.; Fried, A.; Sewell, S.; Cantrell, C.; Shetter, R. (1997) Photochemical modeling of hydroxyl and its relationship to other species during the Tropospheric OH Photochemistry Experiment. J. Geophys. Res. (Atmos.) 102: 6467-6493.
McKenna, D. S.; Konopka, P.; Grooß, J.-U.; Günther, G.; Müller, R.; Spang, R.; Offermann, D.; Orsolini, Y. (2002) A new chemical Lagrangian model of the stratosphere (CLaMS) 1. formulation of advection and mixing. J. Geophys. Res. 107(D16): 10.1029/2000JD000114.
Meagher, J. F.; Cowling, E. B.; Fehsenfeld, F. C.; Parkhurst, W. J. (1998) Ozone formation and transport in southeastern United States: overview of the SOS Nashville/Middle Tennessee Ozone Study. J. Geophys. Res. [Atmos.] 103: 22,213-22,223.
Mendoza-Dominguez, A.; Russell, A. G. (2000) Iterative inverse modeling and direct sensitivity analysis of a photochemical air quality model. Environ. Sci. Technol. 3: 4974-4981.
Mendoza-Dominguez, A.; Russell, A. G. (2001) Estimation of emission adjustments from the application of four-dimensional data assimilation to photochemical air quality modeling. Atmos. Environ. 35: 2879-2894.
Meng, Z.; Seinfeld, J. H. (1996) Time scales to achieve atmospheric gas-aerosol equilibrium for volatile species. Atmos. Environ. 30: 2889-2900.
Meng, Z.; Dabdub, D.; Seinfeld, J. H. (1997) Chemical coupling between atmospheric ozone and particulate matter. Science (Washington, DC) 277: 116-119.
Mentel, T. F.; Sohn, M.; Wahner, A. (1999) Nitrate effect in the heterogeneous hydrolysis of dinitrogen pentoxide on aqueous aerosols. Phys. Chem. Chem. Phys. 1: 5451-5457.
Merrill, J. T.; Moody, J. L. (1996) Synoptic meteorology and transport during the North Atlantic Regional Experiment (NARE) intensive: overview. J. Geophys. Res. [Atmos.] 101: 28,903-28,921.
Meyers, T.; Sickles, J.; Dennis, R.; Rusell, K.; Galloway, J.; Church, T. (2001) Atmospheric nitrogen deposition to coastal estuaries and their watersheds. In: Valigura, R. A.; Alexander, R. B.; Castro, M. S.; Meyers, T. P.; Paerl, H. W.; Stacey, P. E.; Turner, R. E., eds. Nitrogen Loading in Coastal Water Bodies: an Atmospheric Perspective. Washington, DC: AGU Press.
Meyrahn, H.; Pauly, J.; Schneider, W.; Warneck, P. (1986) Quantum yields for photodissociation of acetone in air and an estimate for the life time of acetone in the lower troposphere. J. Atmos. Chem. 4: 277-291.
Michel, A. E.; Usher, C. R.; Grassian, V. H. (2002) Heterogeneous and catalytic uptake of ozone on mineral oxides and dusts: a Knudsen cell investigation. Geophys. Res. Lett. 29: DOI:10.1029/2002GL014896.
Michel, A. E.; Usher, C. R.; Grassian, V. H. (2003) Reactive uptake of ozone on mineral oxides and mineral dusts. Atmos. Environ. 37: 3201-3211.
Mickley, L. J.; Murti, P. P.; Jacob, D. J.; Logan, J. A.; Koch, D. M.; Rind, D. (1999) Radiative forcing from tropospheric ozone calculated with a unified chemistry-climate model. J. Geophys. Res. [Atmos.] 104: 30,153-30,172.

Mihelcic, D.; Holland, F.; Hofzumahaus, A.; Hoppe, L.; Konrad, S.; Müsgen, P.; Pätz, H.-W.; Schäfer, H.-J.; Schmitz, T.; Volz-Thomas, A.; Bächmann, K.; Schlomski, S.; Platt, U.; Geyer, A.; Alicke, B.; Moortgat, G. K. (2003) Peroxy radicals during BERLIOZ and Pabstthum: measurements, radical budgets and ozone production. J. Geophys. Res. [Atmos.] 108(D4): 10.1029/2001JD001014.

Milanchus, M. L.; Rao, S. T.; Zurbenko. I. G. (1998) Evaluating the effectiveness of ozone management efforts in the presence of meteorological variability. J. Air Waste Manage. Assoc. 48: 201-215.

Milford, J. B.; Russell, A. G.; McRae, G. J. (1989) A new approach to photochemical pollution control: implications of spatial patterns in pollutant responses to reductions in nitrogen oxides and reactive organic gas emissions. Environ. Sci. Technol. 23: 1290-1301.

Milford, J. B.; Gao, D.; Sillman, S.; Blossey, P.; Russell, A. G. (1994) Total reactive nitrogen (NO_y) as an indicator of the sensitivity of ozone to reductions in hydrocarbon and NO_x emissions. J. Geophys. Res. 99: 3533-3542.

Milne, P. J.; Zika, R. G. (1993) Amino acid nitrogen in atmospheric aerosols: occurrence, sources, and photochemical modification. J. Atmos. Chem. 16: 361-398.

Milne, P. J.; Prados, A. I.; Dickerson, R. R.; Doddrige, B. G.; Riemer, D. D.; Zika, R. G.; Merrill, J. T.; Moody, J. L. (2000) Nonmethane hydrocarbon mixing ratios in continental outflow air from Eastern North America: export of ozone precursors to Bermuda. J. Geophys. Res. [Atmos.] 105: 9981-9990.

Mochida, M.; Hirokawa, J.; Kajii, Y.; Akimoto, H. (1998) Heterogeneous reactions of Cl_2 with sea salts at ambient temperature: implications for halogen exchange in the atmosphere. Geophys. Res. Lett. 25: 3927-3930.

Mohnen, V. A.; Reiter, E. R. (1977) International conference on oxidants, 1976 - analysis of evidence and viewpoints: part III. the issue of stratospheric ozone intrusion. Research Triangle Park, NC: U.S. Environmental Protection Agency, Environmental Sciences Research Laboratory; EPA report no. EPA-600/3-77-115. Available from: NTIS, Springfield, VA; PB-279 010.

Monks, P. S. (2000) A review of the observations and origins of the spring ozone maximum. Atmos. Environ. 34: 3545-3561.

Monson, R. K.; Harley, P. C.; Litvak, M. E.; Wildermuth, M.; Guenther, A. B.; Zimmerman, P. R.; Fall, R. (1994) Environmental and developmental controls over the seasonal pattern of isoprene emission from aspen leaves. Oecologia 99: 260-270.

Moody, J. L.; Oltmans, S. J.; Levy, H., II; Merrill, J. T. (1995) Transport climatology of tropospheric ozone: Bermuda, 1988-1991. J. Geophys. Res. [Atmos.] 100: 7179-7194.

Moody, J. L.; Davenport, J. C.; Merrill, J. T.; Oltmans, S. J.; Parrish, D. D.; Holloway, J. S.; Levy, H., II; Forbes, G. L.; Trainer, M.; Buhr, M. (1996) Meteorological mechanisms for transporting O_3 over the western North Atlantic Ocean: a case study for August 24-29, 1993. J. Geophys. Res. 101(D22): 29,213-29,227.

Moody, J. L.; Wimmers, A. J.; Davenport, J. C. (1999) Remotely sensed specific humidity: development of a derived product from the GOES Imager Channel 3. Geophys. Res. Lett. 26: 59-62.

Moorthi, S.; Suarez, M. J. (1992) Relaxed Arakawa-Schubert: a parameterization of moist convection for general circulation models. Mon. Weather Rev. 120: 978-1002.

Mopper, K.; Kieber, D. J. (2000) Marine photochemistry and its impact on carbon cycling. In: Demers, S.; Vernet, M., eds. Effects of UV Radiation on Marine Ecosystems. New York, NY: Cambridge University Press, Ch.4, pp. 101-129.

Morales-Morales, R. (1998) Carbon monoxide, ozone, and hydrocarbons in the Baltimore metropolitan area [dissertation]. College Park, MD: University of Maryland, Department of Meteorology. Available from: University Microfilms International, Ann Arbor, MI; publication no. 9908993.

Moschonas, N.; Danalatos, D.; Glavas, S. (1999) The effect of O_2 and NO_2 on the ring retaining products of the reaction of toluene with hydroxyl radicals. Atmos. Environ. 33: 111-116.

Mount, G. H.; Eisele, F. L. (1992) An intercomparison of tropospheric OH measurements at Fritz Peak Observatory, Colorado. Science (Washington, DC) 256: 1187-1190.

Mount, G. H.; Williams, E. J. (1997) An overview of the tropospheric OH photochemistry experiment, Fritz Peak/Idaho Hill, Colorado, fall 1993. J. Geophys. Res. [Atmos.] 102: 6171-6186.

Mozurkewich, M. (1995) Mechanisms for the release of halogens from sea-salt particles by free radical reactions. J. Geophys. Res. (Atmos.) 100: 14,199-14,207.

Müller, J.-F.; Brasseur, G. (1995) IMAGES: a three-dimensional chemical transport model of the global troposphere. J. Geophys. Res. (Atmos.) 100: 16,445-16,490.

Müller, J.-F.; Brasseur, G. (1999) Sources of upper tropospheric HO_x: a three-dimensional study. J. Geophys. Res. (Atmos.) 104: 1705-1715.

Munger, J. W.; Fan, S.-M.; Bakwin, P. S.; Goulden, M. L.; Goldstein, A. H.; Colman, A. S.; Wofsy, S. C. (1998) Regional budgets of nitrogen oxides from continental sources: variations of rates for oxidation and deposition with season and distance from source regions. J. Geophys. Res. (Atmos.) 103: 8355-8368.

Muñoz, M. S. S.; Rossi, M. J. (2002) Heterogeneous reactions of HNO_3 with flame soot generated under different combustion conditions. Reaction mechanism and kinetics. Phys. Chem. Chem. Phys. 4: 5110-5118.

Murphy, D.; Fahey, D. (1994) An estimate of the flux of stratospheric reactive nitrogen and ozone into the troposphere. J. Geophys. Res. (Atmos.) 99: 5325-5332.

Narita S.; Uchiyama S.; Takemi K. (1998) The interference and cross sensitivity for an UV ozone monitor. Ozone Sci. Eng. 20: 495-497.

National Bureau of Standards. (1975) Catalog of NBS standard reference materials, 1975-76 edition. Washington, DC: U.S. Department of Commerce, National Bureau of Standards; NBS special publication no. 260.

National Research Council. (1991) Rethinking the ozone problem in urban and regional air pollution. Washington, DC: National Academy Press.

National Research Council. (1999) Ozone-forming potential of reformulated gasoline. Washington, DC: National Academy of Sciences.

National Research Council. (2002) Estimating the public health benefits of proposed air pollution regulations. Washington, DC: National Academy of Sciences. Available at: http://books.nap.edu/books/0309086094/html/index.html [7 November, 2002].

National Research Council. (2003) Air emissions from animal feeding operations: current knowledge and future needs. Available: http://www.nap.edu/books/0309087058/html/ (5 February 2004).

Neff, J. C.; Holland, E. A.; Dentener, F. J.; McDowell, W. H.; Russell, K. M. (2002) Atmospheric organic nitrogen: implications for the global N cycle. Biogeochemistry 57/58: 99-136.

Neuman, J. A.; Huey, L. G.; Dissly, R. W.; Fehsenfeld, F. C.; Flocke, F.; Holecek, J. C.; Holloway, J. S.; Hübler, G.; Jakoubek, R.; Nicks, D. K., Jr.; Parrish, D. D.; Ryerson, T. B.; Sueper, D. T.; Weinheimer, A. J. (2002) Fast-response airborne in-situ measurements of HNO_3 during the Texas Air Quality Study. J. Geophys. Res. (Atmos.) 107: 10.1029/2001JD001437.

Newberg, J.; Williams, D.; Chu, G.; Matthew, B.; Anastasio, C. (2000) Photoformation of hydroxyl radical in sea-salt particles. In: Preprints of Extended Abstracts presented at the 219th American Chemical Society National Meeting; March; San Francisco, CA. Columbus, OH: American Chemical Society; ENVR 176.

Newchurch, M. J.; Ayoub, M. A.; Oltmans, S.; Johnson, B.; Schmidlin, F. J. (2003) Vertical distribution of ozone at four sites in the United States. J. Geophys. Res. 108(D1): 10.1029/2002JD002059.

Newell, R. E.; Thouret, V.; Cho, J. Y. N.; Stoller, P.; Marenco, A.; Smit, H. G. (1999) Ubiquity of quasi-horizontal layers in the troposphere. Nature (London) 398: 316-319.

Nordmeyer, T.; Wang, W.; Ragains, M. L.; Finlayson-Pitts, B. J.; Spicer, C. W.; Plastridge, R. A. (1997) Unique products of the reaction of isoprene with atomic chlorine: potential markers. Geophys. Res. Lett. 24: 1615-1618.

North American Research Strategy for Tropospheric Ozone (NARSTO) Synthesis Team. (2000) An assessment of tropospheric ozone pollution: a North American perspective. Palo Alto, CA: Electric Power Research Institute.

Notholt, J.; Hjorth, J.; Raes, F. (1992a) Formation of HNO_2 on aerosol surfaces during foggy periods in the presence of NO and NO_2. Atmos. Environ. Part A 26: 211-217.

Notholt, J.; Hjorth, J.; Raes, F.; Schrems, O. (1992b) Simultaneous long path field measurements of HNO_2, CH_2O and aerosol. Ber. Bunsen Ges. Phys. Chem. 96: 290-293.

Nunnermacker, L. J.; Imre, D.; Daum, P. H.; Kleinman, L.; Lee, Y.-N.; Lee, J. H.; Springston, S. R.; Newman, L.; Weinstein-Lloyd, J.; Luke, W. T.; Banta, R.; Alvarez, R.; Senff, C.; Sillman, S.; Holdren, M.; Keigley, G. W.; Zhou, X. (1998) Characterization of the Nashville urban plume on July 3 and July 18, 1995. J. Geophys. Res. 103(D21): 28,129-28,148.

Nunnermacker, L. J.; Kleinman, L. I.; Imre, D.; Daum, P. H.; Lee, Y.-N.; Lee, J. H.; Springston, S. R.; Newman, L.; Gillani, N. (2000) NO_y lifetimes and O_3 production efficiencies in urban and power plant plumes: analysis of field data. J. Geophys. Res. [Atmos.] 105: 9165-9176.

O'Brien, R. J.; Green, P. J.; Nguyen, N.-L.; Doty, R. A.; Dumdel, B. E. (1983) Carbon balances in simulated atmospheric reactions: aromatic hydrocarbons. Environ. Sci. Technol. 17: 183-186.

Odman, M. T.; Ingram, C. I. (1996) Multiscale air quality simulation platform (MAQSIP): source code documentation and validation. Research Triangle Park, NC: MCNC; technical report ENV-96TR002-v1.0. Available: http://www.ce.gatech.edu/~todman/maqsip.pdf (9 September 2003).

Odman, M. T.; Russell, A. G. (1999) Mass conservative coupling of non-hydrostatic meteorological models with air quality models. In: Grying, S.-E.; Batchvarova, E., eds. Air Pollution Modeling and its Application XIII. New York, NY: Plenum Press.

Odum, J. R.; Hoffmann, T.; Bowman, F.; Collins, D.; Flagan, R. C.; Seinfeld, J. H. (1996) Gas/particle partitioning and secondary organic aerosol yields. Environ. Sci. Technol. 30: 2580-2585.

Olsen, M. A.; Stanford, J. L. (2001) Evidence of stratosphere-to-troposphere transport within a mesoscale model and total ozone mapping spectrometer total ozone. J. Geophys. Res. [Atmos.] 106: 27,323-27,334.

Olsen, M. A.; Douglass, A. R.; Schoeberl, M. R. (2002) Estimating downward cross-tropopause flux using column ozone and potential vorticity. J. Geophys. Res. 107(D22): 10.1029/2001JD002041.

Olszyna, K. J.; Bailey, E. M.; Simonaitis, R.; Meagher, J. F. (1994) O_3 and NO_y relationships at a rural site. J. Geophys. Res. [Atmos.] 99: 14,557-14,563.

Oltmans, S. J.; Levy, H., II. (1992) Seasonal cycle of surface ozone over the North Atlantic. Nature 358: 392-394.

Oltmans, S. J.; Levy, H., II; Harris, J. M.; Merrill, J. T.; Moody, J. L.; Lathrop, J. A.; Cuevas, E.; Trainer, M.; O'Neill, M. S.; Prospero, J. M.; Vömel, H.; Johnson, B. J. (1996) Summer and spring ozone profiles over the North Atlantic from ozonesonde observations. J. Geophys. Res. 101: 29,179-29,200.

Oltmans, S. J.; Lefohn, A. S.; Scheel, H. E.; Harris, J. M.; Levy, H., II; Galbally, I. E.; Brunke, E.-G.; Meyer, C. P.; Lathrop, J. A.; Johnson, B. J.; Shadwick, D. S.; Cuevas, E.; Schmidlin, F. J.; Tarasick, D. W.; Claude, H.; Kerr, J. B.; Uchino, O.; Mohnen, V. (1998) Trends of ozone in the troposphere. Geophys. Res. Lett. 25: 139-142.

Orlando, J. J.; Tyndall, G. S.; Paulson, S. E. (1999) Mechanism of the OH-initiated oxidation of methacrolein. Geophys. Res. Lett. 26: 2191-2194.

Padro, J. (1996) Summary of ozone dry deposition velocity measurements and model estimates over vineyard, cotton, grass and deciduous forest in summer. Atmos. Environ. 30: 2363-2369.

Palmer, P. I.; Jacob, D. J.; Fiore, A. M.; Martin, R. V.; Chance, K.; Kuruso, T. P. (2003) Mapping isoprene emissions over North America using formaldehyde column observations from space. J. Geophys. Res. 108(D6): 10.1029/2002JD002153.

Pandis, S. N.; Paulson, S. E.; Seinfeld, J. H.; Flagan, R. C. (1991) Aerosol formation in the photooxidation of isoprene and β-pinene. Atmos. Environ. Part A 25: 997-1008.

Pandis, S. N.; Harley, R. A.; Cass, G. R.; Seinfeld, J. H. (1992) Secondary organic aerosol formation and transport. Atmos. Environ. Part A 26: 2269-2282.

Papagni, C.; Arey, J.; Atkinson, R. (2001) Rate constants for the gas-phase reactions of OH radicals with a series of unsaturated alcohols. Int. J. Chem. Kinet. 33: 142-147.

Park, R. J.; Stenchikov, G. L.; Pickering; Dickerson, R. R.; Allen, D. J.; Kondragunta, S. (2001) Regional air pollution and its radiative forcing: studies with a single column chemical and radiation transport model. J. Geophys. Res. [Atmos.] 106: 28,751-28,770.

Parrish, D. D.; Fehsenfeld, F. C. (2000) Methods for gas-phase measurements of ozone, ozone precursors and aerosol precursors. Atmos. Environ. 34: 1921-1957.

Parrish, D. D.; Trainer, M.; Buhr, M. P.; Watkins, B. A.; Fehsenfeld, F. C. (1991) Carbon monoxide concentrations and their relatin to concentrations of total reactive oxided nitrogen at two rural U.S. sites. J. Geophys. Res. (Atmos.) 96: 9309-9320.

Parrish, D. D.; Hahn, C. J.; Williams, E. J.; Norton, R. B.; Fehsenfeld, F. C.; Singh, H. B.; Shetter, J. D.; Gandrud, B. W.; Ridley, B. A. (1992) Indications of photochemical histories of Pacific air masses from measurements of atmospheric trace species at Point Arena, California. J. Geophys. Res. [Atmos.] 97: 15,883-15,901.

Parrish, D. D.; Hahn, C. J.; Williams, E. J.; Norton, R. B.; Fehsenfeld, F. C.; Singh, H. B.; Shetter, J. D.; Gandrud, B. W.; Ridley, B. A. (1993) Reply [to Comment on "Indications of photochemical histories of Pacific air masses from measurements of atmospheric trace species at Point Arena, California" by D. D. Parrish et al.]. J. Geophys. Res. (Atmos.) 98(D8): 14,995-14,997.

Parrish, D. D.; Trainer, M.; Young, V.; Goldan, P. D.; Kuster, W. C.; Jobson, B. T.; Fehsenfeld, F. C.; Lonneman, W. A.; Zika, R. D.; Farmer, C. T.; Riemer, D. D.; Rodgers, M. O. (1998) Internal consistency tests for evaluation of measurements of anthropogenic hydrocarbons in the troposphere. J. Geophys. Res. (Atmos.) 103(D17): 22,339-22,359.

Parrish, D. D.; Ryerson, T. B.; Holloway, J. S.; Trainer, M.; Fehsenfeld, F. C. (1999) Does pollution increase or decrease tropospheric ozone in winter-spring? Atmos. Environ. 33: 5147-5149.

Parrish, D. D.; Holloway, J. S.; Jakoubek, R.; Trainer, M.; Ryerson, T. B.; Hübler, G.; Fehsenfeld, F. C.; Moody, J. L.; Cooper. O. R. (2000) Mixing of anthropogenic pollution with stratospheric ozone: a case study from the North Atlantic wintertime troposphere. J. Geophys. Res. [Atmos.] 105: 24,363-24,374.

Parrish, D. D.; Trainer, M.; Hereid, D.; Williams, E. J.; Olszyna, K. J.; Harley, R. A.; Meagher, J. F.; Fehsenfeld, F. C. (2002) Decadal change in carbon monoxide to nitrogen oxide ratio in U.S. vehicular emissions J. Geophys. Res. (Atmos.) 107(D13): 10.1029/2001JD000720.

Paul, J. W.; Beauchamp, E. G. (1993) Nitrogen availability for corn in soils amended with urea, cattle slurry, and solid and composted manures. Can. J. Soil Sci. 73: 253-266.

Paul, J. W.; Beauchamp, E. G.; Zhang, X. (1993) Nitrous and nitric oxide emissions during nitrification and denitrification from manure-amended soil in the laboratory. Can. J. Soil Sci. 73: 539-553.
Penner, J. E. (1995) Carbonaceous aerosols influencing atmospheric radiation: black and organic carbon. In: Charlson, R. J.; Heintzenberg, J., eds. Aerosol Forcing of Climate. New York, NY: John Wiley and Sons; pp. 91-108.
Penrose, W. R..; Pan, L.; Stetter, J. R.; Ollison, W. M. (1995) Sensitive measurement of ozone using amperometric gas sensors. Anal. Chim. Acta 313: 209-219.
Perry, R. A.; Atkinson, R.; Pitts, J. N., Jr. (1977) Kinetics and mechanism of the gas phase reaction of OH radicals with aromatic hydrocarbons over the temperature range 296-473 K. J. Phys. Chem. 81: 296-304.
Petriconi, G. L.; Papee, H. M. (1972) On the photolytic separation of halogens from sea water concentrates. Water Air Soil Pollut. 1: 117-131.
Pickering, K. E.; Dickerson, R. R.; Huffman, G. J.; Boatman, J. F.; Schanot, A. (1988) Trace gas transport in the vicinity of frontal convective clouds. J. Geophys. Res. 93: 759-773.
Pickering, K. E.; Thompson, A. M.; Dickerson, R. R.; Luke, W. T.; McNamara, D. P.; Greenberg, J. P.; Zimmerman, P. R. (1990) Model calculations of tropospheric ozone production potential following observed convective events. J. Geophys. Res. [Atmos.] 95: 14,049-14,062.
Pickering, K. E.; Thompson, A. M.; Scala, J. R.; Tao, W.-K.; Simpson, J.; Garstang, M. (1991) Photochemical ozone production in tropical squall line convection during NASA Global Tropospheric Experiment/Amazon Boundary Layer Experiment 2A. J. Geophys. Res. 96: 3099-3114.
Pickering, K. E.; Thompson, A. M.; Scala, J. R.; Tao, W.-K.; Simpson, J. (1992a) Ozone production potential following convective redistribution of biomass burning emissions. J. Atmos. Chem. 14: 297-313.
Pickering, K. E.; Thompson, A. M.; Scala, J. R.; Tao, W.-K.; Dickerson, R. R.; Simpson, J. (1992b) Free tropospheric ozone production following entrainment of urban plumes into deep convection. J. Geophys. Res. 97(D16): 17985-18,000.
Pickering, K. E.; Scala, J. R.; Thompson, A. M.; Tao, W.-K.; Simpson, J. (1992c) A regional estimate of the convective transport of CO from biomass burning. Geophys. Res. Lett. 19: 289-292.
Pickering, K. E.; Thompson, A. M.; Tao, W.-K.; Kucsera, T. L. (1993) Upper tropospheric ozone production following mesoscale convection during STEP/EMEX. J. Geophys. Res. 98: 8737-8749.
Pickering, K. E.; Thompson, A. M.; Tao, W.-K.; Rood, R. B.; McNamara, D. P.; Molod, A. M. (1995) Vertical transport by convective clouds: comparisons of three modeling approaches. Geophys. Res. Lett. 22: 1089-1092.
Pickering, K. E.; Thompson, A. M.; Wang, Y.; Tao, W.-K.; McNamara, D. P.; Kirchhoff, W. J. H.; Heikes, B. G.; Sachse, G. W.; Bradshaw, J. D.; Gregory, G. L.; Blake, D. R. (1996) Convective transport of biomass burning emissions over Brazil during TRACE A. J. Geophys. Res. [Atmos.] 101: 23,993-24,012.
Pickering, K. E.; Wang, Y.; Tao, W.-K.; Price, C.; Müller, J.-F. (1998) Vertical distributions of lightning NO_x for use in regional and global chemical transport models. J. Geophys. Res. [Atmos.] 103: 31,203-31,216.
Pickering, K. E.; Thompson, A. M.; Kim, H.; DeCaria, A. J.; Pfister, L.; Kucsera, T. L.; Witte, J. C.; Avery, M. A.; Blake, D. R.; Crawford, J. H.; Heikers, B. G.; Sachse, G. W.; Sandholm, S. T.; Talbot, R. W. (2001) Trace gas transport and scavenging ini PEM-Tropics B South Pacific Convergence Zone convection. J. Geophys. Res. [Atmos.] 106: 32,591-32,602.
Pierce, T. E.; Waldruff, P. S. (1991) PC-BEIS: a personal computer version of the biogenic emissions inventory system. J. Air Waste Manage. Assoc. 41: 937-941.
Pierce, T; Geron, C.; Bender, L.; Dennis, R.; Tonnesen, G.; Guenther, A. (1998) Influence of increased isoprene emissions on regional ozone modeling. J. Geophys. Res. (Atmos.) 103: 25,611-25,630.
Pierson, W. R.; Gertler, A. W.; Bradow, R. L. (1990) Comparison of the SCAQS tunnel study with historical data. Presented at: 83rd annual meeting & exhibition of the Air and Waste Management Association; June; Pittsburgh, PA. Pittsburgh, PA: Air and Waste Management Association; paper no. 90-175.3.
Pinto, J. P.; Bruhl, C.; Thompson, A. M. (1993) The current and future envirionmental role of atmospheric methane. In: Khalil, M. A. K., ed. Atmospheric methane sources, sinks, and role in global change, p. 514-531. (NATO ASI Series, v. 113).
Piotrowicz, S. R.; Bezdek, H. F.; Harvey, G. R.; Springer-Young, M.; Hanson, K. J. (1991) On the ozone minimum over the equatorial Pacific Ocean. J. Geophys. Res. 96: 18,679-18,687.
Pippin, M. R.; Bertman, S.; Thornberry, T.; Town, M.; Carroll, M. A.; Sillman, S. (2001) Seasonal variation of PAN, PPN, MPAN and O_3 at the upper midwest PROPHET site. J. Geophys. Res. (Atmos.) 106: 24,451-24,463.

Pitari, G.; Grassi, B.; Visconti, G. (1997) Results of a chemical transport model with interactive aerosol microphysics. In: Bojkov, R.; Visconti, G., eds. Proceedings of the XVIII Quadrennial Ozone Symposium; September 1996; L'Aquila, Italy, pp. 759-762.

Pitts, J. N., Jr.; Sanhueza, E.; Atkinson, R.; Carter, W. P. L.; Winer, A. M.; Harris, G. W.; Plum, C. N. (1984a) An investigation of the dark formation of nitrous acid in environmental chambers. Int. J. Chem. Kinet. 16: 919-939.

Pitts, J. N., Jr.; Biermann, H. W.; Atkinson, R.; Winer, A. M. (1984b) Atmospheric implications of simultaneous nighttime measurements of NO_3 radicals and HONO. Geophys. Res. Lett. 11: 557-560.

Placet, M.; Mann, C. O.; Gilbert, R. O.; Niefer, M. J. (2000) Emissions of ozone precursors from stationary sources: a critical review. Atmos. Environ. 34: 2183-2204.

Plummer, D. A.; McConnell, J. C.; Shepson, P. B.; Hastie, D. R.; Niki, H. (1996) Modeling of ozone formation at a rural site in southern Ontario. Atmos. Environ. 30: 2195-2217.

Pokharel, S. S.; Bishop, G. A.; Stedman, D. H. (2002) An on-road motor vehicle emissions inventory for Denver: an efficient alternative to modeling. Atmos. Environ. 36: 5177-5184.

Poppe, D.; Wallasch, M.; Zimmermann, J. (1993) The dependence of the concentration of OH on its precursors under moderately polluted conditions: a model study. J. Atmos. Chem. 16: 61-78.

Poppe, D.; Zimmermann, J.; Bauer, R.; Brauers, T.; Brüning, D.; Callies, J.; Dorn, H.-P.; Hofzumahaus, A.; Johnen, F.-J.; Khedim, A.; Koch, H.; Koppmann, R.; London, H.; Müller, K.-P.; Neuroth, R.; Plass-Dülmer, C.; Platt, U.; Rohrer, F.; Röth, E.-P.; Rudolph, J.; Schmidt, U.; Wallasch, M.; Ehhalt, D. H. (1994) Comparison of measured OH concentrations with model calculations. J. Geophys. Res. [Atmos.] 99: 16,633-16,642.

Poppe, D.; Zimmerman, J.; Dorn, H. P. (1995) Field data and model calculations for the hydroxyl radical. J. Atmos. Sci. 52: 3402-3407.

Poulida, O.; Dickerson, R. R.; Heymsfield, A. (1996) Troposphere-stratosphere exchange in a midlatitude mesoscale convective complex: 1. Observations. J. Geophys. Res. [Atmos.] 101: 6823-6836.

Prados, A. I. (2000) The export of ozone and other atmospheric trace species from North America: observations and numerical simulations [dissertation]. College Park, MD: The University of Maryland.

Prados, A. I.; Dickerson, R. R.; Doddridge, B. G.; milne, P. A.; Moody, J. L.; Merrill, J. T. (1999) Transport of ozone and pollutants from North America to the North Atlantic Ocean during the 1996 AEROCE intensive experiment. J. Geophys. Res. 104: 26,219-26,233.

Prather, M.; Ehhalt, D. (2001) Atmospheric chemistry and greenhouse gases. In: Houghton, J. T.; Ding, Y.; Griggs, D. J.; Noguer, M.; van der Linden, P. J.; Dai, X.; Maskell, K.; Johnson, C. A., eds. Climate Change 2001: The Scientific Basis; pp. 239-287. Cambridge, MA: Cambridge University Press. Available: http://www.grida.no/climate/ipcc_tar/wg1/ (20 January 2004).

Prather, M. J.; Jacob, D. J. (1997) A persistent imbalance in HO_x and NO_x photochemistry in the upper troposphere driven by deep tropical convection. Geophys. Res. Lett. 24: 3189-3192.

Prenni, A. J.; DeMott, P. J.; Kreidenweis, S. M. (2003) Water uptake of internally mixed particles containing ammomium sulfate and dicarboxylic acids. Atmos. Environ. 37: 4243-4251.

Prévôt, A. S. H.; Staehelin, J.; Kok, G. L.; Schillawski, R. D.; Neininger, B.; Staffelbach, T.; neftel, A.; Wernli, H.; Dommen, J. (1997) The Milan photooxidant plume. J. Geophys. Res. (Atmos.) 102: 23,375-23,388.

Price, J. D.; Vaughan, G. (1993) The potential for stratosphere-troposphere exchange in cut-off-low systems. Q. J. R. Meteorol. Soc. 119: 343-365.

Price, C.; Penner, J.; Prather, M. (1997) NO_x from lightning: 1. Global distribution based on lightning physics. J. Geophys. Res. [Atmos.] 102: 5929-5941.

Pszenny, A. A. P.; Keene, W. C.; Jacob, D. J.; Fan, S.; Maben, J. R.; Zetwo, M. P.; Springer-Young, M.; Galloway, J. N. (1993) Evidence of inorganic chlorine gases other than hydrogen chloride in marine surface air. Geophys. Res. Lett. 20: 699-702.

Pszenny, A. A. P.; Moldanova, J.; Keene, W. C.; Sander, R.; Maben, J. R.; Martinez, M.; Crutzen, P. J.; Perner, D.; Prinn, R. G. (2003) Halogen cycling and aerosol pH in the Hawaiian marine boundary layer. Atmos. Chem. Phys. Disc. 3: 4701-4753.

Pun, B. K.; Seigneur, C.; Grosjean, D.; Saxena, P. (2000) Gas-phase formation of water-soluble organic compounds in the atmosphere: a retrosynthetic analysis. J. Atmos. Chem. 35: 199-223.

Quigley, D. C.; Hornafius, J. S.; Luyendyk, B. P.; Francis, R. D.; Clark, J.; Washburn, L. (1999) Decrease in natural marine hydrocarbon seepage near Coal Oil Point, California, associated with offshore oil production. Geol. 27: 1047-1050.

Rancher, J.; Kritz, M. A. (1980) Diurnal fluctuations of Br and I in the tropical marine atmosphere. J. Geophys. Res. 85: 5581-5587.

Rao, S. T.; Zurbenko, I. G. (1994) Detecting and tracking changes in ozone air quality. J. Air Waste Manage. Assoc. 44: 1089-1092.

Rao, S. T.; Zurbenko, I. G.; Neagu, R.; Porter, P. S.; Ku, J. Y.; Henry, R. F. (1997) Space and time scales in ambient ozone data. Bull. Am. Meteorol. Soc. 78: 2153-2166.

Rao, S. T.; Ku, J. Y.; Berman, S. (2003) Summertime characteristics of the atmospheric boundary layer and relationships to ozone levels over the eastern United States. Pure Appl. Geophys. 160: 21-55.

Reed, R. J. (1955) A study of a characteristic type of upper-level frontogenesis. J. Meteorol. 12: 226-237.

Regener, E. (1941) Ozonschicht und atmospharische turbulenz. Ber. Dtsch. Wetterdienstes US-Zone No. 11: 45-57.

Reid, J. P.; Sayer, R. M. (2003) Heterogeneous atmospheric aerosol chemistry: laboratory studies of chemistry on water droplets. Chem. Soc. Rev. 32: 70-79.

Reisinger, A. R. (2000) Unidentified interference in DOAS measurements of ozone. Appl. Spectrosc. 54: 72-79.

Reissell, A.; Arey, J.; Atkinson, R. (2001) Atmospheric chemistry of camphor. Int. J. Chem. Kinet. 33: 56-63.

Reitebuch, O.; Strassburger, A.; Emeis, S.; Kuttler, W. (2000) Nocturnal secondary ozone concentration maxima analysed by sodar observation and surface measurements. Atmos. Environ. 34: 4315-4329.

Reiter, E. R. (1963) A case study of radioactive fallout. J. Appl. Meteorol. 2: 691-705.

Reiter, E. R. (1975) Stratospheric-tropospheric exchange processes. Rev. Geophys. Space Phys. 13: 459-474.

Reiter, E. R.; Mahlman, J. D. (1965) Heavy radioactive fallout over the southern United States, November 1962. J. Geophys. Res. 70: 4501-4520.

Reithmeier, C.; Sausen, R. (2002) ATTILA: atmospheric tracer transport in a Lagrangian model. Tellus 54B: 278-299.

Ren, X. R.; Harder, H.; Martinez, M.; Lesher, R. L.; Oliger, A.; Shirley, T.; Adams, J.; Simpas, J. B.; Brune, W. H. (2003) HOx concentrations and OH reactivity observations in New York City during PMTACS-NY2001. Atmos. Environ. 37: 3627-3637.

Reynolds, S.; Michaels, H.; Roth, P.; Tesche, T. W.; McNally, D.; Gardner, L.; Yarwood, G. (1996) Alternative base cases in photochemical modeling: their construction, role, and value. Atmos. Environ. 30: 1977-1988.

Ridley, B. A.; Carroll, M. A.; Dunlap, D. D.; Trainer, M.; Sachse, G. W.; Gregory, G. L.; Condon, E. P. (1989) Measurements of NO_x over the eastern Pacific ocean and southwestern United States during the spring 1984 NASA GTE aircraft program. J. Geophys. Res. [Atmos.] 94: 5043-5067.

Ridley, B. A.; Walega, J. G.; Lamarque, J.-F.; Grahek, F. E.; Trainer, M.; Hübler, G.; Lin, X.; Fehsenfeld, F. C. (1998) Measurements of reactive nitrogen and ozone to 5-km altitude in June 1990 over the southeastern United States. J. Geophys. Res. 103: 8369-8388.

Riemer, D. D.; Apel, E. C. (2001) Confirming the presence and extent of oxidation by Cl in the Houston, Texas urban area using specific isoprene oxidation products as tracers. Miami, FL: University of Miami, Rosenstiel School of Marine and Atmospheric Science. Available: http://clearinghouse.ces.utexas.edu/TexAQS/DB_Files/ConfirmingPresenceandExtentOfOxidationByCI.pdf (5 February 2004).

Riemer, N.; Vogel, H.; Vogel, B.; Schell, B.; Ackermann, I.; Kessler, C.; Hass, H. (2003) Impact of the heterogeneous hydrolysis of N_2O_5 on chemistry and nitrate aerosol formation in the lower troposphere under photosmog conditions. J. Geophys. Res. (Atmos.) 108(D4): 10.1029/2002JD002436.

Roberts, J. M.; Williams, J.; Baumann, K.; Buhr, M. P.; Goldan, P. D.; Holloway, J.; Hübler, G.; Kuster, W. C.; McKeen, S. A.; Ryerson, T. B.; Trainer, M.; Williams, E. J.; Fehsenfeld, F. C.; Bertman, S. B.; Nouaime, G.; Seaver, C.; Grodzinsky, G.; Rodgers, M.; Young, V. L. (1998) Measurements of PAN, PPN, and MPAN made during the 1994 and 1995 Nashville Intensives of the Southern Oxidant Study: implications for regional ozone production from biogenic hydrocarbons. J. Geophys. Res. [Atmos.] 103: 22,473-22,490.

Robinson, G. N.; Worsnop, D. R.; Jayne, J. T.; Kolb, C. E.; Davidovits, P. (1997) Heterogeneous uptake of $ClONO_2$ and N_2O_5 by sulfuric acid solutions. J. Geophys. Res. (Atmos.) 102: 3583-3601.

Rodgers, M. O.; Davis, D. D. (1989) A UV-photofragmentation/laser-induced fluorescence sensor for the atmospheric detection of HONO. Environ. Sci. Technol. 23: 1106-1112.

Roelofs, G. J.; Scheeren, H. A.; Heland, J.; Ziereis, H.; Lelieveld, J. (2003) A model study of ozone in the eastern Mediterranean free troposphere during MINOS (August 2001). Atmos. Chem. Phys. 3: 1199-1210.

Rogers, J. D. (1990) Ultraviolet absorption cross sections and atmospheric photodissociation rate constants of formaldehyde. J. Phys. Chem. 94: 4011-4015.

Roselle, S. J. (1994) Effects of biogenic emission uncertainties on regional photochemical modeling of control strategies. Atmos. Environ. 28: 1757-1772.

Rudich, Y.; Talukdar, R. K.; Fox, R. W.; Ravishankara, A. R. (1996) Rate coefficients for reactions of NO_3 with a few olefins and oxygenated olefins. J. Phys. Chem. 100: 5374-5381.

Rudolph, J.; Ramacher, B.; Plass-Dülmer, C.; Müller, K.-P.; Koppmann, R. (1997) The indirect determination of chlorine atom concentration in the troposphere from changes in the patterns of non-methane hydrocarbons. Tellus B 49: 592-601.

Ruppert, L.; Becker, K. H. (2000) A product study of the OH radical-initiated oxidation of isoprene: formation of C_5-unsaturated diols. Atmos. Environ. 34: 1529-1542.

Russell, K. M. (2002) Characterization and dry deposition of atmospheric nitrogen at the mid-Atlantic United States coast [dissertation]. Richmond, VA: University of Virginia. Available from: University Microfilms, Ann Arbor, MI; AADAA-13044880.

Russell, A.; Dennis, R. (2000) NARSTO critical review of photochemical models and modeling. Atmos. Environ. 34: 2283-2324.

Ryan, W. F.; Doddridge, B. G.; Dickerson, R. R.; Morales, R. M.; Hallock, K. A.; Roberts, P. T.; Blumenthal, D. L.; Anderson, J. A.; Civerolo, K. (1998) Pollutant transport during a regional O_3 episode in the mid-Atlantic states. J. Air Waste Manage. Assoc. 48: 786-797.

Ryerson, T. B.; Buhr, M. P.; Frost, G. J.; Goldan, P. D.; Holloway, J. S.; Hübler, G.; Jobson, B. T.; Kuster, W. C.; McKeen, S. A.; Parrish, D. D.; Roberts, J. M.; Sueper, D. T.; Trainer, M.; Williams, J.; Fehsenfeld, F. C. (1998) Emissions lifetimes and ozone formation in power plant plumes. J. Geophys. Res. 103(D17): 22,569-22,583.

Ryerson, T. B.; Williams, E J.; Fehsenfeld, F. C. (2000) An efficient photolysis system for fast-response NO_2 measurements. J. Geophys. Res. (Atmos.) 105(D21): 26,447-26,461.

Ryerson, T. B.; Trainer, M.; Holloway, J. S.; Parrish, D. D.; Huey, L. G.; Sueper, D. T.; Frost, G. J.; Donnelly, S. G.; Schauffler, S.; Atlas, E. L.; Kuster, W. C.; Goldan, P. D.; Hübler, G.; Meagher, J. F.; Fehsenfeld, F. C. (2001) Observations of ozone formation in power plant plumes and implications for ozone control strategies. Science (Washington, DC) 292: 719-723.

Saathoff, H.; Naumann, K. H.; Riemer, N.; Kamm, S.; Möhler, O.; Schurath, U.; Vogel, H.; Vogel, B. (2001) The loss of NO_2, HNO_3,,NO_3/N_2O_5 and $HO_2/HOONO_2$ on soot aerosol: a chamber and modeling study. Geophys. Res. Lett. 28: 1957-1960.

Sakamaki, F.; Hatakeyama, S.; Akimoto, H. (1983) Formation of nitrous acid and nitric oxide in the heterogeneous dark reaction of nitrogen dioxide and water vapor in a smog chamber. Int. J. Chem. Kinet. 15: 1013-1029.

Sakugawa, H.; Kaplan, I. R. (1989) H_2O_2 and O_3 in the atmosphere of Los Angeles and its vicinity: factors controlling their formation and their role as oxidants of SO_2. J. Geophys. Res. [Atmos.] 94: 12,957-12,973.

Salmond, J. A.; McKendry, I. G. (2002) Secondary ozone maxima in a very stable nocturnal boundary layer: observations from the Lower Fraser Valley, BC. Atmos. Environ. 36: 5771-5782.

Samson, P. J.; Shi, B. (1988) A meteorological investigation of high ozone values in American cities. Ann Arbor, MI: University of Michigan, Space Physics Research Laboratory, Department of Atmospheric, Oceanic, and Space Sciences.

Sander, R.; Crutzen, P. J. (1996) Model study indicating halogen activation and ozone destruction in polluted air masses transported to the sea. J. Geophys. Res. [Atmos.] 101: 9121-9138.

Sander, R.; Rudich, Y.; Von Glasow, R.; Crutzen, P. J. (1999) The role of $BrNO_3$ in marine tropospheric chemistry: a model study. Geophys. Res. Lett. 26: 2858-2860.

Sander, R.; Keene, W. C.; Pszenny, A. A. P.; Arimoto, R. Ayers, G. P.; Chainey, J. M.; Crutzen, P. J.; Duce, R. A.; Huebert, B. J.; Maenhaut, W.; Turekian, V. C.; Van Dingenan, R. (2003) Inorganic bromine in the marine boundary layer: a critical review. Atmos. Chem. Phys. 3: 1301-1336.

Santer, B. D.; Wehner, M. F.; Wigley, T. M. L.; Sausen, R.; Meehl, G. A.; Taylor, K. E.; Ammann, C.; Arblaster, J.; Washington, W. M.; Boyle, J. S.; Bruggemann, W. (2003) Contributions of anthropogenic and natural forcing to recent tropopause height changes. Science 301: 479-483.

Sarwar, G.; Corsi, R.; Kumura, Y.; Allen, D.; Weschler, C. J. (2002) Hydroxyl radicals in indoor environments. Atmos. Environ. 36: 3973-3988.

Sauer, F.; Schaefer, C.; Neeb, P.; Horie, O.; Moortgat, G. (1999) Formation of hydrogen peroxide in the ozonolysis of isoprene and simple alkenes. Atmos. Environ. 33: 229-241.

Sawyer, R. F.; Harley, R. A.; Cadle, S. H.; Norbeck, J. M.; Slott, R.; Bravo, H. A. (2000) Mobile sources critical review: 1998 NARSTO assessment. Atmos. Environ. 34: 2161-2181.

Saxena, P.; Hildemann, L. M.; McMurry, P. H.; Seinfeld, J. H. (1995) Organics alter hygroscopic behavior of atmospheric particles. J. Geophys. Res. [Atmos.] 100: 18,755-18,770.

Saylor, R. D. (1997) An estimate of the potential significance of heterogeneous loss to aerosols as an additional sink for hydroperoxy radicals in the troposphere. Atmos. Environ. 31: 3653-3658.

Scala, J. M.; Garstang, M.; Tao, W.-K.; Pickering, K. E.; Thompson, A. M.; Simpson, J.; Kirchhoff, V. W. J. H.; Browell, E. V.; Sachse, G. W.; Torres. A. L.; Gregory, G. L.; Rasmussen, R. W.; Khalil, M. A. K. (1990) Cloud draft structure and trace gas transport. J. Geophys. Res. 95: 17,015-17,030.

Schere, K. L.; Wayland, R. A. (1989) Development and evaluation of the regional oxidant model for the northeastern United States. In: Schneider, T.; Lee, S. D.; Wolters, G. J. R.; Grant, L. D., eds. Atmospheric ozone research and its policy implications: proceedings of the 3rd US-Dutch international symposium; May 1988; Nijmegen, The Netherlands. Amsterdam, The Netherlands: Elsevier Science Publishers; pp. 613-622. (Studies in environmental science 35).

Schere, K. L.; Wayland, R. A. (1989) EPA regional oxidant model (ROM2.0): evaluation on 1980 NEROS data bases. Research Triangle Park, NC: U.S. Environmental Protection Agency, Atmospheric Research and Exposure Assessment Laboratory; report no. EPA/600/3-89/057. Available from: NTIS, Springfield, VA; PB89-200828/HSU.

Schichtel, B. A.; Husar, R. B. (1998) Eastern U.S. transport climatology during average, high and low ozone days. Online paper 98-A884. Available: http://capita.wustl.edu/capita/CapitaReports (30 October 2003).

Schichtel, B. A.; Husar, R. B. (2001) Eastern North American transport climatology during high- and low-ozone days. Atmos. Environ. 35: 1029-1038.

Schneider, M.; Ballschmiter, K. (1999) C_3-C_{14}-alkyl nitrates in remote South Atlantic air. Chemosphere 38: 233-244.

Schneider, M.; Luxenhofer, O.; Deissler, A.; Ballschmiter, K. (1998) C_1-C_{15} alkyl nitrates, benzyl nitrate, and bifunctional nitrates: Measurements in California and South Atlantic air and global comparison using C_2Cl_4 and $CHBr_3$ as marker molecules. Environ. Sci. Technol. 32: 3055-3062.

Schubert, S. D.; Rood, R. B.; Pfaendtner, J. (1993) An assimilated dataset for earth science applications. Bull. Am. Meteorol. Soc. 74: 2331-2342.

Schultz, M. G.; Jacob, D. J.; Bradshaw, J. D.; Sandholm, S. T.; Dibb, J. E.; Talbot, R. W.; Singh, H. B. (2000) Chemical NO_x budget in the upper troposphere over the tropical South Pacific. J. Geophys. Res. 105: 6669-6679.

Schumann, U.; Schlager, H.; Arnold, F.; Ovarlez, J.; Kelder, H.; Hov, Ø.; Hayman, G.; Isaksen, I. S. A.; Staehelin, J.; Whitefield, P. D. (2000) Pollution from aircraft emissions in the North Atlantic flight corridor: overview on the POLINAT projects. J. Geophys. Res. 105(D3): 10.1029/1999JD900941.

Schutze, M.; Herrmann, H. (2002) Determination of phase transfer parameters for the uptake of HNO_3, N_2O_5 and O_3 on single aqueous drops. Phys. Chem. Chem. Phys. 4: 60-67.

Scudlark, J. R.; Russell, K. M.; Galloway, J. N.; Church, T. M.; Keene, W. C. (1998) Dissolved organic nitrogen in precipitation at the mid-Atlantic U.S. coast—methods evaluation and preliminary data. Atmos. Environ. 32: 1719-1728.

Seaman, N. L. (2000) Meteorological modeling for air quality assessments. Atmos. Environ. 34: 2231-2259.

Seila, R. L.; Lonneman, W. A.; Meeks, S. A. (1989) Determination of C_2 to C_{12} ambient air hydrocarbons in 39 U.S. cities from 1984 through 1986. Research Triangle Park, NC: U.S. Environmental Protection Agency, Atmospheric Research and Exposure Assessment Laboratory; report no. EPA/600/3-89/058.

Seinfeld, J. H. (1988) Ozone air quality models: a critical review. JAPCA 38: 616-645.

Seinfeld, J. H. (1989) Urban air pollution: state of the science. Science (Washington, DC) 243: 745-752.

Seinfeld, J. H.; Pandis, S. N. (1998) Atmospheric chemistry and physics: from air pollution to climate change. New York, NY: John Wiley & Sons, Inc.

Senff, C. J.; Hardesty, R. M.; Alvarez, R. J., II; Mayor, S. D. (1998) Airborne lidar characterization of power plant plumes during the 1995 Southern Oxidants Study. J. Geophys. Res. [Atmos.] 103: 31,173-31,189.

Seo, K.-H.; Bowman, K. P. (2001) A climatology of isentropic cross-tropopause exchange. J. Geophys. Res. [Atmos.] 106: 28,159-28,172.

Seo, K.-H.; Bowman, K. P. (2002) Lagrangian estimate of global stratosphere-troposphere mass exchange. J. Geophys. Res. (Atmos.) 107(D21): 10.1029/2002JD002441.

Sexton, K. (1982) Evidence of an additive effect for small city plumes. Presented at: 75th annual meeting of the Air Pollution Control Association; June; New Orleans, LA. Pittsburgh, PA: Air Pollution Control Association; paper no. 82-31.4.

Sexton, K.; Westberg, H. (1980) Elevated ozone concentrations measured downwind of the Chicago-Gary urban complex. J. Air Pollut. Control Assoc. 30: 911-914.

Sexton, F. W.; Michie, R. A., Jr.; McElroy, F. F.; Thompson, V. L. (1981) Technical assistance document for the calibration and operation of automated ambient non-methane organic compound analyzers. Research Triangle Park, NC: U.S. Environmental Protection Agency, Environmental Monitoring Systems Laboratory; report no. EPA-600/4-81-015. Available from: NTIS, Springfield, VA; PB82-147406.

Sexton, F. W.; Michie, R. M., Jr.; McElroy, F. F.; Thompson, V. L. (1982) A comparative evaluation of seven automated ambient nonmethane organic compound analyzers. Research Triangle Park, NC: U.S. Environmental Protection Agency, Environmental Monitoring Systems Laboratory; report no. EPA-600/4-82-046. Available from: NTIS, Springfield, VA; PB82-230798.

Shafran, P. C.; Seaman, N. L.; Gayno, G. A. (2000) Evaluation of numerical predictions of boundary layer structure during the Lake Michigan ozone study. J. Appl. Meteorol. 39: 412-420.

Shapiro, R. (1977) Genetic effects of bisulfite (sulfur dioxide). Mutat. Res. 39: 149-175.

Shapiro, M. A. (1980) Turbulent mixing within tropopause folds as a mechanism for the exchange of chemical constituents between the stratosphere and troposphere. J. Atmos. Sci. 37: 994-1004.

Sharkey, T. D.; Singsaas, E. L.; Vanderveer, P. J.; Geron, C. D. (1996) Field measurements of isoprene emission from trees in response to temperature and light. Tree Physiol. 16: 649-654.

Shepson, P. B.; Edney, E. O.; Corse, E. W. (1984) Ring fragmentation reactions on the photooxidations of toluene and *o*-xylene. J. Phys. Chem. 88: 4122-4126.

Shepson, P. B.; Mackay, E.; Muthuramu, K. (1996) Henry's Law constants and removal processes for several atmospheric β-hydroxy alkyl nitrates. Environ. Sci. Technol. 30: 3618-3623.

Shetter, R. E.; Junkermann, W.; Swartz, W. H.; Frost, G. J.; Crawford, J. H.; Lefer, B. L.; Barrick, J. D.; Hall, S. R.; Hofzumahaus, A.; Bais, A.; Calvert, J. G.; Cantrell, C. A.; Madronich, S.; Müller, M.; Kraus, A.; Monks, P. S.; Edwards, G. D.; McKenzie, R.; Johnston, P.; Schmitt, R.; Griffioen, E.; Krol, M.; Kylling, A.; Dickerson, R. R.; Lloyd, S. A.; Martin, T.; Gardiner, B.; Mayer, B.; Pfister, G.; Roeth, E. P.; Koepke, P.; Ruggaber, A.; Schwander, H.; Van Weele, M. (2003) Photolysis frequency of NO_2: Measurement and modeling during the International Photolysis Frequency Measurement and Modeling intercomparison (IPMMI). J. Geophys. Res. (Atmos.) 108(D16): 10.1029/2002JD002932.

Sillman, S. (1995) The use of NO_y, H_2O_2 and HNO_3 as indicators for O_3-NO_x-ROG sensitivity in urban locations. J. Geophys. Res. 100: 14,175-14,188.

Sillman, S. (1999) The relation between ozone, NO_x and hydrocarbons in urban and polluted rural environments. Atmos. Environ. 33: 1821-1845.

Sillman, S. (2000) Ozone production efficiency and loss of NO_x in power plant plumes: photochemical model and interpretation of measurements in Tennessee. J. Geophys. Res. [Atmos.] 105: 9189-9202.

Sillman, S.; He, D.-Y. (2002) Some theoretical results concerning O_3-NO_x-VOC chemistry and NO_x-VOC indicators. J. Geophys. Res. (Atmos.) 107: 10.1029/2001JD001123.

Sillman, S.; Samson, P. J. (1995) Impact of temperature on oxidant photochemistry in urban, polluted rural and remote environments. J. Geophys. Res. [Atmos.] 100: 11,497-11,508.

Sillman, S.; Logan, J. A.; Wofsy, S. C. (1990) The sensitivity of ozone to nitrogen oxides and hydrocarbons in regional ozone episodes. J. Geophys. Res. [Atmos.] 95: 1837-1851.

Sillman, S.; Al-Wali, K. I.; Marsik, F. J.; Nowacki, P.; Samson, P. J.; Rodgers, M. O.; Garland, L. J.; Martinez, J. E.; Stoneking, C.; Imhoff, R.; Lee, J.-H.; Newman, L.; Weinstein-Lloyd, J.; Aneja, V. P. (1995) Photochemistry of ozone formation in Atlanta, GA–models and measurements. Atmos. Environ. 29: 3055-3066.

Sillman, S.; He, D.; Cardelino, C.; Imhoff, R. E. (1997) The use of photochemical indicators to evaluate ozone-NO_x-hydrocarbon sensitivity: case studies from Atlanta, New York, and Los Angeles. J. Air Waste Manage. Assoc. 47: 1030-1040.

Sillman, S.; He, D.; Pippin, M. R.; Daum, P. H.; Imre, D. G.; Kleinman, L. I.; Lee, J. H.; Weinstein-Lloyd, J. (1998) Model correlations for ozone, reactive nitrogen, and peroxides for Nashville in comparison with measurements: implications for O_3-NO_x-hydrocarbon chemistry. J. Geophys. Res. [Atmos.] 103: 22,629-22,644.

Sillman, S.; Vautard, R.; Menut, L.; Kley, D. (2003) O_3-NO_x-VOC sensitivity and NO_x-VOC indicators in Paris: results from models and atmospheric pollution over the Paris area (ESQUIF) measurements. J. Geophys. Res. (Atmos.) 108: 10.1029/2002JD001561.

Singh, H. B.; Ludwig, F. L.; Johnson, W. B. (1977) Ozone in clean remote atmospheres: concentrations and variabilities. New York, NY: Coordinating Research Council, Inc.; report no. CRC-APRAC CAPA-15-76. Available from: NTIS, Springfield, VA; PB-272290.

Singh, H. B.; Viezee, W.; Johnson, W. B.; Ludwig, F. L. (1980) The impact of stratospheric ozone on tropospheric air quality. J. Air Pollut. Control Assoc. 30: 1009-1017.

Singh, H. B.; Kanakidou, M.; Crutzen, P. J.; Jacob, D. J. (1995) High concentrations and photochemical fate of oxygenated hydrocarbons in the global troposphere. Nature (London) 378: 50-54.

Singh, H. B.; Gregory, G. L.; Anderson, B.; Browell, E.; Sachse, G. W.; Davis, D. D.; Crawford, J.; Bradshaw, J. D.; Talbot, R.; Blake, D. R.; Thornton, D.; Newell, R.; Merrill, J. (1996a) Low ozone in the marine boundary layer of the tropical Pacific Ocean: photochemical loss, chlorine atoms, and entrainment. J. Geophys. Res. [Atmos.] 101: 1907-1917.

Singh, H. B.; Herlth, D.; Kolyer, R.; Salas, L.; Bradshaw, J. D.; Sandholm, S. T.; Davis, D. D.; Crawford, J.; Kondo, Y.; Koike, M.; Talbot, R.; Gregory, G. L.; Sachse, G. W.; Browell, E.; Blake, D. R.; Rowland, F. S.; Newell, R.; Merrill, J.; Heikes, B.; Liu, S. C.; Crutzen, P. J.; Kanakidou, M. (1996b) Reactive nitrogen and ozone over the western Pacific: distribution, partitioning, and sources. J. Geophys. Res. 101: 1793-1808.

Singh, M. P.; McNider, R. T.; Meyers, R.; Shekhar, G. (1997) Nocturnal wind structure and dispersion of pollutants: an analytical study. Atmos. Environ. 31: 105-115.

Singh, H. B.; Salas, L. J.; Chatfield, R. B.; Czech, E.; Fried, A.; Walega, J.; Evans, M. J.; Field, B. D.; Jacob, D. J.; Blake, D.; Heikes, B.; Talbot, R.; Sachse, G.; Crawford, J. H.; Avery, M. A.; Sandholm, S.; Fuelberg, H. (2004) Analysis of the atmospheric distribution, sources, and sinks of oxygenated volatile organic chemicals based on measurements over the Pacific during TRACE-P. J. Geophys. Res. (Atmos.) 109(D15S07): 10.1029/2003JD003883.

Sirju, A. P.; Shepson, P. B. (1995) Laboratory and field investigation of the DNPH cartridge technique for the measurement of atmospheric carbonyl compounds. Environ. Sci. Technol. 29: 384-392.

Skiba, U. ; Fowler, D.; Smith, K.A. (1997) Nitric oxide emissions from agricultural soils in temperate and tropical climates: sources, controls and mitigation options. Nutrient Cycling Agroecosystems. 48 (1-2): 139-153.

Slemr, F.; Seiler, W. (1984) Field measurements of NO and NO_2 emissions from fertilized and unfertilized soils. J. Atmos. Chem. 2: 1-24.

Slemr, J.; Slemr, F.; Partridge, R.; D'Souza, H.; Schmidbauer, N. (2002) Accurate Measuements of Hydrocarbons in the Atmosphere (AMOHA): three European intercomparisons. J. Geophys. Res. [Atmos.] 107(D19): 10.1020/2001JD001357.

Smith, F.; Strong, R. (1977) Independent performance audits on rams station sensors - audit #4. interim report. Research Triangle Park, NC: Research Triangle Institute; EPA contract no. 68-02-2407.

Smith, A. M.; Rigler, E.; Kwok, E. S. C.; Atkinson, R. (1996) Kinetics and products of the gas-phase reactions of 6-methyl-5-hepten-2-one and *trans*-cinnamaldehyde with OH and NO_3 radicals and O_3 at 29672K. Environ. Sci. Technol. 30: 1781-1785.

Smith, D. F.; McIver, C. D.; Kleindienst, T. E. (1998) Primary product distribution from the reaction of hydroxyl radicals with toluene at ppb NO_x mixing ratios. J. Atmos. Chem. 30: 209-228.

Smith, D. F.; Kleindienst, T. E.; McIver, C. D. (1999) Primary product distributions from the reaction of OH with *m*-, *p*-xylene, 1,2,4- and 1,3,5-trimethylbenzene. J. Atmos. Chem. 34: 339-364.

Spicer, C. W.; Chapman, E. G.; Finlayson-Pitts, B. J.; Plastridge, R. A.; Hubbe, J. M.; Fast, J. D.; Berkowitz, C. M. (1998) Unexpectedly high concentrations of molecular chlorine in coastal air (letter). Nature (London) 394: 353-356.

Spicer, C. W.; Billick, I. H.; Yanagisawa, Y. (2001) Nitrous acid interference with passive NO_2 measurement methods and the impact on indoor NO_2 data. Indoor Air 11: 156-161.

Spivakovsky, C. M.; Logan, J. A.; Montzka, S. A.; Balkanski, Y. J.; Foreman-Fowler, M.; Jones, D. B. A.; Horowitz, L. W.; Fusco, A. C.; Brenninkmeijer, C. A. M.; Prather, M. J.; Wofsy, S. C.; McElroy, M. B. (2000) Three-dimensional climatological distribution of tropospheric OH: update and evaluation. J. Geophys. Res. (Atmos.) 105: 8931-8980.

Spokes, L. J.; Yeatman, S. G.; Cornell, S. E.; Jickells, T. D. (2000) Nitrogen deposition to the eastern Atlantic Ocean, the importance of south-easterly flow. Tellus Ser. B 52B: 37-49.

Sprenger, M.; Wernli, H. (2003) A northern hemispheric climatology of cross-tropopause exchange for the ERA 15 time period (1979-1993). J. Geophys. Res. 108(D12): 10.1029/2002JD002636.

Sprenger, M.; Maspoli, M. C.; Wernli, H. (2003) Tropopause folds and cross-tropopause exchange: a global investigation based upon ECMWF analyses for the time period March 2000 to February 2001. J. Geophys. Res. (Atmos.) 108(D12): 10.1029/2002JD002587.

Sprengnether, M.; Demerjian, K. L.; Donahue, N. M.; Anderson, J. G. (2002) Product analysis of the OH oxidation of isoprene and 1,3-butadiene in the presence of NO J. Geophys. Res. (Atmos.) 107(D15): 10.1029/2001JD000716.

Sprung, D.; Jost, C.; Reiner, T.; Hansel, A.; Wisthaler, A. (2001) Acetone and acetonitrile in the tropical Indian ocean boundary layer and free troposphere: aircraft-based intercomparison of AP-CIMS and PTR-MS measurements. J. Geophys. Res. 106: 28,511-28,528.

Staffelbach, T.; Neftel, A.; Blatter, A.; Gut, A.; Fahrni, M.; Stähelin, J.; Prévôt, A.; Hering, A.; Lehning, M.; Neininger, B.; Bäumle, M.; Kok, G. L.; Dommen, J.; Hutterli, M.; Anklin, M. (1997) Photochemical oxidant formation over southern Switzerland 1. results from summer 1994. J. Geophys. Res. (Atmos.) 102: 23,345-23,362.

Staudt, A. C.; Jacob, D. J.; Ravetta, F.; Logan, J. A.; Bachiochi, D.; Krishnamurti, T. N.; Sandholm, S. T>; Ridley, B. A.; Singh, H. B.; Talbot, R. W. (2003) Sources and chemistry of nitrogen oxides over the tropical Pacific. J. Geophys. Res. (Atmos.) 108(8239): 10.1029/2002JD002139.

Stedman, D. H.; Bishop, G.; Peterson, J. E.; Guenther, P. L. (1991) On-road CO remote sensing in the Los Angeles Basin: final report. Sacramento, CA: California Air Resources Board, ARB Contract No. A932-189.

Stehr, J. W.; Dickerson, R. R.; Hallock-Waters, K. A.; Doddridge, B. G.; Kirk, D. (2000) Observations of NO_y , CO, and SO_2 and the origin of reactive nitrogen J. Geophys. Res. 105(D3): 3553-3563.

Stein, A. F.; Lamb, D. (2002) Chemical indicators of sulfate sensitivity to nitrogen oxides an volatile organic compounds. J. Geophys. Res. (Atmos.) 107: 10.1029/2001JD001088.

Stein, A. F.; Lamb, D. (2003) Empirical evidence for the low- and high-NO_x photochemical regimes of sulfate and nitrate formation. Atmos. Environ. 37: 3615-3625.

Stein, A. F.; Lamb, D.; Draxler, R. R. (2000) Incorporation of detailed chemistry into a three-dimensional Lagrangian-Eulerian hybrid model: application to regional tropospheric ozone. Atmos. Environ. 34: 4361-4372.

Stenchikov, G.; Dickerson, R.; Pickering, K.; Ellis, W. Jr.; Doddridge, B.; Kondragunta, S.; Poulida, O.; Scala, J.; Tao, W.-K. (1996) Stratosphere-troposphere exchange in a midlatitude mesoscale convective complex. 2. Numerical simulation. J. Geophys. Res. [Atmos.] 101: 6837-6851.

Stevens, R. K.; Drago, R. J.; Mamane, Y. (1993) A long path differential optical absorption spectrometer and EPA-approved fixed-point methods intercomparison. Atmos. Environ. Part B 27: 231-236.

Steyn, D. J.; Bottenheim, J. W.; Thomson, R. B. (1997) Overview of tropospheric ozone in the Lower Fraser Valley, and the Pacific '93 field study. Atmos. Environ. 31: 2025-2036.

Stith, J.; Dye, J.; Ridley, B.; Laroche, P.; Defer, E.; Baumann, K.; Hübler, G.; Zerr, R.; Venticinque, M. (1999) NO signatures from lightning flashes. J. Geophys. Res. [Atmos.] 101: 6837-6851.

Stockwell, W. R.; Middleton, P.; Chang, J. S.; Tang, X. (1990) The second generation Regional Acid Deposition Model chemical mechanism for regional air quality modeling. J. Geophys. Res. [Atmos.] 95: 16,343-16,367.

Stockwell, W. R.; Kirchner, F.; Kuhn, M.; Seefeld, S. (1997) A new mechanism for regional atmospheric chemistry modeling. J. Geophys. Res. 102(D22): 25847-25879.

Stohl, A. (2001) A 1-year Lagrangian "climatology" of airstreams in the Northern Hemisphere troposphere and lowermost stratosphere. J. Geophys. Res. (Atmos.) 106: 7263-7279.

Stohl, A.; Trickl, T. (1999) A textbook example of long-range transport: simultaneous observation of ozone maxima of stratospheric and North American origin in the free troposphere of Europe. J. Geophys. Res. 104(D23): 30,445-30,462.

Stohl, A.; Spichtinger-Rakowsky, N.; Bonasoni, P.; Feldmann, H.; Memmesheimer, M.; Scheel, H. E.; Trickly, T.; Hübener, S.; Ringer, W.; Mandl, M. (2000) The influence of stratospheric intrusions on alpine ozone concentrations. Atmos. Environ. 34: 1323-1354.

Stohl, A.; Trainer, M.; Ryerson, T. B.; Holloway, J. S.; Parrish, D. D. (2002) Export of NO_y from the North American boundary layer during 1996 and 1997 North Atlantic Regional Experiments. J. Geophys. Res. 107(D11): 10.1029/2001JD000519.

Stohl, A.; Bonasoni, P.; Cristofanelli, P.; Collins, W.; Feichter, J.; Frank, A.; Forster, C.; Gerasopoulos, E.; Gäggeler, H.; James, P.; Kentarchos, T.; Kromp-Kolb, H.; Krüger, B.; Land, C.; Meloen, J.; Papayannis, A.; Priller, A.; Seibert, P.; Sprenger, M.; Roelofs, G. J.; Scheel, H. E.; Schnabel, C.; Siegmund, P.; Tobler, L.; Trickl, T.; Wernli, H.; Wirth, V.; Zanis, P.; Zerefos, C. (2003) Stratosphere-troposphere exchange: a review and what we have learned from STACCATO. J. Geophys. Res. 108(D12): 10.1029/2002JD002490.

Stroud, C.; Madronich, S.; Atlas, E.; Ridley, B.; Flocke, F.; Weinheimer, A.; Talbot, B.; Fried, A.; Wert, B.; Shetter, R.; Lefer, B.; Coffey, M.; Heikes, B.; Blake, D. (2003) Photochemistry in the arctic free troposphere: NO_x budget and the role of odd nitrogen reservoir recycling. Atmos. Environ. 37: 3351-3364.

Stull, R. B. (1985) A fair-weather cumulus cloud classification scheme for mixed layer studies. J. Clim. Appl. Meteorol. 24: 49-56.

Stull, R. B. (1988) An introduction to boundary layer meteorology. Dordrecht, The Netherlands: Kluwer Academic Publishers, pp. 9-16; 499-506. (Atmospheric Sciences Library, v. 13).

Stull, R.B. (1999) An introduction to boundary layer meteorology. Dordrecht, The Netherlands: Kluwer Academic Publishers; pp. 9-15, 500-505.

Stull, R. B. (2000) Meteorology for scientists and engineers: a technical companion book to C. Donald Ahrens' Meteorology Today. 2nd ed. New York, NY: Brooks Cole.
Sturges, W. T.; Barrie, L. A. (1988) Chlorine Bromine and Iodine in Arctic aerosols. Atmos. Environ. 22: 1179-1194.
Stutz, J.; Platt, U. (1996) Numerical analysis and estimation of the statistical error of differential optical absorption spectroscopy measurements with least-squares methods. Appl. Opt. 35: 6041-6053.
Stutz, J.; Hebestreit, K.; Alicke, B.; Platt, U. (1999) Chemistry of halogen ozides in the troposphere: comparison of model calculations with recent field data. J. Atmos. Chem. 34: 65-85.
Stutz, J.; Ackermann, R.; Fast, J. D.; Barrie, L. (2002) Atmospheric reactive chlorine and bromine at the Great Salt Lake, Utah. Geophys. Res. Lett. 29: 10.1029/2002GL014812.
Suhre, K.; Cammas, J.-P.; Nédelec, P.; Rosset, R.; Marenco, A.; Smit, H. G. J. (1997) Ozone-rich transients in the upper equatorial Atlantic troposphere (letter). Nature 388: 661-663.
Sundet, J. K. (1997) Model studies with a 3-D global CTM using ECMWF data [thesis]. Oslo, Norway: University of Oslo, Department of Geophysics.
Svensson, R.; Ljungstroem, E.; Lindqvist, O. (1987) Kinetics of the reaction between nitrogen dioxide and water vapour. Atmos. Environ. 21: 1529-1539.
Talbot, R. W.; Vijgen, A. S.; Harris, R. C. (1990) Measuring tropospheric HNO_3: problems and prospects for nylon filter and mist chamber. J. Geophys. Res. [Atmos.] 95: 7553-7542.
Tan, D.; Faloona, I.; Simpas, J. B.; Brune, W.; Shepson, P. B.; Couch, T. L.; Sumner, A. L.; Carroll, M. A.; Thornberry, T.; Apel, E.; Riemer, D.; Stockwell, W. (2001) HO_x budgets in a deciduous forest: results from the PROPHET summer 1998 campaign. J. Geophys. Res. (Atmos.) 106: 24,407-24,427.
Tanaka, P. L.; Oldfield, S.; Neece, J. D.; Mullins, C. B.; Allen, D. T. (2000) Anthropogenic sources of chlorine and ozone formation in urban atmospheres. Environ. Sci. Technol. 34: 4470-4473.
Tanaka, P. L.; Riemer, D. D.; Chang, S.; Yarwood, G.; McDonald-Buller, E. C.; Apel, E. C.; Orlando, J. J.; Silva, P. J.; Jimenez, J. L.; Canagaratna, M. R.; Neece, J. D.; Mullins, C. B.; Allen, D. T. (2003a) Direct evidence for chlorine-enhanced urban ozone formation in Houston, Texas. Atmos. Environ. 37: 1393-1400.
Tanaka, P. L.; McDonald-Buller, E. C.; Chang, S.; Yarwood, G.; Kimura, Y.; Neece, J. D.; Mullins, C. B.; Allen, D. T. (2003b) Development of a chlorine mechanism for use in the Carbon Bond IV chemistry model. J. Geophys. Res. [Atmos.] 108(D4): art. no. 4145.
Tanner, R. L.; Kelly, T. J.; Dezaro, D. A.; Forrest, J. (1989) A comparison of filter, denuder, and real-time chemiluminescence techniques for nitric acid determination in ambient air. Atmos. Environ. 23: 2213-2222.
Tao, W.-K.; Simpson, J. (1993) The Goddard Cumulus Ensemble Model. Part I: model description. Terr. Atmos. Oceanic Sci. (TAO) 4: 35-71.
Taubman, B. F.; Marufu, L. T.; Piety, C. A.; Doddridge, B. G.; Stehr, J. W.; Dickerson, R. R. (2004) Airborne characterization of the chemical, optical, and meteorological properties, and origins of a combined ozone-haze episode over the eastern United States. J. Atmos. Sci. 61: 1781-1793.
Tesche, T. W.; Roth, P. M.; Reynolds, S. D.; Lurmann, F. W. (1993) Scientific assessment of the urban airshed model (UAM-IV). Washington, DC: American Petroleum Institute; API publication no. 4556.
Thielman, A.; Prévôt, A. S. H.; Grüebler, F. C.; Staelhelin, J. (2001) Empirical ozone isopleths as a tool to identify ozone production regimes. Geophys. Res. Lett. 28: 2369-2372.
Thielman, A.; Prévôt, A. S. H.; Staelhelin, J. (2002) Sensitivity of ozone production derived from field measurements in the Italian Po basin. J. Geophys. Res. (Atmos.) 107(D22): 10.1029/2000JD000119.
Thompson, A. M. (1992) The oxidizing capacity of the Earth's atmosphere: probable past and future changes. Science (Washington, DC) 256: 1157-1165.
Thompson, A. M.; Stewart, R. W. (1991) Effect of chemical kinetics uncertainties on calculated constituents in a tropospheric photochemical model. J. Geophys. Res. 96(D7): 13,089-13,108.
Thompson, A. M.; Pickering, K. E.; Dickerson, R. R.; Ellis, W. G., Jr.; Jacob, D. J.; Scala, J. R.; Tao, W.-K.; McNamara, D. P.; Simpson, J. (1994) Convective-transport over the central United States and its role in regional CO and O_3 budgets. J. Geophys. Res. [Atmos.] 99: 18,703-18,711.
Thompson, A. M.; Singh, H. B.; Schlager, H. (2000) Subsonic assessment ozone and nitrogen oxide experiment (SONEX) and pollution from aircraft emissions in the North Atlantic Flight Corridor (POLINAT 2). J. Geophys. Res. 105: 3595-3603.
Thornton, J. A.; Wooldridge, P. J.; Cohen, R. C. (2000) Atmospheric NO_2: in situ laser-induced fluorescence detection at parts per trillion mixing ratios. Anal. Chem. 72: 528-539.
Thornton, J. A.; Braban, C. F.; Abbatt, J. P. D. (2003) N_2O_5 hydrolysis on sub-micron organic aerosol: the effect of relative humidity, particle phase and particle size. Phys. Chem. Chem. Phys. 5: 4593-4603.

Tie, X. X.; Emmons, L.; Horowitz, L.; Brasseur, G.; Ridley, ,B.; Atlas, E.; Stround, C.; Hess, P.; Klonecki, A.; Madronich, S.; Talbot, R.; Dibb, J. (2003) Effect of sulfate aerosol on tropospheric NO_x and ozone budgets: model simulations and TOPSE evidence. J. Geophys. Res. (Atmos.) 108(D4): 10.1029/2001JD001508.
Tonnesen, G. S.; Dennis, R. L. (2000a) Analysis of radical propagation efficiency to assess ozone sensitivity to hydrocarbons and NO_x 1. Local indicators of odd oxygen production sensitivity. J. Geophys. Res. (Atmos.) 105: 9213-9225.
Tonnesen, G. S.; Dennis, R. L. (2000b) Analysis of radical propagation efficiency to assess ozone sensitivity to hydrocarbons and NO_x 2. Long-lived species as indicators of ozone concentration sensitivity. J. Geophys. Res. 105: 9227-9241.
Trainer, M.; Buhr, M. P.; Curran, C. M.; Fehsenfeld, F. C.; Hsie, E. Y.; Liu, S. C.; Norton, R. B.; Parrish, D. D.; Williams, E. J.; Gandrud, B. W.; Ridley, B. A.; Shetter, J. D.; Allwine, E. J.; Westberg, H. H. (1991) Observations and modeling of the reactive nitrogen photochemistry at a rural site. J. Geophys. Res. [Atmos.] 96: 3045-3063.
Trainer, M.; Parrish, D. D.; Buhr, M. P.; Norton, R. B.; Fehsenfeld, F. C.; Anlauf, K. G.; Bottenheim, J. W.; Tang, Y. Z.; Wiebe, H. A.; Roberts, J. M.; Tanner, R. L.; Newman, L.; Bowersox, V. C.; Meagher, J. F.; Olszyna, K. J.; Rodgers, M. O.; Wang, T.; Berresheim, H.; Demerjian, K. L.; Roychowdhury, U. K. (1993) Correlation of ozone with NO_y in photochemically aged air. J. Geophys. Res. [Atmos.] 98: 2917-2925.
Trainer, M.; Ridley, B. A.; Buhr, M. P.; Kok, G.; Walega, J.; Hübler, G.; Parrish, D. D.; Fehsenfeld, F. C. (1995) Regional ozone and urban plumes in the southeastern United States: Birmingham, a case study. J. Geophys. Res. [Atmos.] 100: 18,823-18,834.
Trainer, M.; Parrish, D. D.; Golday, P. D.; Roberts, J.; Fehsenfeld, F. C. (2000) Review of observation-based analysis of the regional factors influencing ozone concentrations. Atmos. Environ. 34: 2045-2061.
Traub, M.; Fischer, H.; De Reus, M.; Kormann, R.; Heland, J.; Ziereis, H.; Schlager, H.; Holzinger, R.; Williams, J.; Warneke, C.; De Gouw, J.; Lelieveld, J. (2003) Chemical characteristics assigned to trajectory clusters during the MINOS campaign. Atmos. Chem. Phys. 3: 459-468.
Tseng, R.-S.; Viechnicki, J. T.; Skop, R. A.; Brown, J. W. (1992) Sea-to-air transfer of surface-active organic compounds by bursting bubbles. J. Geophys. Res. (Atmos.) 97: 5201-5206.
Tuazon, E. C.; MacLeod, H.; Atkinson, R.; Carter, W. P. L. (1986) α-Dicarbonyl yields from the NO_x–air photooxidations of a series of aromatic hydrocarbons in air. Environ. Sci. Technol. 20: 383-387.
Tully, F. P.; Ravishankara, A. R.; Thompson, R. L.; Nicovich, J. M.; Shah, R. C.; Kreutter, N. M.; Wine, P. H. (1981) Kinetics of the reactions of hydroxyl radical with benzene and toluene. J. Phys. Chem. 85: 2262-2269.
Turekian, V. C.; Macko, S. A.; Keene, W. C. (2003) Concentrations, isotopic compositions, and sources of size-resolved, particulate organic carbon and oxalate in near-surface marine air at Bermuda during spring. J. Geophys. Res. (Atmos.) 108(D5): 10.1029/2002JD002053.
U.S. Congress. (1990) Clean Air Act amendments of 1990, PL 101-549, November 15. Washington, DC: U.S. Government Printing Office.
U.S. Environmental Protection Agency. (1991) Guideline for regulatory application of the urban airshed model. Research Triangle Park, NC: Office of Air Quality Planning and Standards; report no. EPA-450/4-91-013. Available from: NTIS, Springfield, VA; PB92-108760/HSU.
U.S. Environmental Protection Agency. (1993a) Air quality criteria for oxides of nitrogen. Research Triangle Park, NC: Office of Health and Environmental Assessment, Environmental Criteria and Assessment Office; report nos. EPA/600/8-91/049aF-cF. 3v. Available from: NTIS, Springfield, VA; PB95-124533, PB95-124525, and PB95-124517.
U.S. Environmental Protection Agency. (1993) Regional interim emission inventories (1987-1991), v. II: emission summaries. Research Triangle Park, NC: Office of Air Quality Planning and Standards; report no. EPA-454/R-93-021b. Available from: NTIS, Springfield, VA; PB93-236115.
U.S. Environmental Protection Agency. (1996) Air quality criteria for ozone and related photochemical oxidants, v. I-III. Research Triangle Park, NC: Office of Research and Development; report no. EPA/600/P-93/004aF-cF. Available from: NTIS, Springfield, VA; PB96-185582. PB96-185590, and PB96-185608. Available: www.epa.gov/ncea/ozone.htm [25 February 2002].
U.S. Environmental Protection Agency. (1997) National air pollutant emission trends 1990-1996. Research Triangle Park, NC: Office of Air Quality Planning and Standards; report no. EPA/454/R-97/011. Available from: NTIS, Springfield, VA.
U.S. Environmental Protection Agency (1999).

U.S. Environmental Protection Agency. (2000) Air quality criteria for carbon monoxide. Research Triangle Park, NC: National Center for Environmental Assessment; report no. EPA/600/P-99/001F. Available: http://www.epa.gov/ncea/pdfs/coaqcd.pdf (7 May 2003).
U.S. Environmental Protection Agency. (2001) National air quality and emissions trends report, 1999. Research Triangle Park, NC: Office of Air Quality Planning and Standards; report no. EPA 454/R-01-004. Available: http://www.epa.gov/oar/aqtrnd99/ [7 May 2003].
U.S. Environmental Protection Agency. (2003) Air quality criteria for ozone and related photochemical oxidants. Research Triangle Park, NC: Office of Research and Development: manuscript in preparation.
Underwood, G. M.; Song, C. H.; Phadnis, M.; Carmichael, G. R.; Grassian, V. H. (2001) Heterogeneous reactions of NO_2 and HNO_3 on oxides and mineral dust: a combined laboratory and modeling study. J. Geophys. Res. [Atmos.] 106: 18,055-18,066.
Usher, C. R.; Michel, A. E.; Stec, D.; Grassian, V. H. (2003) Laboratory studies of ozone uptake on processed mineral dust. Atmos. Environ. 37: 5337-5347.
Valente, R. J.; Imhoff, R. E.; Tanner, R. L.; Meagher, J. F.; Daum, P. H.; Hardesty, R. M.; Banta, R. M.; Alvarez, R. J.; McNider, R. T.; Gillani, N. V. (1998) Ozone production during an urban air stagnation episode over Nashville, Tennessee. J. Geophys. Res. [Atmos.] 103: 22,555-22,568.
Van Aardenne, J. A.; Dentener, F. J.; Olivier, J. G. J.; Goldewijk, C. G. M. K.; Lelieveld, J. (2001) A 1 ° x 1° resolution data set of historical anthropogenic trace gas emissions for the period 1980-1990. Glob. Biogeochem. Cycles 15: 909-928.
Vandaele, A. C.; Tsouli, A.; Carleer, M.; Colin, R. (2002) UV Fourier transform measurements of tropospheric O_3, NO_2, SO_2, benzene, and toluene. Environ. Pollut. 116: 193-201.
Vaughan, W. M.; Chan, M.; Cantrell, B.; Pooler, F. (1982) A study of persistent elevated pollution episodes in the northeastern United States. Bull. Am. Meteorol. Soc. 63: 258-266.
Vautard, R.; Martin, D.; Beekman, M.; Drobinski, P.; Friedrich, R.; Jaubertie, A.; Kley, D.; Lattuati, M.; Moral, P.; Neininger, B.; Theloke, J. (2002) Paris emission inventory diagnostics from the ESQUIF airborne measurements and a chemistry transport model. J. Geophys. Res. (Atmos.) 108(D17): 10.1029/2002JD002797.
Viezee, W.; Johnson, W. B.; Singh, H. B. (1979) Airborne measurements of stratospheric ozone intrusions into the troposphere over the United States [final report]. Menlo Park, CA: SRI International; SRI project 6690.
Viezee, W.; Singh, H. B. (1982) Contribution of stratospheric ozone to ground-level ozone concentrations - a scientific review of existing evidence. Research Triangle Park, NC: U.S. Environmental Protection Agency, Environmental Science Research Laboratory; grant CR-809330010.
Vogt, R.; Crutzen, P. J.; Sander, R. (1996) A mechanism for halogen release from sea-salt aerosol in the remote marine boundary layer. Nature 383: 327-330.
Vogt, R.; Sander, R.; Von Glasow, R.; Crutzen, P. J. (1999) Iodine chemistry and its role in halogen activation and ozone loss in the marine boundary layer: a model study. J. Atmos. Chem. 32: 375-395.
Volz-Thomas, A.; Geiss, H.; Hofzumahaus, A.; Becker, K.-H. (2003) Introduction to special section: photochemistry experiment in BERLIOZ. J. Geophys. Res. [Atmos.] 108(D4): 10.1029/JD002029.
Von Glasow, R.; Sander, R.; Bott, A.; Crutzen, P. J. (2002a) Modeling halogen chemistry in the marine boundary layer. 1. Cloud-free MBL. J. Geophys. Res. 107(D17): 10.1029/2001JD000942.
Von Glasow, Sander, R.; Bott, A.; Crutzen, P. J. (2002b) Modeling halogen chemistry in the marine boundary layer. 2. Interactions with sulfur and cloud-covered MBL. J. Geophys. Res. 107(D17): 10.1029/2001JD000943.
Vuilleumier, L.; Bamer, J. T.; Harley, R. A.; Brown, N. J. (2001) Evaluation of nitrogen dioxide photolysis rates in an urban area using data from the 1997 Southern California Ozone Study. Atmos. Environ. 35: 6525-6537.
Vukovich, F. M. (1995) Regional-scale boundary layer ozone variations in the eastern United States and their association with meteorological variations. Atmos. Environ. 29: 2259-2273.
Vukovich, F. M. (1997) Time scales of surface ozone variations in the regional, non-urban environment. Atmos. Environ. 31:1513-1530.
Vukovich, R. M.; Ching, J. K. S. (1990) A semi-impirical approach to estimate vertical transport by nonprecipitating convective clouds on a regional scale. Atmos. Environ. 24A: 2153-2168.
Vukovich, F. M.; Bach, W. D., Jr.; Crissman, B. W.; King, W. J. (1977) On the relationship between high ozone in the rural surface layer and high pressure systems. Atmos. Environ. 11: 967-983.
Wagner, T.; Platt, U. (1998) Satellite mapping of enhanced BrO concentrations in the troposphere. Nature (London) 395: 486-490.
Wagner, V.; Jenkin, M. E.; Saunders, S. M.; Stanton, K.; Wirtz, M.; Pilling, J. (2003) Modelling of the photooxidation of toluene: conceptual ideas for validating detailed mechanisms. Atmos. Chem. Phys. 3: 89-106.

Wahner, A.; Mentel, T. F.; Sohn, M.; Stier, J. (1998) Heterogeneous reaction of N_2O_5 on sodium nitrate aerosol. J. Geophys. Res. (Atmos.) 103: 31,103-31,112.

Wainman, T.; Zhang, J.; Weschler, C. J.; Lioy, P. J. (2000) Ozone and limonene in indoor air: a source of submicron particle exposure. Environ. Health Perspect. 108: 1139-1145.

Walcek, C. J.; Taylor, G. R. (1986) A theoretical method for computing vertical distributions of acidity and sulfate production within cumulus clouds. J. Atmos. Sci. 43: 339-355.

Walcek, C. J.; Stockwell, W. R.; Chang, J. S. (1990) Theoretical estimates of the dynamic, radiative and chemical effects of clouds on tropospheric trace gases. Atmos. Res. 25: 53-69.

Walega, J. G.; Stedman, D. H.; Shetter, R. E.; Mackay, G. I.; Iguchi, T.; Schiff, H. I. (1984) Comparison of a chemiluminescent and a tunable diode laser absorption technique for the measurement of nitrogen oxide, nitrogen dioxide, and nitric acid. Environ. Sci. Technol. 18: 823-826.

Wang, Y.; Tao, W.-K.; Pickering, K. E.; Thompson, A. M.; Kain, J. S.; Adler, R. F.; Simpson, J.; Keehn, P. R.; Lai, G. S. (1996) Mesoscale model simulations of TRACE A and preliminary regional experiment for storm-scale operational and research meteorology convective systems and associated tracer transport. J. Geophys. Res. [Atmos.] 101: 24,013-24,027.

Wang, Y.; DeSilva, A. W.; Goldenbaum, G. C.; Dickerson, R. R. (1998) Nitric oxide production by simulated lightning: dependence on current, energy, and pressure. J. Geophys. Res. [Atmos.] 103: 19,149-19,159.

Wang, Y.; Logan, J. A.; Jacob, D. J. (1998) Global simulation of tropospheric O_3-NO_x-hydrocarbon chemistry, 2. Model evaluation and global ozone budget. J. Geophys. Res. (Atmos.) 103: 10,727-10,755.

Wang, L. H.; Milford, J. B.; Carter, W. P. L. (2000a) Reactivity estimates for aromatic compounds. Part I: uncertainty in chamber-derived parameters. Atmos. Environ. 34: 4337-4348.

Wang, L. H.; Milford, J. B.; Carter, W. P. L. (2000b) Reactivity estimates for aromatic compounds. Part 2. uncertainty in incremental reactivities. Atmos. Environ. 4349-4360.

Warneke, C.; Van Der Veen, C.; Luxembourg, S.; De Gouw, J. A.; Kok, A. (2001) Measurements of benzene and toluene in ambient air using proton-transfer-reaction mass spectrometry: calibration, humidity dependence, and field intercomparison. Int. J. Mass Spectrom. 207: 167-182.

Watson, J. G.; Chow, J. C.; Fujita, E. M. (2001) Review of volatile organic compound source apportionment by chemical mass balance. Atmos. Environ. 35: 1567-1584.

Wayne, R. P. (2000) Chemistry of Atmospheres: an introduction to the chemistry of the atmospheres of Earth, the planets, and their satellites. 3rd ed. New York, NY: Oxford University Press, Inc.

Wayne, R. P.; Barnes, I.; Biggs, P.; Burrows, J. P.; Canosa-Mas, C. E.; Hjorth, J.; Le Bras, G.; Moortgat, G. K.; Perner, D.; Poulet, G.; Restelli, G.; Sidebottom, H. (1991) The nitrate radical: physics, chemistry, and the atmosphere. Atmos. Environ. Part A 25: 1-203.

Wingenter, O. W.; Kubo, M. K.; Blake, N. J.; Smith, T. W., Jr.; Blake, D. R.; Rowland, F. S. (1996) Hydrocarbon and halocarbon measurements as photochemical and dynamical indicators of atmospheric hydroxyl, atomic chlorine, and vertical mixing obtained during Langrangian flights. J. Geophys. Res. (Atmos.) 101(D1): 4331-4340.

Wingenter, O. W.; Blake, D. R.; Blake, N. J.; Sive, B. C.; Rowland, F. S.; Atlas, E.; Flocke, F. (1999) Tropospheric hydroxyl and atomic chlorine concentrations, and mixing timescales determined from hydrocarbon and halocarbon measurements made over the Southern Ocean. J. Geophys. Res. (Atmos.) 104(D17): 21819-21828.

Wennberg, P. O.; Cohen, R. C.; Stimpfle, R. M.; Koplow, J. P.; Anderson, J. G.; Salawitch, R. J.; Fahey, D. W.; Woodbridge, E. L.; Keim, E. R.; Geo, R. S.; Webster, C. R.; May, R. D.; Toohey, D. W.; Avallone, L. M.; Proffitt, M. H.; Loewenstein, M.; Podolske, J. R.; Chan, K. R.; Wofsy, S. C. (1994) Removal of stratospheric O_3 by radicals - in situ measurements of OH, HO_2, NO, NO_2, CLO, and BRO. Science 266: 398-404.

Wennberg, P. O.; Hanisco, T. F.; Jaeglé, L.; Jacob, D. J.; Hintsa, E. J.; Lanzendorf, E. J.; Anderson, J. G.; Gao, R.-S.; Keim, E. R.; Donnelly, S. G.; Del Negro, L. A.; Fahey, D. W.; McKeen, S. A.; Salawitch, R. J.; Webster, C. R.; May, R. D.; Herman, R. L.; Proffitt, M. H.; Margitan, J. J.; Atlas, E. L.; Schauffler, S. M.; Flocke, F.; McElroy, C. T.; Bui, T. P. (1998) Hydrogen radicals, nitrogen radicals, and the production of O_3 in the upper troposphere. Science (Washington, DC) 279: 49-53.

Wernli, H.; Bourqui, M. (2002) A Lagrangian "1-year climatology" of (deep) cross-tropopause exchange in the extratropical Northern Hemisphere. J. Geophys. Res. (Atmos.) 107(D1-D2): 10.1029/2001JD000812.

Wesely, M. L.; Hicks, B. B. (2000) A review of the current status of knowledge on dry deposition. Atmos. Environ. 34: 2261-2282.

Westberg, H.; Zimmerman, P. (1993) Analytical methods used to identify nonmethane organic compounds in ambient atmospheres. In: Newman, L., ed. Measurement challenges in atmospheric chemistry. Washington, DC: American Chemical Society, pp. 275-291.

Whitby, K. T. (1978) The physical characteristics of sulfur aerosols. Atmos. Environ. 12: 135-159.
Wild, O.; Prather, M. J. (2000) Excitation of the primary tropospheric chemical mode in a global CTM. J. Geophys. Res. (Atmos.) 105: 24,647-24,660.
Williams, E. J.; Guenther, A.; Fehsenfeld, F. C. (1992) An inventory of nitric oxide emissions from soils in the United States. J. Geophys. Res. [Atmos.] 97: 7511-7519.
Williams, J.; Roberts, J. M.; Fehsenfeld, F. C.; Bertman, S. B.; Buhr, M. P.; Goldan, P. D.; Hubler, G.; Kuster, W. C.; Ryerson, T. B.; Trainer, M.; Young, V. (1997) Regional ozone from biogenic hydrocarbons deduced from airborne measurements of PAN, PPN, and MPAN. Geophys. Res. Lett. 24: 1099-1102.
Williams, E. J.; Baumann, K.; Roberts, J. M.; Bertman, S. B.; Norton, R. B.; Fehsenfeld, F. C.; Springston, S. R.; Nunnermacker, L. J.; Newman, L.; Olszyna, K.; Meagher, J.; Hartsell, B.; Edgerton, E.; Pearson, J. R.; Rodgers, M. O. (1998) Intercomparison of ground-based NO_y measurement techniques. J. Geophys. Res. 103: 22,261-22,280.
Wimmers, A. J. (2003) (dissertation). Charlottesville, VA: University of Virginia, R. J. Reynolds Institute for Environmental Science.
Wimmers, A. J.; Moody, J. L. (2001) A fixed-layer estimation of upper-tropospheric specific humidity from the GOES water vapor channel: parameterization and validation of the altered brightness temperature product. J. Geophys. Res. [Atmos.] 106: 17,115-17,132.
Wimmers, A. J.; Moody, J. L. (2004a) Tropopause folding at satellite-observed spatial gradients: 1. Verification of an empirical relationship. J. Geophys. Res. [Atmos.] 109(D19306): 10.1029/2003JD004145.
Wimmers, A. J.; Moody, J. L. (2004b) Tropopause folding at satellite-observed spatial gradients: 2. Development of an empirical model. J. Geophys. Res. [Atmos.] 109(D19307): 10.1029/2003JD004146.
Wimmers, A. J.; Moody, J. L.; Browell, E. V.; Hair, J. W.; Grant, W. B.; Butler, C. F.; Fenn, M. A.; Schmidt, C. C.; Li, J.; Ridley, B. A. (2003) Signatures of tropopause folding in satellite imagery. J. Geophys. Res. (Atmos.) 108(D4): 10.1029/2001JD001358.
Winer, A. M.; Peters, J. W.; Smith, J. P.; Pitts, J. N., Jr. (1974) Response of commercial chemiluminescent NO-NO_2 analyzers to other nitrogen-containing compounds. Environ. Sci. Technol. 8: 1118-1121.
Winer, A. M.; Arey, J.; Atkinson, R.; Aschmann, S. M.; Long, W. D.; Morrison, C. L.; Olszyk, D. M. (1992) Emission rates of organics from vegetation in California's Central Valley. Atmos. Environ. Part A 26: 2647-2659.
Winner, D. A.; Cass, G. R. (2001) Modeling the long-term frequency distribution of regional ozone concentrations using synthetic meteorology. Environ. Sci. Technol. 35: 3718-3726.
Witter, M.; Berndt, T.; Böge, O.; Stratmann, F.; Heintzenberg, J. (2002) Gas-phase ozonolysis: rate coefficients for a series of terpenes and rate coefficients and OH yields for 2-methyl-2-butene and 2,3-dimethyl-2-butene. Int. J. Chem. Kinet. 34: 394-403.
Wolff, G. T. (1993) On a NO_x-focused control strategy to reduce O_3. J. Air Waste Manage. Assoc. 43: 1593-1596.
Wolff, G. T.; Korsog, P. E. (1992) Ozone control strategies based on the ratio of volatile organic compounds to nitrogen oxides. J. Air Waste Manage. Assoc. 42: 1173-1177.
Wolff, G. T.; Lioy, P. J. (1978) An empirical model for forecasting maximum daily ozone levels in the northeastern U.S. J. Air Pollut. Control Assoc. 28: 1034-1038.
Wolff, G. T.; Lioy, P. J. (1980) Development of an ozone river associated with synoptic scale episodes in the eastern United States. Environ. Sci. Technol. 14: 1257-1260.
Wolff, G. T.; Lioy, P. J.; Meyers, R. E.; Cederwall, R. T.; Wight, G. D.; Pasceri, R. E.; Taylor, R. S. (1977) Anatomy of two ozone transport episodes in the Washington, D.C., to Boston, Mass., corridor. Environ. Sci. Technol. 11: 506-510.
Wolff, G. T.; Lioy, P. J.; Wight, G. D.; Meyers, R. E.; Cederwall, R. T. (1977) An investigation of long-range transport of ozone across the midwestern and eastern United States. Atmos. Environ. 11: 797-802.
Wolff, G. T.; Lioy, P. J.; Wight, G. D.; Pasceri, R. E. (1977) Aerial investigation of the ozone plume phenomenon. J. Air Pollut. Control Assoc. 27: 460-463.
Wolff, G. T.; Lioy, P. J.; Wight, G. D.; Pasceri, R. E. (1977) Aerial investigation of photochemical oxidants over the northeast. In: Bufalini, J. J.; Lonneman, W. A., eds. Proceedings of symposium on 1975 northeast oxidant transport study; January 1976; Research Triangle Park, NC. Research Triangle Park, NC: U.S. Environmental Protection Agency, Environmental Sciences Research Laboratory; pp. 70-86; EPA report no. EPA-600/3-77-017. Available from: NTIS, Springfield, VA; PB-265370.
World Meteorological Organization. (1990) Scientific assessment of stratospheric ozone: 1989. Volume II. Appendix: AFEAS report. Geneva, Switzerland: Global Ozone Research Monitoring Project; report no. 20.
World Meteorological Organization. (1992) Scientific assessment of ozone depletion: 1991 [preprint]. Geneva, Switzerland: World Meteorological Organization; report no. 25.

Wright, E. S.; Vang, M. J.; Finkelstein, J. N.; Mavis, R. D. (1982) Changes in phospholipid biosynthetic enzymes in type II cells and alveolar macrophages isolated from rat lungs after NO_2 exposure. Toxicol. Appl. Pharmacol. 66: 305-311.

Wunderli, S.; Gehrig, R. (1991) Influence of temperature on formation and stability of surface PAN and ozone. A two year field study in Switzerland. Atmos. Environ. Part A 25: 1599-1608.

Yienger, J. J.; Levy, H., II. (1995) Empirical model of global soil-biogenic NO_x emissions. J. Geophys. Res. 100(D6): 11,447-11,464.

Young, V. L.; Kieser, B. N.; Chen, S. P.; Nii, H. (1997) Seasonal trends and local influences on nonmethane hydrocarbon concentrations in the Canadian boreal forest. J. Geophys. Res. (Atmos.) 102: 5913-5918.

Yu, J.; Jeffries, H. E. (1997) Atmospheric photooxidation of alkylbenzenes II. evidence of formation of epoxide intermediates. Atmos. Environ. 31: 2281-2287.

Yu, J.; Jeffries, H. E.; Sexton, K. G. (1997) Atmospheric photooxidation of alkylbenzenes I. carbonyl product analyses. Atmos. Environ. 31: 2261-2280.

Yung, Y. L.; Pinto, J. P.; Watson, R. T.; Sander, S. P. (1980) Atmospheric bromine and ozone perturbations in the lower stratosphere. J. Atmos. Sci. 37: 339-353.

Zafiriou, O. C.; True, M. B. (1979) Nitrate photolysis in seawater by sunlight. Mar. Chem. 8: 33-42.

Zanis, P.; Trickl, T.; Stohl, A.; Wernli, H.; Cooper, O.; Zerefos, C.; Gaeggeler, H.; Schnabel, C.; Tobler, L.; Kubik, P. W.; Priller, A.; Scheel, H. E.; Kanter, H. J.; Cristofanelli, P.; Forster, C.; James, P.; Gerasopoulos, E.; Delcloo, A.; Papayannis, A.; Claude, H. (2003) Forecast, observation and modelling of a deep stratospheric intrusion event over Europe. Atmos. Chem. Phys. 3: 763-777.

Zenker, T.; Fischer, H.; Nikitas, C.; Parchatka, U.; Harris, G. W.; Mihelcic, D.; Müsgen, P.; Pätz, H. W.; Schultz, M.; Volz-Thomas, A.; Schmitt, R.; Behmann, T.; Wiessenmayer, M.; Burrows, J. P. (1998) Intercomparison of NO, NO_2, NO_y, O_3, and RO_x measurements during the oxidizing capacity of the tropospheric atmosphere (OCTA) campaign 1993 at Izana. J. Geophys. Res. [Atmos.] 103: 13,615-13,634.

Zhang, Y.; Carmichael, G. R. (1999) The role of mineral aerosol in tropospheric chemistry in East Asia--a model study. J. Appl. Meteorol. 38: 353-366.

Zhang, J. S.; Rao, S. T. (1999) The role of vertical mixing in the temporal evolution of ground-level ozone concentrations. J. Appl. Meteorol. 38: 1674-1691.

Zhang, D.-L.; Zheng, W.-Z. (2004) Diurnal cycles of surface winds and temperatures as simulated by five boundary layer parameterizations. J. Appl. Meteorol. 43: 157-169.

Zhang, S.-H.; Shaw, M.; Seinfeld, J. H.; Flagan, R. C. (1992) Photochemical aerosol formation from α-pinene and β-pinene. J. Geophys. Res. [Atmos.] 97: 20,717-20,729.

Zhang et al., 1997.

Zhang, K.; Juiting, M.; Civerolo, K. C.; Berman, S.; Ku, J.; Rao, S. T.; Doddridge, B.; Philbrick, R. C.; Clark, R. (2001) Numerical investigation of boundary layer evolution and nocturnal low-level jets: local versus non-local PBL schemes. Environ. Fluid Mech. 1: 171-208.

Zhang, D.; Lei, W. F.; Zhang, R. Y. (2002) Mechanism of OH formation from ozonolysis of isoprene: kinetics and product yields. Chem. Phys. Lett. 358: 171-179.

Zhang, D.; Zang, J.; Shi, G.; Iwasaka, Y.; Matsuki, A.; Trochkine, D. (2003) Mixture state of individual Asian dust particles at a coastal site of Qingdao, China. Atmos. Environ. 37: 3895-3901.

Zhou, X.; Mopper, K. (1990) Determination of photochemically produced hydroxyl radicals in seawater and freshwater. Mar. Chem. 30: 71-88.

Zimmermann, J.; Poppe, D. (1993) Nonlinear chemical couplings in the tropospheric NO_x–HO_x gas phase chemistry. J. Atmos. Chem. 17: 141-155.

Zondlo, M. A.; Barone, S. B.; Tolbert, M. A. (1998) Condensed-phase products in heterogeneous reactions: N_2O_5, $ClONO_2$, and HNO_3 reacting on ice films at 185 K. J. Phys. Chem. A 102: 5735-5748.

3. ENVIRONMENTAL CONCENTRATIONS, PATTERNS, AND EXPOSURE ESTIMATES

3.1 INTRODUCTION

Identification and Use of Existing Air Quality Data

Topics discussed in this chapter include the characterization of ambient air quality data for ozone (O_3), the uses of these data in assessing the exposure of vegetation to O_3, concentrations of O_3 in microenvironments, and a discussion of the currently available human exposure data and exposure model development. The information contained in this chapter pertaining to ambient concentrations is taken primarily from the U.S. Environmental Protection Agency Air Quality System (AQS; formerly the AIRS database). The AQS contains readily accessible detailed, hourly data that has been subject to the Agency's quality control and assurance procedures. Data available in AQS were collected from 1979 to 2001. As discussed in previous versions of the O_3 Air Quality Criteria Document or AQCD (U.S. Environmental Protection Agency, 1986, 1996), the data available prior to 1979 may be unreliable due to calibration problems and uncertainties.

As indicated in the 1996 O_3 AQCD (U.S. Environmental Protection Agency, 1996), O_3 is the only photochemical oxidant other than nitrogen dioxide (NO_2) that is routinely monitored and for which a comprehensive aerometric database exists. Data for peroxyacetyl nitrate (PAN) and hydrogen peroxide (H_2O_2) have been obtained only as part of special research field investigations. Consequently, no data on nationwide patterns of occurrence are available for these non-O_3 oxidants; nor are extensive data available on the relationships of levels and patterns of these oxidants to those of O_3.

Characterizing Ambient Ozone Concentrations

In this chapter, data are analyzed for the purpose of providing information on specific issues of exposure-response relationships that are considered in the later chapters addressing O_3 exposure effects. It is important to distinguish among concentration, exposure, and dose when using air quality data to assess human health and vegetation effects. For this chapter, the following definitions apply.

The "concentration" of a specific air pollutant is typically defined as the amount (mass) of that material per unit volume of air. Air pollution monitors measure pollutant concentrations, which may or may not provide accurate exposure estimates. However, most of the data presented herein are expressed as "mixing ratios" in terms of a volume-to-volume ratio, expressed as parts per million (ppm) or parts per billion (ppb). Data expressed this way are often referred to as concentrations, both in the literature and in the text, following common usage.

The term "exposure" may generally be defined as the concentration of a pollutant encountered by the subject (animal, human, or plant) for a duration of time. Exposure implies that such an encounter leads to intake through the contact surface. A measured concentration functions as a surrogate for an exposure only to the degree to which it represents concentrations actually experienced by the subject under otherwise similar conditions.

The term "dose" is defined as that mass of pollutant delivered to a target. This term has numerous quantitative descriptions, so the context of the use of this term and the units within the document must be considered. A more in-depth description of exposure and dose appears later in this chapter for humans and in Chapter 9 for vegetation and ecosystems.

In summarizing the hourly average concentrations in this chapter, specific attention is given to the relevance of the exposure indicators used. For example, for human health considerations, concentration (or exposure) indicators such as the daily maximum 1-h average concentrations, as well as the number of daily maximum 8-h average concentrations, are used to characterize information in the population-oriented monitor locations. For vegetation, several different types of exposure indicators are used. The peak-weighted, cumulative exposure indicators used in this chapter for characterizing vegetation exposures are SUM06 and SUM08 (the sums of all hourly average concentrations $\geq$ 0.06 and 0.08 ppm, respectively) and W126 (the sum of the hourly average concentrations that have been weighted according to a sigmoid function [see Lefohn and Runeckles, 1987] that is based on a hypothetical vegetation response). Further discussion of these exposure indices is presented in Chapter 9.

Hourly average concentration information is summarized for urban versus rural or nonurban (i.e., forested and agricultural) areas in the United States in Annex AX3. The distribution of O_3 or its precursors at a rural site near an urban source is affected by wind direction (i.e., whether the rural site is located up- or downwind from the source of O_3 precursors). It is difficult to apply land use designations to the generalization of exposure regimes that may be experienced in urban versus rural areas, because the land use characterization of "rural" does not imply that a specific location is isolated from anthropogenic influences. Rather, the characterization implies only the current use of the land. Since it is possible for O_3 produced from urban area emissions to be transported to more rural downwind locations, elevated O_3 concentrations can occur at considerable distances from urban centers. Nitrogen oxides (NO_x) often depress O_3 concentrations through titration in urban cores with heavy traffic. Due to the less chemical scavenging in nonurban areas, O_3 tends to persist longer in nonurban than in urban areas; thus, exposures may be greater in downwind nonurban locations. For example, Logan (1989) has noted that hourly average O_3 concentrations above 0.08 ppm are common in rural areas of the eastern United States in spring and summer, but are unusual at remote western sites. Consequently, for the purposes of comparing exposure regimes that may be characteristic of clean locations in the United States with those that are urban influenced (i.e., located in either urban or rural locations), this chapter characterizes data collected from those stations whose locations appear to be isolated from large-scale anthropogenic influences (i.e., relatively clean remote sites) in Annex AX3, Section AX3.2.

Acknowledging the photochemical and insolation-dependent nature of O_3 formation, the U.S. Environmental Protection Agency (U.S. EPA) has established allowable "ozone seasons" for the required measurement of ambient O_3 concentrations for different locations within the United States and the U.S. territories (CFR, 2000). Table 3-1 shows the O_3 seasons during which continuous, hourly averaged O_3 concentrations must be monitored.

The use of ambient monitoring data in epidemiological studies provides the exposure indicator for individuals exercising outside and serves as a measure of relative exposures since ambient photochemical production is the major source of O_3. The lack of association between ambient air concentration and total exposure results in some misclassification when using monitoring data or ambient air modeling results as surrogates for exposure. The reliance on monitoring data from a single site or averaged over large regions as exposure surrogates may not adequately represent regional variations or differences in exposures with location and activity. This may increase the potential for misclassification of both absolute and relative exposures. Exposure models rather than chemistry transport models (CTMs) have been used to refine population exposure estimates, decreasing misclassification of exposures. For cohort studies, exposure measurements using passive personal samplers combined with modeling can provide

Table 3-1. Ozone Monitoring Seasons by State

State	Start Month — End	State	Start Month — End
Alabama	March — October	Nevada	January — December
Alaska	April — October	New Hampshire	April — September
Arizona	January — December	New Jersey	April — October
Arkansas	March — November	New Mexico	January — December
California	January — December	New York	April — October
Colorado	March — September	North Carolina	April — October
Connecticut	April — September	North Dakota	May — September
Delaware	April — October	Ohio	April — October
District of Columbia	April — October	Oklahoma	March — November
Florida	March — October	Oregon	May — September
Georgia	March — October	Pennsylvania	April — October
Hawaii	January — December	Puerto Rico	January — December
Idaho	April — October	Rhode Island	April — September
Illinois	April — October	South Carolina	April — October
Indiana	April — September	South Dakota	June — September
Iowa	April — October	Tennessee	March — October
Kansas	April — October	Texas[1]	January — December
Kentucky	March — October	Texas[1]	March — October
Louisiana	January — December	Utah	May — September
Maine	April — September	Vermont	April — September
Maryland	April — October	Virginia	April — October
Massachusetts	April — September	Washington	May — September
Michigan	April — September	West Virginia	April — October
Minnesota	April — October	Wisconsin	April 15 — October 15
Mississippi	March — October	Wyoming	April — October
Missouri	April — October	American Samoa	January — December
Montana	June — September	Guam	January — December
Nebraska	April — October	Virgin Islands	January — December

[1] The ozone season is defined differently in different sections of Texas.

Source: CFR (2000).

detailed individual exposure data to minimize misclassification. Improvements in models will help better characterize exposures by location for activities deemed most likely to increase risk, such as exercise, and for sensitive populations.

3.2 AMBIENT AIR QUALITY DATA FOR OZONE

Ozone Air Quality at Urban, Suburban, and Nonurban Sites

Often there is a difference in the distribution of hourly average concentrations between urban and nonurban areas. Ozone concentrations measured at center-city sites are often lower than at surrounding rural sites. In some urban areas, maximum hourly average concentrations exceed 0.120 ppm. However, only about 1% of the hourly average concentrations generally exceed 0.100 ppm at sites in these areas. Furthermore, monitoring sites in polluted areas tend to experience frequent hourly average O_3 concentrations at or near minimum detectable levels. The highest values of the second highest daily maximum of the O_3 hourly average concentrations are observed in the Texas Gulf Coast and Southern California, but high levels of O_3 also occur in the Northeast Corridor, and other heavily populated regions of the United States as shown in Figure 3-1 and Table 3-2. Metropolitan Statistical Areas (MSAs), which experience elevated second highest daily maximum hourly average concentrations, also experience elevated fourth highest 8-h daily maximum concentrations. There are considerably more MSAs and Consolidated Metropolitan Statistical Areas (CMSAs) that experience fourth highest 8-h daily maximum concentrations $\geq$ 0.085 ppm than MSAs and CMSAs that experience second highest daily maximum hourly average concentrations $\geq$ 0.125 ppm (Figure 3-2 and Table 3-3).

It is difficult to identify a set of unique O_3 distribution patterns that adequately describes the hourly average concentrations experienced at monitoring sites in nonurban locations, because many nonurban sites in the United States are influenced by local sources of pollution or long-range transport of O_3 or its precursors. Using hourly averaged data from AQS for a select number of rural monitoring sites, Table 3-4 summarizes the percentiles of the hourly average O_3 concentrations, the number of occurrences of the hourly average concentration $\geq$ 0.08 and 0.10 ppm, the 7-month sum of all hourly average concentrations $\geq$ 0.06 ppm, and the 7-month W126 exposure index. Note the large variation in the number of hourly average concentrations

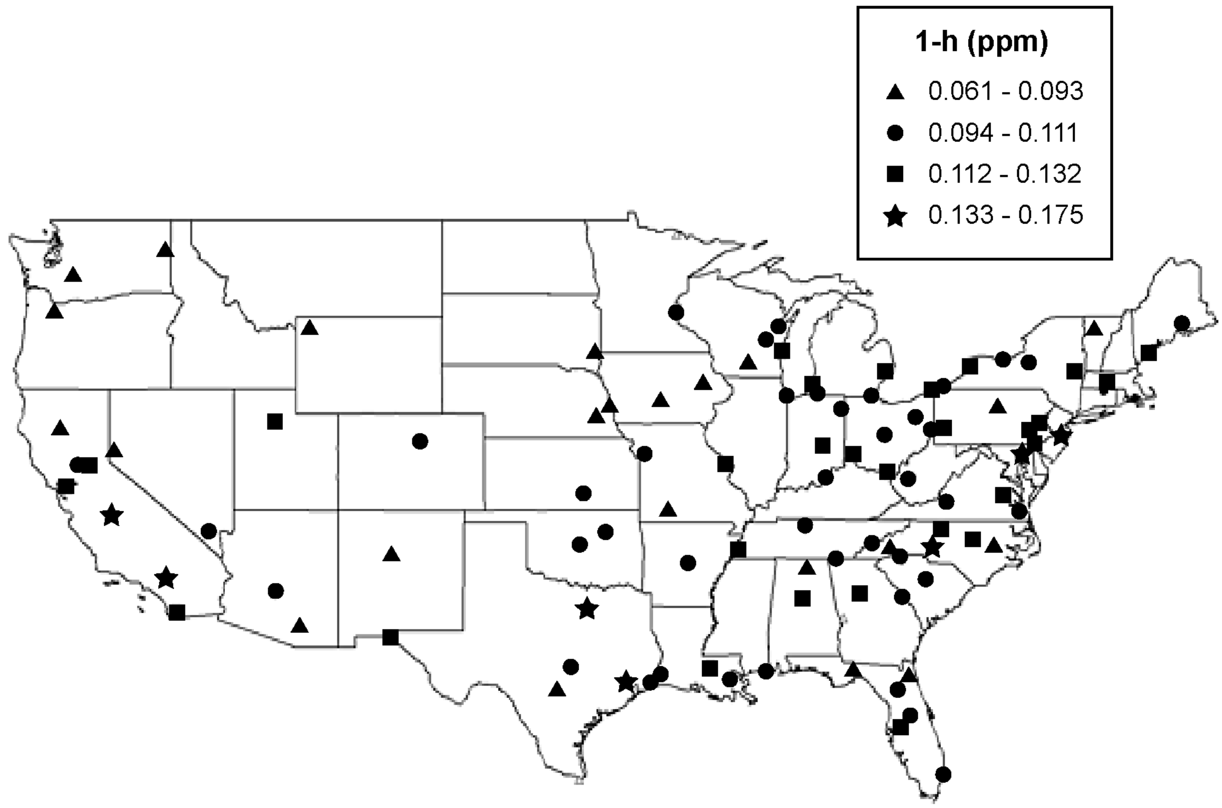

Figure 3-1. Second highest daily maximum 1-h O_3 concentrations.

Source: U.S. Environmental Protection Agency (2003a).

≥ 0.08 and 0.10 ppm. The sites are influenced either by local sources or by transport of O_3 or its precursors.

Ozone Air Quality Data at Relatively Remote Monitoring Sites

In characterizing hourly average concentration data obtained at nonurban locations, it is important to carefully quantify the distribution of the hourly average concentrations that are folded into the cumulative exposure indices used in predicting vegetation effects. For example, in 2001, although the Crestline, CA site in the San Bernardino National Forest and the Cove Mountain site in the Great Smoky Mountains National Park experience similar cumulative exposures (i.e., SUM06 and W126 values), the Crestline site experienced considerably more high hourly average concentrations ≥ 0.10 ppm (i.e., 369) than the Cove Mountain site (i.e., 5).

Table 3-2. The Second Highest Daily Maximum One-Hour Ozone Concentration (ppm) by Metropolitan Statistical Area (MSA) or Consolidated Metropolitan Statistical Area (CMSA) for the Years 1999 to 2001

MSA/CMSA	1999	2000	2001
Albany-Schenectady-Troy, NY MSA	0.107	0.088	0.112
Albuquerque, NM MSA	0.097	0.093	0.088
Allentown-Bethlehem-Easton, PA MSA	0.126	0.114	0.126
Altoona, PA MSA	0.111	0.104	0.107
Appleton-Oshkosh-Neenah, WI MSA	0.105	0.085	0.102
Asheville, NC MSA	0.099	0.107	0.091
Atlanta, GA MSA	0.156	0.158	0.125
Augusta-Aiken, GA-SC MSA	0.108	0.115	0.103
Austin-San Marcos, TX MSA	0.110	0.107	0.097
Bakersfield, CA MSA	0.136	0.142	0.134
Bangor, ME MSA	0.088	.	0.105
Barnstable-Yarmouth, MA MSA	0.127	0.107	0.139
Baton Rouge, LA MSA	0.121	0.139	0.117
Beaumont-Port Arthur, TX MSA	0.103	0.160	0.103
Bellingham, WA MSA	0.062	0.063	0.061
Benton Harbor, MI MSA	0.107	0.107	0.117
Biloxi-Gulfport-Pascagoula, MS MSA	0.107	0.135	0.099
Birmingham, AL MSA	0.131	0.127	0.114
Boston-Worcester-Lawrence, MA-NH-ME-CT CMSA	0.125	0.101	0.136
Brownsville-Harlingen-San Benito, TX MSA	0.075	0.080	0.074
Buffalo-Niagara Falls, NY MSA	0.102	0.105	0.116
Burlington, VT MSA	0.093	0.080	0.083
Canton-Massillon, OH MSA	0.108	0.104	0.106
Cedar Rapids, IA MSA	0.096	0.083	0.084
Champaign-Urbana, IL MSA	0.108	0.084	0.080
Charleston, WV MSA	0.130	0.094	0.107
Charleston-North Charleston, SC MSA	0.101	0.105	0.085
Charlotte-Gastonia-Rock Hill, NC-SC MSA	0.130	0.141	0.142

Table 3-2 (cont'd). The Second Highest Daily Maximum One-Hour Ozone Concentration (ppm) by Metropolitan Statistical Area (MSA) or Consolidated Metropolitan Statistical Area (CMSA) for the Years 1999 to 2001

MSA/CMSA	1999	2000	2001
Chattanooga, TN-GA MSA	0.122	0.124	0.107
Chicago-Gary-Kenosha, IL-IN-WI CMSA	0.126	0.102	0.124
Chico-Paradise, CA MSA	0.110	0.091	0.100
Cincinnati-Hamilton, OH-KY-IN CMSA	0.119	0.110	0.115
Clarksville-Hopkinsville, TN-KY MSA	0.115	0.108	0.096
Cleveland-Akron, OH CMSA	0.118	0.110	0.118
Colorado Springs, CO MSA	0.075	0.088	0.085
Columbia, SC MSA	0.117	0.116	0.107
Columbus, GA-AL MSA	0.110	0.114	0.090
Columbus, OH MSA	0.144	0.117	0.111
Corpus Christi, TX MSA	0.103	0.099	0.092
Dallas-Fort Worth, TX CMSA	0.154	0.126	0.137
Davenport-Moline-Rock Island, IA-IL MSA	0.099	0.089	0.089
Dayton-Springfield, OH MSA	0.127	0.106	0.100
Daytona Beach, FL MSA	0.087	0.088	0.085
Decatur, AL MSA	0.103	0.110	0.087
Decatur, IL MSA	0.102	0.092	0.078
Denver-Boulder-Greeley, CO CMSA	0.105	0.107	0.105
Des Moines, IA MSA	0.083	0.082	0.069
Detroit-Ann Arbor-Flint, MI CMSA	0.121	0.102	0.122
Dover, DE MSA	0.120	0.126	0.117
Duluth-Superior, MN-WI MSA	0.082	0.074	0.071
El Paso, TX MSA	0.108	0.122	0.116
Elkhart-Goshen, IN MSA	0.085	0.080	0.066
Elmira, NY MSA	0.092	0.089	0.094
Erie, PA MSA	0.112	0.095	0.104
Eugene-Springfield, or MSA	0.084	0.078	0.081
Evansville-Henderson, IN-KY MSA	0.114	0.097	0.095

Table 3-2 (cont'd). The Second Highest Daily Maximum One-Hour Ozone Concentration (ppm) by Metropolitan Statistical Area (MSA) or Consolidated Metropolitan Statistical Area (CMSA) for the Years 1999 to 2001

MSA/CMSA	1999	2000	2001
Fargo-Moorhead, ND-MN MSA	0.073	0.073	0.069
Fayetteville, NC MSA	0.120	0.106	0.108
Flagstaff, AZ-UT MSA	0.086	0.082	0.074
Fort Collins-Loveland, CO MSA	0.089	0.096	0.088
Fort Myers-Cape Coral, FL MSA	0.096	0.091	0.079
Fort Pierce-Port St. Lucie, FL MSA	0.083	0.079	0.095
Fort Wayne, IN MSA	0.101	0.099	0.098
Fresno, CA MSA	0.145	0.146	0.146
Gainesville, FL MSA	0.098	0.096	0.096
Grand Rapids-Muskegon-Holland, MI MSA	0.116	0.123	0.118
Green Bay, WI MSA	0.097	0.090	0.107
Greensboro-Winston-Salem-High Point, NC MSA	0.126	0.116	0.122
Greenville, NC MSA	0.109	0.109	0.091
Greenville-Spartanburg-Anderson, SC MSA	0.122	0.115	0.108
Harrisburg-Lebanon-Carlisle, PA MSA	0.126	0.110	0.105
Hartford, CT MSA	0.161	0.116	0.139
Hickory-Morganton-Lenoir, NC MSA	0.115	0.107	0.099
Honolulu, HI MSA	0.054	0.048	0.051
Houma, LA MSA	.	0.124	0.106
Houston-Galveston-Brazoria, TX CMSA	0.203	0.194	0.170
Huntington-Ashland, WV-KY-OH MSA	0.122	0.094	0.113
Huntsville, AL MSA	0.106	0.111	0.088
Indianapolis, IN MSA	0.114	0.102	0.114
Jackson, MS MSA	0.110	0.099	0.095
Jacksonville, FL MSA	0.103	0.114	0.093
Jamestown, NY MSA	0.103	0.113	0.109
Janesville-Beloit, WI MSA	0.105	0.098	0.093
Johnson City-Kingsport-Bristol, TN-VA MSA	0.111	0.126	0.110

Table 3-2 (cont'd). The Second Highest Daily Maximum One-Hour Ozone Concentration (ppm) by Metropolitan Statistical Area (MSA) or Consolidated Metropolitan Statistical Area (CMSA) for the Years 1999 to 2001

MSA/CMSA	1999	2000	2001
Johnstown, PA MSA	0.107	0.104	0.106
Kalamazoo-Battle Creek, MI MSA	0.103	0.090	0.101
Kansas City, MO-KS MSA	0.116	0.124	0.108
Knoxville, TN MSA	0.129	0.131	0.109
Lafayette, LA MSA	0.094	0.123	0.090
Lake Charles, LA MSA	0.127	0.133	0.105
Lakeland-Winter Haven, FL MSA	0.101	0.102	0.109
Lancaster, PA MSA	0.127	0.107	0.127
Lansing-East Lansing, MI MSA	0.101	0.091	0.106
Laredo, TX MSA	0.084	0.085	0.071
Las Cruces, NM MSA	0.102	0.123	0.104
Las Vegas, NV-AZ MSA	0.097	0.094	0.100
Lawton, OK MSA	0.089	0.094	0.094
Lexington, KY MSA	0.114	0.086	0.092
Lima, OH MSA	0.107	0.100	0.096
Lincoln, NE MSA	0.062	0.072	0.061
Little Rock-North Little Rock, AR MSA	0.107	0.114	0.102
Longview-Marshall, TX MSA	0.134	0.131	0.111
Los Angeles-Riverside-Orange County, CA CMSA	0.159	0.174	0.175
Louisville, KY-IN MSA	0.124	0.112	0.106
Macon, GA MSA	0.133	0.131	0.115
Madison, WI MSA	0.098	0.087	0.088
McAllen-Edinburg-Mission, TX MSA	0.086	0.088	0.092
Medford-Ashland, OR MSA	.	0.079	0.081
Melbourne-Titusville-Palm Bay, FL MSA	0.087	0.093	0.094
Memphis, TN-AR-MS MSA	0.130	0.123	0.121
Merced, CA MSA	0.125	0.120	0.113
Miami-Fort Lauderdale, FL CMSA	0.113	0.094	0.106

Table 3-2 (cont'd). The Second Highest Daily Maximum One-Hour Ozone Concentration (ppm) by Metropolitan Statistical Area (MSA) or Consolidated Metropolitan Statistical Area (CMSA) for the Years 1999 to 2001

MSA/CMSA	1999	2000	2001
Milwaukee-Racine, WI CMSA	0.122	0.098	0.122
Minneapolis-St. Paul, MN-WI MSA	0.088	0.089	0.109
Mobile, AL MSA	0.104	0.118	0.095
Modesto, CA MSA	0.111	0.110	0.111
Monroe, LA MSA	0.097	0.103	0.090
Montgomery, AL MSA	0.110	0.111	0.094
Nashville, TN MSA	0.123	0.122	0.110
New London-Norwich, CT-RI MSA	0.127	0.135	0.109
New Orleans, LA MSA	0.117	0.124	0.111
NY-Northern NJ-Long Island, NY-NJ-CT-PA CMSA	0.154	0.136	0.146
Norfolk-Virginia Beach-Newport News, VA-NC MSA	0.135	0.099	0.100
Ocala, FL MSA	0.097	0.093	0.089
Oklahoma City, OK MSA	0.097	0.100	0.097
Omaha, NE-IA MSA	0.093	0.083	0.076
Orlando, FL MSA	0.101	0.106	0.108
Owensboro, KY MSA	0.102	0.082	0.086
Parkersburg-Marietta, WV-OH MSA	0.123	0.105	0.108
Pensacola, FL MSA	0.106	0.118	0.098
Peoria-Pekin, IL MSA	0.099	0.083	0.084
Philadelphia-Wilmington-Atlantic City, PA-NJ-DE-MD CMSA	0.152	0.128	0.131
Phoenix-Mesa, AZ MSA	0.119	0.107	0.106
Pittsburgh, PA MSA	0.132	0.111	0.112
Pittsfield, MA MSA	0.092	.	0.112
Portland, ME MSA	0.120	0.089	0.124
Portland-Salem, OR-WA CMSA	0.094	0.082	0.093
Providence-Fall River-Warwick, RI-MA MSA	0.133	0.118	0.144
Provo-Orem, UT MSA	0.109	0.095	0.094
Raleigh-Durham-Chapel Hill, NC MSA	0.134	0.116	0.113

Table 3-2 (cont'd). The Second Highest Daily Maximum One-Hour Ozone Concentration (ppm) by Metropolitan Statistical Area (MSA) or Consolidated Metropolitan Statistical Area (CMSA) for the Years 1999 to 2001

MSA/CMSA	1999	2000	2001
Reading, PA MSA	0.128	0.105	0.125
Redding, CA MSA	0.113	0.098	0.093
Reno, NV MSA	0.097	0.088	0.090
Richmond-Petersburg, VA MSA	0.133	0.112	0.119
Roanoke, VA MSA	.	0.095	0.101
Rochester, NY MSA	0.101	0.088	0.100
Rockford, IL MSA	0.093	0.084	0.086
Rocky Mount, NC MSA	0.104	0.106	0.099
Sacramento-Yolo, CA CMSA	0.137	0.134	0.129
Salinas, CA MSA	0.075	0.084	0.078
Salt Lake City-Ogden, UT MSA	0.112	0.100	0.118
San Antonio, TX MSA	0.109	0.095	0.092
San Diego, CA MSA	0.114	0.123	0.118
San Francisco-Oakland-San Jose, CA CMSA	0.144	0.126	0.118
San Luis Obispo-Atascadero-Paso Robles, CA MSA	0.094	0.082	0.092
Santa Barbara-Santa Maria-Lompoc, CA MSA	0.095	0.100	0.103
Sarasota-Bradenton, FL MSA	0.112	0.107	0.114
Savannah, GA MSA	0.107	0.102	0.085
Scranton-Wilkes-Barre-Hazleton, PA MSA	0.115	0.093	0.104
Seattle-Tacoma-Bremerton, WA CMSA	0.091	0.095	0.088
Sharon, PA MSA	0.108	0.098	0.113
Sheboygan, WI MSA	0.130	0.106	0.122
Shreveport-Bossier City, LA MSA	0.108	0.129	0.105
Sioux Falls, SD MSA	0.068	0.076	0.088
South Bend, IN MSA	0.107	0.095	0.108
Spokane, WA MSA	0.073	0.082	0.084
Springfield, IL MSA	0.099	0.100	0.095
Springfield, MA MSA	0.113	0.099	0.132

Table 3-2 (cont'd). The Second Highest Daily Maximum One-Hour Ozone Concentration (ppm) by Metropolitan Statistical Area (MSA) or Consolidated Metropolitan Statistical Area (CMSA) for the Years 1999 to 2001

MSA/CMSA	1999	2000	2001
Springfield, MO MSA	0.095	0.092	0.091
St. Louis, MO-IL MSA	0.128	0.123	0.122
State College, PA MSA	0.099	0.109	0.097
Steubenville-Weirton, OH-WV MSA	0.111	0.100	0.096
Stockton-Lodi, CA MSA	0.130	0.111	0.112
Syracuse, NY MSA	0.099	0.083	0.097
Tallahassee, FL MSA	0.094	0.092	0.085
Tampa-St. Petersburg-Clearwater, FL MSA	0.116	0.108	0.118
Terre Haute, IN MSA	0.093	0.088	0.096
Toledo, OH MSA	0.128	0.095	0.111
Tucson, AZ MSA	0.092	0.085	0.084
Tulsa, OK MSA	0.116	0.122	0.107
Tyler, TX MSA	0.118	.	0.098
Utica-Rome, NY MSA	0.089	0.083	0.100
Victoria, TX MSA	0.102	0.094	0.085
Visalia-Tulare-Porterville, CA MSA	0.125	0.119	0.126
Washington-Baltimore, DC-MD-VA-WV CMSA	0.152	0.128	0.142
Wausau, WI MSA	0.095	0.081	0.078
West Palm Beach-Boca Raton, FL MSA	0.104	0.093	0.098
Wheeling, WV-OH MSA	0.100	0.093	0.104
Wichita, KS MSA	0.095	0.093	0.096
Williamsport, PA MSA	0.091	0.092	0.094
Wilmington, NC MSA	0.081	0.097	0.089
York, PA MSA	0.121	0.112	0.104
Youngstown-Warren, OH MSA	0.109	0.097	0.105
Yuba City, CA MSA	0.106	0.101	0.105

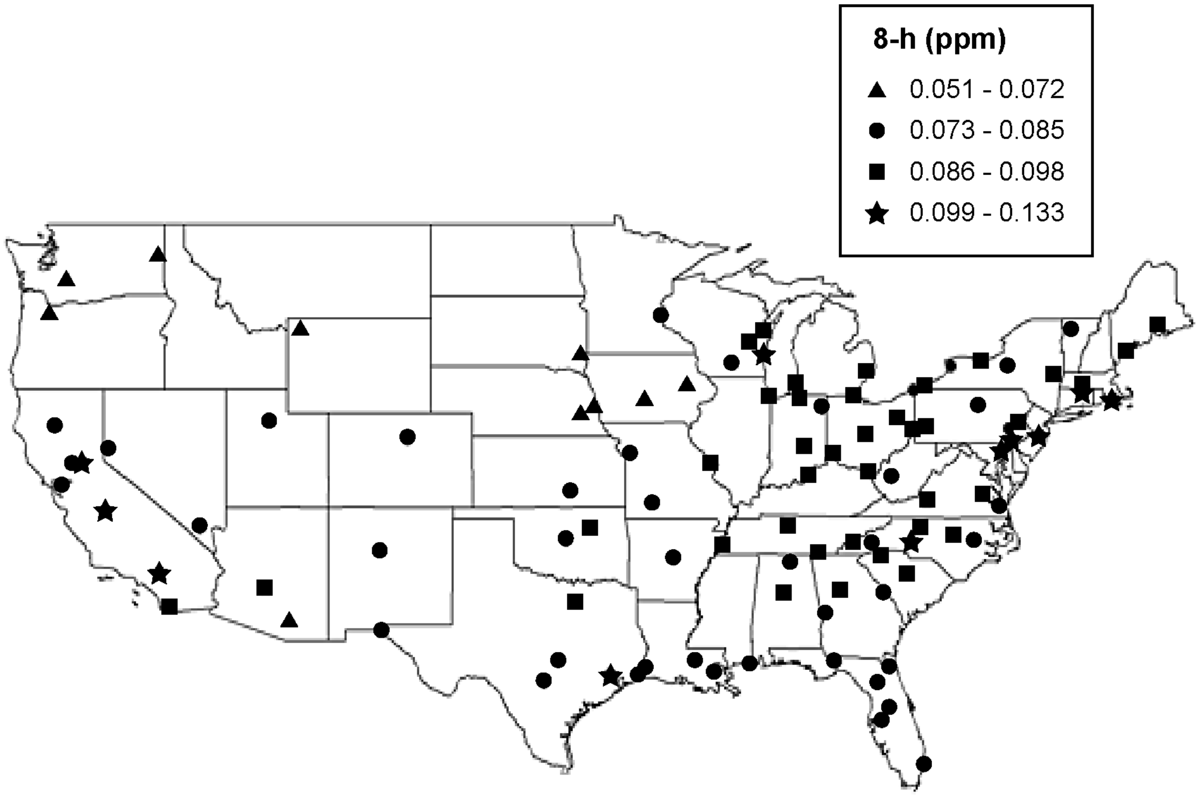

Figure 3-2. Fourth highest 8-h daily maximum O_3 concentration.

Source: U.S. Environmental Protection Agency (2003a).

It is important to characterize hourly average O_3 concentrations at relatively remote monitoring sites so that assessments of the possible effects of O_3 on human health and vegetation use ranges of hourly average concentrations in their experiments that mimic the range of O_3 exposures that occur under ambient conditions. No hourly average concentrations ≥ 0.08 ppm were observed at monitoring sites in Redwood NP (CA), Olympic NP (WA), Glacier NP (MT), Denali NP (AK), Badlands (SD), and Custer NF (MT) during the months of April to October from 1988 to 2001 (Table 3-5). There were eight occurrences of hourly average concentrations ≥ 0.08 ppm from April to October of 1997 at the monitoring site in Theodore Roosevelt NP (ND). However, no hourly average concentrations ≥ 0.08 ppm were observed from April to October in any other year at this site. Except for 1988, the year in which there were major forest fires at Yellowstone NP (WY), the monitoring site located there experienced no hourly average

Table 3-3. The Fourth Highest Daily Maximum Eight-Hour Ozone Concentration (ppm) by Metropolitan Statistical Area (MSA) or Consolidated Metropolitan Statistical Area (CMSA) for the Years 1999 to 2001

MSA/CMSA	1999	2000	2001
Albany-Schenectady-Troy, NY MSA	0.092	0.072	0.090
Albuquerque, NM MSA	0.076	0.076	0.074
Allentown-Bethlehem-Easton, PA MSA	0.107	0.092	0.094
Altoona, PA MSA	0.091	0.080	0.083
Appleton-Oshkosh-Neenah, WI MSA	0.087	0.068	0.087
Asheville, NC MSA	0.084	0.090	0.076
Atlanta, GA MSA	0.126	0.113	0.092
Augusta-Aiken, GA-SC MSA	0.090	0.093	0.082
Austin-San Marcos, TX MSA	0.099	0.088	0.080
Bakersfield, CA MSA	0.109	0.111	0.109
Bangor, ME MSA	0.080	.	0.088
Barnstable-Yarmouth, MA MSA	0.101	0.083	0.105
Baton Rouge, LA MSA	0.100	0.101	0.084
Beaumont-Port Arthur, TX MSA	0.077	0.097	0.081
Bellingham, WA MSA	0.050	0.052	0.050
Benton Harbor, MI MSA	0.096	0.077	0.088
Biloxi-Gulfport-Pascagoula, MS MSA	0.097	0.091	0.083
Birmingham, AL MSA	0.100	0.099	0.089
Boston-Worcester-Lawrence, MA-NH-ME-CT CMSA	0.098	0.082	0.101
Brownsville-Harlingen-San Benito, TX MSA	0.066	0.064	0.063
Buffalo-Niagara Falls, NY MSA	0.090	0.085	0.102
Burlington, VT MSA	0.079	0.071	0.076
Canton-Massillon, OH MSA	0.091	0.087	0.089
Cedar Rapids, IA MSA	0.076	0.075	0.069
Champaign-Urbana, IL MSA	0.094	0.073	0.073
Charleston, WV MSA	0.104	0.085	0.083
Charleston-North Charleston, SC MSA	0.084	0.082	0.071
Charlotte-Gastonia-Rock Hill, NC-SC MSA	0.107	0.101	0.103

Table 3-3 (cont'd). The Fourth Highest Daily Maximum Eight-Hour Ozone Concentration (ppm) by Metropolitan Statistical Area (MSA) or Consolidated Metropolitan Statistical Area (CMSA) for the Years 1999 to 2001

MSA/CMSA	1999	2000	2001
Chattanooga, TN-GA MSA	0.098	0.098	0.087
Chicago-Gary-Kenosha, IL-IN-WI CMSA	0.102	0.086	0.099
Chico-Paradise, CA MSA	0.087	0.086	0.088
Cincinnati-Hamilton, OH-KY-IN CMSA	0.096	0.093	0.088
Clarksville-Hopkinsville, TN-KY MSA	0.092	0.088	0.082
Cleveland-AKRON, OH CMSA	0.103	0.085	0.099
Colorado Springs, CO MSA	0.064	0.070	0.070
Columbia, SC MSA	0.094	0.097	0.091
Columbus, GA-AL MSA	0.097	0.094	0.079
Columbus, OH MSA	0.103	0.091	0.090
Corpus Christi, TX MSA	0.085	0.083	0.077
Dallas-Fort Worth, TX CMSA	0.112	0.102	0.098
Davenport-Moline-Rock Island, IA-IL MSA	0.083	0.077	0.079
Dayton-Springfield, OH MSA	0.096	0.088	0.084
Daytona Beach, FL MSA	0.075	0.076	0.073
Decatur, AL MSA	0.092	0.091	0.077
Decatur, IL MSA	0.087	0.077	0.071
Denver-Boulder-Greeley, CO CMSA	0.081	0.083	0.082
Des Moines, IA MSA	0.073	0.071	0.060
Detroit-Ann Arbor-Flint, MI CMSA	0.096	0.082	0.095
Dover, DE MSA	0.097	0.093	0.091
Duluth-Superior, MN-WI MSA	0.074	0.065	0.062
El Paso, TX MSA	0.071	0.084	0.078
Elkhart-Goshen, IN MSA	0.077	0.063	0.055
Elmira, NY MSA	0.082	0.073	0.082
Erie, PA MSA	0.096	0.078	0.089
Eugene-Springfield, OR MSA	0.068	0.047	0.066
Evansville-Henderson, IN-KY MSA	0.098	0.085	0.081

Table 3-3 (cont'd). The Fourth Highest Daily Maximum Eight-Hour Ozone Concentration (ppm) by Metropolitan Statistical Area (MSA) or Consolidated Metropolitan Statistical Area (CMSA) for the Years 1999 to 2001

MSA/CMSA	1999	2000	2001
Fargo-Moorhead, ND-MN MSA	0.066	0.057	0.060
Fayetteville, NC MSA	0.100	0.086	0.084
Flagstaff, AZ-UT MSA	0.076	0.071	0.070
Fort Collins-Loveland, CO MSA	0.074	0.078	0.070
Fort Myers-Cape Coral, FL MSA	0.081	0.077	0.068
Fort Pierce-Port St. Lucie, FL MSA	0.071	0.071	0.075
Fort Wayne, IN MSA	0.090	0.091	0.082
Fresno, CA MSA	0.105	0.114	0.113
Gainesville, FL MSA	0.080	0.080	0.079
Grand Rapids-Muskegon-Holland, MI MSA	0.103	0.080	0.095
Green Bay, WI MSA	0.085	0.071	0.088
Greensboro-Winston-Salem-High Point, NC MSA	0.100	0.094	0.096
Greenville, NC MSA	0.093	0.082	0.077
Greenville-Spartanburg-Anderson, SC MSA	0.100	0.089	0.090
Harrisburg-Lebanon-Carlisle, PA MSA	0.104	0.088	0.091
Hartford, CT MSA	0.107	0.089	0.102
Hickory-Morganton-Lenoir, NC MSA	0.094	0.091	0.088
Honolulu, HI MSA	0.048	0.044	0.042
Houma, LA MSA	0.087	0.085	0.084
Houston-Galveston-Brazoria, TX CMSA	0.124	0.117	0.110
Huntington-Ashland, WV-KY-OH MSA	0.097	0.083	0.088
Huntsville, AL MSA	0.093	0.088	0.080
Indianapolis, IN MSA	0.096	0.090	0.093
Jackson, MS MSA	0.084	0.080	0.078
Jacksonville, FL MSA	0.080	0.077	0.075
Jamestown, NY MSA	0.092	0.087	0.090
Janesville-Beloit, WI MSA	0.093	0.083	0.084
Johnson City-Kingsport-Bristol, TN-VA MSA	0.089	0.097	0.086

Table 3-3 (cont'd). The Fourth Highest Daily Maximum Eight-Hour Ozone Concentration (ppm) by Metropolitan Statistical Area (MSA) or Consolidated Metropolitan Statistical Area (CMSA) for the Years 1999 to 2001

MSA/CMSA	1999	2000	2001
Johnstown, PA MSA	0.090	0.086	0.090
Kalamazoo-Battle Creek, MI MSA	0.091	0.070	0.085
Kansas City, MO-KS MSA	0.084	0.091	0.079
Knoxville, TN MSA	0.106	0.100	0.093
Lafayette, LA MSA	0.081	0.092	0.077
Lake Charles, LA MSA	0.088	0.090	0.080
Lakeland-Winter Haven, FL MSA	0.078	0.079	0.087
Lancaster, PA MSA	0.102	0.090	0.097
Lansing-East Lansing, MI MSA	0.089	0.077	0.087
Laredo, TX MSA	0.067	0.070	0.063
Las Cruces, NM MSA	0.082	0.081	0.079
Las Vegas, NV-AZ MSA	0.084	0.082	0.082
Lawton, OK MSA	0.082	0.085	0.078
Lexington, KY MSA	0.091	0.077	0.078
Lima, OH MSA	0.093	0.085	0.081
Lincoln, NE MSA	0.053	0.057	0.051
Little Rock-North Little Rock, AR MSA	0.089	0.092	0.080
Longview-Marshall, TX MSA	0.105	0.099	0.082
Los Angeles-Riverside-Orange County, CA CMSA	0.133	0.122	0.133
Louisville, KY-IN MSA	0.103	0.090	0.086
Macon, GA MSA	0.113	0.097	0.086
Madison, WI MSA	0.085	0.071	0.078
McAllen-Edinburg-Mission, TX MSA	0.075	0.077	0.074
Medford-Ashland, OR MSA	.	0.067	0.064
Melbourne-Titusville-Palm Bay, FL MSA	0.077	0.078	0.084
Memphis, TN-AR-MS MSA	0.104	0.093	0.092
Merced, CA MSA	0.105	0.103	0.096
Miami-Fort Lauderdale, FL CMSA	0.077	0.077	0.076

Table 3-3 (cont'd). The Fourth Highest Daily Maximum Eight-Hour Ozone Concentration (ppm) by Metropolitan Statistical Area (MSA) or Consolidated Metropolitan Statistical Area (CMSA) for the Years 1999 to 2001

MSA/CMSA	1999	2000	2001
Milwaukee-Racine, WI CMSA	0.097	0.086	0.102
Minneapolis-St. Paul, MN-WI MSA	0.077	0.072	0.078
Mobile, AL MSA	0.085	0.097	0.078
Modesto, CA MSA	0.090	0.091	0.094
Monroe, LA MSA	0.082	0.081	0.077
Montgomery, AL MSA	0.092	0.086	0.077
Nashville, TN MSA	0.101	0.093	0.086
New London-Norwich, CT-RI MSA	0.096	0.084	0.090
New Orleans, LA MSA	0.091	0.095	0.084
NY-Northern NJ-Long Island, NY-NJ-CT-PA CMSA	0.113	0.114	0.108
Norfolk-Virginia Beach-Newport News, VA-NC MSA	0.097	0.084	0.085
Ocala, FL MSA	0.083	0.079	0.074
Oklahoma City, OK MSA	0.084	0.086	0.082
Omaha, NE-IA MSA	0.080	0.072	0.063
Orlando, FL MSA	0.084	0.081	0.079
Owensboro, KY MSA	0.090	0.074	0.073
Panama City, FL MSA	.	0.092	0.082
Parkersburg-Marietta, WV-OH MSA	0.097	0.087	0.085
Pensacola, FL MSA	0.086	0.096	0.082
Peoria-Pekin, IL MSA	0.082	0.073	0.080
Philadelphia-Wilmington-Atlantic City, PA-NJ-DE-MD CMSA	0.112	0.109	0.105
Phoenix-Mesa, AZ MSA	0.091	0.090	0.086
Pittsburgh, PA MSA	0.101	0.088	0.093
Pittsfield, MA MSA	0.075	.	0.092
Portland, ME MSA	0.089	0.073	0.097
Portland-Salem, or-WA CMSA	0.072	0.065	0.069
Providence-Fall River-Warwick, RI-MA MSA	0.091	0.087	0.105
Provo-Orem, UT MSA	0.083	0.077	0.076

Table 3-3 (cont'd). The Fourth Highest Daily Maximum Eight-Hour Ozone Concentration (ppm) by Metropolitan Statistical Area (MSA) or Consolidated Metropolitan Statistical Area (CMSA) for the Years 1999 to 2001

MSA/CMSA	1999	2000	2001
Raleigh-Durham-Chapel Hill, NC MSA	0.108	0.089	0.089
Reading, PA MSA	0.102	0.084	0.099
Redding, CA MSA	0.094	0.082	0.077
Reno, NV MSA	0.076	0.069	0.075
Richmond-Petersburg, VA MSA	0.100	0.083	0.091
Roanoke, VA MSA	0.089	0.081	0.089
Rochester, NY MSA	0.089	0.073	0.086
Rockford, IL MSA	0.082	0.070	0.078
Rocky Mount, NC MSA	0.092	0.085	0.085
Sacramento-Yolo, CA CMSA	0.106	0.103	0.105
Salinas, CA MSA	0.063	0.063	0.063
Salt Lake City-Ogden, UT MSA	0.080	0.080	0.084
San Antonio, TX MSA	0.091	0.082	0.081
San Diego, CA MSA	0.092	0.095	0.096
San Francisco-Oakland-San Jose, CA CMSA	0.088	0.077	0.081
San Luis Obispo-Atascadero-Paso Robles, CA MSA	0.077	0.070	0.073
Santa Barbara-Santa Maria-Lompoc, CA MSA	0.079	0.080	0.083
Sarasota-Bradenton, FL MSA	0.085	0.086	0.086
Savannah, GA MSA	0.083	0.079	0.067
Scranton-Wilkes-Barre-Hazleton, PA MSA	0.096	0.077	0.088
Seattle-Tacoma-Bremerton, WA CMSA	0.072	0.070	0.071
Sharon, PA MSA	0.091	0.081	0.094
Sheboygan, WI MSA	0.093	0.090	0.102
Shreveport-Bossier city, LA MSA	0.094	0.093	0.084
Sioux Falls, SD MSA	0.058	0.065	0.065
South Bend, IN MSA	0.090	0.081	0.089
Spokane, WA MSA	0.065	0.068	0.071
Springfield, IL MSA	0.075	0.079	0.073

Table 3-3 (cont'd). The Fourth Highest Daily Maximum Eight-Hour Ozone Concentration (ppm) by Metropolitan Statistical Area (MSA) or Consolidated Metropolitan Statistical Area (CMSA) for the Years 1999 to 2001

MSA/CMSA	1999	2000	2001
Springfield, MA MSA	0.094	0.079	0.093
Springfield, MO MSA	0.081	0.078	0.072
St. Louis, MO-IL MSA	0.102	0.088	0.088
State College, PA MSA	0.085	0.079	0.086
Steubenville-Weirton, OH-WV MSA	0.091	0.080	0.086
Stockton-Lodi, CA MSA	0.094	0.082	0.078
Syracuse, NY MSA	0.086	0.074	0.085
Tallahassee, FL MSA	0.081	0.076	0.074
Tampa-St. Petersburg-Clearwater, FL MSA	0.087	0.083	0.085
Terre Haute, IN MSA	0.082	0.075	0.083
Toledo, OH MSA	0.091	0.081	0.092
Tucson, AZ MSA	0.073	0.077	0.069
Tulsa, OK MSA	0.091	0.088	0.095
Tyler, TX MSA	0.097	0.087	0.082
Utica-Rome, NY MSA	0.078	0.067	0.084
Victoria, TX MSA	0.086	0.079	0.073
Visalia-Tulare-Porterville, CA MSA	0.108	0.105	0.104
Washington-Baltimore, DC-MD-VA-WV CMSA	0.113	0.099	0.112
Wausau, WI MSA	0.084	0.073	0.072
West Palm Beach-Boca Raton, FL MSA	0.079	0.075	0.073
Wheeling, WV-OH MSA	0.088	0.071	0.088
Wichita, KS MSA	0.079	0.080	0.084
Williamsport, PA MSA	0.076	0.073	0.080
Wilmington, NC MSA	0.067	0.080	0.078
York, PA MSA	0.094	0.090	0.087
Youngstown-Warren, OH MSA	0.095	0.080	0.093
Yuba City, CA MSA	0.090	0.083	0.084

Table 3-4. Seasonal (April–October) Percentile Distribution of Hourly Ozone Concentrations, Number of Hourly Mean Ozone Occurrences ≥ 0.08 and ≥ 0.10, SUM06, and W126 Values for Selected Rural Ozone Monitoring Sites in 2001. Concentrations in ppm.

			Percentiles									Hourly Mean O_3 Occurrences			
AIRS Site	Name	Min.	10	30	50	70	90	95	99	Max	No. of Hours	≥0.08	≥0.10	SUM06 (ppm-h)	W126 (ppm-h)
RURAL AGRICULTURAL															
170491001	Effingham Co., IL	0.000	0.007	0.021	0.031	0.041	0.056	0.063	0.074	0.094	5076	21	0	24.7	20.7
180970042	Indianapolis, IN	0.000	0.007	0.021	0.033	0.044	0.061	0.068	0.078	0.088	4367	37	0	34.2	25.8
240030014	Anne Arundel, MD	0.000	0.004	0.019	0.031	0.043	0.062	0.072	0.096	0.130	5059	142	34	43.5	35.7
310550032	Omaha, NE	0.000	0.015	0.023	0.030	0.038	0.050	0.056	0.064	0.085	5116	1	0	8.6	10.6
420070002	Beaver Co., PA	0.000	0.020	0.031	0.040	0.050	0.068	0.075	0.089	0.105	5080	156	6	63.2	50.0
510610002	Fauquier Co., VA	0.000	0.004	0.017	0.029	0.041	0.057	0.065	0.079	0.114	5055	48	1	27.4	22.7
551390011	Oshkosh Co., WI	0.002	0.015	0.026	0.035	0.043	0.057	0.065	0.082	0.100	4345	59	1	24.8	22.8
RURAL FOREST															
060430003	Yosemite NP, CA	0.013	0.038	0.046	0.052	0.058	0.069	0.074	0.084	0.114	4619	106	6	86.0	65.6
360310002	Whiteface Mtn., NY	0.000	0.024	0.035	0.043	0.051	0.063	0.070	0.084	0.113	4536	77	4	44.7	37.7
471550101	Smoky Mtns. NP, TN	0.020	0.039	0.050	0.057	0.064	0.075	0.080	0.089	0.106	5074	267	5	149.2	106.5
511130003	Shenandoah NP	0.010	0.035	0.045	0.052	0.059	0.070	0.075	0.089	0.107	4813	157	4	98.5	73.6
RURAL OTHER (I.E., RURAL RESIDENTIAL OR RURAL COMMERCIAL)															
060710005	Crestline, CA	0.000	0.024	0.043	0.055	0.068	0.093	0.107	0.135	0.170	4922	933	369	174.8	144.9
350431001	Sandoval Co., NM	0.000	0.004	0.020	0.033	0.045	0.056	0.061	0.070	0.091	5088	9	0	21.4	20.3
370810011	Guilford Co., NC	0.000	0.003	0.015	0.029	0.043	0.063	0.071	0.087	0.120	4879	111	10	45.4	334.4
371470099	Farmville, NC	—	0.000	0.008	0.021	0.033	0.044	0.061	0.068	0.078	0.097	4882	34	0	36.6

Table 3-5. Seasonal (April – October) Percentile Distribution of Hourly Ozone Concentrations (ppm), Number of Hourly Mean Ozone Occurrences ≥ 0.08 and ≥ 0.10, Seasonal 7-h Average Concentrations, SUM06, and W126 Values for Sites Experiencing Low Maximum Hourly Average Concentrations with Data Capture ≥ 75%

			Percentiles									Hourly Mean O_3 Occurrences				
Site	Year	Min.	10	30	50	70	90	95	99	Max	No. of Obs.	≥ 0.08	≥ 0.10	Seasonal 7-h	SUM06 (ppm-h)	W126 (ppm-h)
Redwood NP 060150002 (California) 235 m	1988	0.002	0.011	0.018	0.023	0.029	0.038	0.041	0.046	0.060	4825	0	0	0.026	1.8	0.1
	1989	0.000	0.010	0.017	0.022	0.027	0.034	0.038	0.042	0.047	4624	0	0	0.024	1.0	0.0
	1990	0.000	0.011	0.018	0.023	0.028	0.035	0.038	0.043	0.053	4742	0	0	0.025	1.2	0.0
	1991	0.001	0.012	0.019	0.025	0.031	0.038	0.041	0.045	0.054	4666	0	0	0.027	1.7	0.0
	1992	0.000	0.010	0.017	0.021	0.026	0.035	0.039	0.045	0.055	4679	0	0	0.023	1.1	0.0
	1993	0.000	0.010	0.017	0.022	0.027	0.035	0.038	0.042	0.054	4666	0	0	0.025	1.1	0.0
	1994	0.001	0.011	0.018	0.024	0.028	0.035	0.038	0.043	0.050	4846	0	0	0.026	0.0	1.2
Olympic NP (Washington) 530090012 125 m	1989	0.000	0.003	0.010	0.015	0.022	0.030	0.035	0.046	0.065	4220	0	0	0.021	0.7	0.1
	1990	0.000	0.005	0.012	0.018	0.023	0.030	0.034	0.043	0.064	4584	0	0	0.022	0.8	0.3
	1991	0.000	0.006	0.014	0.019	0.024	0.033	0.036	0.044	0.056	4677	0	0	0.025	0.9	0.0
	1993	0.000	0.004	0.010	0.016	0.021	0.029	0.034	0.041	0.064	4595	0	0	0.022	0.7	0.3
	1994	0.000	0.006	0.013	0.019	0.025	0.033	0.038	0.043	0.062	4044	0	0	0.025	0.2	0.8
	1995	0.000	0.006	0.014	0.020	0.027	0.037	0.040	0.048	0.077	4667	0	0	0.027	0.8	1.9
	1996	0.000	0.006	0.013	0.019	0.025	0.034	0.038	0.043	0.058	4811	0	0	0.025	0.0	1.0
	1997	0.000	0.005	0.010	0.015	0.022	0.035	0.040	0.046	0.057	4403					
	1998	0.000	0.008	0.014	0.019	0.025	0.033	0.037	0.044	0.063	4792	0	0	0.024	0.3	1.1
	1999	0.000	0.006	0.014	0.019	0.026	0.036	0.039	0.044	0.050	4656	0	0	0.024	0.0	1.1
	2000	0.000	0.006	0.013	0.019	0.025	0.035	0.039	0.045	0.061	4676	0	0	0.024	0.1	1.2
	2001	0.002	0.009	0.017	0.023	0.028	0.036	0.041	0.046	0.055	4643	0	0	0.027	0.0	1.4

Table 3-5 (cont'd). Seasonal (April – October) Percentile Distribution of Hourly Ozone Concentrations (ppm), Number of Hourly Mean Ozone Occurrences ≥0.08 and ≥0.10, Seasonal 7-h Average Concentrations, SUM06, and W126 Values for Sites Experiencing Low Maximum Hourly Average Concentrations with Data Capture ≥75%

			Percentiles									Hourly Mean O_3 Occurrences				
Site	**Year**	**Min.**	**10**	**30**	**50**	**70**	**90**	**95**	**99**	**Max**	**No. of Obs.**	**≥ 0.08**	**≥ 0.10**	**Seasonal 7-h**	**SUM06 (ppm-h)**	**W126 (ppm-h)**
Glacier NP	1989	0.000	0.003	0.015	0.026	0.036	0.046	0.050	0.058	0.067	4770	0	0	0.036	5.9	1.8
300298001 (Montana)	1990	0.000	0.003	0.014	0.026	0.035	0.044	0.047	0.052	0.066	5092	0	0	0.036	4.1	1.3
963 m	1991	0.000	0.001	0.014	0.027	0.036	0.046	0.049	0.056	0.062	5060	0	0	0.036	5.3	0.7
	1992	0.000	0.001	0.013	0.025	0.033	0.043	0.048	0.055	0.077	4909	0	0	0.033	4.1	1.0
	1993	0.000	0.000	0.010	0.020	0.029	0.040	0.044	0.050	0.058	5071	0	0	0.029	0.0	2.3
	1994	0.000	0.001	0.014	0.026	0.036	0.046	0.050	0.056	0.061	5072	0	0	0.036	0.1	5.4
	1995	0.000	0.000	0.010	0.022	0.031	0.041	0.045	0.051	0.066	4744	0	0	0.023	0.3	2.3
	1996	0.000	0.002	0.013	0.025	0.035	0.046	0.051	0.058	0.065	4666	0	0	0.035	1.9	5.4
	1997	0.000	0.000	0.008	0.017	0.026	0.041	0.045	0.053	0.058	4378	0	0	0.027	0.0	2.3
	1998	0.000	0.003	0.013	0.025	0.035	0.047	0.051	0.058	0.064	4649	0	0	0.036	1.4	5.6
	1999	0.000	0.002	0.015	0.026	0.035	0.046	0.051	0.058	0.068	4540	0	0	0.035	1.3	5.4
	2000	0.000	0.001	0.011	0.023	0.033	0.044	0.048	0.055	0.062	4551	0	0	0.033	0.7	3.8
	2001	0.000	0.000	0.013	0.025	0.033	0.042	0.044	0.049	0.057	4643	0	0	0.033	0.0	2.7
Yellowstone NP (Wyoming)	1988	0.002	0.020	0.029	0.037	0.044	0.054	0.058	0.070	0.098	4257	17	0	0.043	14.0	8.9
560391010	1989	0.002	0.018	0.027	0.036	0.044	0.052	0.057	0.063	0.071	4079	0	0	0.042	11.0	6.7
2484 m	1990	0.000	0.015	0.023	0.029	0.036	0.043	0.046	0.053	0.061	4663	0	0	0.034	3.8	0.5
	1991	0.004	0.020	0.030	0.037	0.042	0.048	0.051	0.057	0.064	4453	0	0	0.042	7.7	1.2
	1992	0.001	0.018	0.029	0.036	0.042	0.051	0.056	0.064	0.075	4384	0	0	0.042	10.7	6.3
	1993	0.000	0.018	0.028	0.036	0.042	0.047	0.050	0.054	0.060	4399	0	0	0.041	6.5	0.2
	1994	0.003	0.022	0.033	0.040	0.046	0.053	0.056	0.062	0.072	4825	0	0	0.046	6.0	15.2
	1995	0.004	0.022	0.033	0.040	0.045	0.052	0.055	0.059	0.065	4650	0	0	0.045	2.8	12.5

Table 3-5 (cont'd). Seasonal (April – October) Percentile Distribution of Hourly Ozone Concentrations (ppm), Number of Hourly Mean Ozone Occurrences ≥0.08 and ≥0.10, Seasonal 7-h Average Concentrations, SUM06, and W126 Values for Sites Experiencing Low Maximum Hourly Average Concentrations with Data Capture ≥75%

Site	Year	Min.	Percentiles 10	30	50	70	90	95	99	Max	No. of Obs.	Hourly Mean O_3 Occurrences ≥ 0.08	≥ 0.10	Seasonal 7-h	SUM06 (ppm-h)	W126 (ppm-h)
Yellowstone NP (Wyoming)	1997	0.005	0.026	0.035	0.040	0.045	0.051	0.054	0.060	0.068	4626	0	0	0.043	3.3	12.4
560391011 2468 m	1998	0.004	0.029	0.038	0.043	0.048	0.055	0.058	0.064	0.073	4827	0	0	0.046	9.9	20.0
	1999	0.012	0.033	0.040	0.046	0.051	0.059	0.062	0.069	0.079	4733	0	0	0.049	27.1	29.8
	2000	0.009	0.031	0.039	0.045	0.050	0.057	0.060	0.065	0.074	4678	0	0	0.047	17.0	23.4
	2001	0.012	0.034	0.041	0.046	0.050	0.057	0.060	0.065	0.078	4869	0	0	0.048	16.9	25.6
Denali NP (Alaska)	1988	0.003	0.018	0.024	0.028	0.033	0.044	0.050	0.053	0.056	4726	0	0	0.031	0.0	4.0
022900003 640 m	1990	0.003	0.017	0.024	0.029	0.034	0.040	0.043	0.048	0.050	3978	0	0	0.030	2.1	0.0
	1991	0.005	0.018	0.024	0.028	0.034	0.041	0.043	0.047	0.057	4809	0	0	0.030	2.7	0.0
	1992	0.003	0.016	0.023	0.028	0.034	0.044	0.047	0.050	0.054	4800	0	0	0.031	3.7	0.0
	1993	0.002	0.017	0.023	0.028	0.033	0.041	0.043	0.048	0.055	4773	0	0	0.030	2.6	0.0
	1994	0.003	0.017	0.022	0.027	0.033	0.042	0.045	0.049	0.053	4807	0	0	0.030	0.0	2.9
	1995	0.001	0.013	0.019	0.025	0.032	0.042	0.044	0.052	0.059	4825	0	0	0.028	0.0	3.0
	1996	0.002	0.015	0.022	0.028	0.035	0.044	0.047	0.052	0.063	4831	0	0	0.031	0.1	4.1
	1997	0.001	0.015	0.023	0.030	0.038	0.045	0.048	0.051	0.084	4053	1	0	0.032	0.2	4.0
	1998	0.004	0.018	0.023	0.030	0.036	0.048	0.050	0.055	0.058	4782	0	0	0.032	0.0	6.0
	1999	0.002	0.016	0.024	0.029	0.036	0.045	0.048	0.054	0.058	4868	0	0	0.032	0.0	4.7
	2000	0.003	0.014	0.019	0.025	0.029	0.034	0.036	0.038	0.049	4641	0	0	0.025	0.0	1.0
	2001	0.002	0.016	0.023	0.029	0.036	0.048	0.051	0.055	0.068	4868	0	0	0.032	0.7	11.1
Badlands NP 460711001	1989	0.006	0.020	0.027	0.034	0.041	0.049	0.053	0.060	0.071	4840	0	0	0.040	9.2	3.1
(South Dakota) 730 m	1990	0.006	0.019	0.027	0.032	0.037	0.044	0.048	0.054	0.063	4783	0	0	0.037	4.8	0.8
	1991	0.005	0.020	0.028	0.033	0.040	0.047	0.050	0.056	0.066	4584	0	0	0.038	6.2	0.7

Table 3-5 (cont'd). Seasonal (April – October) Percentile Distribution of Hourly Ozone Concentrations (ppm), Number of Hourly Mean Ozone Occurrences ≥0.08 and ≥0.10, Seasonal 7-h Average Concentrations, SUM06, and W126 Values for Sites Experiencing Low Maximum Hourly Average Concentrations with Data Capture ≥75%

Site	Year	Min.	Percentiles 10	30	50	70	90	95	99	Max	No. of Obs.	Hourly Mean O_3 Occurrences ≥ 0.08	≥ 0.10	Seasonal 7-h	SUM06 (ppm-h)	W126 (ppm-h)
Theod. Roos. NP 380530002 (North Dakota) 730 m	1984	0.000	0.017	0.025	0.032	0.039	0.047	0.050	0.059	0.068	4923	0	0	0.038	7.0	2.8
	1985	0.000	0.019	0.026	0.032	0.038	0.046	0.049	0.054	0.061	4211	0	0	0.038	5.0	0.1
	1986	0.004	0.017	0.027	0.033	0.039	0.047	0.050	0.056	0.062	4332	0	0	0.039	5.5	0.4
	1989	0.004	0.023	0.032	0.039	0.045	0.054	0.058	0.065	0.073	4206	0	0	0.046	14.2	11.0
	1992	0.005	0.019	0.027	0.033	0.039	0.047	0.050	0.056	0.063	4332	0	0	0.040	6.1	0.8
	1993	0.004	0.018	0.025	0.031	0.037	0.045	0.048	0.055	0.064	4281	0	0	0.038	4.6	0.7
	1994	0.000	0.018	0.028	0.035	0.041	0.049	0.052	0.058	0.079	4644	0	0	0.041	1.1	8.4
	1995	0.000	0.018	0.028	0.035	0.041	0.050	0.053	0.058	0.064	4242	0	0	0.042	1.2	7.7
	1996	0.003	0.022	0.031	0.037	0.043	0.051	0.054	0.059	0.064	3651	0	0	0.044	1.8	8.5
	1997	0.000	0.016	0.029	0.037	0.044	0.053	0.058	0.069	0.082	4344	8	0	0.046	11.8	14.6
Theod. Roos. NP 380070002 (North Dakota) 808 m	1999	0.007	0.024	0.031	0.037	0.042	0.049	0.052	0.058	0.070	5105	0	0	0.041	1.6	10
	2000	0.002	0.021	0.031	0.036	0.043	0.050	0.053	0.058	0.066	5105	0	0	0.041	2.3	10.5
	2001	0.002	0.023	0.031	0.036	0.042	0.049	0.052	0.058	0.064	5099	0	0	0.041	1.9	9.2
Custer NF, MT 300870101 (Montana) 1006 m	1978	0.000	0.010	0.020	0.035	0.040	0.050	0.055	0.060	0.070	4759	0	0	0.033	3.0	8.3
	1979	0.010	0.025	0.035	0.040	0.045	0.050	0.055	0.060	0.075	5014	0	0	0.043	7.3	13.2
	1980	0.010	0.025	0.035	0.040	0.050	0.055	0.060	0.065	0.070	4574	0	0	0.043	22.4	19.7
	1983	0.010	0.025	0.035	0.040	0.045	0.05	0.055	0.060	0.065	4835	0	0	0.042	4.2	10.7

concentrations ≥ 0.08 ppm. Ozone hourly average concentrations rarely exceed 0.08 ppm at remote monitoring sites in the western United States. In almost all cases for the above sites, the maximum hourly average concentration was ≤ 0.075 ppm.

The highest hourly average concentrations at several relatively remote monitoring sites do not necessarily occur during the summer months. Similarly, the highest 8-h daily maximum concentrations do not necessarily all occur during the summer. For example, at the Yellowstone National Park site, the first three 8-h daily maximum concentrations occurred in April and May in 1998, and the fourth highest 8-h daily maximum concentration did not occur until July of that year. In 1999, the first three highest 8-h daily maximum concentrations were observed in March and May, and the fourth highest value occurred in April. In 2000, the four highest values occurred in May, June, July, and August.

It is questionable whether the distributions experienced at sites exhibiting low maximum hourly average concentrations in the western United States are representative of sites in the eastern and midwestern United States because of regional differences in sources of precursors and transport patterns. Given the high density of sources in the eastern and midwestern United States, it is unclear whether a site could be found in either of these regions that would not be influenced by the transport of O_3 from urban areas. Thus, with the exception of the Voyageurs National Park site in Minnesota, observations at relatively remote monitoring sites are limited to those obtained in the western United States.

Based on data collected in the 1970s to the mid-1990s, consistent trends in tropospheric O_3 have not been observed at the cleanest sites in the Northern Hemisphere. When assessing possible trends at clean sites, specific attention must be given to the possibility of long-range transport from urban centers. For example, the trends at Whiteface Mountain could provide evidence that background O_3 concentrations have risen by a few ppb in surface air over the United States during the past two decades. However, these trends are probably associated with the transport of regional pollution to the site. The site experiences elevated levels of O_3 during the summer months, and the area is currently designated as in nonattainment for the 1-h standard.

Using (1) a 15-year record of O_3 from Lassen Volcanic National Park, (2) data from two aircraft campaigns, and (3) observations spanning 18 years from five United States west coast marine boundary layer sites, Jaffe et al. (2003) have estimated that the amount of O_3 in air arriving from the Eastern Pacific in spring has increased by approximately 10 ppb from the mid-1980s to the present. This positive trend might be due to increases of emissions of O_3 precursors in Asia. Positive trends in O_3 were found during all seasons. Although the Lassen Volcanic National Park site is not close to any major emission sources or urban centers, it experiences maximum hourly average O_3 concentrations > 0.080 ppm during April-May and > 0.100 ppm during the summertime, suggesting local photochemical production, at least during the summertime. Elevated levels of O_3 occur in the areas to the west (Redding, CA) and to the south (Chico, CA; Tuscan, CA; Red Bluff, CA) of the park site. Hourly average concentration levels occur in the 0.080 to 0.099 ppm range during April and May, and they can be above 0.100 ppm during the summertime at these locations.

Since emissions of O_3 precursors have decreased in California, one of the reasons suggested for the springtime increases in O_3 at Lassen is transport from Asia. However, although emissions of O_3 precursors may have decreased in California as a whole over the monitoring period, there still may be regional increases in areas that could affect air quality in Lassen Volcanic National Park. Thus, at this time, although there is evidence as reported in the literature that some rural locations may be experiencing increasing levels of O_3, there is also evidence that O_3 concentrations at relatively remote monitoring sites, as reported in the chapter, have not increased over the period of record.

3.3 DIURNAL VARIABILITY OF OZONE

Diurnal patterns of O_3 may be expected to vary with location, depending on the balance among the many factors affecting O_3 formation, transport, and destruction. Although they vary with locality, diurnal patterns for O_3 typically show a rise in concentration from low (or levels near minimum detectable amounts) to an early afternoon peak at lower elevation monitoring sites. The 1978 O_3 AQCD (U.S. Environmental Protection Agency, 1978) ascribed the diurnal pattern of concentrations to three simultaneous processes: (1) downward transport of O_3 from layers aloft, (2) destruction of O_3 through contact with surfaces and through reaction with nitric oxide (NO) at ground level, and (3) in situ photochemical production and destruction of O_3.

The form of the average diurnal pattern may provide information on sources, transport, and chemical formation and destruction effects at various sites. Atmospheric conditions leading to limited transport from source regions will produce early afternoon peaks. However, long-range transport processes shift the occurrence of a peak from afternoon to evening or early morning hours.

The U.S. Environmental Protection Agency (1996) discussed diurnal patterns for urban sites. An example was provided for a Philadelphia site for July 13, 1979. On this day, a peak 1-h average concentration of 0.20 ppm, the highest for the month, was reached at 1400 hours, presumably as the result of meteorological factors, such as atmospheric mixing and local photochemical processes. The severe depression of concentrations to below detection limits (less than 0.005 ppm) between 0300 and 0600 hours usually is explained as resulting from the scavenging of O_3 by local NO emissions. In this regard, this site is typical of most urban sites. Diurnal profiles of O_3 can vary from day to day at a specific site because of changes in the various factors that influence concentrations. Composite diurnal data (i.e., concentrations for each hour of the day averaged over multiple days or months) often differ markedly from the diurnal cycle shown by concentrations for a specific day. For urban sites, maximum diurnal variability occurs in the third quarter.

Nonurban O_3 monitoring sites experience differing types of diurnal patterns depending on their location relative to urban source regions. Thus, considerable variations in O_3 concentrations are found among sites characterized as agricultural or forested. Nonurban areas are more likely to show flatter diurnal patterns than sites located in urban areas. Such patterns are based on average concentrations calculated over an extended period and, as indicated earlier, caution is urged in drawing conclusions concerning whether some monitoring sites experience higher cumulative O_3 exposures than other sites. On a daily basis, variations in O_3 concentrations occur from hour to hour, and, in some cases, elevated hourly average concentrations are experienced either during the daytime or nighttime. Because the diurnal patterns represent averaged concentrations calculated over an extended period, the smoothing caused by the averaging tends to mask the elevated hourly average concentrations.

The current forms of the O_3 standards focus on both the highest hourly average concentrations (1-h standard) and, for many monitoring sites, the mid-level hourly average concentrations (8-h standard). Examples provided in this chapter show that urban monitoring sites show a tendency for the highest maximum hourly average concentration to occur from June to August (Figure 3-3). Due to meteorological and other factors, the absolute magnitude of the

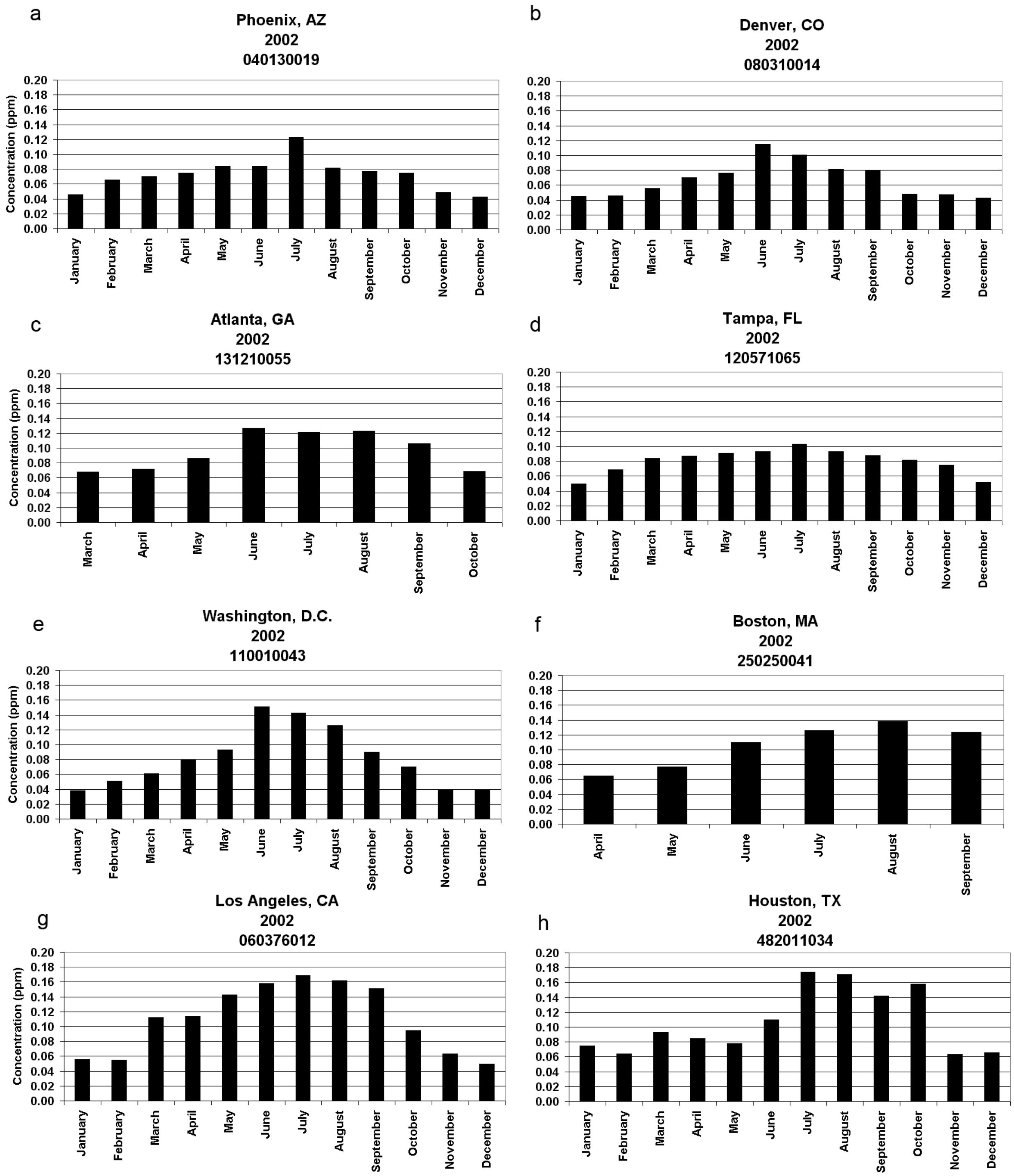

Figure 3-3a-h. Seasonal variations in O_3 concentrations as indicated by the 1-h maximum in each month at selected sites in 2002.

Source: U.S. Environmental Protection Agency (2003a).

maximum hourly average concentrations varies from year to year. For nonurban areas, it is not possible to predict the quarter in which the highest hourly average concentrations occur. There is a tendency for relatively remote monitoring sites to experience their highest average O_3 concentrations during the second quarter (i.e., the months of April or May) versus the third quarter of the year ad for urban sites.

3.4 SPATIAL VARIABILITY OF OZONE

The spatial variability in O_3 concentrations in nine MSAs across the United States was examined. These MSAs were selected to provide (1) information helpful for risk assessments, (2) a general overview of the spatial variability of O_3 in different regions of the country, and (3) insight in to the spatial distribution of O_3 in cities where health outcome studies have been conducted. Statistical analyses of the human health effects of airborne pollutants based on aggregate population time-series data have often relied on ambient concentrations of pollutants measured at one or more central sites in a given metropolitan area. In the particular case of ground-level O_3 pollution, central-site monitoring has been justified as a regional measure of exposure partly on the grounds that correlations between concentrations at neighboring sites measured over time are usually high. In analyses where multiple monitoring sites monitor ambient O_3 concentrations, a summary measure, such as an average, has often been regarded as adequately characterizing the exposure distribution.

For quantifying spatial variability, there were no clearly discernible regional differences in the ranges of parameters analyzed (Table 3-6). Additional urban areas would need to be examined to discern broadscale patterns. The data indicate considerable variability in the concentrations fields. Seasonal means vary within individual urban areas by factors of 1.4 to 4. Intersite correlation coefficients show mixed patterns (i.e., in some urban areas all pairs of sites are moderately to highly correlated and in other areas there is a larger range of correlations). As may be expected, those areas showing a smaller range of seasonal mean concentrations also show a smaller range of intersite correlation coefficients. However, there are a number of cases where sites in an urban area may be moderately to highly correlated, but show substantial differences in absolute concentrations. In many cases, values for the P_{90} can equal or exceed seasonal mean O_3 concentrations.

Table 3-6. Summary Statistics for O_3 (in ppm) Spatial Variability in Selected Urban Areas in the United States

Urban Area	Number of Sites	Minimum Mean Conc.	Maximum Mean Conc.	Minimum Corr. Coeff.	Maximum Corr. Coeff.	Minimum P_{90} [a]	Maximum P_{90}	Minimum COD [b]	Maximum COD
Boston, MA	18	0.021	0.033	0.46	0.93	0.012	0.041	0.17	0.45
New York, NY	29	0.015	0.041	0.45	0.96	0.0080	0.044	0.17	0.55
Philadelphia, PA	12	0.020	0.041	0.79	0.95	0.011	0.036	0.23	0.46
Washington, DC	20	0.022	0.041	0.72	0.97	0.010	0.032	0.17	0.45
Charlotte, NC	8	0.031	0.043	0.48	0.95	0.012	0.038	0.17	0.32
Atlanta, GA	12	0.023	0.047	0.63	0.94	0.013	0.045	0.24	0.55
Tampa, FL	9	0.024	0.035	0.74	0.94	0.011	0.025	0.20	0.35
Detroit, MI	7	0.022	0.037	0.74	0.96	0.0090	0.027	0.19	0.36
Chicago, IL	24	0.015	0.039	0.38	0.96	0.0080	0.043	0.16	0.50
Milwaukee, WI	9	0.027	0.038	0.73	0.96	0.0090	0.025	0.18	0.33
St. Louis, MO	17	0.022	0.038	0.78	0.96	0.0090	0.031	0.15	0.41
Baton Rouge, LA	7	0.018	0.031	0.81	0.95	0.0090	0.029	0.23	0.41
Dallas, TX	10	0.028	0.043	0.67	0.95	0.011	0.033	0.16	0.36
Houston, TX	13	0.016	0.036	0.73	0.96	0.0090	0.027	0.20	0.38
Denver, CO	8	0.022	0.044	0.60	0.92	0.013	0.044	0.16	0.46
El Paso, TX	4	0.022	0.032	0.81	0.94	0.012	0.023	0.24	0.31
Salt Lake City, UT	8	0.029	0.048	0.52	0.92	0.012	0.043	0.13	0.51
Phoenix, AZ	15	0.021	0.058	0.29	0.95	0.011	0.057	0.15	0.61
Seattle, WA	5	0.015	0.038	0.63	0.94	0.0080	0.024	0.16	0.46
Portland, OR	5	0.015	0.036	0.73	0.91	0.011	0.025	0.20	0.50
Fresno, CA	6	0.030	0.047	0.90	0.97	0.0090	0.027	0.17	0.40
Bakersfield, CA	8	0.028	0.047	0.23	0.96	0.013	0.052	0.20	0.58
Los Angeles, CA	14	0.010	0.042	0.42	0.95	0.010	0.053	0.22	0.59
Riverside, CA	18	0.018	0.054	0.38	0.95	0.013	0.057	0.15	0.64

[a] P_{90} = 90th percentile absolute difference in concentrations.
[b] COD = coefficient of divergence for different site pairs.

3.5 TRENDS IN OZONE CONCENTRATIONS

Ozone concentrations and, thus, O_3 exposures, change from year to year. From 1983 to 2002, extremely high O_3 levels occurred in 1983 and 1988 in some areas of the United States (Figures 3-4 and 3-5). These levels were likely due, in part, to hot and dry, stagnant weather conditions. The annual second highest 1-h average O_3 concentrations were the lowest in 2000 (U.S. Environmental Protection Agency, 2003b). These low levels may have been due to meteorological conditions that were less favorable for O_3 formation and to recently implemented control measures. For the period 1983 to 2002, 1-h and 8-h O_3 concentrations decreased in most areas of the country. On a nationwide basis, a 22% decrease was observed in the second highest 1-h average concentration and a 14% decrease in the annual fourth highest annual daily maximum concentration was observed from 1983 to 2002. The Northeast and Pacific Southwest exhibited the most substantial improvement for 1-h and 8-h O_3 levels. The Mid-Atlantic and North Central regions experienced minimal decreases in 8-h O_3 levels. In contrast, the Pacific Northwest region showed a slight increase in 8-h O_3 concentrations.

From 1993 to 2002, the nationwide trend in 8-h O_3 concentration shows a 4% increase, and the nationwide trend in 1-h O_3 shows a 2% decrease. However, these trends were not statistically significant. Ozone concentrations varied slightly during this 10-year period but, overall, showed no significant change.

Regional trends provide additional information that can increase our understanding of the patterns of change of O_3 levels (Section AX3). The trend in 8-h O_3 concentrations for the Pacific Southwest shows a 29% decrease from 1983 to 2002. When considering the Los Angeles area separately, the trend for Los Angeles shows a 49% decrease for the same 20-year period, with a 15% decrease for other locations in the Pacific Southwest. For 1993 to 2002, the Pacific Southwest experienced an overall 13% decrease in 8-h O_3. However, when considering Los Angeles separately, the Los Angeles area shows a 28% decrease for the 10-year period, while the Pacific Southwest without Los Angeles has a 5% decrease.

It is important to note that year-to-year changes in ambient O_3 trends are influenced by meteorological conditions, population growth, and changes in emission levels of O_3 precursors (i.e., volatile organic compounds [VOCs] and NO_x) resulting from ongoing control measures. On a nationwide basis, the trends analyses provide an indication that a slowing down of improvement in O_3 air quality has occurred. Information provided in the literature indicates that

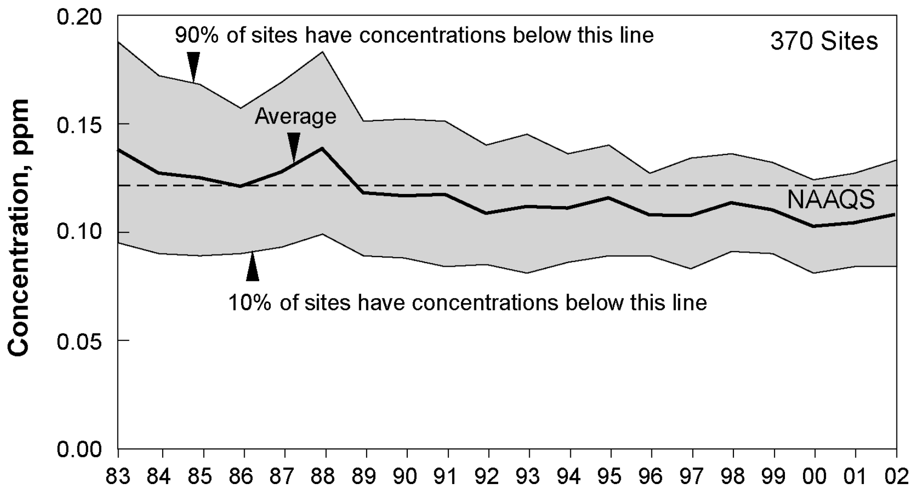

1983–2002: 22% decrease
1993–2002: 2% decrease

Figure 3-4. Trends for 1983 – 2002 period for the annual second maximum 1-h average concentration.

Source: U.S. Environmental Protection Agency (2003b).

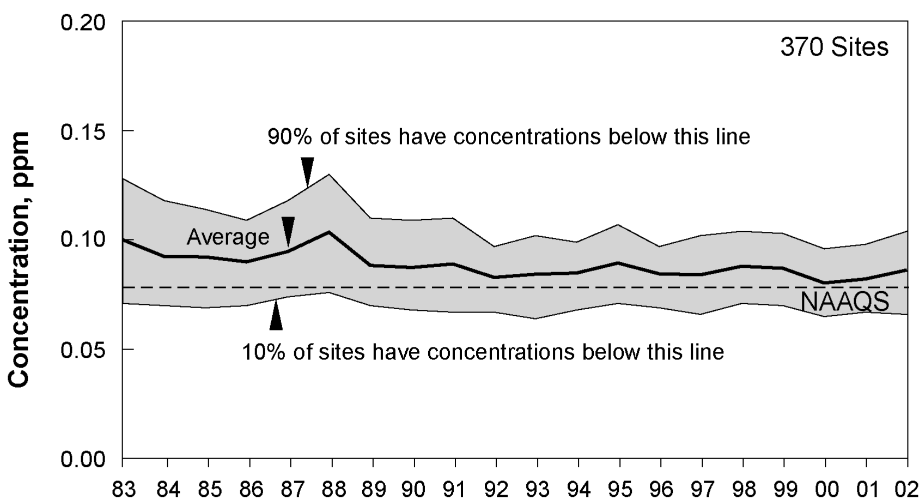

1983–2002: 14% decrease
1993–2002: 4% increase

Figure 3-5. Trends for 1983 – 2002 period for the annual fourth maximum 8-h average concentration.

Source: U.S. Environmental Protection Agency (2003b).

the higher concentrations may be reduced at a faster rate than the lower values. Using models, several investigators have commented on the difficulty in reducing the mid-level hourly average concentrations while reducing the fourth highest 8-h average daily maximum concentration. Using ambient O_3 concentrations in conjunction with photochemical models to determine the technical feasibility of reducing hourly average concentrations, some investigators have reported that various combinations of VOCs and NO_x emission reductions were effective in lowering modeled peak 1-h O_3 concentrations. However, VOC emissions reductions were found to have only a modest impact on modeled peak 8-h O_3 concentrations. It has been reported that 70 to 90% NO_x emissions reductions were required to reduce peak 8-h O_3 concentrations to the desired level. Some investigators have noted that when anthropogenic VOC and NO_x emissions are reduced significantly, the primary sources of O_3 precursors are biogenic emissions and CO from anthropogenic sources. Chemical process analysis results indicated that slowly reacting pollutants such as CO could be contributing from 10 to 20% of the O_3 produced. Several investigators have proposed that the effect of Asian emissions on surface O_3 concentrations might be responsible for explaining the inability of the emissions reductions to effect a rapid change in the mid-level concentrations. However, as described in the chapter, inconsistent trends results do not indicate that either the low or the high end of the hourly average concentration distributions are increasing and, thus, the effect of Asian emissions on surface O_3 concentrations in the western United States is not clear at this time.

U.S. Environmental Protection Agency (2003b) reported that 28 of the national parks in the United States had sufficient O_3 data for calculating trends for the 10-year period 1993 to 2002. Seven monitoring sites in five of these parks experienced statistically significant upward trends in 8-h O_3 levels: Great Smoky Mountains (Tennessee), Craters of the Moon (Idaho), Mesa Verde (Colorado), Denali (Alaska), and Acadia (Maine). Monitoring data for one park, Saguaro (Arizona), showed statistically significant improvements over the same time period. For the remaining 22 parks with O_3 trends data, the 8-h O_3 levels at 13 parks increased only slightly between 1993 and 2002, while five parks showed decreasing levels and four showed levels unchanging. Using all available data for the national parks, additional analyses of the hourly average concentration data were performed to characterize trends using the (a) seasonal W126 and SUM06 cumulative exposure indices, (b) fourth highest of the 1-h daily maximum average concentrations over a 3-year period for January through December, and (c) 3-year average of the fourth highest daily maximum 8-h average concentration.

Table 3-7 summarizes the results of the analysis. Caution is urged in interpreting the table. The use of the significance levels 0.2, 0.1, and 0.05 indicates varying levels of uncertainty. As indicated above, the use of a specific concentration index (e.g., 8-h average concentration) will provide a different history than the use of an alternative index, such as the W126 or SUM06 cumulative exposure index. Both the 1-h and 8-h indices are extreme value metrics that focus on the highest levels in the distribution of the hourly average concentrations. On the other hand, the W126 and SUM06 exposure indices accumulate the hourly average concentrations mainly in the upper half of the distribution. Changes in the magnitude of the extreme value statistics may or may not result in a significant change in the entire percentile distribution of the hourly average concentrations.

3.6 RELATIONSHIPS BETWEEN OZONE AND OTHER SPECIES

Correlations between Ozone and other Species

In order to understand relationships among atmospheric species, an important distinction must be made between primary (directly emitted) species and secondary (photochemically produced) species. In general, it is more likely that primary species will be more highly correlated with each other, and that secondary species will be more highly correlated with each other. By contrast, primary species are less likely to be correlated with secondary species. Secondary reaction products tend to correlate with each other, but there is considerable variation. Some species (e.g., O_3 and organic nitrates) are closely related photochemically and correlate with each other strongly. Others (e.g., O_3 and H_2O_2) show a more complex correlation pattern. Further details are given in Annex AX3 in Section AX3.7.

Relationships between primary and secondary components are illustrated by considering data for O_3 and $PM_{2.5}$. Ozone and $PM_{2.5}$ concentrations observed at a monitoring site in Fort Meade, MD are plotted as conditional means in Figure 3-6, based on data collected between July 1999 and July 2001. As can be seen from the figure, $PM_{2.5}$ tends to be negatively correlated with O_3 to the left of the inflection point (at about 30 ppbv O_3) and tends to be positively correlated with O_3 to the right of the inflection point. Data to the left of the minimum in $PM_{2.5}$ were

Table 3-7. Trends at National Parks in the United States (1981 – 2001 or available data period)

Site	AIRS ID	W126 (Seasonal)	SUM06 (Seasonal)	8-h (Annual)	1-h (Annual)
Acadia NP	230090003	NS	NS	NS	NS
Acadia NP ACAD	230090101	NS	NS	*(-)	***(-)
Acadia NP Cadillac Mountain	230090102			*(+)	NS
Acadia NP MARS/PRIMENet Site	230090103	NS	NS	NS	**(-)
Big Bend NP BIBE	480430101	NS	NS	NS	NS
Brigantine (FWS) BRIG	340010005	***(-)	***(-)	***(-)	***(-)
Canyonlands NP CANY	490370101	***(+)	***(+)	*(+)	**(+)
Cape Cod NS CACO	250010002	NS	NS	NS	***(-)
Cape Romain (FWS) CARO	450190046	NS	NS	NS	NS
Chamizal NMEM CHAM	481410044	***(+)	**(+)	NS	NS
Channel Islands NP CHIS	060832012	NS	NS	NS	***(-)
Chiricahua NM (NDDN CNM167)	040038001	NS	*(+)	NS	**(-)
Congaree Swamp NM COSW	450791006	NS	NS	*(-)	*(-)
Cowpens NB COWP	450210002	*(+)	*(+)	NS	*(+)
Craters of the Moon NM CRMO	160230101	*(+)	NS	***(+)	NS
Death Valley NP DEVA	060270101	NS	NS	NS	NS
Denali NP DENA	022900003	NS	NS	*(+)	NS
Everglades NP EVER	120250030	NS	NS	NS	*(-)
Glacier NP (NDDN GNP168) GLAC	300298001	NS	NS	NS	NS
Great Basin NP GRBA	320330101	**(+)	*(+)	NS	NS

Table 3-7 (cont'd). Trends at National Parks in the United States (1981 – 2001 or available data period)

Site	AIRS ID	W126 (Seasonal)	SUM06 (Seasonal)	8-h (Annual)	1-h (Annual)
Grand Canyon NP (NDDN GCN174)	040058001	NS	*(+)	NS	NS
Great Smoky Mountains NP (Cades Cove) GSCC	470090102	NS	NS	NS	
Great Smoky Mountains NP (Clingmans Dome) GSCD	471550102			NS	NS
Great Smoky Mountains NP (Cove Mountain) GSCM	471550101	**(+)	**(+)	***(+)	***(+)
Great Smoky Mountains NP (Look Rock) GSLR	470090101	***(+)	**(+)	NS	***(+)
Hawaii Volcanoes NP HAVO	150010005			NS	NS
Joshua Tree NP	060719002	***(-)	*(-)	***(-)	***(-)
Lassen Volcanic NP LAVO	060893003	**(+)	NS	NS	NS
Mammoth Cave NP MACA	210610500	NS	NS	**(-)	NS
Mammoth Cave NP MACA	210610501	NS	NS	*(-)	**(-)
Mesa Verde NP MEVE	080830101	**(+)	*(+)	NS	***(+)
Mount Rainier NP MORA	530531010	NS	NS	NS	NS
North Cascade NP NOCA	530570013	NS	NS	NS	**(+)
Olympic NP OLYM	530090012	NS	NS	NS	*(-)
Petrified Forest NP PEFO	040010012	NS	NS	NS	***(+)
Pinnacles NM PINN	060690003	*(-)	**(-)	**(-)	***(-)
Rocky Mountain NP ROMO	080690007	***(+)	***(+)	NS	*(+)
Saguaro NM SAGU	040190021	NS	NS	NS	**(-)
Sequoia/Kings Canyon NPs (Ash Mountain) SEAM	061070005	***(-)	***(-)	NS	NS
Sequoia/Kings Canyon NPs (Lookout Point) SELP	061070008			NS	NS

Table 3-7 (cont'd). Trends at National Parks in the United States (1981 – 2001 or available data period)

Site	AIRS ID	W126 (Seasonal)	SUM06 (Seasonal)	8-h (Annual)	1-h (Annual)
Sequoia/Kings Canyon NPs (Lower Kaweah) SELK	061070006	NS	NS	NS	NS
Shenandoah NP (Big Meadows) SVBM	511130003	NS	NS	NS	***(+)
Voyageurs NP VOYA	271370034	**(-)	**(-)	*(-)	***(-)
Yellowstone NP YELL	560391010	NS	NS	NS	NS
Yellowstone NP YELL	560391011	NS	NS	NS	**(+)
Yosemite NP (Camp Mather) YOCM	061090004			*(+)	***(0)
Yosemite NP (Turtleback Dome) YOTD	060430003	NS	NS	***(-)	***(-)
Yosemite NP (Wawona Valley) YOWV	060430004	*(-)	*(-)	***(-)	**(-)

* 0.20 level of significance
** 0.10 level of significance
*** 0.05 level of significance
NS Not significant

W126 (seasonal) = cumulative W126 exposure (as described by Lefohn and Runeckles [1987]) over a 24-h period for the period April – October.
SUM06 (seasonal) = cumulative exposure of hourly average concentrations $\geq$ 0.06 ppm over a 24-h period for the April – October period.
8-h (annual) = 3-year average of the fourth highest 8-h daily maximum average concentration for January – December.
1-h (annual) = fourth highest 1-h daily maximum average concentration over a 3-year period for January – December.

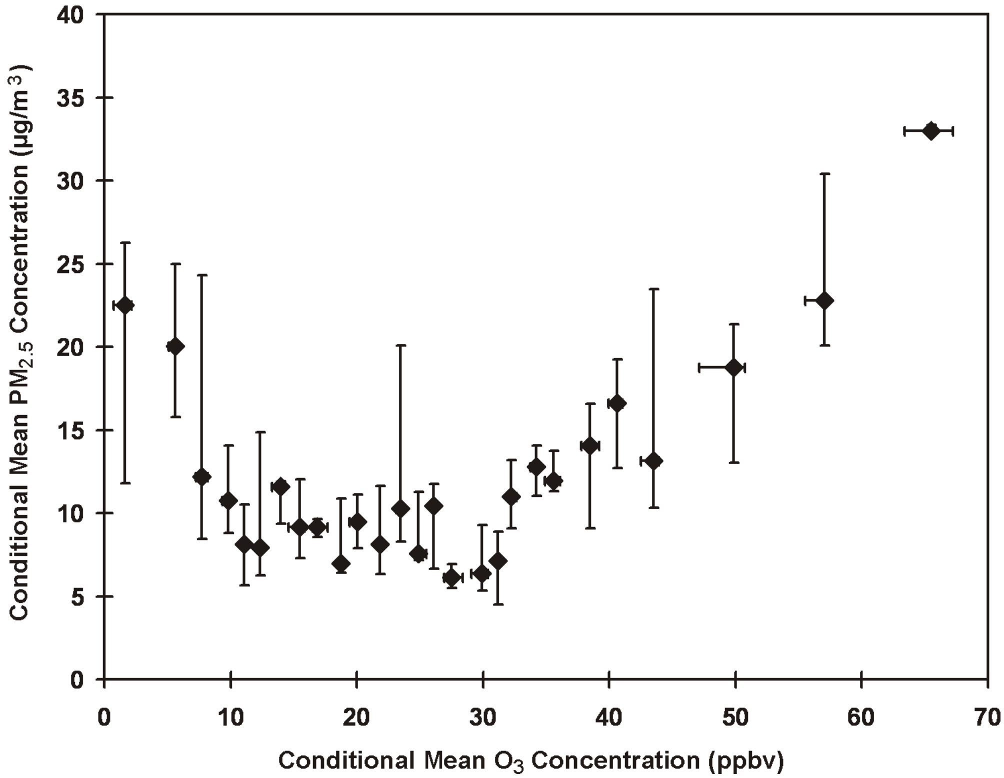

Figure 3-6. Conditional mean $PM_{2.5}$ concentrations versus O_3 concentrations observed at Fort Meade, MD from July 1999 to July 2001.

Source: Chen (2002).

collected mainly during the cooler months of the year, while data to the right of the minimum were collected during the warmer months. This situation arises because $PM_{2.5}$ contains a large secondary component during the summer, and has a larger primary component during winter. During the winter, O_3 comes mainly from the free troposphere, above the planetary boundary layer and, thus, may be considered a tracer for relatively clean air, and it is titrated with NO in the polluted boundary layer. Unfortunately, data for $PM_{2.5}$ and O_3 are collected concurrently at relatively few sites in the United States throughout an entire year, so these results, while highly instructive are not readily extrapolated to areas where appreciable photochemical activity occurs throughout the year.

Co-Occurrence of Ozone with other Pollutants

The characterization of co-occurrence patterns under ambient conditions is important for relating human health and vegetation effects under ambient conditions to controlled research results as described in Annex AX3.8. Several attempts have been made to characterize gaseous air pollutant mixtures. The previous 1996 O_3 AQCD discussed various patterns of pollutant mixtures of SO_2, NO_2, and O_3. Pollutant combinations can occur at or above a threshold concentration at either the same or different times.

The 1996 O_3 AQCD noted that studies of the joint occurrence of gaseous NO_2/O_3 and SO_2/O_3 reached two conclusions: (1) hourly simultaneous and daily simultaneous-only co-occurrences are fairly rare (when both pollutants were present at an hourly average concentration $\geq$ 0.05 ppm) and (2) when co-occurrences are present, complex-sequential and sequential-only co-occurrence patterns predominate. Year-to-year variability was found to be insignificant.

Using 2001 hourly data for O_3 and NO_2, the co-occurrence patterns for the data show similar results from previous studies; most of the collocated monitoring sites experienced fewer than 10 co-occurrences as shown in Figure 3-7. Using 2001 data, co-occurrence analyses for O_3 and SO_2 showed results similar to those published previously - that most of the collocated monitoring sites analyzed experienced fewer than 10 co-occurrences, as shown in Figure 3-8.

Since 1999, monitoring stations across the United States have routinely measured 24-h average concentrations for $PM_{2.5}$. Daily co-occurrence of $PM_{2.5}$ and O_3 over a 24-h period was also characterized. Because $PM_{2.5}$ data are mostly summarized as 24-h average concentrations in the AQS database, a daily co-occurrence of O_3 and $PM_{2.5}$ was subjectively defined as an hourly average O_3 concentration $\geq$ 0.05 ppm and a $PM_{2.5}$ 24-h concentration $\geq$ 40 $\mu g/m^3$ (corresponding to the EPA's Air Quality Index, Level of Concern for $PM_{2.5}$) occurring during the same 24-h period. Using 2001 data from the AQS database, the daily co-occurrence of $PM_{2.5}$ and O_3 was infrequent (Figure 3-9). There are limited data available on the co-occurrence of O_3 and other pollutants (e.g., acid precipitation and acidic cloudwater). In most cases, routine monitoring data are not available from which to draw general conclusions.

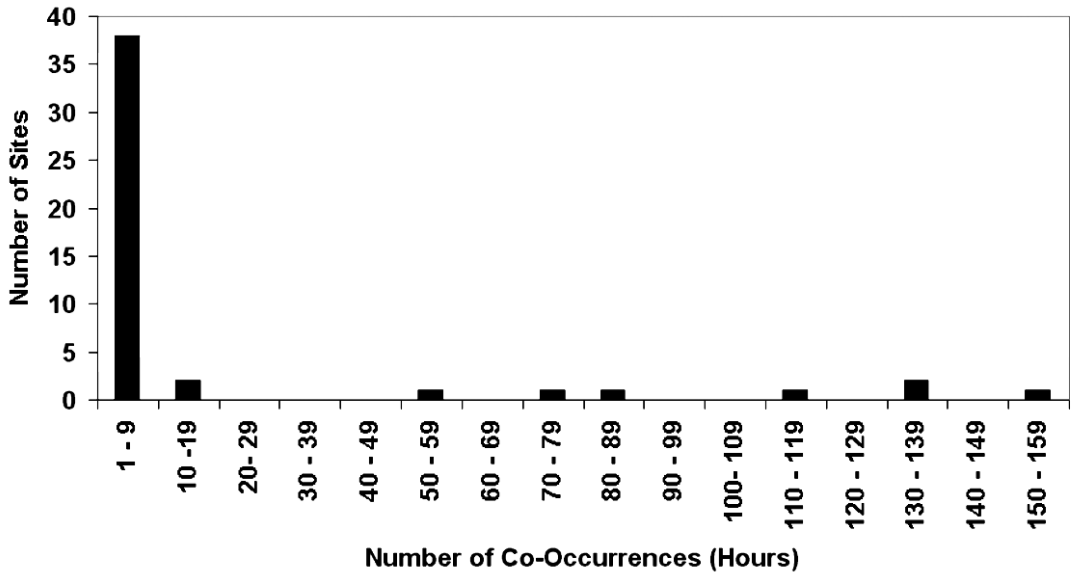

Figure 3-7. The co-occurrence pattern for O_3 and nitrogen dioxide using 2001 data from the AQS. There is co-occurrence when hourly average concentrations of O_3 and another pollutant are both ≥ 0.05 ppm.

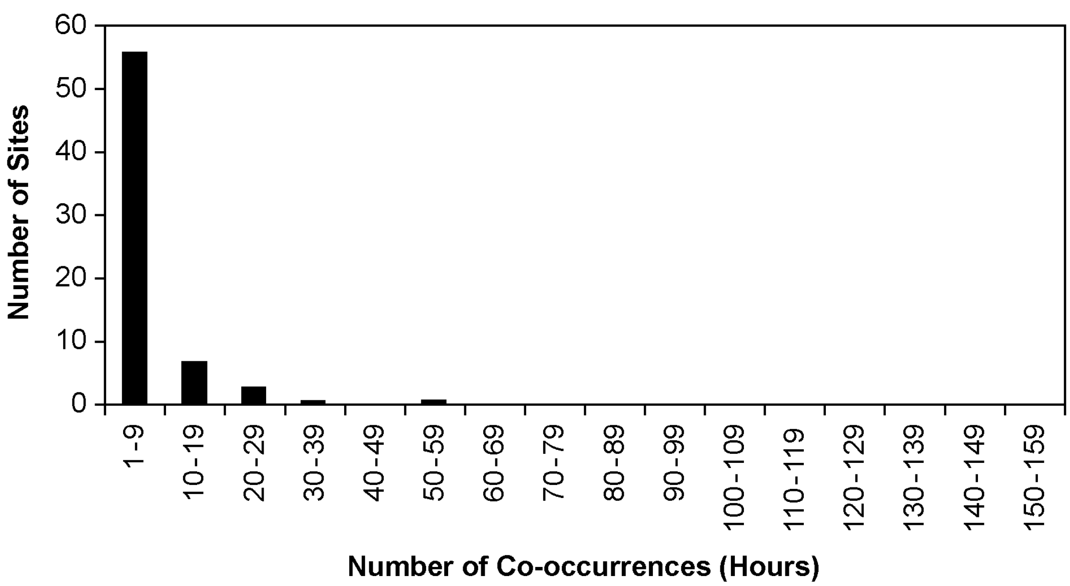

Figure 3-8. The co-occurrence pattern for O_3 and sulfur dioxide using 2001 data from AQS. There is co-occurrence when hourly average concentrations of O_3 and another pollutant are both ≥ 0.05 ppm.

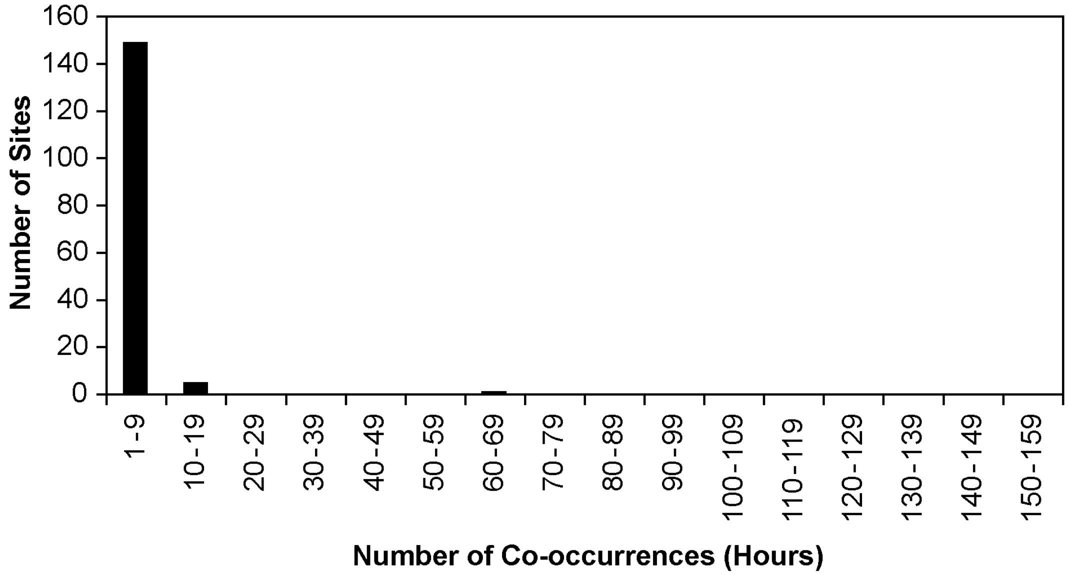

Figure 3-9. The co-occurrence pattern for O_3 and $PM_{2.5}$ using 2001 data from AQS.

3.7 POLICY RELEVANT BACKGROUND OZONE CONCENTRATIONS

Background O_3 concentrations used for NAAQS-setting purposes are referred to as Policy Relevant Background (PRB) O_3 concentrations. They are used by the EPA to assess risks to human and ecosystem health and to provide risk estimates associated with O_3 produced by anthropogenic sources in North America (defined here as the continental North America). Policy Relevant Background concentrations are those concentrations that would result in the United States in the absence of anthropogenic emissions in North America. Policy Relevant Background concentrations include contributions from natural sources everywhere in the world and from anthropogenic sources outside North America. Issues concerning the methodology for calculating PRB O_3 concentrations are described in detail in Annex AX3, Section AX3.9.

Contributions to PRB O_3 include photochemical interactions involving natural emissions of VOCs, NO_x, and CO; the long-range transport of O_3 and its precursors from outside North America; and stratospheric-tropospheric exchange (STE). Processes involved in STE are described in detail in Annex AX2.3. Natural sources of O_3 precursors include biogenic emissions, wildfires, and lightning. Biogenic emissions from agricultural activities are not considered in the formation of PRB O_3.

Springtime maxima are observed at relatively clean (Annex AX3 and Figures 3-10a,b) national parks mainly in the western United States and at a number of other relatively unpolluted monitoring sites throughout the Northern Hemisphere. The major issues concerning the calculation of PRB O_3 center on the capability of the current generation of global-scale, three-dimensional, CTMs to simulate the causes of high O_3 concentrations observed at monitoring sites in relatively unpolluted areas of the United States from late winter through spring (i.e., February through June). The issues raised do not affect interpretations of the causes of summertime O_3 episodes as strongly. Summertime O_3 episodes are mainly associated with slow-moving high-pressure systems characterized by limited mixing between the planetary boundary layer and the free troposphere, as noted in Annex AX2, Section AX2.3.

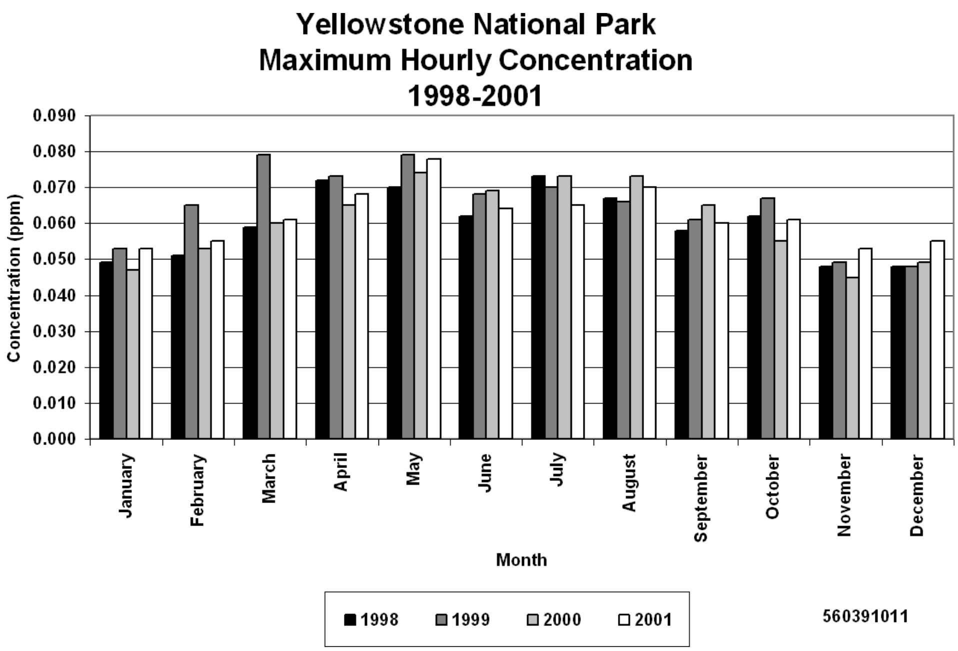

Figure 3-10a. Monthly maximum hourly average O_3 concentrations at Yellowstone National Park, Wyoming, in 1998, 1999, 2000, and 2001.

Source: U.S. Environmental Protection Agency (2003a).

A large number of case studies document the occurrence of STE in mid- and high latitudes in Europe, Asia, and North America mainly during winter and spring. These studies were based on aircraft, satellite, and ground-based measurements. Considerable uncertainty exists in the

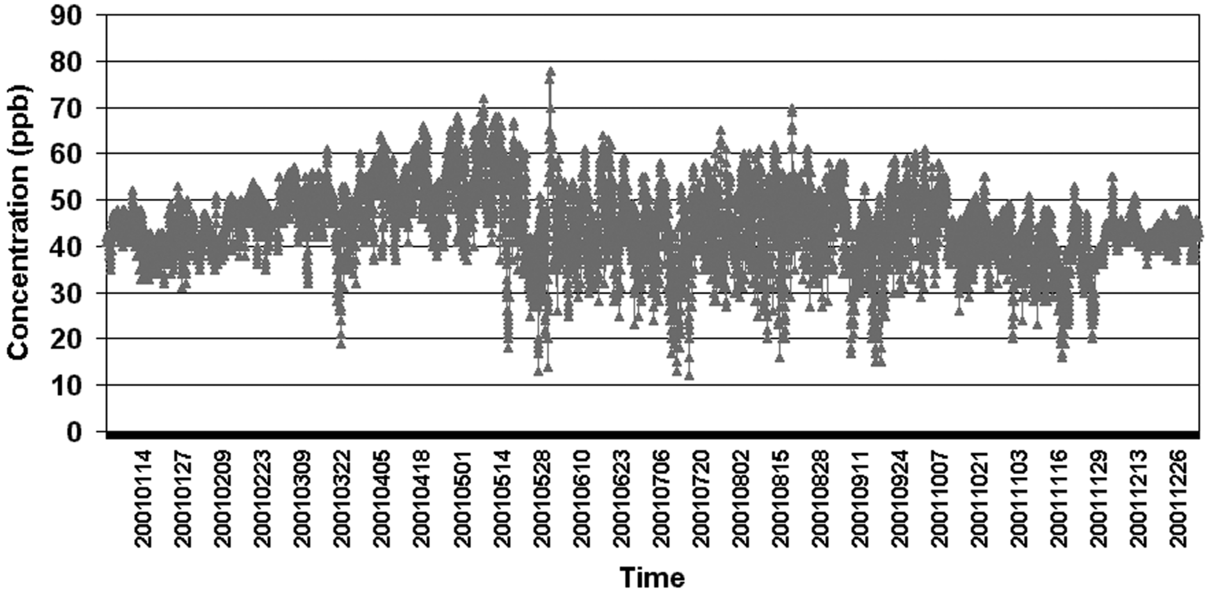

Figure 3-10b. Hourly average O_3 concentrations at Yellowstone National Park, Wyoming for the period January to December 2001.

Source: U.S. Environmental Protection Agency (2003a).

magnitude of the exchange; however, these studies have found that STE occurs year long, but with a distinct preference for the transport of O_3 directly to the middle and lower troposphere during late winter and spring. Transport to the upper troposphere basically occurs throughout the year.

Springtime maxima in tropospheric O_3 observed at high latitudes are also associated with the winter buildup of O_3 precursors and thermally labile reservoir species such as PAN and other reactive nitrogen species. These pollutants originate from all continents in the Northern Hemisphere. Ozone precursor concentrations reach a maximum in late March; and as sunlight returns to the Arctic, photochemical reactions generate tropospheric O_3 (Section AX3.9.1). The contribution of Asian sources to the U.S. levels is also largest during spring, reflecting the efficient lifting of Asian pollution ahead of cold fronts originating in Siberia and transport in strong westerly winds across the Pacific. The longer lifetime of O_3 during spring also contributes to springtime maxima (Wang et al., 1998) (e.g., Hudman et al., 2004).

Estimates of PRB concentrations cannot be obtained solely by examining measurements of O_3 obtained at relatively remote monitoring sites (RRMS) in the United States (Annex AX3, Section AX3.2.3) because of the long-range transport from anthropogenic source regions within North America. It should also be noted that it is impossible to determine sources of O_3 without ancillary data that could be used as tracers of sources or to calculate photochemical production and loss rates. The current definition of PRB implies that only CTMs can be used to estimate the range of PRB values. On the synoptic and larger spatial scales at least, all evidence indicates that global CTMs are adequate tools to investigate the factors controlling tropospheric O_3; and three-dimensional CTMs, as typified by Fiore et al. (2003) appear to offer the best methodology for estimating PRB concentrations that can not be measured directly (Annex AX3, Section AX3.9.2), at least for averaging periods of longer than one hour.

Previous estimates of background O_3 concentrations, based on different concepts of background, are given in Table 3-8. Results from global three-dimensional CTMs, where the background is estimated by zeroing anthropogenic emissions in North America (Table 3-8) are on the low end of the 25 to 45 ppbv range. Lefohn et al. (2001) have argued that frequent occurrences of O_3 concentrations above 50 to 60 ppbv at remote northern U.S. sites in spring are mainly stratospheric in origin. Fiore et al. (2003a) used a global CTM to determine the origin of the high-O_3 events reported by Lefohn et al. (2001), and to conduct a more general quantitative analysis of background O_3 as a function of season, site location, and local O_3 concentration.

Figure 3-11 shows a comparison between observations obtained at CASTNet sites and model results of Fiore et al. (2003a). They classified the CASTNet monitoring sites into low-lying surface sites (generally < 1.5 km) and elevated sites (> 1.5 km). All elevated sites are in the West. Results were then aggregated to construct the cumulative probability distributions shown in Figure 3-11, for the 58 surface sites and the 12 elevated sites, and for the three seasons. The calculated mean background at the surface sites in spring is 27 ppbv as compared to 23 ppbv in summer and fall. At these sites, the background is highest for O_3 concentrations near the center of the distribution, and decline as total surface O_3 concentrations increase, for reasons summarized above and discussed by Fiore et al. (2002a). At the elevated sites, the calculated mean background is 36 ppbv in spring versus 30 ppbv in the other seasons. Background concentrations in the fall resemble those in summer but show less variability and do not exceed 40 ppbv anywhere in this analysis.

Table 3-8. Previous Estimates of Background O_3 in Surface Air Over the United States

Study	Method	Time Period	Region	Background Estimate (ppbv)
Trainer et al. (1993)	y-intercept of O_3 vs. NO_y-NO_x regression line[a]	Summer 1988	Eastern United States	30-40
Hirsch et al. (1996)	y-intercept of O_3 vs. NO_y-NO_x regression line	May-Sep 1990-1994	Harvard Forest[b]	25 (Sept) – 40 (May)
Altshuller and Lefohn (1996)	y-intercept of O_3 vs. NO_y regression line, and observations at remote/rural sites	Apr-Oct 1988-1993	Continental United States	25-45 (inland)[c] 25-35 (coastal)
Liang et al. (1998)	Sensitivity simulation in a 3-D model with anthropogenic NO_x emissions in the continental U.S. set to zero	Full year	Continental United States	20-30 (East) 20-40 (West) (spring maximum)
Lin et al. (2000)	Median O_3 values for the lowest 25th percentiles of CO and NO_y concentrations	1990-1998	Harvard Forest	35 (fall) – 45 (spring)
Fiore et al. (2002a)	O_3 produced outside of the North American boundary layer in a global 3-D model	Summer 1995	Continental United States	15-30 (East) 25-35 (West)

[a] NO_y is the chemical family including NO_x and its oxidation products; NO_y-NO_x denotes the chemically processed component of NO_y.
[b] rural site in central Massachusetts.
[c] seasonal 7-h daylight average.

Source: Fiore et al. (2003a).

Major conclusions from the Fiore et al. (2003a) study (which are discussed in detail in Annex AX3, Sections AX3.9.3 and AX3.9.4) are:

- PRB O_3 concentrations in U.S. surface air are generally 15 to 35 ppbv. They decline from spring to summer and are generally < 25 ppbv under the conditions conducive to high-O_3 episodes.
- PRB O_3 concentrations can be represented as a function of season, altitude, and total surface O_3 concentration, as illustrated in Figure 3-11.
- High-elevation sites (> 2 km) do occasionally experience high PRB concentrations in spring (40 to 50 ppbv) due to free-tropospheric influence which includes a 4 to 12 ppbv contribution from hemispheric pollution (O_3 produced from anthropogenic emissions outside North America). These sites cannot be viewed as representative of low-elevation surface sites (Cooper and Moody, 2000), where the background is consistently lower.

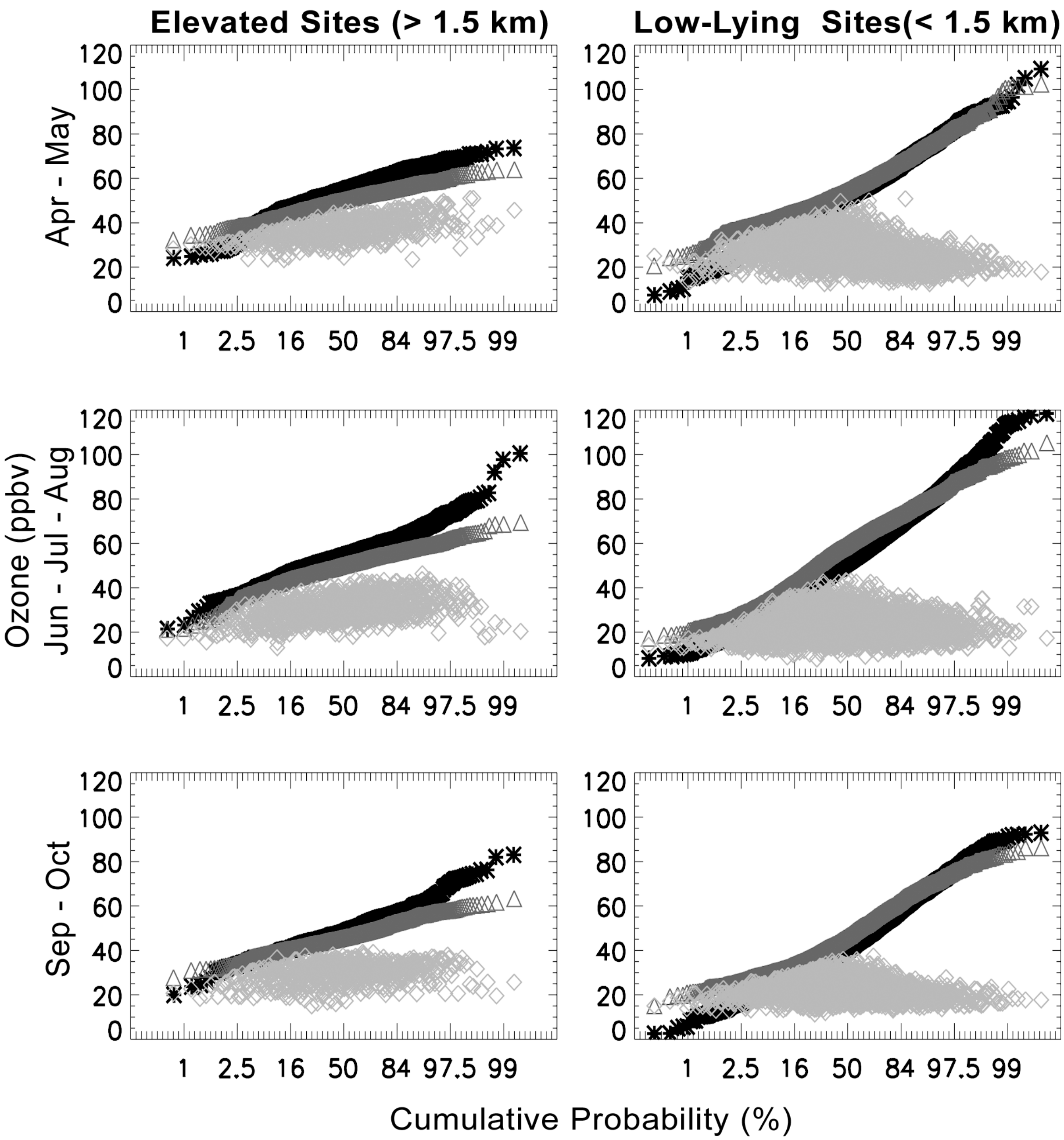

Figure 3-11. Estimates of background contribution to surface afternoon (13 to 17 LT) O_3 concentrations in the United States as a function of local O_3 concentration, site altitude, and season. The figure shows cumulative probability distributions of O_3 concentrations for the observations (asterisks) and the model (triangles). The corresponding distribution of background O_3 concentrations is shown as grey diamonds.

Source: Fiore et al. (2003a).

- The stratospheric contribution to surface O_3 is of minor importance, typically well < 20 ppbv. While stratospheric intrusions might occasionally elevate surface O_3 at high-altitude sites, these events are rare.

Appropriate background concentrations should thus be allowed to vary as a function of season, altitude, and total O_3 level. The diamonds in Figure 3-11 can be applied for this purpose. In particular, the depletion of the background during high-O_3 events should be taken into account (i.e., background O_3 is depleted by reactions in the atmosphere and by deposition to the surface but is not replenished at a significant rate in the stable, polluted boundary layer). This depletion is shown mainly in the right-hand panels of Figure 3-11 for the highest O_3 values. Note that the model is generally able to reproduce the overall frequency distributions in Figure 3-11. Underpredictions, especially at the upper end of the frequency distribution during the warmer months, are likely related to sub-grid-scale processes that the model cannot resolve explicitly. The highest observed O_3 concentrations in all three seasons and at all altitudes are associated with regional pollution (i.e., North American anthropogenic emissions), rather than stratospheric influence.

Chemistry transport models should be evaluated with observations given earlier in Chapter 3, in Annex AX3, and in Figure 3-12 (over appropriate averaging periods), and be able to simulate the processes summarized in Chapter 2. Higher resolution models capable of spatially and temporally resolving stratospheric intrusions and capable of resolving O_3 variability on hourly timescales have not been applied to this problem. Ebel et al. (1991) have demonstrated that regional scale CTMs could be used to study individual stratospheric intrusions. As an example of the utility of different types of models, Zanis et al. (2003) were able to forecast, observe, and model a stratospheric intrusion (maximum penetration depth was to slightly > 2 km altitude) that occurred from June 20 to 21, 2001, over a large swath of central Europe. Roelofs et al. (2003) compared results from six global tropospheric CTMs with lidar observations obtained during that event and concluded that the models qualitatively captured the features of this intrusion. It was also found that the coarser resolution models overestimated transport to lower altitudes. The use of higher resolution models, perhaps nested inside the coarser resolution models, may have helped solve this problem. They would also better address issues related to temporal (i.e., 1-h versus 8-h averages) and spatial (i.e., populated versus remote areas) scales needed by policymakers.

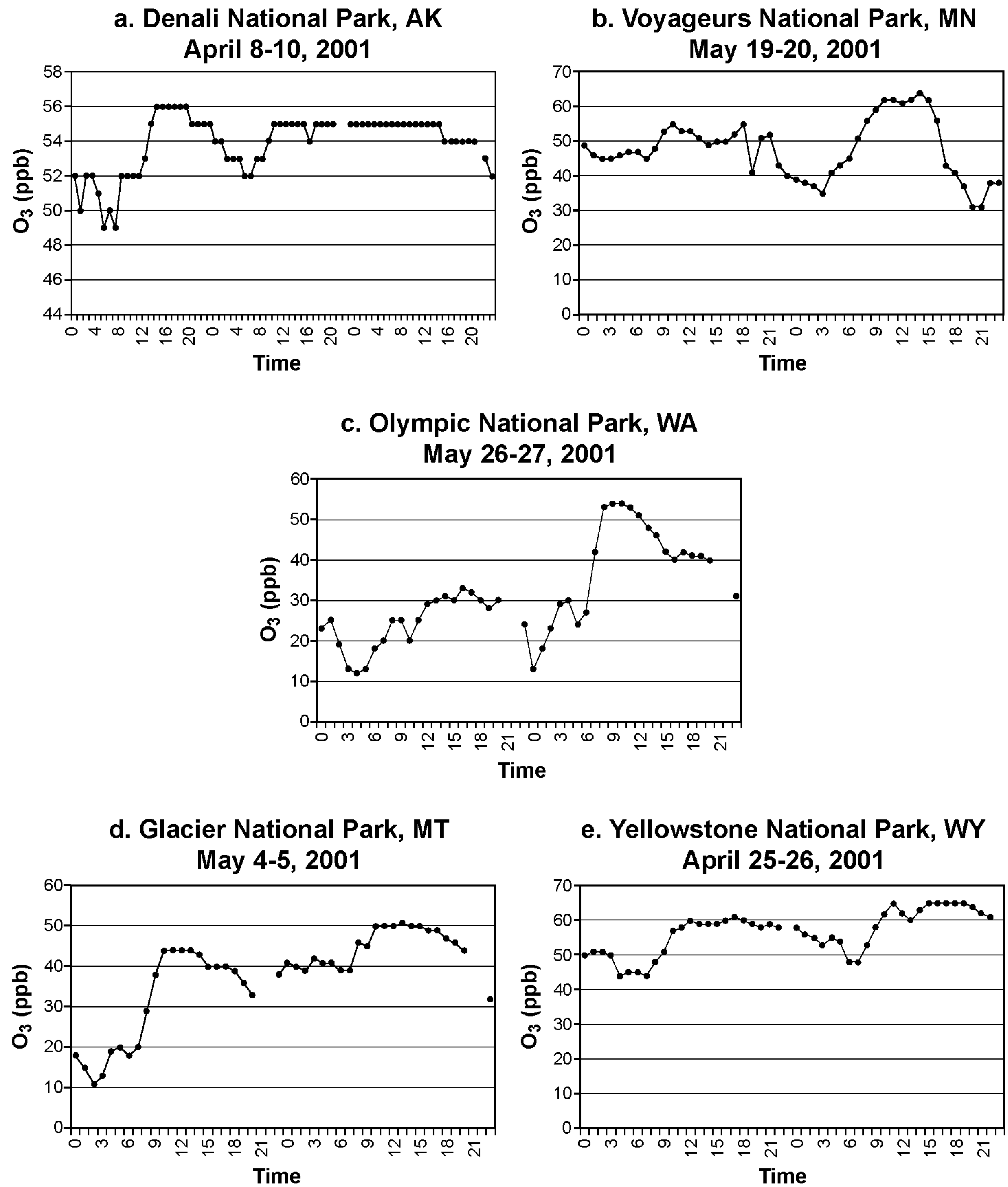

Figure 3-12. Time-series of hourly average ozone concentrations observed at five national parks: Denali, AK; Voyageur, MN; Olympic, WA; Glacier, MT; and Yellowstone, WY.

Although many of the features of the day-to-day variability of O_3 at relatively remote monitoring sites in the United States are simulated reasonably well by Fiore et al. (2003), uncertainties in the calculation of the temporal variability of O_3 originating from different sources on shorter time scales that must be recognized. The uncertainties stem in part from seasonal variability in the STE of O_3 that is too low (Fusco and Logan, 2003), the geographical variability of this exchange, and the variability in the exchange between the free troposphere and the planetary boundary layer in the model.

Ideally, the predictions resulting from an ensemble of models should be compared with each other and with observations so that the range of uncertainty inherent in the model predictions can be evaluated.

3.8 INDOOR SOURCES AND EMISSIONS OF OZONE

Ozone enters the indoor environment primarily through infiltration from outdoors and through building components, such as windows, doors, and ventilation systems. There are also a few indoor sources of O_3 (photocopiers, facsimile machines, and laser printers and electrostatic air cleaners and precipitators) (Weschler, 2000). Generally O_3 emissions from office equipment and air cleaners are low except under improper maintenance conditions. Reported O_3 emissions from office equipment range from 1300 to 7900 μg/h (Leovic et al., 1998, 1996). Most air cleaners (particulate ionizers) emitted no or only a small amount (56 to 2757 μg/h) of O_3 during operation (Niu et al., 2001). Emissions from O_3 generators can range from tens to thousands of micrograms per hour (Weschler, 2000; U.S. Environmental Protection Agency, 1996).

Factors Affecting Ozone Concentrations Indoors

The concentration of O_3 in indoor environments is dependent on the outdoor O_3 concentration, the air exchange rate (AER) or outdoor infiltration, indoor circulation rate, and O_3 removal processes through contact with indoor surfaces and reactions with other indoor pollutants. Since O_3 concentrations are generally higher during the warmer months, indoor concentrations will likely be highest during that time period. (See earlier discussion on ambient concentrations of O_3.)

The AER, the balance of the flow of air in and out of a microenvironment, is greatest in a residential building when a window or door is open (Johnson et al., 2004; Howard-Reed et al., 2002). The opening of windows or doors is dependent on the building occupancy, season, housing density, the presence of air conditioning and wind speed (Johnson and Long, 2004). When windows and doors are closed, the dominant mechanism controlling AERs is infiltration through unintentional openings in the building envelope. One of the most comprehensive evaluations of AERs for residential structures was reported by Murray and Burmaster (1995) and includes AERs for 2,844 residential structures in four different regions by season (winter, spring, summer, and fall). The AER for all seasons across all regions was 0.76 h^{-1} (arithmetic mean). Table 3-9 lists the mean AER for the seasons and regions. The AERs were generally higher during the warm seasons, when ambient O_3 concentrations are highest.

Average mean (median) AERs of 2.45 (2.24), 1.35 (1.09), and 2.22 (1.79) h^{-1} were reported by Lagus Applied Technology, Inc. (1995) for schools, offices, and retail establishments in California. The AERs for schools, offices, and retail establishments in Oregon and Washington were 0.32, 0.31, and 1.12 h^{-1} (Turk et al., 1989), considerably less than that reported by Lagus Applied Technology. Park et al. (1998) reported AERs ranging from 1.0 to 47.5 h^{-1} for stationary vehicles under varying ventilating conditions. Where available, AERs for other studies are included in Table 3-10.

The most important removal process for O_3 in the indoor environment is deposition on and reaction with indoor surfaces. The rate of deposition is material-specific. The removal rate will depend on the indoor dimensions, surface coverings, and furnishings. Smaller rooms generally have larger surface-to-volume ratio (A/V) and remove O_3 faster. Fleecy materials, such as carpets, have larger surface-to-volume ratios and remove O_3 faster than smooth surfaces (Weschler, 2000). However, the rate of O_3 reaction with carpet diminishes with cumulative O_3 exposure (Morrison et al., 2000; Morrison and Nazaroff, 2002). Weschler (2000) compiled the O_3 removal rates for a variety of microenvironments. Generally, the removal rates ranged between 3.0 and 4.3 k_d (A/V)/h^{-1}. The highest removal rate, 7.6 k_d (A/V)/h^{-1}, was noted for a clean room (Weschler et al, 1989).

Ozone reacts with terpenes from wood products, solvents, or odorants to produce submicron particles (Nazaroff and Weschler, 2004; Wainman et al., 2000; Weschler and Shields, 1999; Grosjean and Grosjean, 1996, 1998), possibly resulting in $PM_{2.5}$ concentrations > 20 μg/m^3

Table 3-9. Air Exchange Rates in Residences by Season and Region of the Country*

Season[a]	Region	Sample Size	Mean	Std Dev
All	All	2844	0.76	0.88
1	All	1139	0.55	0.46
2	All	1051	0.65	0.57
3	All	529	1.5	1.53
4	All	125	0.41	0.58
1	1	161	0.36	0.28
1	2	428	0.57	0.43
1	3	96	0.47	0.4
1	4	454	0.63	0.52
2	1	254	0.44	0.31
2	2	43	0.52	0.91
2	3	165	0.59	0.43
2	4	589	0.77	0.62
3	1	5[b]	0.82	0.69
3	2	2[b]	1.31	na
3	3	34	0.68	0.5
3	4	488	1.57	1.56
4	1	47	0.25	0.15
4	2	23[b]	0.35	0.18
4	3	37	0.51	0.25
4	4	18[b]	0.72	1.43

* The data does not represent all areas of the country.
[a] Season 1: December, January, February; Season 2: March, April, May; Season 3: June, July, August; Season 4: September, October, November.
[b] Note: Small sample size, n < 25.
[c] Estimated using locations of residences evaluated in the region.

Source: Adapted from Murray and Burmaster (1995).

Table 3-10. Indoor/Outdoor Ozone Concentrations in Various Microenvironments

Location and Ventilation Conditions	Indoor/Outdoor Concentrations	Comments	Reference
New England States (9) Fall	20 ppb/40 ppb	Schools represented a variety of environmental conditions - varying ambient O_3 concentrations, sources, geographic locations, population density, traffic patterns, building types. Average O_3 concentrations were low in the morning and peaked during the early afternoon. O_3 concentrations averaged for all schools monitored.	NESCAUM (2002)
Mexico City, School Windows/Doors Open (27) Windows/Doors Closed Cleaner Off (41) Windows/Doors Closed Cleaner On (47)	0 to 247 ppb/ 64 to 361 ppb	Study conducted over 4 d period during winter months. Two-minute averaged measurements were taken both inside and outside of the school every 30 min from 10 a.m. to 4 p.m. Estimated air exchange rates were 1.1, 2.1, and 2.5 h^{-1} for low, medium, and high flow rates. Ozone concentrations decreased with increasing relative humidity.	Gold et al. (1996)
Mexico City Homes Schools	5 ppb/27ppb (7 d) 7 ppb/37 ppb (14 d) 22 ppb/56 to 733 ppb	Ozone monitoring occurred between September and July. Study included 3 schools and 145 homes. Most of the homes were large and did not have air conditioning. Ninety-two percent of the homes had carpeting, 13% used air filters, and 84% used humidifiers. Thirty-five percent opened windows frequently, 43% sometimes, and 22% never between 10 a.m. and 4 p.m. Ozone was monitored at the schools sites from 8 a.m. to 1 p.m. daily for 14 consecutive days. Homes were monitored for continuous 24-h periods for 7 and 14 consecutive days.	Romieu et al. (1998)
Boston, MA, Homes (9) Winter - continuously Summer - continuously	 0 to 20.4 ppb/4.4 to 24.5 ppb 0 to 34.2 ppb/8.2 to 51.8 ppb	Study examined the potential for O_3 to react with VOCs to form acid aerosols. Carbonyls were formed. No clear trend of O_3 with AERs. The average AER was 0.9 h^{-1} during the winter and 2.6 h^{-1} during the summer. Four residences in winter and nine in summer with over 24 h samples collected.	Reiss et al. (1995)
Los Angeles, Homes (239)	13 ppb/37 ppb	Four hundred and eighty-one samples collected inside and immediately outside of home from February to December. Concentrations based on 24-h average O_3 concentrations indoors and outdoors. Low outdoor concentrations resulted in low indoor concentrations. However, high outdoor concentrations resulted in a range of indoor concentrations.	Avol et al. (1998)

Table 3-10 (cont'd). Indoor/Outdoor Ozone Concentrations in Various Microenvironments

Location and Ventilation Conditions	Indoor/Outdoor Concentrations	Comments	Reference
Burbank, CA	0.2/21.1 ppb	Major source of O_3 was transport from outdoors. From early spring to late fall O_3 concentrations peaked during the early afternoon and approach zero at sunset. AER ranged from 1.0 to 1.9 h^{-1}.	Weschlov et al. (1994)
Telephone Switching Station			
Munich Germany		Indoor concentrations were dependent on the type of ventilation.	Jakobi and Fabian (1997)
Office	0.4/0.9 ppb		
Gymnasium	0.49/0.92 ppb		
Classroom	0.54/0.77 ppb		
Residence			
Bedroom	0.47/1.0 ppb		
Livingroom	0.74/1.0 ppb		
Montpellier, France, Homes (110)	15.5/32.0 ppb	Ozone measurements were made over 5-d periods in and outside of 21 homes during the summer and winter months. The winter I/O ratio was 0.31 compared to 0.46 during the summer months.	Bernard et al. (1999)
Southern CA, Homes		Ozone measurements were taken at 119 homes (57 in Upland and 62 in towns located in the mountains) during April and May. Concentrations were based on average monthly outdoor concentrations and average weekly indoor concentrations. Indoor based on the home location, number of bedrooms, and the presence of an air conditioner.	Geyh et al. (2000) Lee et al. (2002)
Upland	11.8/48.2 ppb		
Mountains	2.8/35.7 ppb		
Krakow, Poland, Museums		Ozone continuously monitored at five museums and cultural centers. Monitoring conducted during the summer months for 21 to 46 h or 28 to 33 days at each of the sites. The indoor concentration was found to be dependent on the ventilation rate, i.e., when the ventilation rate was high the indoor O_3 concentrations approached that of ambient O_3. Rooms sequestered from the outdoor air or where air was predominantly recycled through charcoal filters the ozone levels indoors were greatly reduced.	Salmon et al. (2000)
Cloth Hall	3.2/25.7-27.4 ppb		
Matejko	8.5/20.0 ppb		
Wawel Castle	2.5/14.7 ppb		
National	1.5/11.0 ppb		
Buildings, Greece		There was no heating/air conditioning system in the building at Thessalonki. Windows were kept closed during the entire monitoring period. Complete air exchange took place every 3 h. The air conditioning system in continuous use at the Athens site recirculated the air. Complete air exchange was estimated to be 1 h. Monitoring lasted for 30 days at each site but only the 7 most representative days were used.	Drakou et al. (1995)
Thessalonki	9.39/15.48 ppb		
Athens	8.14/21.66 ppb		

Table 3-10 (cont'd). Indoor/Outdoor Ozone Concentrations in Various Microenvironments

Location and Ventilation Conditions	Indoor/Outdoor Concentrations	Comments	Reference
Patrol cars, NC	11.7/28.3 ppb	Patrol cars were monitored Mon. through Thurs. between the hours of 3 p.m. to midnight on 25 occasions during the months of Aug., Sept., and Oct. Outdoor O_3 concentrations were taken from ambient monitoring station. Air inside the patrol car was recirculated cool air.	Riediker et al. (2003)
University of CA Photocopy room	< 20 ppm/—	Room volume was 40 m^3. Ozone concentrations increased proportionately with increasing use of photocopier.	Black et al. (2000)
Home/office O_3 generators	14 to 200 ppb/—	Room volume was 27 m^3. Doors and windows were closed. Heating/air conditioning and mechanical ventilation systems were off. Ozone generator was operated for 90 min. High ozone concentrations noted when O_3 generator used at high setting. AER was o.3 h^{-1}.	Steiber et al. (1995)

(Wainman et al., 2000). Indoor hydroxy radical (•OH) concentrations increase nonlinearly with increased indoor O_3 concentrations and indoor alkene emissions. Sarwar et al. (2002) suggested that the •OH reacts with terpenes to produce products with low vapor pressures that contribute to fine particle growth.

Monitored and Modeled Ozone Concentration in Microenvironments

Ozone concentrations in various microenvironments under a variety of environmental conditions have been reported in the literature. In the absence of an indoor O_3 source, concentrations of O_3 indoors are lower than that found in the ambient air. Ozone concentrations in microenvironments were found to be primarily controlled by ambient O_3 concentrations and the AER; they increase with increasing AER. To a lesser extent, O_3 concentrations in microenvironments are influenced by the ambient temperature, time of day, indoor characteristics (e.g., presence of carpeting), and the presence of other pollutants in the microenvironment. Table 3-9 describes the findings of the available studies.

Estimates of indoor O_3 concentrations may be made using a simple one-compartment mass balance model. The model takes into account the effects of ventilation, filtration, heterogeneous removal, direct emission, and photolytic and thermal and chemical reactions. The simplest form of the model is represented by the following differential equation:

$$\frac{dC_{IN}}{dt} = vC_{OUT} + \frac{S}{V} - vC_{IN}$$

where dC_{IN} is the indoor pollutant concentration (mass/volume), dt is time in hours, v is the air exchange rate, C_{OUT} is the outdoor pollutant concentration (mass/volume), V is the volume of the microenvironment, and S is the indoor source emission rate. When the model was used to estimate indoor O_3 concentrations, indoor concentrations were found to be 33% of outdoor O_3 concentrations (Freijer and Bloemen, 2000). A more in-depth discussion of the mass balance model has been reported in Nazaroff and Cass (1986).

3.9 HUMAN EXPOSURE TO OZONE

Humans are exposed to O_3 and related photochemical oxidants through the exchange boundary, the skin and the openings into the body such as the mouth, the nostrils, and punctures and lesions in the skin (U.S. Environmental Protection Agency, 1992; Federal Register, 1986). Inhalation exposure to O_3 and related photochemical oxidants is determined by pollutant concentrations measured in the breathing zone that is not affected by exhaled air as the individual moves through time and space.

Quantification of Exposure

Ambient O_3 concentrations vary with time of day (peaking during the latter portion of the day) and season and among locations. Consequently, exposure to O_3 will change as a function of time of day and as an individual moves among locations. A hypothetical exposure is demonstrated in Figure 3-13. The actual dose received also changes during the day and is dependent on the O_3 concentration in the breathing zone and the individual's breathing rate, which is, in turn, dependent on the individual's level of exertion.

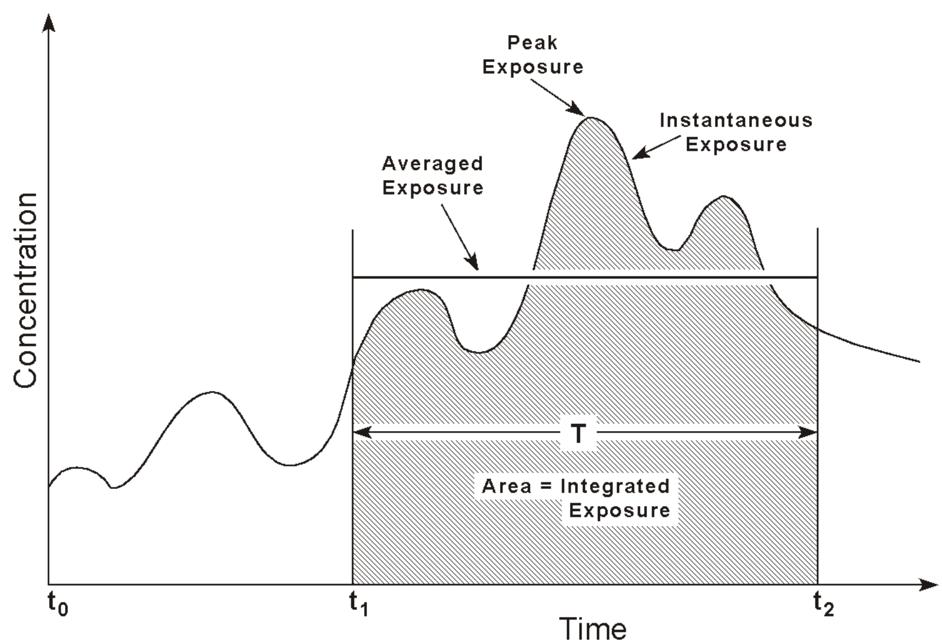

Figure 3-13. Ozone exposure time profile.

When measuring or modeling exposure to O_3 and related photochemical oxidants consideration should be given to the diurnal weekly (weekday-weekend) and seasonal variability. Peak concentrations, lasting for several hours, typically occur towards the latter portion of the day during the summer months. Regional O_3 episodes often co-occur with high concentrations of airborne fine particles, making it difficult to assess O_3 dynamics and exposure patterns. Also, while there are few indoor O_3 sources, O_3 will react with materials and other pollutants in the indoor environment in an analogous fashion to that occurring in the ambient atmosphere, potentially exposing subjects to other more toxic pollutants (Nazaroff and Weschler, 2004; Lee and Hogsett, 1999; Wainman et al., 2000; Weschler and Shields, 1997). (See discussion on O_3 atmospheric chemistry and indoor sources and concentrations earlier in this chapter.)

Personal Exposure and Ambient Concentrations

The two methods for measuring personal exposure are (a) the direct method, using a personal exposure monitor (PEM) consisting of a passive sampler worn around the breathing zone, and (b) the indirect method, which measures or estimates the O_3 concentrations through the use of models or biomarkers of exposure in all of the microenvironments the individual encounters (Ott, 1982, 1985). The concept of microenvironment is important in the understanding of human exposure modeling. Often identified with a perfectly mixed compartment, microenvironments are more recently viewed as a controlled volume, indoors or outdoors, that can be characterized using a set of either mechanistic or phenomenological governing equations. This allows for a nonhomogeneous environment, including sources and sinks within the microenvironment. Microenvironments include indoor residences, other indoor locations, outdoors near roadways, other outdoor locations, and in-vehicles.

Although it is difficult to develop passive monitors for personal exposure measurements because of problems in identifying chemical or trapping reagents that can react with O_3, several modified passive samplers have been developed for use in personal O_3 exposure measurements (Bernard et al., 1999; Koutrakis et al., 1993; Avol et al., 1998; Geyh et al., 1997, 1999). Some personal exposure measurements using passive samplers show O_3 exposures below those O_3 concentrations measured at outdoor stationary sites (Delfino et al., 1996; Avol et al., 1998; Sarnat et al., 2000; Geyh et al., 2000; Brauer and Brook, 1997). However, other studies have found strong correlations between O_3 measured at stationary sites and personal monitored concentrations (Liard et al., 1999; Bauer and Brook, 1997; Linn et al., 1996; Lee et al., 2004; Avol et al., 1998; O'Neill et al., 2003) when the time spent outdoors, age, gender, and occupation of the subjects were considered.

Hourly O_3 concentrations from monitoring stations have been used as surrogates of exposure in epidemiological studies in evaluating exposure-related health effects. Routinely collected ambient data, though readily available and convenient, may not represent true exposure and may tend to underestimate the effect of the air pollutant on health (Krzyznowki, 1997). In some instances, ambient O_3 monitors are located in areas outside the breathing zone of the general population. Studies on the effect of elevation on O_3 concentrations found that concentrations increased with increasing elevation (Väkeva et al., 1999; Johnson, 1997). Further, since O_3 monitors are frequently located on rooftops in urban settings, the concentrations measured there may overestimate the exposure to individuals outdoors in streets and parks, locations where people exercise and maximum O_3 exposure is likely to occur. Accordingly, the resulting exposure measurement error and its effect on the estimates of relative risk should be taken into consideration.

There are three components to exposure measurement error: (1) the use of aggregate, rather than individual, exposure data; (2) the difference between the average personal exposure and the true ambient concentration; and (3) the difference between true and measured ambient concentration levels. Zeger et al. (2000) indicated that the first and third error components are largely Berksonian errors and would not significantly bias the risk estimate. The error resulting from the difference between the personal and ambient concentration levels, however, may introduce bias, especially if indoor sources are associated with ambient levels. (See discussion on indoor sources of O_3 earlier in this chapter.)

Studies by Brauer and Brook (1997), Chang et al. (2000), Lee et al. (2004), Liard et al. (1999), Linn et al. (1996), Liu et al. (1995,1997), O'Neill et al. (2003), Delfino et al. (1996), Avol et al. (1998b), and Sarnat et al. (2001) examined the relationship between ambient O_3 concentrations from a central monitoring site and personal O_3 exposure. Sarnat et al. (2001), found that averaged 24-h O_3 concentrations from a stationary monitoring site were not significantly associated with O_3 concentrations from personal monitors in several exposed groups in Baltimore, MD. The mixed regression effect estimates were $\beta = 0.01$ ($t = 1.21$) and

$\beta = 0.00$ ($t = 0.03$), for summer and winter, respectively. In contrast, O'Neill et al. (2003) found a statistically significant association between personal and ambient O_3 concentrations in Mexico City outdoor workers ($\beta = 0.56$, $t = 8.52$). The subjects in the Sarnat et al. (2001) study spent less than 6% of their time outdoors, whereas the personal exposure data from O'Neill et al. (2003) were from subjects who spent the entire measurement period outdoors. Brauer and Brook (1997) observed that the averaged personal O_3 measurements and ambient concentrations were well correlated after stratifying groups by time spent outdoors. Lee et al. (2004) also observed that personal O_3 exposure was positively correlated with time spent outdoors ($r = 0.19$, $p < 0.01$) and negatively correlated with time spent indoors ($r = -0.17$, $p < 0.01$). Liu et al. (1995) found that after adjusting for time spent in various indoor and outdoor microenvironments (i.e., car with windows open, car with windows closed, school, work, home, outdoors near home, outdoors other than near home), mean 12-h ambient O_3 concentrations explained 32% of the variance seen in personal exposure during the summer months. Delfino et al. (1996) reported a moderate correlation ($r = 0.45$; range: 0.36 to 0.69) between personal exposure and ambient O_3 concentrations measured at a stationary site. When asthmatic subjects were measured over a 12-h period during the daytime, the mean personal exposures were only 27% of the measured ambient concentrations. Chang et al. (2000) compared 1-h personal and ambient O_3 measurements in several microenvironments in Baltimore, MD. There was no correlation between personal exposure and ambient O_3 concentrations in the indoor residence ($r = 0.09$ and $r = 0.05$, for summer and winter, respectively), although a moderate correlation was found for indoor microenvironments other than the residence ($r = 0.34$ in summer, $r = 0.46$ in winter). The correlation between personal exposure and ambient O_3 in outdoor environments near and away from roadways was moderate to high ($0.68 \le r \le 0.91$). Liard et al. (1999) found a high variance in O_3 measurements from stationary monitoring sites and PEMs in adults and children monitored three times for 4 consecutive day intervals. For each period, all adults wore the O_3 monitors over the same 4 days. However, when personal measurements from all subjects were aggregated for each of the exposure periods, the mean personal O_3 exposure was found to be highly correlated with the corresponding 4-day mean ambient concentration ($r = 0.83$, $p <0.05$). Similarly, a study of Los Angeles school children by Linn et al. (1996) found that 24-h average ambient O_3 concentrations from a central site were well-correlated ($r = 0.61$) with averaged personal O_3 exposure. Results from these studies suggest that although O_3 concentrations from stationary ambient monitoring site do not explain the variance of individual personal O_3 exposures, they may serve as surrogate measures for aggregate personal exposures.

Modeled Personal Exposures

Exposure modeling is often used in evaluating exposure to large populations over time. The use of models is complicated by the fact that O_3 is a secondary pollutant with complex nonlinear and multiscale dynamics in space and time. Ozone is formed in the atmosphere through a series of chemical reactions involving the precursors VOCs and NO_x. Therefore, O_3 exposures may be affected by: (1) emission levels and spatiotemporal patterns of VOCs and NO_x; (2) ambient atmospheric as well as indoor microenvironmental transport, removal and mixing processes; and (3) chemical transformations that take place over a multitude of spatial scales. The transformations are dependent on the presence of co-occurring pollutants and the nature of surfaces interacting with the pollutants.

Exposure models may be classified as (1) potential exposure models, typically the maximum outdoor concentrations versus "actual" exposure, including locally modified microenvironmental outdoor and indoor exposures; (2) population versus "specific individual" based exposure models; (3) deterministic versus probabilistic models; and (4) observation versus mechanistic air quality model driven estimates of spatially and temporally varying O_3 concentrations.

There are several steps involved in defining exposure models. The steps are based on frameworks described in the literature over the last 20 years and the structure of various existing inhalation exposure models (NEM/pNEM, HAPEM, SHEDS, REHEX, EDMAS, MENTOR-OPERAS, APEX, AIRPEX, AIRQUIS). The steps include (1) estimation/determination of the background or ambient levels of O_3; (2) estimation/determination of levels and temporal profiles of O_3 in various microenvironments; (3) characterization of relevant attributes of individuals or populations under study (age, gender, weight, occupation, other physiological characteristics); (4) development of activity event or exposure event sequences; (5) determination of appropriate inhalation rates during the exposure events; (6) determination of dose; (7) determination of event-specific exposure and intake dose distributions for selected time periods; and (8) extrapolation of population sample (or cohort) exposures and doses to the entire populations of interest. Figure 3-14 provides a conceptual overview of the pNEM exposure model. A more detailed overview of an exposure model can be found in Annex AX3.

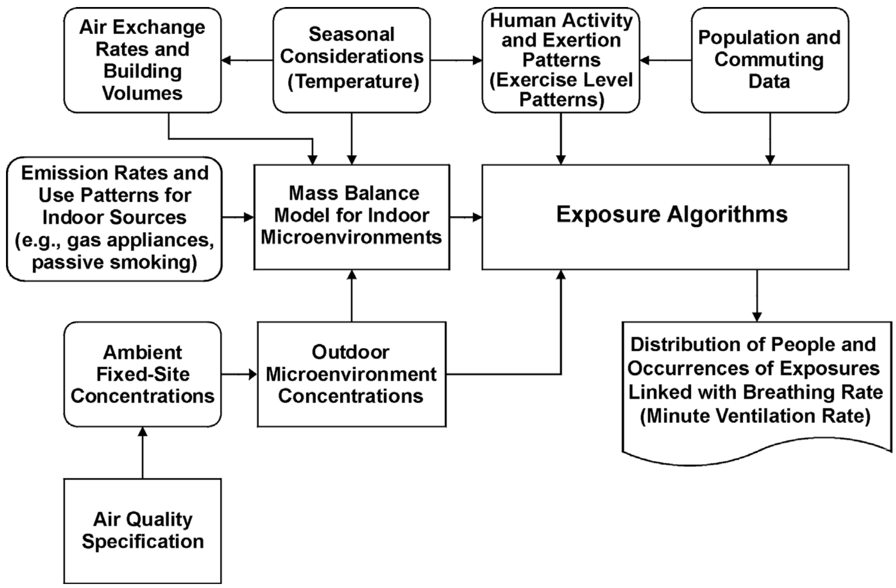

Figure 3-14. Conceptual overview of pNEM. Model inputs (e.g., activity patterns, ambient monitoring data, air exchange rates) are in round-corner boxes and model calculations are shown in rectangles.

Source: Johnson et al. (1999).

Outdoor concentrations of O_3 are estimated either through emissions-based mechanistic modeling, or through ambient-data-based modeling. Emissions-based models determine the spatiotemporal fields of the O_3 concentrations using precursor emissions and meteorological conditions as inputs. (They are described in Annex AX2, Section AX2.5). The ambient-data-based models determine spatial or spatiotemporal distributions of O_3 through the use of interpolation schemes. The kriging approach provides standard procedures for generating an interpolated O_3 spatial distribution for a given period of time (Georgopoulos et al., 1997a,b). The Spatio-Temporal Random Field (STRF) approach has been used to interpolate monitoring data in both space and time (Christakos and Vyas, 1998a,b). The STRF approach can analyze information on temporal trends which cannot be directly incorporated by kriging.

Several approaches are available for modeling microenvironmental concentrations: empirical, mass balance, and detailed computational fluid dynamics (CFD) models. Empirical relationships provide the basis for future, "prognostic" population exposure models. Mass balance modeling is the most common approach used to model pollutant concentrations in enclosed microenvironments. Mass balance modeling ranges from very simple formulations, assuming ideal (homogeneous) mixing and only linear physicochemical transformations with sources and sinks, to models that take into account complex multi-phase chemical and physical interactions and nonidealities in mixing. The pNEM/O_3 model, discussed later in this chapter, includes a sophisticated mass balance model for indoor and vehicle microenvironments (Johnson, 2003). CFD models take into account the complex, multiphase processes that affect indoor concentrations of interacting gas phase pollutants, such as the interactions of O_3 with indoor sinks and sources (surfaces, gas releases) and with entrained gas (Sarwar et al., 2001, 2002; Sørensen and Weschler, 2002).

To estimate the actual O_3 dose delivered to the lung, information on the concentration, minute ventilation rate, activity level, and the morphology of the respiratory tract are needed. Limited data have been compiled for ventilation rates for different age groups, both healthy and compromised individuals, at varies levels of activity (Klepeis et al., 1996, 2001; Avol et al., 1998b; Adams, 1993). Based on the available information, the highest level of outdoor activity occurs during the spring and summer months, during the mid- to late afternoon and early evening, the times when O_3 concentrations are highest. Children are likely more susceptible to the effects of O_3 than other groups. School-age children spend more time outdoors engaged in high level activities than do other groups and breath more air in than adults relative to body surface area, breathing frequency, and heart rate. Asthmatic children spend the same amount of time outdoors as other more healthy children but the time spent engaged in high levels of activity are less.

Estimates of activity level have been compiled based on questionnaire data. The National Human Activity Pattern Survey (NHAPS), a probability-based telephone survey, was conducted in the early 1990s. The survey concluded that outdoor work-related activities were highest during the springtime and were more frequent during the morning and early afternoon. Exercise/sports-related activities were highest from noon to 3 p.m. during the summer months. During the spring months, exercise/sports-related activities were highest from mid- to late afternoon (Klepeis et al., 1996, 2001). A pilot study by Gonzalez et al. (2003) evaluated the use of retrospective questionnaires for reconstructing past time-activity and location pattern information. Ozone concentration estimates using ambient stationary monitors and estimates derived from diaries and questionnaires differed slightly. However, both estimates were greater than O_3 personal exposure measurements.

Existing comprehensive inhalation exposure models (NEM and pNEM) (Johnson, 2003), (SHEDS) Burke et al., 2001; McCurdy et al., 2000), and the Air Pollutants Exposure model (APEX version 3) treat human activity patterns as sequences of exposure events in which each event is defined by a geographic location and microenvironment and then assigned activity diary records from the CHAD (Consolidated Human Activities Database; www.epa.gov/chadnet1) (Glen et al., 1997; McCurdy, 2000; McCurdy et al., 2000). There are now about 22,600 person-days of sequential daily activity pattern data in CHAD representing all ages and both genders. The data for each subject consist of one or more days of sequential activities, in which each activity is defined by start time, duration, activity type (140 categories), and microenvironment classification (110 categories). Activities vary from 1 min to 1 h in duration. Activities longer than 1 h are subdivided into clock-hour durations to facilitate exposure modeling. A distribution of values for the ratio of oxygen uptake rate to body mass (referred to as metabolic equivalents or METs) is provided for each activity type listed.

pNEM divides the population of interest into representative cohorts based on the combinations of demographic characteristics (age, gender, and employment), home/work district, and residential cooking fuel. APEX and SHEDS generate a population demographic file containing a user-defined number of person-records for each census tract of the population based on proportions of characteristic variables (age, gender, employment and housing) obtained for the population of interest, and then assigns the matching activity information from CHAD to each individual record of the population based on the characteristic variables.

An important source of uncertainty in existing exposure modeling involves the creation of multiday, seasonal, or year long exposure activity sequences based on 1- to 3-day activity data for any given individual from CHAD. Currently, appropriate longitudinal data are not available and the existing models use various rules to derive longer-term activity sequences utilizing 24-h activity data from CHAD.

Of the above models, only NEM/pNEM have been used extensively in O_3 exposure modeling. The pNEM probabilistic model builds on the earlier NEM deterministic exposure model. The model take into consideration the temporal and spatial distribution of people and O_3 in the area of consideration, variations in O_3 concentrations in the microenvironment, and the effects of exercise increased ventilation on O_3 uptake. There are three versions of the pNEM/O_3 model: (1) general population (Johnson et al., 1996a), (2) outdoor workers (Johnson et al., 1996b), and (3) outdoor children (Johnson et al., 1996c, 1997). The pNEM models have been applied to nine urban areas and a summer camp. The models used activity data from the Cincinnati Activity Diary Study (CADS) along with time/activity data from several other studies. Data from stationary monitoring sites were used to estimate outdoor O_3 exposure. Indoor O_3 decay was assumed to be proportional to the indoor O_3 concentration. An algorithm assigned the EVR associated with each exposure event. The EVR for the outdoor children model was generated using a module based on heart rate data by Spier et al. (1992) and Linn et al. (1992).

Exposure to Related Photochemical Oxidants

A variety of related photochemical oxidants produced outdoors, such as PAN and peroxypropionyl nitrate (PPN) can infiltrate into indoor environments. These compounds are thermally unstable and decompose to peroxacetyl radicals and NO_2. Exposure to related photochemical oxidants have not been measured, nor are these compounds routinely monitored at stationary monitoring sites. Available monitored concentrations of related photochemical oxidants may be found in Annex AX3.

3.10 SUMMARY OF KEY POINTS

Ozone monitored in the United States during “ozone season” vary in length depending on location. The O_3 season extends all year long in the Southwest. In most other areas of the country, the O_3 season typically last from April to October. Median O_3 concentrations averaged over the appropriate O_3 season are about 0.035 ppm. The daily maximum 1-h O_3 concentrations could have been much higher in large urban areas or in areas downwind of large urban areas. For example, in Houston, TX the daily maximum 1-h O_3 concentrations reached 0.202 ppm in

1999 and reached 0.161 ppm in 2000. Although daily maximum 1-h average O_3 concentrations in some areas of the United States downwind of major sources of O_3 precursors can exceed 0.120 ppm, only about 1% of hourly average O_3 concentrations exceed 0.100 ppm at sites in these areas.

Daily maximum 8-h average O_3 concentrations are lower than the maximum 1-h O_3 concentrations but they are highly correlated. Within individual MSAs, O_3 concentrations tend to be well correlated across monitoring sites. However, there can be substantial variations in O_3 concentrations. Ozone in city centers tends to be lower than in regions either upwind or downwind because of titration by NO emitted by motor vehicles.

Ozone concentrations tend to peak in early- to mid-afternoon in areas where there is strong photochemical activity and later in the day in areas where transport is more important in determining the O_3 abundance. Summertime maxima in O_3 concentrations occur in areas in the United States where there is substantial photochemical activity involving O_3 precursors emitted from human activities. Monthly maxima can occur anytime from June through August. However, springtime maxima are observed in national parks, mainly in the western United States and at a number of other relatively unpolluted monitoring sites throughout the Northern Hemisphere. For example, the highest O_3 concentrations at Yellowstone National Park tend to occur during April and May. Generally, monthly minima O_3 concentrations tend to occur from November through February at polluted sites and during the fall at relatively remote sites.

Nationwide, 1-h O_3 concentrations decreased approximately 29% from 1980 to 2003 and approximately 16% from 1990 to 2003. The 8-h O_3 concentration decreased approximately 21% since 1980 and approximately 9% since 1990. Ozone concentrations have continued to decrease nationwide, but the rate of decrease has slowed since 1990. However, these trends have not been uniform across the United States. In general, reductions in O_3 have been largest in New England and states along the West Coast and smallest in states in the Midwest. Downward trends in O_3 in California have been driven mainly by trends in Southern California, with reductions in other areas not being as large.

Sufficient data are not available for other oxidants (e.g., H_2O_2, PAN) and oxidation products (e.g., HNO_3, H_2SO_4) in the atmosphere to relate concentrations of O_3 to these species. Data for these species are only obtained as part of specialized field studies. In general, secondary species, such as HNO_3, H_2SO_4, H_2O_2, and PAN, are expected to be at least moderately correlated with O_3. On the other hand, primary species are expected to be more highly correlated with each other than with secondary species, provided that the primary species originate from common sources. The relationship of O_3 to $PM_{2.5}$ is complex because PM is not a distinct chemical species, but is a mix of primary and secondary species. $PM_{2.5}$ concentrations were positively correlated with O_3 during summer, but negatively correlated with O_3 during winter at Ft. Meade, MD. More data are needed before this result can be applied to other areas.

Co-occurrences of O_3 (defined when both pollutants are present at an hourly average concentration of $\geq$ 0.05 ppm) with NO_2 and SO_2 are rare. For example, there were fewer than 10 co-occurrences with either NO_2 or SO_2 in 2001. The number of co-occurrences for O_3 and $PM_{2.5}$ (defined as an hourly average O_3 concentration $\geq$0.05 ppm and a 24-h average $PM_{2.5}$ concentration $\geq$ 40 $\mu g/m^3$ occurring during the same 24-h period) also tended to be infrequent (< 10 times) at most sites, but there were up to 20 such co-occurrences at a few sites.

Policy relevant O_3 background concentrations are used for assessing risks to human health associated with O_3 produced from anthropogenic sources in continental North America. Because of the nature of the definition of PRB concentrations, they cannot be directly derived from monitored concentrations, instead they must be derived from modeled estimates. Current model estimates indicate that the PRB concentrations in the United States ambient air are generally 0.015 ppm to 0.035 ppm. They decline from spring to summer and are generally < 0.025 ppm under conditions conducive to high O_3 episodes. PRB concentrations can be higher, especially at elevated sites during spring, due to enhanced contributions from hemispheric pollution and stratospheric exchange.

Humans are exposed to O_3 either outdoors or in various micro-environments. Ozone in indoor environments results mainly from infiltration from outdoors. Once indoors, O_3 is removed by deposition on and reaction with surfaces and reaction with other pollutants in the indoor environment such as terpenes (e.g., wood products, solvents, odorants) to produce ultrafine particles. Personal exposure to O_3 tends to be positively associated with time spent outdoors. Although O_3 concentrations obtained at stationary monitoring sites may not explain the variance in individual personal exposures, they may serve a surrogate measures for aggregate personal exposures.

REFERENCES

Adams, W. C. (1993) Measurement of breathing rate and volume in routinely performed daily activities [final report]. Sacramento, CA: California Environmental Protection Agency, Air Resources Board; contract no. A033-205.

Altshuller, A. P.; Lefohn, A. S. (1996) Background ozone in the planetary boundary layer over the United States. J. Air Waste Manage. Assoc. 46: 134-141.

Avol, E. L.; Navidi, W. C.; Colome, S. D. (1998a) Modeling ozone levels in and around southern California homes. Environ. Sci. Technol. 32: 463-468.

Avol, E. L.; Navidi, W. C.; Rappaport, E. B.; Peters, J. M. (1998) Acute effects of ambient ozone on asthmatic, wheezy, and healthy children. Cambridge, MA: Health Effects Institute; research report no. 82.

Bernard, N. L.; Gerber, M. J.; Astre, C. M.; Saintot, M. J. (1999) Ozone measurement with passive samplers: validation and use for ozone pollution assessment in Montpellier, France. Environ. Sci. Technol. 33: 217-222.

Black, D. R.; Harley, R. A.; Hering, S. V.; Stolzenburg, M. R. (2000) A new, portable, real-time monitor. Environ. Sci. Technol. 34: 3031-3040.

Brauer, M.; Brook, J. R. (1997) Ozone personal exposures and health effects for selected groups residing in the Fraser Valley. In: Steyn, D. G.; Bottenheim, J. W., eds. The Lower Fraser Valley Oxidants/Pacific '93 Field Study. Atmos. Environ. 31: 2113-2121.

Burke, J. M.; Zufall, M. J.; Özkaynak, H. (2001) A population exposure model for particulate matter: case study results for $PM_{2.5}$ in Philadelphia, PA. J. Exposure Anal. Environ. Epidemiol. 11: 470-489.

Chang, L.-T.; Koutrakis, P.; Catalano, P. J.; Suh, H. H. (2000) Hourly personal exposures to fine particles and gaseous pollutants—results from Baltimore, Maryland. J. Air Waste Manage. Assoc. 50: 1223-1235.

Christakos, G.; Vyas, V. M. (1998a) A composite space/time approach to studying ozone distribution over eastern United States. Atmos. Environ. 32: 2845-2857.

Christakos, G.; Vyas, V. M. (1998b) A novel method for studying population health impacts of spatiotemporal ozone distribution. Soc. Sci. Med. 47: 1051-1066.

Code of Federal Regulations. (2000) Appendix D to part 58—Network design for state and local air monitoring stations (SLAMS), national air monitoring stations (NAMS), and photochemical assessment monitoring stations (PAMS). C. F. R. 40: pt. 58, app. D.

Cooper, O. R.; Moody, J. L. (2000) Meteorological controls on ozone at an elevated eastern United States regional background monitoring site. J. Geophys. Res. [Atmos.] 105: 6855-6869.

Delfino, R. J.; Coate, B. D.; Zeiger, R. S.; Seltzer, J. M.; Street, D. H.; Koutrakis, P. (1996) Daily asthma severity in relation to personal ozone exposure and outdoor fungal spores. Am. J. Respir. Crit. Care Med. 154: 633-641.

Drakou, G.; Zerefos, C.; Ziomas, I. (1995) A preliminary study on the relationship between outdoor and indoor air pollution levels. Fresenius' Environ. Bull. 4: 689-694.

Ebel, A.; Hass, H.; Jakobs, J. H.; Laube, M.; Memmesheimer, M.; Oberreuter, A. (1991) Simulation of ozone intrusion caused by a tropopause fold and cut-off low. Atmos. Environ. Part A 25: 2131-2144.

Federal Register. (1986) Guidelines for estimating exposures. F. R. (September 24) 51: 34,042-34,054.

Fiore, A. M.; Jacob, D. J.; Bey, I.; Yantosca, R. M.; Field, B. D.; Fusco, A. C.; Wilkinson, J. G. (2002) Background ozone over the United States in summer: origin, trend, and contribution to pollution episodes. J. Geophys. Res. (Atmos.) 107(D15): 10.1029/2001JD000982.

Fiore, A.; Jacob, D. J.; Liu, H.; Yantosca, R. M.; Fairlie, T. D.; Li, Q. (2003) Variability in surface ozone background over the United States: implications for air quality policy. J. Geophys. Res. (Atmos.) 108(D24): 10.1029/2003JD003855.

Freijer, J. I.; Bloemen, H. J. T. (2000) Modeling relationships between indoor and outdoor air quality. J. Air Waste Manage. Assoc. 50: 292-300.

Fusco, A. C.; Logan, J. A. (2003) Analysis of 1970-1995 trends in tropospheric ozone at Northern Hemisphere midlatitudes with the GEOS-CHEM model. J. Geophys. Res. (Atmos.) 108: 10.1029/2002JD002742.

Georgopoulos, P. G.; Arunachalam, S.; Wang, S. (1997a) Alternative metrics for assessing the relative effectiveness of NO_x and VOC emission reductions in controlling ground-level ozone. J. Air Waste Manage. Assoc. 47: 838-850.

Georgopoulos, P. G.; Walia, A.; Roy, A.; Lioy, P. J. (1997b) Integrated exposure and dose modeling and analysis system. 1. Formulation and testing of microenvironmental and pharmacokinetic components. Environ. Sci. Technol. 31: 17-27.

Geyh, A. S.; Wolfson, J. M.; Koutrakis, P.; Mulik, J. D.; Avol, E. L. (1997) Development and evaluation of a small active ozone sampler. Environ. Sci. Technol. 31: 2326-2330.

Geyh, A. S.; Roberts, P. T.; Lurmann, F. W.; Schoell, B. M.; Avol, E. L. (1999) Initial field evaluation of the Harvard active ozone sampler for personal ozone monitoring. J. Exposure Anal. Environ. Epidemiol. 9: 143-149.

Geyh, A. S.; Xue, J.; Özkaynak, H.; Spengler, J. D. (2000) The Harvard Southern California chronic ozone exposure study: assessing ozone exposure of grade-school-age children in two southern California communities. Environ. Health Perspect. 108: 265-270.

Glen, G.; Lakkadi, Y.; Tippett, J. A.; del Valle-Torres, M. (1997) Development of NERL/CHAD: the National Exposure Research Laboratory consolidated human activity database. Research Triangle Park, NC: U.S. Environmental Protection Agency, Office of Research and Development; contract no. 68-D5-0049.

Gold, D. R.; Allen, G.; Damokosh, A.; Serrano, P.; Hayes, C.; Castillejos, M. (1996) Comparison of outdoor and classroom ozone exposures for school children in Mexico City. J. Air Waste Manage. Assoc. 46: 335-342.

Gonzales, M.; Ngo, L.; Hammond, S. K.; Tager, I. (2003) Validation of a questionnaire and microenvironmental model for estimating past exposures to ozone. Int. J. Environ. Health Res. 13: 249-260.

Grosjean, E.; Grosjean, D. (1996) Carbonyl products of the gas phase reaction of ozone with symmetrical alkenes. Environ. Sci. Technol. 30: 2036-2044.

Grosjean, E.; Grosjean, D. (1998) The gas-phase reaction of alkenes with ozone: formation yields of carbonyls from biradicals in ozone-alkene-cyclohexane experiments. Atmos. Environ. 32: 3393-3402.

Hirsch, A. I.; Munger, J. W.; Jacob, D. J.; Horowitz, L. W.; Goldstein, A. H. (1996) Seasonal variation of the ozone production efficiency per unit NOx at Harvard Forest, Massachusetts. J. Geophys. Res. [Atmos.] 101: 12,659-12,666.

Howard-Reed, C.; Wallace, L. A.; Ott, W. R. (2002) The effect of opening windows on air change rates in two homes. J. Air Waste Manage Assoc. 52: 147-159.

Hudman, R. C.; Jacob, D. J.; Cooper, O. C.; Evans, M. J.; Heald, C. L.; Park, R. J.; Fehsenfeld, F.; Flocke, F.; Holloway, J.; Hubler, G.; Kita, K.; Koike, M.; Kondo, Y.; Neuman, A.; Nowak, J.; Oltmans, S.; Parrish, D.; Roberts, J. M.; Ryerson, T. (2004) Ozone production in transpacific Asian pollution plumes and implications for ozone air quality in California. J. Geophys. Res. (Atmos.) 109(D23): 10.1029/2004JD004974.

Jakobi, G.; Fabian, P. (1997) Indoor/outdoor concentrations of ozone and peroxyacetyl nitrate (PAN). Int. J. Biometeorol. 40: 162-165.

Johnson, T. (1997) A pilot study in Los Angeles to measure personal ozone exposures during scripted activities. Washington, DC: American Petroleum Institute, Health and Environmental Sciences Department; API publication no. DR 218.

Johnson, T. (2003) A guide to selected algorithms, distributions, and databases used in exposure models developed by the Office of Air Quality Planning and Standards. Research Triangle Park, NC: U.S. Environmental Protection Agency, Office of Research and Development; EPA grant no. CR827033. Available: http://www.epa.gov/ttn/fera/data/human/report052202.pdf [9 April, 2004].

Johnson, T.; Long, T. (2004) Determining the frequency of open windows in residences: a pilot study in Durham, North Carolina during varying temperature conditions. J. Exposure Anal. Environ. Epidemiol.: 10.1038/sj.jea.7500409.

Johnson, T.; Capel, J.; McCoy, M. (1996a) Estimation of ozone exposures experienced by urban residents using a probabilistic version of NEM and 1990 population data. Research Triangle Park, NC: U.S. Environmental Protection Agency, Office of Air Quality Planning and Standards; contract no. 68-DO-0062.

Johnson, T.; Capel, J.; McCoy, M.; Mozier, J. W. (1996b) Estimation of ozone exposures experienced by outdoor workers in nine urban areas using a probabilistic version of NEM. Research Triangle Park, NC: U.S. Environmental Protection Agency, Office of Air Quality Planning and Standards; contract no. 63-D-30094, work assignment nos. 0-1 and 1-4.

Johnson, T.; Capel, J.; Mozier, J.; McCoy, M. (1996c) Estimation of ozone exposures experienced by outdoor children in nine urban areas using a probabilistic version of NEM. Research Triangle Park, NC: U.S. Environmental Protection Agency, Office of Air Quality Planning and Standards; contract no. 63-D-30094.

Johnson, T.; Mozier, J.; Capel, J. (1997) Supplement to "Estimation of ozone exposures experienced by outdoor children in nine urban areas using a probabilistic version of NEM (April 1996)". Research Triangle Park, NC: U.S. Environmental Protection Agency, Office of Air Quality Planning and Standards.

Johnson, T.; Mihlan, G.; LaPointe, J.; Fletcher, K.; Capel, J. (1999) Estimation of carbon monoxide exposures and associated carboxyhemoglobin levels in Denver residents using pNEM/CO (version 2.0) [draft]. Research Triangle Park, NC: U.S. Environmental Protection Agency, Office of Air Quality Planning and Standards; March 15.

Johnson, T.; Myers, J.; Kelly, T.; Wisbith, A.; Ollison, W. (2004) A pilot study using scripted ventilation conditions to identify key factors affecting indoor pollutant concentrations and air exchange rate in a residence. J. Exposure Anal. Environ. Epidemiol. 14: 1-22.
Klepeis, N. E.; Tsang, A. M.; Behar, J. V. (1996) Analysis of the national human activity pattern survey (NHAPS) respondents from a standpoint of exposure assessment. Washington, DC: U.S. Environmental Protection Agency, Office of Research and Development; report no. EPA/600/R-96/074.
Klepeis, N. E.; Nelson, W. C.; Ott. W. R.; Robinson, J. P. Tsang, A. M.; Switzer, P.; Behar, J. V.; Hern, S. C.; Engelmann, W. H. (2001) The National Human Activity Pattern Survey (NHAPS): a resource for assessing exposure to environmental pollutants. J. Exposure Anal. Environ. Epidemiol. 11: 231-252.
Koutrakis, P.; Sioutas, C.; Ferguson, S. T.; Wolfson, J. M.; Mulik, J. D.; Burton, R. M. (1993) Development and evaluation of a glass honeycomb denuder/filter pack system to collect atmospheric gases and particles. Environ. Sci. Technol. 27: 2497-2501.
Krzyzanowski, M. (1997) Methods for assessing the extent of exposure and effects of air pollution. Occup. Environ. Med. 54: 145-151.
Lagus Applied Technology, Inc. (1995) Air change rates in non-residential buildings in California. Sacramento, CA: California Energy Commission; contract no. 400-91-034; July.
Lee, E. H.; Hogsett, W. E. (1999) Role of concentrations and time of day in developing ozone exposure indices for a secondary standard. J. Air Waste Manage. Assoc. 49: 669-681.
Lee, K.; Xue, J.; Geyh, A. S.; Ozkaynak, H.; Leaderer, B. P.; Weschler, C. J.; Spengler, J. D. (2002) Nitrous acid, nitrogen dioxide, and ozone concentrations in residential environments. Environ. Health Perspect. 110: 145-150.
Lee, K.; Parkhurst, W. J.; Xue, J.; Özkaynak, H.; Neuberg, D.; Spengler, J. D. (2004) Outdoor/indoor/personal ozone exposures of children in Nashville, Tennessee. J. Air Waste Manage. Assoc. 54: 352-359.
Lefohn, A. S.; Runeckles, V. C. (1987) Establishing standards to protect vegetation - ozone exposure/dose considerations. Atmos. Environ. 21: 561-568.
Lefohn, A. S.; Oltmans, S. J.; Dann, T.; Singh, H. B. (2001) Present-day variability of background ozone in the lower troposphere. J. Geophys. Res. [Atmos.] 106: 9945-9958.
Leovic, K. W.; Sheldon, L. S.; Whitaker, D. A.; Hetes, R. G.; Calcagni, J. A.; Baskir, J. N. (1996) Measurement of indoor air emissions from dry-process photocopy machines. J. Air Waste Manage. Assoc. 46: 821-829.
Leovic, K.; Whitaker, D.; Northeim, C.; Sheldon, L. (1998) Evaluation of a test method for measuring indoor air emissions from dry-process photocopiers. J. Air Waste Manage. Assoc. 48: 915-923.
Liang, J.; Horowitz, L. W.; Jacob, D. J.; Wang, Y.; Fiore, A. M.; Logan, J. A.; Gardner, G. M.; Munger, J. W. (1998) Seasonal budgets of reactive nitrogen species and ozone over the United States, and export fluxes to the global atmosphere. J. Geophys. Res. (Atmos.) 103: 13,435-13,450.
Liard, R.; Zureik, M.; Le Moullec, Y.; Soussan, D.; Glorian, M.; Grimfeld, A.; Neukirch, F. (1999) Use of personal passive samplers for measurement of NO_2, NO, and O_3 levels in panel studies. Environ. Res. 81: 339-348.
Lin, C.-Y.; Jacob, D. J.; Munger, J. W.; Fiore, A. M. (2000) Increasing background ozone in surface air over the United States. Geophys. Res. Lett. 27: 3465-3468.
Linn, W. S.; Shamoo, D. A.; Hackney, J. D. (1992) Documentation of activity patterns in 'high-risk' groups exposed to ozone in the Los Angeles area. In: Tropospheric ozone and the environment II: effects, modeling and control: papers from an Air & Waste Management Association international specialty conference; November, 1991; Atlanta, GA. Pittsburgh, PA: Air & Waste Management Association; pp. 701-712. (A&WMA publication TR-20).
Linn, W. S.; Shamoo, D. A.; Anderson, K. R.; Peng, R.-C.; Avol, E. L.; Hackney, J. D.; Gong, H., Jr. (1996) Short-term air pollution exposures and responses in Los Angeles area schoolchildren. J. Exposure Anal. Environ. Epidemiol. 6: 449-472.
Liu, L.-J. S.; Koutrakis, P.; Leech, J.; Broder, I. (1995) Assessment of ozone exposures in the greater metropolitan Toronto area. J. Air Waste Manage. Assoc. 45: 223-234.
Liu, L.-J. S.; Delfino, R.; Koutrakis, P. (1997) Ozone exposure assessment in a southern California community. Environ. Health Perspect. 105: 58-65.
Logan, J. A. (1989) Ozone in rural areas of the United States. J. Geophys. Res. [Atmos.] 94: 8511-8532.
McCurdy, T. (2000) Conceptual basis for multi-route intake dose modeling using an energy expenditure approach. J. Exposure Anal. Environ. Epidemiol. 10: 86-97.
McCurdy, T.; Glen, G.; Smith, L.; Lakkadi, Y. (2000) The National Exposure Research Laboratory's Consolidated Human Activity Database. J. Exposure Anal. Environ. Epidemiol. 10: 566-578.

Morrison, G. C.; Nazaroff, W. W. (2000) The rate of ozone uptake on carpets: experimental studies. Environ. Sci. Technol. 34: 4963-4968.

Morrison, G. C.; Nazaroff, W. W. (2002) Ozone interactions with carpet: secondary emissions of aldehydes. Environ. Sci. Technol. 36: 2185-2192.

Murray, D. M.; Burmaster, D. E. (1995) Residential air exchange rates in the United States: empirical and estimated parametric distributions by season and climatic region. Risk Anal. 15: 459-465.

Nazaroff, W. W.; Cass, G. R. (1986) Mathematical modeling of chemically reactive pollutants in indoor air. Environ. Sci. Technol. 20: 924-934.

Nazaroff, W. W.; Weschler, C. J. (2004) Cleaning products and air fresheners: exposure to primary and secondary air pollutants. Atmos. Environ. 38: 2841-2865.

Niu, J.; Tung, T. C. W.; Burnett, J. (2001) Ozone emission rate testing and ranking method using environmental chamber. Atmos. Environ. 35: 2143-2151.

Northeast States for Coordinated Air Use Management (NESCAUM). (2002) Indoor/outdoor school air monitoring project. Boston, MA. Available: http://www.nescaum.org/pdf/schoolmonitoring.pdf [29 October, 2003].

O'Neill, M. S.; Ramirez-Aguilar, M.; Meneses-Gonzalez, F.; Hernández-Avila, M.; Geyh, A. S.; Sienra-Monge, J. J.; Romieu, I. (2003) Ozone exposure among Mexico City outdoor workers. J. Air Waste Manage. Assoc. 53: 339-346.

Ott, W. R. (1982) Concepts of human exposure to air pollution. Environ. Int. 7: 179-196.

Ott, W. R. (1985) Total human exposure: an emerging science focuses on humans as receptors of environmental pollution. Environ. Sci. Technol. 19: 880-886.

Park, J.-H.; Spengler, J. D.; Yoon, D.-W.; Dumyahn, T.; Lee, K.; Ozkaynak, H. (1998) Measurement of air exchange rate of stationary vehicles and estimation of in-vehicle exposure. J. Exposure Anal. Environ. Epidemiol. 8: 65-78.

Reiss, R.; Ryan, P. B.; Koutrakis, P.; Tibbetts, S. J. (1995) Ozone reactive chemistry on interior latex paint. Environ. Sci. Technol. 29: 1906-1912.

Riediker, M.; Williams, R.; Devlin, R.; Griggs, T.; Bromberg, P. (2003) Exposure to particulate matter, volatile organic compounds, and other air pollutants inside patrol cars. Environ. Sci. Technol. 37: 2084-2093.

Roelofs, G. J.; Scheeren, H. A.; Heland, J.; Ziereis, H.; Lelieveld, J. (2003) A model study of ozone in the eastern Mediterranean free troposphere during MINOS (August 2001). Atmos. Chem. Phys. 3: 1199-1210.

Romieu, I.; Lugo, M. C.; Colome, S.; Garcia A. M.; Avila, M. H.; Geyh, A.; Velasco, S. R.; Rendon, E. P. (1998) Evaluation of indoor ozone concentration and predictors of indoor-outdoor ratio in Mexico City. J. Air Waste Manage. Assoc. 48: 327-335.

Salmon, L. G.; Cass, G. R.; Bruckman, K.; Haber, J. (2000) Ozone exposure inside museums in the historic central district of Krakow, Poland. Atmos. Environ. 34: 3823-3832.

Sarnat, J. A.; Koutrakis, P.; Suh, H. H. (2000) Assessing the relationship between personal particulate and gaseous exposures of senior citizens living in Baltimore, MD. J. Air Waste Manage. Assoc. 50: 1184-1198.

Sarnat, J. A.; Schwartz, J.; Catalano, P. J.; Suh, H. H. (2001) Gaseous pollutants in particulate matter epidemiology: confounders or surrogates? Environ. Health Perspect. 109: 1053-1061.

Sarwar, M.; Corsi, R.; Kimura, Y.; Allen, D.; Weschler, C. (2001) Hydroxyl radicals in indoor environments. In: Proceedings of the Air & Waste Management Association's 94th Annual Conference & Exhibition; June; Orlando, FL. Pittsburgh, PA: Air & Waste Management Association.

Sarwar, G.; Corsi, R.; Kumura, Y.; Allen, D.; Weschler, C. J. (2002) Hydroxyl radicals in indoor environments. Atmos. Environ. 36: 3973-3988.

Sørensen, D. N.; Weschler, C. J. (2002) Modeling-gas phase reactions in indoor environments using computational fluid dynamics. Atmos. Environ. 36: 9-18.

Spier, C. E.; Little, D. E.; Trim, S. C.; Johnson, T. R.; Linn, W. S.; Hackney, J. D. (1992) Activity patterns in elementary and high school students exposed to oxidant pollution. J. Exposure Anal. Environ. Epidemiol. 2: 277-293.

Steiber, R. S. (1995) Ozone generators in indoor air settings. Research Triangle Park, NC: U.S. Environmental Protection Agency, National Risk Management Research Laboratory; report no. EPA-600/R-95-154. Available from: NTIS, Springfield, VA; PB96-100201.

Trainer, M.; Parrish, D. D.; Buhr, M. P.; Norton, R. B.; Fehsenfeld, F. C.; Anlauf, K. G.; Bottenheim, J. W.; Tang, Y. Z.; Wiebe, H. A.; Roberts, J. M.; Tanner, R. L.; Newman, L.; Bowersox, V. C.; Meagher, J. F.; Olszyna, K. J.; Rodgers, M. O.; Wang, T.; Berresheim, H.; Demerjian, K. L.; Roychowdhury, U. K. (1993) Correlation of ozone with NO_y in photochemically aged air. J. Geophys. Res. [Atmos.] 98: 2917-2925.

Turk, B. H.; Grimsrud, D. T.; Brown, J. T.; Geisling-Sobotka, K. L.; Harrison, J.; Prill, R. J. (1989) Commercial building ventilation rates and particle concentrations. ASHRAE Trans. 95(part 1): 422-433.

U.S. Environmental Protection Agency. (1978) Air quality criteria for ozone and other photochemical oxidants. Research Triangle Park, NC: Office of Health and Environmental Assessment, Environmental Criteria and Assessment Office; report no. EPA-600/8-78-004. Available from: NTIS, Springfield, VA; PB80-124753.

U.S. Environmental Protection Agency. (1986) Air quality criteria for ozone and other photochemical oxidants. Research Triangle Park, NC: Office of Health and Environmental Assessment, Environmental Criteria and Assessment Office; report nos. EPA-600/8-84-020aF-eF. 5v. Available from: NTIS, Springfield, VA; PB87-142949.

U.S. Environmental Protection Agency. (1992) Guidelines for exposure assessment. Washington, DC: Risk Assessment Forum, USEPA 600Z-92/001.

U.S. Environmental Protection Agency. (1996) Air quality criteria for ozone and related photochemical oxidants. Research Triangle Park, NC: Office of Research and Development; report nos. EPA/600/AP-93/004aF-cF. 3v. Available from: NTIS, Springfield, VA; PB96-185582, PB96-185590, and PB96-185608. Available: http://cfpub2.epa.gov/ncea/.

U.S. Environmental Protection Agency. (2003a) Technology Transfer Network: Air Quality System (AQS). Washington, DC: Office of Air and Radiation. Available: http://www.epa.gov/ttn/airs/airsaqs/ [1 April, 2004].

U.S. Environmental Protection Agency. (2003b) Latest findings on national air quality: 2002 status and trends. Research Triangle Park, NC: Office of Air Quality Planning and Standards; report no. EPA/454/K-03-001. Available: http://www.epa.gov/airtrends/2002_airtrends_final.pdf [18 December, 2003]. Available: NTIS, Springfield, VA; PB2004-100183.

Väkevä, M.; Hämeri, K.; Kulmala, M.; Lahdes, R.; Ruuskanen, J.; Laitinen, T. (1999) Street level versus rooftop concentrations of submicron aerosol particles and gaseous pollutants in an urban street canyon. Atmos. Environ. 33: 1385-1397.

Wainman, T.; Zhang, J.; Weschler, C. J.; Lioy, P. J. (2000) Ozone and limonene in indoor air: a source of submicron particle exposure. Environ. Health Perspect. 108: 1139-1145.

Weschler, C. J. (2000) Ozone in indoor environments: concentration and chemistry. Indoor Air 10: 269-288.

Weschler, C. J.; Shields, H. C. (1997) Potential reactions among indoor pollutants. Atmos. Environ. 31: 3487-3495.

Weschler, C. J.; Shields, H. C. (1999) Indoor ozone/terpene reactions as a source of indoor particles. Atmos. Environ. 33: 2301-2312.

Weschler, C. J.; Shields, H. C.; Naik, D. V. (1989) Indoor ozone exposures. JAPCA 39: 1562-1568.

Weschler, C. J.; Shields, H. C.; Naik, D. V. (1994) Indoor chemistry involving O3, NO, and NO2 as evidenced by 14 months of measurements at a site in southern California. Environ. Sci. Technol. 28: 2120-2132.

Zanis, P.; Trickl, T.; Stohl, A.; Wernli, H.; Cooper, O.; Zerefos, C.; Gaeggeler, H.; Schnabel, C.; Tobler, L.; Kubik, P. W.; Priller, A.; Scheel, H. E.; Kanter, H. J.; Cristofanelli, P.; Forster, C.; James, P.; Gerasopoulos, E.; Delcloo, A.; Papayannis, A.; Claude, H. (2003) Forecast, observation and modelling of a deep stratospheric intrusion event over Europe. Atmos. Chem. Phys. 3: 763-777.

Zeger, S. L.; Thomas, D.; Dominici, F.; Samet, J. M.; Schwartz, J.; Dockery, D.; Cohen, A. (2000) Exposure measurement error in time-series studies of air pollution: concepts and consequences. Environ. Health Perspect. 108: 419-426.

ANNEX AX3. ENVIRONMENTAL CONCENTRATIONS, PATTERNS, AND EXPOSURE ESTIMATES

AX3.1 INTRODUCTION

Identification and Use of Existing Air Quality Data

The effects of ozone (O_3) on humans, animals, and vegetation have received extensive examination and are discussed in detail subsequent annexes. As indicated in the previous document, Air Quality Criteria for Ozone and Related Oxidants (1996 O_3 AQCD; U.S. Environmental Protection Agency, 1996a), most of the human and welfare effects research has focused on evaluating impacts on health or vegetation from exposure to O_3 that simulate ambient O_3 exposures (e.g., matching the occurrence of hourly average concentrations or more prolonged times of exposure). The information contained within this annex on concentrations was obtained from extensive monitoring in the United States can be useful both for linking anthropogenic emissions of O_3 precursors with health and welfare effects and for augmenting exposure assessment and epidemiology studies.

The information obtained for this annex is primarily available from a database that has been designed to archive air quality data from a network of monitoring stations that have been established to determine compliance with the National Ambient Air Quality Standards (NAAQS) defined in 40 CFR 50. Air quality monitoring is conducted continuously through the National Air Monitoring Network, which consists of monitoring stations defined in 40 CFR 58.20. State and Local Ambient Monitoring Stations (SLAMS) are located throughout the United States. National Ambient Monitoring Stations (NAMS) are located in areas where possible human exposure to air contaminants could potentially be a risk. NAMS are used to provide data for national policy and trend analysis and to give the public information about air quality in major metropolitan areas. These monitoring stations are required in urban areas with populations greater than 200,000 and are selected from a subset of the State and Local Air Monitoring Stations (SLAMS) network. The data from all of these sites are gathered and stored in the U.S. Environmental Protection Agency Air Quality System (AQS; formerly the AIRS database). These available data were collected from 1979 to 2001. As discussed in the previous versions of the O_3 AQCD (U.S. Environmental Protection Agency, 1986, 1996a), the data available prior to

1979 may be considered unreliable due to calibration problems and uncertainties. The AQS contains readily accessible detailed, hourly data that has been subject to the Agency's quality control and assurance procedures. The information has been summarized in a series of tables and graphs to better describe the current O_3 situation. Most of the field data were collected by the various state agencies and O_3 working groups for regulation and enforcement of O_3 levels, but the information may also be used to determine trends and patterns for O_3 surface concentrations. In the sections that follow, the hourly averaged ambient O_3 data have been summarized in different ways to reflect the interests of those who wish to know more about the potential for O_3 exposure of humans and the environment. This annex is not meant to be an exposure assessment for ambient O_3; rather, this annex elucidates the features of O_3 concentration patterns and exposure possibilities.

As indicated in the previous O_3 AQCD (U.S. Environmental Protection Agency, 1996a), O_3 is the only photochemical oxidant, other than nitrogen dioxide (NO_2), that is routinely monitored and for which a comprehensive aerometric database exists. Data for peroxyacetyl nitrate (PAN) and hydrogen peroxide (H_2O_2) have been obtained only as part of special research field investigations. Consequently, no data on nationwide patterns of occurrence are available for these non-O_3 oxidants; nor are extensive data available on the correlations of levels and patterns of these oxidants with those of O_3.

Characterizing Ambient Ozone Concentrations

In this annex, data are analyzed for the purpose of providing focus on specific issues of exposure-response relationships that are considered in the later annexes addressing O_3 exposure effects. It is important to distinguish among concentration, exposure, and dose when using air quality data to assess human health and vegetation effects. For this annex, the following definitions apply:

(1) The "concentration" of a specific air pollutant is typically defined as the amount (mass) of that material per unit volume of air. Air pollution monitors measure pollutant concentrations, which may or may not provide accurate exposure estimates. However, most of the data presented herein are expressed as a "mixing ratio" in terms of a volume-to-volume ratio expressed as parts per million (ppm) or parts per billion (ppb).

(2) The term “exposure” is defined as the concentration of a pollutant encountered by the subject (animal, human, or plant) for a duration of time. Exposure implies that such an encounter leads to intake (i.e., through the respiratory tract or stomata). It is expressed in terms of ppm × time.

(3) The term “dose” is defined as that mass of pollutant delivered to a target. This term has numerous quantitative descriptions (e.g., micrograms of O_3 per square centimeter of lung epithelium per minute), so the context of the use of this term and the units within the document must be considered.

The dose incurred by an organism (e.g., plant, animal, or human) is a more complicated measure involving the concentration, the exposure duration, and the volume of delivered air (e.g., through inhalation). These distinctions become important because the concentration of an airborne contaminant that is measured in an empty room or at a stationary outdoor monitor is not in fact an exposure. A measured concentration functions as a surrogate for an exposure only to the degree to which it represents concentrations actually experienced by individuals under otherwise similar conditions.

Concentrations of airborne contaminants for vegetation are considered to represent an exposure when a plant is subjected to them over a specified time period. As indicated in Chapter 9, dose has been defined historically by air pollution vegetation researchers as ambient air quality concentration multiplied by time (O’Gara, 1922). However, a more rigorous definition was required. Runeckles (1974) introduced the concept of “effective dose” as the amount or concentration of pollutant that is adsorbed by vegetation, in contrast to that which is present in the ambient air. Fowler and Cape (1982) developed this concept further and proposed that the “pollutant adsorbed dose” be defined in units of grams per square meter (of ground or leaf area) and could be obtained as the product of concentration, time, and stomatal (or canopy) conductance for the gas in question. Taylor et al. (1982) suggested internal flux (milligrams per square meter per hour) as a measure of the dose to which plants respond. In this annex, dose will be taken to signify, for the purposes of vegetation, that amount of pollutant absorbed by the plant.

Although parallel mathematical definitions to quantify exposure and dose have been employed in animal and human health effects research, the equivalent biologic effects between species and plants induced by a specific dose is at present difficult to define. In order to characterize the specific doses responsible for affecting human health and vegetation, there has to be a linkage between exposure and actual dose. Unfortunately, it is difficult to predict this relationship, even with the available models. For example, the sensitivity of vegetation to O_3 as a function of time of day, period of growth, or edaphic conditions can determine the severity of response (see Chapter 9). Similarly, in animals and humans, additional factors such as the state of the organism's susceptibility, physical activity, demographic characteristics will substantially modulate the intensity and persistence of response. Because not enough is known to quantify the links between exposure, dosage, and vegetation and human effects, routine monitoring for O_3 is summarized as hourly average concentrations. Whenever the information is available the exposure or dose will be reported as well. Most of the information provided in this annex is characterized in terms of concentration and exposure.

For many years, as indicated in Chapter 9, air pollution specialists have explored alternative mathematical approaches for summarizing ambient air quality information in biologically meaningful forms that can serve as alternatives for characterizing dose. Extensive research has focused on identifying indicators of concentration and duration (exposure) that are firmly founded on biological principles for vegetation. Many of these indicators have been based on research results indicating that the magnitude of vegetation responses to air pollution is determined more as a function of the magnitude of the concentration than of the length of the exposure (U.S. Environmental Protection Agency, 1996a). Short-term (1-h), high O_3 concentrations ($\geq$ 0.1 ppm) have been identified by many researchers as being more important than long-term, low O_3 concentrations in inducting visible injury and damage to vegetation (see Chapter 9 for further discussion).

Long-term, average concentrations (e.g., 7-h seasonal daylight average concentrations) were used initially as an exposure indicator to describe O_3 concentrations over time when assessing vegetation effects (Heck et al., 1982). The 1996 O_3 AQCD (U.S. Environmental Protection Agency, 1996a) concluded that higher concentrations of O_3 should be given more weight than lower concentrations (see Chapter 9 for further details). Similar observations on the importance of peak concentration on the magnitude of response have been reported in human studies (Hazucha et al., 1992; Adams, 2003) (see Chapter 6; Annex 6, Section AX6.2.4 for further discussion). They reported that a triangular pattern of exposure elicited substantially greater functional response than the same O_3 dose with an even concentration profile. These findings suggest that a similar approach as employed in assessing damage to vegetation should be used in human studies (i.e., that higher concentration should be given more weight in deriving exposure dose).

As outlined in the 1996 O_3 AQCD, several investigators have suggested additional representations other than strict concentration analysis for assessing O_3 impact on human health and other welfare issues (see Chapter 9 for information concerning the use of "effective flux" as a way to predict potential vegetation effects). Many of these methodologies examine the relationships between concentration, exposure, and dose.

In summarizing the hourly average concentrations in this annex, specific attention is given to the relevance of the exposure indicators used. For example, for human health considerations, concentration (or exposure) indicators such as the daily maximum 1-h average concentrations, as well as the number of daily maximum 8-h average concentrations, are used to characterize information in the population-oriented locations. For vegetation, several different types of exposure indicators are used. Several exposure indicators that use either a threshold or a sigmoidal weighting scheme are used in this annex to provide insight concerning the O_3 exposures that are experienced at a select number of rural monitoring sites in the United States. The peak-weighted, cumulative-exposure indicators used in this annex are SUM06 and SUM08 (the sums of all hourly average concentrations $\geq$ 0.06 and 0.08 ppm, respectively) and W126 (the sum of the hourly average concentrations that have been weighted according to a sigmoid function [see Lefohn and Runeckles, 1987] that is based on a hypothetical vegetation response). Further discussion of these exposure indices is presented in Chapter 9.

The exposure indicators used for human health considerations are in mixing ratios (i.e., parts per million), whereas the indicators used for vegetation (e.g., SUM06, SUM08, W126) are in parts per million-hour (ppm-h). Although ppm are mixing ratios, they are commonly referred to as concentrations and will be referred to as concentrations in this chapter. The magnitude of the peak-weighted, cumulative indicators at specific sites can be compared with those values experienced at areas that experience low hourly average maximum concentrations. In some cases, to provide more detailed information about the distribution patterns for a specific O_3 exposure regime, the percentile distribution of the hourly average concentrations (in ppm) is given. For further clarification of the determination and rationale for the exposure indicators that are used for assessing human health and vegetation effects, the reader is encouraged to read Section AX3.10 in this annex as well as Chapter 9.

To obtain a better understanding of the potential effect of ambient O_3 concentrations on human health and vegetation, hourly average concentration information was summarized for urban versus rural (forested and agricultural) areas in the United States. A land use characterization of rural does not imply that any specific location is isolated from anthropogenic influences. For example, Logan (1989) has noted that hourly average O_3 concentrations above 0.08 ppm are common in rural areas of the eastern United States in spring and summer, but are unusual at remote western sites. Consequently, for the purposes of comparing exposure regimes that may be characteristic of clean locations in the United States with those that are urban influenced (i.e., located in either urban or rural locations), this annex characterizes data collected from those stations whose locations appear to be isolated from large-scale anthropogenic influences.

Long-term (multiyear) patterns and trends are available only from stationary ambient monitors; data on indoor concentrations are collected predominantly in selected settings during comparatively short-term studies. Data from the indoor and outdoor environments are reviewed here separately.

Ambient air means the portion of the atmosphere, external to buildings, to which the general public has access (CFR, 2000a). The 1-h and/or the 8-h O_3 ambient air quality standards are respectively met at an air quality monitoring site when the second highest daily maximum 1-h average O_3 concentration is $\leq$ 0.12 ppm and/or the average of the annual fourth-highest daily maximum 8-h average O_3 concentration is $\leq$ 0.08 ppm, as determined in accordance with Appendix I to 40 CFR Part 50 (CFR, 2000a).

Acknowledging the photochemical and insulation-dependent nature of O_3 formation, the U.S. Environmental Protection Agency (U.S. EPA) has established allowable "ozone seasons" for the required measurement of ambient O_3 concentrations for different locations within the United States and U.S. territories (CFR, 2000b). Table AX3-1 shows the summarized O_3 seasons during which continuous, hourly averaged O_3 concentrations must be monitored.

In Section AX3.2, surface O_3 concentrations are characterized and the difficulties of characterizing background O_3 concentrations for controlled exposure studies and for assessing the health benefits associated with setting the NAAQS are discussed. In addition, hourly averaged concentrations obtained by several monitoring networks have been characterized for urban and rural areas. The diurnal variations for the various urban and rural locations are found

Table AX3-1. Ozone Monitoring Seasons by State

State	Start Month — End	State	Start Month — End
Alabama	March — October	Nevada	January — December
Alaska	April — October	New Hampshire	April — September
Arizona	January — December	New Jersey	April — October
Arkansas	March — November	New Mexico	January — December
California	January — December	New York	April — October
Colorado	March - September	North Carolina	April — October
Connecticut	April — September	North Dakota	May — September
Delaware	April — October	Ohio	April — October
District of Columbia	April — October	Oklahoma	March — November
Florida	March — October	Oregon	May — September
Georgia	March — October	Pennsylvania	April — October
Hawaii	January — December	Puerto Rico	January — December
Idaho	April — October	Rhode Island	April — September
Illinois	April — October	South Carolina	April — October
Indiana	April — September	South Dakota	June — September
Iowa	April — October	Tennessee	March — October
Kansas	April — October	Texas[1]	January — December
Kentucky	March — October	Texas[1]	March — October
Louisiana	January — December	Utah	May — September
Maine	April — September	Vermont	April — September
Maryland	April — October	Virginia	April — October
Massachusetts	April — September	Washington	May — September
Michigan	April — September	West Virginia	April — October
Minnesota	April — October	Wisconsin	April 15 — October 15
Mississippi	March — October	Wyoming	April — October
Missouri	April — October	American Samoa	January — December
Montana	June — September	Guam	January — December
Nebraska	April — October	Virgin Islands	January — December

[1]The ozone season is defined differently in different sections of Texas.

Source: CFR (2000b).

in Section AX3.3, where urban and rural patterns are described. In Section AX3.4, seasonal patterns of the 1-h and 8-h average concentrations are discussed. Spatial variations that occur within urban areas, between rural and urban areas, as well as variations with elevation are discussed in Section AX3.5. Section AX3.6 of this annex summarizes the historical trends for 1980 to 2001 on a national scale and for selected cities. The most recent U.S. EPA trends results are also presented. Section AX3.7 describes available information for the concentrations and patterns of related photochemical oxidants. Section AX3.8 describes the co-occurrence patterns of O_3 with NO_2, sulfur dioxide (SO_2), and 24-h $PM_{2.5}$. Indoor O_3 concentrations, including sources and factors affecting indoor O_3 concentrations, are described in Section AX3.9. Section AX3.10 describes human population exposure measurement methods, factors influencing exposure, and exposure models.

AX3.2 SURFACE OZONE CONCENTRATIONS

Data for O_3 concentrations in a number of different environments, ranging from urban to remote, are summarized and characterized in this section. The characterization of the variability of O_3 concentrations in these different environments receives the main emphasis. Another important issue relates to the determination of background concentrations. There are a number of different uses of the term background depending on the context in which it is used. Various definitions of background have been covered in the 1996 O_3 AQCD (U.S. Environmental Protection Agency, 1996a) and in Air Quality Criteria for Particulate Matter (PM AQCD; U.S. Environmental Protection Agency, 1996b). This section deals with the characterization of background O_3 concentrations that are used for two main purposes: (1) performing experiments relating the effects of exposure to O_3 on humans, animals, and vegetation; and (2) assessing the health benefits associated with setting different levels of the NAAQS for O_3. Ozone background concentrations used for NAAQS setting purposes are referred to as policy relevant background (PRB) concentrations. PRB concentrations are defined by the U.S. EPA Office of Air Quality Programs and Standards (OAQPS) as those concentrations that would be observed in the United States if anthropogenic sources of O_3 precursors were turned off in continental North America (the United States, Canada and Mexico), i.e., the definition includes O_3 formed from natural sources everywhere in the world and from anthropogenic O_3 precursors outside of North

America. The 1996 O_3 AQCD considered two possible methods for quantifying background O_3 concentrations for the two purposes mentioned above. The first method was to estimate, using mathematical models and historical data, unpolluted and natural background levels not susceptible to human influence. The second method was to use the distribution of hourly average O_3 concentrations observed at clean, relatively remote monitoring sites (RRMS) in the United States (i.e., those which experience low maximum hourly concentrations). Because of a lack of simulations by available numerical models, the second method was employed in the 1996 O_3 AQCD.

Sections AX3.2.1 and AX3.2.2 review data for O_3 concentrations in urban and nonurban (but influenced by urban emissions) environments. Section AX3.2.3 reviews the data from relatively clean remote sites, addresses the issue of how to use these data to help set background levels for controlled exposure studies, and presents evidence of trends in O_3 concentrations at these sites. The characterization of PRB O_3 concentrations will be the subject of Section AX3.2.4. Two alternative approaches for establishing PRB concentrations are presented: the first uses data from relatively clean, remote monitoring sites and the second uses numerical models. The strengths and weaknesses of each approach are presented in the hopes of stimulating discussion that will resolve issues related to the use of either of these alternative methods.

AX3.2.1 Urban Area Concentrations

Often there is a difference in the distribution of hourly average concentrations between urban and nonurban areas. For example, it is possible for urban emissions, as well as O_3 produced from urban area emissions, to be transported to more rural locations downwind. This can result in elevated O_3 concentrations at considerable distances from urban centers (U.S. Environmental Protection Agency, 1996a). Urban O_3 concentrations often are depressed because of titration by NO_x (Stasiuk and Coffey, 1974). The phenomenon, where O_3 concentrations measured at center-city sites are lower than some rural locations, was reported by Reagan (1984) and Lefohn et al. (1987). Because of the absence of chemical scavenging, O_3 tends to persist longer in nonurban than in urban areas (U.S. Environmental Protection Agency, 1996a).

Table AX3-2 summarizes the percentile distribution for the hourly average concentrations at specific monitoring sites for the period of April 1999 through October 2001. As can be seen

Table AX3-2. Summary of Percentiles of Hourly Average Concentrations (ppm) for the April to October Period

AQS*	Name	Area	Year	Min.	Percentiles 10	30	50	70	90	95	99	Max.	Number of Observations
Georgia													
131210055	Fulton Co.	Atlanta	1999	0.001	0.005	0.017	0.032	0.051	0.082	0.097	0.124	0.157	4880
131210055	Fulton Co.	Atlanta	2000	0.002	0.002	0.013	0.027	0.044	0.071	0.082	0.105	0.162	5021
131210055	Fulton Co.	Atlanta	2001	0.002	0.002	0.011	0.023	0.037	0.062	0.072	0.087	0.118	5071
North Carolina													
371191009	Mecklenberg, Co.	Charlotte	1999	0.005	0.005	0.021	0.034	0.050	0.073	0.086	0.106	0.122	5090
371191009	Mecklenberg, Co.	Charlotte	2000	0.005	0.005	0.019	0.034	0.048	0.068	0.078	0.098	0.144	5066
371191009	Mecklenberg, Co.	Charlotte	2001	0.005	0.005	0.020	0.032	0.046	0.067	0.076	0.092	0.128	5096
Connecticut													
90013007	Fairfield, Co.	Stratford	1999	0.000	0.010	0.025	0.035	0.045	0.060	0.070	0.095	0.158	4342
90013007	Fairfield, Co.	Stratford	2000	0.000	0.009	0.022	0.031	0.041	0.056	0.064	0.090	0.14	4655
90013007	Fairfield, Co.	Stratford	2001	0.000	0.011	0.026	0.037	0.046	0.061	0.072	0.096	0.148	4364
California													
60710005	San Bernardino Co.	Los Angeles	1999	0.000	0.023	0.042	0.054	0.070	0.094	0.106	0.132	0.174	4910
60710005	San Bernardino Co.	Los Angeles	2000	0.000	0.017	0.037	0.050	0.064	0.087	0.098	0.123	0.176	4922
60710005	San Bernardino Co.	Los Angeles	2001	0.005	0.024	0.043	0.055	0.068	0.093	0.107	0.135	0.170	4922
Texas													
482010055	Harris Co.	Houston	1999	0.000	0.004	0.014	0.025	0.040	0.070	0.086	0.120	0.202	4942
482010055	Harris Co.	Houston	2000	0.000	0.004	0.014	0.023	0.036	0.062	0.077	0.105	0.161	4889
482010055	Harris Co.	Houston	2001	0.000	0.001	0.011	0.022	0.034	0.058	0.073	0.102	0.173	4897

Table AX3-2 (cont'd). Summary of Percentiles of Hourly Average Concentrations (ppm) for the April to October Period

AQS*	Name	Area	Year	Min.	Percentiles 10	30	50	70	90	95	99	Max.	Number of Observations
Louisiana													
220331001	E. Baton Rouge	Baton Rouge	1999	0.000	0.006	0.018	0.032	0.047	0.069	0.079	0.101	0.128	4932
220331001	E. Baton Rouge	Baton Rouge	2000	0.000	0.007	0.018	0.030	0.045	0.066	0.075	0.092	0.151	5034
220331001	E. Baton Rouge	Baton Rouge	2001	0.000	0.004	0.014	0.024	0.037	0.056	0.065	0.082	0.101	5000
Maryland													
240251001	Edgewood	DC	1999	0.000	0.000	0.016	0.030	0.042	0.064	0.076	0.102	0.156	5067
240251001	Edgewood	DC	2000	0.000	0.002	0.017	0.028	0.040	0.060	0.070	0.092	0.125	5102
240251001	Edgewood	DC	2001	0.000	0.002	0.020	0.034	0.047	0.068	0.080	0.107	0.156	5106
Rhode Island													
440030002	Kent Co.	Providence	1999	0.000	0.005	0.018	0.029	0.039	0.055	0.068	0.093	0.131	3718
440030002	Kent Co.	Providence	2000	0.000	0.004	0.018	0.030	0.039	0.056	0.063	0.089	0.121	3979
440030002	Kent Co.	Providence	2001	0.000	0.007	0.023	0.035	0.045	0.061	0.075	0.103	0.136	3902
Wisconsin													
550590019	Kenosha	Chicago	1999	0.002	0.012	0.029	0.039	0.049	0.068	0.079	0.100	0.126	4331
550590019	Kenosha	Chicago	2000	0.002	0.014	0.025	0.033	0.042	0.056	0.064	0.081	0.118	4193
550590019	Kenosha	Chicago	2001	0.002	0.013	0.028	0.037	0.047	0.065	0.076	0.098	0.134	4305

*Formerly the AIRS database.

from inspection of Table AX3-2, there are relatively few occurrences of high 1-h average O_3 concentrations (e.g., hourly average concentrations > 0.120 ppm). For example, maximum hourly average O_3 monitoring sites at Charlotte, NC; Stratford, CT; Baton Rouge, LA; Providence, RI; and Chicago, IL experience concentrations above 0.120 ppm. However, approximately only 1% of the hourly average concentrations generally exceed 0.100 ppm at these sites. Monitoring sites in polluted areas such as these also tend to experience frequent hourly average O_3 concentrations at or near minimum detectable levels. Table AX3-2 illustrates that, for several of the sites listed, except for Atlanta, District of Columbia, Los Angeles, and Houston, high hourly average concentrations (e.g., > 0.120 ppm) occur less than 1% of the time and therefore, as indicated above, are associated with occasional episodes.

The second highest daily maximum 1-h O_3 concentrations observed in U.S. Metropolitan Statistical Areas (MSAs) and in Consolidated Metropolitan Statistical Areas (CMSAs) for the years 1999 to 2001 are summarized in Table AX3-3 and shown graphically in Figure AX3-1. MSAs and CMSAs represent politically defined units and often do not reflect the influence of physical or other features on the distribution of air pollutants. As an example, the Los Angeles MSA includes a monitoring site in Lancaster, CA, which is located on the other side of the San Gabriel Mountains from the main urban area. Annual mean concentrations of $PM_{2.5}$ at this site were approximately half of those in the Los Angeles basin during 1999 and 2000 (Pinto et al., 2004). Large gradients in pollutant concentrations exist due to the presence of topographic barriers or simply because of the large area of the MSA (e.g., San Bernadino County) with attendant large gradients in population densities. As a result, when monitors are pooled together from disparate areas or when averages over several urban monitors are taken to represent conditions at remote sites, the potential for exposure misclassification exists. The highest values of the second highest daily maximum O_3 concentrations are observed in the Texas Gulf Coast and Southern California, but high levels of O_3 also occur in the Northeast Corridor and other heavily populated regions of the United States.

Table AX3-4 illustrates the percentiles of hourly average concentrations and the fourth highest daily maximum 8-h average concentration for the April to October period for specific monitoring sites that experience 3-year averages of the fourth highest 8-h concentration between 0.080 and 0.085 ppm. Note that year-to-year variation of the fourth highest 8-h daily maximum

Table AX3-3. The Second Highest Daily Maximum One-Hour Ozone Concentration (ppm) by Metropolitan Statistical Area (MSA) or Consolidated Metropolitan Statistical Area (CMSA) for the Years 1999 to 2001

MSA/CMSA	1999	2000	2001
Albany-Schenectady-Troy, NY MSA	0.107	0.088	0.112
Albuquerque, NM MSA	0.097	0.093	0.088
Allentown-Bethlehem-Easton, PA MSA	0.126	0.114	0.126
Altoona, PA MSA	0.111	0.104	0.107
Appleton-Oshkosh-Neenah, WI MSA	0.105	0.085	0.102
Asheville, NC MSA	0.099	0.107	0.091
Atlanta, GA MSA	0.156	0.158	0.125
Augusta-Aiken, GA-SC MSA	0.108	0.115	0.103
Austin-San Marcos, TX MSA	0.110	0.107	0.097
Bakersfield, CA MSA	0.136	0.142	0.134
Bangor, ME MSA	0.088	.	0.105
Barnstable-Yarmouth, MA MSA	0.127	0.107	0.139
Baton Rouge, LA MSA	0.121	0.139	0.117
Beaumont-Port Arthur, TX MSA	0.103	0.160	0.103
Bellingham, WA MSA	0.062	0.063	0.061
Benton Harbor, MI MSA	0.107	0.107	0.117
Biloxi-Gulfport-Pascagoula, MS MSA	0.107	0.135	0.099
Birmingham, AL MSA	0.131	0.127	0.114
Boston-Worcester-Lawrence, MA-NH-ME-CT CMSA	0.125	0.101	0.136
Brownsville-Harlingen-San Benito, TX MSA	0.075	0.080	0.074
Buffalo-Niagara Falls, NY MSA	0.102	0.105	0.116
Burlington, VT MSA	0.093	0.080	0.083
Canton-Massillon, OH MSA	0.108	0.104	0.106
Cedar Rapids, IA MSA	0.096	0.083	0.084
Champaign-Urbana, IL MSA	0.108	0.084	0.080
Charleston, WV MSA	0.130	0.094	0.107
Charleston-North Charleston, SC MSA	0.101	0.105	0.085
Charlotte-Gastonia-Rock Hill, NC-SC MSA	0.130	0.141	0.142

Table AX3-3 (cont'd). The Second Highest Daily Maximum One-Hour Ozone Concentration (ppm) by Metropolitan Statistical Area (MSA) or Consolidated Metropolitan Statistical Area (CMSA) for the Years 1999 to 2001

MSA/CMSA	1999	2000	2001
Chattanooga, TN-GA MSA	0.122	0.124	0.107
Chicago-Gary-Kenosha, IL-IN-WI CMSA	0.126	0.102	0.124
Chico-Paradise, CA MSA	0.110	0.091	0.100
Cincinnati-Hamilton, OH-KY-IN CMSA	0.119	0.110	0.115
Clarksville-Hopkinsville, TN-KY MSA	0.115	0.108	0.096
Cleveland-Akron, OH CMSA	0.118	0.110	0.118
Colorado Springs, CO MSA	0.075	0.088	0.085
Columbia, SC MSA	0.117	0.116	0.107
Columbus, GA-AL MSA	0.110	0.114	0.090
Columbus, OH MSA	0.144	0.117	0.111
Corpus Christi, TX MSA	0.103	0.099	0.092
Dallas-Fort Worth, TX CMSA	0.154	0.126	0.137
Davenport-Moline-Rock Island, IA-IL MSA	0.099	0.089	0.089
Dayton-Springfield, OH MSA	0.127	0.106	0.100
Daytona Beach, FL MSA	0.087	0.088	0.085
Decatur, AL MSA	0.103	0.110	0.087
Decatur, IL MSA	0.102	0.092	0.078
Denver-Boulder-Greeley, CO CMSA	0.105	0.107	0.105
Des Moines, IA MSA	0.083	0.082	0.069
Detroit-Ann Arbor-Flint, MI CMSA	0.121	0.102	0.122
Dover, DE MSA	0.120	0.126	0.117
Duluth-Superior, MN-WI MSA	0.082	0.074	0.071
El Paso, TX MSA	0.108	0.122	0.116
Elkhart-Goshen, IN MSA	0.085	0.080	0.066
Elmira, NY MSA	0.092	0.089	0.094
Erie, PA MSA	0.112	0.095	0.104
Eugene-Springfield, OR MSA	0.084	0.078	0.081
Evansville-Henderson, IN-KY MSA	0.114	0.097	0.095

Table AX3-3 (cont'd). The Second Highest Daily Maximum One-Hour Ozone Concentration (ppm) by Metropolitan Statistical Area (MSA) or Consolidated Metropolitan Statistical Area (CMSA) for the Years 1999 to 2001

MSA/CMSA	1999	2000	2001
Fargo-Moorhead, ND-MN MSA	0.073	0.073	0.069
Fayetteville, NC MSA	0.120	0.106	0.108
Flagstaff, AZ-UT MSA	0.086	0.082	0.074
Fort Collins-Loveland, CO MSA	0.089	0.096	0.088
Fort Myers-Cape Coral, FL MSA	0.096	0.091	0.079
Fort Pierce-Port St. Lucie, FL MSA	0.083	0.079	0.095
Fort Wayne, IN MSA	0.101	0.099	0.098
Fresno, CA MSA	0.145	0.146	0.146
Gainesville, FL MSA	0.098	0.096	0.096
Grand Rapids-Muskegon-Holland, MI MSA	0.116	0.123	0.118
Green Bay, WI MSA	0.097	0.090	0.107
Greensboro-Winston-Salem-High Point, NC MSA	0.126	0.116	0.122
Greenville, NC MSA	0.109	0.109	0.091
Greenville-Spartanburg-Anderson, SC MSA	0.122	0.115	0.108
Harrisburg-Lebanon-Carlisle, PA MSA	0.126	0.110	0.105
Hartford, CT MSA	0.161	0.116	0.139
Hickory-Morganton-Lenoir, NC MSA	0.115	0.107	0.099
Honolulu, HI MSA	0.054	0.048	0.051
Houma, LA MSA	.	0.124	0.106
Houston-Galveston-Brazoria, TX CMSA	0.203	0.194	0.170
Huntington-Ashland, WV-KY-OH MSA	0.122	0.094	0.113
Huntsville, AL MSA	0.106	0.111	0.088
Indianapolis, IN MSA	0.114	0.102	0.114
Jackson, MS MSA	0.110	0.099	0.095
Jacksonville, FL MSA	0.103	0.114	0.093
Jamestown, NY MSA	0.103	0.113	0.109
Janesville-Beloit, WI MSA	0.105	0.098	0.093
Johnson City-Kingsport-Bristol, TN-VA MSA	0.111	0.126	0.110

Table AX3-3 (cont'd). The Second Highest Daily Maximum One-Hour Ozone Concentration (ppm) by Metropolitan Statistical Area (MSA) or Consolidated Metropolitan Statistical Area (CMSA) for the Years 1999 to 2001

MSA/CMSA	1999	2000	2001
Johnstown, PA MSA	0.107	0.104	0.106
Kalamazoo-Battle Creek, MI MSA	0.103	0.090	0.101
Kansas City, MO-KS MSA	0.116	0.124	0.108
Knoxville, TN MSA	0.129	0.131	0.109
Lafayette, LA MSA	0.094	0.123	0.090
Lake Charles, LA MSA	0.127	0.133	0.105
Lakeland-Winter Haven, FL MSA	0.101	0.102	0.109
Lancaster, PA MSA	0.127	0.107	0.127
Lansing-East Lansing, MI MSA	0.101	0.091	0.106
Laredo, TX MSA	0.084	0.085	0.071
Las Cruces, NM MSA	0.102	0.123	0.104
Las Vegas, NV-AZ MSA	0.097	0.094	0.100
Lawton, OK MSA	0.089	0.094	0.094
Lexington, KY MSA	0.114	0.086	0.092
Lima, OH MSA	0.107	0.100	0.096
Lincoln, NE MSA	0.062	0.072	0.061
Little Rock-North Little Rock, AR MSA	0.107	0.114	0.102
Longview-Marshall, TX MSA	0.134	0.131	0.111
Los Angeles-Riverside-Orange County, CA CMSA	0.159	0.174	0.175
Louisville, KY-IN MSA	0.124	0.112	0.106
Macon, GA MSA	0.133	0.131	0.115
Madison, WI MSA	0.098	0.087	0.088
McAllen-Edinburg-Mission, TX MSA	0.086	0.088	0.092
Medford-Ashland, OR MSA	.	0.079	0.081
Melbourne-Titusville-Palm Bay, FL MSA	0.087	0.093	0.094
Memphis, TN-AR-MS MSA	0.130	0.123	0.121
Merced, CA Msa	0.125	0.120	0.113
Miami-Fort Lauderdale, FL CMSA	0.113	0.094	0.106

Table AX3-3 (cont'd). The Second Highest Daily Maximum One-Hour Ozone Concentration (ppm) by Metropolitan Statistical Area (MSA) or Consolidated Metropolitan Statistical Area (CMSA) for the Years 1999 to 2001

MSA/CMSA	1999	2000	2001
Milwaukee-Racine, WI CMSA	0.122	0.098	0.122
Minneapolis-St. Paul, MN-WI MSA	0.088	0.089	0.109
Mobile, AL MSA	0.104	0.118	0.095
Modesto, CA MSA	0.111	0.110	0.111
Monroe, LA MSA	0.097	0.103	0.090
Montgomery, AL MSA	0.110	0.111	0.094
Nashville, TN MSA	0.123	0.122	0.110
New London-Norwich, CT-RI MSA	0.127	0.135	0.109
New Orleans, LA MSA	0.117	0.124	0.111
NY-Northern NJ-Long Island, NY-NJ-CT-PA CMSA	0.154	0.136	0.146
Norfolk-Virginia Beach-Newport News, VA-NC MSA	0.135	0.099	0.100
Ocala, FL MSA	0.097	0.093	0.089
Oklahoma City, OK MSA	0.097	0.100	0.097
Omaha, NE-IA MSA	0.093	0.083	0.076
Orlando, FL MSA	0.101	0.106	0.108
Owensboro, KY MSA	0.102	0.082	0.086
Parkersburg-Marietta, WV-OH MSA	0.123	0.105	0.108
Pensacola, FL MSA	0.106	0.118	0.098
Peoria-Pekin, IL MSA	0.099	0.083	0.084
Phil-Wilmington-Atlantic City, PA-NJ-DE-MD CMSA	0.152	0.128	0.131
Phoenix-Mesa, AZ MSA	0.119	0.107	0.106
Pittsburgh, PA MSA	0.132	0.111	0.112
Pittsfield, MA MSA	0.092	.	0.112
Portland, ME MSA	0.120	0.089	0.124
Portland-Salem, OR-WA CMSA	0.094	0.082	0.093
Providence-Fall River-Warwick, RI-MA MSA	0.133	0.118	0.144
Provo-Orem, UT MSA	0.109	0.095	0.094
Raleigh-Durham-Chapel Hill, NC MSA	0.134	0.116	0.113

Table AX3-3 (cont'd). The Second Highest Daily Maximum One-Hour Ozone Concentration (ppm) by Metropolitan Statistical Area (MSA) or Consolidated Metropolitan Statistical Area (CMSA) for the Years 1999 to 2001

MSA/CMSA	1999	2000	2001
Reading, PA MSA	0.128	0.105	0.125
Redding, CA MSA	0.113	0.098	0.093
Reno, NV MSA	0.097	0.088	0.090
Richmond-Petersburg, VA MSA	0.133	0.112	0.119
Roanoke, VA MSA	.	0.095	0.101
Rochester, NY MSA	0.101	0.088	0.100
Rockford, IL MSA	0.093	0.084	0.086
Rocky Mount, NC MSA	0.104	0.106	0.099
Sacramento-Yolo, CA CMSA	0.137	0.134	0.129
Salinas, CA MSA	0.075	0.084	0.078
Salt Lake City-Ogden, UT MSA	0.112	0.100	0.118
San Antonio, TX MSA	0.109	0.095	0.092
San Diego, CA MSA	0.114	0.123	0.118
San Francisco-Oakland-San Jose, CA CMSA	0.144	0.126	0.118
San Luis Obispo-Atascadero-Paso Robles, CA MSA	0.094	0.082	0.092
Santa Barbara-Santa Maria-Lompoc, CA MSA	0.095	0.100	0.103
Sarasota-Bradenton, FL MSA	0.112	0.107	0.114
Savannah, GA MSA	0.107	0.102	0.085
Scranton-Wilkes-Barre-Hazleton, PA MSA	0.115	0.093	0.104
Seattle-Tacoma-Bremerton, WA CMSA	0.091	0.095	0.088
Sharon, PA MSA	0.108	0.098	0.113
Sheboygan, WI MSA	0.130	0.106	0.122
Shreveport-Bossier City, LA MSA	0.108	0.129	0.105
Sioux Falls, SD MSA	0.068	0.076	0.088
South Bend, IN MSA	0.107	0.095	0.108
Spokane, WA MSA	0.073	0.082	0.084
Springfield, IL MSA	0.099	0.100	0.095
Springfield, MA MSA	0.113	0.099	0.132

Table AX3-3 (cont'd). The Second Highest Daily Maximum One-Hour Ozone Concentration (ppm) by Metropolitan Statistical Area (MSA) or Consolidated Metropolitan Statistical Area (CMSA) for the Years 1999 to 2001

MSA/CMSA	1999	2000	2001
Springfield, MO MSA	0.095	0.092	0.091
St. Louis, MO-IL MSA	0.128	0.123	0.122
State College, PA MSA	0.099	0.109	0.097
Steubenville-Weirton, OH-WV MSA	0.111	0.100	0.096
Stockton-Lodi, CA MSA	0.130	0.111	0.112
Syracuse, NY MSA	0.099	0.083	0.097
Tallahassee, FL MSA	0.094	0.092	0.085
Tampa-St. Petersburg-Clearwater, FL MSA	0.116	0.108	0.118
Terre Haute, IN MSA	0.093	0.088	0.096
Toledo, OH MSA	0.128	0.095	0.111
Tucson, AZ MSA	0.092	0.085	0.084
Tulsa, OK MSA	0.116	0.122	0.107
Tyler, TX MSA	0.118	.	0.098
Utica-Rome, NY MSA	0.089	0.083	0.100
Victoria, TX MSA	0.102	0.094	0.085
Visalia-Tulare-Porterville, CA MSA	0.125	0.119	0.126
Washington-Baltimore, DC-MD-VA-WV CMSA	0.152	0.128	0.142
Wausau, WI MSA	0.095	0.081	0.078
West Palm Beach-Boca Raton, FL MSA	0.104	0.093	0.098
Wheeling, WV-OH MSA	0.100	0.093	0.104
Wichita, KS MSA	0.095	0.093	0.096
Williamsport, PA MSA	0.091	0.092	0.094
Wilmington, NC MSA	0.081	0.097	0.089
York, PA MSA	0.121	0.112	0.104
Youngstown-Warren, OH MSA	0.109	0.097	0.105
Yuba City, CA MSA	0.106	0.101	0.105

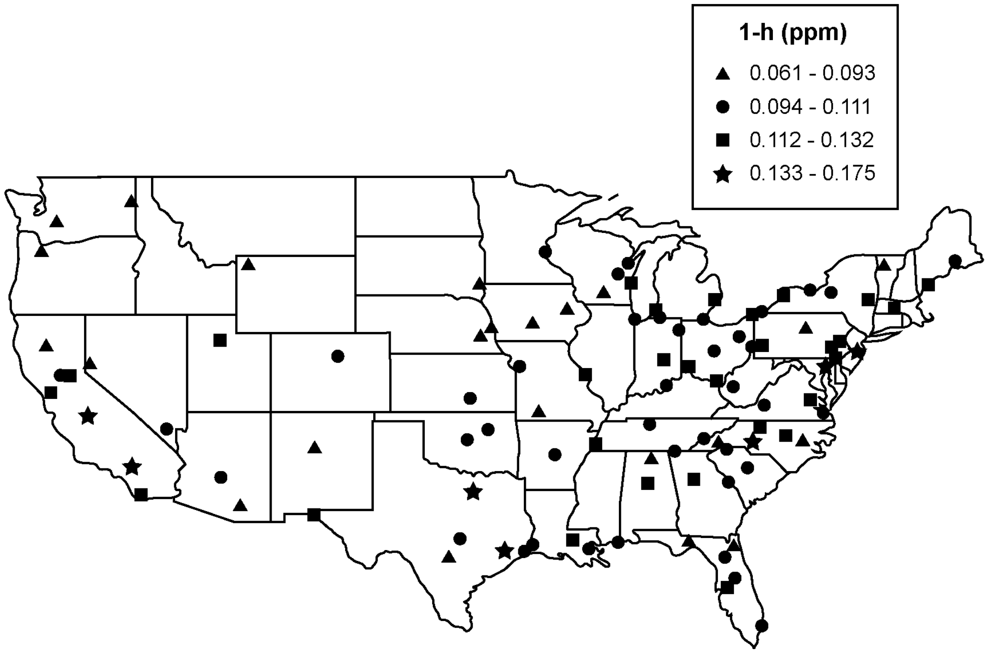

Figure AX3-1. Second highest daily maximum 1-h O_3 concentrations in 2001.

Source: U.S. Environmental Protection Agency (2003a).

concentration affects the 3-year average, and thus one might anticipate annual variability of the 3-year average concentrations above and below specific thresholds, such as 0.085 ppm.

Table AX3-5 summarizes the fourth highest daily maximum 8-h average O_3 concentrations by MSA for the years 1999 to 2001. The data are shown as a map in Figure AX3-2. The data have been reported for the O_3 season as summarized in Table AX3-1. In some cases, high concentrations occur in the fall and winter periods as well as in the summertime. A comparison of Tables AX3-3 and AX3-5 shows that the MSAs, which experience high second daily maximum hourly average concentrations, also experience elevated fourth highest 8-h daily maximum concentrations. However, there are considerably more MSAs and CMSAs that experience fourth highest 8-h daily maximum concentrations ≥ 0.085 ppm than MSAs and CMSAs that experience second highest daily maximum hourly average concentrations ≥ 0.125 ppm.

Table AX3-4. Percentiles of Hourly Average Concentrations (ppm) and Fourth Highest Eight-Hour Daily Maximum Concentration for the April to October Period

AIRS Site	Name	Area	Year	Min.	Percentiles 10	30	50	70	90	95	99	Max.	4th High 8-h Avg	Number of Observations
Alabama														
011030011	Morgan Co.	Decatur	2000	0.000	0.006	0.023	0.036	0.051	0.070	0.078	0.090	0.116	0.091	4169
011030011	Morgan Co.	Decatur	2001	0.000	0.003	0.018	0.031	0.043	0.061	0.068	0.079	0.107	0.077	4641
Arizona														
040139508	Maricopa Co.	Phoenix	1999	0.031	0.048	0.055	0.060	0.064	0.073	0.077	0.088	0.098	0.086	4922
040139508	Maricopa Co.	Phoenix	2000	0.019	0.042	0.049	0.056	0.063	0.072	0.077	0.084	0.095	0.082	4991
040139508	Maricopa Co.	Phoenix	2001	0.024	0.044	0.053	0.058	0.063	0.072	0.076	0.085	0.098	0.085	5042
Kentucky														
210470006	Christian Co.	Clarksville	1999	0.000	0.022	0.03	0.04	0.06	0.071	0.08	0.092	0.12	0.092	5017
210470006	Christian Co.	Clarksville	2000	0.001	0.019	0.030	0.040	0.050	0.064	0.070	0.082	0.104	0.081	4944
210470006	Christian Co.	Clarksville	2001	0.002	0.021	0.032	0.040	0.051	0.065	0.071	0.081	0.096	0.082	5108
New York														
360551004	Monroe Co.	Rochester	1999	0.000	0.005	0.017	0.027	0.038	0.061	0.069	0.088	0.104	0.088	3649
360551004	Monroe Co.	Rochester	2000	0.000	0.004	0.018	0.027	0.035	0.050	0.057	0.071	0.100	0.073	4855
360551004	Monroe Co.	Rochester	2001	0.001	0.007	0.021	0.030	0.040	0.055	0.063	0.080	0.099	0.084	5014
North Carolina														
370210030	Buncombe Co.	Asheville	1999	0.000	0.006	0.020	0.033	0.046	0.064	0.073	0.086	0.115	0.084	5053
370210030	Buncombe Co.	Asheville	2000	0.000	0.003	0.015	0.028	0.042	0.061	0.070	0.087	0.108	0.090	4864
370210030	Buncombe Co.	Asheville	2001	0.000	0.005	0.018	0.030	0.043	0.059	0.066	0.078	0.1	0.076	4777

Table AX3-4 (cont'd). Percentiles of Hourly Average Concentrations (ppm) and Fourth Highest Eight-Hour Daily Maximum Concentration for the April to October Period

AIRS Site	Name	Area	Year	Min.	Percentiles 10	30	50	70	90	95	99	Max.	4th High 8-h Avg	Number of Observations
Ohio														
390810016	Jefferson Co.	Steubenville	1999	0.000	0.001	0.012	0.027	0.041	0.063	0.073	0.086	0.113	0.088	4764
390810016	Jefferson Co.	Steubenville	2000	0.000	0.002	0.012	0.025	0.039	0.058	0.066	0.079	0.103	0.080	4897
390810016	Jefferson Co.	Steubenville	2001	0.000	0.003	0.014	0.027	0.041	0.063	0.072	0.086	0.104	0.086	4688
Pennsylvania														
420274000	Centre Co.	State College	1999	0.001	0.014	0.025	0.034	0.046	0.060	0.068	0.083	0.109	0.085	5122
420274000	Centre Co.	State College	2000	0.000	0.009	0.021	0.031	0.040	0.056	0.063	0.077	0.109	0.075	5089
420274000	Centre Co.	State College	2001	0.000	0.011	0.025	0.034	0.044	0.060	0.068	0.082	0.091	0.082	5090
Texas														
480290032	Bextar Co.	San Antonio	1999	0.000	0.006	0.017	0.027	0.038	0.059	0.070	0.091	0.120	0.091	4720
480290032	Bextar Co.	San Antonio	2000	0.000	0.006	0.014	0.021	0.031	0.048	0.058	0.075	0.096	0.077	4932
480290032	Bextar Co.	San Antonio	2001	0.000	0.005	0.014	0.022	0.031	0.046	0.055	0.074	0.095	0.078	4920

Table AX3-5. The Fourth Highest Daily Maximum Eight-Hour Ozone Concentration (ppm) by Metropolitan Statistical Area (MSA) or Consolidated Metropolitan Statistical Area (CMSA) for the Years 1999 to 2001

MSA/CMSA	1999	2000	2001
Albany-Schenectady-Troy, NY MSA	0.092	0.072	0.090
Albuquerque, NM MSA	0.076	0.076	0.074
Allentown-Bethlehem-Easton, PA MSA	0.107	0.092	0.094
Altoona, PA MSA	0.091	0.080	0.083
Appleton-Oshkosh-Neenah, WI MSA	0.087	0.068	0.087
Asheville, NC MSA	0.084	0.090	0.076
Atlanta, GA MSA	0.126	0.113	0.092
Augusta-Aiken, GA-SC MSA	0.090	0.093	0.082
Austin-San Marcos, TX MSA	0.099	0.088	0.080
Bakersfield, CA MSA	0.109	0.111	0.109
Bangor, ME MSA	0.080	.	0.088
Barnstable-Yarmouth, MA MSA	0.101	0.083	0.105
Baton Rouge, LA MSA	0.100	0.101	0.084
Beaumont-Port Arthur, TX MSA	0.077	0.097	0.081
Bellingham, WA MSA	0.050	0.052	0.050
Benton Harbor, MI MSA	0.096	0.077	0.088
Biloxi-Gulfport-Pascagoula, MS MSA	0.097	0.091	0.083
Birmingham, AL MSA	0.100	0.099	0.089
Boston-Worcester-Lawrence, MA-NH-ME-CT CMSA	0.098	0.082	0.101
Brownsville-Harlingen-San Benito, TX MSA	0.066	0.064	0.063
Buffalo-Niagara Falls, NY MSA	0.090	0.085	0.102
Burlington, VT MSA	0.079	0.071	0.076
Canton-Massillon, OH MSA	0.091	0.087	0.089
Cedar Rapids, IA MSA	0.076	0.075	0.069
Champaign-Urbana, IL MSA	0.094	0.073	0.073
Charleston, WV MSA	0.104	0.085	0.083
Charleston-North Charleston, SC MSA	0.084	0.082	0.071
Charlotte-Gastonia-Rock Hill, NC-SC MSA	0.107	0.101	0.103

Table AX3-5 (cont'd). The Fourth Highest Daily Maximum Eight-Hour Ozone Concentration (ppm) by Metropolitan Statistical Area (MSA) or Consolidated Metropolitan Statistical Area (CMSA) for the Years 1999 to 2001

MSA/CMSA	1999	2000	2001
Chattanooga, TN-GA MSA	0.098	0.098	0.087
Chicago-Gary-Kenosha, IL-IN-WI CMSA	0.102	0.086	0.099
Chico-Paradise, CA MSA	0.087	0.086	0.088
Cincinnati-Hamilton, OH-KY-IN CMSA	0.096	0.093	0.088
Clarksville-Hopkinsville, TN-KY MSA	0.092	0.088	0.082
Cleveland-Akron, OH CMSA	0.103	0.085	0.099
Colorado Springs, CO MSA	0.064	0.070	0.070
Columbia, SC MSA	0.094	0.097	0.091
Columbus, GA-AL MSA	0.097	0.094	0.079
Columbus, OH MSA	0.103	0.091	0.090
Corpus Christi, TX MSA	0.085	0.083	0.077
Dallas-Fort Worth, TX CMSA	0.112	0.102	0.098
Davenport-Moline-Rock Island, IA-IL MSA	0.083	0.077	0.079
Dayton-Springfield, OH MSA	0.096	0.088	0.084
Daytona Beach, FL MSA	0.075	0.076	0.073
Decatur, AL MSA	0.092	0.091	0.077
Decatur, IL MSA	0.087	0.077	0.071
Denver-Boulder-Greeley, CO CMSA	0.081	0.083	0.082
Des Moines, IA MSA	0.073	0.071	0.060
Detroit-Ann Arbor-Flint, MI CMSA	0.096	0.082	0.095
Dover, DE MSA	0.097	0.093	0.091
Duluth-Superior, MN-WI MSA	0.074	0.065	0.062
El Paso, TX MSA	0.071	0.084	0.078
Elkhart-Goshen, IN MSA	0.077	0.063	0.055
Elmira, NY MSA	0.082	0.073	0.082
Erie, PA MSA	0.096	0.078	0.089
Eugene-Springfield, OR MSA	0.068	0.047	0.066
Evansville-Henderson, IN-KY MSA	0.098	0.085	0.081

Table AX3-5 (cont'd). The Fourth Highest Daily Maximum Eight-Hour Ozone Concentration (ppm) by Metropolitan Statistical Area (MSA) or Consolidated Metropolitan Statistical Area (CMSA) for the Years 1999 to 2001

MSA/CMSA	1999	2000	2001
Fargo-Moorhead, ND-MN MSA	0.066	0.057	0.060
Fayetteville, NC MSA	0.100	0.086	0.084
Flagstaff, AZ-UT MSA	0.076	0.071	0.070
Fort Collins-Loveland, CO MSA	0.074	0.078	0.070
Fort Myers-Cape Coral, FL MSA	0.081	0.077	0.068
Fort Pierce-Port St. Lucie, FL MSA	0.071	0.071	0.075
Fort Wayne, IN MSA	0.090	0.091	0.082
Fresno, CA MSA	0.105	0.114	0.113
Gainesville, FL MSA	0.080	0.080	0.079
Grand Rapids-Muskegon-Holland, MI MSA	0.103	0.080	0.095
Green Bay, WI MSA	0.085	0.071	0.088
Greensboro-Winston-Salem-High Point, NC MSA	0.100	0.094	0.096
Greenville, NC MSA	0.093	0.082	0.077
Greenville-Spartanburg-Anderson, SC MSA	0.100	0.089	0.090
Harrisburg-Lebanon-Carlisle, PA MSA	0.104	0.088	0.091
Hartford, CT MSA	0.107	0.089	0.102
Hickory-Morganton-Lenoir, NC MSA	0.094	0.091	0.088
Honolulu, HI MSA	0.048	0.044	0.042
Houma, LA MSA	0.087	0.085	0.084
Houston-Galveston-Brazoria, TX CMSA	0.124	0.117	0.110
Huntington-Ashland, WV-KY-OH MSA	0.097	0.083	0.088
Huntsville, AL MSA	0.093	0.088	0.080
Indianapolis, IN MSA	0.096	0.090	0.093
Jackson, MS MSA	0.084	0.080	0.078
Jacksonville, FL MSA	0.080	0.077	0.075
Jamestown, NY MSA	0.092	0.087	0.090
Janesville-Beloit, WI MSA	0.093	0.083	0.084
Johnson City-Kingsport-Bristol, TN-VA MSA	0.089	0.097	0.086

Table AX3-5 (cont'd). The Fourth Highest Daily Maximum Eight-Hour Ozone Concentration (ppm) by Metropolitan Statistical Area (MSA) or Consolidated Metropolitan Statistical Area (CMSA) for the Years 1999 to 2001

MSA/CMSA	1999	2000	2001
Johnstown, PA MSA	0.090	0.086	0.090
Kalamazoo-Battle Creek, MI MSA	0.091	0.070	0.085
Kansas City, MO-KS MSA	0.084	0.091	0.079
Knoxville, TN MSA	0.106	0.100	0.093
Lafayette, LA MSA	0.081	0.092	0.077
Lake Charles, LA MSA	0.088	0.090	0.080
Lakeland-Winter Haven, FL MSA	0.078	0.079	0.087
Lancaster, PA MSA	0.102	0.090	0.097
Lansing-East Lansing, MI MSA	0.089	0.077	0.087
Laredo, TX MSA	0.067	0.070	0.063
Las Cruces, NM MSA	0.082	0.081	0.079
Las Vegas, NV-AZ MSA	0.084	0.082	0.082
Lawton, OK MSA	0.082	0.085	0.078
Lexington, KY MSA	0.091	0.077	0.078
Lima, OH MSA	0.093	0.085	0.081
Lincoln, NE MSA	0.053	0.057	0.051
Little Rock-North Little Rock, AR MSA	0.089	0.092	0.080
Longview-Marshall, TX MSA	0.105	0.099	0.082
Los Angeles-Riverside-Orange County, CA CMSA	0.133	0.122	0.133
Louisville, KY-IN MSA	0.103	0.090	0.086
Macon, GA MSA	0.113	0.097	0.086
Madison, WI MSA	0.085	0.071	0.078
McAllen-Edinburg-Mission, TX MSA	0.075	0.077	0.074
Medford-Ashland, OR MSA	.	0.067	0.064
Melbourne-Titusville-Palm Bay, FL MSA	0.077	0.078	0.084
Memphis, TN-AR-MS MSA	0.104	0.093	0.092
Merced, CA MSA	0.105	0.103	0.096
Miami-Fort Lauderdale, FL CMSA	0.077	0.077	0.076

Table AX3-5 (cont'd). The Fourth Highest Daily Maximum Eight-Hour Ozone Concentration (ppm) by Metropolitan Statistical Area (MSA) or Consolidated Metropolitan Statistical Area (CMSA) for the Years 1999 to 2001

MSA/CMSA	1999	2000	2001
Milwaukee-Racine, WI CMSA	0.097	0.086	0.102
Minneapolis-St. Paul, MN-WI MSA	0.077	0.072	0.078
Mobile, AL MSA	0.085	0.097	0.078
Modesto, CA MSA	0.090	0.091	0.094
Monroe, LA MSA	0.082	0.081	0.077
Montgomery, AL MSA	0.092	0.086	0.077
Nashville, TN MSA	0.101	0.093	0.086
New London-Norwich, CT-RI MSA	0.096	0.084	0.090
New Orleans, LA MSA	0.091	0.095	0.084
NY-Northern NJ-Long Island, NY-NJ-CT-PA CMSA	0.113	0.114	0.108
Norfolk-Virginia Beach-Newport News, VA-NC MSA	0.097	0.084	0.085
Ocala, FL MSA	0.083	0.079	0.074
Oklahoma City, OK MSA	0.084	0.086	0.082
Omaha, NE-IA MSA	0.080	0.072	0.063
Orlando, FL MSA	0.084	0.081	0.079
Owensboro, KY MSA	0.090	0.074	0.073
Panama City, FL MSA	.	0.092	0.082
Parkersburg-Marietta, WV-OH MSA	0.097	0.087	0.085
Pensacola, FL MSA	0.086	0.096	0.082
Peoria-Pekin, IL MSA	0.082	0.073	0.080
Phil-Wilmington-Atlantic City, PA-NJ-DE-MD CMSA	0.112	0.109	0.105
Phoenix-Mesa, AZ MSA	0.091	0.090	0.086
Pittsburgh, PA MSA	0.101	0.088	0.093
Pittsfield, MA MSA	0.075	.	0.092
Portland, ME MSA	0.089	0.073	0.097
Portland-Salem, OR-WA CMSA	0.072	0.065	0.069
Providence-Fall River-Warwick, RI-MA MSA	0.091	0.087	0.105
Provo-Orem, UT MSA	0.083	0.077	0.076

Table AX3-5 (cont'd). The Fourth Highest Daily Maximum Eight-Hour Ozone Concentration (ppm) by Metropolitan Statistical Area (MSA) or Consolidated Metropolitan Statistical Area (CMSA) for the Years 1999 to 2001

MSA/CMSA	1999	2000	2001
Raleigh-Durham-Chapel Hill, NC MSA	0.108	0.089	0.089
Reading, PA MSA	0.102	0.084	0.099
Redding, CA MSA	0.094	0.082	0.077
Reno, NV MSA	0.076	0.069	0.075
Richmond-Petersburg, VA MSA	0.100	0.083	0.091
Roanoke, VA MSA	0.089	0.081	0.089
Rochester, NY MSA	0.089	0.073	0.086
Rockford, IL MSA	0.082	0.070	0.078
Rocky Mount, NC MSA	0.092	0.085	0.085
Sacramento-Yolo, CA CMSA	0.106	0.103	0.105
Salinas, CA MSA	0.063	0.063	0.063
Salt Lake City-Ogden, UT MSA	0.080	0.080	0.084
San Antonio, TX MSA	0.091	0.082	0.081
San Diego, CA MSA	0.092	0.095	0.096
San Francisco-Oakland-San Jose, CA CMSA	0.088	0.077	0.081
San Luis Obispo-Atascadero-Paso Robles, CA MSA	0.077	0.070	0.073
Santa Barbara-Santa Maria-Lompoc, CA MSA	0.079	0.080	0.083
Sarasota-Bradenton, FL MSA	0.085	0.086	0.086
Savannah, GA MSA	0.083	0.079	0.067
Scranton-Wilkes-Barre-Hazleton, PA MSA	0.096	0.077	0.088
Seattle-Tacoma-Bremerton, WA CMSA	0.072	0.070	0.071
Sharon, PA MSA	0.091	0.081	0.094
Sheboygan, WI MSA	0.093	0.090	0.102
Shreveport-Bossier City, LA MSA	0.094	0.093	0.084
Sioux Falls, SD MSA	0.058	0.065	0.065
South Bend, IN MSA	0.090	0.081	0.089
Spokane, WA MSA	0.065	0.068	0.071
Springfield, IL MSA	0.075	0.079	0.073

Table AX3-5 (cont'd). The Fourth Highest Daily Maximum Eight-Hour Ozone Concentration (ppm) by Metropolitan Statistical Area (MSA) or Consolidated Metropolitan Statistical Area (CMSA) for the Years 1999 to 2001

MSA/CMSA	1999	2000	2001
Springfield, MA MSA	0.094	0.079	0.093
Springfield, MO MSA	0.081	0.078	0.072
St. Louis, MO-IL MSA	0.102	0.088	0.088
State College, PA MSA	0.085	0.079	0.086
Steubenville-Weirton, OH-WV MSA	0.091	0.080	0.086
Stockton-Lodi, CA MSA	0.094	0.082	0.078
Syracuse, NY MSA	0.086	0.074	0.085
Tallahassee, FL MSA	0.081	0.076	0.074
Tampa-St. Petersburg-Clearwater, FL MSA	0.087	0.083	0.085
Terre Haute, IN MSA	0.082	0.075	0.083
Toledo, OH MSA	0.091	0.081	0.092
Tucson, AZ MSA	0.073	0.077	0.069
Tulsa, OK MSA	0.091	0.088	0.095
Tyler, TX MSA	0.097	0.087	0.082
Utica-Rome, NY MSA	0.078	0.067	0.084
Victoria, TX MSA	0.086	0.079	0.073
Visalia-Tulare-Porterville, CA MSA	0.108	0.105	0.104
Washington-Baltimore, DC-MD-VA-WV CMSA	0.113	0.099	0.112
Wausau, WI MSA	0.084	0.073	0.072
West Palm Beach-Boca Raton, FL MSA	0.079	0.075	0.073
Wheeling, WV-OH MSA	0.088	0.071	0.088
Wichita, KS MSA	0.079	0.080	0.084
Williamsport, PA MSA	0.076	0.073	0.080
Wilmington, NC MSA	0.067	0.080	0.078
York, PA MSA	0.094	0.090	0.087
Youngstown-Warren, OH MSA	0.095	0.080	0.093
Yuba City, CA MSA	0.090	0.083	0.084

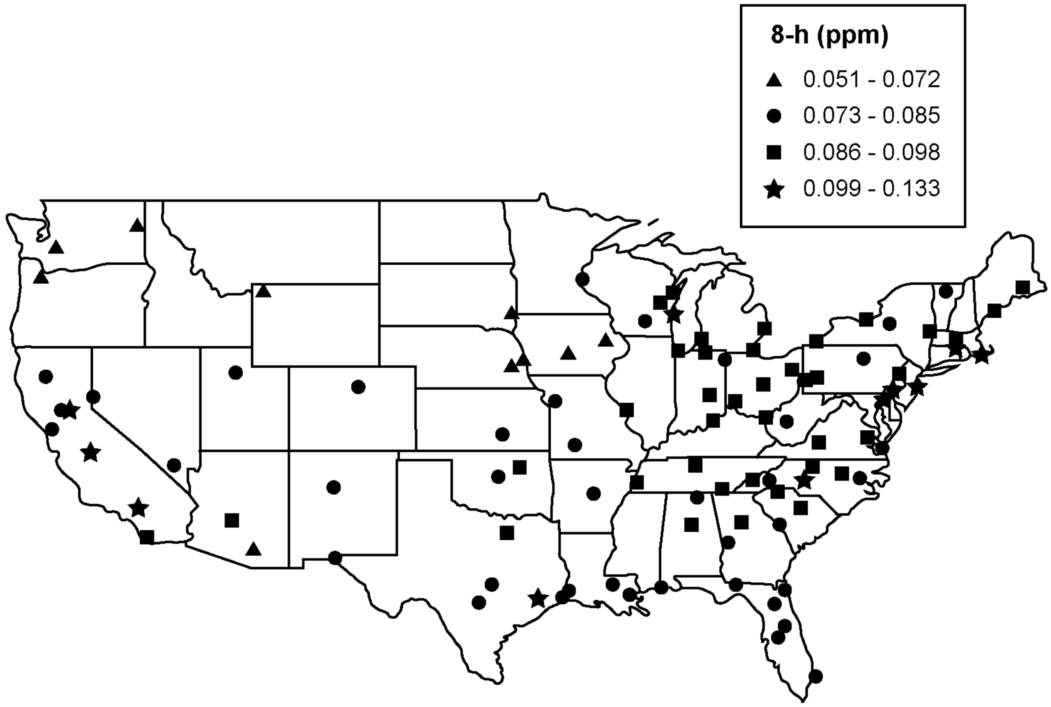

Figure AX3-2. Fourth highest 8-h daily maximum O_3 concentration in 2001.

Source: U.S. Environmental Protection Agency (2003a).

There has been considerable interest in possibly substituting one index for another when attempting to relate O_3 exposure with an effect. For example, using O_3 ambient air quality data, McCurdy (1988) compared the number of exceedances of 0.12 ppm and the number of occurrences of the daily maximum 8-h average concentrations ≥ 0.08 ppm and reported that a positive correlation (r = 0.79) existed between the second-highest 1-h daily maximum in a year and the expected number of days with an 8-h daily maximum average concentration ≥ 0.08 ppm O_3. In this case, the predictive strength of using one O_3 exposure index to predict another is not strong. However, such may not be the case when relating the second highest daily maximum 1-h average concentration with the fourth highest 8-h daily maximum concentration that occurs over an O_3 season. Figure AX3-3 below shows the scatter diagram for the two exposure indices for all urban sites in the AQS database for 2001. The diagram shows that there is a fairly close relationship between the two indices. Figure AX3-4 shows a similar diagram using the rural (sites designated as rural in the AQS database) monitors that measured O_3 concentrations in

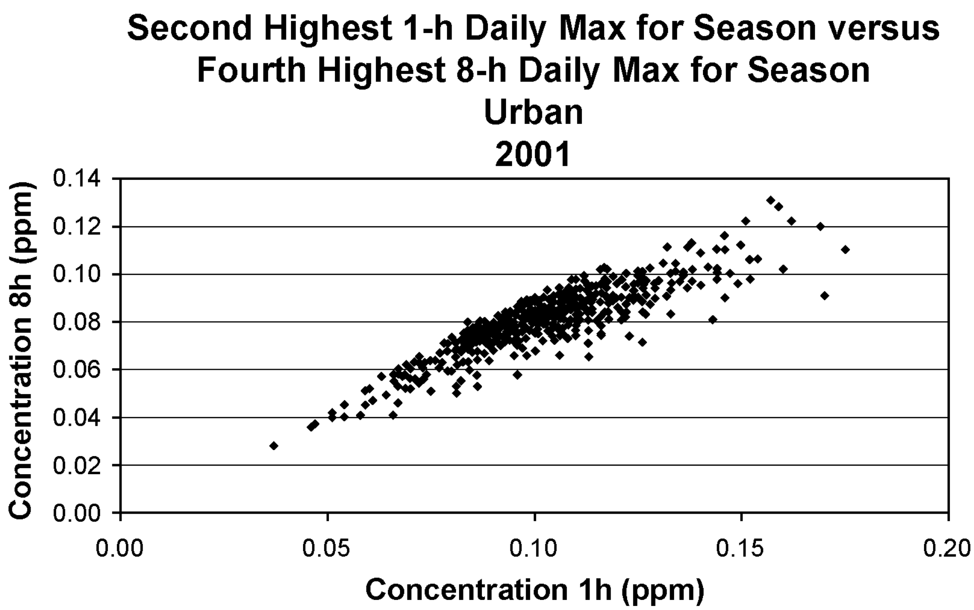

Figure AX3-3. The relationship between the second highest 1-h average daily maximum concentration and the fourth highest 8-h average daily maximum concentration at urban sites for 2001 for the O_3 season.

Source: U.S. Environmental Protection Agency (2003a).

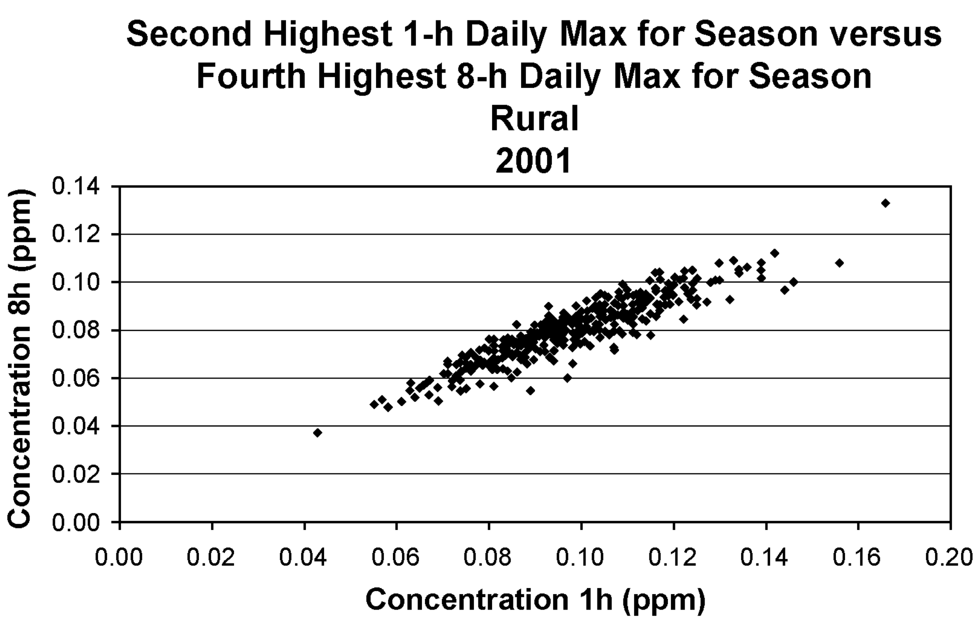

Figure AX3-4. The relationship between the second highest 1-h average daily maximum concentration and the fourth highest 8-h average daily maximum concentration at rural sites for 2001 for the O_3 season.

Source: U.S. Environmental Protection Agency (2003a).

2001. Using air quality data from the AQS database for 2001, both Figure AX3-3 and Figure AX3-4 appear to show similar relationships for both urban and rural monitors. Thus, as indicated in Tables AX3-3 and AX3-5, there is a pattern for those MSAs with high second daily maximum hourly average concentrations to experience elevated fourth highest 8-h daily maximum concentrations.

For analyzing the results of epidemiological time-series studies, the percentiles of the pooled data have been characterized for all monitoring sites across the United States. All of the hourly average concentrations from all monitoring sites have been combined. Table AX3-6 shows the results of pooling all data in the AQS database for 1996 to 2000 for sites within MSAs and outside of MSAs. The following tables have 5-year means and selected percentiles of hourly, daily, daily maximum 1-h, and daily 1000-1800 hours 8-h averaged O_3 concentrations. These were calculated from 1996 to 2000 O_3 data for the months April through September. The source of the data used was AQS AMP350 national-level hourly O_3 raw data files. Some data completeness requirements were imposed:

(1) All hours in the 8-h period (1000-1800 hours) were required for that day to be included.

(2) At least 75% of available days were required for a monitor to be used.

(3) At least 75% of the hours in a day were required for a 24-h average to be computed and used.

The data have been characterized by the hourly average concentrations, the 8-h daily maximum concentrations, and the 24-h average concentrations, as well as the mean concentrations for the specific averaging times.

As pointed out by the U.S. Environmental Protection Agency (1986), a familiar measure of O_3 air quality is the number or percentage of days on which some specific concentration is equaled or exceeded. This measure, however, does not shed light on one of the more important questions regarding the effects of O_3 on both people and plants: what is the possible significance of high concentrations lasting 1 h or longer and then recurring on 2 or more successive days? The recurrence of high O_3 concentrations on consecutive days was examined in four cities (one site in each city) by the U.S. Environmental Protection Agency (1986). The numbers of multiday events were tallied by length of event (i.e., number of consecutive days) using data for

Table AX3-6. Summary of Percentiles of Pooled Data Across Monitoring Sites for 1996 – 2000[a]

			Percentiles										
Pooled Group/ Avg. Time	**Number of Values**	**Mean**	**1**	**5**	**10**	**25**	**30**	**50**	**70**	**75**	**90**	**95**	**99**
Daily 1-h Maximum Concentrations													
Monitors in MSAs	536,824	58	20	29	34	44	47	56	67	70	85	95	118
Monitors not in MSAs	104,798	57	22	30	35	45	47	55	65	68	80	88	105
8-h Daily Maximum Concentrations (1000 – 1800 hours)													
Monitors in MSAs	536,824	47	13	21	26	35	38	46	55	58	70	78	93
Monitors not in MSAs	104,798	48	16	24	29	37	38	47	55	58	68	74	87
24-h Average Concentrations													
Monitors in MSAs	536,148	34	9	15	18	25	27	33	39	41	49	55	67
Monitors not in MSAs	104,689	38	12	18	21	28	30	37	44	46	55	61	73
Hourly Average Concentrations													
Monitors in MSAs	1,265,0861	33	0	2	6	17	20	32	43	47	62	71	91
Monitors not in MSAs	2,453,249	38	0	6	12	24	27	37	48	51	63	71	86

[a]Concentrations in ppb.

the daylight hours (0600 to 2000 hours) in the second and third quarters of 1979 through 1981. These sites were selected because they included areas known to experience high O_3 concentrations (e.g., California), and because they represent different geographic regions of the country (West, Southwest, and East).

Because of the importance of episodes and respites in assessing possible biological impacts, the U.S. Environmental Protection Agency (1986) commented on the number of O_3 episodes, the length of episodes, and the time between episodes. The agency concluded that its analysis showed variations among sites in the lengths of episodes as well as the respite periods. In its discussion, the U.S. Environmental Protection Agency (1986) defined a day or series of days on which the daily 1-h maximum reached or exceeded the specified level as an "exposure," the intervening day or days when that level was not reached was called a "respite." Four O_3 concentrations were selected: 0.06, 0.12, 0.18, and 0.24 ppm. At the Dallas site, for example, the concentration value was $\geq$ 0.06 ppm for more than 7 days in a row. The Pasadena site experienced 10 such exposures, but these 10 exposure events spanned 443 days; in Dallas, 11 exposures spanned only 168 days. At the lowest concentration ($\geq$ 0.06 ppm), the Dallas station recorded more short-term (< 7 days) exposures (45 exposures over 159 days) than the Pasadena station (14 exposures over 45 days) because the daily 1-h maximum statistic in Pasadena remained above 0.06 ppm for such protracted periods. At concentrations $\geq$ 0.12 ppm, the lengthy exposures at the Pasadena site resolved into numerous shorter exposures, whereas in Dallas the exposures markedly dwindled in number and duration.

An interesting observation first reported and studied in the 1970s is that O_3 concentrations in some locations are actually higher on weekends than on weekdays although the atmospheric levels of O_3 precursors are lower on weekends compared with weekdays (Cleveland et al., 1974; Lebron, 1975). The weekly cycles of atmospheric O_3 are of interest, because they provide information about the response of O_3 to changes in anthropogenic emissions from weekdays to weekends. Heuss et al. (2003) described the results of a nationwide analysis of weekday/weekend differences that demonstrated significant variation across the United States. The authors reported that weekend 1-h or 8-h maximum O_3 varied from 15% lower than weekday levels to 30% higher. The weekend O_3 increases were primarily found in and around large coast cities in California and large cities in the Midwest and Northeast Corridor. Many sites that experienced elevated weekday O_3 also had higher O_3 on weekends even though the traffic and O_3 precursor levels were substantially reduced on weekends. The authors reported that detailed studies of this phenomenon indicated that the primary cause of the higher O_3 on weekends was the reduction in oxides of nitrogen emissions on weekends in a volatile organic compound (VOC)-limited chemical regime. Heuss et al. (2003) hypothesized that the lower O_3 on weekends in other locations may result from NO_x reductions in a NO_x-limited regime.

Pun et al. (2003) described the day-of-week behavior for O_3 in Chicago, Philadelphia, and Atlanta. In Chicago and Philadelphia, maximum 1-h average O_3 increases on weekends. In Atlanta, O_3 builds up from Mondays to Fridays and declines during the weekends. Fujita et al. (2003) pointed out that since the mid-1970s, O_3 levels in portions of California's South Coast Air Basin on weekends have been as high as or higher than levels on weekdays, even though emissions of O_3 precursors are lower on weekends. The authors reported that the analysis of the ambient data indicates that the intensity and spatial extent of the weekend O_3 effect are correlated with day-of-week variations in the extent of O_3 inhibition caused by titration with nitric oxide (NO), reaction of hydroxyl radical (OH) with nitrogen dioxide (NO_2), and the rate of O_3 accumulation. Blanchard and Tanebaum (2003) noted that despite significantly lower O_3 precursor levels on weekends, 20 of 28 South Coast Air Basin sites showed statistically significant higher mean O_3 levels on Sundays than on weekdays. Chinkin et al. (2003) noted that ambient O_3 levels in California's South Coast Air Basin can be as much as 55% higher on weekends than on weekdays under comparable meteorological conditions.

AX3.2.2 Nonurban Area Concentrations

It is difficult to identify a set of unique O_3 distribution patterns that adequately describes the hourly average concentrations experienced at monitoring sites in nonurban locations, because many nonurban sites in the United States are influenced by local sources of pollution or long-range transport of O_3 or its precursors (U.S. Environmental Protection Agency, 1996a). At most of the RRMS characterized in Section AX3.2.3, the maximum hourly average concentrations were below 0.08 ppm. Unlike these RRMS, urban-influenced nonurban sites sometimes show frequent hourly average concentrations near the minimum detectable level, but often show occurrences of hourly average concentrations > 0.10 ppm. The frequent occurrence of hourly average concentrations near the minimum detectable level is indicative of scavenging processes (i.e., by NO); the presence of high hourly average concentrations can be attributable to the influence of either local generation or the long-range transport of O_3. For example, the U.S. Environmental Protection Agency (2003a) reported that Whiteface Mountain (NY) experienced a 3-year average of the fourth highest 8-h daily maximum concentration of 0.086 ppm for the period of 2000 to 2002. In 2002, the maximum hourly average concentration reached 0.113 ppm (U.S. Environmental Protection Agency, 2003b). Similarly, for the period of 2000 to 2002, high-elevation sites in the Great Smoky Mountain National Park in North Carolina and Tennessee experienced a 3-year average of the fourth highest 8-h daily maximum concentrations > 0.085 ppm. In the Great Smoky Mountain National Park, maximum hourly average concentrations reached ~0.12 ppm. These sites are influenced by the long-range transport of O_3. Using hourly averaged data from the AQS database for a select number of rural monitoring sites, Table AX3-7 summarizes the percentiles of the hourly average O_3 concentrations, the number of occurrences of the hourly average concentration ≥ 0.08 and 0.10 ppm, the 7-month sum of all hourly average concentrations ≥0.06 ppm, and the 7-month W126 exposure index. Note the large variation in the number of hourly average concentrations ≥ 0.08 and 0.10 ppm. These sites are influenced either by local sources or by transport of O_3 or its precursors. The maximum hourly average concentrations are generally > 0.10 ppm, and the occurrence of hourly average concentrations near minimum detectable levels indicates NO_x scavenging processes. Also note that in 2001, although the Crestline, CA site in the San Bernardino National Forest and the Cove Mountain site in the Great Smoky Mountains National Park experienced similar cumulative exposures (SUM06 and W126 values), the Crestline site experienced considerably more high hourly average concentrations ≥ 0.10 ppm (369) than the Cove Mountain site (5).

Taylor et al. (1992) have summarized the O_3 concentrations that were experienced at 10 Electric Power Research Institute (EPRI) Integrated Forest Study sites in North America. The authors reported that in 1988 all sites experienced maximum hourly average concentrations > 0.08 ppm. In almost all cases, the sites experienced multiple occurrences above 0.08 ppm. This implies that, although the sites were located in remote forested areas, the sites experienced elevated O_3 concentrations that were more than likely due to long-range transport of O_3 or its precursors.

Ozone concentrations in the Shenandoah National Park exhibit some features in common with both urban and rural areas on a seasonal basis. During some years, maximum hourly average concentrations exceed 0.12 ppm, although some sites in the park exhibit hourly average

Table AX3-7. Seasonal (April through October) Percentile Distribution of Hourly Ozone Concentrations, Number of Hourly Mean Ozone Occurrences ≥ 0.08 and ≥ 0.10, SUM06, and W126 Values for Selected Rural Ozone Monitoring Sites in 2001. Concentrations in ppm.

			Percentiles									Hours			
AIRS Site	Name	Min.	10	30	50	70	90	95	99	Max.	No. of Hours	≥0.08	≥ 0.10	SUM06 (ppm-h)	W126 (ppm-h)
RURAL AGRICULTURAL															
170491001	Effingham Co., IL	0.000	0.007	0.02	0.031	0.041	0.056	0.06	0.07	0.1	5076	21	0	24.7	20.7
180970042	Indianapolis, IN	0.000	0.007	0.021	0.033	0.044	0.061	0.068	0.078	0.1	4367	37	0	34.2	25.8
240030014	Anne Arundel, MD	0.000	0.004	0.019	0.031	0.043	0.062	0.072	0.096	0.13	5059	142	34	43.5	35.7
310550032	Omaha, NE	0.000	0.015	0.023	0.030	0.038	0.050	0.056	0.064	0.1	5116	1	0	8.6	10.6
420070002	Beaver Co., PA	0.000	0.020	0.031	0.040	0.050	0.068	0.075	0.089	0.11	5080	156	6	63.2	50.0
510610002	Fauquier Co., VA	0.000	0.004	0.017	0.029	0.041	0.057	0.065	0.08	0.11	5055	48	1	27.4	22.7
551390011	Oshkosh Co., WI	0.002	0.02	0.026	0.035	0.043	0.057	0.065	0.082	0.1	4345	59	1	24.8	22.8
RURAL FOREST															
060430003	Yosemite NP, CA	0.013	0.038	0.046	0.052	0.058	0.069	0.074	0.084	0.11	4619	106	6	86.0	65.6
360310002	Whiteface Mtn., NY	0.000	0.024	0.035	0.043	0.051	0.063	0.070	0.084	0.11	4536	77	4	44.7	37.7
471550101	Smoky Mtns. NP, TN	0.020	0.039	0.050	0.057	0.064	0.075	0.080	0.089	0.11	5074	267	5	149.2	106.5
511130003	Shenandoah NP	0.010	0.035	0.045	0.052	0.059	0.070	0.075	0.089	0.11	4813	157	4	98.5	73.6
RURAL OTHER (I.E., RURAL RESIDENTIAL OR RURAL COMMERCIAL)															
060710005	Crestline, CA	0.000	0.024	0.043	0.055	0.068	0.093	0.107	0.135	0.17	4922	933	369	174.8	144.9
350431001	Sandoval Co., NM	0.000	0.004	0.020	0.033	0.045	0.056	0.061	0.070	0.1	5088	9	0	21.4	20.3
370810011	Guilford Co., NC	0.000	0.003	0.015	0.029	0.043	0.063	0.071	0.087	0.12	4879	111	10	45.4	334.4
371470099	Farmville, NC	—	0.000	0.008	0.021	0.033	0.044	0.061	0.068	0.1	0.097	4882	34	0	36.6

concentrations near the minimum detectable level. Taylor and Norby (1985) have characterized O_3 episodes, which they defined as any day in which a 1-h mean O_3 concentration was > 0.08 ppm. Based on a 4-year monitoring period in Shenandoah National Park, the probability was 80% that any given episode during the growing season would last 2 or more days, whereas the probabilities of episodes lasting for periods greater than 3, 4, and 5 days were 30, 10, and 2%, respectively. Single-day O_3 episodes were infrequent. Taylor and Norby (1985) noted that, given the frequency of respites, there was a 50% probability that a second episode would occur within 2 weeks.

Because of a lack of air quality data collected at rural and remote locations, interpolation techniques must be used to estimate O_3 exposures in these areas. In the absence of actual O_3 data, interpolation techniques have been applied to the estimation of O_3 exposures across the United States (Reagan, 1984; Lefohn et al., 1987; Knudsen and Lefohn, 1988). "Kriging," a mathematical interpolation technique (Matheron, 1963), has been used in the analyses of air quality data (Grivet, 1980; Faith and Sheshinski, 1979) and was used to provide estimates of seasonal O_3 values for the National Crop Loss Assessment Network (NCLAN) for 1978 through 1982 (May to September of each year) (Reagan, 1984). These values, along with updated values, coupled with exposure-response models, were used to predict agriculturally related economic benefits anticipated by lower O_3 levels in the United States (Adams et al., 1985, 1989).

The U.S. Environmental Protection Agency (1996a) concluded that the higher hourly average concentrations (≥ 0.10 ppm) should be provided greater weight than the mid-level (0.06 to 0.099 ppm) and lower hourly average concentrations in predicting injury and yield reduction for agricultural crops and forests. The most recent findings concerning the importance of the higher hourly average concentrations in comparison to the mid-level and lower values will be discussed in Chapter 9. For 2001, ordinary kriging was used to estimate the seasonal W126, SUM06, and number of hours ≥ 0.10 ppm (N100), using hourly average concentrations accumulated over a 24-h period. As discussed in Chapter 9, the correlation between the number of occurrences of hourly average concentrations ≥ 0.10 ppm and the magnitude of the W126 and SUM06 values is not strong. Because of this, the N100 was also estimated, along with the W126 and SUM06 exposure indices. For the period of April through September, the estimates of the seasonal W126, SUM06, and N100 exposure index values were made for each 0.5˚ by 0.5˚ cell in the continuous United States. The kriged values, the variance, and the 95% error bound for each 0.5° by 0.5° cell were estimated. Because of the concern for inner-city depletion caused by NO_x scavenging, data from specific monitoring stations located in large metropolitan areas were not included in the analysis.

Figure AX3-5 shows the kriged values for the 24-h cumulative seasonal W126 exposure index and the N100 index for 2001 for the eastern United States. Note that for some of the areas with elevated W126 values (e.g., > 35 ppm-h), the number of hourly average concentrations was estimated to be < 22. Figure AX3-6 illustrates the kriged values using the 24-h cumulative seasonal SUM06 exposure index and the N100 index for 2001 for the eastern United States. Figures AX3-7 and AX3-8 show the W126 and SUM06 values, respectively, with the N100 values for the central United States region. For 2001, the number of hourly average concentrations ≥ 0.10 ppm was usually < 22 for the 6-month period. Figures AX3-9 and AX3-10 illustrate the W126 and SUM06 values, respectively, for the western United States region. Note that in the Southern California and Central California areas, the number of hourly average concentrations ≥ 0.10 ppm was in the range of 48 to 208 for the 6-month period. This is considerably greater than the frequency of occurrences for the higher hourly average concentrations experienced in the eastern and central United States.

Due to the scarcity of monitoring sites across the United States, especially in the Rocky Mountain region, the uncertainty in the estimates for the various exposure indices vary. Figures AX3-11 through AX3-19 illustrate the 95% confidence intervals associated with the indices by region. In some cases, the uncertainty in the estimates of the exposure indices is great. However, based on the actual hourly average concentrations measured, the pattern of distinct differences across the regions in the United States for the number of hourly average concentrations ≥ 0.10 ppm is real even though at times the uncertainty in the kriged estimates may be large.

AX3.2.3 Ozone Concentrations Observed at Relatively Remote Monitoring Sites

Hourly average concentrations used in controlled O_3 exposures for both human health and vegetation studies appear to be lower than those experienced at RRMS in the United States or in other parts of the world (see Chapter 9). This might have implications for human health (see Annex AX6) and vegetation effects. This concern is relevant to those using exposure

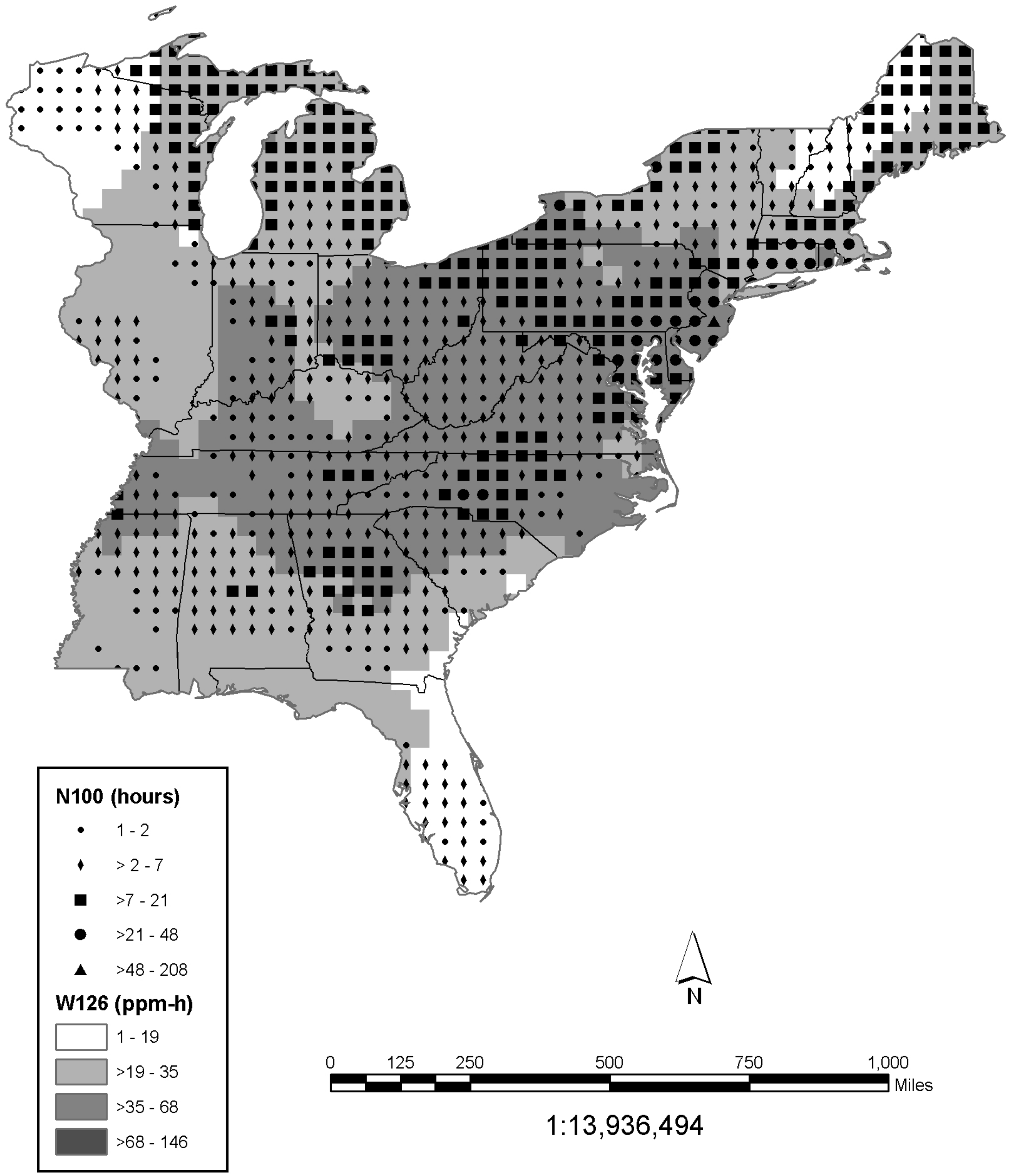

Figure AX3-5. Six-month (April to September) 24-h cumulative W126 exposure index with the number of hourly average concentrations ≥ 0.10 ppm (N100) occurring during 2001 for the eastern United States.

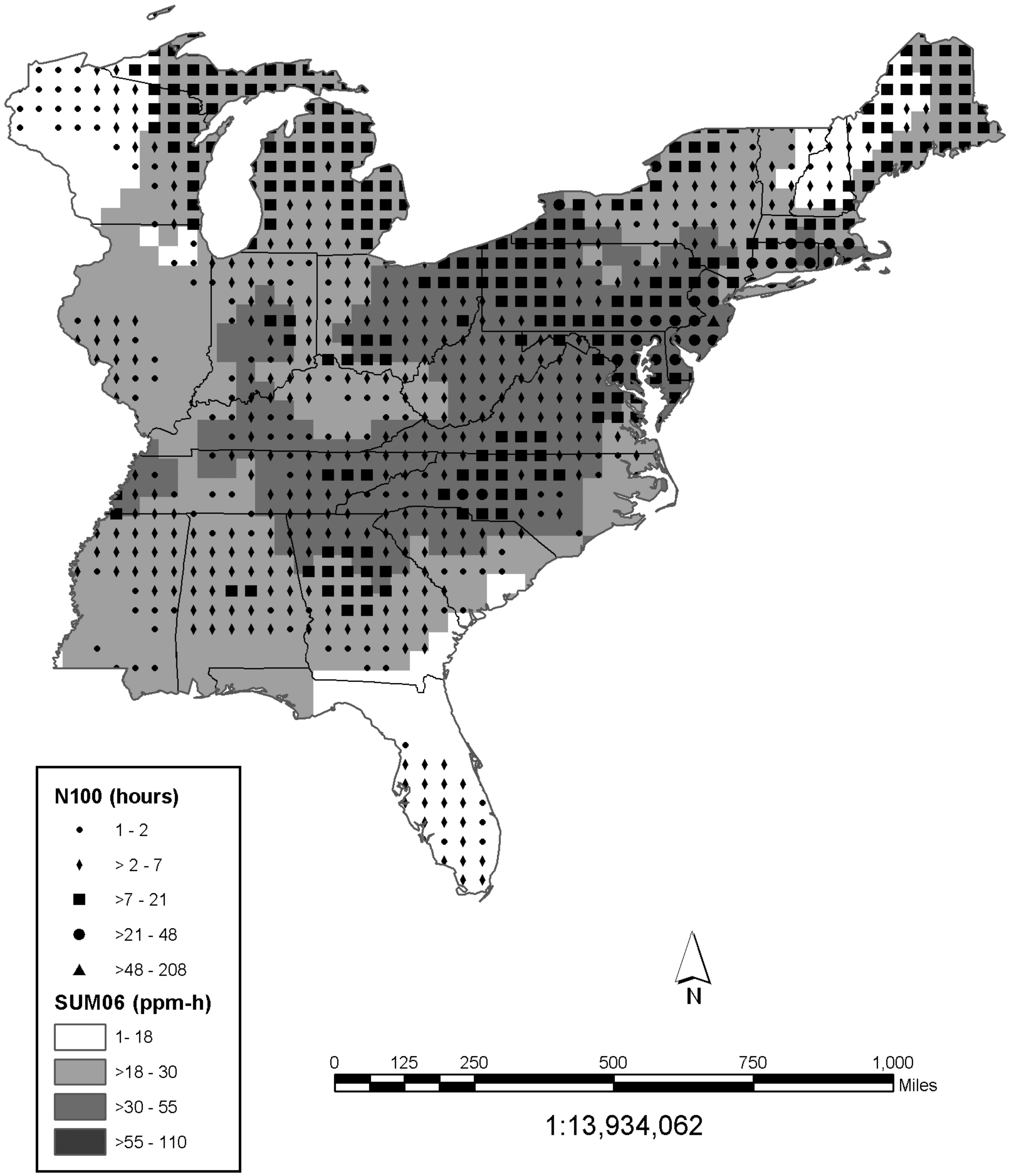

Figure AX3-6. Six-month (April to September) 24-h cumulative SUM06 exposure index with the number of hourly average concentrations ≥ 0.10 ppm (N100) occurring during 2001 for the eastern United States.

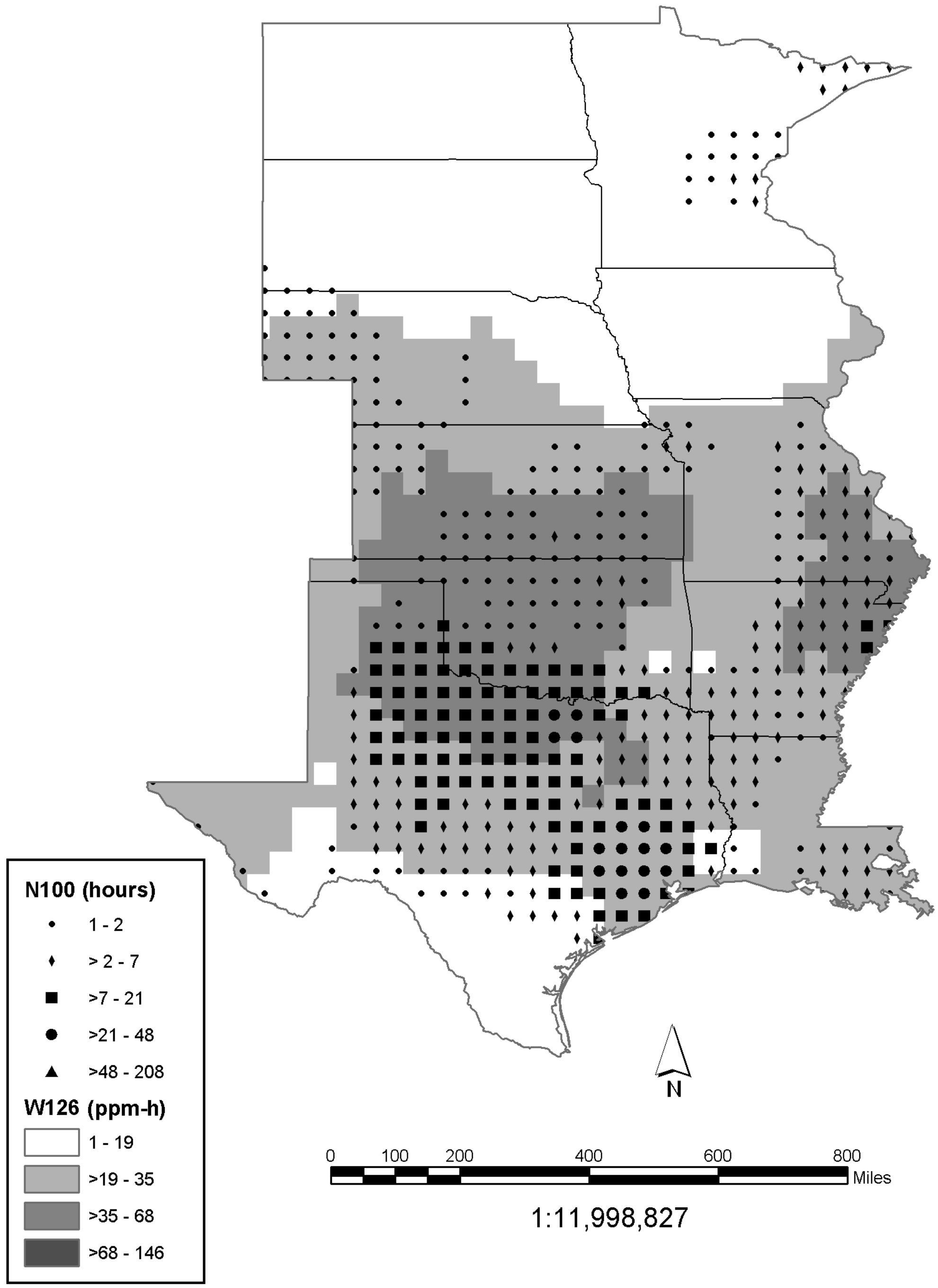

Figure AX3-7. Six-month (April to September) 24-h cumulative W126 exposure index with the number of hourly average concentrations ≥ 0.10 ppm (N100) occurring during 2001 for the central United States.

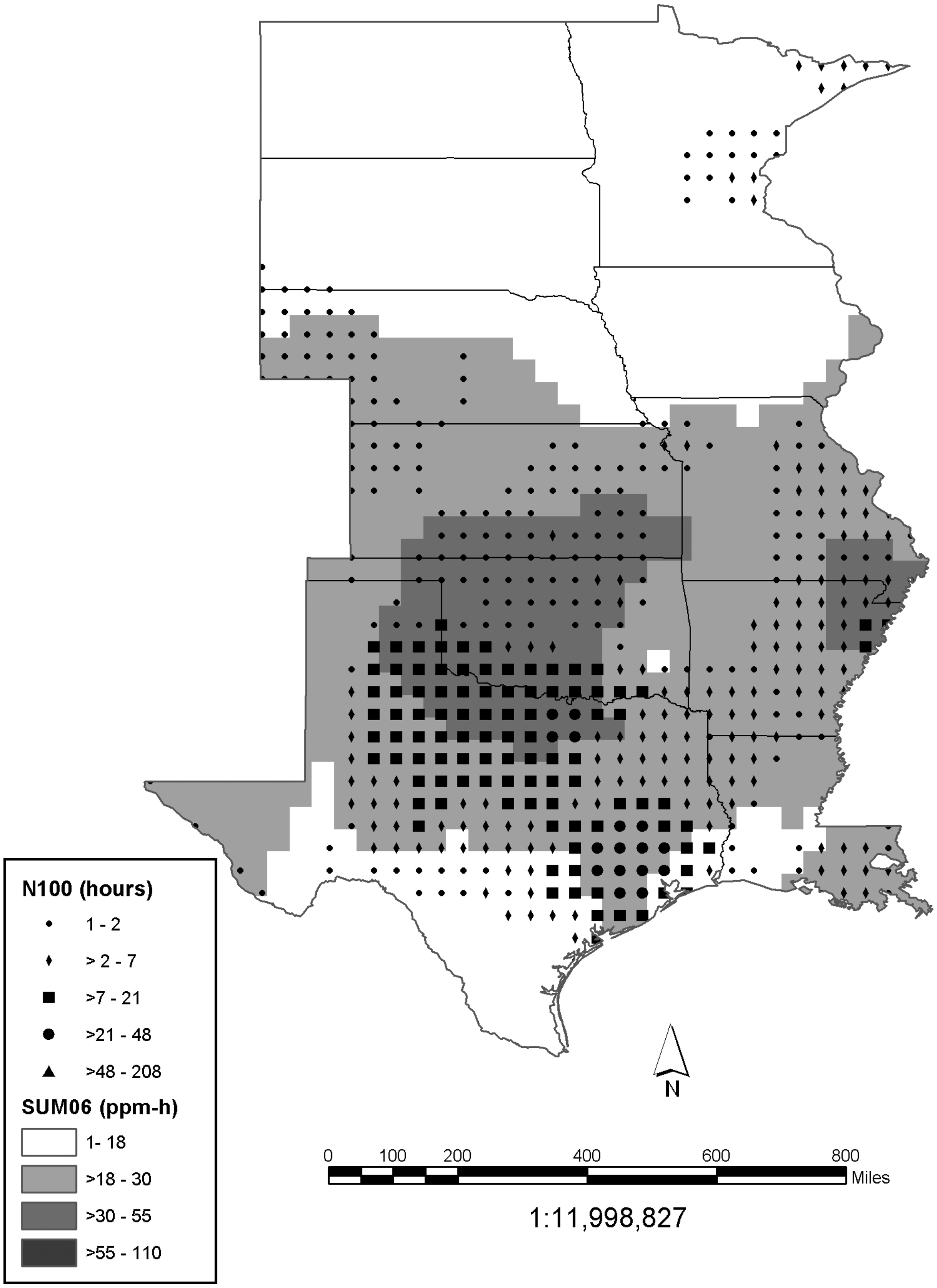

Figure AX3-8. Six-month (April to September) 24-h cumulative SUM06 exposure index with the number of hourly average concentrations ≥ 0.10 ppm (N100) occurring during 2001 for the central United States.

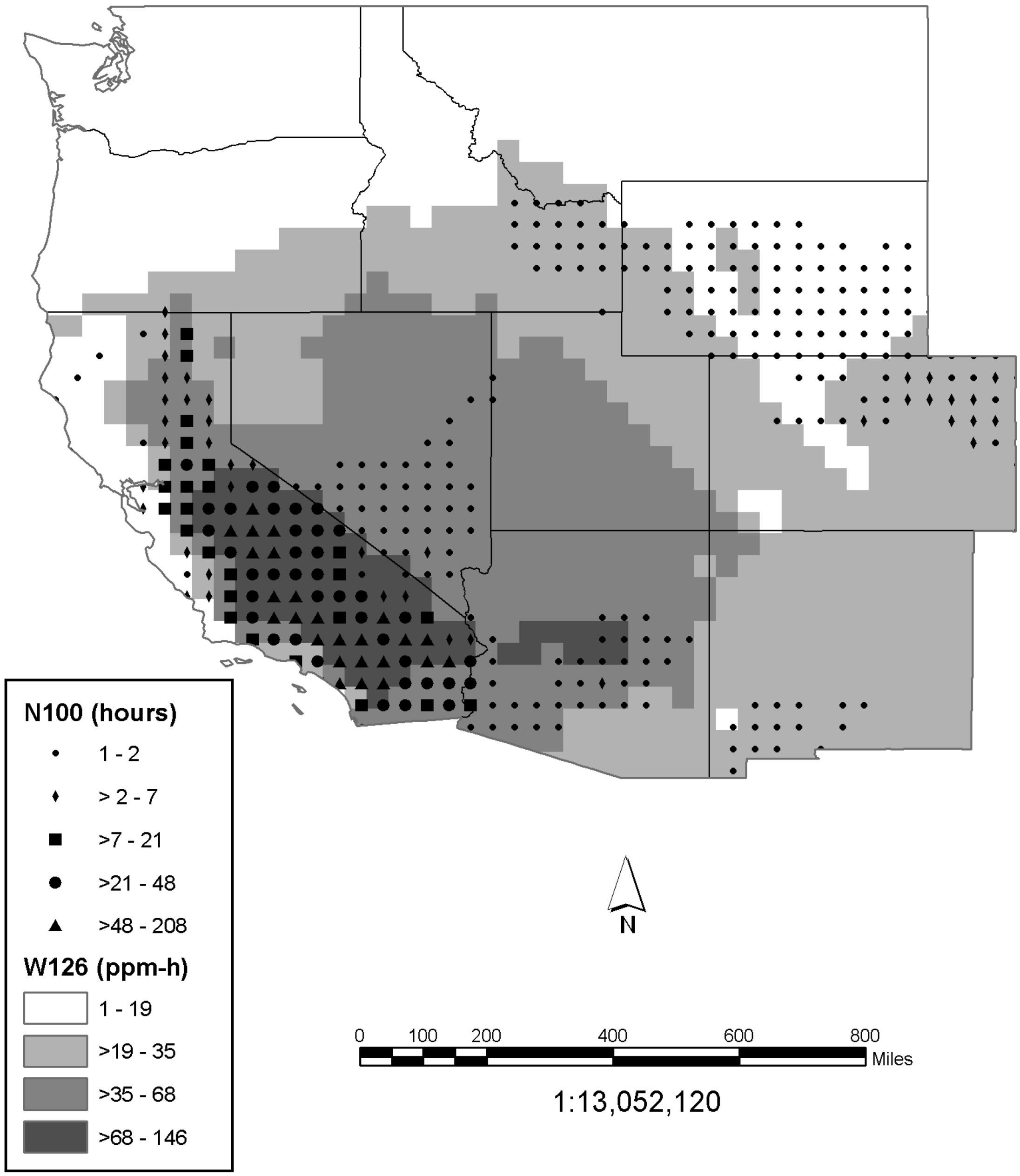

Figure AX3-9. Six-month (April to September) 24-h cumulative W126 exposure index with the number of hourly average concentrations ≥ 0.10 ppm (N100) occurring during 2001 for the western United States.

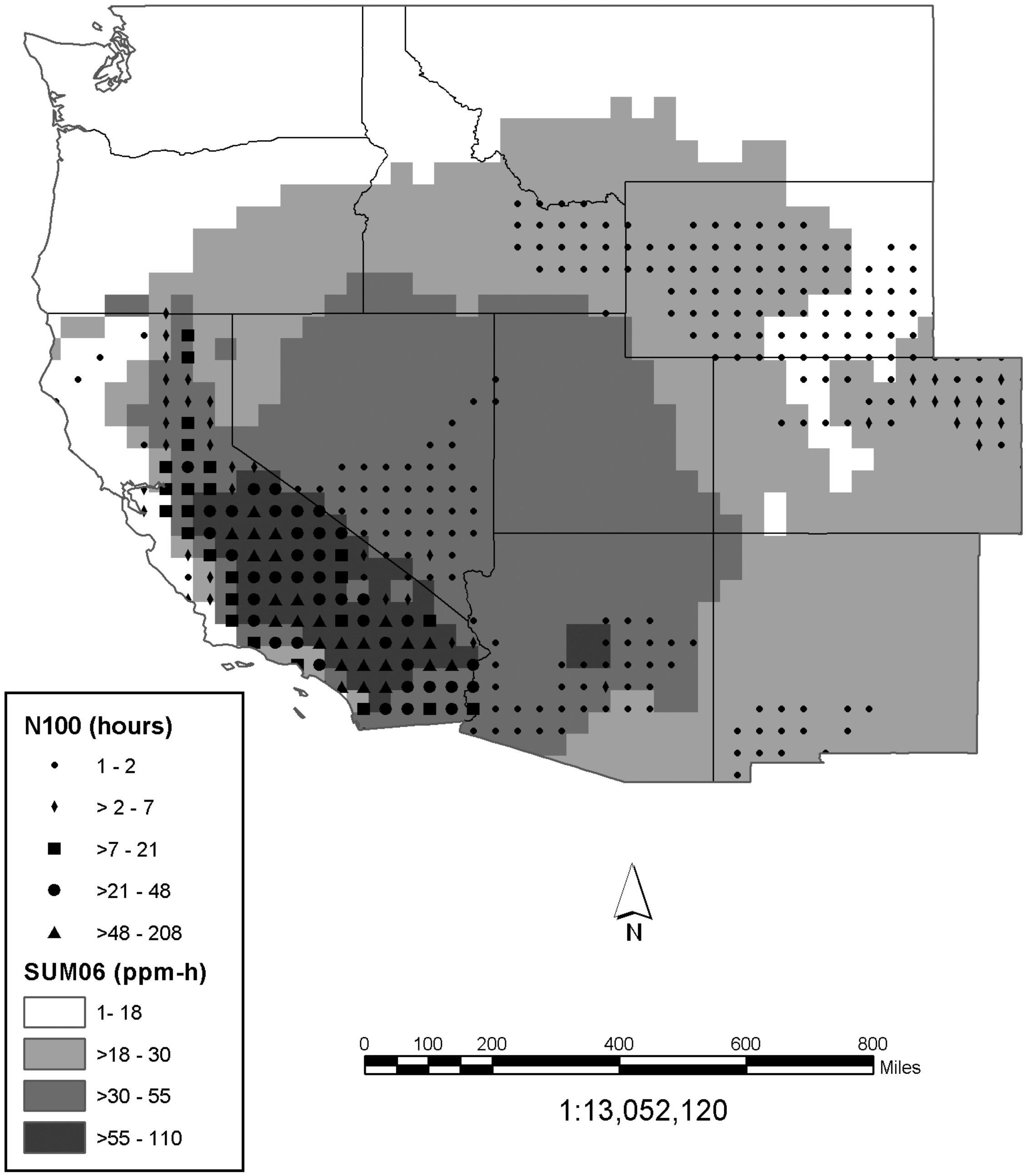

Figure AX3-10. Six-month (April to September) 24-h cumulative SUM06 exposure index with the number of hourly average concentrations ≥ 0.10 ppm (N100) occurring during 2001 for the western United States.

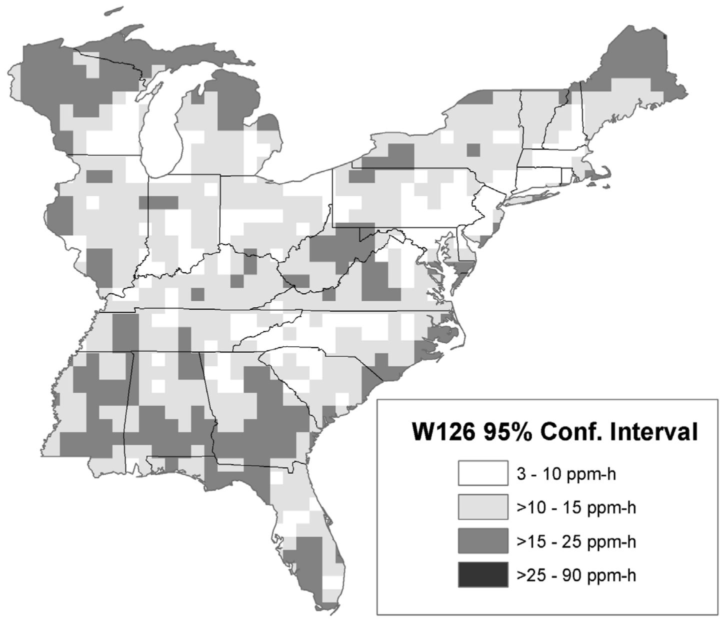

Figure AX3-11. The 95% confidence interval for the 6-month (April to September) 24-h cumulative W126 exposure index for 2001 for the eastern United States.

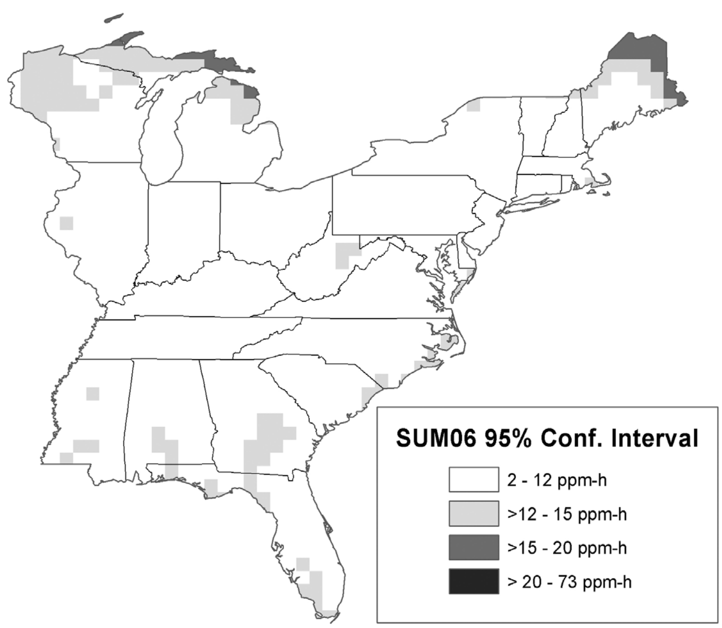

Figure AX3-12. The 95% confidence interval for the 6-month (April to September) 24-h cumulative SUM06 exposure index for 2001 for the eastern United States.

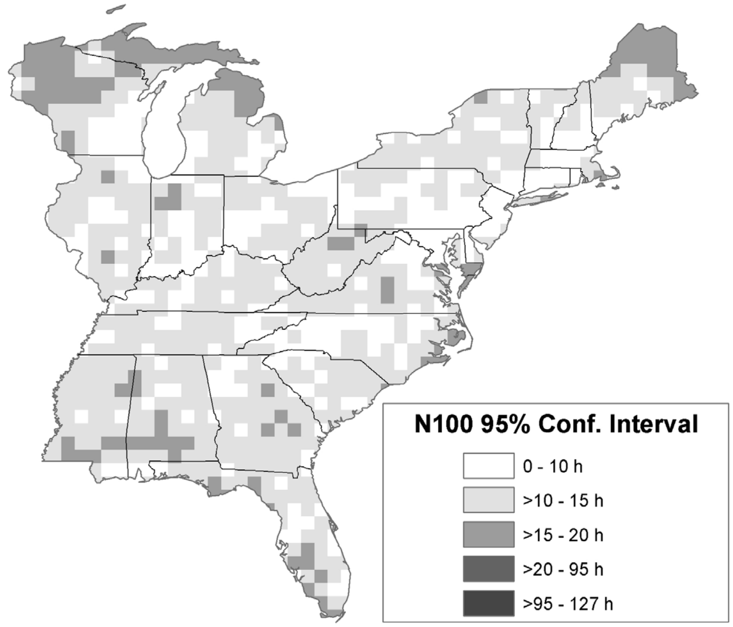

Figure AX3-13. The 95% confidence interval for the 6-month (April to September) 24-h cumulative N100 exposure index for 2001 for the eastern United States.

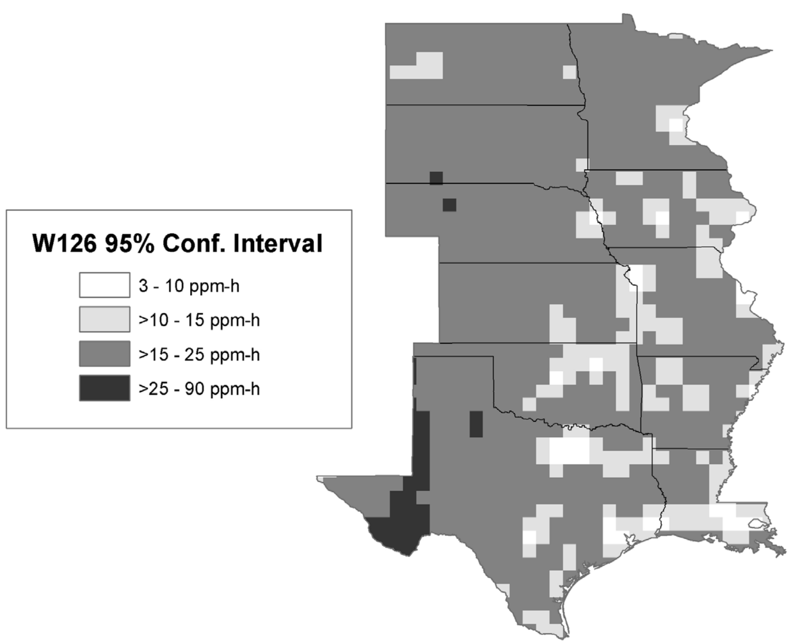

Figure AX3-14. The 95% confidence interval for the 6-month (April to September) 24-h cumulative W126 exposure index for 2001 for the central United States.

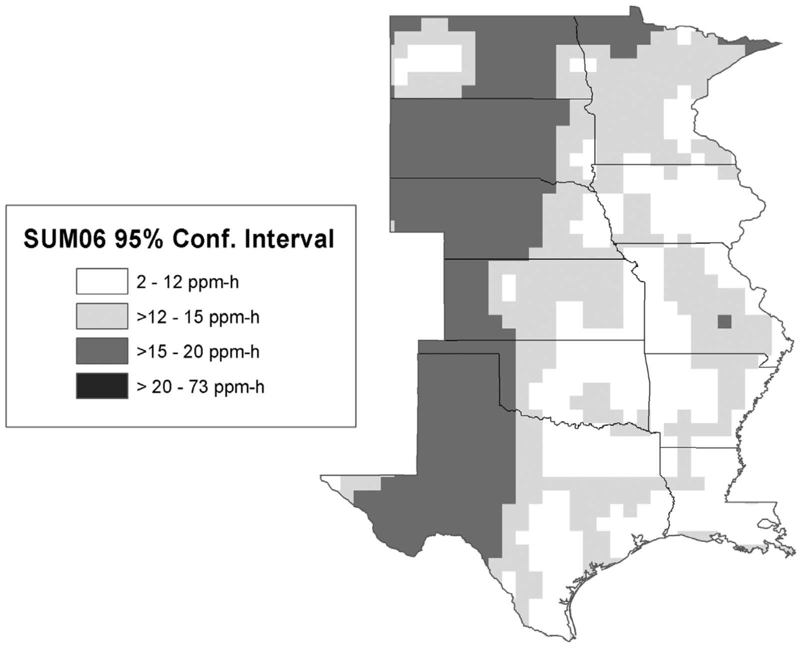

Figure AX3-15. The 95% confidence interval for the 6-month (April to September) 24-h cumulative SUM06 exposure index for 2001 for the central United States.

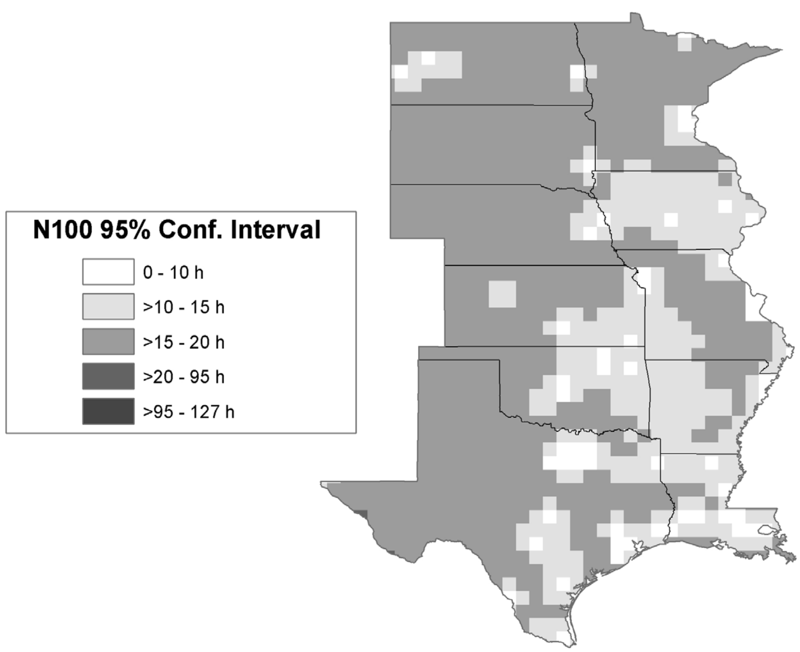

Figure AX3-16. The 95% confidence interval for the 6-month (April to September) 24-h cumulative N100 exposure index for 2001 for the central United States.

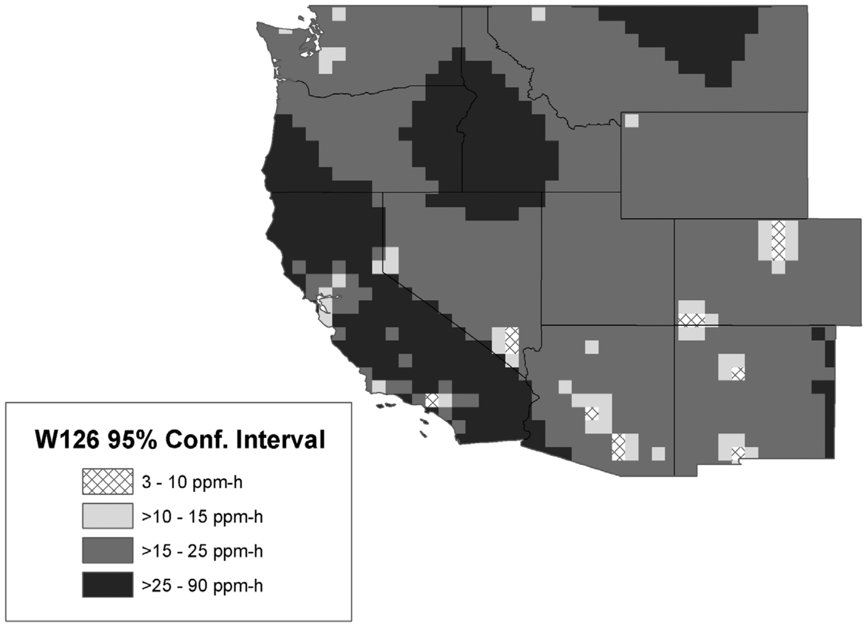

Figure AX3-17. The 95% confidence interval for the 6-month (April to September) 24-h cumulative W126 exposure index for 2001 for the western United States.

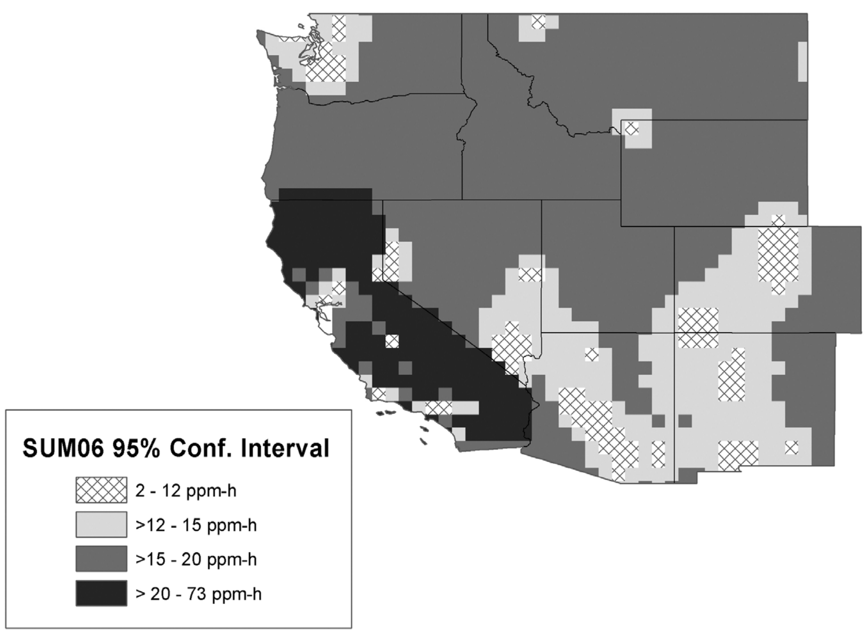

Figure AX3-18. The 95% confidence interval for the 6-month (April to September) 24-h cumulative SUM06 exposure index for 2001 for the western United States.

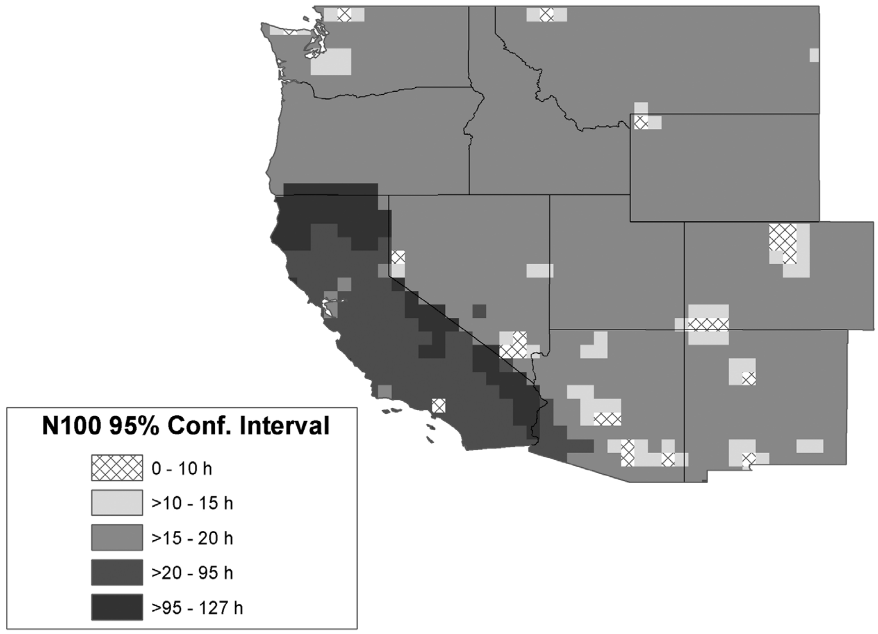

Figure AX3-19. The 95% confidence interval for the 6-month (April to September) 24-h cumulative N100 exposure index for 2001 for the western United States.

indices (e.g., 8-h average concentrations, SUM06, W126, etc.) to predict effects when the control exposure regimes are based on O_3 concentrations that are below background levels that cannot be controlled with emission reductions (Tingey et al., 2002).

The 1996 O_3 AQCD (U.S. Environmental Protection Agency, 1996a) concluded that the annual average background concentration of O_3 near sea level ranged from 0.020 to 0.035 ppm and that, during the summer, the 1-h daily maximum ranged from 0.03 to 0.05 ppm. The 1996 O_3 AQCD also included O_3 hourly average concentrations measured at several clean, RRMS mostly located in the western United States. Table AX3-8 provides an updated summary of the characterization of the hourly average concentrations recorded from 1988 to 2001 at some of the monitoring sites previously analyzed. The percentile distribution of the hourly average concentrations (April to October), number of hourly average occurrences $\geq$ 0.08 and $\geq$ 0.10 ppm, seasonal 7-h average concentrations, the SUM06, and W126 values were characterized for those site years with a data capture of $\geq$ 75%. From 1988 to 2001, no hourly average concentrations

Table AX3-8. Seasonal (April to October) Percentile Distribution of Hourly Ozone Concentrations (ppm), Number of Hourly Mean Ozone Occurrences ≥ 0.08 and ≥ 0.10, Seasonal 7-h Average Concentrations, SUM06, and W126 Values for Sites Experiencing Low Maximum Hourly Average Concentrations with Data Capture of ≥ 75%

			Percentiles									Hours				
Site	**Year**	**Min.**	**10**	**30**	**50**	**70**	**90**	**95**	**99**	**Max.**	**No. of Obs.**	**≥ 0.08**	**≥ 0.10**	**Seasonal 7-h**	**SUM06 (ppm-h)**	**W126 (ppm-h)**
Redwood NP 060150002 (California) 235 m	1988	0.002	0.011	0.018	0.023	0.029	0.038	0.041	0.046	0.06	4825	0	0	0.026	1.8	0.1
	1989	0.000	0.010	0.017	0.022	0.027	0.034	0.038	0.042	0.047	4624	0	0	0.024	1.0	0.0
	1990	0.000	0.011	0.018	0.023	0.028	0.035	0.038	0.043	0.053	4742	0	0	0.025	1.2	0.0
	1991	0.001	0.012	0.019	0.025	0.031	0.038	0.041	0.045	0.054	4666	0	0	0.027	1.7	0.0
	1992	0.000	0.010	0.017	0.021	0.026	0.035	0.039	0.045	0.055	4679	0	0	0.023	1.1	0.0
	1993	0.000	0.010	0.017	0.022	0.027	0.035	0.038	0.042	0.054	4666	0	0	0.025	1.1	0.0
	1994	0.001	0.011	0.018	0.024	0.028	0.035	0.038	0.043	0.050	4846	0	0	0.026	0.0	1.2
Olympic NP (Washington) 530090012 125 m	1989	0.000	0.003	0.010	0.015	0.022	0.030	0.035	0.046	0.065	4220	0	0	0.021	0.7	0.1
	1990	0.000	0.005	0.012	0.018	0.023	0.030	0.034	0.043	0.064	4584	0	0	0.022	0.8	0.3
	1991	0.000	0.006	0.014	0.019	0.024	0.033	0.036	0.044	0.056	4677	0	0	0.025	0.9	0.0
	1993	0.000	0.004	0.010	0.016	0.021	0.029	0.034	0.041	0.064	4595	0	0	0.022	0.7	0.3
	1994	0.000	0.006	0.013	0.019	0.025	0.033	0.038	0.043	0.062	4044	0	0	0.025	0.2	0.8
	1995	0.000	0.006	0.014	0.020	0.027	0.037	0.040	0.048	0.077	4667	0	0	0.027	0.8	1.9
	1996	0.000	0.006	0.013	0.019	0.025	0.034	0.038	0.043	0.058	4811	0	0	0.025	0.0	1.0
	1997	0.000	0.005	0.010	0.015	0.022	0.035	0.040	0.046	0.057	4403					
	1998	0.000	0.008	0.014	0.019	0.025	0.033	0.037	0.044	0.063	4792	0	0	0.024	0.3	1.1
	1999	0.000	0.006	0.014	0.019	0.026	0.036	0.039	0.044	0.050	4656	0	0	0.024	0.0	1.1
	2000	0.000	0.006	0.013	0.019	0.025	0.035	0.039	0.045	0.061	4676	0	0	0.024	0.1	1.2
	2001	0.002	0.009	0.017	0.023	0.028	0.036	0.041	0.046	0.055	4643	0	0	0.027	0.0	1.4

Table AX3-8 (cont'd). Seasonal (April to October) Percentile Distribution of Hourly Ozone Concentrations (ppm), Number of Hourly Mean Ozone Occurrences ≥0.08 and ≥ 0.10, Seasonal 7-h Average Concentrations, SUM06, and W126 Values for Sites Experiencing Low Maximum Hourly Average Concentrations with Data Capture of ≥ 75%

			Percentiles									Hours				
Site	Year	Min.	10	30	50	70	90	95	99	Max.	No. of Obs.	≥ 0.08	≥ 0.10	Seasonal 7-h	SUM06 (ppm-h)	W126 (ppm-h)
Glacier NP 300298001 (Montana) 963 m	1989	0.000	0.003	0.015	0.026	0.036	0.046	0.050	0.058	0.067	4770	0	0	0.036	5.9	1.8
	1990	0.000	0.003	0.014	0.026	0.035	0.044	0.047	0.052	0.066	5092	0	0	0.036	4.1	1.3
	1991	0.000	0.001	0.014	0.027	0.036	0.046	0.049	0.056	0.062	5060	0	0	0.036	5.3	0.7
	1992	0.000	0.001	0.013	0.025	0.033	0.043	0.048	0.055	0.077	4909	0	0	0.033	4.1	1
	1993	0.000	0.000	0.010	0.020	0.029	0.040	0.044	0.050	0.058	5071	0	0	0.029	0.0	2.3
	1994	0.000	0.001	0.014	0.026	0.036	0.046	0.050	0.056	0.061	5072	0	0	0.036	0.1	5.4
	1995	0.000	0.000	0.010	0.022	0.031	0.041	0.045	0.051	0.066	4744	0	0	0.023	0.3	2.3
	1996	0.000	0.002	0.013	0.025	0.035	0.046	0.051	0.058	0.065	4666	0	0	0.035	1.9	5.4
	1997	0.000	0.000	0.008	0.017	0.026	0.041	0.045	0.053	0.058	4378	0	0	0.027	0.0	2.3
	1998	0.000	0.003	0.013	0.025	0.035	0.047	0.051	0.058	0.064	4649	0	0	0.036	1.4	5.6
	1999	0.000	0.002	0.015	0.026	0.035	0.046	0.051	0.058	0.068	4540	0	0	0.035	1.3	5.4
	2000	0.000	0.001	0.011	0.023	0.033	0.044	0.048	0.055	0.062	4551	0	0	0.033	0.7	3.8
	2001	0.000	0.000	0.013	0.025	0.033	0.042	0.044	0.049	0.057	4643	0	0	0.033	0.0	2.7
Yellowstone NP (Wyoming) 560391010 2484 m	1988	0.002	0.020	0.029	0.037	0.044	0.054	0.058	0.070	0.098	4257	17	0	0.043	14.0	8.9
	1989	0.002	0.018	0.027	0.036	0.044	0.052	0.057	0.063	0.071	4079	0	0	0.042	11.0	6.7
	1990	0.000	0.015	0.023	0.029	0.036	0.043	0.046	0.053	0.061	4663	0	0	0.034	3.8	0.5
	1991	0.004	0.020	0.030	0.037	0.042	0.048	0.051	0.057	0.064	4453	0	0	0.042	7.7	1.2
	1992	0.001	0.018	0.029	0.036	0.042	0.051	0.056	0.064	0.075	4384	0	0	0.042	10.7	6.3
	1993	0.000	0.018	0.028	0.036	0.042	0.047	0.050	0.054	0.060	4399	0	0	0.041	6.5	0.2
	1994	0.003	0.022	0.033	0.040	0.046	0.053	0.056	0.062	0.072	4825	0	0	0.046	6.0	15.2
	1995	0.004	0.022	0.033	0.040	0.045	0.052	0.055	0.059	0.065	4650	0	0	0.045	2.8	12.5

Table AX3-8 (cont'd). Seasonal (April to October) Percentile Distribution of Hourly Ozone Concentrations (ppm), Number of Hourly Mean Ozone Occurrences ≥0.08 and ≥ 0.10, Seasonal 7-h Average Concentrations, SUM06, and W126 Values for Sites Experiencing Low Maximum Hourly Average Concentrations with Data Capture of ≥ 75%

			Percentiles									Hours				
Site	**Year**	**Min.**	**10**	**30**	**50**	**70**	**90**	**95**	**99**	**Max.**	**No. of Obs.**	**≥ 0.08**	**≥ 0.10**	**Seasonal 7-h**	**SUM06 (ppm-h)**	**W126 (ppm-h)**
Yellowstone NP (Wyoming)	1997	0.005	0.026	0.035	0.040	0.045	0.051	0.054	0.060	0.068	4626	0	0	0.043	3.3	12.4
560391011 2468 m	1998	0.004	0.029	0.038	0.043	0.048	0.055	0.058	0.064	0.073	4827	0	0	0.046	9.9	20.0
	1999	0.012	0.033	0.040	0.046	0.051	0.059	0.062	0.069	0.079	4733	0	0	0.049	27.1	29.8
	2000	0.009	0.031	0.039	0.045	0.050	0.057	0.060	0.065	0.074	4678	0	0	0.047	17.0	23.4
	2001	0.012	0.034	0.041	0.046	0.050	0.057	0.060	0.065	0.078	4869	0	0	0.048	16.9	25.6
Denali NP (Alaska)	1988	0.003	0.018	0.024	0.028	0.033	0.044	0.050	0.053	0.056	4726	0	0	0.031	0.0	4.0
022900003 640 m	1990	0.003	0.017	0.024	0.029	0.034	0.040	0.043	0.048	0.050	3978	0	0	0.030	2.1	0.0
	1991	0.005	0.018	0.024	0.028	0.034	0.041	0.043	0.047	0.057	4809	0	0	0.030	2.7	0.0
	1992	0.003	0.016	0.023	0.028	0.034	0.044	0.047	0.050	0.054	4800	0	0	0.031	3.7	0.0
	1993	0.002	0.017	0.023	0.028	0.033	0.041	0.043	0.048	0.055	4773	0	0	0.030	2.6	0.0
	1994	0.003	0.017	0.022	0.027	0.033	0.042	0.045	0.049	0.053	4807	0	0	0.030	0.0	2.9
	1995	0.001	0.013	0.019	0.025	0.032	0.042	0.044	0.052	0.059	4825	0	0	0.028	0.0	3.0
	1996	0.002	0.015	0.022	0.028	0.035	0.044	0.047	0.052	0.063	4831	0	0	0.031	0.1	4.1
	1997	0.001	0.015	0.023	0.030	0.038	0.045	0.048	0.051	0.084	4053	1	0	0.032	0.2	4.0
	1998	0.004	0.018	0.023	0.030	0.036	0.048	0.050	0.055	0.058	4782	0	0	0.032	0.0	6.0
	1999	0.002	0.016	0.024	0.029	0.036	0.045	0.048	0.054	0.058	4868	0	0	0.032	0.0	4.7
	2000	0.003	0.014	0.019	0.025	0.029	0.034	0.036	0.038	0.049	4641	0	0	0.025	0.0	1.0
	2001	0.002	0.016	0.023	0.029	0.036	0.048	0.051	0.055	0.068	4868	0	0	0.032	0.7	11.1
Badlands NP 460711001	1989	0.006	0.020	0.027	0.034	0.041	0.049	0.053	0.060	0.071	4840	0	0	0.040	9.2	3.1
(South Dakota) 730 m	1990	0.006	0.019	0.027	0.032	0.037	0.044	0.048	0.054	0.063	4783	0	0	0.037	4.8	0.8
	1991	0.005	0.020	0.028	0.033	0.040	0.047	0.050	0.056	0.066	4584	0	0	0.038	6.2	0.7

Table AX3-8 (cont'd). Seasonal (April to October) Percentile Distribution of Hourly Ozone Concentrations (ppm), Number of Hourly Mean Ozone Occurrences ≥0.08 and ≥ 0.10, Seasonal 7-h Average Concentrations, SUM06, and W126 Values for Sites Experiencing Low Maximum Hourly Average Concentrations with Data Capture of ≥ 75%

			Percentiles									Hours				
Site	Year	Min.	10	30	50	70	90	95	99	Max.	No. of Obs.	≥ 0.08	≥ 0.10	Seasonal 7-h	SUM06 (ppm-h)	W126 (ppm-h)
Theod. Roos. NP 380530002 (North Dakota) 730 m	1984	0.000	0.017	0.025	0.032	0.039	0.047	0.050	0.059	0.068	4923	0	0	0.038	7.0	2.8
	1985	0.000	0.019	0.026	0.032	0.038	0.046	0.049	0.054	0.061	4211	0	0	0.038	5.0	0.1
	1986	0.004	0.017	0.027	0.033	0.039	0.047	0.050	0.056	0.062	4332	0	0	0.039	5.5	0.4
	1989	0.004	0.023	0.032	0.039	0.045	0.054	0.058	0.065	0.073	4206	0	0	0.046	14.2	11.0
	1992	0.005	0.019	0.027	0.033	0.039	0.047	0.050	0.056	0.063	4332	0	0	0.040	6.1	0.8
	1993	0.004	0.018	0.025	0.031	0.037	0.045	0.048	0.055	0.064	4281	0	0	0.038	4.6	0.7
	1994	0.000	0.018	0.028	0.035	0.041	0.049	0.052	0.058	0.079	4644	0	0	0.041	1.1	8.4
	1995	0.000	0.018	0.028	0.035	0.041	0.050	0.053	0.058	0.064	4242	0	0	0.042	1.2	7.7
	1996	0.003	0.022	0.031	0.037	0.043	0.051	0.054	0.059	0.064	3651	0	0	0.044	1.8	8.5
	1997	0.000	0.016	0.029	0.037	0.044	0.053	0.058	0.069	0.082	4344	8	0	0.046	11.8	14.6
Theod. Roos. NP 380070002 (North Dakota) 808 m	1999	0.007	0.024	0.031	0.037	0.042	0.049	0.052	0.058	0.070	5105	0	0	0.041	1.6	10
	2000	0.002	0.021	0.031	0.036	0.043	0.050	0.053	0.058	0.066	5105	0	0	0.041	2.3	10.5
	2001	0.002	0.023	0.031	0.036	0.042	0.049	0.052	0.058	0.064	5099	0	0	0.041	1.9	9.2
Custer NF, MT 300870101 (Montana) 1006 m	1978	0.000	0.010	0.020	0.035	0.040	0.050	0.055	0.060	0.070	4759	0	0	0.033	3.0	8.3
	1979	0.010	0.025	0.035	0.040	0.045	0.050	0.055	0.060	0.075	5014	0	0	0.043	7.3	13.2
	1980	0.010	0.025	0.035	0.040	0.050	0.055	0.060	0.065	0.070	4574	0	0	0.043	22.4	19.7
	1983	0.010	0.025	0.035	0.040	0.045	0.05	0.055	0.060	0.065	4835	0	0	0.042	4.2	10.7

≥ 0.08 ppm were observed at monitoring sites in Redwood NP (CA), Olympic NP (WA), Glacier NP (MT), Denali NP (AK), Badlands (SD), and Custer NF (MT) during the months of April to October. There were eight occurrences of hourly average O_3 concentrations ≥ 0.08 ppm from April to October of 1997 at the monitoring site in Theodore Roosevelt NP (ND). However, no hourly average concentrations ≥ 0.08 ppm were observed from April to October in any other year at this site. Except for 1988, the year in which there were major forest fires at Yellowstone NP (WY), the monitoring site located there experienced no hourly average concentrations ≥ 0.08 ppm. Logan (1989) noted that O_3 hourly average concentrations rarely exceed 0.08 ppm at remote monitoring sites in the western United States. In almost all cases for the above sites, the maximum hourly average concentration was ≤ 0.075 ppm. The top 10 daily maximum 8-h average concentrations for sites experiencing low maximum hourly average concentrations with a data capture of ≥ 75% are summarized in Table AX3-9. Figure AX3-20 shows the 3-year average of the fourth highest 8-h daily maximum concentration at Olympic (WA), Glacier (MT), Yellowstone (WY), and Denali (AK) National Parks for 1999 to 2001. The highest 8-h daily maximum concentrations do not necessarily all occur during the summer months. For example, at the Yellowstone National Park site, the first three highest 8-h daily maximum concentrations occurred in April and May in 1998, and the fourth highest, 8-h daily maximum concentration did not occur until July of that year. In 1999, the first three highest, 8-h daily maximum concentrations were observed in March and May, and the fourth highest value occurred in April. In 2000, the four highest values occurred in May, June, July, and August.

The 1996 O_3 AQCD (U.S. Environmental Protection Agency, 1996a) noted that the 7-month (April to October) average of the 7-h daily average concentrations (0900 to 1559 hours) observed at the Theodore Roosevelt National Park monitoring site in North Dakota were 0.038, 0.039, and 0.039 ppm, respectively, for 1984, 1985, and 1986 and concluded that the range of 7-h seasonal averages for the Theodore Roosevelt National Park site was representative of the range of maximum daily 8-h average O_3 concentrations that may occur at other fairly clean sites in the United States and other locations in the Northern Hemisphere. However, as shown in Table AX3-9 and Figure AX3-20, the representative (as given by the fourth highest) daily maximum 8-h average O_3 concentrations at fairly clean sites in the United States are higher than the 0.038 and 0.039 ppm values cited in the 1996 O_3 AQCD, and more appropriate values should be used.

Table AX3-9. The Top 10 Daily Maximum 8-h Average Concentrations (ppm) for Sites Experiencing Low Maximum Hourly Average Concentrations with Data Capture of ≥ 75%

Site	Year	1	2	3	4	5	6	7	8	9	10
Redwood NP 060150002 (California) 235 m	1988	0.061	0.058	0.053	0.052	0.049	0.047	0.046	0.046	0.045	0.045
	1989	0.044	0.043	0.043	0.043	0.042	0.042	0.042	0.042	0.041	0.041
	1990	0.051	0.048	0.048	0.047	0.047	0.046	0.045	0.044	0.043	0.043
	1991	0.048	0.047	0.046	0.045	0.045	0.045	0.044	0.044	0.043	0.043
	1992	0.060	0.053	0.045	0.045	0.045	0.044	0.044	0.043	0.043	0.042
	1993	0.049	0.046	0.043	0.043	0.043	0.042	0.042	0.042	0.041	0.041
	1994	0.048	0.048	0.046	0.046	0.045	0.044	0.044	0.043	0.043	0.043
Olympic NP 530090012 (Washington) 125 m	1989	0.054	0.052	0.047	0.044	0.044	0.044	0.042	0.042	0.038	0.038
	1990	0.056	0.048	0.046	0.046	0.043	0.040	0.040	0.039	0.038	0.038
	1991	0.050	0.048	0.045	0.043	0.042	0.041	0.041	0.041	0.041	0.041
	1993	0.055	0.052	0.044	0.042	0.040	0.039	0.038	0.038	0.037	0.037
	1994	0.050	0.046	0.042	0.042	0.042	0.042	0.041	0.041	0.040	0.040
	1995	0.064	0.063	0.050	0.049	0.045	0.045	0.044	0.044	0.044	0.044
	1996	0.046	0.046	0.046	0.046	0.043	0.042	0.041	0.041	0.041	0.040
	1997	0.052	0.051	0.046	0.045	0.045	0.045	0.044	0.043	0.042	0.042
	1998	0.051	0.050	0.049	0.046	0.044	0.043	0.042	0.041	0.041	0.041
	1999	0.045	0.044	0.044	0.043	0.043	0.042	0.042	0.042	0.042	0.041
	2000	0.051	0.051	0.048	0.047	0.045	0.044	0.043	0.042	0.042	0.042
	2001	0.051	0.050	0.047	0.045	0.045	0.044	0.044	0.044	0.043	0.043

Table AX3-9 (cont'd). The Top 10 Daily Maximum 8-h Average Concentrations (ppm) for Sites Experiencing Low Maximum Hourly Average Concentrations with Data Capture of ≥ 75%

Site	Year	1	2	3	4	5	6	7	8	9	10
Glacier NP 300298001 (Montana) 963 m	1989	0.062	0.061	0.060	0.059	0.058	0.057	0.056	0.056	0.056	0.056
	1990	0.058	0.057	0.055	0.054	0.053	0.053	0.052	0.052	0.052	0.052
	1991	0.060	0.057	0.057	0.057	0.056	0.055	0.055	0.054	0.054	0.053
	1992	0.062	0.056	0.055	0.054	0.054	0.054	0.053	0.053	0.053	0.053
	1993	0.055	0.052	0.051	0.051	0.050	0.050	0.049	0.049	0.049	0.048
	1994	0.057	0.057	0.056	0.056	0.055	0.055	0.055	0.055	0.054	0.053
	1995	0.061	0.055	0.053	0.052	0.052	0.052	0.051	0.051	0.051	0.050
	1996	0.059	0.059	0.058	0.058	0.057	0.057	0.055	0.056	0.055	0.055
	1997	0.056	0.054	0.052	0.052	0.052	0.051	0.050	0.050	0.050	0.050
	1998	0.060	0.059	0.058	0.058	0.056	0.056	0.055	0.055	0.055	0.054
	1999	0.065	0.065	0.060	0.058	0.056	0.055	0.055	0.055	0.055	0.054
	2000	0.059	0.058	0.058	0.056	0.054	0.052	0.051	0.050	0.050	0.050
	2001	0.054	0.052	0.049	0.049	0.049	0.048	0.047	0.047	0.047	0.047
Yellowstone NP 560391010 (Wyoming) 2484 m	1988	0.068	0.068	0.067	0.066	0.066	0.066	0.064	0.064	0.063	0.061
	1989	0.067	0.065	0.064	0.063	0.063	0.061	0.061	0.061	0.061	0.060
	1990	0.057	0.056	0.054	0.054	0.053	0.052	0.050	0.050	0.049	0.048
	1991	0.059	0.058	0.058	0.057	0.056	0.056	0.056	0.055	0.055	0.055
	1992	0.066	0.064	0.064	0.063	0.063	0.061	0.061	0.059	0.059	0.058
	1993	0.057	0.054	0.054	0.054	0.053	0.053	0.053	0.052	0.052	0.052
	1994	0.067	0.063	0.063	0.061	0.061	0.061	0.061	0.061	0.059	0.059
	1995	0.064	0.062	0.061	0.060	0.059	0.059	0.059	0.059	0.059	0.058

Table AX3-9 (cont'd). The Top 10 Daily Maximum 8-h Average Concentrations (ppm) for Sites Experiencing Low Maximum Hourly Average Concentrations with Data Capture of ≥ 75%

Site	Year	1	2	3	4	5	6	7	8	9	10
Yellowstone NP 560391011 (Wyoming) 2468 m	1997	0.065	0.065	0.062	0.061	0.061	0.060	0.057	0.056	0.056	0.056
	1998	0.069	0.068	0.066	0.066	0.063	0.063	0.061	0.061	0.061	0.060
	1999	0.078	0.074	0.073	0.071	0.070	0.070	0.070	0.069	0.068	0.067
	2000	0.070	0.069	0.067	0.065	0.065	0.065	0.064	0.064	0.063	0.063
	2001	0.068	0.068	0.066	0.066	0.065	0.064	0.064	0.064	0.064	0.063
Denali NP 022900003 (Alaska) 640 m	1988	0.055	0.054	0.054	0.053	0.053	0.053	0.052	0.052	0.052	0.052
	1990	0.049	0.048	0.048	0.048	0.048	0.047	0.047	0.046	0.046	0.046
	1991	0.054	0.054	0.050	0.050	0.047	0.046	0.046	0.046	0.045	0.044
	1992	0.053	0.052	0.052	0.051	0.050	0.050	0.049	0.049	0.049	0.049
	1993	0.053	0.053	0.051	0.048	0.048	0.047	0.047	0.046	0.046	0.046
	1994	0.053	0.051	0.049	0.049	0.049	0.048	0.048	0.048	0.048	0.048
	1995	0.058	0.056	0.056	0.054	0.051	0.050	0.049	0.046	0.046	0.046
	1996	0.058	0.053	0.053	0.053	0.052	0.052	0.052	0.052	0.051	0.051
	1997	0.054	0.053	0.052	0.051	0.051	0.050	0.050	0.049	0.049	0.049
	1998	0.057	0.056	0.056	0.055	0.054	0.054	0.054	0.054	0.053	0.053
	1999	0.056	0.056	0.054	0.054	0.054	0.053	0.053	0.053	0.052	0.051
	2000	0.046	0.046	0.044	0.044	0.044	0.043	0.043	0.042	0.042	0.042
	2001	0.061	0.058	0.057	0.055	0.055	0.055	0.053	0.053	0.053	0.053
Badlands NP 460711001 (South Dakota) 730 m	1989	0.069	0.066	0.064	0.063	0.060	0.058	0.057	0.057	0.057	0.057
	1990	0.061	0.059	0.055	0.055	0.054	0.052	0.052	0.051	0.051	0.050
	1991	0.058	0.058	0.056	0.056	0.056	0.055	0.055	0.054	0.054	0.053

Table AX3-9 (cont'd). The Top 10 Daily Maximum 8-h Average Concentrations (ppm) for Sites Experiencing Low Maximum Hourly Average Concentrations with Data Capture of ≥ 75%

Site	Year	1	2	3	4	5	6	7	8	9	10
Theod. Roos. NP 380530002 (North Dakota) 730 m	1984	0.064	0.062	0.062	0.062	0.059	0.058	0.057	0.057	0.057	0.057
	1985	0.058	0.055	0.055	0.054	0.054	0.054	0.053	0.053	0.053	0.052
	1986	0.059	0.058	0.057	0.056	0.055	0.055	0.054	0.053	0.053	0.052
	1989	0.073	0.069	0.066	0.065	0.065	0.064	0.063	0.063	0.063	0.063
	1992	0.060	0.059	0.058	0.058	0.056	0.056	0.056	0.054	0.054	0.054
	1993	0.062	0.059	0.056	0.056	0.055	0.053	0.052	0.052	0.052	0.052
	1994	0.066	0.064	0.058	0.058	0.057	0.056	0.056	0.056	0.056	0.055
	1995	0.060	0.059	0.058	0.058	0.058	0.058	0.057	0.057	0.056	0.055
	1996	0.060	0.059	0.059	0.059	0.058	0.058	0.057	0.057	0.057	0.056
	1997	0.080	0.073	0.072	0.071	0.069	0.068	0.066	0.066	0.063	0.063
Theod. Roos. NP 380070002 (North Dakota) 808 m	1999	0.063	0.060	0.059	0.058	0.057	0.057	0.057	0.056	0.056	0.056
	2000	0.062	0.061	0.060	0.059	0.059	0.057	0.057	0.057	0.057	0.057
	2001	0.060	0.059	0.059	0.058	0.058	0.057	0.057	0.056	0.055	0.055
Custer NF, MT 300870101 (Montana) 1006 m	1978	0.069	0.065	0.063	0.062	0.061	0.061	0.060	0.060	0.060	0.058
	1979	0.073	0.066	0.066	0.065	0.063	0.060	0.060	0.060	0.059	0.059
	1980	0.069	0.069	0.069	0.068	0.067	0.067	0.066	0.066	0.064	0.064
	1983	0.064	0.061	0.060	0.060	0.059	0.058	0.058	0.058	0.056	0.056

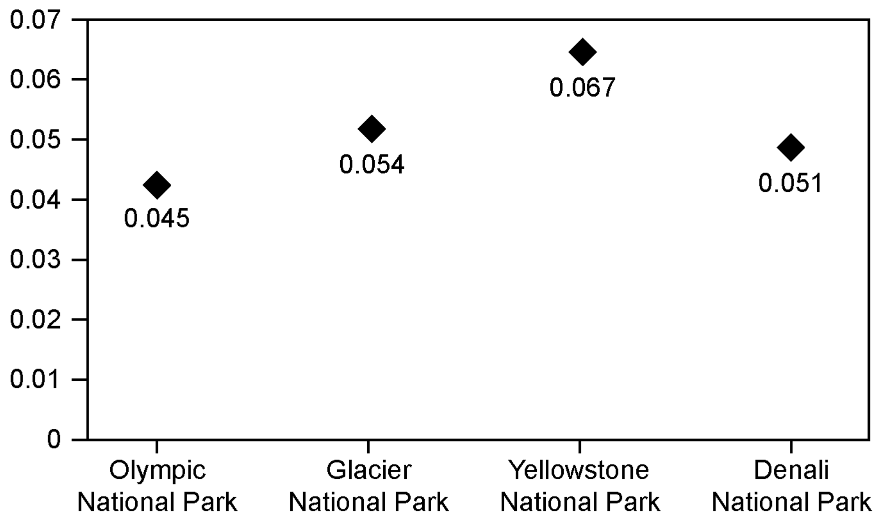

Figure AX3-20. Three-year average of the fourth highest 8-h daily maximum concentration at Olympic (WA), Glacier (MT), Yellowstone (WY), and Denali (AK) National Parks for 1999 to 2001.

It is questionable whether the distributions experienced at sites exhibiting low maximum hourly average concentrations in the western United States are representative of sites in the eastern and midwestern United States because of regional differences in sources of precursors and local meteorological conditions that affect patterns of transport. As described in the 1996 O_3 AQCD, the O_3 monitoring site in the Ouachita National Forest, AR experienced distributions of hourly average concentrations similar to some of the western sites. However, since 1993, this site has seen significant shifts, both increases and decreases, in hourly average concentrations. Figure AX3-21 illustrates the changes that have occurred from 1991 to 2001. The large changes in hourly average O_3 concentrations observed at the Ouachita National Forest may indicate that this rural site is influenced by the transport of pollution. Given the high density of sources in the eastern and midwestern United States, it is unclear whether a site could be found in either of these regions that would not be influenced by the transport of O_3 from urban areas. Thus, with the exception of the Voyageurs National Park site, observations in this section are limited to those obtained at relatively clean, remote sites in western North America.

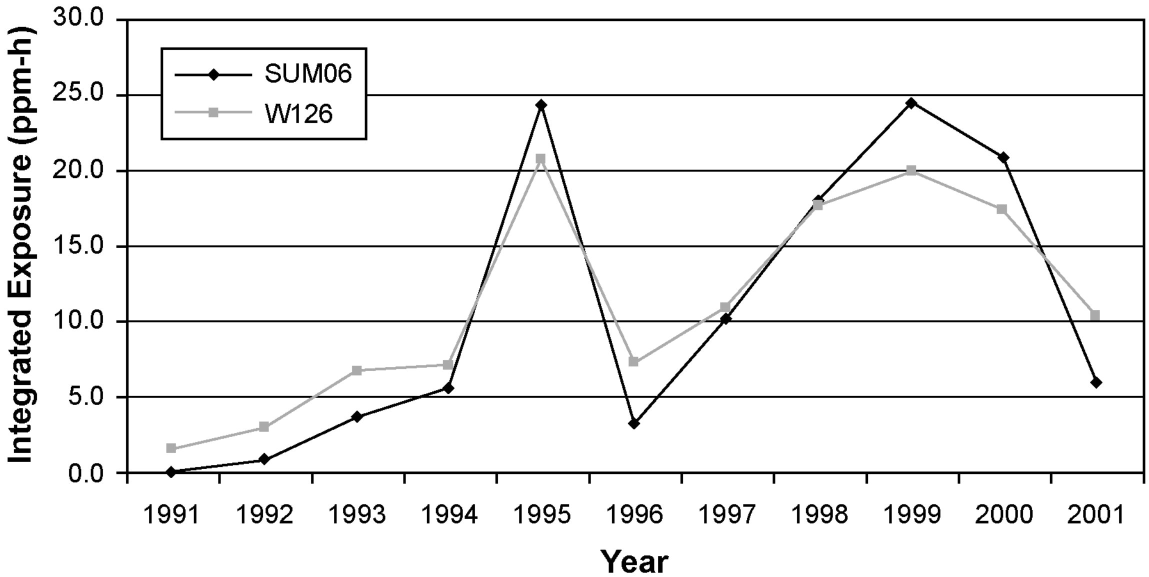

Figure AX3-21. Seasonal SUM06 and W126 exposure indices for the Ouachita National Forest for the period of 1991 to 2001.

Evidence for Trends in Ozone Concentrations at Rural Sites in the United States

Based on data collected in the 1970s to the middle 1990s, consistent trends in tropospheric O_3 at the cleanest sites in the world have not been observed across the Northern Hemisphere. Oltmans et al. (1998) concluded that since the early 1980s, based on four high-latitude stations in Canada, O_3 amounts throughout the troposphere at these stations has declined significantly. Changes in O_3 concentrations since the early 1970s have been relatively small at two stations in the eastern United States (Whiteface Mountain, NY and Wallops Island, VA). Oltmans et al. (1998) noted that in the eastern United States, the station at Whiteface Mountain showed an overall increase with almost no change after the mid-1980s, consistent with the pattern seen at other sites in mid-latitudes of the Northern Hemisphere. The authors noted that little change was noted in the troposphere throughout the 25-year measurement period at Wallops Island. At two high altitude sites (Zugspitze and Hohenpeissenberg, Germany), Oltmans et al. (1998) noted that O_3 amounts increased rapidly into the mid-1980s, but increased less rapidly (and at some other sites, not at all) since then. Increases at a Japanese ozonesonde station (Tsukuba) have been largest in the lower troposphere, but have slowed in the recent decade (Oltmans et al., 1998). Fiore et al. (2002a) pointed out that the trends at Whiteface Mountain, as reported by Oltmans et al. (1998), provide some evidence that during the past two decades background O_3 concentrations have risen by a few ppb in the surface air over the United States. However, the trends observed at Whiteface Mountain are probably associated with the transport of regional pollution to the site, because the site experiences elevated levels of O_3 during the summer months and the area is currently designated as in nonattainment for the 1-h standard.

Data from monitoring stations in national parks in the United States show conflicting evidence of trends. Statistically significant increases in 8-h O_3 concentrations have occurred during the period of 1992 to 2001 (U.S. Environmental Protection Agency, 2002) in the Great Smoky Mountains (TN), Craters of the Moon (ID), Mesa Verde (CO), and Mammoth Cave (KY) National Parks. In contrast, statistically significant decreases in 8-h O_3 concentrations have occurred over the same time period in the Saguaro (AZ) and Sequoia (CA) National Parks. In addition, no statistically significant changes in the 8-h O_3 concentrations have been observed at the remaining 26 national parks where O_3 monitoring takes place (U.S. Environmental Protection Agency, 2002). Yellowstone NP (WY) is an apparent exception[1] (see Figure AX3-22). Table AX3-10 shows the trends, using the Kendall's tau test (Lefohn and Shadwick, 1991), for the 30th percentiles of the hourly average concentrations at four relatively remote national park sites in the western United States. As can be seen from inspection of Table AX3-10, no trends were observed at the 5% significance level for these sites. As an example of high time resolution data obtained at RRMS, hourly average concentrations at Yellowstone NP for 2001 are shown in Figure AX3-23.

[11]U.S. EPA (2002) indicated that 8-h O_3 concentrations in Yellowstone National Park (WY) had increased during the period from 1987 to 2001. However, in reanalyses completed for this document, a Mann-Kendall test using the data collected at Yellowstone AQS sites for the periods 1987 to 1996, 1996 to 2000, and 1987 to 2000 showed, at the 5% confidence level, that an increase did not occur. The monitoring site in Yellowstone was physically moved in 1996 from AQS (ID 560391010) to AQS (ID 560391011). The difference between this analysis and that contained in U.S. Environmental Protection Agency (2002) may be due to (a) a change in location of the actual O_3 monitor in 1996 has resulted in two distinct sets of data being generated that should not be combined for trends analysis and/or (b) the use by the EPA of data for only the 10-year periods, 1991 to 2000 and 1992 to 2001, provides a different representation of what has actually occurred at the site over the period of record of 1987 to 2001.

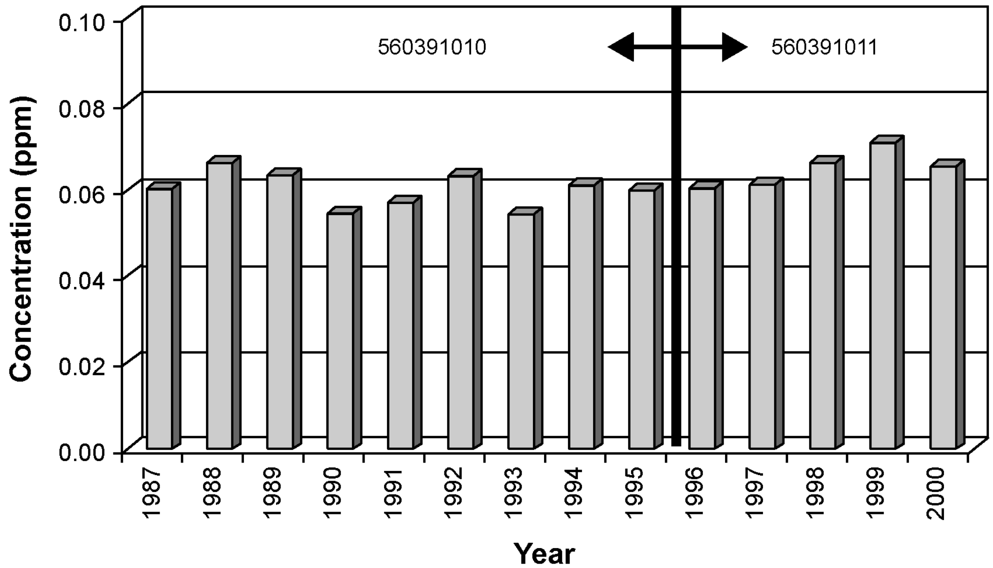

Figure AX3-22. The fourth highest 8-hour concentration at Yellowstone National Park. In 1996, the Yellowstone AIRS site (AIRS ID 560391010) was physically moved (AIRS ID 560391011).

Table AX3-10. Trends (Using Kendall's tau) for the 30th Percentile at National Park Service Monitoring Sites[1]

AQS ID	Site Name	Monitoring Period	Median Difference (ppm/year)	Median Relative Level (%/year)	Level of Significance of Difference
22900003	Denali NP	1988-2000	−0.00014286	−0.59524	0.141
300298001	Glacier NP	1989-2000	−0.00023611	−1.63360	0.098
530090012	Olympic NP	1987-2000	0.00016667	1.38889	0.141
560391010	Yellowstone NP	1988-1996	0.00070833	2.48457	0.089

[1]Years in which data capture was > 75%.

Lin et al. (2000) examined the long-term trend of background O_3 in surface air over the United States from 1980 to 1998 using monthly probability distributions of daily maximum 8-h average concentrations at a large collection of rural sites in the AQS database. As shown in Table AX3-11, reported O_3 concentrations decreased at the high end of the frequency

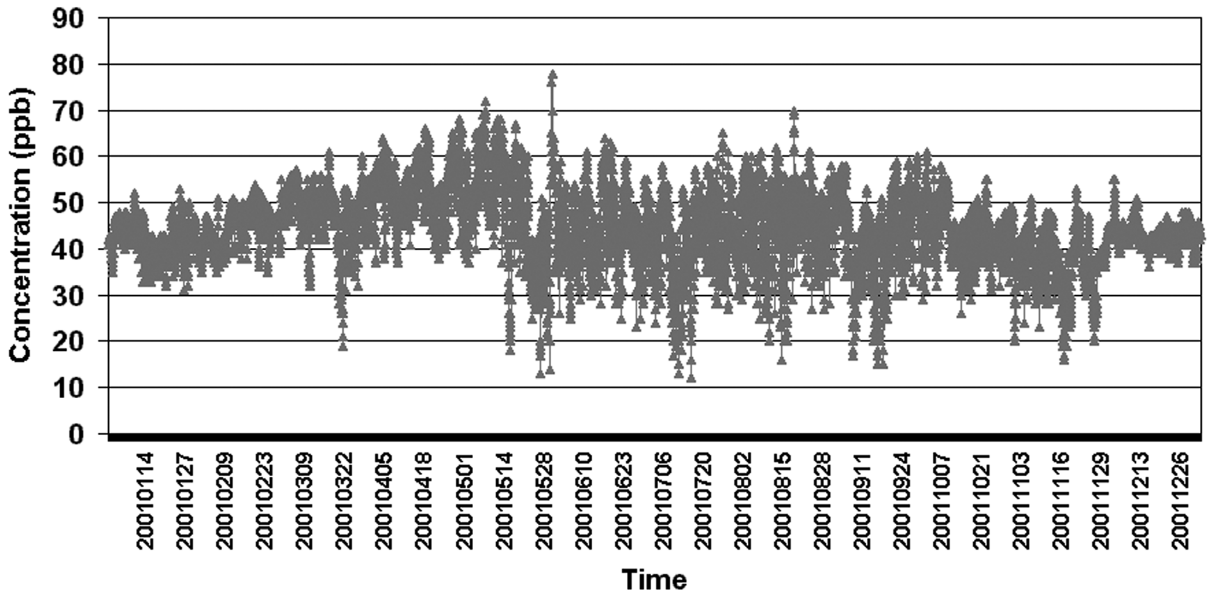

Figure AX3-23. Hourly average O_3 concentrations at Yellowstone National Park, Wyoming for the period of January to December 2001.

Source: U.S. Environmental Protection Agency (2003a).

distribution but increased at the lower end of the distribution. The increase was statistically significant at the 5% level in spring and fall. The authors hypothesized that the increase was due to the long-range transport of pollutants from Asia. The largest increase observed by Lin et al. (2000) was in the northeastern United States which, as they noted, was inconsistent with the hypothesis that the increase was attributable to transport from Asia. It is interesting to note that many of the rural sites (identification of sites provided by Lin, included in the Lin et al. (2000) analysis (e.g., Crestline [CA], Rockdale [GA], Edgewood [MD], Camden [NJ], Guilford [NC], and Sumner [TN]) are heavily influenced by transport from polluted areas: 66% of the O_3 monitoring sites used in the Lin et al. (2000) analysis exceeded the national 8-h O_3 standard for the 3-year period from 1998 to 2000. It should be noted that in the AQS database, the land use designation of rural does not mean that the site is mostly isolated from the long-range transport of episodic occurrences of O_3 concentrations that occur in or near urban areas. As noted in the 1996 O_3 AQCD, a land use characterization of rural does not imply that a specific location is isolated from anthropogenic influences.

Table AX3-11. Long-Term Trend of Background Ozone

AQS ID	Site Name	County	Land Use	8-h Avg (1998-2000)
10735002	Jefferson Co.	Jefferson Co.	Rural – Residential	0.092
40132001	Glendale	Maricopa Co.	Rural – Residential	0.075
40191018	Tucson	Pima Co.	Rural – Desert	0.072
51191002	North Little Rock	Pulaski Co.	Rural – Forest	0.087
60012001	Hayward	Alameda Co.	Rural – Residential	
60652002	Indio	Riverside Co.	Rural	0.090
60690002	Hollister	San Benito Co.	Rural – Residential	0.073
60710005	Crestline	San Bernardino	Rural – Residential	0.146
60731006	San Diego Co.	San Diego Co.	Rural – Residential	0.100
60830008	Capitan	Santa Barbara Co.	Rural	0.063
60833001	Santa Barbara Co.	Santa Barbara Co.	Rural – Agricultural	0.066
61113001	El Rio	Ventura Co.	Rural – Agricultural	0.068
80013001	Welby	Adams Co.	Rural – Agricultural	0.072
90131001	Stafford	Tolland Co.	Rural – Forest	0.089
121035002	Tarpon Springs	Pinellas Co.	Rural – Residential	0.082
132151003	Muscogee Co.	Muscogee Co.	Rural – Agricultural	0.093
132470001	Rockdale Co.	Rockdale Co.	Rural – Agricultural	0.111
171192007	Madison Co.	Madison Co.	Rural – Agricultural	0.086
180970042	Indianapolis	Marion Co.	Rural – Agricultural	0.088
201730001	Sedgwick Co.	Sedgwick Co.	Rural – Agricultural	0.077
210150003	Boone Co.	Boone Co.	Rural – Agricultural	0.086
210670001	Fayette Co.	Fayette Co.	Rural – Agricultural	0.076
210910012	Hancock Co.	Hancock Co.	Rural – Residential	0.089
220331001	E. Baton Rge, PA	E. Baton Rge, PA	Rural – Agricultural	0.094
220470002	Iberville, PA	Iberville, PA	Rural – Residential	0.088
220950002	St John Bap., PA	St John Bap., PA	Rural – Industrial	0.087
230052003	Cape Elizabeth	Cumberland Co.	Rural – Residential	0.077
240030014	Anne Arundel Co.	Anne Arundel Co.	Rural – Agricultural	0.107
240251001	Edgewood	Harford Co.	Rural – Commercial	0.1

Table AX3-11 (cont'd). Long-Term Trend of Background Ozone

AQS ID	Site Name	County	Land Use	8-h Avg (1998-2000)
240313001	Rockville	Montgomery Co.	Rural – Residential	0.09
240330002	Greenbelt	Prince Georges	Rural – Agricultural	0.099
250171801	Sudbury	Middlesex Co.	Rural – Agricultural	0.085
260370001	Clinton Co.	Clinton Co.	Rural – Agricultural	0.079
260492001	Genesee Co.	Genesee Co.	Rural	0.086
260812001	Kent Co.	Kent Co.	Rural – Agricultural	0.087
290470003	Clay Co.	Clay Co.	Rural – Residential	0.086
290470005	Clay Co.	Clay Co.	Rural – Agricultural	0.089
291831002	St Charles Co.	St Charles Co.	Rural – Agricultural	0.094
291890006	St Louis Co.	St Louis Co.	Rural – Residential	0.090
310550032	Omaha	Douglas Co.	Rural – Agricultural	0.071
340010005	Atlantic Co.	Atlantic Co.	Rural – Residential	0.090
340071001	Camden Co.	Camden Co.	Rural – Commercial	0.101
340190001	Flemington	Hunterdon Co.	Rural – Agricultural	0.098
340273001	Morris Co.	Morris Co.	Rural – Agricultural	0.096
350011012	Bernalillo Co.	Bernalillo Co.	Rural – Desert	0.075
350130008	Dona Ana Co.	Dona Ana Co.	Rural – Agricultural	0.073
360310002	Essex Co.	Essex Co.	Rural	0.08
360631006	Niagara Co.	Niagara Co.	Rural – Agricultural	0.085
360650004	Oneida Co.	Oneida Co.	Rural – Forest	0.073
361173001	Wayne Co.	Wayne Co.	Rural – Agricultural	0.081
370810011	Guilford Co.	Guilford Co.	Rural – Residential	0.094
371191005	Mecklenburg Co.	Mecklenberg Co.	Rural – Industrial	0.098
371191009	Mecklenburg Co.	Mecklenberg Co.	Rural – Agricultural	0.104
390230001	Clark Co.	Clark Co.	Rural – Agricultural	0.093
390610010	Hamilton Co.	Hamilton Co.	Rural – Industrial	0.085
391331001	Portage Co.	Portage Co.	Rural – Agricultural	0.093
391351001	Preble Co.	Preble Co.	Rural – Agricultural	0.08
401430174	Glenpool	Tulsa Co.	Rural – Agricultural	0.081

Table AX3-11 (cont'd). Long-Term Trend of Background Ozone

AQS ID	Site Name	County	Land Use	8-h Avg (1998-2000)
410050004	Clackamas Co.	Clackamas Co.	Rural – Agricultural	0.072
410090004	Columbia Co.	Columbia Co.	Rural – Agricultural	0.056
420430401	Harrisburg	Dauphin Co.	Rural – Commercial	0.090
420990301	Perry Co.	Perry Co.	Rural	0.085
450150002	Berkeley Co.	Berkeley Co.	Rural – Industrial	0.081
450230002	Chester Co.	Chester Co.	Rural – Commercial	0.088
450370001	Edgefield Co.	Edgefield Co.	Rural – Agricultural	0.085
450791002	Richland Co.	Richland Co.	Rural – Agricultural	0.095
470370026	Nashville-Davidson	Davidson Co.	Rural – Forest	0.091
470650028	Chattanooga	Hamilton Co.	Rural – Forest	0.097
470651011	Hamilton Co.	Hamilton Co.	Rural – Agricultural	0.097
471571004	Shelby Co.	Shelby Co.	Rural – Agricultural	0.097
471632002	Sullivan Co.	Sullivan Co.	Rural – Residential	0.091
471650007	Sumner Co.	Sumner Co.	Rural – Industrial	0.100
510410004	Chesterfield Co.	Chesterfield Co.	Rural – Residential	0.087
510850001	Hanover Co.	Hanover Co.	Rural – Agricultural	0.100
530330010	King Co.	King Co.	Rural – Forest	0.063
551390011	Oshkosh	Winnebago Co.	Rural – Agricultural	0.076

Source: Lin et al. (2000).

Using a 15-year record of O_3 from Lassen Volcanic National Park, a rural elevated site in northern California; data from two aircraft campaigns; and observations spanning 18 years from five U.S. West Coast, marine boundary layer sites, Jaffe et al. (2003) reported that O_3 in air arriving from the eastern Pacific in spring has increased by approximately 10 ppb from the mid-1980s to the present. They concluded that this positive trend is due to increases of emissions of O_3 precursors in Asia. They found positive trends in O_3 occurring during all seasons. They also noted that diurnal variations during summer were about 21 ppb, but only about 6 ppb during spring. Although Lassen Volcanic National Park site is not close to any major emission sources or urban centers, the site experiences maximum hourly average O_3 concentrations above 0.080 ppm during April to May and above 0.100 ppm during the summertime (U.S. Environmental Protection Agency, 2003a), suggesting local photochemical production, at least during summer. However, local springtime photochemical production cannot be ruled out. The authors suggested that the likely cause for the spring increases is transport from Asia, because emissions of precursors have decreased in California over the monitoring period. The springtime increases appears to be inconsistent with the summer increases, when there is evidence for the occurrence of more localized photochemical activity. Although emissions of O_3 precursors may have decreased in California as a whole over the monitoring period, there still may be regional increases in areas that could affect air quality in Lassen.

Thus, although there is evidence as reported in the literature that some locations may be experiencing increased levels of O_3 at some rural locations, there is also evidence that O_3 concentrations at RRMS have not experienced increasing levels for the period of record.

AX3.3 DIURNAL PATTERNS IN OZONE CONCENTRATION

AX3.3.1 Introduction

By definition, diurnal variations are those that occur during a 24-h period. Diurnal patterns of O_3 may be expected to vary with location, depending on the balance among the many factors affecting O_3 formation, transport, and destruction. Although they vary with locality, diurnal patterns for O_3 typically show a rise in concentration from low (or near minimum detectable amounts) to an early afternoon peak at lower elevation monitoring sites. The diurnal pattern of O_3 concentrations has been ascribed to three simultaneous processes: (1) downward transport of O_3 from layers aloft, (2) destruction of O_3 through contact with surfaces and through reaction with NO at ground level, and (3) in situ photochemical production of O_3 (U.S. Environmental Protection Agency, 1978; Coffey et al., 1977; Mohnen et al., 1977; Reiter, 1977a).

The form of an average diurnal pattern may provide information on sources, transport, and chemical formation and destruction effects at various sites (Lefohn, 1992). Atmospheric conditions leading to limited transport from source regions will produce early afternoon peaks. However, long-range transport processes will influence the actual timing of a peak, from afternoon to evening or early morning hours. Investigators have used diagrams that illustrate composite diurnal patterns as a means to describe qualitatively the differences in O_3 exposures between sites (Lefohn and Jones, 1986; Böhm et al., 1991). Monitoring data programs, such as the National Air Pollution Background Network (NAPBN), the Electric Power Research Institute's Sulfate Regional Air Quality Study, and the Mountain Cloud Chemistry Program (U.S. Environmental Protection Agency, 1996a), provide opportunities to characterize O_3 diurnal patterns at diverse sites. For example, the Mountain Cloud Chemistry Program characterized hourly O_3 concentrations at Shenandoah National Park and Whiteface Mountain at different elevations. This information is very useful when characterizing the diurnal patterns in similar locations, but at different elevations. Although it might appear that composite diurnal pattern diagrams could be used to quantify the differences in O_3 exposures between sites, caution in their use for this purpose is urged (Lefohn et al., 1991). The average diurnal patterns are derived from long-term calculations of the hourly average concentrations, and the resulting diagram cannot adequately identify, at most sites, the presence of high hourly average concentrations and, thus, may not adequately distinguish O_3-exposure differences among sites. Logan (1989) noted that diurnal variation of O_3 did not reflect the presence of high hourly average concentrations.

Unique families of diurnal average profiles exist, and it is possible to distinguish between two types of O_3 monitoring sites. A seasonal diurnal diagram provides the investigator with the opportunity to identify whether more scavenging occurs at a specific O_3 monitoring site than at any other site. Ozone is rapidly depleted near the surface below the nocturnal inversion layer (Berry, 1964). Mountainous sites, which are above the nocturnal inversion layer, do not necessarily experience this depletion (Stasiuk and Coffey, 1974). Taylor and Hanson (1992) reported similar findings, using data from the Integrated Forest Study. The authors reported that intraday variability was most significant for the low-elevation sites due to the pronounced daily amplitude in O_3 concentration between the predawn minimum and mid-afternoon-to-early evening maximum. The authors reported that interday variation was more significant in the high-elevation sites. Ozone trapped below the inversion layer is depleted by dry deposition and chemical reactions if other reactants are present in sufficient quantities (Kelly et al., 1984). Above the nocturnal inversion layer, dry deposition does not generally occur, and the concentration of O_3 scavengers is generally lower, so O_3 concentrations remain fairly constant

(Wolff et al., 1987). A flat diurnal pattern is usually interpreted as indicating a lack of efficient scavenging of O_3 or a lack of photochemical precursors, whereas a varying diurnal pattern is taken to indicate the opposite.

As indicated above, with the composite diagrams alone, it is difficult to quantify the daily or long-term exposures of O_3. For example, the diurnal patterns for two such sites are illustrated in Figure AX3-24. The Jefferson County, KY site, characterized as a suburban-residential site in the AQS database, is urban-influenced and experiences elevated levels of O_3 and NO_x. The Oliver County, ND site, characterized as rural-agricultural, is fairly isolated from urban-influenced sources and hourly average O_3 concentrations are mostly < 0.09 ppm. The flat diurnal pattern observed for the Oliver County site is usually interpreted as indicating a lack of efficient scavenging of O_3 or a lack of photochemical precursors, whereas the varying diurnal pattern observed at the Jefferson County site may be interpreted to indicate the opposite. Logan (1989) described the diurnal pattern for several rural sites in the United States (Figure AX3-25) and noted that average daily profiles showed a broad maximum from about 1200 hours until about 1800 hours at all the eastern sites, except for the peak of Whiteface Mountain, NY. Logan (1989) noted that the maximum concentrations were higher at the Sulfate Regional Experiment Program (SURE) sites than at the Western NAPBN sites in the East, because the latter were situated in more remote or coastal locations.

An analysis that identified when the highest hourly average concentrations were observed at rural agricultural and forested sites was described in 1996 O_3 AQCD. A review of the hourly average data collected at all rural agricultural and forested sites in Environmental Protection Agency's AQS database for 1990 to 1992 was undertaken to evaluate the percentage of time hourly average concentrations ≥ 0.1 ppm occurred during the period of 0900 to 1559 hours in comparison with the 24-h period. It was found that 70% of the rural-agricultural and forested sites used in the analysis experienced at least 50% of the occurrences ≥ 0.1 ppm during the period of 0900 to 1559 hours when compared to the 24-h period. When O_3 monitoring sites in California were eliminated, approximately 73% of the remaining sites experienced at least 50% of the occurrences ≥ 0.10 ppm during the daylight 7-h period when compared with the 24-h period.

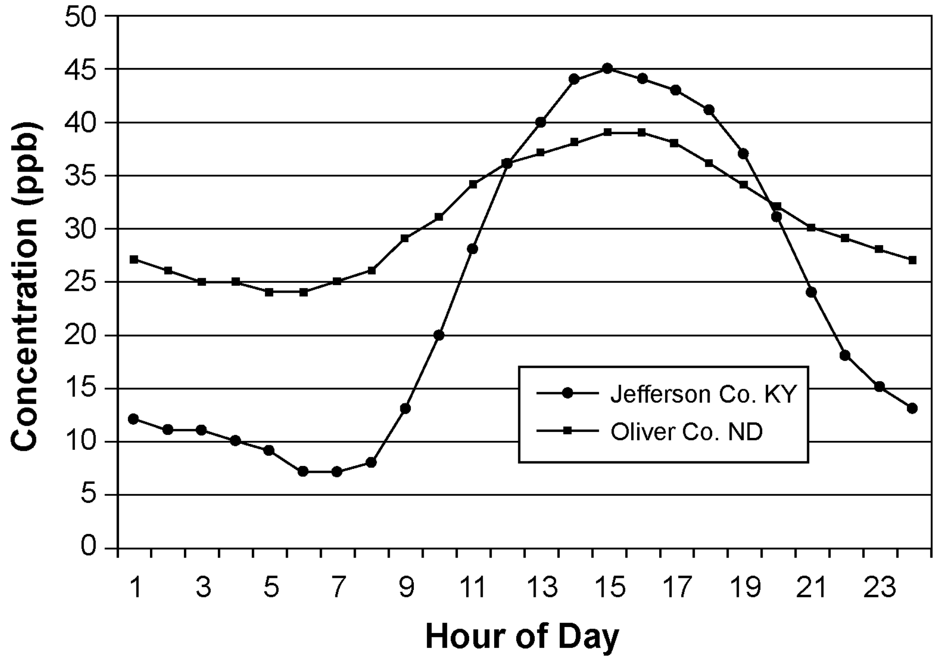

Figure AX3-24. The comparison of the seasonal (April-October) diurnal patterns for urban-influenced (Jefferson County, KY) and a rural-influenced (Oliver County, ND) monitoring sites using 2002 hourly data.

AX3.3.2 Diurnal Patterns in Urban Areas

The 1996 O_3 AQCD (U.S. Environmental Protection Agency, 1996a) discussed diurnal patterns for urban sites. Figure AX3-26a,b shows the diurnal pattern of O_3 concentrations on August 3, 2004 at several sites in Maryland. On this day, a peak 1-h average concentration of 0.20 ppm, the highest for the month, was reached at 1400 hours, presumably as the result of meteorological factors, such as atmospheric mixing and local photochemical processes. The severe depression of concentrations to below detection limits (< 0.005 ppm) between 0300 and 0600 hours usually is explained as resulting from the scavenging of O_3 by local NO emissions. In this regard, this station is typical of most urban locations.

Diurnal profiles of O_3 concentrations can vary from day to day at a specific site, because of changes in the various factors that influence concentrations. Composite diurnal data (i.e., concentrations for each hour of the day averaged over multiple days or months) often differ

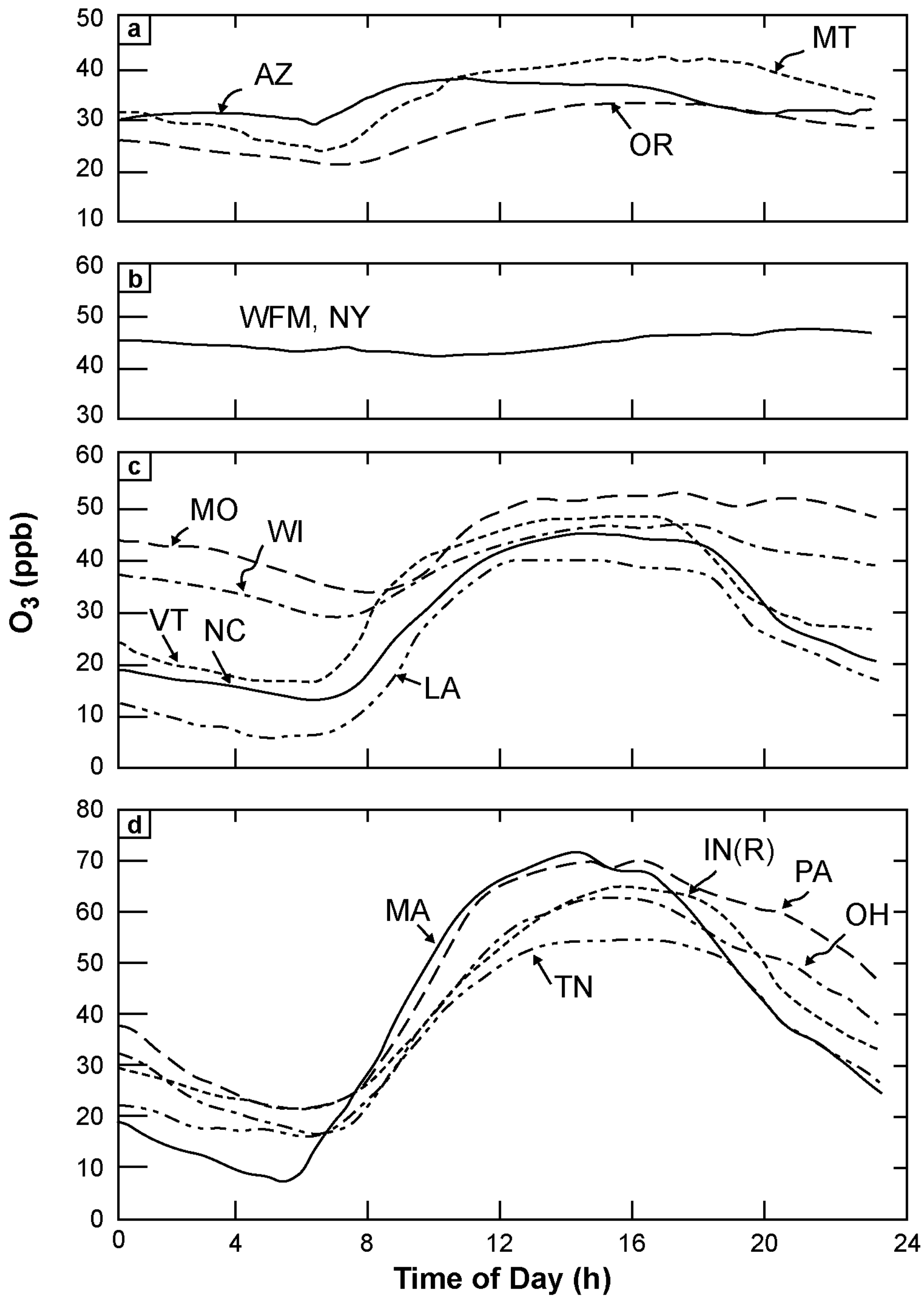

Figure AX3-25a-d. Diurnal behavior of O_3 at rural sites in the United States in July. Sites are identified by the state in which they are located. (a) Western National Air Pollution Background Network sites (NAPBN); (b) Whiteface Mountain (WFM) located at 1.5 km above sea level; (c) eastern NAPBN sites; and (d) sites selected from the Electric Power Research Institute's Sulfate Regional Air Quality Study. IN(R) refers to Rockport.

Source: Logan (1989).

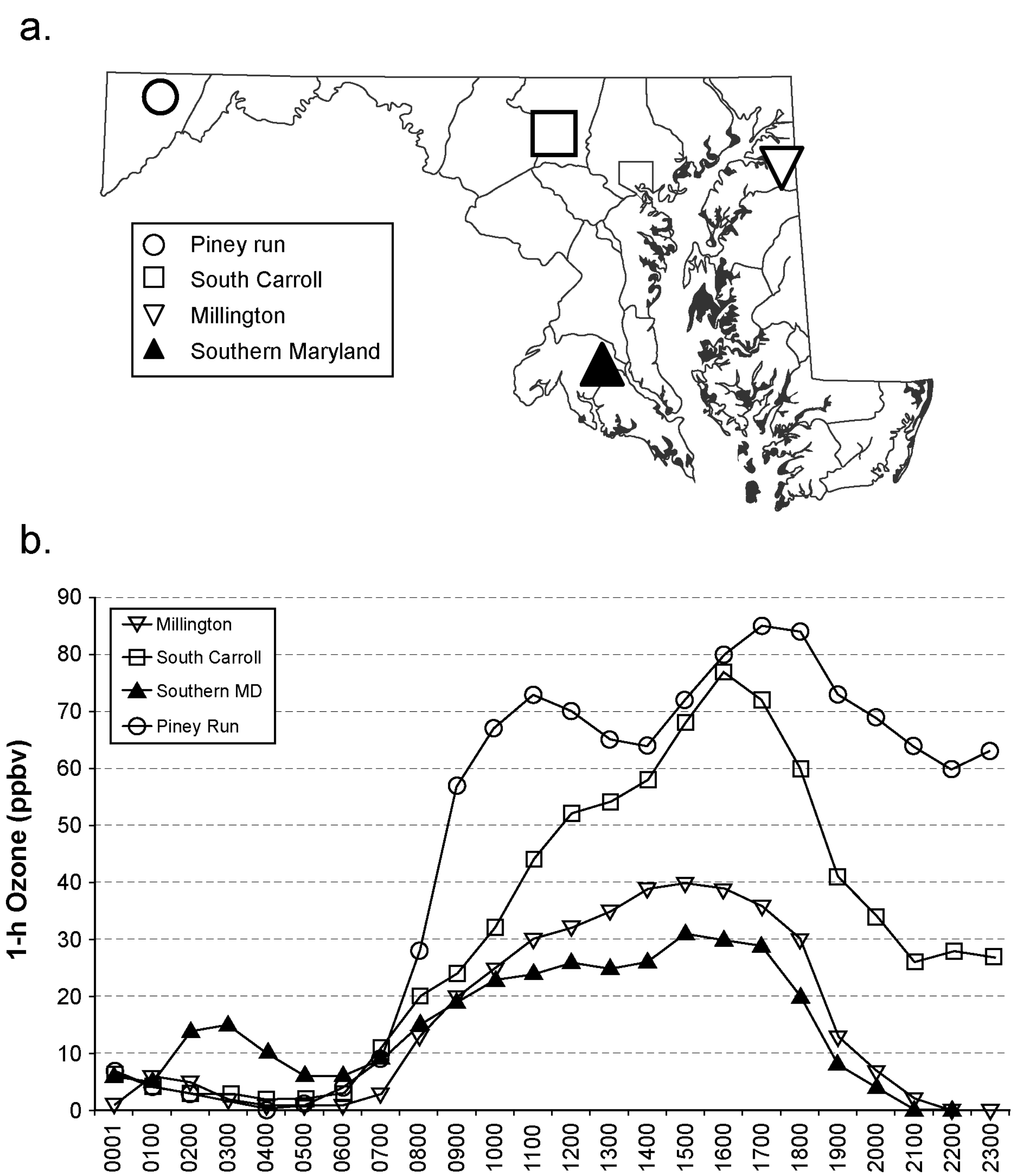

Figure AX3-26a,b. Diurnal pattern of 1-h O_3 concentration on August 3, 2004 at various sites in Maryland.

Source: Piety (2004).

markedly from the diurnal cycle shown by concentrations for a specific day. In Figures AX3-27 through AX3-29, diurnal data for 2 consecutive days are compared with composite diurnal data (1-month averages of hour-by-hour measurements) at three different kinds of sites: (1) center city-commercial (Washington, DC); (2) rural-near urban (St. Louis, MO); and (3) suburban-residential (Alton, IL). Several obvious points of interest present themselves in these figures: at some sites, peaks can occur at virtually any hour of the day or night, but these peaks may not show up strongly in the longer-term average data; some sites may be exposed to multiple peaks during a 24-h period; and disparities, some of them large, can exist between peaks (the diurnal data) and the 1-month average (the composite diurnal data) of hourly O_3 concentrations.

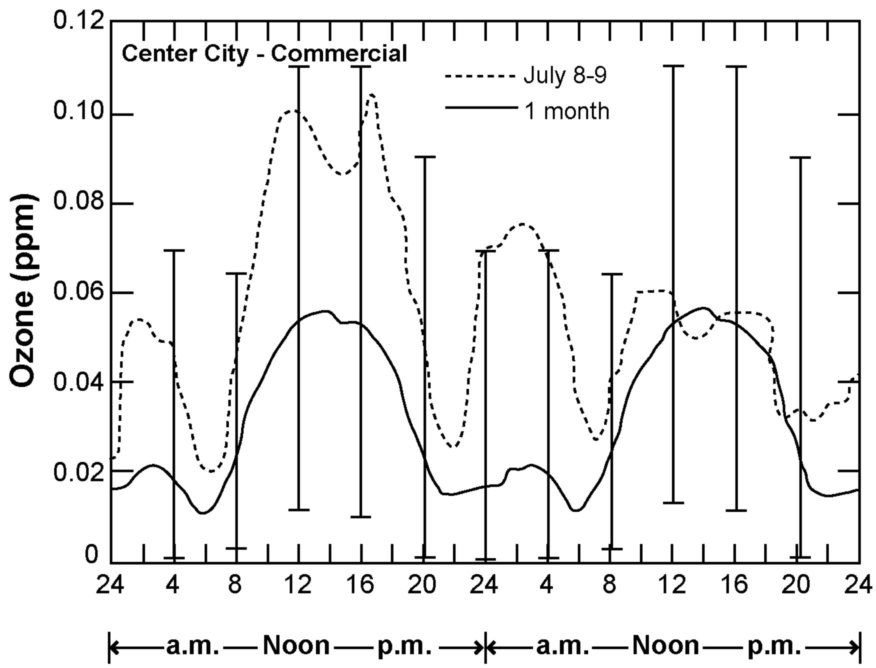

Figure AX3-27. Diurnal and 1-month composite diurnal variations in O_3 concentrations, Washington, DC July 1981.

Source: U.S. Environmental Protection Agency (1986).

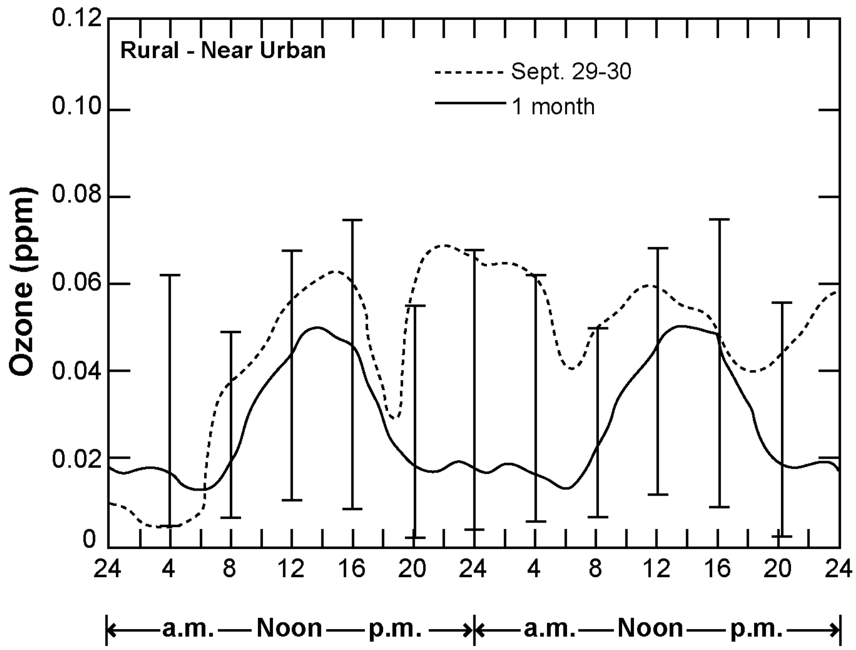

Figure AX3-28. Diurnal and 1-month composite diurnal variations in O_3 concentrations, St. Louis County, MO September 1981.

Source: U.S. Environmental Protection Agency (1986).

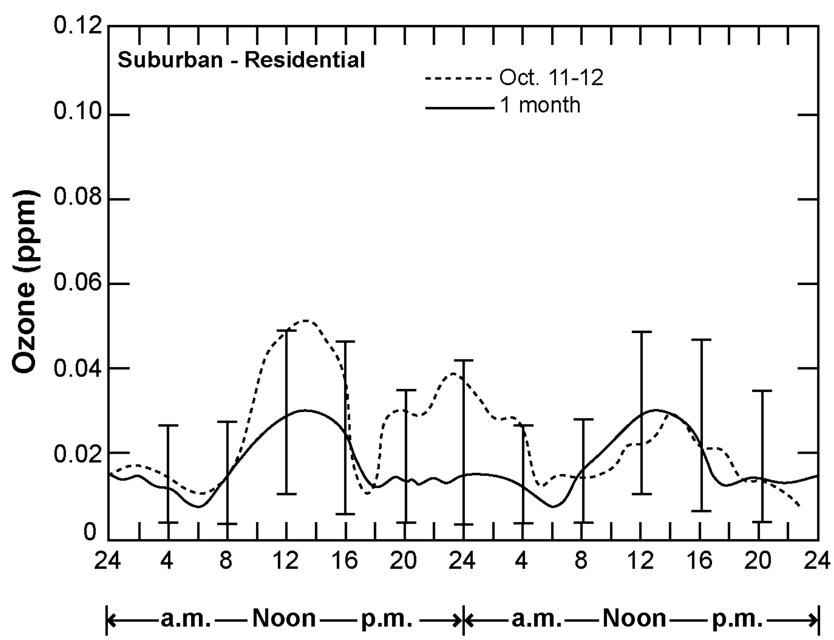

Figure AX3-29. Diurnal and 1-month composite diurnal variations in O_3 concentrations, Alton, IL October 1981 (fourth quarter).

Source: U.S. Environmental Protection Agency (1986).

When diurnal or short-term composite diurnal O_3 concentrations are compared with longer-term composite diurnal O_3 concentrations, the peaks are smoothed as the averaging period is lengthened. Figure AX3-30 demonstrates the effects of lengthening the period of time over which values are averaged. This figure shows a composite diurnal pattern calculated on a 3-month basis. Although seasonal differences are observed, the comparison of the 3-month average of the fourth quarter (Figure AX3-30) with 1-month composite diurnal concentrations for October (Figure AX3-29) at the Alton, IL site readily demonstrates the smoothing out of peak concentrations as the averaging period is lengthened. As indicated in the 1996 O_3 AQCD, the smoothing of the higher average concentrations using longer-term averages makes it difficult to identify those exposure regimes that affect human health and vegetation.

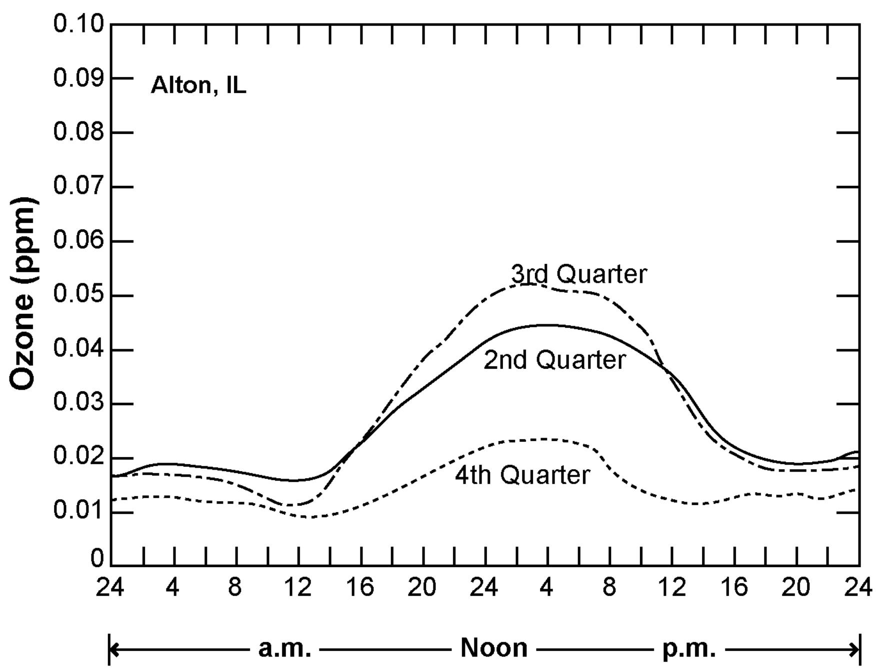

Figure AX3-30. Composite diurnal patterns of O_3 concentrations by quarter, Alton, IL October 1981.

Source: U.S. Environmental Protection Agency (1986).

AX3.3.3 Diurnal Patterns in Nonurban Areas

Nonurban areas only marginally affected by transported O_3 usually have a flatter diurnal profile than sites located in urban areas. Furthermore, nonurban O_3 monitoring sites experience differing types of diurnal patterns (Böhm et al., 1991; Lefohn, 1992). As indicated earlier, O_3 concentrations at a specific location are influenced by local emissions and by long-range transport from both natural and anthropogenic sources. Thus, considerable variation of O_3 exposures is found among sites characterized as agricultural or forested, with no preference for maximum diurnal patterns to occur in either the second or third quarter.

The diurnal patterns for several agricultural sites have been characterized (U.S. Environmental Protection Agency, 1996a). Figures AX3-31 and AX3-32 show some typical patterns of exposure. As discussed in the U.S. Environmental Protection Agency (1996a), the six sites, whose diurnal patterns are illustrated in Figure AX3-31, represent counties with high soybean, wheat, or hay production. The two figures show a distinct afternoon maximum with the lowest concentrations occurring in the early morning and evening hours. Quarterly composite diurnal patterns clearly show the division of the afternoon O_3 concentrations into two seasonal patterns: the low, "winter," levels in the first and fourth quarters of the year; and the high, "summer," levels in the second and third quarters.

Remote forested sites experience unique patterns of O_3 concentrations (Evans et al., 1983; Lefohn, 1984). Figure AX3-33 shows diurnal patterns for several national forest sites in the EPA AQS database for 2002. Several of the sites analyzed exhibit fairly flat average diurnal patterns. Such a pattern is based on average concentrations calculated over an extended period, and caution is urged in drawing conclusions concerning whether some monitoring sites illustrated in the figure experience higher cumulative O_3 exposures than other sites. Variation in O_3 concentration occurs from hour to hour on a daily basis, and, in some cases, elevated hourly average concentrations are experienced either during daytime or nighttime periods (Lefohn and Mohnen, 1986; Lefohn and Jones, 1986; Logan, 1989; Lefohn et al., 1990a; Taylor et al., 1992). Because the diurnal patterns represent averaged concentrations calculated over an extended period, the smoothing of the averaging tends to mask the elevated hourly average concentrations.

Lefohn et al. (1990b) characterized O_3 concentrations at high-elevation monitoring sites. The authors reported that a fairly flat diurnal pattern for the Whiteface Mountain summit site

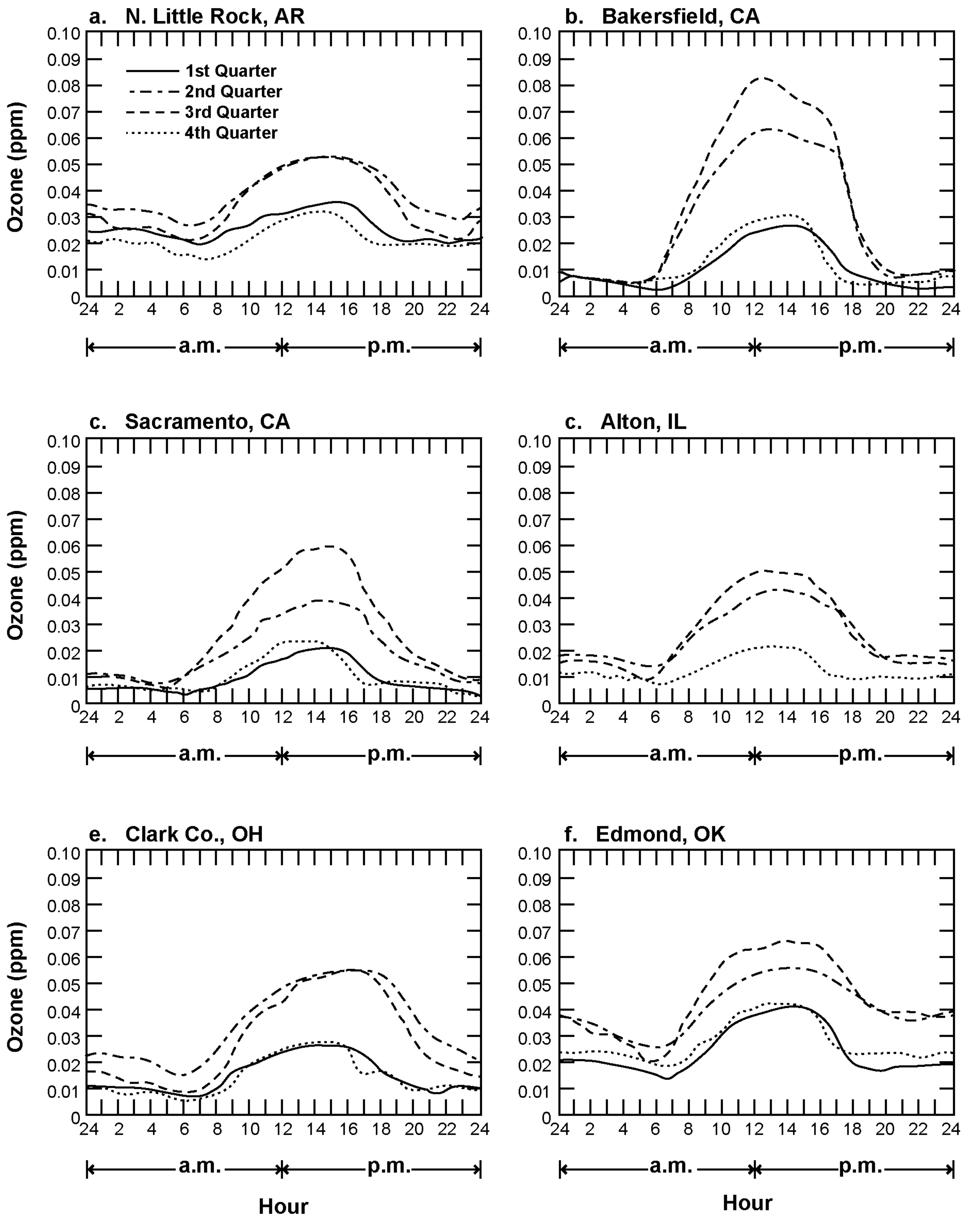

Figure AX3-31a-f. Quarterly composite diurnal patterns of O_3 concentrations at selected sites representing potential for exposure of major crops, 1981.

Source: U.S. Environmental Protection Agency (1986).

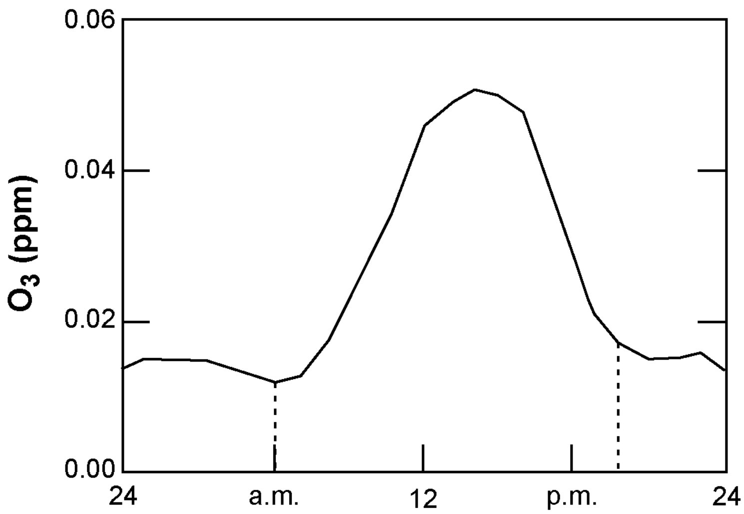

Figure AX3-32. Composite diurnal O_3 pattern at a rural National Crop Loss Assessment Network site in Argonne, IL August 6 through September 30, 1980.

Source: U.S. Environmental Protection Agency (1986).

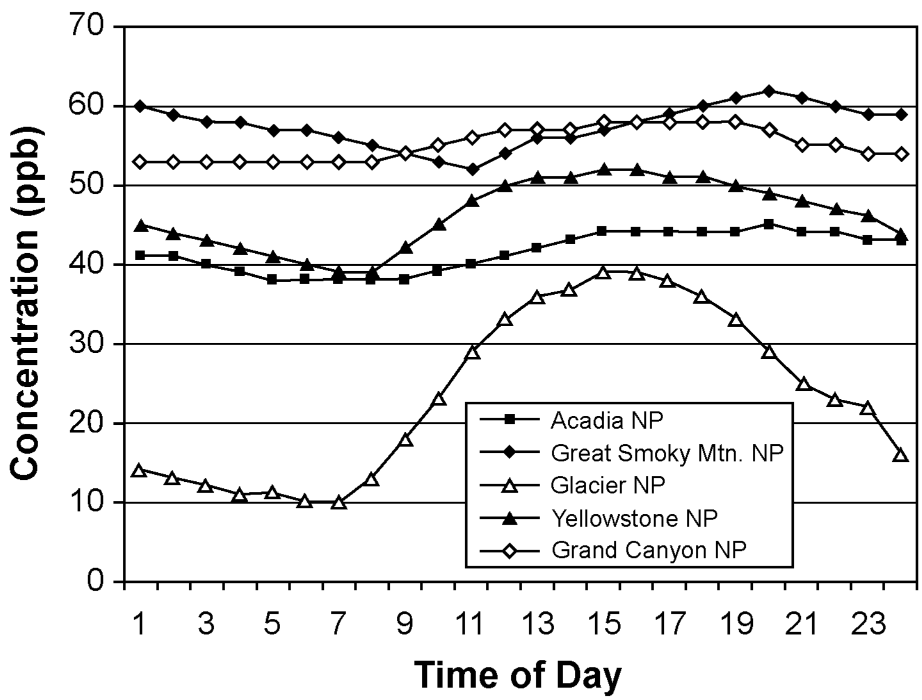

Figure AX3-33. Composite diurnal O_3 pattern at selected national forest sites in the United States using 2002 hourly average concentration data.

Source: U.S. Environmental Protection Agency (2003a).

(WF1) was observed (Figure AX3-34a), with the maximum hourly average concentrations occurring in the late evening or early morning hours. A similar pattern was observed for the mid-elevation site at Whiteface Mountain (WF3). The site at the base of Whiteface Mountain (WF4) showed the typical diurnal pattern expected from sites that experience some degree of O_3 scavenging. More variation in the diurnal pattern for the highest Shenandoah National Park sites occurred than for the higher elevation Whiteface Mountain sites, with the typical variation for urban-influenced sites in the diurnal pattern at the lower elevation Shenandoah National Park site (Figure AX3-34b). Aneja and Li (1992), in their analysis of the five high-elevation Mountain Cloud Chemistry Program (MCCP) sites, noted the presence of the flat diurnal pattern typical of high-elevation sites that has been described previously in the literature. Aneja and Li (1992) noted that the peak of the diurnal patterns over the period of May to October (1986 to 1988) occurred between 1800 and 2400 hours for the five sites, whereas the minimum was observed between 0900 and 1200 hours. However, it is important to note that, as indicated by Lefohn et al. (1990b), the flat diurnal pattern was not observed for all high-elevation sites.

As mentioned earlier, nonurban areas only marginally affected by transported O_3 usually have a flatter diurnal profile than sites located in urban areas. Nonurban O_3 monitoring sites experience differing types of diurnal patterns, as shown in this section. The difference in diurnal patterns may influence the potential for O_3 exposures to affect vegetation.

AX3.4 SEASONAL PATTERNS IN OZONE CONCENTRATIONS

AX3.4.1 Urban Area Seasonal Patterns

Seasonal variations in O_3 concentrations in 1981 were described by the U.S. Environmental Protection Agency (1996a). The current forms of the O_3 standards focus on both the highest hourly average concentrations (1-h standard) and, for many monitoring sites, the mid-level hourly average concentrations (8-h standard). The description that follows uses the highest hourly average concentration as an indication of exposure. Figure AX3-35 shows the single 1-h maximum concentrations within the month for eight sites across the United States for 2002. Data from all eight monitoring sites show a tendency for the highest maximum hourly average concentration to occur in the June to August period. Because of annual variability, the general weather conditions in a given year may be more favorable for the formation of O_3 and other

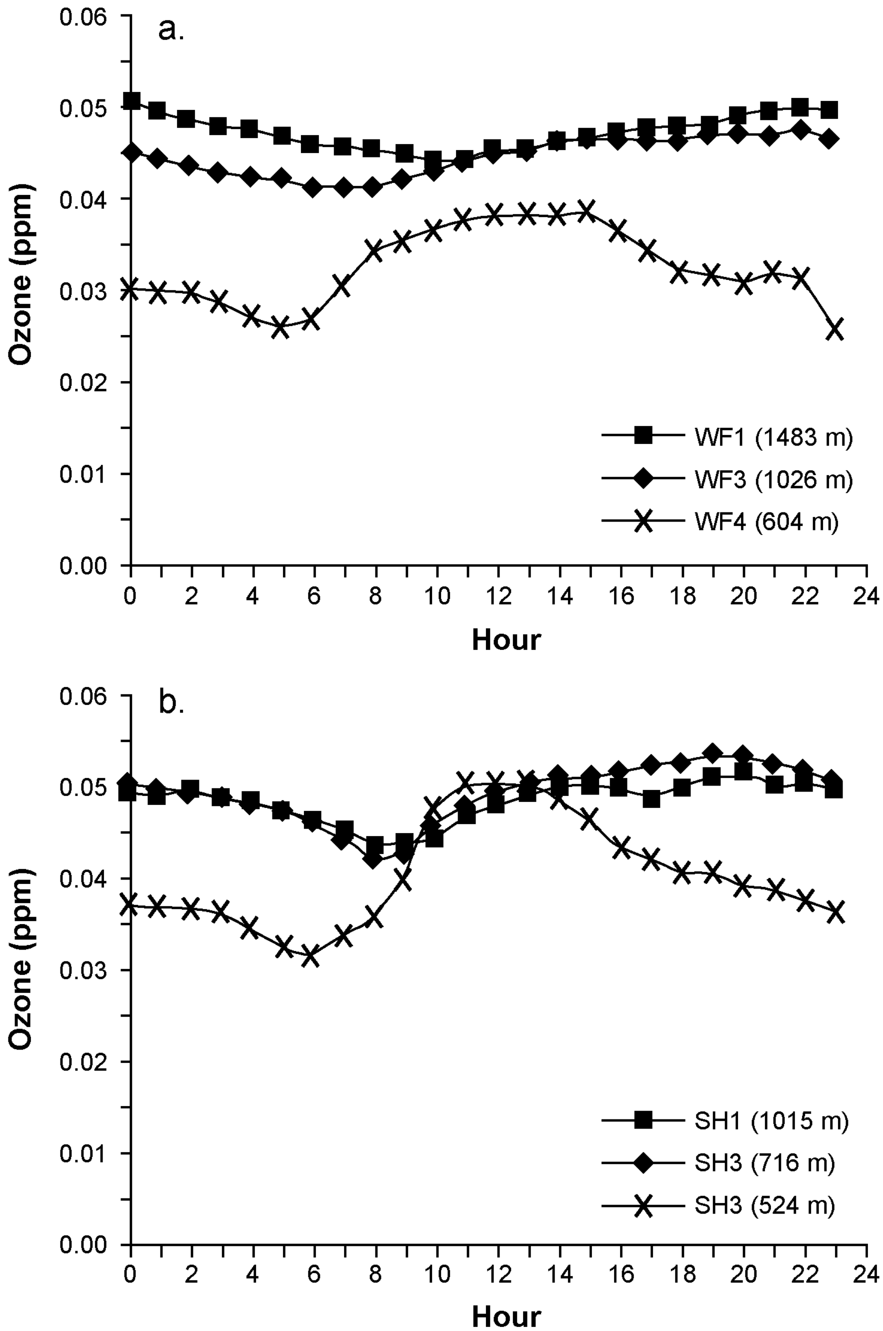

Figure AX3-34a,b. **Composite diurnal pattern at (a) Whiteface Mountain, NY and (b) the Mountain Cloud Chemistry Program Shenandoah National Park site for May to September 1987.**

Source: Lefohn et al. (1990a).

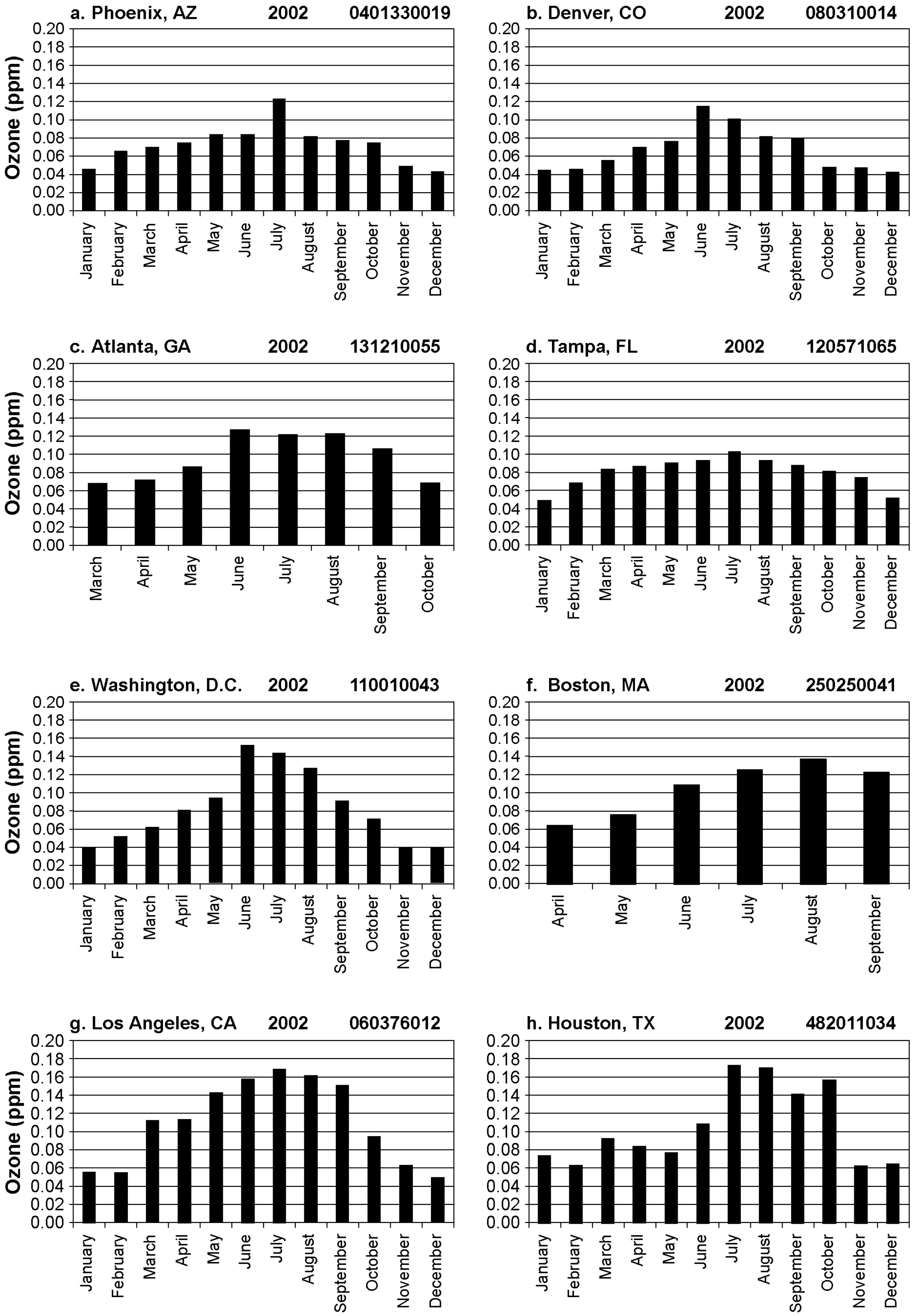

Figure AX3-35a-h. Seasonal variations in O_3 concentrations as indicated by the 1-h maximum in each month at selected sites, 2002.

Source: U.S. Environmental Protection Agency (2003a).

oxidants than during the prior or following year. For example, 1988 was a hot, dry year during which some of the highest O_3 concentrations of the last 16 years occurred, whereas 1989 was a cold, wet year during which some of the lowest concentrations occurred (U.S. Environmental Protection Agency, 1996a).

AX3.4.2 Seasonal Patterns in Nonurban Areas

For the purpose of assessing possible vegetative effects, it is important to characterize the seasons in which the highest O_3 concentrations would be expected to occur in nonurban areas. However, for nonurban areas, it is not possible to generalize the quarters in which the highest hourly average concentrations occur. Many RRMS tend to experience their highest average O_3 concentrations during the second quarter (i.e., the months of April or May) versus the third quarter of the year (Evans et al., 1983; Singh et al., 1978; Lefohn et al., 2001). This observation has been attributed either to stratospheric intrusions or to an increasing frequency of slow-moving, high-pressure systems that promote the formation of O_3 (U.S. Environmental Protection Agency, 1996a). Figure AX3-23 illustrates the hourly average concentrations for Yellowstone National Park (WY) for the period of January to December 2001. Note that at the Yellowstone National Park site, the highest hourly average concentrations tend to occur during the April to May period. Lefohn et al. (2001) and Monks (2000) noted that this was also observed for other RRMS in North America and northern Europe.

The highest O_3 concentrations tend to occur in rural-forested areas during different times of the year. The different patterns may be associated with the observations by Logan (1989) that spring and summer O_3 concentrations in rural areas of the eastern United States is severely impacted by anthropogenic, and possibly natural emissions of NO_x and hydrocarbons, and that O_3 episodes occur when the weather is particularly conducive to photochemical formation of O_3. Taylor et al. (1992) reported that for 10 forest sites in North America, the temporal patterns of O_3 during quarterly or annual periods exhibited less definitive patterns. Based on the exposure index selected, different patterns were reported. Meagher et al. (1987) reported that for rural O_3 sites in the southeastern United States, the daily maximum 1-h average concentration was found to peak during the summer months. Taylor and Norby (1985) reported that Shenandoah National Park experienced both the highest frequency of episodes and the highest mean duration of exposure events during the month of July.

Aneja and Li (1992) reported that the maximum monthly O_3 levels at several rural sites occurred in either the spring or the summer (May to August), and the minimum occurred in the fall (September and October). The timing of the maximum monthly values differed across sites and years. However, in 1988, an exceptionally high O_3 concentration year occurred, and the highest monthly average concentration occurred in June for almost all of the five sites investigated. June 1988 was also the month in which the greatest number of O_3 episodes occurred in the eastern United States.

Lefohn et al. (1990a) have characterized the O_3 concentrations for several sites in the United States that experience low maximum hourly average concentrations. Of the three western national forest sites evaluated by Lefohn et al. (1990a), only Apache National Forest (AZ) experienced its maximum monthly mean concentration in the spring. The Apache National Forest site was above mean nocturnal inversion height, and no decrease of concentrations occurred during the evening hours. This site also experienced the highest hourly maximum concentration, as well as the highest W126 O_3 exposures. The Custer (MT) and Ochoco National Forest (OR) sites experienced most of their maximum monthly mean concentrations in the summer. The White River Oil Shale site in Colorado experienced its maximum monthly mean during the spring and summer months.

For vegetation effects assessment purposes, the W126 sigmoidal weighting exposure index was also used to identify the month of highest O_3 exposure. A somewhat more variable pattern was observed than when the maximum monthly average concentration was used. For some sites, the winter/spring pattern was present; for others, it was not. In some cases, the highest W126 exposures occurred earlier in the year than was indicated by the maximum monthly concentration. For example, in 1979, the Custer National Forest site experienced its highest W126 exposure in April, although the maximum monthly mean occurred in August. In 1980, the reverse occurred.

There was no consistent pattern for those sites located in the continental United States. The Theodore Roosevelt NP, Ochoco, and Custer National Forest sites and the White River Oil Shale site experienced their maximum O_3 exposures during the spring and summer months. The sites experiencing their highest O_3 exposures in the fall-to-spring period did not necessarily also experience the lowest O_3 exposures.

AX3.5 SPATIAL VARIABILITY IN OZONE CONCENTRATIONS

The spatial variability of O_3 concentrations in different environments in the United States occurring across a variety of spatial scales is characterized in this section. This information will be useful for understanding the influence of regional or altitudinal differences in O_3 exposure on vegetation and for establishing the spatial variations in O_3 concentrations as they are used in epidemiologic studies. Intracity variations in O_3 concentrations are described in Section AX3.5.1. Differences in O_3 concentration between urban and nonurban areas are described in Section AX3.5.2. Ozone concentrations at high elevations are characterized in Section AX3.5.3.

AX3.5.1 Spatial Variability of Ozone Concentrations in Urban Areas

The spatial variability in O_3 concentrations in 24 MSAs across the United States is characterized in this section. These areas were chosen to provide analyses to help guide in risk assessments, to provide a general overview of the spatial variability of O_3 in different regions of the country, and also to provide insight in to the spatial distribution of O_3 in cities where health outcome studies have been conducted. Statistical analyses of the human health effects of airborne pollutants based on aggregate population time-series data have often relied on ambient concentrations of pollutants measured at one or more central sites in a given metropolitan area. In the particular case of ground-level O_3 pollution, central-site monitoring has been justified as a regional measure of exposure partly on grounds that correlations between concentrations at neighboring sites measured over time are usually high (U.S. Environmental Protection Agency, 1996a). In analyses where multiple monitoring sites provide ambient O_3 concentrations, a summary measure such as an averaged concentration has often been regarded as adequately characterizing the exposure distribution. Indeed, a number of studies have referred to multiple-site averaging as the method for measuring O_3 exposure (U.S. Environmental Protection Agency, 1996a). It is hoped that the analyses presented here will shed some light on the suitability of this practice. Earlier analyses were reported in the previous O_3 AQCD (U.S. Environmental Protection Agency, 1996a). The analyses presented there concluded that the extent of spatial homogeneity is specific to the MSA under study. In particular, cities with low traffic densities that are located downwind of major sources of precursors are heavily influenced by long range transport and tend to show smaller variability (e.g., New Haven, CT) than those source areas with high traffic densities located upwind (e.g., New York, NY).

Metrics for characterizing spatial variability include the use of Pearson correlation coefficients (r), values of the 90th percentile (P_{90}) absolute difference in concentrations, and coefficients of divergence (COD)[2]. These methods of analysis follow those used for characterizing $PM_{2.5}$ and $PM_{10\text{-}2.5}$ concentrations in Pinto et al. (2004) and in the latest edition of the PM AQCD (U.S. Environmental Agency, 2004). However, the calculations were performed on an hourly basis rather than on a 24-h basis. Data were aggregated over the local O_3 season as indicated in Table AX3-1. The length of the O_3 season varies across the country. In several southwestern states, it lasts all year long. In other areas, such as in New England, it can be 6 months long, but typically it lasts from April through October.

Table AX3-12 shows the urban areas chosen, the range of 24-h average O_3 concentrations over the O_3 season, the range of intersite correlation coefficients, the range of P_{90} differences in O_3 concentrations between site pairs, and the range in COD values. A COD of zero implies that values in both data sets are identical, and a COD of one indicates that two data sets are completely different. In general, statistics were calculated for partial MSAs. This was done so as to obtain reasonable lower estimates of the spatial variability that is present, as opposed to examining the consolidated MSAs. In Boston, MA and New York, NY, this could not be readily done, and so statistics were calculated for the consolidated MSAs. More detailed calculations for a subset of nine MSAs are given in Figures AX3-36 through AX3-44.

As can be seen, there are no clearly discernible regional trends in the ranges of parameters shown. Additional urban areas would need to be examined to discern broadscale patterns. The data indicate considerable variability in the concentration fields. Seasonal means vary within individual urban areas from factors of 1.4 to 4.0.

The highest annual mean O_3 concentration (0.058 ppm) is found in the Phoenix, AZ MSA at a site which is located in the mountains well downwind of the main urban area. The lowest annual mean O_3 concentration (0.010 ppm) was found in Lynwood in the urban core of the

---

[2] The COD is defined as follows:

$$COD_{jk} = \sqrt{\frac{1}{p}\sum_{i=1}^{p}\left(\frac{x_{ij} - x_{ik}}{x_{ij} + x_{ik}}\right)^2} \qquad \text{(AX3-1)}$$

where x_{ij} and x_{ik} represent the 24-h average $PM_{2.5}$ concentration for day i at site j and site k and p is the number of observations.

Table AX3-12. Summary Statistics for Ozone (in ppm) Spatial Variability in Selected U.S. Urban Areas

Urban Area	Number of Sites	Minimum Mean Conc.	Maximum Mean Conc.	Minimum Corr. Coeff.	Maximum Corr. Coeff.	Minimum P_{90}[a]	Maximum P_{90}	Minimum COD[b]	Maximum COD
Boston, MA	18	0.021	0.033	0.46	0.93	0.012	0.041	0.17	0.45
New York, NY	29	0.015	0.041	0.45	0.96	0.0080	0.044	0.17	0.55
Philadelphia, PA	12	0.020	0.041	0.79	0.95	0.011	0.036	0.23	0.46
Washington, DC	20	0.022	0.041	0.72	0.97	0.010	0.032	0.17	0.45
Charlotte, NC	8	0.031	0.043	0.48	0.95	0.012	0.038	0.17	0.32
Atlanta, GA	12	0.023	0.047	0.63	0.94	0.013	0.045	0.24	0.55
Tampa, FL	9	0.024	0.035	0.74	0.94	0.011	0.025	0.20	0.35
Detroit, MI	7	0.022	0.037	0.74	0.96	0.0090	0.027	0.19	0.36
Chicago, IL	24	0.015	0.039	0.38	0.96	0.0080	0.043	0.16	0.50
Milwaukee, WI	9	0.027	0.038	0.73	0.96	0.0090	0.025	0.18	0.33
St. Louis, MO	17	0.022	0.038	0.78	0.96	0.0090	0.031	0.15	0.41
Baton Rouge, LA	7	0.018	0.031	0.81	0.95	0.0090	0.029	0.23	0.41
Dallas, TX	10	0.028	0.043	0.67	0.95	0.011	0.033	0.16	0.36
Houston, TX	13	0.016	0.036	0.73	0.96	0.0090	0.027	0.20	0.38
Denver, CO	8	0.022	0.044	0.60	0.92	0.013	0.044	0.16	0.46
El Paso, TX	4	0.022	0.032	0.81	0.94	0.012	0.023	0.24	0.31
Salt Lake City, UT	8	0.029	0.048	0.52	0.92	0.012	0.043	0.13	0.51
Phoenix, AZ	15	0.021	0.058	0.29	0.95	0.011	0.057	0.15	0.61
Seattle, WA	5	0.015	0.038	0.63	0.94	0.0080	0.024	0.16	0.46
Portland, OR	5	0.015	0.036	0.73	0.91	0.011	0.025	0.20	0.50
Fresno, CA	6	0.030	0.047	0.90	0.97	0.0090	0.027	0.17	0.40
Bakersfield, CA	8	0.028	0.047	0.23	0.96	0.013	0.052	0.20	0.58
Los Angeles, CA	14	0.010	0.042	0.42	0.95	0.010	0.053	0.22	0.59
Riverside, CA	18	0.018	0.054	0.38	0.95	0.013	0.057	0.15	0.64

[a]P90 = 90th percentile absolute difference in concentrations.
[b]COD = coefficient of divergence for different site pairs.

Charlotte - Gastonia - Rock Hill, NC - SC MSA

a.

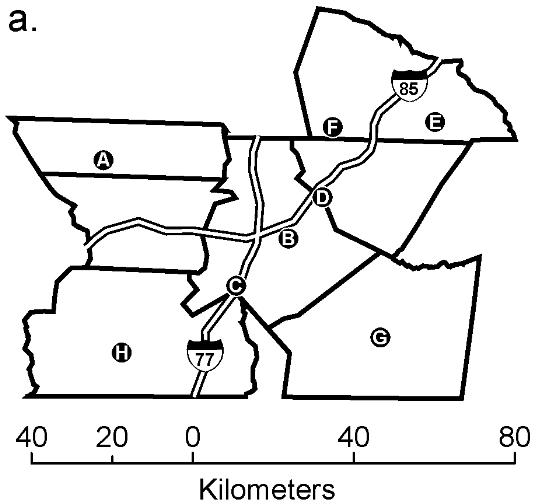

b.

AIRS Site ID	
Site A	37-109-0004
Site B	37-119-0041
Site C	37-119-1005
Site D	37-119-1009
Site E	37-159-0021
Site F	37-159-0022
Site G	37-179-0003
Site H	45-091-0006

c.

Site	A	B	C	D	E	F	G	H
mean (ppm)	0.034	0.034	0.031	0.035	0.039	0.040	0.038	0.035
A	1	0.87 0.020 0.28 4508	0.86 0.021 0.29 4824	0.88 0.019 0.28 4834	0.88 0.021 0.28 4821	0.86 0.023 0.31 4677	0.84 0.023 0.29 4664	0.85 0.021 0.29 4749
B		1	0.93 0.015 0.20 4706	0.95 0.012 0.17 4720	0.91 0.018 0.23 4503	0.87 0.020 0.26 4366	0.90 0.017 0.24 4341	0.82 0.021 0.27 4621
C			1	0.91 0.017 0.21 5045	0.85 0.023 0.28 4821	0.82 0.025 0.30 4677	0.87 0.020 0.27 4657	0.82 0.022 0.30 4955
D				1	0.93 0.015 0.21 4832	0.89 0.018 0.25 4688	0.87 0.019 0.25 4664	0.81 0.022 0.27 4968
E					1	0.89 0.016 0.22 4684	0.88 0.018 0.22 4651	0.83 0.021 0.24 4744
F						1	0.81 0.022 0.26 4510	0.81 0.021 0.23 4608
G							1	0.83 0.019 0.26 4582
H								1

Key
Pearson correlation coefficient
90th %-ile difference in concentration
Coefficient of divergence
Number of paired observations

Figure AX3-36. Locations of O_3 sampling sites (a) by AQS ID# (b) and intersite correlation statistics (c) for the Charlotte, NC-Gastonia-Rock Hill, SC MSA. The mean observed O_3 concentration at each site is given above its letter code. For each data pair, the Pearson correlation coefficient, 90th percentile difference in absolute concentrations, the coefficient of divergence, and number of observations are given.

Los Angeles MSA. CO and NO_x monitors at this site recorded the highest concentrations in California, indicating that titration of O_3 by NO freshly emitted from tail pipes of motor vehicles is responsible for the low O_3 values that are found. Ratios of highest to lowest mean O_3 concentrations in these two MSAs are among the highest shown in Table AX3-12. Both of these MSAs are characterized by sunny, warm climates; sources of precursors that are associated with

Baton Rouge, LA MSA

a.

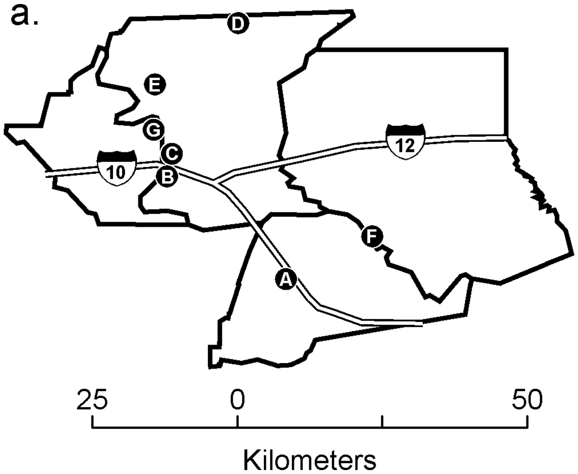

b.

AIRS Site ID	
Site A	22-005-0004
Site B	22-033-0003
Site C	22-033-0009
Site D	22-033-0013
Site E	22-033-1001
Site F	22-063-0002
Site G	22-121-0001

c.

Site	A	B	C	D	E	F	G
mean (ppm)	0.022	0.023	0.023	0.025	0.026	0.025	0.023
A	**1**	0.88 0.015 0.32 8378	0.86 0.016 0.33 8242	0.90 0.015 0.32 8342	0.87 0.017 0.36 8381	0.94 0.011 0.28 8382	0.86 0.016 0.33 8360
B		**1**	0.95 0.009 0.23 8159	0.87 0.015 0.29 8266	0.92 0.012 0.27 8301	0.86 0.016 0.32 8302	0.93 0.010 0.26 8281
C			**1**	0.87 0.015 0.30 8224	0.92 0.012 0.27 8171	0.86 0.017 0.32 8260	0.94 0.010 0.23 8157
D				**1**	0.93 0.011 0.24 8266	0.93 0.012 0.24 8379	0.88 0.015 0.28 8251
E					**1**	0.89 0.015 0.29 8306	0.94 0.011 0.25 8290
F						**1**	0.86 0.016 0.31 8292
G							**1**

Key
Pearson correlation coefficient
90th %-ile difference in concentration
Coefficient of divergence
Number of paired observations

Figure AX3-37. Locations of O_3 sampling sites (a) by AQS ID# (b) and intersite correlation statistics (c) for the Baton Rouge, LA MSA. The mean observed O_3 concentration at each site is given above its letter code. For each data pair, the Pearson correlation coefficient, 90th percentile difference in absolute concentrations, the coefficient of divergence, and number of observations are given.

O_3 titration to varying degrees in their urban centers; and with maximum O_3 found well downwind of the urban centers. Intersite correlation coefficients show mixed patterns, i.e., in some urban areas all pairs of sites are moderately to highly correlated, while other areas show a very large range of values. As may be expected, those areas which show smaller ratios of seasonal mean concentrations also exhibit a smaller range of intersite correlation coefficients. Within the examined urban areas , P_{90} values were evenly distributed between all site pairs

Detroit - Ann Arbor - Fling, MI CMSA

a.

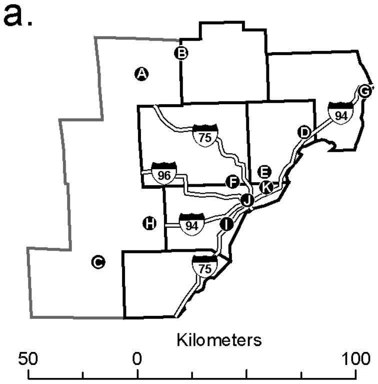

b.

AIRS Site ID	
Site A	26-049-0021
Site B	26-049-2001
Site C	26-091-0007
Site D	26-099-0009
Site E	26-099-1003
Site F	26-125-0001
Site G	26-147-0005
Site H	26-161-0008
Site I	26-163-0001
Site J	26-163-0016
Site K	26-163-0019

c.

Site	A	B	C	D	E	F	G	H	I	J	K
mean (ppm)	0.033	0.035	0.037	0.032	0.031	0.028	0.031	0.032	0.026	0.028	0.028
A	1	0.93 0.012 0.20 4333	0.84 0.019 0.24 4151	0.84 0.019 0.26 4253	0.86 0.019 0.27 4341	0.86 0.020 0.30 4103	0.81 0.020 0.26 4338	0.86 0.019 0.27 4163	0.82 0.024 0.35 4228	0.84 0.022 0.32 4324	0.85 0.020 0.29 4247
B		1	0.84 0.019 0.22 4152	0.86 0.017 0.25 4252	0.85 0.020 0.28 4341	0.84 0.023 0.33 4104	0.82 0.019 0.25 4339	0.84 0.021 0.28 4164	0.81 0.025 0.37 4230	0.81 0.024 0.36 4323	0.84 0.021 0.32 4248
C			1	0.85 0.020 0.27 4072	0.86 0.020 0.28 4159	0.87 0.022 0.32 3930	0.78 0.023 0.27 4156	0.92 0.015 0.25 4164	0.84 0.025 0.37 4049	0.86 0.023 0.35 4143	0.86 0.021 0.32 4068
D				1	0.91 0.014 0.26 4260	0.88 0.019 0.31 4022	0.86 0.017 0.25 4259	0.86 0.019 0.27 4086	0.84 0.022 0.34 4148	0.87 0.020 0.31 4245	0.90 0.016 0.27 4193
E					1	0.94 0.014 0.24 4112	0.83 0.020 0.27 4346	0.89 0.017 0.25 4172	0.88 0.020 0.31 4235	0.94 0.013 0.24 4330	0.96 0.010 0.19 4255
F						1	0.83 0.021 0.29 4109	0.91 0.015 0.25 3944	0.85 0.020 0.31 4000	0.93 0.013 0.23 4093	0.93 0.014 0.24 4025
G							1	0.79 0.022 0.28 4169	0.76 0.024 0.36 4233	0.80 0.022 0.33 4329	0.83 0.020 0.29 4255
H								1	0.88 0.019 0.34 4062	0.89 0.017 0.29 4153	0.89 0.017 0.27 4081
I									1	0.89 0.016 0.29 4217	0.90 0.018 0.29 4144
J										1	0.95 0.011 0.21 4242
K											1

Key
Pearson correlation coefficient
90th %-ile difference in concentration
Coefficient of divergence
Number of paired observations

Figure AX3-38. Locations of O_3 sampling sites (a) by AQS ID# (b) and intersite correlation statistics (c) for the Detroit-Ann Arbor-Flint, MI CMSA. The mean observed O_3 concentration at each site is given above its letter code. For each data pair, the Pearson correlation coefficient, 90th percentile difference in absolute concentrations, the coefficient of divergence, and number of observations are given.

St. Louis, MO - IL CMSA

a.

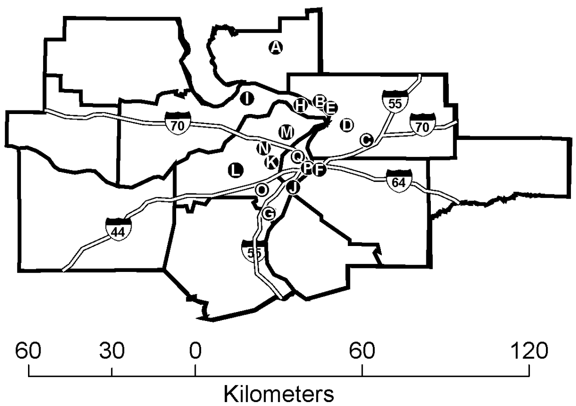

b.

AIRS Site ID	
Site A	17-083-1001
Site B	17-119-0008
Site C	17-119-1009
Site D	17-119-2007
Site E	17-119-3007
Site F	17-163-0010
Site G	29-099-0012
Site H	29-183-1002
Site I	29-183-1004
Site J	29-189-0004
Site K	29-189-0006
Site L	29-189-3001
Site M	29-189-5001
Site N	29-189-7003
Site O	29-510-0007
Site P	29-510-0072
Site Q	29-510-0086

Figure AX3-39. Locations of O_3 sampling sites (a) by AQS ID# (b) and intersite correlation statistics (c) for the St. Louis, MO-IL MSA. The mean observed O_3 concentration at each site is given above its letter code. For each data pair, the Pearson correlation coefficient, 90th percentile difference in absolute concentrations, the coefficient of divergence, and number of observations are given.

considered. The CODs indicate variability among site pairs. However, there are a number of cases where sites in an urban area may be moderately to highly correlated but showed substantial differences in absolute concentrations. In many cases, values for P_{90} equaled or exceeded seasonal mean O_3 concentrations. This was reflected in both values for P_{90} and for the COD.

It is instructive to compare the metrics for spatial variability shown in Table AX3-12 to those calculated for $PM_{2.5}$ and $PM_{10\text{-}2.5}$ in the PM AQCD (U.S. Environmental Agency, 2004). The values for concentrations and concentration differences are unique to the individual species, but the intersite correlation coefficients and the COD values can be directly compared. In general, the variability in O_3 concentrations is larger than for $PM_{2.5}$ concentrations and comparable to that obtained for $PM_{10\text{-}2.5}$. Intersite correlation coefficients in some areas (e.g., Philadelphia, PA; Atlanta, GA; Portland, OR) can be very similar for both $PM_{2.5}$ and for O_3.

St. Louis, MO - IL CMSA

C.

Site	A	B	C	D	E	F	G	H	I	J	K	L	M	N	O	P	Q
mean (ppm)	0.037	0.035	0.031	0.029	0.031	0.028	0.035	0.034	0.035	0.032	0.031	0.025	0.030	0.030	0.028	0.024	0.030
A	1	0.88 0.015 0.19 5055	0.84 0.020 0.26 4935	0.84 0.022 0.29 5032	0.85 0.021 0.29 5021	0.83 0.025 0.38 5045	0.81 0.021 0.28 5049	0.89 0.016 0.21 5052	0.91 0.014 0.20 4735	0.82 0.022 0.28 5077	0.84 0.021 0.29 5073	0.80 0.029 0.37 5075	0.86 0.022 0.31 5077	0.85 0.021 0.32 5071	0.80 0.026 0.36 5035	0.82 0.027 0.40 5034	0.85 0.022 0.34 5065
B		1	0.87 0.017 0.26 4963	0.90 0.016 0.26 5061	0.93 0.013 0.23 5048	0.86 0.021 0.34 5077	0.82 0.019 0.28 5078	0.93 0.012 0.18 5082	0.90 0.014 0.19 4766	0.83 0.020 0.27 5106	0.85 0.018 0.27 5102	0.84 0.024 0.34 5105	0.87 0.019 0.30 5106	0.84 0.020 0.30 5101	0.84 0.022 0.33 5064	0.87 0.022 0.35 5064	0.88 0.018 0.31 5094
C			1	0.92 0.012 0.24 4941	0.88 0.015 0.26 4933	0.92 0.014 0.29 4952	0.87 0.018 0.26 4958	0.90 0.015 0.23 4963	0.88 0.016 0.24 4680	0.88 0.016 0.25 4985	0.87 0.016 0.26 4981	0.85 0.020 0.32 4983	0.90 0.015 0.26 4985	0.88 0.016 0.27 4979	0.86 0.018 0.30 4943	0.88 0.017 0.32 4942	0.91 0.014 0.27 4973
D				1	0.93 0.012 0.22 5024	0.90 0.014 0.29 5050	0.85 0.019 0.26 5055	0.91 0.016 0.23 5058	0.88 0.017 0.25 4742	0.86 0.018 0.27 5083	0.84 0.018 0.27 5079	0.84 0.020 0.30 5081	0.87 0.016 0.27 5085	0.85 0.017 0.28 5077	0.86 0.017 0.28 5042	0.88 0.016 0.29 5040	0.90 0.015 0.27 5073
E					1	0.90 0.015 0.29 5039	0.84 0.019 0.27 5045	0.93 0.013 0.22 5046	0.90 0.015 0.23 4728	0.85 0.018 0.27 5069	0.84 0.018 0.29 5065	0.88 0.018 0.32 5067	0.88 0.016 0.29 5069	0.86 0.017 0.29 5065	0.88 0.016 0.29 5027	0.89 0.017 0.30 5027	0.90 0.015 0.28 5057
F						1	0.90 0.018 0.28 5067	0.90 0.018 0.32 5070	0.89 0.018 0.32 4754	0.91 0.016 0.29 5095	0.88 0.017 0.30 5091	0.90 0.016 0.32 5093	0.92 0.014 0.27 5095	0.91 0.015 0.27 5091	0.92 0.013 0.26 5053	0.92 0.015 0.28 5053	0.94 0.012 0.23 5083
G							1	0.87 0.017 0.23 5075	0.86 0.017 0.24 4756	0.95 0.012 0.22 5100	0.91 0.015 0.25 5096	0.88 0.022 0.33 5098	0.88 0.018 0.27 5100	0.88 0.017 0.26 5094	0.89 0.020 0.29 5058	0.86 0.023 0.35 5057	0.91 0.016 0.26 5088
H								1	0.94 0.011 0.15 4759	0.87 0.017 0.24 5103	0.88 0.016 0.24 5099	0.87 0.022 0.32 5101	0.92 0.015 0.26 5103	0.90 0.015 0.27 5097	0.86 0.020 0.31 5062	0.87 0.022 0.35 5060	0.91 0.015 0.29 5091
I									1	0.86 0.017 0.28 4784	0.90 0.015 0.25 4782	0.88 0.022 0.33 4782	0.91 0.016 0.27 4784	0.90 0.016 0.28 4778	0.85 0.021 0.32 4742	0.86 0.022 0.35 4743	0.90 0.017 0.30 4773
J										1	0.92 0.013 0.26 5124	0.91 0.018 0.30 5126	0.91 0.015 0.24 5128	0.91 0.014 0.23 5122	0.90 0.016 0.25 5086	0.88 0.019 0.30 5085	0.93 0.013 0.22 5116
K											1	0.87 0.019 0.29 5122	0.90 0.015 0.23 5124	0.91 0.014 0.23 5118	0.86 0.018 0.28 5082	0.87 0.020 0.30 5081	0.90 0.015 0.25 5112
L												1	0.88 0.018 0.28 5126	0.90 0.017 0.28 5120	0.90 0.015 0.27 5084	0.88 0.016 0.27 5083	0.92 0.016 0.26 5114
M													1	0.96 0.009 0.18 5122	0.87 0.018 0.26 5086	0.87 0.019 0.29 5085	0.95 0.011 0.21 5116
N														1	0.87 0.017 0.26 5080	0.86 0.019 0.31 5079	0.94 0.011 0.20 5110
O															1	0.92 0.014 0.26 5045	0.92 0.014 0.25 5074
P																1	0.92 0.016 0.28 5074
Q																	1

Key
Pearson correlation coefficient
90th %-ile difference in concentration
Coefficient of divergence
Number of paired observations

Figure AX3-39 (cont'd).

Phoenix - Mesa, AZ MSA

a.

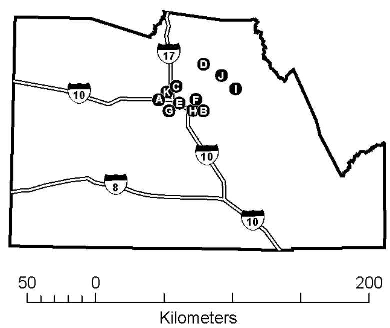

b.

AIRS Site ID	
Site A	04-013-0019
Site B	04-013-1003
Site C	04-013-1004
Site D	04-013-2005
Site E	04-013-3002
Site F	04-013-3003
Site G	04-013-4003
Site H	04-013-4005
Site I	04-013-9702
Site J	04-013-9704
Site K	04-013-9997

c.

Site	A	B	C	D	E	F	G	H	I	J	K
mean (ppm)	0.021	0.025	0.028	0.046	0.021	0.024	0.024	0.028	0.038	0.041	0.024
A	1	0.87 0.017 0.38 7580	0.91 0.018 0.35 8031	0.59 0.046 0.59 7991	0.93 0.012 0.31 7925	0.89 0.016 0.35 7593	0.91 0.014 0.32 7901	0.90 0.017 0.34 6651	0.78 0.034 0.54 8020	0.78 0.037 0.55 8081	0.95 0.011 0.27 7920
B		1	0.90 0.018 0.25 7962	0.69 0.038 0.46 7912	0.89 0.016 0.41 7872	0.92 0.013 0.33 7502	0.89 0.015 0.30 7826	0.93 0.014 0.22 6768	0.83 0.027 0.38 7895	0.85 0.029 0.41 8011	0.90 0.016 0.32 7858
C			1	0.62 0.040 0.47 8377	0.92 0.019 0.40 8326	0.92 0.016 0.34 7965	0.91 0.017 0.28 8273	0.92 0.016 0.24 7022	0.82 0.027 0.39 8367	0.82 0.030 0.41 8468	0.95 0.013 0.28 8319
D				1	0.58 0.047 0.61 8286	0.63 0.043 0.56 7925	0.58 0.042 0.51 8231	0.61 0.043 0.49 6992	0.67 0.025 0.23 8332	0.79 0.018 0.16 8429	0.58 0.045 0.56 8281
E					1	0.92 0.014 0.35 7894	0.94 0.012 0.35 8180	0.93 0.015 0.37 6938	0.82 0.033 0.57 8279	0.80 0.037 0.58 8369	0.95 0.012 0.31 8238
F						1	0.90 0.015 0.35 7863	0.94 0.012 0.30 6599	0.82 0.030 0.50 7913	0.84 0.033 0.52 8009	0.93 0.013 0.31 7846
G							1	0.93 0.014 0.25 6882	0.81 0.029 0.44 8225	0.80 0.033 0.46 8322	0.93 0.013 0.29 8166
H								1	0.82 0.029 0.41 6963	0.83 0.032 0.43 7078	0.93 0.013 0.25 6912
I									1	0.86 0.016 0.17 8411	0.81 0.031 0.50 8265
J										1	0.80 0.035 0.51 8367
K											1

Key
Pearson correlation coefficient
90th %-ile difference in concentration
Coefficient of divergence
Number of paired observations

Figure AX3-40. Locations of O_3 sampling sites (a) by AQS ID# (b) and intersite correlation statistics (c) for the Phoenix-Mesa, AZ MSA. The mean observed O_3 concentration at each site is given above its letter code. For each data pair, the Pearson correlation coefficient, 90th percentile difference in absolute concentrations, the coefficient of divergence, and number of observations are given.

Fresno, CA MSA

a.

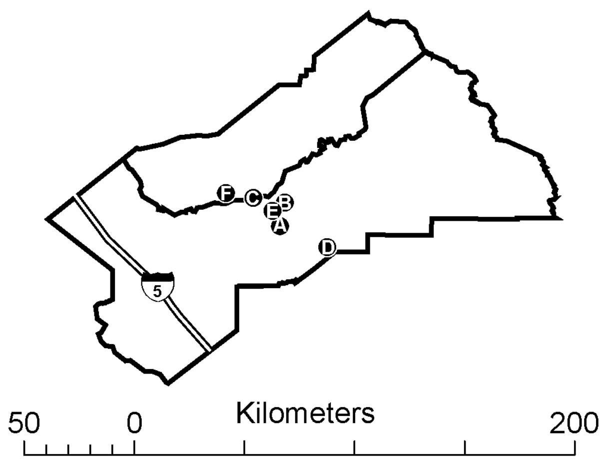

b.

AIRS Site ID	
Site A	06-019-0007
Site B	06-019-0008
Site C	06-019-0242
Site D	06-019-4001
Site E	06-019-5001
Site F	06-039-0004

c.

Site	A	B	C	D	E	F
mean (ppm)	0.031	0.031	0.047	0.040	0.036	0.030
A	1	0.97 0.010 0.19 7804	0.94 0.027 0.34 8124	0.93 0.022 0.25 7950	0.95 0.016 0.19 8066	0.92 0.015 0.25 8055
B		1	0.95 0.026 0.40 7777	0.92 0.022 0.33 7624	0.97 0.013 0.23 7726	0.92 0.017 0.25 7710
C			1	0.92 0.019 0.20 7939	0.93 0.022 0.29 8055	0.94 0.027 0.40 8036
D				1	0.92 0.017 0.22 7876	0.92 0.024 0.32 7873
E					1	0.90 0.022 0.29 7998
F						1

Key
Pearson correlation coefficient
90th %-ile difference in concentration
Coefficient of divergence
Number of paired observations

Figure AX3-41. Locations of O_3 sampling sites (a) by AQS ID# (b) and intersite correlation statistics (c) for the Fresno, CA MSA. The mean observed O_3 concentration at each site is given above its letter code. For each data pair, the Pearson correlation coefficient, 90th percentile difference in absolute concentrations, the coefficient of divergence, and number of observations are given.

However, there is much greater variability in the concentration fields of O_3 as evidenced by the much higher COD values. Indeed, COD values are higher for O_3 than for $PM_{2.5}$ in each of the urban areas examined. In all of the urban areas examined for O_3 some site pairs are always very highly correlated with each other (i.e., r > 0.9) as seen for $PM_{2.5}$. These sites also show less variability in concentration and are probably influenced most strongly by regional production mechanisms.

Bakersfield, CA MSA

a.

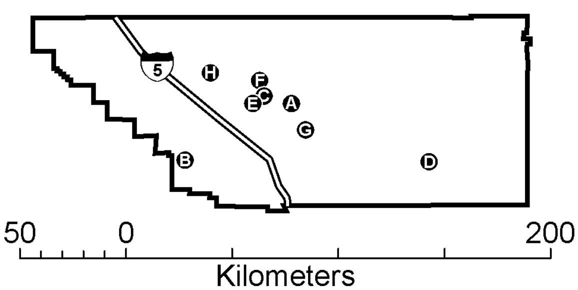

b.

AIRS Site ID	
Site A	06-029-0007
Site B	06-029-0008
Site C	06-029-0010
Site D	06-029-0011
Site E	06-029-0014
Site F	06-029-0232
Site G	06-029-5001
Site H	06-029-6001

c.

Site	A	B	C	D	E	F	G	H
mean (ppm)	0.039	0.047	0.029	0.047	0.030	0.038	0.043	0.030
A	1	0.87 0.026 0.28 8299	0.82 0.030 0.40 7835	0.62 0.038 0.35 8127	0.80 0.032 0.45 8307	0.88 0.019 0.24 7915	0.87 0.022 0.24 8283	0.80 0.031 0.40 8061
B		1	0.76 0.042 0.47 7779	0.68 0.028 0.28 8079	0.75 0.044 0.51 8251	0.87 0.025 0.29 7880	0.89 0.021 0.20 8244	0.75 0.042 0.47 8006
C			1	0.62 0.047 0.48 7612	0.95 0.014 0.30 7791	0.88 0.026 0.37 7469	0.84 0.032 0.43 7772	0.94 0.015 0.29 7549
D				1	0.62 0.047 0.49 8096	0.69 0.033 0.34 7695	0.68 0.032 0.30 8066	0.61 0.047 0.46 7903
E					1	0.86 0.028 0.41 7862	0.84 0.033 0.46 8244	0.96 0.013 0.28 8024
F						1	0.89 0.021 0.25 7843	0.85 0.028 0.37 7626
G							1	0.84 0.033 0.42 8005
H								1

Key
Pearson correlation coefficient
90th %-ile difference in concentration
Coefficient of divergence
Number of paired observations

Figure AX3-42. Locations of O_3 sampling sites (a) by AQS ID# (b) and intersite correlation statistics (c) for the Bakersfield, CA MSA. The mean observed O_3 concentration at each site is given above its letter code. For each data pair, the Pearson correlation coefficient, 90th percentile difference in absolute concentrations, the coefficient of divergence, and number of observations are given.

A number of processes can contribute to spatial variability in O_3 concentrations in urban areas. Ozone formation occurs more or less continuously downwind of sources of precursors, producing a gradient in O_3 concentrations. Ozone ‘titration’ by reaction with NO can deplete O_3 levels near NO sources such as highways and busy streets. Differences in surface characteristics affect the rate of deposition of O_3. Mixing of O_3 from aloft can lead to local enhancements in O_3 concentration.

Los Angeles - Orange County, CA CMSA

a.

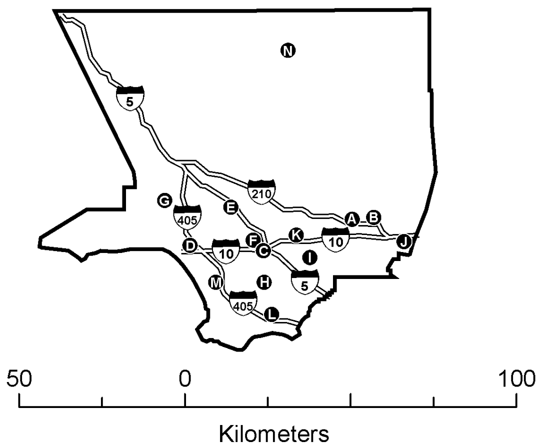

b.

AIRS Site ID	
Site A	06-037-0002
Site B	06-037-0016
Site C	06-037-0030
Site D	06-037-0113
Site E	06-037-1002
Site F	06-037-1103
Site G	06-037-1201
Site H	06-037-1301
Site I	06-037-1601
Site J	06-037-1701
Site K	06-037-2005
Site L	06-037-4002
Site M	06-037-5001
Site N	06-037-9002

Figure AX3-43. Locations of O_3 sampling sites (a) by AQS ID# (b) and intersite correlation statistics (c) for the Los Angeles-Orange County, CA CMSA. The mean observed O_3 concentration at each site is given above its letter code. For each data pair, the Pearson correlation coefficient, 90th percentile difference in absolute concentrations, the coefficient of divergence, and number of observations are given.

Los Angeles - Orange County, CA CMSA

C.

Site	A	B	C	D	E	F	G	H	I	J	K	L	M	N
mean (ppm)	0.021	0.029	0.021	0.020	0.018	0.019	0.021	0.013	0.016	0.013	0.021	0.022	0.027	0.042
A	1	0.95 0.017 0.32 8378	0.87 0.020 0.33 6723	0.64 0.028 0.41 8387	0.88 0.018 0.38 8202	0.85 0.020 0.36 8292	0.82 0.021 0.37 8364	0.72 0.029 0.44 8362	0.89 0.019 0.41 8381	0.91 0.022 0.46 8386	0.91 0.015 0.33 8384	0.61 0.029 0.44 8379	0.55 0.035 0.45 8341	0.58 0.048 0.47 6321
B		1	0.82 0.029 0.36 6722	0.60 0.034 0.42 8386	0.86 0.028 0.44 8201	0.80 0.029 0.45 8291	0.80 0.027 0.42 8363	0.67 0.038 0.53 8361	0.84 0.030 0.52 8380	0.88 0.032 0.59 8385	0.87 0.024 0.39 8383	0.57 0.033 0.47 8378	0.53 0.034 0.46 8340	0.56 0.042 0.42 6321
C			1	0.75 0.021 0.32 6731	0.88 0.018 0.35 6546	0.95 0.010 0.22 6636	0.84 0.019 0.29 6708	0.83 0.020 0.37 6729	0.91 0.013 0.37 6725	0.85 0.020 0.49 6730	0.90 0.017 0.24 6728	0.72 0.022 0.31 6723	0.68 0.030 0.37 6686	0.61 0.048 0.45 4998
D				1	0.76 0.023 0.31 8210	0.82 0.018 0.31 8300	0.73 0.023 0.31 8372	0.77 0.023 0.36 8370	0.77 0.022 0.35 8389	0.69 0.027 0.43 8394	0.73 0.024 0.34 8392	0.75 0.021 0.31 8387	0.81 0.025 0.30 8349	0.62 0.046 0.40 6321
E					1	0.90 0.014 0.29 8184	0.86 0.019 0.31 8187	0.79 0.023 0.35 8185	0.90 0.015 0.33 8204	0.87 0.019 0.38 8210	0.91 0.014 0.28 8207	0.67 0.027 0.37 8202	0.66 0.034 0.37 8164	0.59 0.050 0.45 6322
F						1	0.85 0.018 0.31 8277	0.85 0.019 0.36 8275	0.93 0.012 0.33 8294	0.86 0.019 0.42 8300	0.91 0.015 0.26 8297	0.76 0.021 0.35 8292	0.74 0.029 0.40 8254	0.66 0.047 0.50 6325
G							1	0.74 0.026 0.36 8347	0.86 0.020 0.35 8366	0.84 0.023 0.45 8371	0.86 0.017 0.31 8369	0.67 0.026 0.36 8364	0.68 0.028 0.36 8349	0.70 0.042 0.43 6326
H								1	0.86 0.017 0.26 8364	0.74 0.018 0.37 8369	0.80 0.025 0.38 8367	0.84 0.021 0.35 8362	0.73 0.033 0.43 8324	0.61 0.053 0.51 6299
I									1	0.89 0.016 0.31 8388	0.93 0.015 0.30 8386	0.77 0.022 0.34 8381	0.71 0.032 0.39 8343	0.66 0.048 0.48 6321
J										1	0.90 0.021 0.43 8391	0.67 0.028 0.46 8386	0.62 0.037 0.50 8348	0.63 0.053 0.56 6323
K											1	0.71 0.025 0.37 8384	0.65 0.031 0.40 8346	0.65 0.045 0.46 6321
L												1	0.74 0.025 0.33 8341	0.62 0.043 0.42 6321
M													1	0.63 0.038 0.36 6299
N														1

Key
Pearson correlation coefficient
90th %-ile difference in concentration
Coefficient of divergence
Number of paired observations

Figure AX3-43 (cont'd).

Riverside - Orange County, CS CMSA

a.

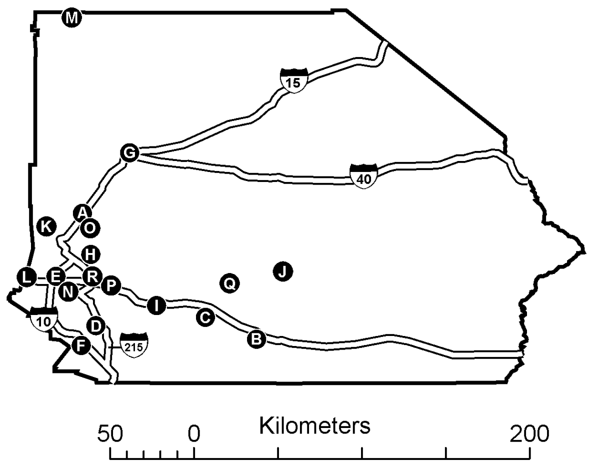

b.

AIRS Site ID	
Site A	06-065-0012
Site B	06-065-2002
Site C	06-065-5001
Site D	06-065-6001
Site E	06-065-8001
Site F	06-065-9001
Site G	06-071-0001
Site H	06-071-0005
Site I	06-071-0012
Site J	06-071-0017
Site K	06-071-0306
Site L	06-071-1004
Site M	06-071-1234
Site N	06-071-2002
Site O	06-071-4001
Site P	06-071-4003
Site Q	06-071-9002
Site R	06-071-9004

Figure AX3-44. Locations of O_3 sampling sites (a) by AQS ID# (b) and intersite correlation statistics (c) for the Riverside-Orange County, CA CMSA. The mean observed O_3 concentration at each site is given above its letter code. For each data pair, the Pearson correlation coefficient, 90th percentile difference in absolute concentrations, the coefficient of divergence, and number of observations are given.

Riverside - Orange County, CS CMSA

C.

Site	A	B	C	D	E	F	G	H	I	J	K	L	M	N	O	P	Q	R
mean (ppm)	0.037	0.035	0.042	0.033	0.026	0.036	0.030	0.047	0.048	0.044	0.032	0.022	0.038	0.020	0.037	0.032	0.040	0.026
A	1	0.71 0.032 0.33 8397	0.77 0.030 0.35 8392	0.84 0.026 0.34 8394	0.79 0.034 0.42 8386	0.81 0.027 0.33 8035	0.76 0.031 0.38 7741	0.70 0.038 0.38 8393	0.69 0.037 0.39 8051	0.69 0.034 0.37 7844	0.75 0.031 0.36 7498	0.76 0.037 0.47 8385	0.55 0.036 0.38 7815	0.75 0.040 0.54 8394	0.76 0.029 0.35 7997	0.81 0.028 0.35 8391	0.53 0.037 0.38 7887	0.80 0.033 0.41 8364
B		1	0.85 0.023 0.25 8394	0.69 0.035 0.34 8395	0.64 0.039 0.42 8388	0.66 0.036 0.33 8040	0.75 0.031 0.33 7919	0.62 0.041 0.33 8393	0.64 0.038 0.34 8233	0.81 0.029 0.30 8017	0.72 0.031 0.34 7678	0.60 0.043 0.46 8389	0.65 0.031 0.31 7990	0.56 0.046 0.51 8395	0.71 0.031 0.31 8179	0.61 0.038 0.37 8392	0.52 0.035 0.33 8059	0.61 0.040 0.42 8369
C			1	0.73 0.037 0.38 8393	0.66 0.044 0.47 8385	0.69 0.036 0.35 8034	0.74 0.035 0.39 7752	0.67 0.036 0.32 8391	0.72 0.030 0.32 8059	0.81 0.025 0.28 7852	0.73 0.034 0.38 7506	0.61 0.049 0.52 8384	0.67 0.030 0.30 7823	0.59 0.052 0.56 8393	0.75 0.030 0.32 8005	0.65 0.039 0.40 8390	0.65 0.031 0.33 7896	0.65 0.045 0.46 8362
D				1	0.90 0.023 0.33 8387	0.91 0.019 0.25 8036	0.79 0.029 0.34 7742	0.70 0.041 0.41 8393	0.68 0.041 0.45 8049	0.67 0.039 0.42 7842	0.77 0.031 0.37 7496	0.87 0.028 0.42 8386	0.57 0.039 0.41 7813	0.84 0.032 0.51 8395	0.75 0.033 0.38 7995	0.87 0.023 0.33 8392	0.47 0.040 0.44 7885	0.89 0.024 0.35 8364
E					1	0.88 0.026 0.36 8028	0.76 0.031 0.38 7735	0.66 0.048 0.51 8385	0.63 0.046 0.54 8042	0.60 0.045 0.51 7835	0.74 0.032 0.42 7490	0.92 0.017 0.34 8378	0.50 0.042 0.50 7806	0.93 0.018 0.43 8387	0.69 0.037 0.46 7988	0.87 0.025 0.39 8384	0.42 0.042 0.52 7878	0.94 0.015 0.36 8356
F						1	0.76 0.031 0.33 7402	0.64 0.042 0.37 8034	0.62 0.039 0.39 7709	0.63 0.037 0.36 7487	0.74 0.031 0.37 7171	0.83 0.032 0.43 8027	0.54 0.037 0.36 7610	0.81 0.034 0.53 8036	0.70 0.032 0.35 7640	0.82 0.026 0.31 8033	0.44 0.039 0.38 7545	0.85 0.028 0.35 8010
G							1	0.68 0.042 0.40 7740	0.68 0.041 0.43 8067	0.75 0.035 0.40 7758	0.85 0.022 0.33 7684	0.72 0.035 0.41 7740	0.68 0.033 0.39 7669	0.68 0.038 0.49 7744	0.78 0.029 0.36 7861	0.72 0.032 0.37 7739	0.46 0.038 0.41 7592	0.73 0.033 0.40 7720
H								1	0.72 0.030 0.26 8047	0.65 0.033 0.26 7840	0.74 0.038 0.40 7494	0.66 0.051 0.56 8384	0.59 0.037 0.27 7811	0.65 0.054 0.59 8393	0.80 0.030 0.31 7993	0.71 0.041 0.39 8390	0.55 0.036 0.28 7883	0.70 0.047 0.46 8363
I									1	0.73 0.022 0.19 7983	0.70 0.039 0.43 7836	0.63 0.049 0.59 8047	0.64 0.027 0.24 7940	0.60 0.052 0.61 8051	0.78 0.030 0.34 8059	0.68 0.040 0.42 8046	0.63 0.024 0.16 7899	0.65 0.046 0.48 8027
J										1	0.72 0.035 0.41 7576	0.57 0.048 0.56 7840	0.73 0.024 0.21 7677	0.54 0.051 0.59 7844	0.74 0.028 0.32 7826	0.60 0.041 0.39 7839	0.57 0.025 0.21 7689	0.58 0.046 0.45 7820
K											1	0.70 0.036 0.44 7494	0.64 0.032 0.40 7430	0.67 0.039 0.51 7498	0.84 0.024 0.34 7626	0.70 0.033 0.41 7493	0.49 0.037 0.42 7352	0.72 0.034 0.42 7477
L												1	0.46 0.044 0.54 7814	0.95 0.013 0.40 8386	0.68 0.041 0.50 7993	0.88 0.027 0.43 8383	0.38 0.045 0.55 7885	0.92 0.018 0.40 8357
M													1	0.42 0.048 0.57 7815	0.65 0.028 0.31 7817	0.49 0.039 0.40 7811	0.50 0.023 0.22 7665	0.49 0.042 0.45 7796
N														1	0.64 0.043 0.54 7996	0.87 0.029 0.50 8392	0.38 0.047 0.58 7887	0.93 0.019 0.45 8364
O															1	0.72 0.033 0.37 7992	0.58 0.030 0.33 7842	0.70 0.037 0.43 7973
P																1	0.46 0.039 0.41 7882	0.92 0.020 0.33 8361
Q																	1	0.45 0.041 0.46 7866
R																		1

Key
Pearson correlation coefficient
90th %-ile difference in concentration
Coefficient of divergence
Number of paired observations

Figure AX3-44 (cont'd).

AX3.5.2 Urban-Nonurban Concentration Differences

Research performed and published in the 1970s and 1980s provides an excellent framework for discussing the differences in urban and nonurban concentrations. Diurnal concentration data presented earlier indicate that peak O_3 concentrations can occur later in the day in rural areas than in urban, with the distances downwind from urban centers generally determining how much later the peaks occur. Meagher et al. (1987) reported that O_3 levels for five rural sites in the Tennessee Valley region of the southeastern United States were found to equal or exceed urban values for the same region. Data presented in the 1978 O_3 AQCD demonstrated that peak O_3 concentrations in rural areas generally are lower than those in urban areas, but that average concentrations in rural areas are comparable to or even higher than those in urban areas (U.S. Environmental Protection Agency, 1978). Reagan (1984) noted that O_3 concentrations measured near "population-oriented" areas were depressed compared to more isolated areas. As noted earlier, urban O_3 values are often depressed because of titration by NO (Stasiuk and Coffey, 1974). In reviewing the NCLAN's use of kriging to estimate the 7-h seasonal average O_3 levels, Lefohn et al. (1987) found that the 7-h values derived from kriging for sites located in rural areas tended to be lower than the actual values due to the use of data from urban areas to estimate rural area values. In addition to the occurrence of higher average concentrations and occasionally higher peak concentrations of O_3 in nonurban than in urban areas, it is well documented that O_3 persists longer in nonurban than in urban areas (Coffey et al., 1977; Wolff et al., 1977; Isaksen et al., 1978). The absence of chemical scavengers appears to be the main reason. Ozone is a secondary pollutant and its source is distributed more uniformly over much broader spatial scales compared to primary pollutants such as CO, SO_2, etc. However, this does not mean that variability in O_3 does not exist on smaller spatial scales.

AX3.5.3 Ozone Concentrations at High Elevations

The distributions of hourly average concentrations experienced at high-elevation cities are similar to those experienced in low-elevation cities. For example, the distribution of hourly average concentrations for several O_3 sites located in Denver were similar to distributions observed at many low-elevation sites elsewhere in the United States. However, the use of absolute concentrations (e.g., in units of micrograms per cubic meter) in assessing the possible impacts of O_3 on vegetation at high-elevation sites instead of mixing ratios (e.g., parts per million) may be an important consideration (see Chapter 9, for further considerations about exposure and effective dose considerations for vegetation assessments).

Concentrations of O_3 vary with altitude and latitude. Although a number of reports contain data on O_3 concentrations at high altitudes (e.g., Coffey et al., 1977; Reiter, 1977b; Singh et al., 1977; Evans et al., 1985; Lefohn and Jones, 1986), fewer reports present data for different elevations in the same locality. Monitoring data collected by the MCCP provide useful information for investigating O_3 exposure differences at different elevations. When applying different exposure indices to the MCCP data, there appears to be no consistent conclusion concerning the relationship between O_3 exposure and elevation.

Lefohn et al. (1990a) summarized the characterization of gaseous exposures at rural sites in 1986 and 1987 at several MCCP high-elevation sites. Aneja and Li (1992) have summarized the O_3 concentrations for 1986 to 1988. Table AX3-13 summarizes the sites characterized by Lefohn et al. (1990a). Table AX3-14 summarizes the concentrations and exposures that occurred at several of the sites for the period 1987 to 1988. In 1987, the 7- and 12-h seasonal means were similar at the Whiteface Mountain WF1 and WF3 sites (Figure AX3-45a). The 7-h mean values were 0.0449 and 0.0444 ppm, respectively, and the 12-h mean values were 0.0454 and 0.0444 ppm, respectively. Note that, in some cases, the 12-h mean was slightly higher than the 7-h mean value. This resulted when the 7-h mean period (0900 to 1559 hours) did not capture the period of the day when the highest hourly mean O_3 concentrations were experienced. A similar observation was made, using the 1987 data, for the MCCP Shenandoah National Park sites. The 7-h and 12-h seasonal means were similar for the SH1 and SH2 sites (Figure AX3-45b). Based on cumulative indices, the Whiteface Mountain summit (1,483-m) site (WF1) experienced a higher exposure than the WF3 (1,026-m) site (Figure AX3-45c). Both the sum of the concentrations $\geq$ 0.07 ppm (SUM07) and the number of hourly concentrations $\geq$ 0.07 ppm were higher at the WF1 site than at the WF3 site. The site at the base of the mountain (WF4) experienced the lowest exposure of the three O_3 sites. Among the MCCP Shenandoah National Park sites, the SH2 site experienced marginally higher O_3 exposures, based on the index that sums all of the hourly average concentrations (referred to as "total dose" in Figure AX3-45c) and sigmoidal values, than the SH1 high-elevation site (Figure AX3-45d). The reverse was true for the sums of the concentrations $\geq$ 0.07 ppm and the number of hourly concentrations $\geq$ 0.07 ppm.

Table AX3-13. Description of Mountain Cloud Chemistry Program Sites

Site	Elevation (m)	Latitude			Longitude		
Howland Forest (HF1), ME	65	458˚	11'		68˚	46'	
Mt. Moosilauke (MS1), NH	1,000	438˚	59'	18"	71˚	48'	28"
Whiteface Mountain (WF1), NY	1483	448˚	23'	26"	73˚	51'	34"
Shenandoah NP (SH1), VA	1,015	38˚	37'	12"	78˚	20'	48"
Shenandoah NP (SH2), VA	716	38˚	37'	30"	78˚	21'	13"
Shenandoah NP (SH3), VA	524	38˚	37'	45"	78˚	21'	28"
Whitetop Mountain (WT1), VA	1,689	36˚	38'	20"	81˚	36'	21"
Mt. Mitchell (MM1), NC	2006	35˚	44'	15"	82˚	17'	15"
Mt. Mitchell (MM2), NC	1760	35˚	45'		82˚	15'	

Table AX3-14. Seasonal (April-October) Percentiles, SUM06, SUM08, and W126 Values for the MCCP Sites

Site	Year	Min.	10	30	50	70 (ppm)	90	95	99	Max.	No. Obs.	SUM06	SUM08 (ppm-h)	W126
Howland Forest, ME (HF1)	1987	.000	.013	.021	.028	.035	.046	.052	.065	.076	4766	5.9	0.0	7.7
	1988	.000	.012	.021	.028	.036	.047	.054	.076	.106	4786	10.9	2.9	11.6
Mt. Moosilauke, NH (MS1)	1987	.006	.027	.036	.045	.053	.065	.074	.086	.102	4077	45.0	9.5	40.1
	1988	.010	.026	.033	.043	.055	.076	.087	.113	.127	2835	51.9	21.2	43.4
Whiteface Mountain, NY (WF1) (36-031-0002)	1987	.011	.029	.037	.046	.053	.067	.074	.087	.104	4703	63.5	12.2	50.5
	1988	.014	.025	.033	.043	.056	.078	.089	.110	.135	4675	94.4	40.8	78.3
Whiteface Mountain, NY (WF3)	1987	.010	.025	.033	.039	.047	.064	.075	.091	.117	4755	45.4	14.4	40.3
Whiteface Mountain, NY (WF4)	1987	.000	.011	.023	.031	.041	.056	.065	.081	.117	4463	23.8	5.1	21.3
Mt. Mitchell, NC (MM1)	1987	.008	.034	.044	.051	.058	.067	.074	.085	.105	3539	59.4	7.8	46.5
	1988	.011	.038	.054	.065	.075	.095	.106	.126	.145	2989	145.1	69.7	116.6
	1989	.010	.038	.047	.054	.059	.068	.072	.081	.147	2788	54.8	3.5	40.7
	1992	.005	.036	.043	.048	.053	.063	.069	.081	.096	3971	37.8	4.4	36.7
Mt. Mitchell, NC (MM2)	1987	.017	.032	.042	.049	.056	.067	.073	.083	.096	3118	47.0	5.1	37.4
	1988	.009	.029	.041	.050	.060	.080	.092	.110	.162	2992	68.7	28.1	57.7
Shenandoah Park, VA (SH1)	1987	.000	.023	.036	.044	.054	.069	.076	.085	.135	3636	54.2	8.5	42.0
	1988	.006	.024	.036	.047	.058	.077	.087	.103	.140	3959	80.9	29.6	67.2
Shenandoah Park, VA (SH2)	1987*	.003	.027	.040	.049	.059	.071	.077	.086	.145	2908	55.7	7.8	41.8
	1988	.006	.029	.042	.054	.064	.083	.095	.108	.145	4661	133.8	55.8	109.4

Table AX3-14 (cont'd). Seasonal (April-October) Percentiles, SUM06, SUM08, and W126 Values for the MCCP Sites

Site	Year	Min.	10	30	50	70 (ppm)	90	95	99	Max.	No. Obs.	SUM06	SUM08 (ppm-h)	W126
Shenandoah Park, VA (SH3)	1987	.000	.018	.029	.037	.047	.061	.068	.080	.108	3030	23.1	2.6	19.2
	1988	.000	.020	.031	.040	.051	.067	.076	.097	.135	4278	52.3	15.6	44.2
Whitetop Mountain, VA (WT1)	1987	0.01	.038	.051	.059	.066	.078	.085	.096	.111	4326	147.7	32.4	105.7
	1988	.000	.030	.046	.058	.068	.084	.094	.119	.163	3788	133.8	51.0	102.8

*Calculations based on a May-September season.

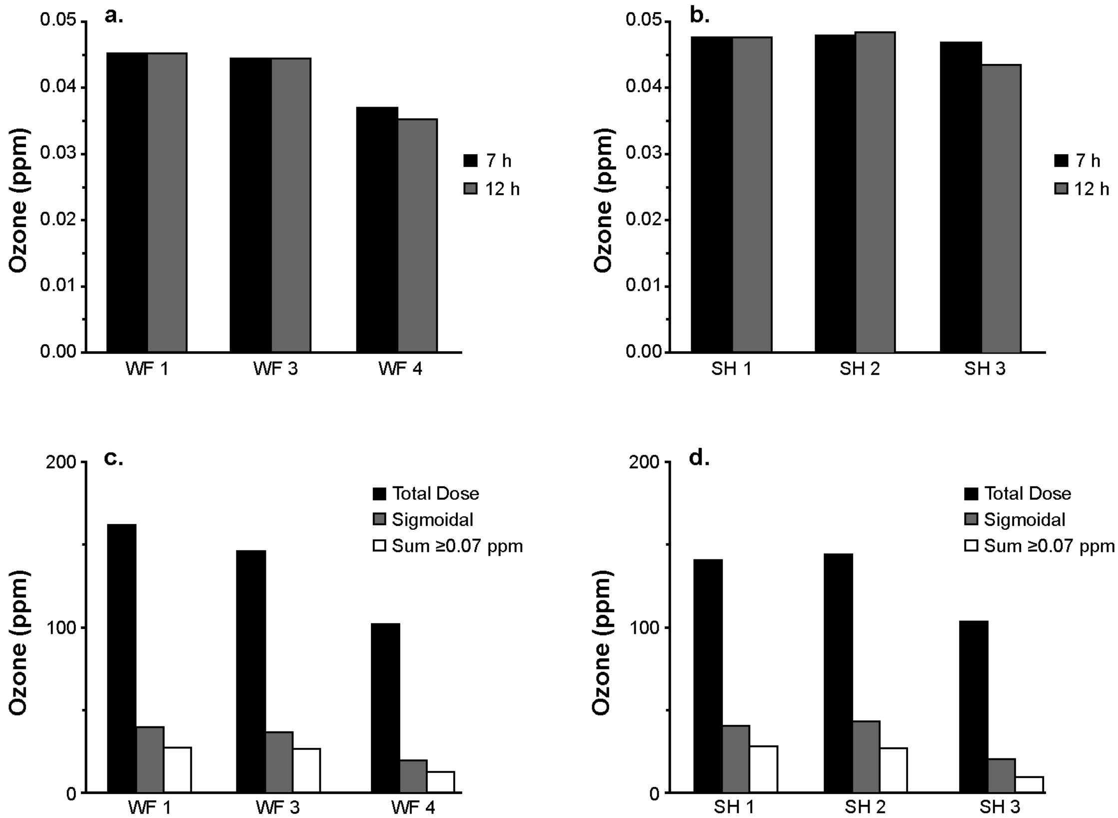

Figure AX3-45a-d. Seven- and 12-h seasonal means at (a) Whiteface Mountain and (b) Shenandoah National Park for May to September 1987, and integrated exposures at (c) Whiteface Mountain and (d) Shenandoah National Park for May to September 1987.

Source: Lefohn et al. (1990a).

When the Big Meadows, Dickey Ridge, and Sawmill Run, Shenandoah National Park, data for 1983 to 1987 were compared, it again was found that the 7-h and 12-h seasonal means were insensitive to the different O_3 exposure patterns. A better resolution of the differences was observed when the cumulative indices were used (Figure AX3-46). There was no evidence that the highest elevation site, Big Meadows, consistently had experienced higher O_3 exposures than the other sites. In 2 of the 5 years, the Big Meadows site experienced lower exposures than the Dickey Ridge and Sawmill Run sites, based on the sum of all concentration or sigmoidal indices. For 4 of the 5 years, the SUM07 index yielded the same result.

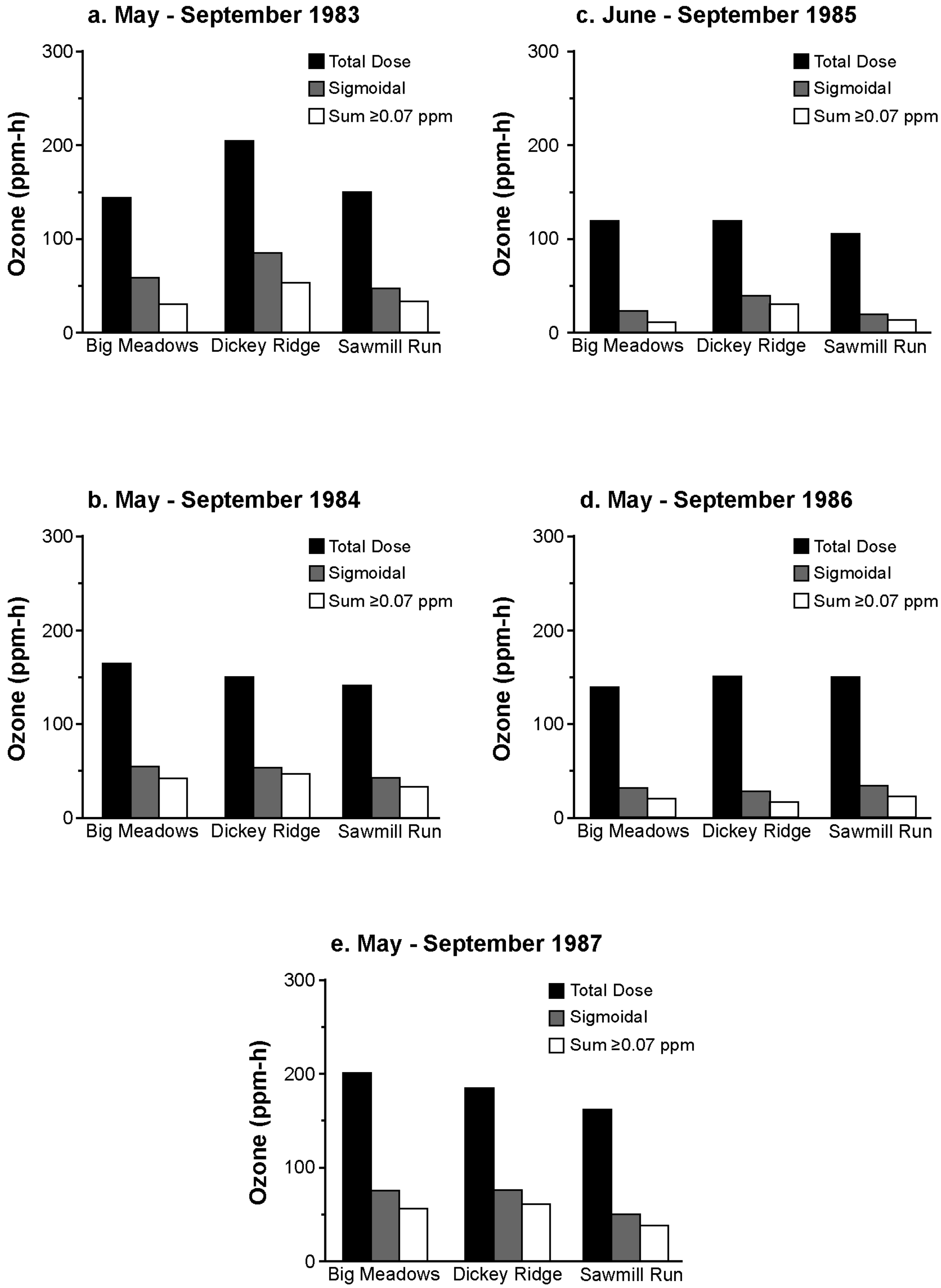

Figure AX3-46a-e. Integrated exposures for three non-Mountain Cloud Chemistry Program Shenandoah National Park sites, 1983 to 1987.

Source: Lefohn et al. (1990b).

Taylor et al. (1992) indicated that the forests they monitored experienced differences in O_3 exposure. The principal spatial factors underlying this variation were elevation, proximity to anthropogenic sources of oxidant precursors, regional-scale meteorological conditions, and airshed dynamics between the lower free troposphere and the surface boundary layer. Table AX3-15 summarizes the exposure values for the 10 EPRI Integrated Forest Study sites located in North America.

An important issue for assessing possible impacts of O_3 at high-elevation sites that requires further attention is the use of mixing ratios (e.g., parts per million) instead of absolute concentration (e.g., in units of micrograms per cubic meter) to describe O_3 concentration. In most cases, mixing ratios or mole fractions are used to describe O_3 concentrations. Lefohn et al. (1990b) pointed out that the manner in which concentration is reported may be important when assessing the potential impacts of air pollution on high-elevation forests. Concentration varies as a function of altitude. Although the change in concentration is small when the elevational difference between sea level and the monitoring site is small, it becomes substantial at high-elevation sites. Given the same part-per-million value experienced at both a high- and low-elevation site, the absolute concentrations (i.e., micrograms per cubic meter) at the two elevations will be different, because both O_3 and ambient air are gases, and changes in pressure directly affect their volume. According to Boyle's law, if the temperature of a gas is held constant, the volume occupied by the gas varies inversely with the pressure (i.e., as pressure decreases, volume increases). This pressure effect must be considered when measuring absolute pollutant concentrations. At any given sampling location, normal atmospheric pressure variations have very little effect on air pollutant measurements. However, when mass/volume units of concentration are used and pollutant concentrations measured at significantly different altitudes are compared, pressure (and, hence, volume) adjustments are necessary. In practice, the summit site at Whiteface Mountain had a slightly higher O_3 exposure than the two low-elevation sites (Lefohn et al., 1991). However, at Shenandoah National Park sites, the higher elevation site experienced lower exposures than lower elevation sites in some years.

These exposure considerations are trivial at low-elevation sites. However, when one compares exposure-effects results obtained at high-elevation sites with those from low-elevation sites, the differences may become significant (Lefohn et al., 1990b). In particular, assuming that the sensitivity of the biological target is identical at both low and high elevations, some

Table AX3-15. Summary Statistics for 11 Integrated Forest Study Sites[a]

Site	Year	Quarter	24-h	12-h	7-h	1-h Max.	SUM06 10^3 ppb-h	SUM08 10^3 ppb-h
HIGH ELEVATION SITES								
Whiteface Mtn, NY	1987	2	42	43	42	104	13.2	2.5
	1987	3	45	44	43	114	30.1	11.8
	1988	2	49	50	49	131	33.5	13.9
	1988	3	44	43	43	119	22.6	10.4
Great Smoky Mtns NP	1987	2	54	52	49	99	57.1	10.9
	1987	3	53	51	49	95	34.3	8.8
	1988	2	71	70	68	119	126.3	61.2
	1988	3	59	57	55	120	74.7	22.2
Coweeta Hydrologic Lab, NC	1987	2	50	48	47	85	32.4	2.6
	1987	3	47	44	42	95	24.1	2.4
	1988	2	61	59	59	104	81.6	18.5
	1988	3	57	54	51	100	63.6	19.8
LOW ELEVATION SITES								
Huntington Forest, NY	1987	2	36	42	42	88	9.8	0.9
	1987	3	24	32	33	76	5.4	0.2
	1988	2	40	46	46	106	19.2	6.1
	1988	3	37	46	48	91	18.6	2.7
Howland, ME	1987	2	34	39	39	69	1.9	0.0
	1987	3	26	32	31	76	3.8	0.0
	1988	2	36	41	41	90	8.1	2.9
	1988	3	24	30	30	71	1.7	0.0
Oak Ridge, TN	1987	2	42	53	50	112	39.5	13.5
	1987	3	29	44	41	105	24.3	9.0
	1988	2	40	57	58	104	26.4	9.8
	1988	3	32	47	51	122	19.7	7.7

Table AX3-15 (cont'd). Summary Statistics for 11 Integrated Forest Study Sites.[a]

Site	Year	Quarter	24-h	12-h	7-h	1-h Max.	SUM06 10^3 ppb-h	SUM08 10^3 ppb-h
LOW ELEVATION SITES (cont'd)								
Thompson Forest, WA	1987	2	36	43	41	103	10.7	3.6
	1987	3	30	36	34	94	10.3	2.1
	1988	2	32	39	37	103	8.1	2.3
	1988	3	32	39	36	140	13.5	6.7
B.F. Grant Forest, GA	1987	2	32	46	48	99	26.1	5.1
	1987	3	33	52	54	102	31.3	10.3
	1988	2	47	63	64	127	53.1	21.9
	1988	3	32	47	48	116	24.1	7.4
Gainesville, FL	1987	2	42	53	50	[b]	[b]	[b]
	1987	3	29	44	41	[b]	[b]	[b]
	1988	2	35	48	51	84	23.4	0.5
	1988	3	20	29	30	70	1.9	0.1
Duke Forest, NC	1987	2	38	48	52	100	29.2	7.8
	1987	3	52	59	50	124	[b]	[b]
	1988	2	54	69	75	115	[b]	[b]
	1988	3	38	51	54	141	52.9	23.4
Nordmoen, Norway	1987	2	32	40	41	75	2.4	0.0
	1987	3	14	18	20	32	0.0	0.0
	1988	2	22	28	29	53	0.0	0.0
	1988	3	11	15	16	30	0.0	0.0

[a]Concentration in ppb.
[b]Data were insufficient to calculate statistic.

Source: Taylor et al. (1992).

adjustment will be necessary when attempting to link experimental data obtained at low-elevation sites with air quality data monitored at the high-elevation stations. This topic is further discussed in Annex AX4 when considering effective dose considerations for predicting vegetation effects associated with O_3.

AX3.6 TRENDS IN OZONE CONCENTRATIONS

AX3.6.1 National Assessment of Trends

Ozone concentrations and, thus, exposure, change from year to year. During the period 1983 to 2002, extremely high O_3 levels occurred in 1983 and 1988 in some areas of the United States. These levels more than likely were attributable, in part, to hot, dry, stagnant conditions. However, the U.S. Environmental Protection Agency (2003b) reported that a downward national trend in 1-h and 8-h O_3 levels occurred, for the period 1983 to 2002, in most geographic areas in the country (Figures AX3-47 and AX3-48). These low levels may have been due to meteorological conditions that were less favorable for O_3 formation and to recently implemented control measures. On a national assessment basis, the U.S. Environmental Protection Agency (2003b) reported a 22% decrease in the second maximum 1-h average O_3 concentration for the period 1983 to 2002 and a 14% decrease for the annual fourth highest annual daily maximum concentration during the same 20-year period. The Northeast and Pacific Southwest exhibited the most substantial improvement for 1-h and 8-h O_3 levels. The Mid-Atlantic and North Central regions experienced minimal decreases in 8-h O_3 levels. In contrast, the Pacific Northwest region showed a slight increase in the 8-h O_3 over the period 1983 to 2002.

For the 10-year period of 1993 to 2002, the national trend in 8-h O_3 concentration shows a 4% increase and the national trend in 1-h O_3 shows a 2% decrease. However, standard statistical tests show that these trends were not statistically significant. Ozone concentrations varied slightly during this 10-year period but showed no real change overall.

AX3.6.2 Regional Trends

Regional trends provide additional information that can increase our understanding of the patterns of change of O_3 levels. Figures AX3-49 and AX3-50 illustrate the 20-year trend for both 1- and 8-h O_3, averaged across regional boundaries. For example, the trend in 8-h O_3

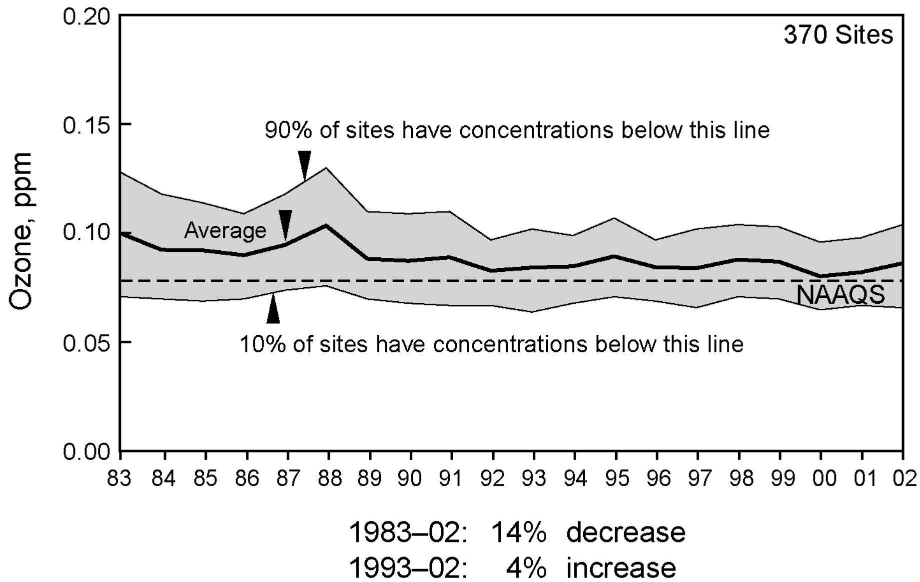

Figure AX3-47. Trends for 1983 to 2002 period for the annual second maximum 1-h average O_3 concentration.

Source: U.S. Environmental Protection Agency (2003b).

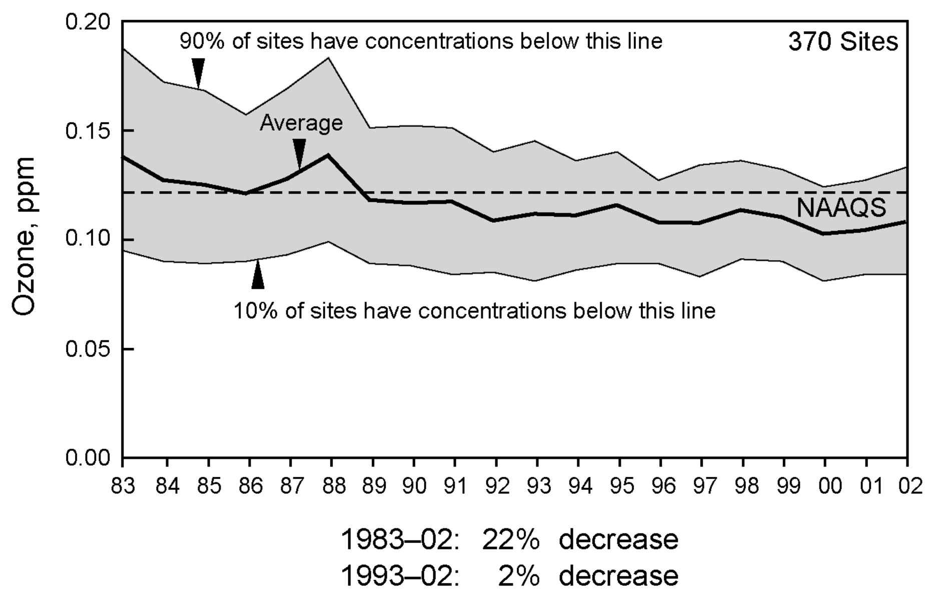

Figure AX3-48. Trends for 1983 to 2002 period for the annual fourth maximum 8-h average O_3 concentration.

Source: U.S. Environmental Protection Agency (2003b).

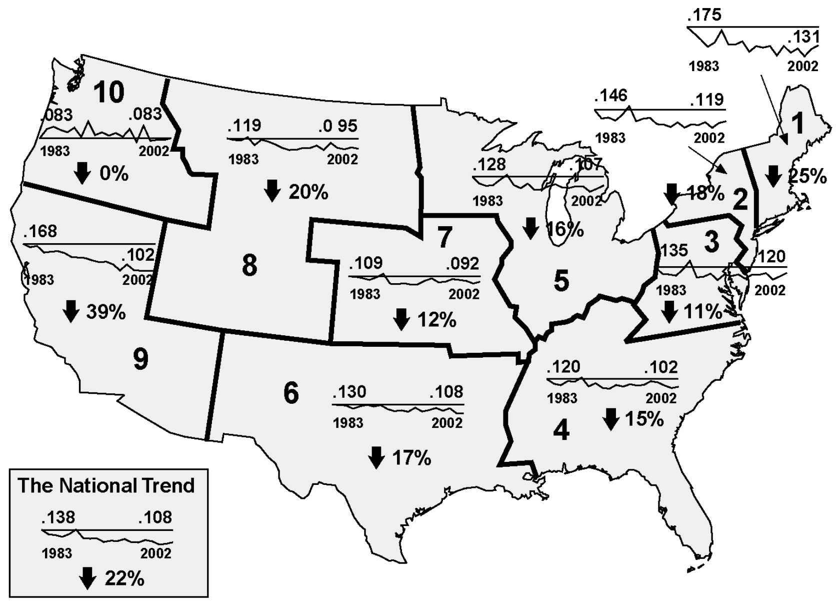

Figure AX3-49. Trend in 1-h O_3 level (based on annual second highest daily maximum concentration) for 1983 to 2002 averaged across EPA regional office boundaries.

Source: U.S. Environmental Protection Agency (2003b).

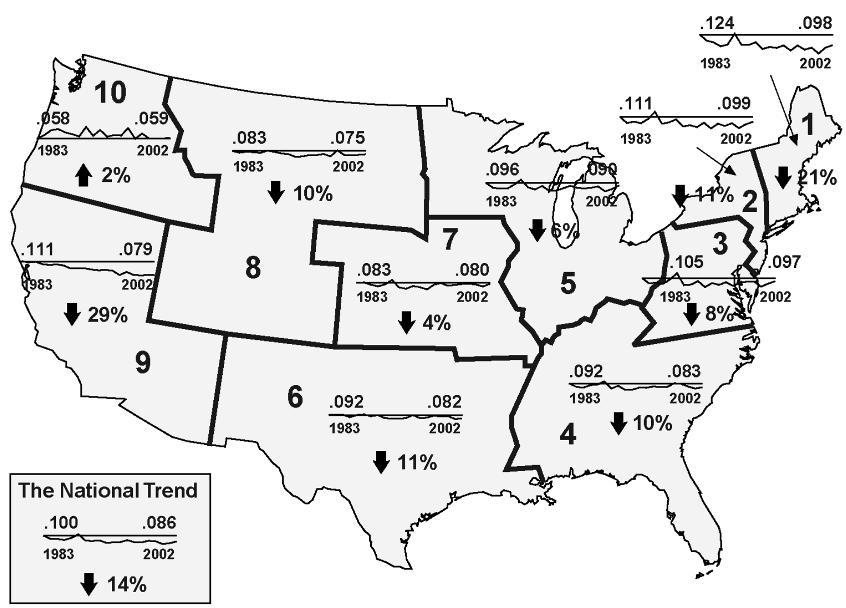

Figure AX3-50. Trend in 8-h O_3 level (based on annual fourth highest maximum concentration) for 1983 to 2002 averaged across EPA regional office boundaries.

Source: U.S. Environmental Protection Agency (2003b).

concentrations for the Pacific Southwest shows the 20-year trend (1983 to 2002) as a 29% decrease. When considering the Los Angeles area separately, the trend for Los Angeles shows a 49% decrease for the 20-year period, compared to a 15% decrease for other locations in the Pacific Southwest. For the 10-year period of 1993 to 2002, the Pacific Southwest has an overall 13% decrease in 8-h O_3. However, when considering Los Angeles separately, the Los Angeles area has a 28% decrease for the 10-year period, while the Pacific Southwest without Los Angeles has a 5% decrease. This illustrates that national assessments for O_3 do not describe trends completely, particularly where control measures such as those implemented in Los Angeles have had a significant effect in reducing O_3 concentrations (U.S. Environmental Protection Agency, 2003b).

It is important to note that year-to-year changes in ambient O_3 trends are influenced by meteorological conditions, population growth, and changes in emission levels of O_3 precursors (i.e.,VOCs and NO_x) resulting from ongoing control measures. For example, to further evaluate the 10-year 8-h O_3 trends, U.S. Environmental Protection Agency (2003b) applied a model to the annual rate of change in O_3 based on measurements in 53 metropolitan areas. This model adjusted the O_3 data in these areas to account for the influence of local meteorological conditions, including surface temperature and wind speed. Figure AX3-51 shows the aggregated trend in 8-h O_3 for these 53 areas adjusted for meteorological conditions for the 10-year period of 1993 to 2002. The figure also shows the aggregated trend for these areas unadjusted for meteorology as well as the national average in 8-h O_3. From this figure, the meteorologically adjusted trend for this 10-year period can be seen as relatively flat, which agrees with the pattern observed without applying meteorologically adjusted methods.

Furthermore, preliminary examination of meteorologically adjusted 8-h O_3 on a subregional basis in the eastern United States reveals a pattern of increasing O_3 through 1998, followed by a period of generally improving O_3 air quality. The U.S. Environmental Protection Agency (2003b) has attributed this reversal to the implementation of regional NO_x reductions from power plants.

Data from the EPA's AQS database were used to characterize the year-to-year variability in the fourth highest daily maximum 1-h concentration over 3 years for the period of 1980 to 2001 at specific monitoring sites located in several metropolitan areas across the United States. Figures AX3-52 through AX3-59 illustrate the reduction in the fourth highest daily maximum

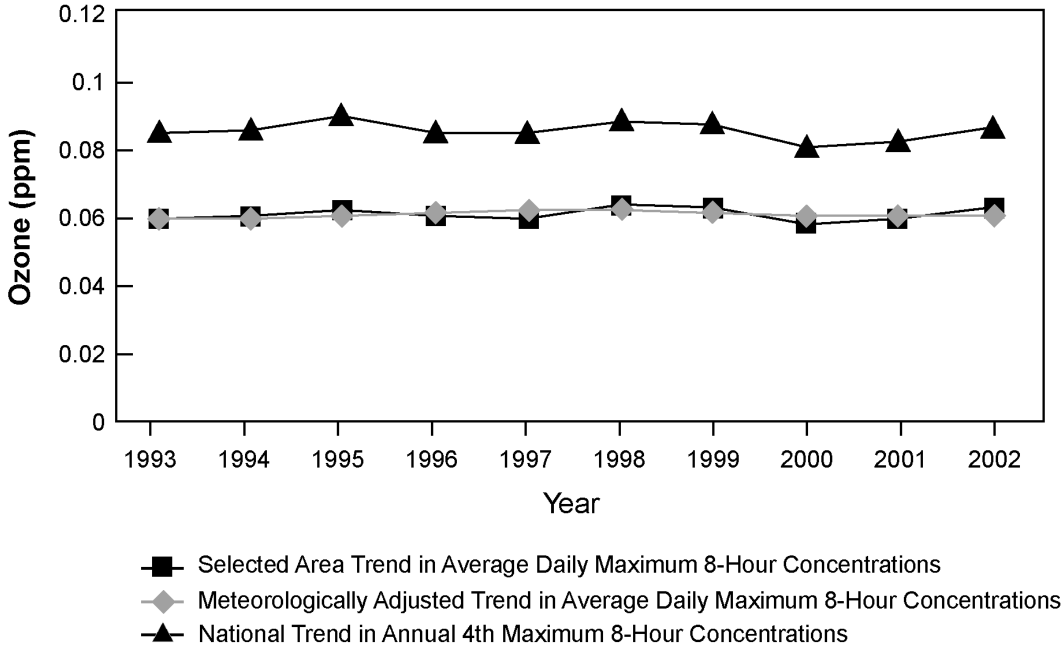

Figure AX3-51. Comparison of actual and meteorological adjusted 8-h O_3 trends for the period 1993 to 2003.

Source: U.S. Environmental Protection Agency (2003b).

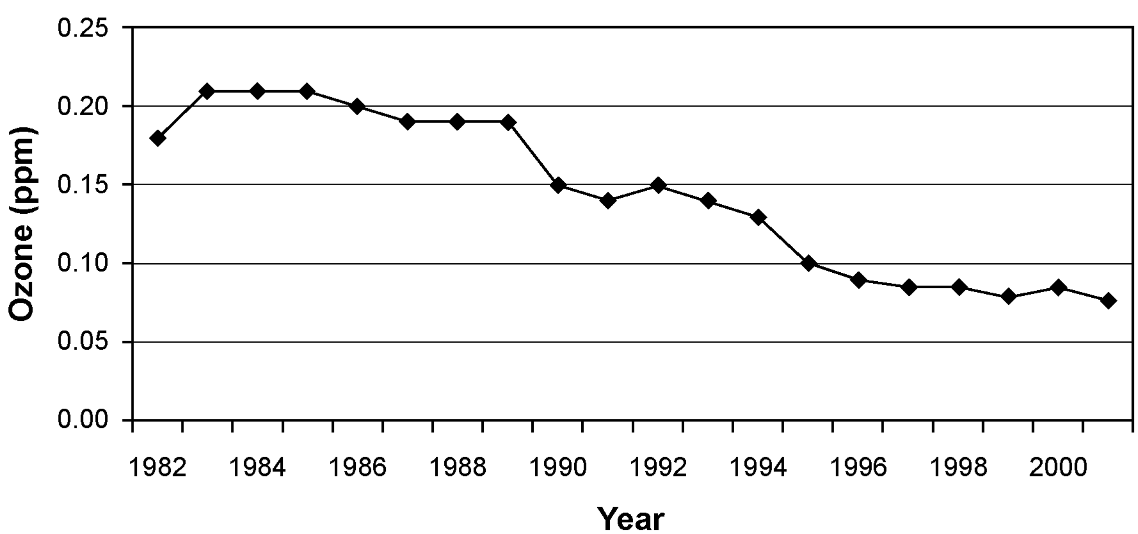

Figure AX3-52. Trend in the 4th highest daily maximum 1-h O_3 concentration over 3 years for the period of 1980 to 2001 for a monitoring site in Los Angeles, CA (060371301).

Source: U.S. Environmental Protection Agency (2003a).

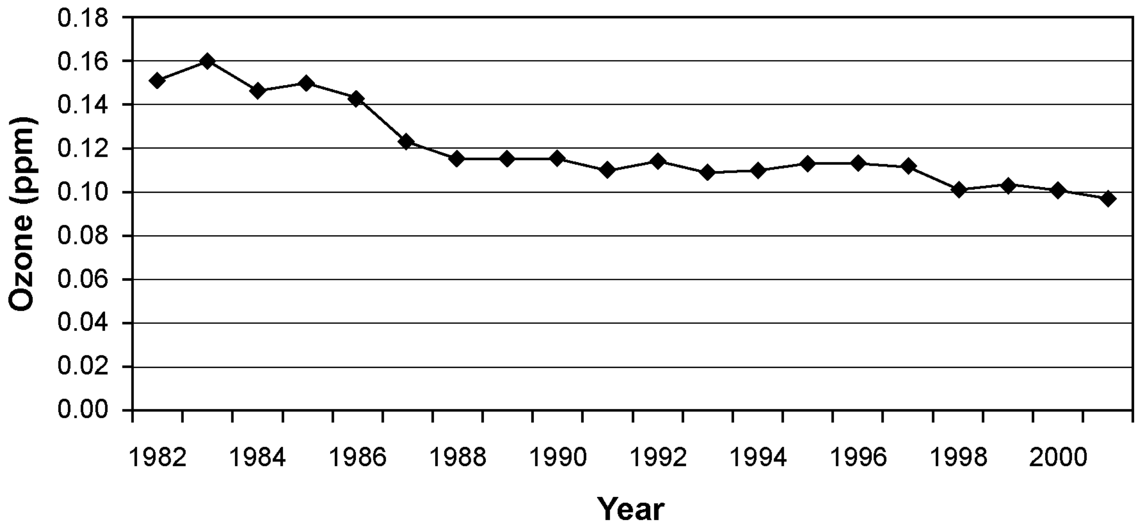

Figure AX3-53. Trend in the 4th highest daily maximum 1-h O_3 concentration over 3 years for the period of 1980 to 2001 for a monitoring site in Phoenix, AZ (040133002).

Source: U.S. Environmental Protection Agency (2003a).

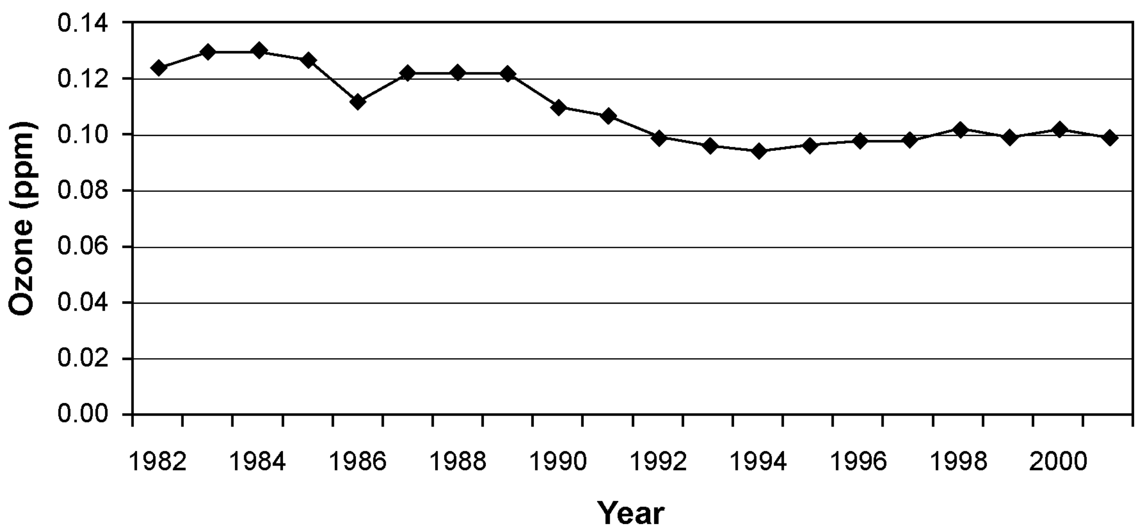

Figure AX3-54. Trend in the 4th highest daily maximum 1-h O_3 concentration over 3 years for the period of 1980 to 2001 for a monitoring site in Denver, CO (080590002).

Source: U.S. Environmental Protection Agency (2003a).

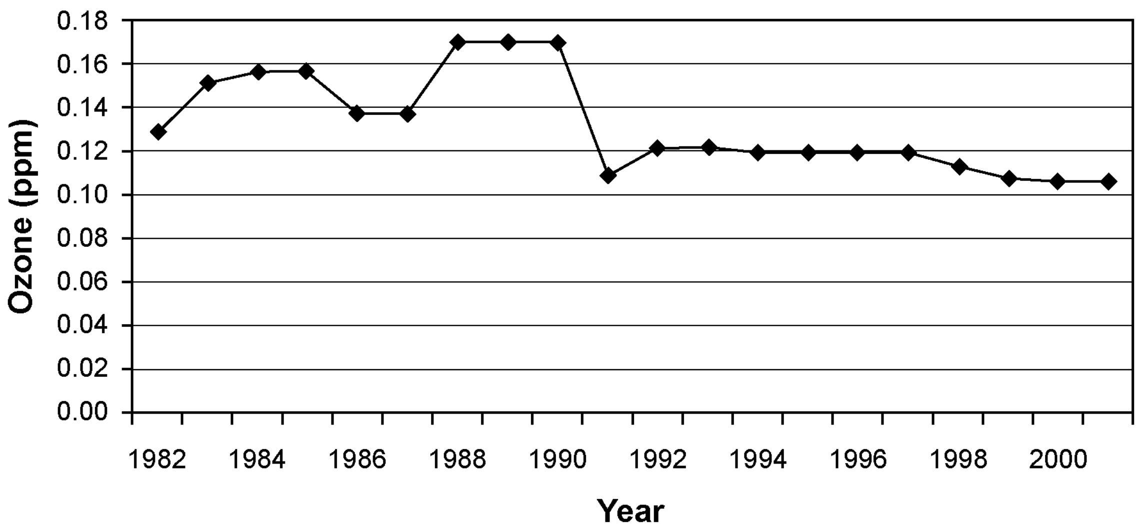

Figure AX3-55. Trend in the 4th highest daily maximum 1-h O_3 concentration over 3 years for the period of 1980 to 2001 for a monitoring site in Chicago, IL (170317002).

Source: U.S. Environmental Protection Agency (2003a).

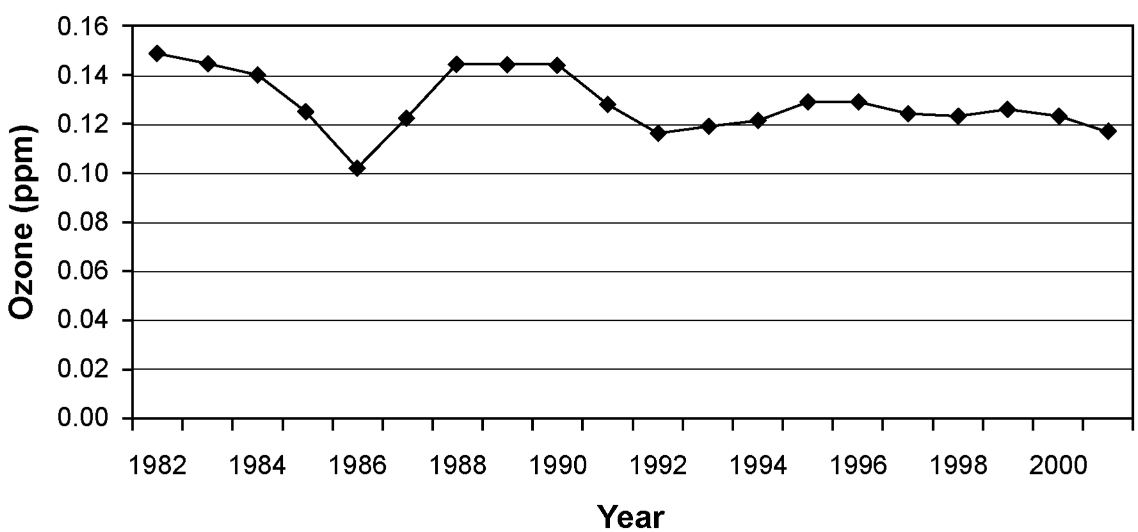

Figure AX3-56. Trend in the 4th highest daily maximum 1-h O_3 concentration over 3 years for the period of 1980 to 2001 for a monitoring site in Detroit, MI (260990009).

Source: U.S. Environmental Protection Agency (2003a).

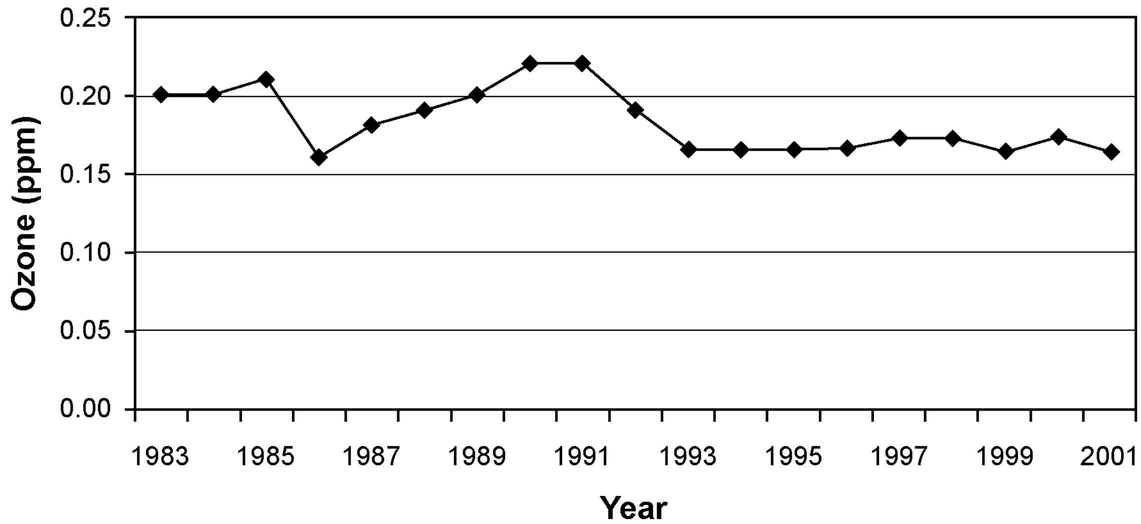

Figure AX3-57. Trend in the 4th highest daily maximum 1-h O_3 concentration over 3 years for the period of 1980 to 2001 for a monitoring site in Houston, TX (482011037).

Source: U.S. Environmental Protection Agency (2003a).

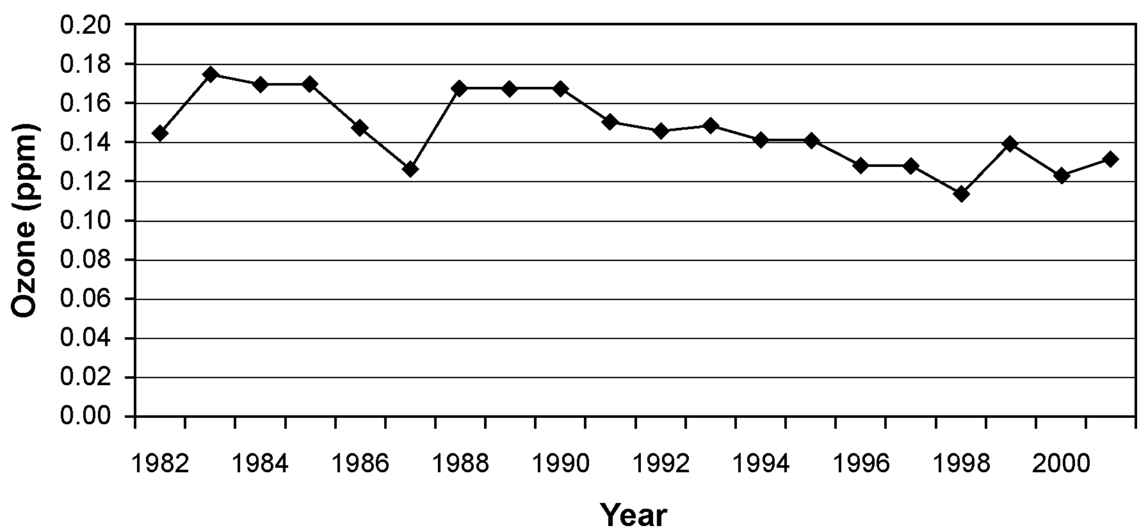

Figure AX3-58. Trend in the 4th highest daily maximum 8-h O_3 concentration averaged over 3 years for the period of 1980 to 2001 for a monitoring site in Fairfield, CN (090013007).

Source: U.S. Environmental Protection Agency (2003a).

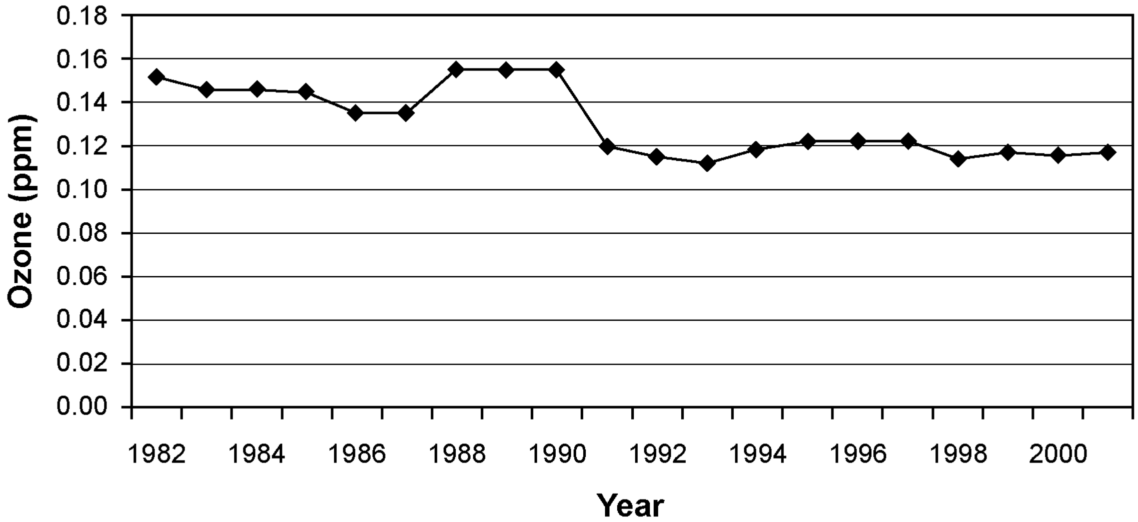

Figure AX3-59. Trend in the 4th highest daily maximum 8-h O_3 concentration averaged over 3 years for the period of 1980 to 2001 for a monitoring site in Washington, DC (110010025).

Source: U.S. Environmental Protection Agency (2003a).

1-h concentration over 3 years for monitoring sites in Los Angeles, California; Phoenix, Arizona; Denver, Colorado; Chicago, Illinois; Detroit, Michigan; Houston, Texas; Fairfield, Connecticut; and Washington, D.C. Figures AX3-60 through AX3-67 illustrate the trends using the fourth highest daily maximum 8-h concentration averaged over 3 years for the same monitoring sites for the same period of time.

As described in Section AX3.6.1, the U.S. Environmental Protection Agency (2003b), on a national assessment basis, reported a 22% decrease in the second maximum 1-h average concentration for the period of 1983 to 2002 and a nonsignificant decrease of 2% for the period of 1993 to 2002. For the annual fourth highest daily maximum 8-h concentration, the U.S. Environmental Protection Agency (2003b) reported a 14% decrease for the period 1983 to 2002 and a nonsignificant increase of 4% for the 10-year period 1993 to 2002. The implication of these figures is that a slowing of improvement has occurred, which is illustrated for many of the monitoring sites described in Figures AX3-52 through AX3-67 for both the fourth highest daily maximum 1-h concentration over 3 years and the fourth highest daily maximum 8-h concentration averaged over 3 years.

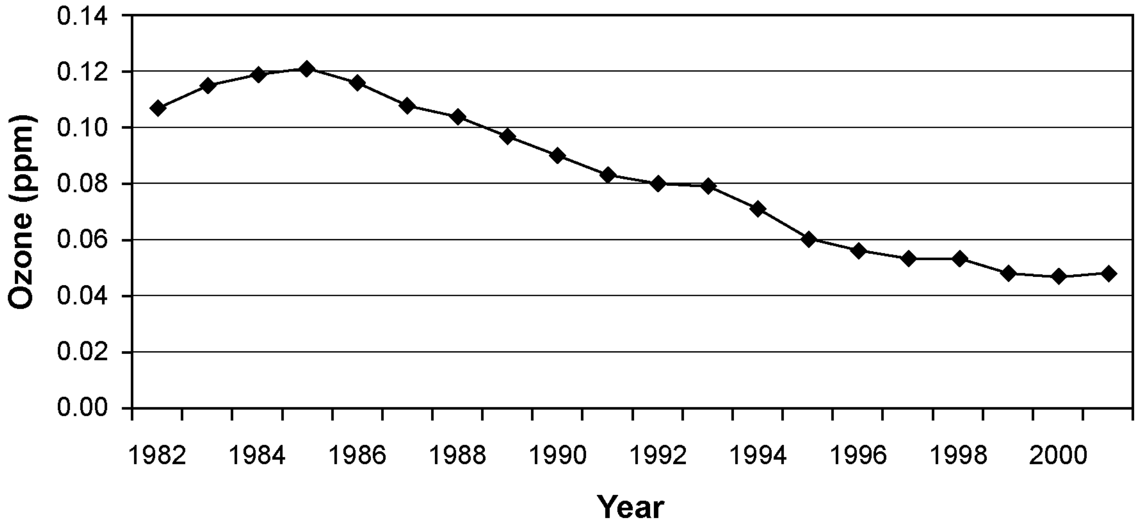

Figure AX3-60. Trend in the 4th highest daily maximum 8-h O_3 concentration averaged over 3 years for the period of 1980 to 2001 for a monitoring site in Los Angeles, CA (060371301).

Source: U.S. Environmental Protection Agency (2003a).

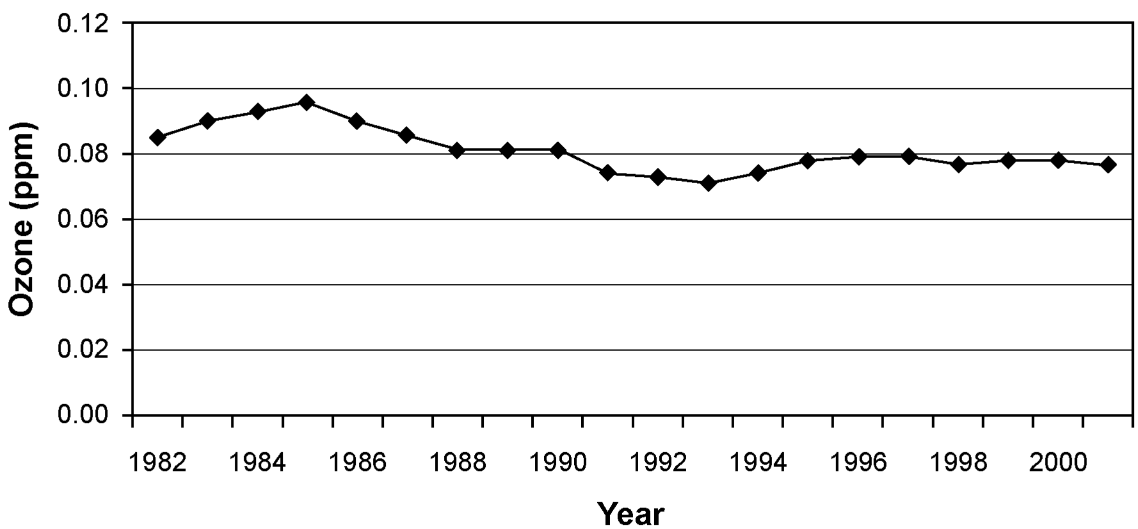

Figure AX3-61. Trend in the 4th highest daily maximum 8-h O_3 concentration averaged over 3 years for the period of 1980 to 2001 for a monitoring site in Phoenix, AZ (040133002).

Source: U.S. Environmental Protection Agency (2003a).

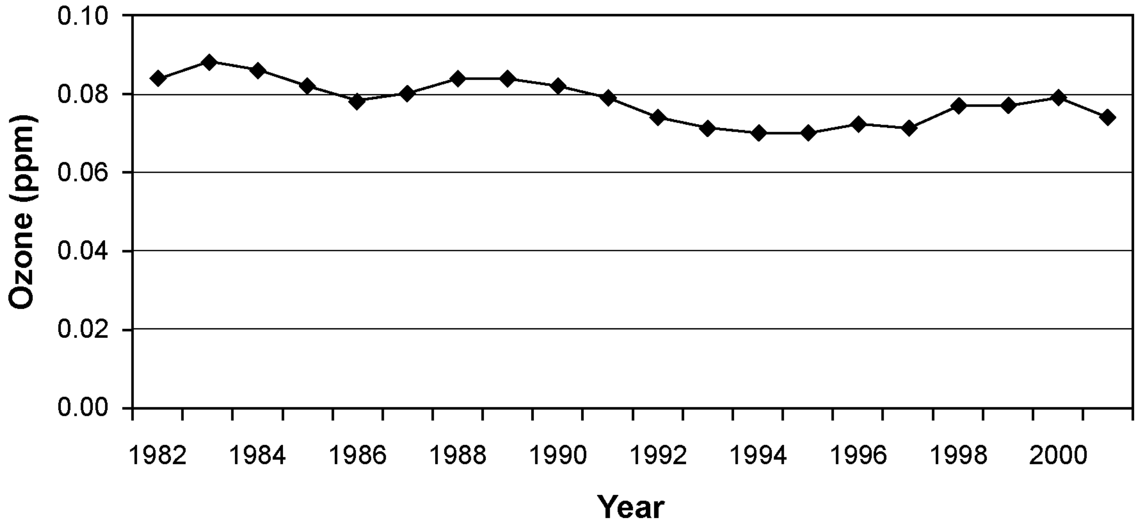

Figure AX3-62. Trend in the 4th highest daily maximum 8-h O_3 concentration averaged over 3 years for the period of 1980 to 2001 for a monitoring site in Denver, CO (080590002).

Source: U.S. Environmental Protection Agency (2003a).

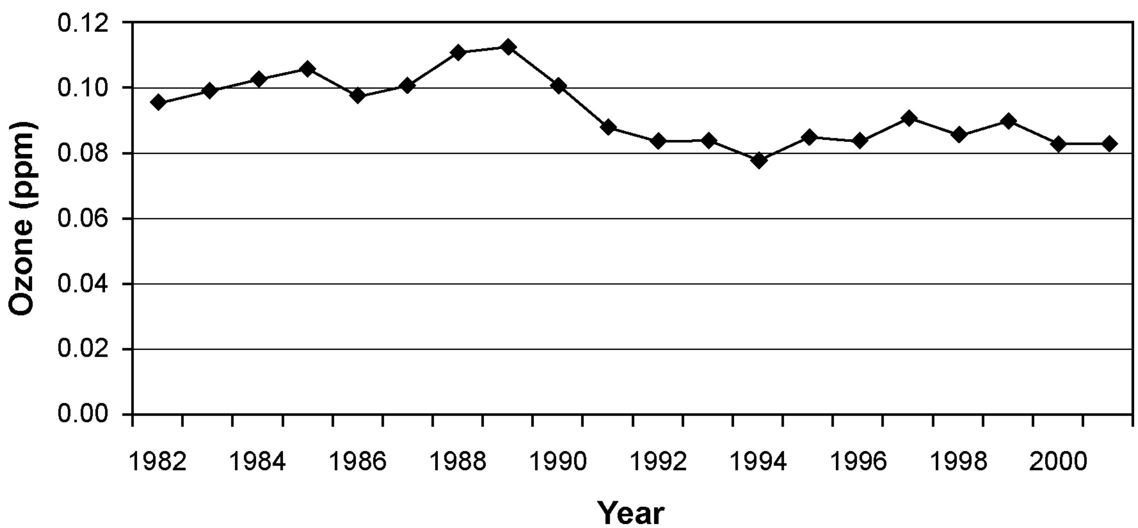

Figure AX3-63. Trend in the 4th highest daily maximum 8-h O_3 concentration averaged over 3 years for the period in 1980 to 2001 for a monitoring site in Chicago, IL (170317002).

Source: U.S. Environmental Protection Agency (2003a).

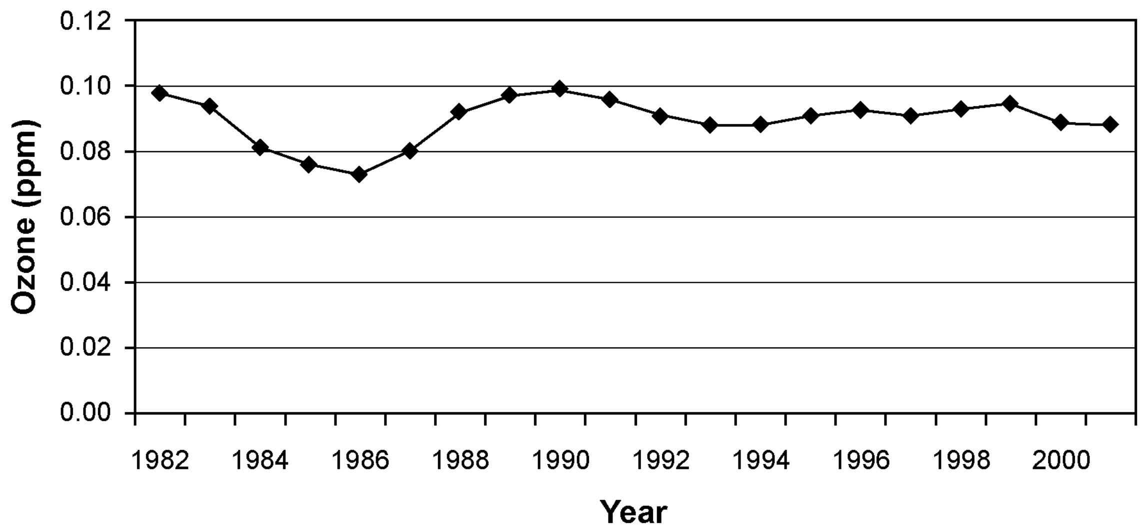

Figure AX3-64. Trend in the 4th highest daily maximum 8-h O_3 concentration averaged over 3 years for the period of 1980 to 2001 for a monitoring site in Detroit, MI (260990009).

Source: U.S. Environmental Protection Agency (2003a).

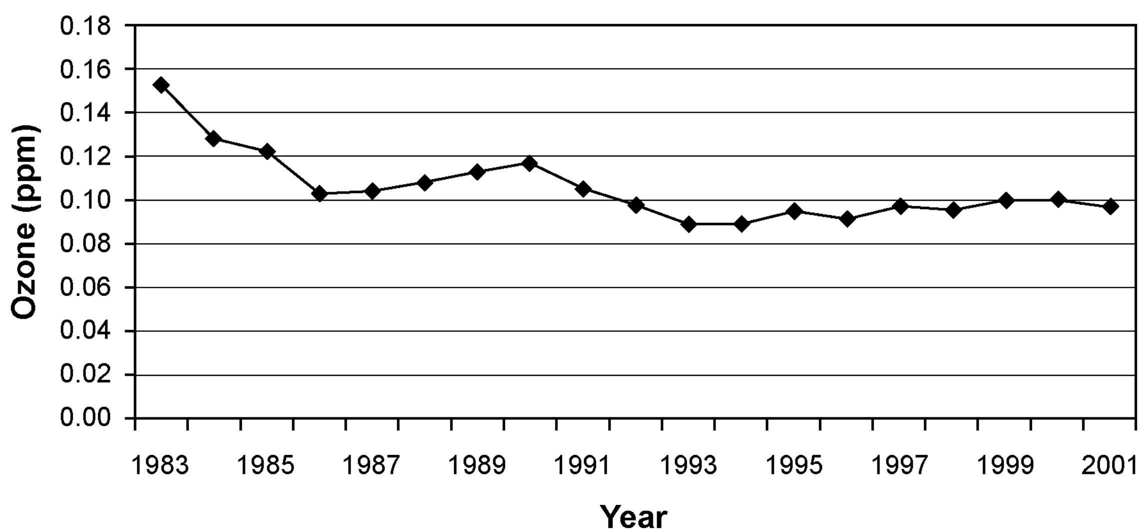

Figure AX3-65. Trend in the 4th highest daily maximum 8-h O_3 concentration averaged over 3 years for the period of 1980 to 2001 for a monitoring site in Houston, TX (482011037).

Source: U.S. Environmental Protection Agency (2003a).

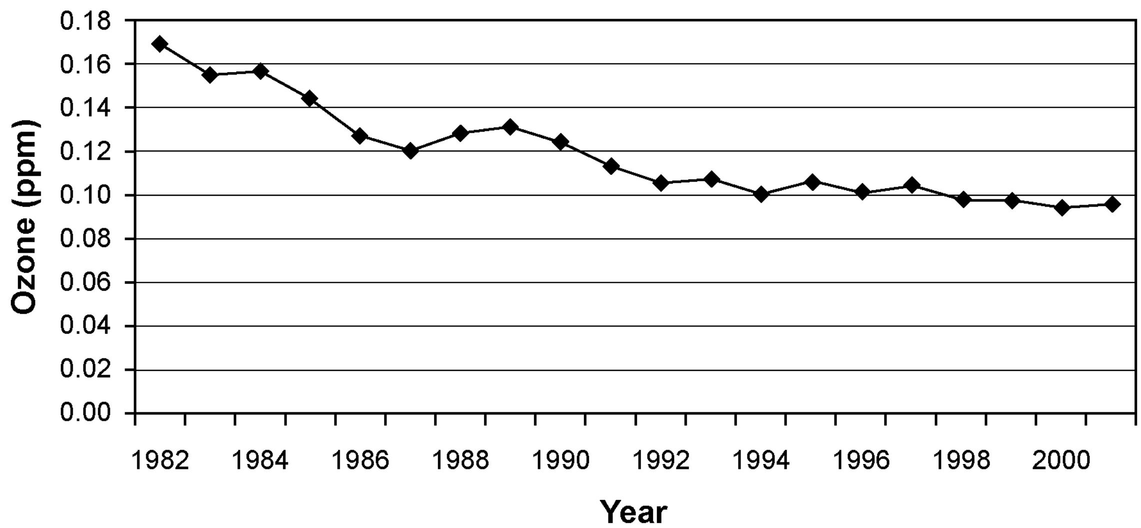

Figure AX3-66. Trend in the 4th highest daily maximum 8-h O_3 concentration averaged over 3 years for the period of 1980 to 2001 for a monitoring site in Fairfield, CN (090013007).

Source: U.S. Environmental Protection Agency (2003a).

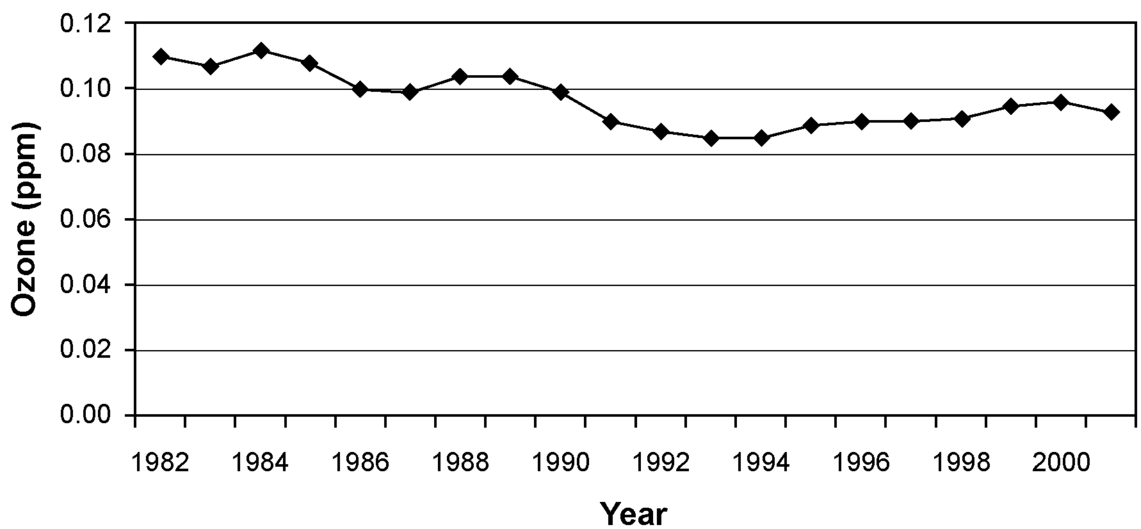

Figure AX3-67. Trend in the 4th highest daily maximum 8-h O_3 concentration averaged over 3 years for the period of 1980 to 2001 for a monitoring site in Washington, DC (110010025).

Source: U.S. Environmental Protection Agency (2003a).

AX3.6.3 Disproportionate Reductions in Hourly Average Concentrations

Figure AX3-68 shows that the higher hourly average concentrations (i.e., > 0.09 ppm) decreased at a faster rate (i.e., at a greater negative rate per year) than the hourly average concentrations in the mid-level range. The numbers of hourly average concentrations in the low end of the distribution also decreased. The result was that, in some cases, the hourly average concentrations in the 0.030 to 0.050 ppm range increased as the peak hourly average concentrations were reduced. Apparently, both the high and low ends of the distribution were moving toward the center of the distribution of the hourly average concentrations.

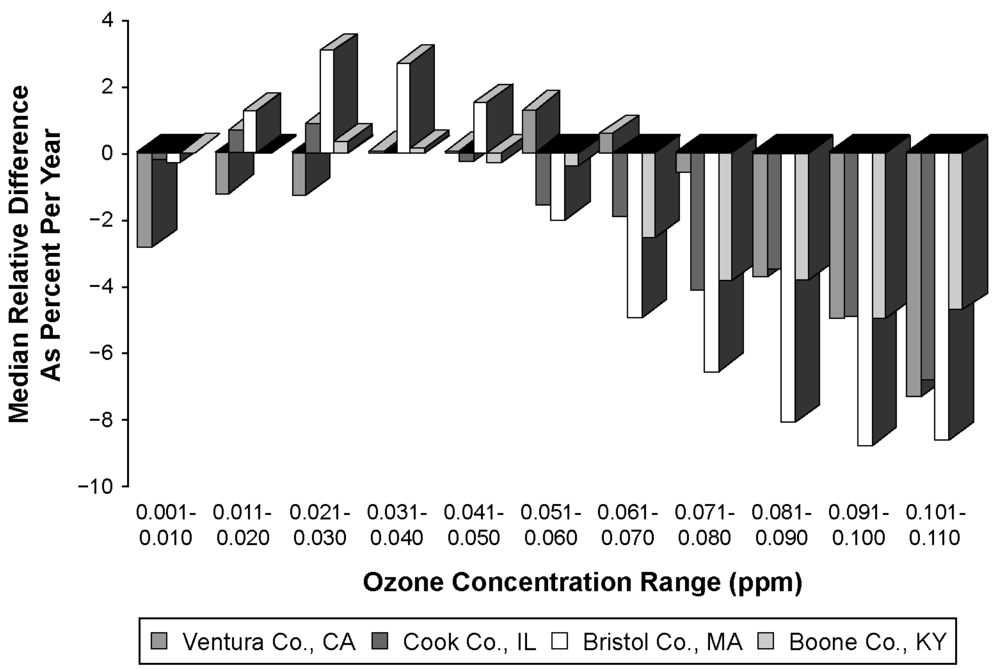

Figure AX3-68. Changes in the distribution of hourly average O_3 concentrations over time for monitoring sites in Ventura County (CA), Cook County (IL), Bristol County (MA), and Boone County (KY).

Source: Adopted from Lefohn et al. (1998).

Lefohn et al. (1998) have commented on the slowing of the rate of decline in monitoring sites that were experiencing statistically significant reductions. The authors identified those sites that demonstrated a significant reduction in O_3 levels for the period of 1980 to 1995. Using data from the sites that experienced reduced O_3 levels over this period of time, the researchers investigated whether the rate of decline of the mid-level hourly average O_3 concentrations (0.06 to 0.099 ppm) was similar to the rate experienced by the high hourly average concentrations ($\geq$ 0.10 ppm). Lefohn et al. (1998) reported that there was a greater resistance to reducing the hourly average concentrations in the mid-range than the hourly average concentrations at the higher concentration range.

Information in the literature provides some indication that the higher concentrations may be reduced at a faster rate than the lower concentrations. The U.S. Environmental Protection Agency (1985) reported that the application of the first-generation regional oxidant model resulted in emissions controls reducing peak concentrations by considerably larger percentages than median or mean concentration values. The emissions controls had no significant effect on concentrations below approximately the 90th percentile value (i.e., 0.080 to 0.090 ppm in the summer and approximately 0.070 ppm in the spring). Roselle and Schere (1995) described similar observations. The U.S. Environmental Protection Agency (1997) noted in its examination of air quality over the last 25 years that, for sites that historically showed improvements, somewhat larger reductions occurred at the higher hourly average concentrations than at the middle or lower values. Yeng and Miller (2002) analyzed monitoring data from 10 stations in Connecticut for the period of 1981 to 1997. The authors noted that emissions reductions in the area had been successful in reducing the hourly O_3 average concentrations but that the lower values actually increased as emissions reductions occurred. Yeng and Miller (2002) concluded that the resistance to reducing the mid-level concentrations was related to a combination of natural factors and area-wide background concentrations of precursors from nonpoint anthropogenic sources. Likewise, Bravo et al. (2003) have reported that the higher hourly average concentrations were reduced at a faster rate than the mid-level values when surface O_3 concentrations in Mexico City were reduced.

Using models, several investigators have commented on the difficulty in reducing the mid-level hourly average O_3 concentrations while reducing the fourth highest 8-h average daily maximum concentration. Saylor et al. (1999) noted that for the Atlanta, GA area, NO_x emissions reductions greater than 60 to 75% would be required to reduce the mid-level hourly average concentrations. Similarly, Winner and Cass (2000) noted that the higher hourly average concentrations were reduced much faster than the mid-level values during simulation modeling for the Los Angeles area. Reynolds et al. (2003, 2004) analyzed ambient O_3 concentrations used in conjunction with the application of photochemical modeling to determine the technical feasibility of reducing hourly average concentrations in central California in the eastern United States. Various combinations of VOC and NO_x emission reductions were effective in lowering modeled peak 1-h O_3 concentrations. However, VOC emissions reductions were found to have only a modest impact on modeled peak 8-h O_3 concentrations. Reynolds et al. (2003) reported that 70 to 90% NO_x emissions reductions were required to reduce peak 8-h O_3 concentrations to the desired level in central California. Anthropogenic NO_x emissions reductions of 46 to 86% of 1996 base case values were needed to reach the desired level of the 8-h value in some areas in the eastern United States (Reynolds et al., 2004).

Reynolds et al. (2003, 2004) commented on possible chemical explanations for the observation that more prominent trends in peak 1-h O_3 levels than in peak 8-h O_3 concentrations or in occurrences of mid-level (i.e., 0.06 to 0.09 ppm) concentrations have been reported. The authors noted that when anthropogenic VOC and NO_x emissions are reduced significantly, the primary sources of O_3 precursors are biogenic emissions and CO from anthropogenic sources. Chemical process analysis results indicated that a slowly reacting pollutant such as CO could be contributing on the order of 10 to 20% of the O_3 produced. The authors recommended that further work focus on the need to confirm that biogenic emissions have not been significantly overestimated in the most recent emission inventories and on the examination of the effects of CO reductions. Several investigators have proposed that the effect of Asian emissions on surface O_3 concentrations might be responsible for explaining the ineffectiveness of the emissions reductions affecting the mid-level concentrations (Jacob et al., 1999; Lin et al., 2000; Jaffe et al., 2003; Vingarzan and Taylor, 2003). However, as described in Section AX3.2.3, inconsistent trends results using data collected at RRMS in the western United States do not indicate that either the low or the high end of the hourly average concentration distributions are increasing and, thus, the effect of Asian emissions on surface O_3 concentrations in the western United States is not clear at this time.

AX3.6.4 Trends in National Parks in the United States

The U.S. Environmental Protection Agency (2003b) reported that 28 of the national parks in the United States had sufficient O_3 trend data for the 10-year period of 1993 to 2002. Seven monitoring sites in five of these parks experienced statistically significant upward trends in 8-h O_3 levels: Great Smoky Mountains (TN), Craters of the Moon (ID), Mesa Verde (CO), Denali (AK), and Acadia (ME). Monitoring data for one park showed statistically significant improvements over the same time period: Saguaro (AZ). For the remaining 22 parks with O_3 trends data, the 8-h O_3 levels at 13 parks increased only slightly between 1993 and 2002, while five parks showed decreasing levels and 4 parks were unchanged.

Air quality in our national parks is important for both human health and welfare (e.g., vegetation) considerations. As noted, the U.S. Environmental Protection Agency (2003b), using 10 years of data and the fourth highest 8-h average of the daily maximum O_3 concentration, has characterized the trending in our national parks. As indicated in the U.S. Environmental Protection Agency (2003b) results, using different exposure indices (e.g., 1-h and 8-h values), different trending results occur. Using all available data for the national parks, an additional analysis of the hourly average concentration data was performed to characterize the trending using the (a) seasonal W126 and SUM06 cumulative exposure indices, (b) fourth highest of the 1-h daily maximum average concentrations over a 3-year period for January to December, and (c) running 3-year average of the annual fourth highest daily maximum 8-h average concentration.

For the seasonal (April to October) W126 and SUM06 exposure indices, all available data were used. At the time of the analysis, in most cases National Park Service data were available for the period of 1988 to 2001. However, a few of the monitoring sites had data that began in 1981. At least 75% of the data had to be available for each year over the 7-month season (April to October) for a site to be included in the analysis. The Kendall's K statistic (Mann-Kendall test) was used to identify linear trends as described in Lefohn and Shadwick (1991). Estimates of the rate of change (Sen estimate of the slope) for the index were calculated. Table AX3-16 summarizes the results of the analysis. Caution is urged in interpreting the table. The use of the significance levels of 0.2, 0.1, and 0.05 indicates varying levels of uncertainty. As indicated above, the use of a specific exposure index (e.g., 8-h average concentration) will provide a different trending pattern than the use of an alternative index, such as the W126 or SUM06 cumulative exposure index. Both the 1-h and 8-h indices are extreme value metrics that focus on the highest levels in the distribution of the hourly average concentrations. On the other hand, the W126 and SUM06 exposure indices accumulate the hourly average concentrations mainly in the

Table AX3-16. Trends at National Parks in the United States (1981 to 2001 or available data period)

Site	AIRS ID	W126 (Seasonal)	SUM06 (Seasonal)	8-h (Annual)	1-h (Annual)
Acadia NP	230090003	NS	NS	NS	NS
Acadia NP ACAD	230090101	NS	NS	*(−)	***(−)
Acadia NP Cadillac Mountain	230090102			*(+)	NS
Acadia NP MARS/PRIMENet Site	230090103	NS	NS	NS	**(−)
Big Bend NP BIBE	480430101	NS	NS	NS	NS
Brigantine (FWS) BRIG	340010005	***(−)	***(−)	***(−)	***(−)
Canyonlands NP CANY	490370101	***(+)	***(+)	*(+)	**(+)
Cape Cod NS CACO	250010002	NS	NS	NS	***(−)
Cape Romain (FWS) CARO	450190046	NS	NS	NS	NS
Chamizal NMEM CHAM	481410044	***(+)	**(+)	NS	NS
Channel Islands NP CHIS	060832012	NS	NS	NS	***(−)
Chiricahua NM (NDDN CNM167)	040038001	NS	*(+)	NS	**(−)
Congaree Swamp NM COSW	450791006	NS	NS	*(−)	*(−)
Cowpens NB COWP	450210002	*(+)	*(+)	NS	*(+)
Craters of the Moon NM CRMO	160230101	*(+)	NS	***(+)	NS
Death Valley NP DEVA	060270101	NS	NS	NS	NS
Denali NP DENA	022900003	NS	NS	*(+)	NS
Everglades NP EVER	120250030	NS	NS	NS	*(−)
Glacier NP (NDDN GNP168) GLAC	300298001	NS	NS	NS	NS
Great Basin NP GRBA	320330101	**(+)	*(+)	NS	NS

Table AX3-16 (cont'd). Trends at National Parks in the United States (1981 to 2001 or available data period)

Site	AIRS ID	W126 (Seasonal)	SUM06 (Seasonal)	8-h (Annual)	1-h (Annual)
Grand Canyon NP (NDDN GCN174)	040058001	NS	*(+)	NS	NS
Great Smoky Mountains NP (Cades Cove) GSCC	470090102	NS	NS	NS	
Great Smoky Mountains NP (Clingmans Dome) GSCD	471550102			NS	NS
Great Smoky Mountains NP (Cove Mountain) GSCM	471550101	**(+)	**(+)	***(+)	***(+)
Great Smoky Mountains NP (Look Rock) GSLR	470090101	***(+)	**(+)	NS	***(+)
Hawaii Volcanoes NP HAVO	150010005			NS	NS
Joshua Tree NP	060719002	***(−)	*(−)	***(−)	***(−)
Lassen Volcanic NP LAVO	060893003	**(+)	NS	NS	NS
Mammoth Cave NP MACA	210610500	NS	NS	**(−)	NS
Mammoth Cave NP MACA	210610501	NS	NS	*(−)	**(−)
Mesa Verde NP MEVE	080830101	**(+)	*(+)	NS	***(+)
Mount Rainier NP MORA	530531010	NS	NS	NS	NS
North Cascade NP NOCA	530570013	NS	NS	NS	**(+)
Olympic NP OLYM	530090012	NS	NS	NS	*(−)
Petrified Forest NP PEFO	040010012	NS	NS	NS	***(+)
Pinnacles NM PINN	060690003	*(−)	**(−)	**(−)	***(−)
Rocky Mountain NP ROMO	080690007	***(+)	***(+)	NS	*(+)
Saguaro NM SAGU	040190021	NS	NS	NS	**(−)
Sequoia/Kings Canyon NPs (Ash Mountain) SEAM	061070005	***(−)	***(−)	NS	NS
Sequoia/Kings Canyon NPs (Lookout Point) SELP	061070008			NS	NS

Table AX3-16 (cont'd). Trends at National Parks in the United States (1981 to 2001 or available data period)

Site	AIRS ID	W126 (Seasonal)	SUM06 (Seasonal)	8-h (Annual)	1-h (Annual)
Sequoia/Kings Canyon NPs (Lower Kaweah) SELK	061070006	NS	NS	NS	NS
Shenandoah NP (Big Meadows) SVBM	511130003	NS	NS	NS	***(+)
Voyageurs NP VOYA	271370034	**(−)	**(−)	*(−)	***(−)
Yellowstone NP YELL	560391010	NS	NS	NS	NS
Yellowstone NP YELL	560391011	NS	NS	NS	**(+)
Yosemite NP (Camp Mather) YOCM	061090004			*(+)	***(0)
Yosemite NP (Turtleback Dome) YOTD	060430003	NS	NS	***(−)	***(−)
Yosemite NP (Wawona Valley) YOWV	060430004	*(−)	*(−)	***(−)	**(−)

* 0.20 level of significance
** 0.10 level of significance
*** 0.05 level of significance
NS Not significant

W126 (seasonal) is the cumulative W126 exposure (as described by Lefohn and Runeckles [1987]) over a 24-h period for the period of April to October.
SUM06 (seasonal) is the cumulative exposure of hourly average concentrations ≥ 0.06 ppm over a 24-h period for the period of April to October.
8-h (annual) is the 3-year average of the annual fourth highest 8-h daily maximum average concentration for the period of January to December.
1-h (annual) is the fourth highest 1-h daily maximum average concentration over a 3-year period for January to December.

middle level of the distribution to the highest values. Changes in the magnitude of the extreme value statistics may or may not necessarily imply a change in the entire distribution of the hourly average concentrations. Thus, in interpreting Table AX3-16, it is suggested that, for a specific monitoring site, the pattern of trending for all four metrics be evaluated. In addition, because of the variability in the number of years when valid data were available, focus should be on the 0.05 level of significance. For example, Joshua Tree National Park in California shows a pattern where three of the four exposure metrics show a decrease trend in O_3 levels at the 0.05 level of significance. Clearly, one would suspect that a strong trend is occurring at this site. Alternatively, Yellowstone National Park in Wyoming shows no significant change using three of the four metrics, while the 1-h index showed an increase at the 0.10 level of significance. The trend at this site should be watched over the next several years to observe whether the statistical significance levels of the metrics increase.

AX3.7 RELATIONS BETWEEN OZONE, OTHER OXIDANTS, AND OXIDATION PRODUCTS

Tabulations of measurements of PAN and peroxypropionyl nitrate (PPN, $CH_3CH_2C(O)OONO_2$) concentrations were given in the 1996 O_3 AQCD (U.S. Environmental Protection Agency, 1996a). Measurements were summarized for rural and urban areas in the United States, Canada, France, Greece, and Brazil. The use of measurements from aboard serve to illustrate or support certain U.S. results as well as to demonstrate the widespread presence of PANs in the atmosphere. Additional data for H_2O_2 were also presented in the 1996 O_3 AQCD. Data for these species are obtained as part of specialized field studies and not as part of routine monitoring operations and thus are highly limited in their ranges of applicability. As a result, it is difficult to relate the concentrations of O_3, other oxidants, and oxidation products on the basis of rather sparse data sets. This information is simply not available for a large number of environments. Instead, it might be more instructive to examine the relations between O_3 and other products of atmospheric reactions on the basis of current understanding of atmospheric photochemical processes.

In order to understand co-occurrence between atmospheric species, an important distinction must be made between primary (directly emitted) species and secondary (photochemically produced) species. In general, it is more likely that primary species will be more highly correlated with each other, and that secondary species will be more highly correlated with each other than will species from mixed classes. By contrast, primary and secondary species are less likely to be correlated with each other. Secondary reaction products tend to correlate with each other, but there is considerable variation. Some species (e.g., O_3 and organic nitrates) are closely related photochemically and correlate with each other strongly. Others (e.g., O_3 and H_2O_2) show a more complex correlation pattern.

Although NO_2 is produced mainly by the reaction of directly emitted NO with O_3 with some contributions from direct emissions, in practice, it behaves like a primary species. The timescale for conversion of NO to NO_2 is fast (5 min or less), so NO and NO_2 ambient concentrations rapidly approach values determined by the photochemical steady state. The sum NO + NO_2 (NO_x) behaves like a typical primary species, while NO and NO_2 reflect some additional complexity based on photochemical interconversion. As a primary species, NO_2 generally does not correlate with O_3 in urban environments. In addition, chemical interactions among O_3, NO and NO_2 have the effect of converting O_3 to NO_2 and vice versa, which can result in a significant anti-correlation between O_3 and NO_2.

Organic nitrates consist of PAN, a number of higher-order species with photochemistry similar to PAN (e.g., PPN), and species such as alkyl nitrates with somewhat different photochemistry. These species are produced by a photochemical process very similar to that of O_3. Photochemical production is initiated by the reaction of primary and secondary VOCs with OH radicals, the resulting organic radicals subsequently react with NO_2 (producing PAN and analogous species) or with NO (producing alkyl nitrates). The same sequence (with organic radicals reacting with NO) leads to the formation of O_3.

In addition, at warm temperatures, the concentration of PAN forms a photochemical steady state with its radical precursors on a timescale of roughly 30 minutes. This steady state value increases with the ambient concentration of O_3 (Sillman et al., 1990). Ozone and PAN may show different seasonal cycles, because they are affected differently by temperature. Ambient O_3 increases with temperature, driven in part by the photochemistry of PAN (see description above). By contrast, the photochemical lifetime of PAN decreases rapidly with increasing temperature. The ratio O_3/PAN should show seasonal changes, with highest ratios in summer, although there is no evidence from measurements. Measured ambient concentrations

(Figure AX3-69) show a strong correlation between O_3 and PAN, and between O_3 and other organic nitrates (Pippin et al., 2001; Roberts et al., 1998).

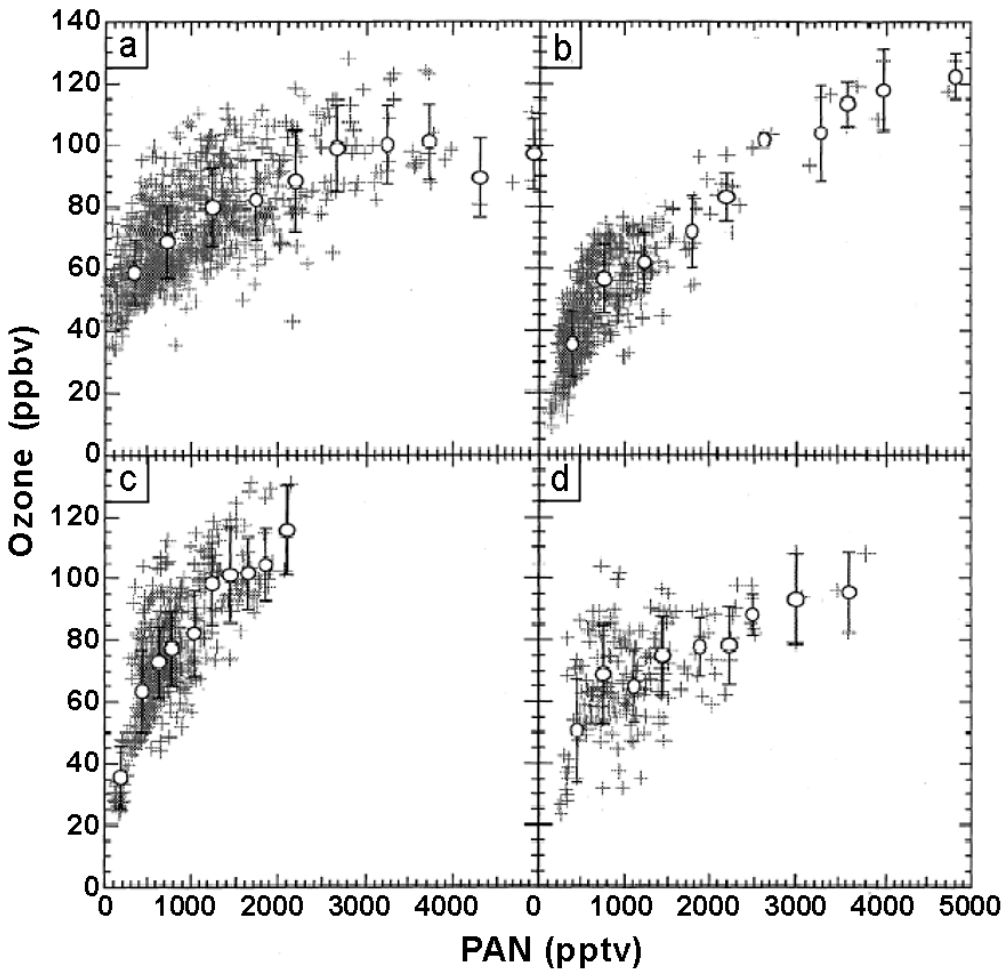

Figure AX3-69a-d. Measured O_3 (ppbv) versus PAN (pptv) in Tennessee, including (a) aircraft measurements, and (b, c, and d) suburban sites near Nashville.

Source: Roberts et al. (1998).

Aerosol nitrate is formed primarily by the combination of nitrate (supplied by HNO_3) with ammonia, and may be limited by the availability of either nitrate or ammonia. Nitrate is expected to correlate loosely with O_3 (see above), whereas ammonia is not expected to correlate with O_3.

Individual primary VOCs are generally highly correlated with each other and with NO_x (Figure AX3-70). A summary of the results of a number of field studies of the concentrations of precursors including NO_x and nonmethane organic compounds (NMOCs) are summarized in the 1996 O_3 AQCD. Although H_2O_2 is produced from photochemistry that is closely related to O_3, it does not show a consistent pattern of correlation with O_3. Hydrogen peroxide is produced in abundance along with O_3 only when O_3 is produced under NO_x-limited conditions. When the photochemistry is NO_x-saturated much less H_2O_2 is produced. In addition, increasing NO_x tends to slow the formation of H_2O_2 under NO_x-limited conditions.

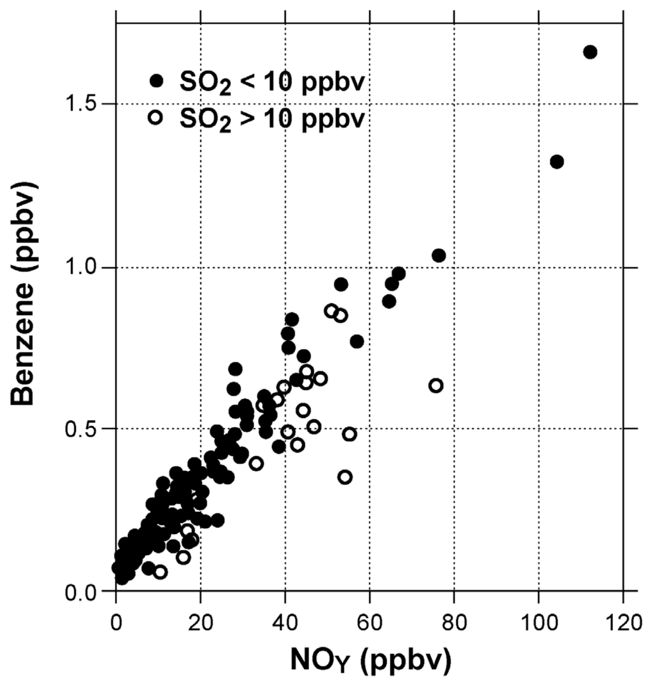

Figure AX3-70. Measured correlation between benzene and NO_y at a measurement site in Boulder, CO. Instances with SO_2 > 10 ppb are identified separately (open circles), because these may reflect different emission sources.

Source: Goldan et al. (1995).

Measurements associated with the Southern Oxidant Study (SOS) in Tennessee (Sillman et al., 1998) and during the North Atlantic Regional Experiment (NARE) (Daum et al., 1996) showed that elevated O_3 was accompanied by relatively high H_2O_2 (3 ppb), much higher than background values reported over the North Atlantic. However, very low H_2O_2 was found in Los Angeles, even in the presence of high O_3 (Sakugawa and Kaplan, 1989).

Elevated O_3 is generally accompanied by elevated HNO_3, although the correlation is not as strong as between O_3 and organic nitrates. Ozone often correlates with HNO_3, because they have the same precursor (NO_x). However, HNO_3 can be produced in significant quantities in winter, even when O_3 is low. The ratio between O_3 and HNO_3 also shows great variation in air pollution events, with NO_x-saturated environments having much lower ratios of O_3 to HNO_3 (Ryerson et al., 2001).

Relations between primary and secondary components discussed above are illustrated by considering data for O_3 and $PM_{2.5}$. Ozone and $PM_{2.5}$ concentrations observed at a monitoring site in Fort Meade, MD are plotted as conditional means in Figure AX3-71. These data were collected between July 1999 and July 2001. As can be seen from the figure, $PM_{2.5}$ tends to be anti-correlated with O_3 to the left of the inflection point (at about 30 ppbv O_3) and $PM_{2.5}$ tends to be positively correlated with O_3 to the right of the inflection point. Data to the left of the minimum in $PM_{2.5}$ were collected mainly during the cooler months of the year, while data to the right of the minimum were collected during the warmer months. This situation arises because $PM_{2.5}$ contains a large secondary component during the summer and has a larger primary component during winter. During the winter, O_3 comes mainly from the free troposphere, above the planetary boundary layer and, thus, may be considered a tracer for relatively clean air. Unfortunately, data for $PM_{2.5}$ and O_3 are collected concurrently at relatively few sites in the United States throughout an entire year, so these results, while highly instructive are not readily extrapolated to areas where appreciable photochemical activity occurs throughout the year.

AX3.8 RELATIONSHIP BETWEEN SURFACE OZONE AND OTHER POLLUTANTS

AX3.8.1 Introduction

Several attempts have been made to characterize gaseous air pollutant mixtures (Lefohn and Tingey, 1984; Lefohn et al., 1987). The characterization of co-occurrence patterns under ambient conditions is important for relating human health and vegetation effects to controlled chamber studies and to ambient conditions. Lefohn et al. (1987) discussed the various patterns

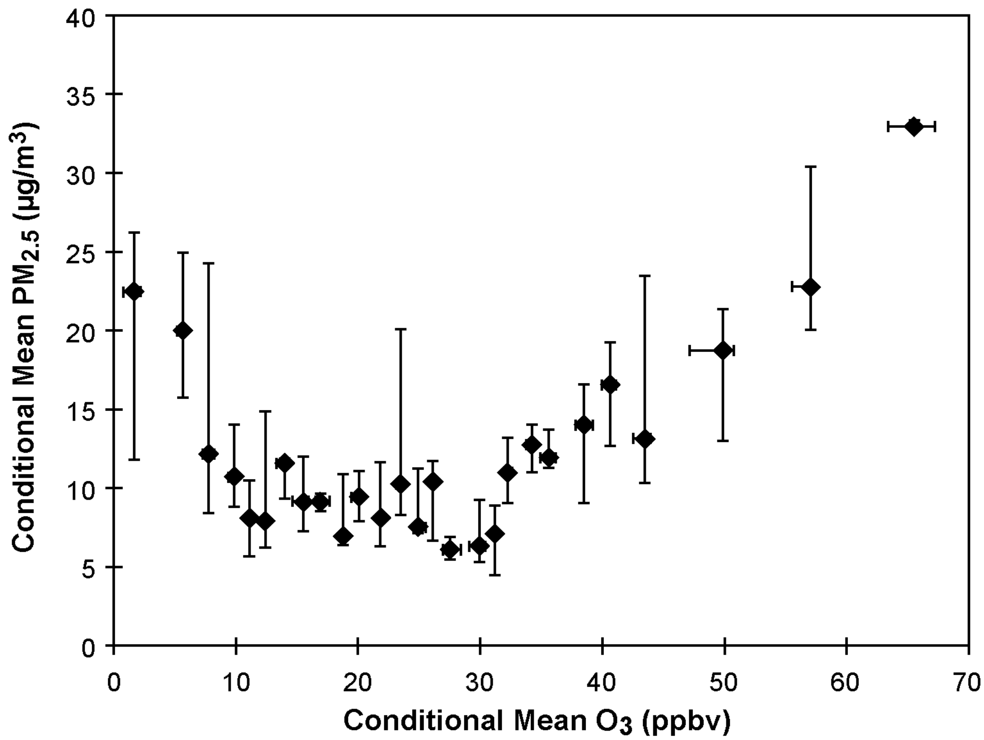

Figure AX3-71. Conditional mean $PM_{2.5}$ concentrations versus conditional mean O_3 concentrations observed at Fort Meade, MD from July 1999 to July 2001.

Source: Chen (2002).

of pollutant exposures. Pollutant combinations can occur at or above a threshold concentration either together or temporally separated from one another. Patterns that show air pollutant pairs appearing at the same hour of the day at concentrations equal to or greater than a minimum hourly mean value were defined as simultaneous-only daily co-occurrences. When pollutant pairs occurred at or above a minimum concentration during the 24-h period, without occurring during the same hour, a "sequential-only" co-occurrence was defined. During a 24-h period, if the pollutant pair occurred at or above the minimum level at the same hour of the day and at different hours during the period, the co-occurrence pattern was defined as "complex-sequential."

For characterizing the different types of co-occurrence patterns for O_3/NO_2, O_3/SO_2, and NO_2/SO_2, Lefohn and Tingey (1984) used a 0.05 ppm threshold to identify the number of hourly simultaneous-only co-occurrences for the period May through September at a large number of air quality urban monitoring sites along with rural sites. The selection of a 0.05-ppm threshold concentration was based on vegetation effects considerations. Data used in the analysis included hourly averaged (1) Environmental Protection Agency Storage and Retrieval of Aerometric Data (SAROAD; now AQS) data for 1981, (2) EPRI-SURE and Eastern Regional Air Quality Study (ERAQS) data for 1978 and 1979, and (3) Tennessee Valley Authority (TVA) data from 1979 to 1982. Lefohn and Tingey (1984) concluded, for the pollutant combinations, that (1) the co-occurrence of two-pollutant mixtures lasted only a few hours per episode and (2) the time interval between episodes was generally large (weeks, sometimes months).

Lefohn et al. (1987), using a 0.03-ppm threshold, grouped air quality data from rural and RRMS (as characterized in the EPA database) within a 24-h period starting at 0000 hours and ending at 2359 hours. Data were analyzed for the May to September period. Data used in the analysis included hourly averaged (1) Environmental Protection Agency AQS (SAROAD) data from 1978 to 1982, (2) EPRI-SURE and –ERAQS data for 1978 and 1979, and (3) TVA data from 1979 to 1982. Patterns that showed air pollutant pairs appearing at the same hour of the day at concentrations equal to or greater than a minimum hourly mean value were defined as simultaneous-only daily co-occurrences. When pollutant pairs occurred at or above a minimum concentration during the 24-h period, without occurring during the same hour, a "sequential-only" co-occurrence was defined. During a 24-h period, if the pollutant pair occurred at or above the minimum level at the same hour of the day and at different hours during the period, the co-occurrence pattern was defined as "complex-sequential." A co-occurrence was not indicated if one pollutant exceeded the minimum concentration just before midnight and the other pollutant exceeded the minimum concentration just after midnight. As will be discussed below, studies of the joint occurrence of gaseous NO_2/O_3 and SO_2/O_3 reached two conclusions: (1) hourly simultaneous and daily simultaneous-only co-occurrences are fairly rare and (2) when co-occurrences are present, complex-sequential and sequential-only co-occurrence patterns predominate. The authors reported that year-to-year variability was found to be insignificant; most of the monitoring sites experienced co-occurrences of any type less than 12% of the 153 days.

Since 1999, monitoring stations across the United States have been routinely measuring the 24-h average concentrations of $PM_{2.5}$. Because of the availability of the $PM_{2.5}$ data, daily co-occurrence of $PM_{2.5}$ and O_3 over a 24-h period was characterized. Because $PM_{2.5}$ data are mostly summarized as 24-h average concentrations in the AQS data base, a daily co-occurrence of O_3 and $PM_{2.5}$ was subjectively defined as when an hourly average O_3 concentration $\geq$ 0.05 ppm and a $PM_{2.5}$ 24-h concentration $\geq$ 40 µg/m^3 occurred over the same 24-h period.

For exploring the co-occurrence of O_3 and other pollutants (e.g., acid precipitation and acidic cloudwater), limited data are available. In most cases, routine monitoring data are not available from which to draw general conclusions. However, published results are reviewed and summarized for the purpose of assessing an estimate of the possible importance of co-occurrence patterns of exposure.

AX3.8.2 Co-Occurrence of Ozone with Nitrogen Oxides

Ozone occurs frequently at concentrations equal to or greater than 0.05 ppm at many rural and remote monitoring sites in the United States (U.S. Environmental Protection Agency, 1996a). Therefore, for many rural locations in the United States, the co-occurrence patterns observed by Lefohn and Tingey (1984) for O_3 and NO_2 were defined by the presence or absence of NO_2. Lefohn and Tingey (1984) reported that most of the sites analyzed experienced fewer than 10 co-occurrences (when both pollutants were present at an hourly average concentration $\geq$ 0.05 ppm). Figure AX3-72 summarizes the simultaneous co-occurrence patterns reported by Lefohn and Tingey (1984). The authors noted that several urban monitoring sites in the South Coast Air Basin experienced more than 450 co-occurrences. For more moderate areas of the country, Lefohn et al. (1987) reported that even with a threshold of 0.03 ppm O_3, the number of co-occurrences with NO_2 was small.

Using 2001 data from the U.S. EPA AQS database, patterns that showed air pollutant pairs of O_3/NO_2 appearing at the same hour of the day at concentrations $\geq$ 0.05 ppm were characterized. The data were not segregated by location settings categories (i.e., rural, suburban, and urban and center city) or land use types (i.e., agricultural, commercial, desert, forest, industrial, mobile, or residential). Data capture was not a consideration in the analysis. The data were characterized over the EPA-defined O_3 season (Table AX3-1). In 2001, there were 341 monitoring sites that co-monitored O_3 and NO_2. Because of possible missing hourly average concentration data during periods when co-monitoring may have occurred, no attempt was made

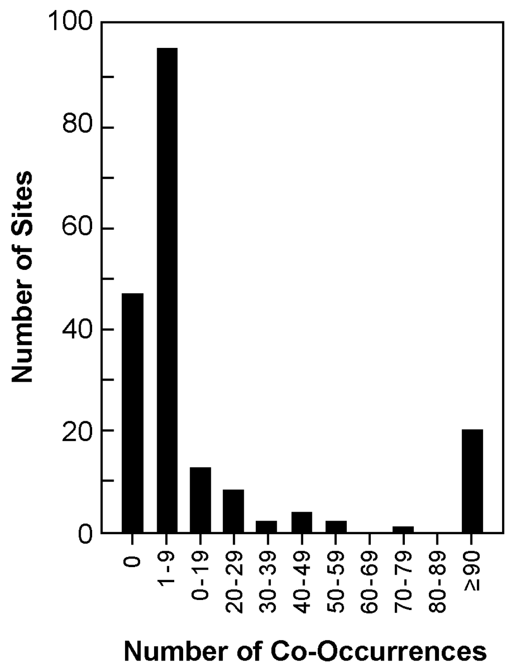

Figure AX3-72. The co-occurrence pattern for O_3 and NO_2.

Source: Lefohn and Tingey (1984).

to characterize the number of co-occurrences in the 0 category. Thus, co-occurrence patterns were identified for those monitoring sites that experienced one or more co-occurrences.

Figure AX3-73 illustrates the results of the analysis. Similar to the analysis summarized by Lefohn and Tingey (1984), most of the collocated monitoring sites analyzed, using the 2001 data, experienced fewer than 10 co-occurrences (when both pollutants were present at an hourly average concentration $\geq$ 0.05 ppm).

AX3.8.3 Co-Occurrence of Ozone with Sulfur Dioxide

Because elevated SO_2 concentrations are mostly associated with industrial activities (U.S. Environmental Protection Agency, 1992), co-occurrence observations are usually associated with monitors located near these types of sources. Lefohn and Tingey (1984) reported that, for the rural and nonrural monitoring sites investigated, most sites experienced fewer than 10 co-occurrences of SO_2 and O_3. Lefohn et al. (1987) reported that even with a threshold of

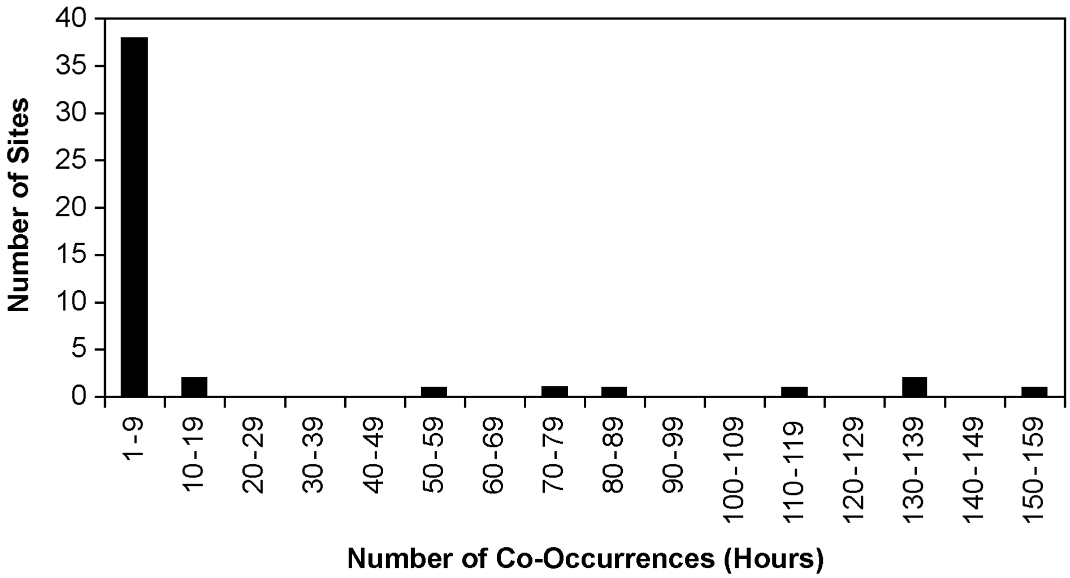

Figure AX3-73. The co-occurrence pattern for O_3 and NO_2 using 2001 data from the AQS.

0.03 ppm O_3, the number of co-occurrences with SO_2 was small. Figure AX3-74 illustrates the simultaneous co-occurrence results reported by Lefohn and Tingey (1984).

Meagher et al. (1987) reported that several documented O_3 episodes at specific rural locations appeared to be associated with elevated SO_2 levels. The investigators defined the co-occurrence of O_3 and SO_2 to be when hourly mean concentrations were $\geq$ 0.10 and 0.01 ppm, respectively.

The above discussion was based on the co-occurrence patterns associated with the presence or absence of hourly average concentrations of pollutant pairs. Taylor et al. (1992) have discussed the joint occurrence of O_3, nitrogen, and sulfur in forested areas using cumulative exposures of O_3 with data on dry deposition of sulfur and nitrogen. The authors concluded in their study that the forest landscapes with the highest loadings of sulfur and nitrogen via dry deposition tended to be the same forests with the highest average O_3 concentrations and largest cumulative exposure. Although the authors concluded that the joint occurrences of multiple pollutants in forest landscapes were important, nothing was mentioned about the hourly co-occurrences of O_3 and SO_2 or of O_3 and NO_2.

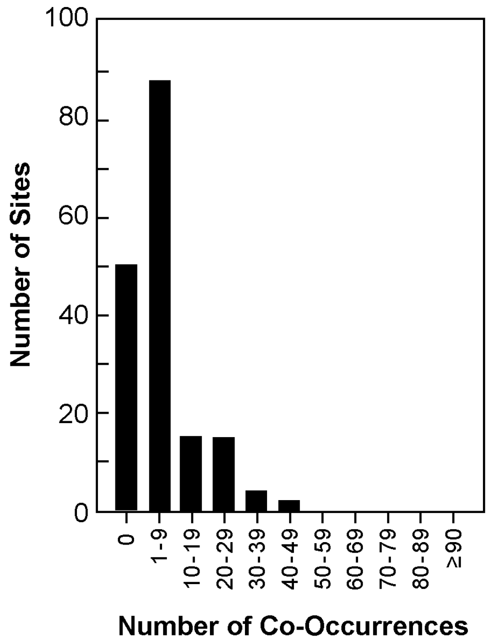

Figure AX3-74. The co-occurrence pattern for O_3 and SO_2.

Source: Lefohn and Tingey (1984).

Using 2001 data from the EPA AQS database, patterns that showed air pollutant pairs of O_3/SO_2 appearing at the same hour of the day at concentrations ≥ 0.05 ppm were characterized. The data were not segregated by location settings categories (i.e., rural, suburban, and urban and center city) or land use types (i.e., agricultural, commercial, desert, forest, industrial, mobile, or residential). Data capture was not a consideration in the analysis. In 2001, there were 246 monitoring sites that co-monitored O_3 and SO_2. As discussed previously, because of possible missing hourly average concentration data during periods when co-monitoring may have occurred, no attempt was made to characterize the number of co-occurrences in the 0 category. Thus, co-occurrence patterns were identified for those monitoring sites that experienced one or more co-occurrences. Figure AX3-75 shows the results from this analysis for the simultaneous co-occurrence of O_3 and SO_2. Similar to the analysis summarized by Lefohn and Tingey (1984), most of the collocated monitoring sites analyzed, using the 2001 data, experienced fewer than 10 co-occurrences (when both pollutants were present at an hourly average concentration ≥ 0.05 ppm).

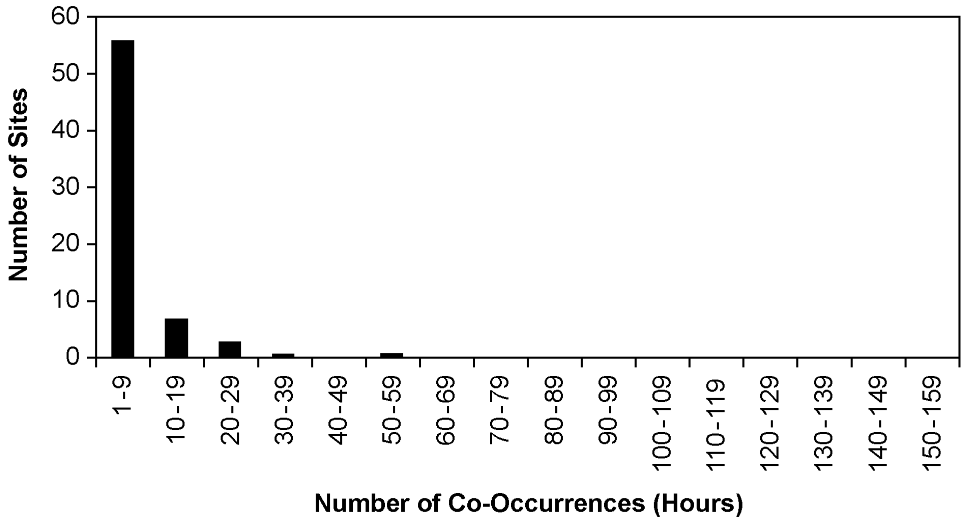

Figure AX3-75. The co-occurrence pattern for O_3 and SO_2 using 2001 data from AQS.

AX3.8.4 Co-Occurrence of Ozone and Daily $PM_{2.5}$

Using 2001 data from the EPA AQS, the daily co-occurrence of $PM_{2.5}$ and O_3 over a 24-h period was characterized. There were 362 sites where $PM_{2.5}$ and O_3 monitors were collocated. As described in the introduction selection of this annex, a daily co-occurrence of O_3 and $PM_{2.5}$ is subjectively defined as an hourly average O_3 concentration ≥ 0.05 ppm and a $PM_{2.5}$ 24-h concentration ≥ 40 μg/m^3 occurring over the same 24-h period. Figure AX3-76 illustrates the daily co-occurrence patterns observed. Using 2001 data from the AQS, the daily co-occurrence of $PM_{2.5}$ and O_3 was infrequent.

AX3.8.5 Co-Occurrence of Ozone with Acid Precipitation

Concern has been expressed about the possible effects on vegetation from co-occurring exposures of O_3 and acid precipitation (Prinz et al., 1985; National Acid Precipitation Assessment Program, 1987; Prinz and Krause, 1989). Little information has been published concerning the co-occurrence patterns associated with the joint distribution of O_3 and acidic deposition (i.e., H^+). Lefohn and Benedict (1983) reviewed the EPA SAROAD monitoring data for 1977 through 1980 and, using National Atmospheric Deposition Program (NADP) and EPRI wet deposition data, evaluated the frequency distribution of pH events for 34 NADP and 8 EPRI

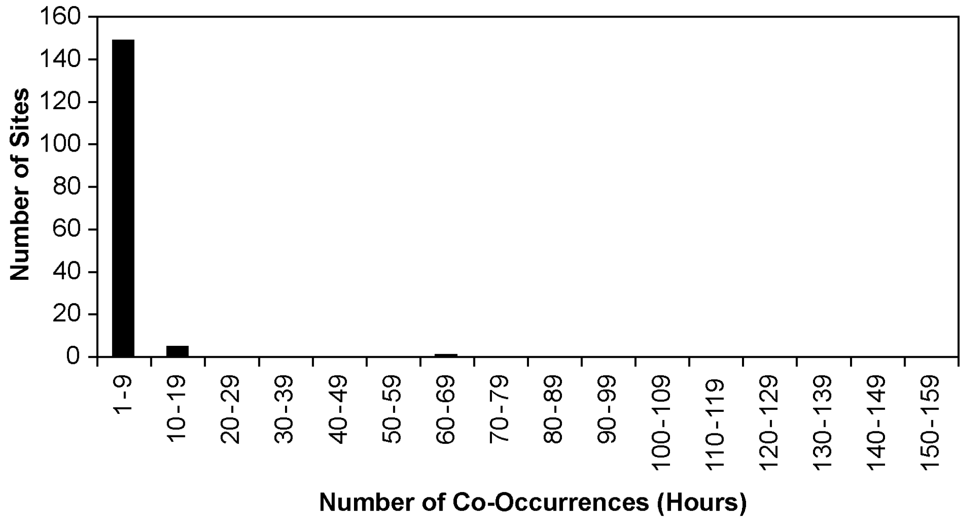

Figure AX3-76. The co-occurrence pattern for O_3 and $PM_{2.5}$ using 2001 data from AQS.

chemistry monitoring sites located across the United States. Unfortunately, there were few sites where O_3 and acidic deposition were co-monitored.

As a result, Lefohn and Benedict (1983) focused their attention on O_3 and acidic deposition monitoring sites that were closest to one another. In some cases, the sites were as far apart as 144 km. Using hourly O_3 monitoring data and weekly and event acidic deposition data from the NADP and EPRI databases, the authors identified specific locations where the hourly mean O_3 concentrations were $\geq$ 0.1 ppm and 20% of the wetfall daily or weekly samples were below pH 4.0. Elevated levels of O_3 were defined as hourly mean concentrations equal to or greater than 0.1 ppm. Although for many cases, experimental research results of acidic deposition on agricultural crops show few effects at pH levels > 3.5 (National Acid Precipitation Assessment Program, 1987), it was decided to use a pH threshold of 4.0 to take into consideration the possibility of synergistic effects between O_3 and acidic deposition.

Based on their analysis, Lefohn and Benedict (1983) identified five sites with the potential for agricultural crops to experience additive, less than additive, or synergistic (i.e., greater than additive) effects from elevated O_3 and H^+ concentrations. The authors stated that they believed, based on the available data, the greatest potential for interaction between acid rain and O_3 concentrations in the United States, with possible effects on crop yields, may be in the most industrialized areas (e.g., Ohio and Pennsylvania). However, they cautioned that, because no documented evidence existed to show that pollutant interaction had occurred under field growth conditions and ambient exposures, their conclusions should only be used as a guide for further research.

In their analysis, Lefohn and Benedict (1983) found no collocated sites. The authors rationalized that data from non-co-monitoring sites (i.e., O_3 and acidic deposition) could be used because O_3 exposures are regional in nature. However, work by Lefohn et al. (1988) has shown that hourly mean O_3 concentrations vary from location to location within a region, and that cumulative indices, such as the percent of hourly mean concentrations $\geq$ 0.07 ppm, do not form a uniform pattern over a region. Thus, extrapolating hourly mean O_3 concentrations from known locations to other areas within a region may provide only qualitative indications of actual O_3 exposure patterns.

In the late 1970s and the 1980s, both the private sector and the government funded research efforts to better characterize gaseous air pollutant concentrations and wet deposition. The event-oriented wet deposition network, EPRI/Utility Acid Precipitation Study Program, and the weekly oriented sampling network, NADP, provided information that can be compared with hourly mean O_3 concentrations collected at several co-monitored locations. No attempt was made to include H^+ cloud deposition information. In some cases, for mountaintop locations (e.g., Clingman's Peak, Shenandoah, Whiteface Mountain, and Whitetop Mountain), the H^+ cloud water deposition is greater than the H^+ deposition in precipitation (Mohnen, 1989), and the co-occurrence patterns associated with O_3 and cloud deposition will be different from those patterns associated with O_3 and deposition by precipitation.

Smith and Lefohn (1991) explored the relationship between O_3 and H^+ in precipitation, using data from sites that monitored both O_3 and wet deposition simultaneously and within one-minute latitude and longitude of each other. The authors reported that individual sites experienced years in which both H^+ deposition and total O_3 exposure were at least moderately high (i.e., annual H^+ deposition $\geq$ 0.5 kg ha^{-1} and an annual O_3 cumulative, sigmoidally weighted exposure (W126) value $\geq$ 50 ppm-h). With data compiled from all sites, it was found that relatively acidic precipitation (pH $\leq$ 4.31 on a weekly basis or pH $\leq$ 4.23 on a daily basis) occurred together with relatively high O_3 levels (i.e., W126 values $\geq$ 0.66 ppm-h for the same week or W126 values $\geq$ 0.18 ppm-h immediately before or after a rainfall event) approximately 20% of the time, and highly acidic precipitation (i.e, pH $\leq$ 4.10 on a weekly basis or pH $\leq$ 4.01

on a daily basis) occurred together with a high O_3 level (i.e., W126 values ≥ 1.46 ppm-h for the same week or W126 values ≥ 0.90 ppm-h immediately before or after a rainfall event) approximately 6% of the time. Whether during the same week or before, during, or after a precipitation event, correlations between O_3 level and pH (or H^+ deposition) were weak to nonexistent. Sites most subject to relatively high levels of both H^+ and O_3 were located in the eastern United States, often in mountainous areas.

AX3.8.6 Co-Occurrence of Ozone with Acid Cloudwater

In addition to the co-occurrence of O_3 and acid precipitation, results have been reported on the co-occurrence of O_3 and acidic cloudwater in high-elevation forests. Vong and Guttorp (1991) characterized the frequent O_3-only and pH-only, single-pollutant episodes, as well as the simultaneous and sequential co-occurrences of O_3 and acidic cloudwater. The authors reported that both simultaneous and sequential co-occurrences were observed a few times each month above the cloud base. Episodes were classified by considering hourly O_3 average concentrations ≥ 0.07 ppm and cloudwater events with pH ≤ 3.2. The authors reported that simultaneous occurrences of O_3 and pH episodes occurred two to three times per month at two southern sites (Mitchell, NC and Whitetop, VA) and the two northern sites (Whiteface Mountain, NY and Moosilauke, NH) averaged one episode per month. No co-occurrences were observed at the central Appalachian site (Shenandoah, VA), due to a much lower cloud frequency. Vong and Guttorp (1991) reported that the simultaneous occurrences were usually of short duration (mean = 1.5 h/episode) and were followed by an O_3-only episode. As would be expected, O_3-only episodes were longer than co-occurrences and pH episodes, averaging an 8-h duration.

AX3.9 THE METHODOLOGY FOR DETERMINING POLICY RELEVANT BACKGROUND OZONE CONCENTRATIONS

AX3.9.1 Introduction

Policy-relevant background (PRB) O_3 concentrations are used by the EPA to assess risks to human and ecosystem health and to provide risk estimates associated with O_3 produced by anthropogenic sources in the continental North America (defined here as the United States, Canada, and Mexico). Policy Relevant Background concentrations are those concentrations that would result in the United States in the absence of anthropogenic emissions in North America. Policy Relevant Background concentrations include contributions from natural sources everywhere in the world and from anthropogenic sources outside North America. They are used for assessing risks to human health in areas where O_3 concentrations exceed the NAAQS.

Contributions to PRB O_3 include: photochemical interactions involving natural emissions of VOCs, NO_x, and CO; the long-range transport of O_3 and its precursors from outside North America; and stratospheric-tropospheric exchange (STE). Processes involved in STE are described in detail in Annex AX2.3. Natural sources of O_3 precursors include biogenic emissions, wildfires, and lightning. Biogenic emissions from agricultural activities are not considered in the formation of PRB O_3.

Most of the issues concerning the calculation of PRB O_3 center on the origin of springtime maxima in surface O_3 concentrations observed at monitoring sites in relatively unpolluted areas of the United States and on the capability of the current generation of global-scale, three-dimensional chemistry transport models to correctly simulate their causes. These issues are related to the causes of the occurrence of high O_3 values, especially those averaged over 1-h to 8-h observed at O_3 monitoring sites during late winter through spring (i.e., February to June). The issues raised do not affect interpretations of the causes of summertime O_3 episodes as strongly. Summertime O_3 episodes are mainly associated with slow-moving high-pressure systems characterized by limited mixing between the planetary boundary layer and the free troposphere (Section AX2.3).

Springtime maxima are observed at national parks mainly in the western United States that are relatively clean (Section AX3.2.2; Figures AX3-77a,b) and at a number of other relatively unpolluted monitoring sites throughout the Northern Hemisphere. Spring maxima in tropospheric O_3 were originally attributed to transport from the stratosphere by Regener (1941) as cited by Junge (1963). Junge (1963) also cited measurements of springtime maxima in O_3 concentrations at Mauna Loa (elevation 3400 m) and at Arkosa, Germany (an alpine location, elevation 1860 m). Measurements of radioactive debris transported downward from the stratosphere as the result of nuclear testing during the 1960s also show springtime maxima (Ludwig et al., 1977). However, more recent studies (Lelieveld and Dentener, 2000; Browell et al., 2003) attribute the springtime maximum in tropospheric O_3 concentrations to tropospheric production rather than transport from the stratosphere.

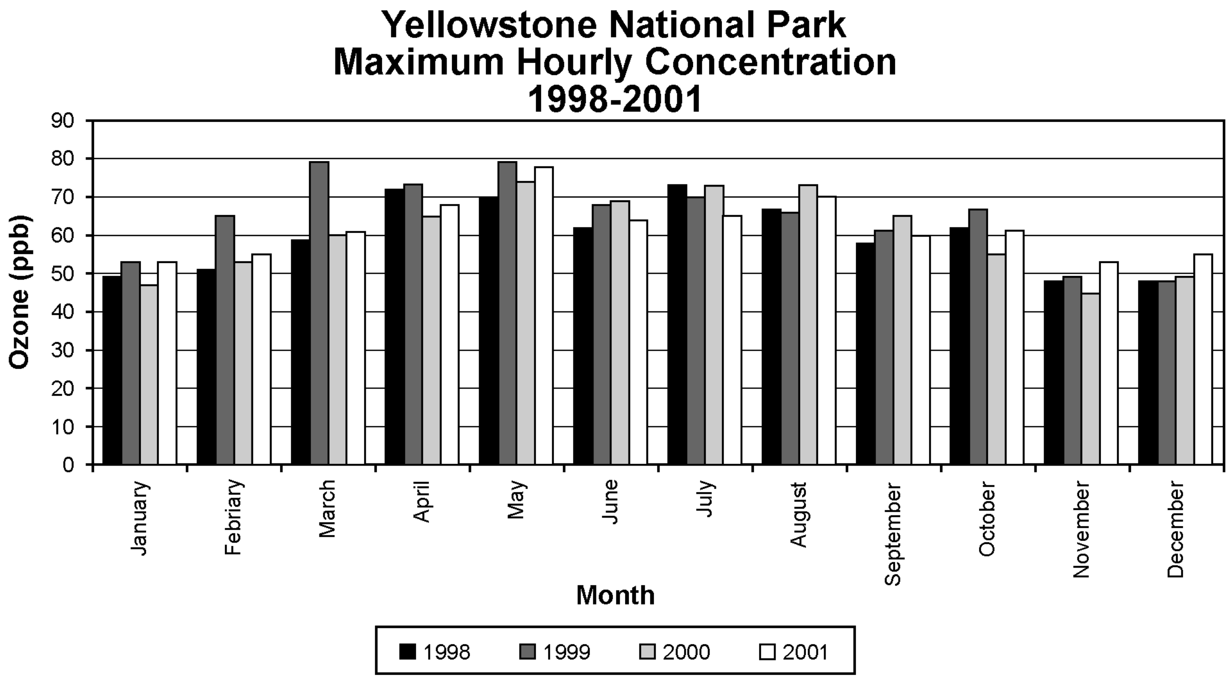

Figure AX3-77a. Monthly maximum hourly average O_3 concentrations at Yellowstone National Park, Wyoming in 1998, 1999, 2000, and 2001.

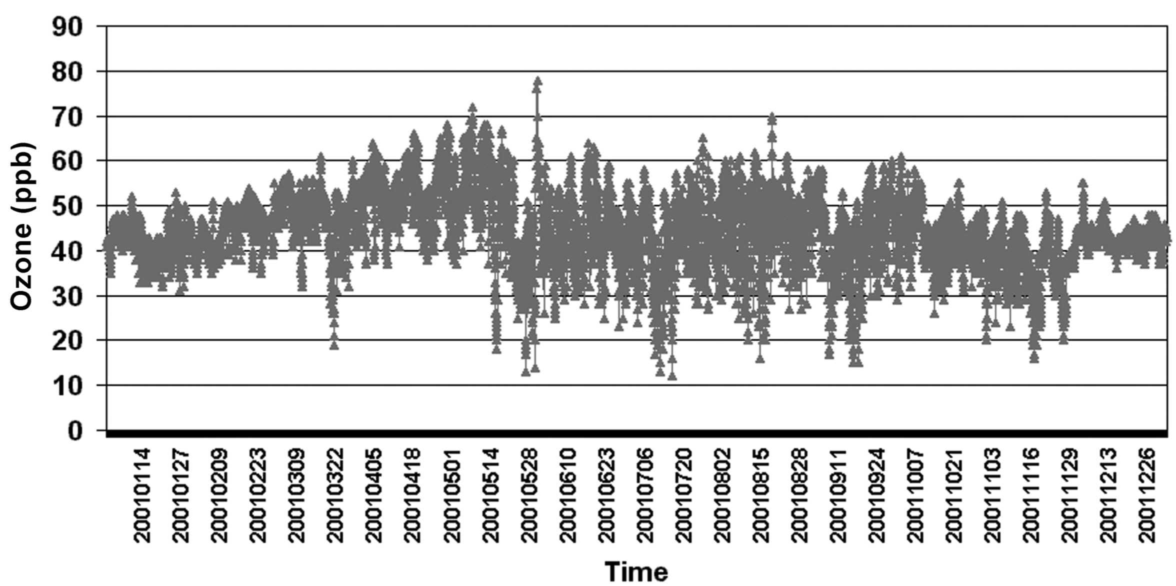

Figure AX3-77b. Hourly average O_3 concentrations at Yellowstone National Park, Wyoming for the period January to December 2001.

Source: U.S. Environmental Protection Agency (2003a).

Springtime O_3 maxima were observed in low-lying surface measurements during the late 19th century. However, these measurements are quantitatively highly uncertain, and extreme caution should be exercised in their use. Concentrations of approximately 0.036 ppm for the daytime average and of 0.030 ppm for the nighttime averages were reported for Zagreb, Croatia using the Schonbein method during the 1890s (Lisac and Grubise, 1991). Of the numerous measurements of tropospheric O_3 made in the 19th century, only the iodine catalyzed oxidation of arsenite has been verified with modern laboratory methods. Kley et al. (1988) reconstructed the apparatus used between 1876 and 1910 in Montsouris, outside Paris, and evaluated it for accuracy and specificity. They concluded that ozone mixing ratios ranged from 5 to 16 ppb with uncertainty of ±2 ppb. Interferences from SO_2 were avoided as the Montsouris data were selected to exclude air from Paris, the only source of high concentrations of SO_2 at that time. Uncertainties in the humidity correction to the Schonbein reading will lead to considerable inaccuracies in the seasonal cycle established by this method (Pavelin et al., 1999). Because of the uncertainties in the earlier methods, it is difficult to quantify the differences between surface O_3 concentrations measured in the last half of the 19th century at certain locations in either Europe or North America with those currently monitored at remote locations in the world.

Observations of O_3 profiles at a large number of sites indicate a positive gradient in O_3 mixing ratios with increasing altitude in the troposphere and a springtime maximum in O_3 concentrations in the upper troposphere (Logan, 1999). As discussed in Section AX2.3.1, STE affects the middle and upper troposphere more than the lower troposphere. It is, therefore, reasonable to suppose that the main cause of this positive gradient is STE. However, deep convection transports pollutants upward and can result in an increase in the pollutant mixing ratio with altitude downwind of surface source regions as shown in Figure AX3-78. This effect can be seen in differences in ozonesonde profiles as one moves eastward across the United States (Newchurch et al., 2003). In addition, O_3 formed by lightning-generated NO_x also contributes to the vertical O_3 gradient. (Lelieveld and Dentener, 2000). This O_3 could be either background or not, depending on the sources of radical precursors. Another contributing factor is the increase of O_3 lifetime with altitude (Wang et al., 1998). Free-tropospheric O_3 is not predominantly of stratospheric origin, nor is it all natural; it is mostly controlled by production within the troposphere and includes a major anthropogenic enhancement (e.g., Berntsen et al., 1997; Roelofs et al., 1997; Wild and Akimoto, 2001).

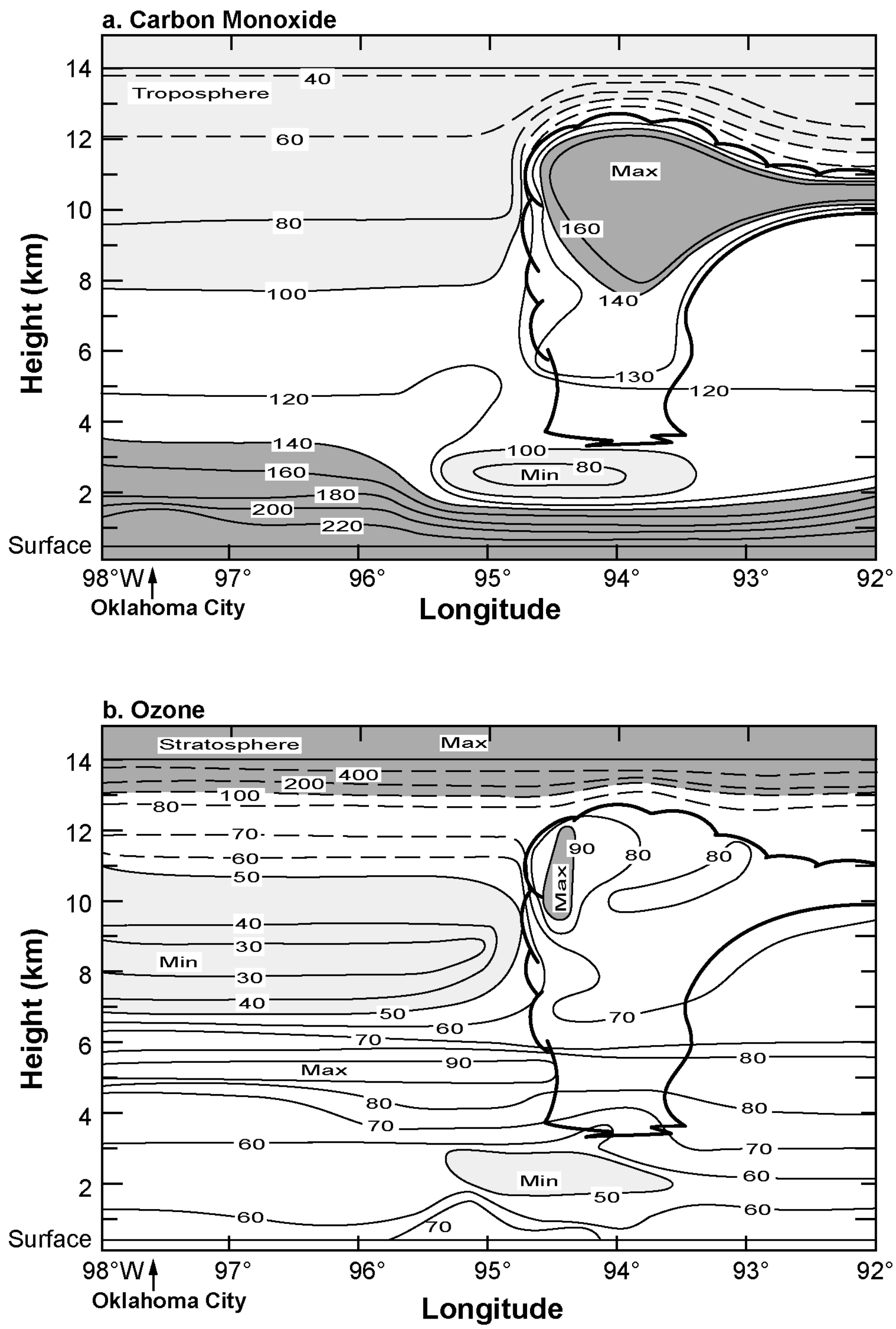

Figure AX3-78. (a) Contour plot of CO mixing ratios (ppbv) observed in and near the June 15, 1985, mesoscale convective complex in eastern Oklahoma. Heavy line shows the outline of the cumulonimbus cloud. Dark shading indicates high CO and light shading indicates low CO. Dashed contour lines are plotted according to climatology since no direct measurements were made in that area. (b) Same as (a) but for O_3 (ppbv).

Source: Dickerson et al. (1987).

Stohl (2001), Wernli and Borqui (2002), Seo and Bowman (2002), James et al. (2003a,b), Sprenger and Wernli (2003), and Sprenger et al. (2003) addressed the spatial and temporal variability in stratosphere to troposphere transport. Both Stohl (2001) and Sprenger et al. (2003) produced 1-year climatologies of tropopause folds based on a 1° by 1° gridded meteorological model data set. They each found that the probability of deep folds (penetrating to the 800 hPa level) was maximum during winter (December through February) with the highest frequency of folding extending from Labrador down the east coast of North America. However, these deep folds occurred in < 1% of the 6-h intervals for which meteorological data was assimilated for grid points in the continental United States, with a higher frequency in Canada. They observed a higher frequency of more shallow folds (penetrating to the upper troposphere) and medium folds (penetrating to levels between 500 and 600 hPa) of about 10% and 1 to 2%, respectively. These events occur preferentially across the subtropics and the southern United States. At higher latitudes, other mechanisms such as the erosion of cut-off lows and the breakup of stratospheric streamers are likely to play an important role in STE. A 15-year model climatology by Sprenger and Wernli (2003) showed the consistent pattern of STE occurring over the primary storm tracks along the Asian and North American coasts. This climatology, and the one of James et al. (2003) both found that recent stratospheric air associated with deep intrusions are relatively infrequent occurrences in these models. Thus, stratospheric intrusions are most likely to directly affect the middle and upper troposphere, not the planetary boundary layer. However, this O_3 can still exchange with the planetary boundary layer through convection or through large-scale subsidence as described later in this subsection and in Sections AX2.3.2, AX2.3.3, and AX2.3.4. These results are in accord with the observations of Galeni et al. (2003) over Greece and those of Ludwig et al. (1977) over the western United States. It should also be remembered that stratospheric O_3 injected into the upper troposphere is subject to chemical destruction as it is transported downward toward the surface.

Ozone concentrations measured at RRMS in the Northern Hemisphere have been compiled by Vingarzan (2004) and are reproduced here in Tables AX3-17, AX3-18, and AX3-19. Data for annual mean/median concentrations show a broad range, as do annual maximum 1-h concentrations. Generally, concentrations increase with elevation and the highest concentrations are found during spring. The overall average of the annual median O_3 concentrations at all sites in the continental United States is about 30 ppb and excluding higher elevation sites it is about

Table AX3-17. Range of Annual (January-December) Hourly Ozone Concentrations (ppb) at Background Sites Around the World (CMDL, 2004)

Location	Elevation (m)	Period of Record	Range of Annual Means
Pt. Barrow, Alaska	11	1992-2001	23-29
Ny Alesund, Svalbard, Spitsbergen[a]	475	1989-1993	28-33[b]
Mauna Loa, Hawaii[c]	3397	1992-2001	37-46[d]

[a]University of Stockholm Meteorological Institute.
[b]Annual medians
[c]10:00 - 18:00 UTC.
[d]High elevation site.

Source: Vingarzan (2004).

Table AX3-18. Range of annual (January-December) Hourly Median and Maximum Ozone Concentrations (ppb) at Background Stations in Protected Areas of the United States (CASTNet, 2004)

Location	Elevation (m)	Period of Record	Range of Annual Medians	Range of Annual Maxima
Denali NP, Alaska	640	1998-2001	29-34	49-68
Glacier NP, Montana	976	1989-2001	19-27	57-77
Voyageurs NP, Minnesota	429	1997-2001	28-35	74-83
Theodore Roosevelt NP, North Dakota	850	1983-2001	29-43	61-82
Yellowstone NP, Wyoming	2469	1996-2001	37-45[a]	68-79[a]
Rocky Mountain NP, Colorado	2743	1994-2001	40-47[a]	68-102[a]
Olympic NP, Washington	125	1998-2001	19-22	50-63
North Cascades NP, Washington	109	1996-2001	14-18	48-69
Mount Rainier NP, Washington	421	1995-2001	38371	54-98
Lassen NP, California	1756	1995-2001	38-43[a]	81-109[a]
Virgin Islands NP, U.S. Virgin Islands	80	1998-2001	19-24	50-64

[a]High elevation site.

Source: Vingarzan (2004).

Table AX3-19. Range of annual (January-December) Hourly Median and Maximum Ozone Concentrations (ppb) at Canadian Background Stations (CAPMoN[a], 2003)

Location	Elevation (m)	Period of Record	Range of Annual Medians	Range of Annual Maxima
Kejimkujik, Nova Scotia[b]	127	1989-2001	25-34	76-116
Montmorency, Quebec	640	1989-1996	28-32	73-99
Algoma, Ontario[a]	411	1988-2001	27-33	76-108
Chalk River, Ontario	184	1988-1996	25-31	79-107
Egbert, Ontario[a]	253	1989-2001	27-32	90-113
E.L.A., Ontario	369	1989-2001	28-33	64-87
Bratt's Lake, Saskatchewan	588	1999-2001	26-29	63-68
Esther, Alberta	707	1995-2001	26-31	63-78
Saturna Island, British Columbia	178	1992-2001	23-27	65-82

[a]Canadian Air and Precipitation Monitoring Network.
[b]Stations affected by long-range transport of anthropogenic emissions.

Source: Vingarzan (2004).

24 ppb. Maximum concentrations may be related to stratospheric intrusions, wildfires, and intercontinental or regional transport of pollution. However, it should be noted that all of these sites are affected by anthropogenic emissions to some extent making an interpretation based on these data alone problematic.

Daily 1-h maximum O_3 concentrations exceeding 50 or 60 ppb are observed during late winter and spring in southern Canada and at sites in national parks as shown in Tables AX3-20, AX3-21, and Figure AX3-79. That these high values can occur during late winter when there are low sun angles and cold temperatures may imply a negligible role for photochemistry and a major role for stratospheric intrusions. However, active photochemistry occurs even at high latitudes during late winter. Rapid O_3 loss, apparently due to multiphase chemistry involving bromine atoms (see Section 2.2.10) occurs in the Arctic marine boundary layer. The Arctic throughout much of winter is characterized by low light levels, temperatures, and precipitation, and can act as a reservoir for O_3 precursors such as PAN and alkyl nitrates, which build up and can then photolyze when sun angles are high enough during late winter and early spring. Long-range transport of total odd nitrogen species (NO_y) (defined in AX2.2.2) and VOCs to Arctic regions can occur from midlatitude-source regions. In addition, O_3 can be transported from tropical areas in the upper troposphere followed by its subsidence at mid and high latitudes (Wang et al., 1998).

Penkett (1983), and later Penkett and Brice (1986), first observed a spring peak in PAN at high northern latitudes and hypothesized that winter emissions transported into the Arctic would be mixed throughout a large region of the free troposphere and transformed into O_3 as solar radiation returned to the Arctic in the spring. Subsequent observations (Dickerson, 1985) confirmed the presence of strata of high concentrations of reactive nitrogen compounds at high latitudes in early spring. Bottenheim et al. (1990, 1993) observed a positive correlation between O_3 and NO_2 in the Arctic spring. Jaffe et al. (1991) found NO_y concentrations approaching 1 ppb in Barrow, Alaska, in the spring and attributed them to long-range transport.

Beine et al. (1997) and Honrath et al. (1997) measured O_3, PAN, and NO_x in Alaska and Svalbard, Norway and concluded that PAN decomposition can lead to photochemical O_3 production. At Poker Flat, Alaska, O_3 production was directly observable. Herring et al. (1997) tracked springtime O_3 maxima in Denali National Park, Alaska, an area one might presume to be pristine. They measured NO_x and hydrocarbons and concluded that, in the spring, O_3 was

Table AX3-20. Number of Hours ≥ 0.05 ppm for Selected Rural O_3 Monitoring in the United States by Month for the Period 1988 to 2001

Site Name	Month	1988	1989	1990	1991	1992	1993	1994	1995	1996	1997	1998	1999	2000	2001
Denali National Park, Alaska	February	0	0	0	0	0	0	0	0		0	0	0	0	14
Denali National Park, Alaska	March	0	0	0	0	0	0	0	0	52	0	122	17	0	24
Denali National Park, Alaska	April	217	0	2	0	64	10	31	21	12	51	236	119	0	302
Denali National Park, Alaska	May	26	1	0	24	10	17	1	54	97	35	79	29	0	98
Denali National Park, Alaska	June	0	0	0	0	0	0	0	0	27	0	0	22	0	6
Yellowstone National Park, Wyoming	February	0		0	11	3	0	21	6	0	1	5	252	23	77
Yellowstone National Park, Wyoming	March	194		2	4	95	26	285	14	7	98	150	509	286	307
Yellowstone National Park, Wyoming	April	228		17	16	217	62	311	185	65	163	385	517	242	461
Yellowstone National Park, Wyoming	May	225		2	10	196	47	180	193	212	216	289	458	240	350
Yellowstone National Park, Wyoming	June	58		67	139	33	28	116	81	94	149	78	212	181	172

Table AX3-20 (cont'd). Number of Hours ≥ 0.05 ppm for Selected Rural O_3 Monitoring in the United States by Month for the Period 1988 to 2001

Site Name	Month	1988	1989	1990	1991	1992	1993	1994	1995	1996	1997	1998	1999	2000	2001
Glacier National Park, Montana	February			0	0	0	0	0	8	0	0	0	0	0	0
Glacier National Park, Montana	March			49	9	24	10	23	40	35	9	6	17	5	4
Glacier National Park, Montana	April			31	64	29	5	45	16	46	52	49	128	16	0
Glacier National Park, Montana	May			20	81	67	41	66	51	51	4	122	103	63	23
Glacier National Park, Montana	June			24	37	31	5	29	13	119	0	3	0	6	0
Voyageurs National Park, Minnesota	February	3	0	0	0	0	43	22	0	0	23	0	6	32	0
Voyageurs National Park, Minnesota	March	6	2	0	0	1	94	10	39	49	220	40	215	60	0
Voyageurs National Park, Minnesota	April	48	0	31	22	27	56	65	30	64	128	254	221	175	0
Voyageurs National Park, Minnesota	May	183	33	14	10	174	78	96	107	111	146	191	247	143	62
Voyageurs National Park, Minnesota	June	92		2	0	55	50	66	190	37	221	25	23	28	95

Table AX3-21. Number of Hours ≥ 0.06 ppm for Selected Rural O_3 Monitoring Sites in the United States by Month for the Period of 1988 to 2001

Site Name	Month	1988	1989	1990	1991	1992	1993	1994	1995	1996	1997	1998	1999	2000	2001
Denali National Park, Alaska	February	0	0	0	0	0	0	0	0		0	0	0	0	0
Denali National Park, Alaska	March	0	0	0	0	0	0	0	0	0	0	0	0	0	0
Denali National Park, Alaska	April	0	0	0	0	0	0	0	0	0	0	0	0	0	0
Denali National Park, Alaska	May	0	0	0	0	0	0	0	0	2	0	0	0	0	9
Denali National Park, Alaska	June	0	0	0	0	0	0	0	0	0	0	0	0	0	2
Yellowstone National Park, Wyoming	February	0		0	0	0	0	0	0	0	0	0	6	0	0
Yellowstone National Park, Wyoming	March	37		0	0	0	0	0	0	0	1	0	120	1	4
Yellowstone National Park, Wyoming	April	59		0	0	29	0	20	4	0	0	64	158	11	77
Yellowstone National Park, Wyoming	May	20		0	0	61	3	42	24	38	26	54	169	49	139
Yellowstone National Park, Wyoming	June	8		7	18	2	1	13	0	0	22	4	27	43	18
Glacier National Park, Montana	February			0	0	0	0	0	0	0	0	0	0	0	0
Glacier National Park, Montana	March			1	0	0	0	0	0	0	0	0	0	0	0

Table AX3-21 (cont'd). Number of Hours ≥ 0.06 ppm for Selected Rural O_3 Monitoring Sites in the United States by Month for the Period of 1988 of 2001

Site Name	Month	1988	1989	1990	1991	1992	1993	1994	1995	1996	1997	1998	1999	2000	2001
Glacier National Park, Montana	April			0	0	1	0	0	0	0	0	2	1	0	0
Glacier National Park, Montana	May			2	7	13	0	0	4	5	0	16	19	8	0
Glacier National Park, Montana	June			0	3	1	0	1	0	16	0	0	0	0	0
Voyageurs National Park, Minnesota	February	1	0	0	0	0	1	8	0	0	0	0	0	0	0
Voyageurs National Park, Minnesota	March	0	0	0	0	0	34	0	5	2	15	0	9	4	0
Voyageurs National Park, Minnesota	April	9	0	1	0	0	5	8	0	17	2	57	24	41	0
Voyageurs National Park, Minnesota	May	77	6	0	0	40	9	40	2	27	46	53	139	43	6
Voyageurs National Park, Minnesota	June	30		0	0	28	17	5	113	12	115	0	5	0	32

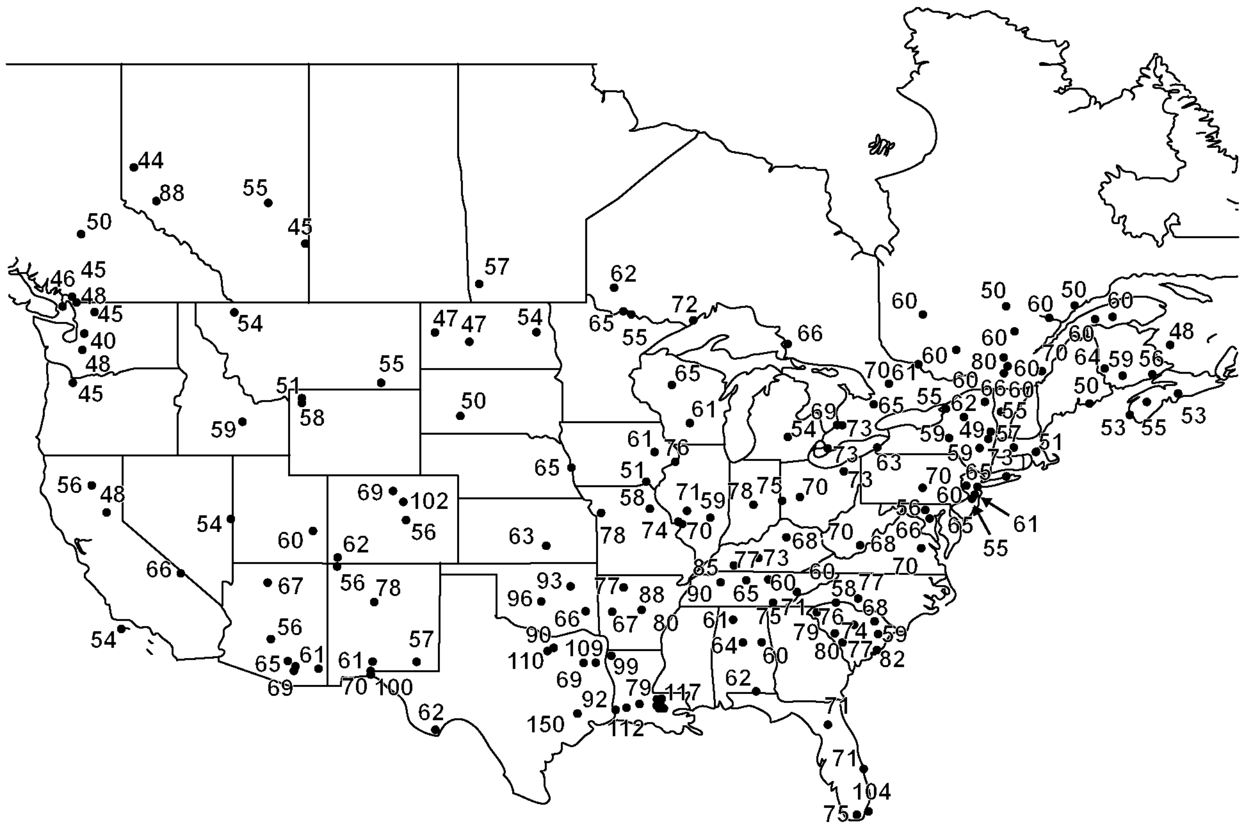

Figure AX3-79. Maximum hourly average O_3 concentrations at rural monitoring sites in Canada and the United States in February from 1980 to 1998.

Source: Lefohn et al. (2001).

produced predominantly by photochemistry at a calculated rate of 1 to 4 ppb/day, implying that the O_3 observed could be produced on timescales ranging from about a week to a month. Solberg et al. (1997) tracked the major components of NO_y in remote Spitsbergen, Norway for the first half of the year 1994. They observed high concentrations of PAN (800 ppt) peaking simultaneously with O_3 (45 to 50 ppb) and attributed this to the long-range transport of pollution and to photochemical smog chemistry. These investigators concluded, in general, that large regions of the Arctic store high concentrations of O_3 precursors in the winter and substantial quantities of O_3 are produced by photochemical reactions in the spring. Although reactions with high-activation-energy barriers may be ineffective, reactions with low- or no activation-energy barriers (such as radical-radical reactions) or negative temperature dependencies will still proceed. Indeed, active photochemistry is observed in the coldest regions of the stratosphere and mesosphere. While it is expected that photochemical production rates of O_3 will increase with decreasing solar zenith angle as one moves southward from the locations noted above, it should not be assumed that photochemical production of O_3 does not occur during late winter and spring at mid- and high-latitudes.

Perhaps the most thorough set of studies investigating causes of springtime maxima in surface O_3 has been performed as part of the AEROCE and NARE studies (cf. Sections AX2.3.4a,b) and TOPSE (Browell et al., 2003). These first two studies found that elevated or surface O_3 > 40 ppb at Bermuda, at least, arises from two distinct sources: the polluted North American continent and the stratosphere. It was also found that these sources mix in the upper troposphere before descending as shown in Figure AX3-80. (In general, air descending behind cold fronts contains contributions from intercontinental transport and the stratosphere.) These studies also concluded that it is impossible to determine sources of O_3 without ancillary data that could be used either as tracers of sources or to calculate photochemical production and loss rates. In addition, subsiding back trajectories do not necessarily imply a free-tropospheric or stratospheric origin for O_3 observed at the surface, since the subsiding conditions are also associated with strong inversions and clear skies that promote O_3 production within the boundary layer. Thus, it would be highly problematic to use observations alone as estimates of PRB O_3 concentrations, especially for sites at or near sea level.

The IPCC Third Assessment Report (TAR) (2001) gave a large range of values for terms in the tropospheric O_3 budget. Estimates of O_3 STE of ozone ranged over a factor of three from 391 to 1440 Tg/year in the twelve models included in the intercomparison; many of the models included in that assessment overestimated O_3 STE. However, the overestimates likely reflected errors in assimilated winds in the upper troposphere (Douglass et al., 2003; Schoeberl et al., 2003; Tan et al., 2004; van Noije et al., 2004). The budgets of tropospheric O_3 calculated since the IPCC TAR are shown in Table AX3-22. Simulation of stratospheric intrusions is notoriously difficult in global models, and O_3 STE is generally parameterized in these models. A model intercomparison looking at actual STE events found significant variations in model results that depended significantly on the type and horizontal resolution of the model (Meloen et al., 2003; Cristofanelli et al., 2003). In particular, it was found that the Lagrangian perspective (as opposed to the Eulerian perspective used in most global scale CTMs) was necessary to

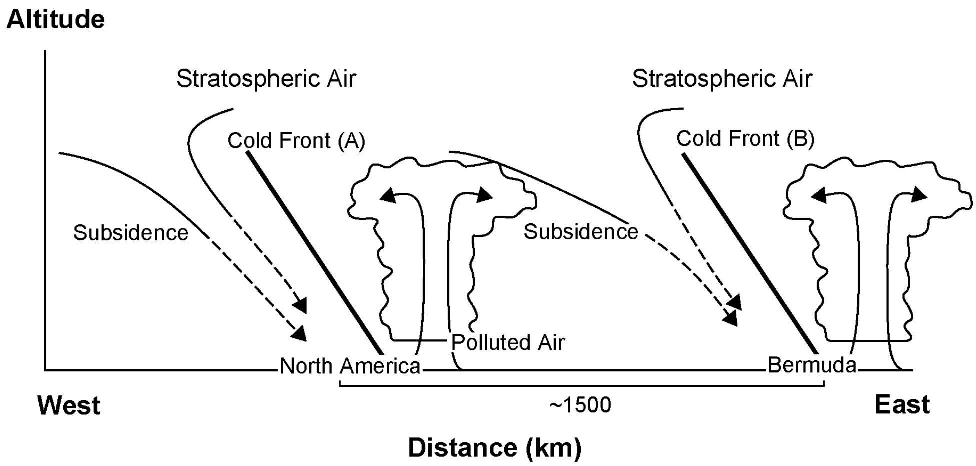

Figure AX3-80. Schematic diagram of a meteorological mechanism involved in high concentrations of ozone found in spring in the lower troposphere off the American East Coast. Subsidence behind the first cold front meets convection ahead of a second cold front such that polluted air and O_3 from the upper troposphere/ lower stratosphere are transported in close proximity (or mixed) and advected over the North Atlantic Ocean. The vertical scale is about 10 km; the horizontal scale about 1500 km. (Note that not all cold fronts are associated with squall lines and that mixing occurs even in their absence.)

Source: Prados (2000).

characterize the depths and residence times of individual events (Sprenger and Wernli, 2003; James et al., 2003a,b). A few studies of the magnitude of the O_3 STE have been made based on chemical observations in the lower stratosphere or combined chemistry and dynamics(e.g., 450 Tg/year net global [Murphy and Fahey, 1994]; 510 Tg/year net global extratropics only [Gettelman et al., 1997]; and 550 ± 140 Tg/year [Olsen et al., 2002]).

Even if the magnitude of cross-tropopause O_3 fluxes in global CTMs are calculated correctly in an annual mean sense, it should be noted that stratospheric intrusions occur episodically following the passage of cold fronts at midlatitudes. Of major concern is the ability of global-scale CTMs to simulate individual intrusions and the effects on surface O_3 concentrations that may result during these events. As noted in Section AX2.3.1, these intrusions occur in “ribbons” ~ 200 to 1000 km long, 100 to 300 km wide, and 1 to 4 km thick. An example of a stratospheric intrusion occurred in Boulder, CO (EPA AQS Site 080130011;

Table AX3-22. Global Budgets of Tropospheric Ozone (Tg year^{-1}) for the Present-day Atmosphere [1]

Reference	Model	Stratosphere-Troposphere Exchange (STE)	Chemical Production [2]	Chemical Loss [2]	Dry Deposition	Burden (Tg)	Lifetime (days) [3]
TAR [4]	11 models	770 ± 400	3420 ± 770	3470 ± 520	770 ± 180	300 ± 30	24 ± 2
Lelieveld and Dentener (2000)		570	3310	3170	710	350	33
Bey et al. (2001) [5]	GEOS-CHEM	470	4900	4300	1070	320	22
Horowitz et al. (2003)	MOZART-2	340	5260	4750	860	360	23
Von Kuhlmann et al. (2003)	MATCH-MPIC	540	4560	4290	820	290	21
Shindell et al. (2003)	GISS	417	NR [6]	NR	1470	349	NR
Park et al. (2004)	UMD-CTM	480	NR	NR	1290	340	NR
Rotman et al. (2004)	IMPACT	660	NR	NR	830	NR	NR
Wong et al. (2004)	SUNYA/UiO GCCM	600	NR	NR	1100	376	NR

[1] From global CTM simulations describing the atmosphere of the last decade of the 20th century.
[2] Chemical production and loss rates are calculated for the odd oxygen family, usually defined as $O_x = O_3 + O + NO_2 + 2NO_3 + 3N_2O_5 + HNO_4 +$ peroxyacylnitrates (and sometimes HNO_3), to avoid accounting for rapid cycling of O_3 with short-lived species that have little implication for its budget. Chemical production is mainly contributed by reactions of NO with peroxy radicals, while chemical loss is mainly contributed by the $O(^1D) + H_2O$ reaction and by the reactions of O_3 with $HO_2^{\bullet}$, •OH, and alkenes. Several models in this table do not report production and loss separately ("NR" entry in the table), reporting instead net production. However, net production is not a useful quantity for budget purposes, because (1) it represents a small residual between large production and loss, (2) it represents the balance between STE and dry deposition, both of which are usually parameterized as a flux boundary condition.
[3] Calculated as the ratio of the burden to the sum of chemical and deposition losses
[4] Means and standard deviations from an ensemble of 11 CTM budgets reported in the IPCC TAR. The mean budget does not balance exactly because only 9 CTMs reported chemical production and loss statistics.
[5] The Martin et al. [2003b] more recent version of GEOS-CHEM gives identical rates and burdens.
[6] Not reported.

formally AIRS) on May 6, 1999 (Lefohn et al., 2001). At 1700 UTC (1000 hours LST) an hourly average concentration of 0.060 ppm was recorded and by 2100 UTC (1400 hours LST), the maximum hourly average O_3 concentration of 0.076 ppm was measured. At 0200 UTC on May 7, 1999 (1900 hours LST on May 6), the hourly average concentration declined to 0.059 ppm. Figure AX3-80 shows the O_3 vertical profile that was recorded at Boulder, CO on May 6, 1999, at 1802 UTC (1102 hours LST). The ragged vertical profile of O_3 at > 4 km reflects stratospheric air that has spiraled downward around an upper-level low and mixed with tropospheric air along the way. Thus, stratospheric air which is normally extremely cold and dry and rich in O_3, loses its characteristics as it mixes downward. This process was described in Section AX2.3.1 and illustrated in Figures AX2-7a,b and c.

The dimensions given above imply that individual intrusions are not resolved properly in the current generation of global-scale CTMs (Figure AX3-81). However, as noted in Section AX2.3.1, penetration of stratospheric air directly to the surface rarely occurs in the continental United States. Rather, intrusions are more likely to affect the middle and upper troposphere, providing a reservoir for O_3 that can exchange with the planetary boundary layer. In this regard, it is important that CTMs be able to spatially and temporally resolve the exchange between the planetary boundary layer and the lower free troposphere properly.

AX3.9.2 CAPABILITY OF GLOBAL MODELS TO SIMULATE TROPOSPHERIC OZONE

The current generation of global CTMs includes detailed representation of tropospheric O_3-NO_x-VOC chemistry. Meteorological information is generally provided by global data assimilation centers. The horizontal resolution is typically a few hundred km, the vertical resolution is 0.1 to 1 km, and the effective temporal resolution is a few hours. These models can simulate most of the observed variability in O_3 and related species, although the coarse resolution precludes simulation of fine-scale structures or localized extreme events. On the synoptic scale, at least, all evidence indicates that global models are adequate tools to investigate the factors controlling tropospheric O_3. Stratosphere-troposphere exchange of O_3 in global models is generally parameterized. The parameterizations are typically constrained to match the global mean O_3 cross-tropopause flux, which is in turn constrained by a number of observational

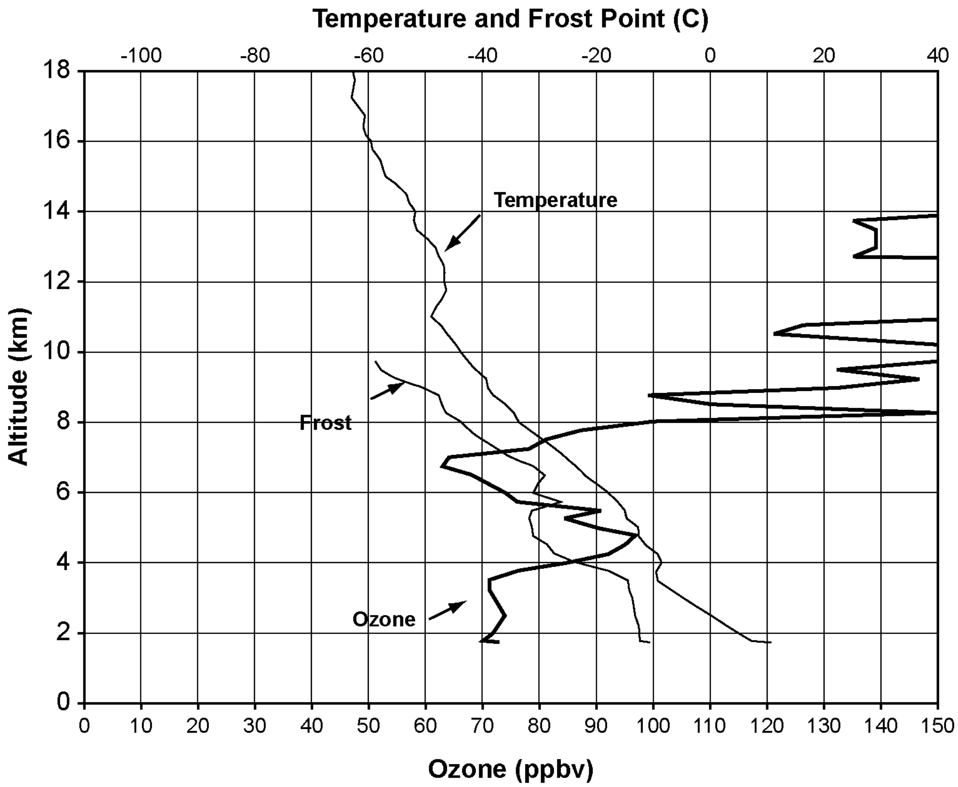

Figure AX3-81. Ozone vertical profile at Boulder, Colorado on May 6, 1999 at 1802 UTC (1102 LST).

Source: Lefohn et al. (2001).

proxies (550 ± 140 Tg O_3 year^{-1} [Olsen et al., 2002]). The model simulations are routinely compared to ozonesonde observations in the middle and upper troposphere to test the simulation of stratospheric influence on tropospheric O_3 (Logan, 1999). Such evaluations show that the parameterized cross-tropopause O_3 flux in global models results in a good simulation of tropospheric O_3, at least in a mean sense; and that the current generation of models can reproduce the tropospheric ozonesonde climatology to within 5 to 10 ppbv, even at mid- and high-northern latitudes in winter, with the correct seasonal cycle.

Fiore et al. (2003a) used the GEOS-CHEM global tropospheric chemistry model to quantify PRB O_3 concentrations across the United States. A net global O_3 flux of 490 Tg O_3 year^{-1} from the stratosphere to the troposphere is imposed in the GEOS-CHEM model, consistent with the range constrained by observations (Olsen et al., 2002). Previous applications of the model have demonstrated that it simulates the tropospheric ozonesonde climatology (Logan, 1999) generally to within 5 to 10 ppbv, including at mid- and high-latitudes (Bey et al., 2001a) over Bermuda in spring (Li et al., 2002) and at sites along the Asian Pacific rim (Liu et al., 2002). The phase of the seasonal cycle is reproduced to within 1 to 2 months (Bey et al., 2001a; Li et al., 2002; Liu et al., 2002). An analysis of the ^{210}Pb-^{7}Be-O_3 relationships observed in three aircraft missions over the western Pacific indicates that the model does not underestimate the stratospheric source of O_3 (Liu et al., 2004). These studies and others (Li et al., 2001; Bey et al., 2001b; Fusco and Logan, 2003) demonstrate that the model provides an adequate simulation of O_3 in the free troposphere at northern midlatitudes, including the mean influence from the stratosphere. However, it cannot capture the structure and enhancements associated with stratospheric intrusions, leading to mean O_3 under-prediction in regions of preferred stratospheric downwelling.

Fiore et al. (2002a, 2003b) presented a detailed evaluation of the model simulation for O_3 and related species in surface air over the United States for the summer of 1995. They showed that the model reproduces important features of observations including the high tail of O_3 frequency distributions at sites in the eastern United States (although sub-grid-scale local peaks are underestimated), the O_3 to (NO_y - NO_x) relationships, and the "piston effect" (the highest O_3 values exhibit the largest response to decreases in U.S. fossil fuel emissions from 1980 to 1995) (Lefohn et al. 1998). Empirical orthogonal functions (EOFs) for the observed regional variability of O_3 over the eastern United States are also well reproduced, indicating that GEOS-CHEM captures the synoptic-scale transport processes modulating surface O_3 concentrations (Fiore et al., 2003b). One model shortcoming relevant for the discussion below is that excessive convective mixing over the Gulf of Mexico and the Caribbean leads to an overestimate of O_3 concentrations in southerly flow over the southeastern United States. Comparison of GEOS-CHEM with the Multiscale Air Quality Simulation Platform (MAQSIP) regional air quality modeling system (Odman and Ingram, 1996) at 36 km^2 horizontal resolution showed that the models exhibit similar skill at capturing the observed variance in O_3 concentrations with comparable model biases (Fiore et al., 2003b).

Simulations to Quantify Background Ozone Over the United States

The sources contributing to the O_3 background over the United States were quantified by Fiore et al. (2003a) with three simulations summarized in Table AX3-23: (1) a standard simulation, (2) a background simulation in which North American anthropogenic NO_x, NMVOC, and CO emissions are set to zero, and (3) a natural O_3 simulation in which global anthropogenic NO_x, NMVOC and CO emissions are set to zero and the CH_4 concentration is set to its 700 ppbv pre-industrial value. Anthropogenic emissions of NO_x, nonmethane volatile organic compounds (NMVOCs), and CO include contributions from fuel use, industry, and fertilizer application. The difference between the standard and background simulations represents regional pollution, i.e., the O_3 enhancement from North American anthropogenic emissions. The difference between the background and natural simulations represents hemispheric pollution, i.e., the O_3 enhancement from anthropogenic emissions outside North America. Methane and NO_x contribute most to hemispheric pollution (Fiore et al., 2002b). A tagged O_3 tracer simulation (Fiore et al., 2002a) was used to isolate the stratospheric contribution to the background and yielded results that were quantitatively consistent with those from a simulation in which O_3 transport from the stratosphere to the troposphere was suppressed (Fusco and Logan, 2003). All simulations were initialized in June 2000; results are reported for March through October 2001.

Table AX3-23. Description of Simulations Used for Source Attribution (Fiore et al., 2003a)

Simulation	Description	Horizontal Resolution
Standard	Present-day emissions as described in the text	2° × 2.5°
Background	North American anthropogenic NO_x, NMVOC, and CO emissions set to zero	2° × 2.5°
Natural	Global anthropogenic NO_x, NMVOC, and CO emissions set to zero and CH_4 concentration set to its 700 ppbv preindustrial value	4° × 5°
Stratospheric	Tagged O_3 tracer originating from the stratosphere in standard simulation	2° × 2.5°

The standard and background simulations were conducted at 2° × 2.5° horizontal resolution, but the natural simulation was conducted at 4° × 5° resolution to save on computational time. There was no significant bias between 4° × 5° and 2° × 2.5° simulations (Fiore et al., 2002a), particularly for a natural O_3 simulation where surface concentrations were controlled by large-scale processes.

AX3.9.3 Mean Background Concentrations: Spatial and Seasonal Variation

The analysis of Fiore et al. (2003a) focused on the 2001 observations from the Clean Air Status and Trends Network (CASTNet) of rural and remote U.S. sites (Lavery et al., 2002) (Figure AX3-82). Figure AX3-83 shows the mean seasonal cycle in afternoon (1300 to 1700 hours LT) O_3 concentrations averaged over the CASTNet stations in each U.S. quadrant. Measured O_3 concentrations (asterisks) are highest in April to May, except in the Northeast where they peak in June. Model results (triangles) are within 3 ppbv and 5 ppbv of the observations for all months in the Northwest and Southwest, respectively. Model results for the Northeast are too high by 5 to 8 ppbv when sampled at the CASTNet sites; the model is lower when the ensemble of grid squares in the region are sampled (squares). The model is 8 to 12 ppbv too high over the Southeast in summer for reasons discussed in Section AX3.9.2.

Results from the background simulation (no anthropogenic emissions in North America; see Table AX3-23) are shown as diamonds in Figure AX3-83. Mean afternoon background O_3 ranges from 20 ppbv in the Northeast in summer to 35 ppbv in the Northwest in spring. It is higher in the West than in the East because of higher elevation, deeper mixed layers, and longer O_3 lifetimes due to the arid climate (Fiore et al., 2002a). It is also higher in spring than in summer, in part because of the seasonal maximum of stratospheric influence (Figure AX3-3) and in part because of the longer lifetime of O_3 (Wang et al., 1998).

Results from the natural O_3 simulation (no anthropogenic emissions anywhere; Table AX3-23) are shown as crosses in Figure AX3-83. Natural O_3 concentrations are also highest in the West and in spring when the influence of stratospheric O_3 on the troposphere peaks (e.g., Holton et al., 1995). Monthly mean natural O_3 concentration ranges are 18 to 23, 18 to 27, 13 to 20, and 15 to 21 ppbv in the Northwest, Southwest, Northeast, and Southeast, respectively. The stratospheric contribution (X's) ranges from 7 ppbv in spring to 2 ppbv in summer.

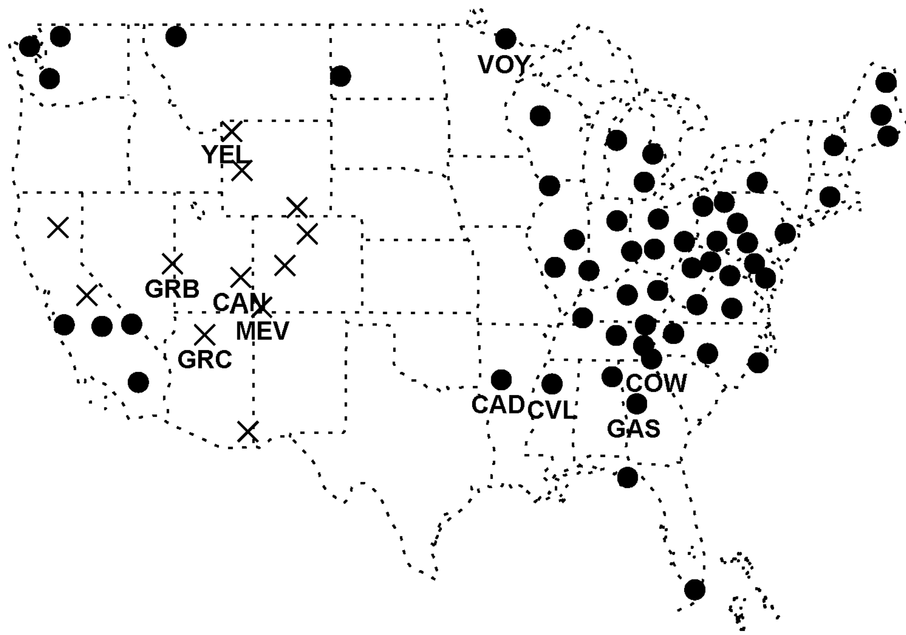

Figure AX3-82. CASTNet stations in the continental United States for 2001. Sites discussed in Section AX3.9.4 are labeled: OY = Voyageurs NP, MI; COW = Coweeta, NC; YEL = Yellowstone NP, WY; CAD = Caddo Valley, AR; CVL = Coffeeville, MS; GAS = Georgia Station, GA; GB = Great Basin, NV; GRC = Grand Canyon, AZ; CAN = Canyonlands, UT; MEV = Mesa Verde, CO. Crosses denote sites > .5 km altitude.

Source: Fiore et al. (2003a).

The difference between the background and natural simulations in Figure AX3-83 represents the monthly mean hemispheric pollution enhancement. This enhancement ranges from 5 to 12 ppbv depending on region and season. It peaks in spring due to a longer O_3 lifetime (Wang et al., 1998) and to e efficient ventilation of pollution from the Asian continent (Liu et al., 2003). In contrast to hemispheric pollution, the regional pollution influence (O_3 produced from North American anthropogenic emissions, shown as the difference between the squares and diamonds) peaks in summer and is highest in the East. For the data in Figure AX3-83, it ranges from 8 ppbv in the northern quadrants in March to over 30 ppbv in the eastern quadrants in summer. Monthly mean observed O_3 concentrations are influenced by both regional and hemispheric pollution in all U.S. regions from March through October.

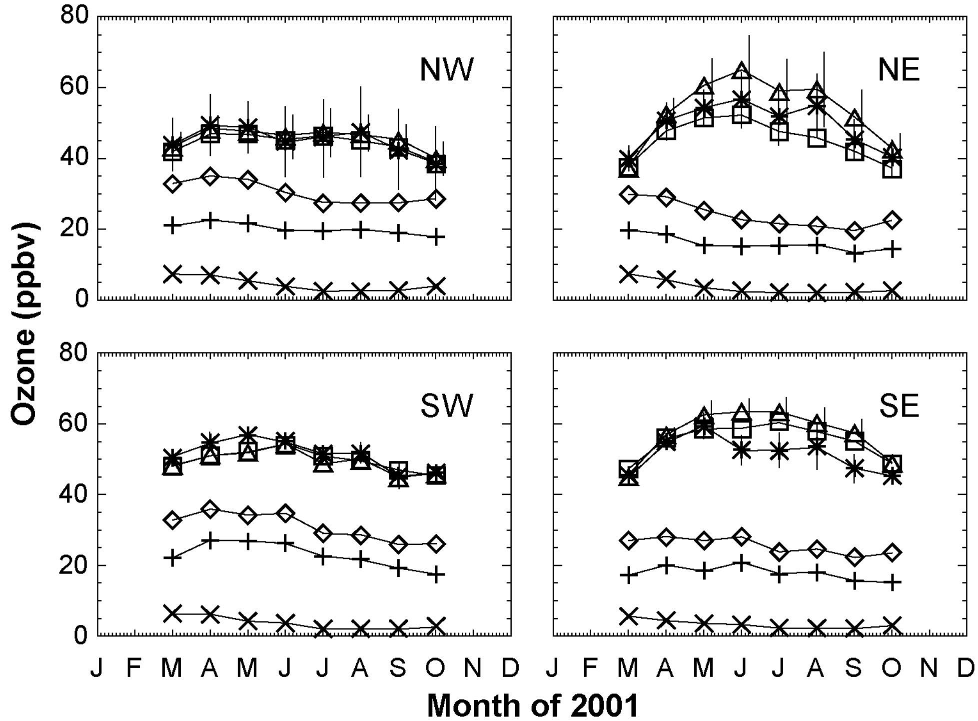

Figure AX3-83. Monthly mean afternoon (1300 to 1700 hours LT) concentrations (ppbv) in surface air averaged over the CASTNet stations (Figure AX3-82) in each U.S. quadrant for March to October 2001. Observations (asterisks) are compared with model values from the standard simulation sampled at the CASTNet sites (triangles) and sampled for the entire quadrant (squares). The vertical lines show the standard deviation in the observed and simulated values. Monthly mean model results for the background (diamonds), natural (crosses), and stratospheric (X's) contributions (Table AX3-23) to surface O_3 are shown. The U.S. quadrants are centered at 98.75° W and 37° N.

Source: Fiore et al. (2003a).

AX3.9.4 Frequency of High-Ozone Occurrences at Remote Sites

Lefohn et al. (2001) pointed out the frequent occurrence of high-O_3 events (> 50 and 60 ppbv) at remote northern U.S. sites in spring. Fiore et al. (2003a) replicated the analysis of Lefohn et al. (2001) at the four CASTNet sites that they examined: Denali National Park (Alaska), Voyageurs National Park (Minnesota), Glacier National Park (Montana), and Yellowstone National Park (Wyoming). The number of times that the hourly O_3 observations at the sites are > 50 and 60 ppbv for each month from March to October 2001 were then calculated (see results in Table AX3-24) and compared with the same statistics for March to June 1988 to 1998 from Lefohn et al. (2001), to place the 2001 statistics in the context of other years. More incidences of O_3 above both thresholds occur at Denali National Park and Yellowstone National Park in 2001 than in nearly all of the years analyzed by Lefohn et al. (2001). The statistics at Glacier National Park, Montana indicate that 2001 had fewer than average incidences of high-O_3 events. At Voyageurs National Park in Minnesota, March and April 2001 had lower-than-average frequencies of high-O_3 events, but May and June were more typical. Overall, 2001 was considered to be a suitable year for analysis of high-O_3 events. Ozone concentrations > 70 and 80 ppbv occurred most often in May through August in 2001 and were found to be associated with regional pollution by Fiore et al. (2003a).

Fiore et al. (2003a) focused their analysis on mean O_3 concentrations during the afternoon hours (1300 to 1700 LT), as the comparison of model results with surface observations is most appropriate in the afternoon when the observations are representative of a relatively deep mixed layer (Fiore et al., 2002a). In addition, the GEOS-CHEM model does not provide independent information on an hour-to-hour basis, because it is driven by meteorological fields that are updated every 6-h and then interpolated. Fiore et al. (2003a) tested whether an analysis restricted to these mean 1300 to 1700 LT surface concentrations captures the same frequency of O_3 > 50 and 60 ppbv that emerges from an analysis of the individual hourly concentrations over 24 hours. Results are reproduced here in Table AX3-24, which shows that the percentage of individual afternoon (1300 to 1700 LT) hours when O_3 > 50 and 60 ppbv at the CASTNet sites is always greater than the percentage of all hourly occurrences above these thresholds, indicating that elevated O_3 concentrations preferentially occur in the afternoon. Furthermore, Table AX3-24 shows that the frequency of observation of high-O_3 events is not diminished when 4-h average (1300 to 1700 LT) concentrations are considered, reflecting persistence in the duration of these events. Model frequencies of high-O_3 events from 1300 to 1700 LT at the CASTNet sites are similar to observations in spring, as shown in Table AX3-24, and about 10% higher in the summer, largely because of the positive model bias in the Southeast discussed in Section AX3.9.2.

Table AX3-24. Number of Hours with Ozone Above 50 or 60 ppbv at U.S. CASTNet Sites in 2001

Site	Mar	Apr	May	Jun	Jul	Aug	Sep	Oct
Observations ≥ 50 ppbv								
Denali NP, Alaska (64˚ N, 149˚ W, 0.6 km)	24	302	98	6	0	0	0	0
Voyageurs NP, Minnesota (48˚ N, 93˚ W, 0.4 km)	0	0	62	95	14	17	33	0
Glacier NP, Montana (49˚ N, 114˚ W, 1.0 km)	4	0	23	0	6	12	0	0
Yellowstone NP, Wyoming (45˚ N, 110˚ W, 2.5 km)	307	461	350	172	140	261	173	77
All CASTNet sites (71)	5468 (11%)	15814 (32%)	17704 (36%)	16150 (33%)	14489 (29%)	15989 (32%)	9874 (20%)	5642 (11%)
All sites, 1300-1700 LT only (hourly data)	1817 (21%)	4684 (56%)	5174 (61%)	4624 (56%)	4613 (54%)	5075 (60%)	3343 (40%)	1945 (23%)
All sites, 1300-1700 LT mean (4-hour average)	435 (20%)	1153 (55%)	1295 (61%)	1147 (55%)	1161 (54%)	1283 (60%)	841 (40%)	478 (22%)
All sites, model 1300-1700 LT mean	254 (12%)	1249 (59%)	1527 (69%)	1505 (71%)	1475 (67%)	1500 (68%)	1080 (51%)	591 (27%)
Observations ≥ 60 ppbv								
Denali NP	0	0	9	2	0	0	0	0
Voyageurs NP	0	0	6	32	0	0	15	0
Glacier NP	0	0	0	0	0	0	0	0
Yellowstone NP	4	77	139	18	6	26	1	2
All sites	519 (1%)	4729 (10%)	8181 (16%)	8199 (17%)	5705 (11%)	7407 (15%)	3492 (7%)	2073 (4%)
All sites, 1300-1700 LT only	235 (3%)	1798 (22%)	2808 (33%)	2721 (33%)	2235 (26%)	2758 (33%)	1416 (17%)	878 (10%)
All sites, 1300-1700 LT mean	56 (3%)	428 (20%)	697 (33%)	671 (32%)	550 (26%)	677 (32%)	358 (17%)	214 (10%)
All sites, model 1300-1700 LT mean	13 (1%)	377 (18%)	834 (38%)	964 (45%)	910 (41%)	834 (38%)	502 (24%)	204 (9%)

Data from 71 U.S. CASTNet sites are included in this analysis: those in Figure AX3-105 plus Denali NP.
Percentages of total occurrences are shown in parentheses.
NP = National Park; LT = Local Time.
Reproduced from Fiore et al. (2003a).

NATURAL VERSUS ANTHROPOGENIC CONTRIBUTIONS TO HIGH-OZONE OCCURRENCES

Figure AX3-84, reproduced from Fiore et al. (2003a), shows probability distributions of daily mean afternoon (1300 to 1700 LT) O_3 concentrations in surface air at the CASTNet sites for March through October 2001. Model distributions for background, natural, and stratospheric O_3 (Table AX3-23) are also shown. The background (long-dashed line) ranges from 10 to 50 ppbv with most values in the 20 to 35 ppbv range. The full 10 to 50 ppbv range of background predicted here encompasses the previous 25 to 45 ppbv estimates shown in Table 3-8. However, background estimates from observations tend to be at the higher end of the range (25 to 45 ppbv), while these results, as well as those from prior modeling studies (Table 3-8) indicate that background O_3 concentrations in surface air are usually below 40 ppbv. The background O_3 concentrations derived from observations may be overestimated if observations at remote and rural sites contain some influence from regional pollution (as shown below to occur in the model), or if the O_3 versus NO_y - NO_x correlation is affected by different relative removal rates of O_3 and NO_y (Trainer et al., 1993). Natural O_3 concentrations (short-dashed line) are generally in the 10 to 25 ppbv range and never exceed 40 ppbv. The range of the hemispheric pollution enhancement (the difference between the background and natural O_3 concentrations) is typically 4 to 12 ppbv and only rarely exceeds 20 ppbv (< 1% total incidences). The stratospheric contribution (dotted line) is always less than 20 ppbv and usually below 10 ppbv. Time series for specific sites are presented below.

CASE STUDIES: INFLUENCE OF THE BACKGROUND ON ELEVATED OZONE EVENTS IN SPRING

High-O_3 events were previously attributed to natural processes by Lefohn et al. (2001) at: Voyageurs National Park, Minnesota in June and Yellowstone National Park, Wyoming in March through May. Fiore et al. (2003a) used observations from CASTNet stations in conjunction with GEOS-CHEM model simulations to deconstruct the observed concentrations into anthropogenic and natural contributions.

At Voyageurs National Park in 2001, O_3 concentrations > 60 ppbv occurred frequently in June but rarely later in summer (Table AX3-24). A similar pattern was observed in 1995 and 1997 and was used to argue that photochemical activity was probably not responsible for these events (Lefohn et al. 2001). Figure AX3-85 from Fiore et al. (2003a) shows that GEOS-CHEM

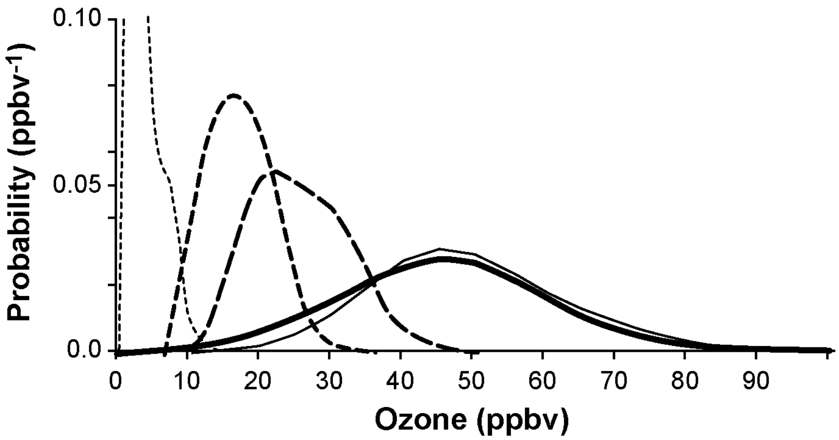

Figure AX3-84. Probability distributions of daily mean afternoon (1300 to 1700 LT) O_3 concentrations in surface air for March through October 2001 at U.S. CASTNet sites (Figure AX3-83): observations (thick solid line) are compared with model results (thin solid line). Additional probability distributions are shown for the simulated background (long-dashed line), natural (short-dashed line), and stratospheric (dotted line) contributions to surface O_3 (Table AX3-23).

Source: Fiore et al. (2003a).

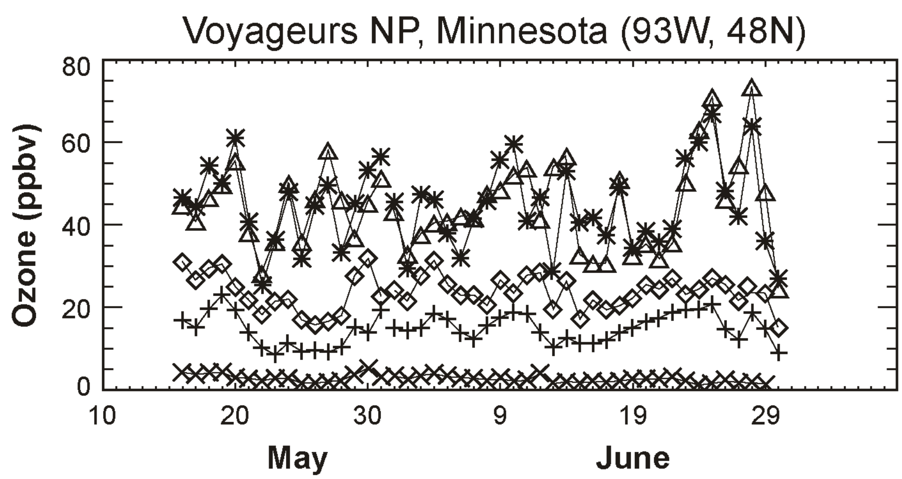

Figure AX3-85. Daily mean afternoon (13 to 17 LT) O_3 concentrations in surface air at Voyageurs National Park (NP), Minnesota in mid-May through June of 2001. Observations (asterisks) are compared with model values from the standard simulation (triangles). The simulated contributions from background (diamonds), natural (crosses), and stratospheric (X's) O_3 are also shown.

Source: Fiore et al. (2003a).

captures much of the day-to-day variability in observed concentrations from mid-May through June, including the occurrence and magnitude of high-O_3 events. The simulated background contribution (diamonds) ranges from 15 to 36 ppbv with a 25 ppbv mean. The natural O_3 level (crosses) is 15 ppbv on average and varies from 9 to 23 ppbv. The stratospheric contribution (X's) is always < 7 ppbv. The dominant contribution to the high-O_3 events on June 26 and 29 is from regional pollution (44 and 50 ppbv on June 26 and 29, respectively, calculated as the difference between the triangles and diamonds in Figure AX3-85). The background contribution (diamonds) is < 30 ppbv on both days, and is composed of a 20 ppbv natural contribution (which includes 2 ppbv of stratospheric origin) and a 5 ppbv enhancement from hemispheric pollution (the difference between the diamonds and crosses). Beyond these two high-O_3 events, Figure AX3-85 shows that regional pollution drives most of the simulated day-to-day variability and explains all events above 50 ppbv. In 2001, monthly mean observed and simulated O_3 concentrations are lower in July (37 and 42 ppbv, respectively) and August (35 and 36 ppbv) than in June (44 and 45 ppbv). Fiore et al. (2003a) hypothesized that the lower mean O_3 and the lack of O_3 > 60 ppbv in July and August reflects a stronger Bermuda high-pressure system sweeping pollution from southern regions eastward before it could reach Voyageurs National Park.

Frequently observed concentrations of O_3 between 60 to 80 ppbv at Yellowstone NP in spring (Figures AX3-77a,b) have been attributed by Lefohn et al. (2001) to natural sources, because they occur before local park traffic starts and back-trajectories do not suggest influence from long-range transport of anthropogenic sources. More hours with O_3 > 60 ppbv occur in April and May of 2001 (Table AX3-24) than in the years analyzed by Lefohn et al. (2001). Fiore et al. (2003a) used GEOS-CHEM to interpret these events; results are shown in Figure AX3-86. The mean background, natural, and stratospheric O_3 contributions in March to May are higher at Yellowstone (38, 22, and 8 ppbv, respectively) as compared to 27, 18, and 5 ppbv at the two eastern sites previously discussed. The larger stratospheric contribution at Yellowstone reflects the high elevation of the site (2.5 km). Fiore et al. (2003a) argued that the background at Yellowstone National Park should be considered an upper limit for U.S. PRB O_3 concentrations, because of its high elevation. While Yellowstone receives a higher background concentration than the eastern sites, the model shows that regional pollution from North American anthropogenic emissions (difference between the triangles and diamonds) contributes an

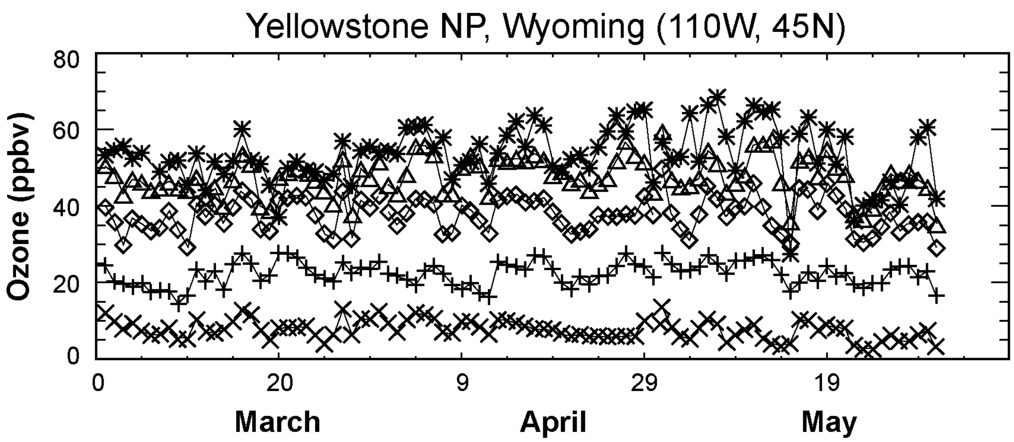

Figure AX3-86. Same as Figure AX3-85 but for Yellowstone National Park, Wyoming in March to May 2001. Observations (asterisks) are compared with model values from the standard simulation (triangles). The simulated contributions from background (diamonds), natural (crosses), and stratospheric (X's) O_3 are also shown.

Source: Fiore et al. (2003a).

additional 10 to 20 ppbv to the highest observed concentrations in April and May. One should not assume that regional photochemistry is inactive in spring.

Higher-altitude western sites are more frequent recipients of subsidence events that transport high concentrations of O_3 from the free troposphere to the surface. Cooper and Moody (2000) cautioned that observations from elevated sites are not generally representative of lower-altitude sites. At Yellowstone, the background O_3 rarely exceeds 40 ppbv, but it is even lower in the East. This point is illustrated in Figure AX3-87, from Fiore et al. (2003a), with time series at representative western and southeastern CASTNet sites for the month of March, when the relative contribution of the background should be high. At the western sites, the background is often near 40 ppbv but total surface O_3 concentrations are rarely above 60 ppbv. While variations in the background play a role in governing the observed total O_3 variability at these sites, regional pollution also contributes. Background concentrations are lower (often < 30 ppbv) in the southeastern states where regional photochemical production drives much of the observed variability. Cooper and Moody (2000) have previously shown that the high O_3 concentrations at an elevated, regionally representative site in the eastern United States in spring

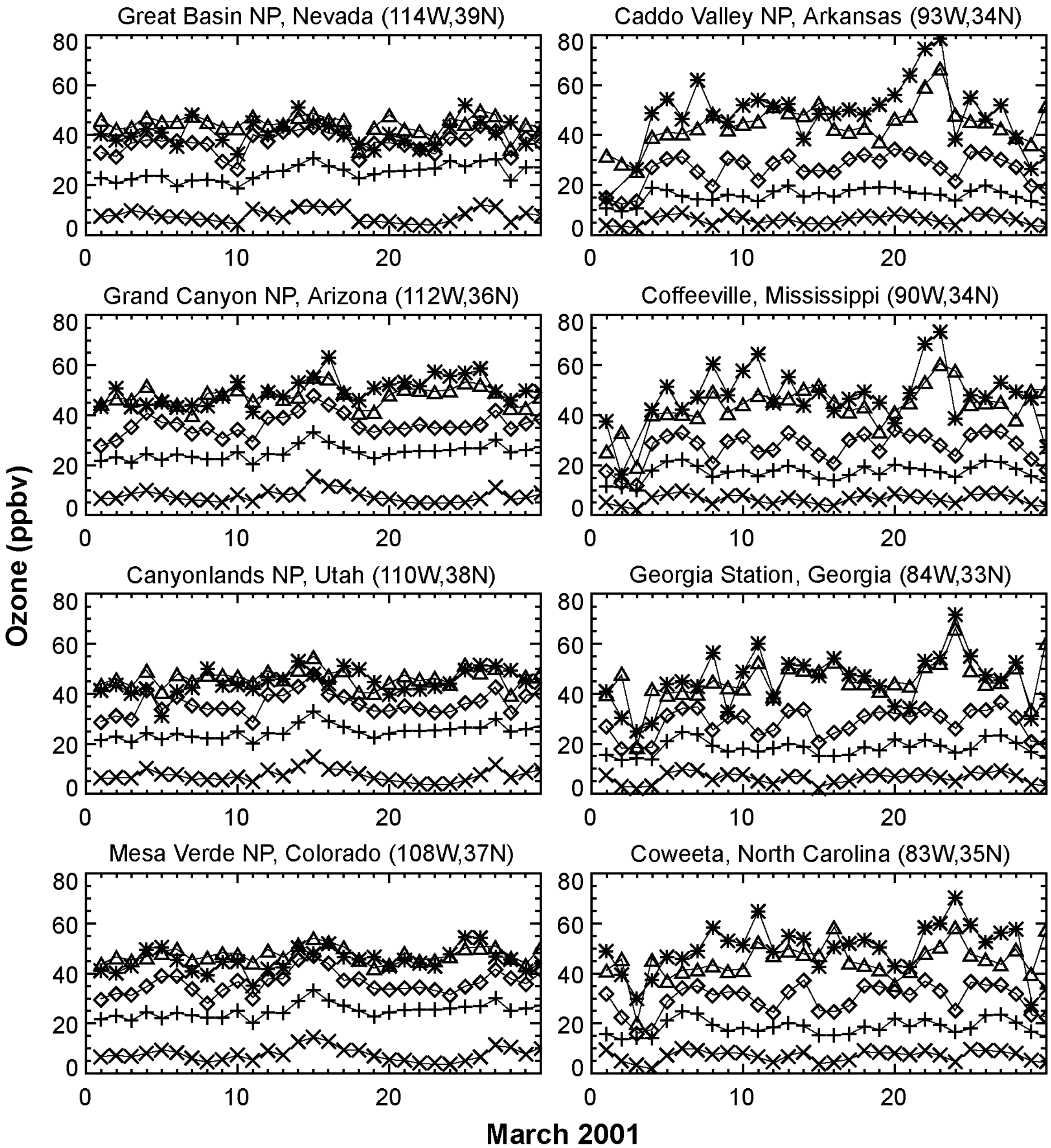

Figure AX3-87. Same as Figure AX3-86 but for March of 2001 at selected western (left column) and southeastern (right column) sites. Observations (asterisks) are compared with model values from the standard simulation (triangles). The simulated contributions from background (diamonds), natural (crosses), and stratospheric (X's) O_3 are also shown.

Source: Fiore et al. (2003a).

coincide with high temperatures and anticyclonic circulation, conditions conducive to photochemical O_3 production. Peak O_3 concentrations in this region, mainly at lower elevations, are associated with lower background concentrations because chemical and depositional loss during stagnant meteorological conditions suppress mixing between the boundary layer and the free troposphere (Fiore et al., 2002a). Surface O_3 concentrations > 80 ppbv could conceivably occur when stratospheric intrusions reach the surface. However, based on information given in Section AX2.3.2, these events are rare.

AX3.10 INDOOR SOURCES AND CONCENTRATIONS

In the past, indoor O_3 concentrations/exposure were not considered of importance. However, since most people spend a significant amount of time indoors, most exposure to air pollutants of outdoor origin occur indoors. This section will address the sources and concentrations of indoor O_3. This section will also briefly discuss those factors that affect indoor O_3 concentrations. A comprehensive review of O_3 in the indoor environment appears in Weschler (2000).

AX3.10.1 Sources and Emissions of Indoor Ozone

Ozone enters the indoor environment primarily through infiltration from outdoors through cracks and crevices in the building envelope (unintentional and uncontrolled ventilation) and through building components such as windows and doors and ventilation systems (natural and controlled ventilation). Natural ventilation is driven by the natural forces of wind and temperature. Possible indoor sources of O_3 include office equipment (photocopiers, facsimile machines, and laser printers) and air cleaners (electrostatic air filters and precipitators and O_3 generators). Generally O_3 emissions from photocopiers and laser printers are limited due to installed filtering systems (Black and Worthan, 1999; Leovic et al., 1996; Aldrich et al., 1995). However, emissions increase under improper maintenance conditions (Leovic et al., 1996). Well-maintained photocopiers and laser printers usually emit low levels of O_3 by catalytically reducing the O_3 to oxygen (Aldrich et al., 1995). Leovic et al. (1996, 1998) measured O_3 emissions from four dry-process photocopiers. Ozone emissions ranged from 1300 to 7900 µg/h.

Most electrostatic air filters and precipitators are designed to minimize the production of O_3. However, if excessive arcing occurs, the units can emit a significant amount of O_3 into the indoor environment (Weschler, 2000). Niu et al. (2001) measured O_3 emissions from 27 air cleaners that used ionization processes to remove particulates. The test were conducted in a $2 \times 2 \times 1.60\ m^3$ stainless steel environmental chamber. The tests were terminated after 1.5 h if no increase in O_3 concentration was noted. If an increase in O_3 was noted, the test was continued, in some cases, for up to 20 h. Most of the evaluated units emitted no O_3 or only small amounts. Five units were found to emit O_3 ranging from 56 to 2757 µg/h.

There are many brands and models of O_3 generators commercially available. The amount of O_3 emitted by each unit depends on the size of the unit. Ozone emission rates have been reported to range from tens to thousands of micrograms per hour (Weschler, 2000; Steiber, 1995). Ozone emissions supposedly can be regulated using the units control features. However, available information suggests that O_3 output may not be proportional to the control setting. Some units are equipped with a sensor that automatically controls O_3 output by turning the unit on and off. The effectiveness of the sensor is unknown (U.S. Environmental Protection Agency, 2002).

AX3.10.2 Factors Affecting Ozone Concentrations Indoors

In the absence of an indoor source, O_3 concentrations in indoor environments will depend on the outdoor O_3 concentration, the air exchange rate (AER) or outdoor infiltration, indoor circulation rate, O_3 removal by indoor surfaces, reactions with other indoor pollutants, and temperature and humidity. Indoor O_3 concentrations generally closely track outdoor O_3 concentrations. Since outdoor O_3 concentrations are generally higher during the warmer months, indoor concentrations will also be highest during that time period. (See discussion on ambient concentrations of O_3 earlier in this chapter.)

Air Exchange Rates

Indoor O_3 increases with increasing air exchange rate (Gold et al., 1996; Lee et al., 1999; Jakobi and Fabian, 1997). The AER is the balance of the flow of air in and out of a microenvironment. Infiltration through unintentional openings in the building envelope is the dominant mechanism for residential air exchange. However, natural ventilation, airflow through opened windows and doors, also influences air exchange in residential buildings. Forced or mechanical ventilation is the dominant mechanism for air exchange in nonresidential buildings.

Air exchange rates vary depending on the temperature differences, wind effects, geographical region, type of heating/mechanical ventilation system, and building type (U.S. Environmental Protection Agency, 1997; Weschler and Shields, 2000; Colome et al., 1994; Johnson et al., 2004). Air exchange rates are generally higher during the summer and lower during the winter months (Wilson et al., 1996; Murray and Burmaster, 1995; Colome et al., 1994; Research Triangle Institute, 1990).

Howard-Reed et al. (2002) determined that opening a window or exterior door causes the greatest increase in AERs with differences between the indoor and outdoor temperature being important when the windows were closed. Johnson and Long (2004) conducted a pilot study to evaluate the frequency that windows were left open in a community. They found that a visual 2-h survey could be used to estimate the frequency that windows are left open. The occupancy, season, housing density, absence of air conditioning, and wind speed were factors in whether the windows were open.

Johnson et al. (2004) conducted a study using scripted ventilation conditions to identify those factors that affected air exchange inside a test house in Columbus, OH. The test house was a wood-framed, split-level structure with aluminum siding covering the wood outer walls. The house had one exterior door located in the front and another at the rear of the house, single-pane glazed windows, central gas heat, a window air-conditioning unit, and ceiling fans in three rooms. Eighteen scenarios with unique air flow conditions were evaluated to determine the effect on the AER. The elements of the scenarios included: exteriors doors open/closed, interior doors open/closed, heater on/off, air conditioner on/off, a ceiling fans on/off. The lower level was sealed off during the study. The various scenarios were evaluated during the winter season. The average AER for all scenarios ranged from 0.36 to 15.8 h^{-1}. When all windows and doors were closed, the AER ranged from 0.36 to 2.29 h^{-1} (0.77 h^{-1} geometric mean). When at least one exterior door or window was open the AER ranged from 0.5 to 15.8 h^{-1} (1.98 h^{-1} geometric mean).

One of the most comprehensive evaluations of AERs for residential structures was conducted by Murray and Burmaster (1995) using data compiled by Brookhaven National Laboratories. The analysis used data on AERs for 2,844 residential structures in four regions based on heating degree days. Data were also separated by seasons (winter, spring, summer, and fall). The AER for all seasons across all regions was 0.76 h^{-1} (arithmetic). Table AX3-25 lists the mean AER for the various seasons and regions. The data does not represent all areas of the country.

Air exchange rates for 49 nonresidential buildings (14 schools, 22 offices, and 13 retail establishments) in California were reported by Lagus Applied Technology, Inc. (1995). Average mean (median) AERs were 2.45 (2.24), 1.35 (1.09), and 2.22 (1.79) h^{-1} for schools, offices, and retail establishments, respectively. Air infiltration rates for 40 of the 49 buildings were 0.32, of 0.31, and 1.12 h^{-1} for schools, offices, and retail establishments, respectively. Air exchange rates for 40 nonresidential buildings in Oregon and Washington (Turk et al., 1989) averaged 1.5 (1.3) h^{-1} (mean median). The geometric mean of the AERs for six garages was 1.6 h^{-1} (Marr et al., 1998). Park et al. (1998) reported AERs for three stationary cars (cars varied by age) under different ventilation conditions. Air exchange rates ranged from 1.0 to 3.0 h^{-1} for windows closed and fan off, 13.3 to 23.5 h^{-1} for windows opened and fan off, 1.8 to 3.7 h^{-1} for windows closed and fan on recirculation (two cars tested), and 36.2 to 47.5 h^{-1} for windows closed and fan on fresh air (one car tested). An average AER of 13.1 h^{-1} was reported by Ott et al. (1992) for a station wagon moving at 20 mph with the windows closed.

Ozone Removal Processes

The most important removal process for O_3 in the indoor environment is deposition on indoor surfaces. When O_3 enters the indoor environment it is deposited on and reacts with indoor surfaces. The rate of deposition is material specific. The removal rate will depend on the indoor dimensions, surface coverings, and furnishings. Smaller rooms generally have larger surface-to-volume ratios (A/V) and remove O_3 faster. Fleecy materials, such as carpets, have larger A/V ratios and remove O_3 faster than smooth surfaces (Weschler, 2000). Weschler et al. (1992) found that O_3 reacts with carpet, decreasing O_3 concentrations and increasing emissions of formaldehyde, acetaldehyde, and other C_5–C_{10} aldehydes. Off-gassing of 4-phenylcyclohexene, 4-vinylcyclohexene, and styrene was reduced. The rate of O_3 reaction with carpet diminishes with cumulative O_3 exposure (Morrison and Nazaroff, 2000, 2002). Reiss et al. (1995) reported significant quantities of acetic acid and smaller quantities of formic acid off-gassing from O_3 reactions with latex paint. The emission rate also was relative

Table AX3-25. Air Exchange Rates in Residences by Season and Region of the Country

Season[a]	Region	Sample Size	Mean	Std. Dev.	Total in Region	Average No. of Days Heated[c]	Std. Dev. of Heating Degree Days[c]
All	All	2844	0.76	0.88	2844		
1	All	1139	0.55	0.46			
2	All	1051	0.65	0.57			
3	All	529	1.5	1.53			
4	All	125	0.41	0.58			
All	1	467	0.4	0.3	467	7324	468
All	2	496	0.55	0.48	496	5751	336
All	3	332	0.55	0.42	332	4333	729
All	4	1549	0.98	1.09	1549	1995	115
1	1	161	0.36	0.28			
1	2	428	0.57	0.43			
1	3	96	0.47	0.4			
1	4	454	0.63	0.52			
2	1	254	0.44	0.31			
2	2	43	0.52	0.91			
2	3	165	0.59	0.43			
2	4	589	0.77	0.62			
3	1	5[b]	0.82	0.69			
3	2	2[b]	1.31	na			
3	3	34	0.68	0.5			
3	4	488	1.57	1.56			
4	1	47	0.25	0.15			
4	2	23[b]	0.35	0.18			
4	3	37	0.51	0.25			
4	4	18[b]	0.72	1.43			

[a]Season 1: December, January, February; Season 2: March, April, May; Season 3: June, July, August; Season 4: September, October, November.
[b]Note: Small sample size, n < 25.
[c]Estimated using locations of residences evaluated in the region.

Source: Adapted from Murry and Burmaster (1995).

humidity-dependent, increasing with higher relative humidity. Klenø et al. (2001) evaluated O_3 removal by several aged (1- to 120-month) but not used building materials (nylon carpet, linoleum, painted gypsum board, hand polished stainless steel, oiled beech parquet, melamine-coated particle board, and glass plate). Initially, O_3 removal was high for all specimens tested with the exception of the glass plate. Ozone removal for one carpet specimen and the painted gypsum board remained high throughout the study. For the oiled beech parquet and melamine-coated particle board, O_3 removal leveled off to a moderate rate. Morrison et al. (1998) reported that little O_3 (~9%) is removed by the ductwork of lined ventilation systems. The removal efficiency decreases with continued exposure to O_3, and unlined ductwork is less efficient in removing O_3. Liu and Nazaroff (2001) reported that O_3 is scavenged by fiberglass insulation. More O_3 was scavenged (60 to 90%) by fiberglass that had not been previously exposed. Table AX3-26 lists the removal rates for O_3 in different indoor environments.

Jaboki and Fabian (1997) found the O_3 decays exponentially. They examined O_3 decay in several closed rooms and in a car after a period of intensive ventilation. Figure AX3-88 plots the O_3 decay rates in these environments.

Several studies have examined factors within homes that may scavenge O_3 and lead to decreased O_3 concentrations. Ozone reacts indoors with NO_x and VOCs in an analogous fashion to that occurring in the ambient atmosphere (Lee et al., 1999; Wainman et al., 2000; Weschler and Shields, 1997). These reactions produce related oxidant species while reducing indoor O_3 levels. Lee et al. (1999) studied 43 homes in Upland, CA in the Los Angeles metropolitan region and reported that O_3 declined faster in homes with more bedrooms, greater amounts of carpeting, and lower ceilings (all of which alter the A/V ratio) and with the use of air conditioning. Homes with air conditioning had indoor/outdoor (I/O) ratios of 0.07, 0.09, and 0.11. Homes without air conditioning had an I/O ratio of 0.68 ± 0.18. Closed windows and doors combined with the use of an air cleaner resulted in an I/O ratio of 0.15. The O_3 I/O ratio was < 0.2 in homes with gas stoves.

Ozone reacts with terpenes from wood products, solvents, or odorants to produce submicron particles (Wainman et al., 2000; Weschler and Shields, 1999; Grosjean and Grosjean, 1996, 1998). Wainman et al. (2000) suggested that the $PM_{2.5}$ concentrations could be in excess of 20 $\mu g/m^3$ in the indoor environment as a result of O_3/terpene reactions. Indoor hydroxy radical (HO•) concentrations increase nonlinearly with increased indoor O_3 concentrations and

Table AX3-26. Rate Constants (h^{-1}) for the Removal of Ozone by Surfaces in Different Indoor Environments

Indoor environment	Surface Removal Rate, k_d (A/V), h^{-1}	Reference
Aluminum Room (11.9 m^3)	3.2	Mueller et at. (1973)
Stainless Steel Room (14.9 m^3)	1.4	
Bedroom (40.8 m^3)	7.2	
Office (55.2 m^3)	4.0	
Home (no forced air)	2.9	Sabersky et al. (1973)
Home (forced air)	5.4	
Department Store	4.3	Thompson et al. (1973)
Office (24.1 m^3)	4.0	Allen et al. (1978)
Office (20.7 m^3)	4.3	
Office/Lab	4.3	Shair and Heitner (1974)
Office/Lab	3.2	Shair (1981)
Office/Lab	3.6	
13 Buildings, 24 ventilation systems	3.6[a]	Nazaroff and Cass (1986)
Museum	4.3	
Museum	4.3	
Office/Lab	4	Weschler et al. (1989)
Office/Lab	3.2	
Office	2.5	
Lab	2.5	
Cleanroom	7.6	
Telephone Office	0.8 – 1.0[b]	Weschler et at. (1994)[b]
43 Homes	2.8 ± 1.3	Lee et al. (1999)

[a] A/V = assumes surface area to volume ratio = 2.8 m^{-1}
[b] Large office, small A/V

Source: Weschler (2000).

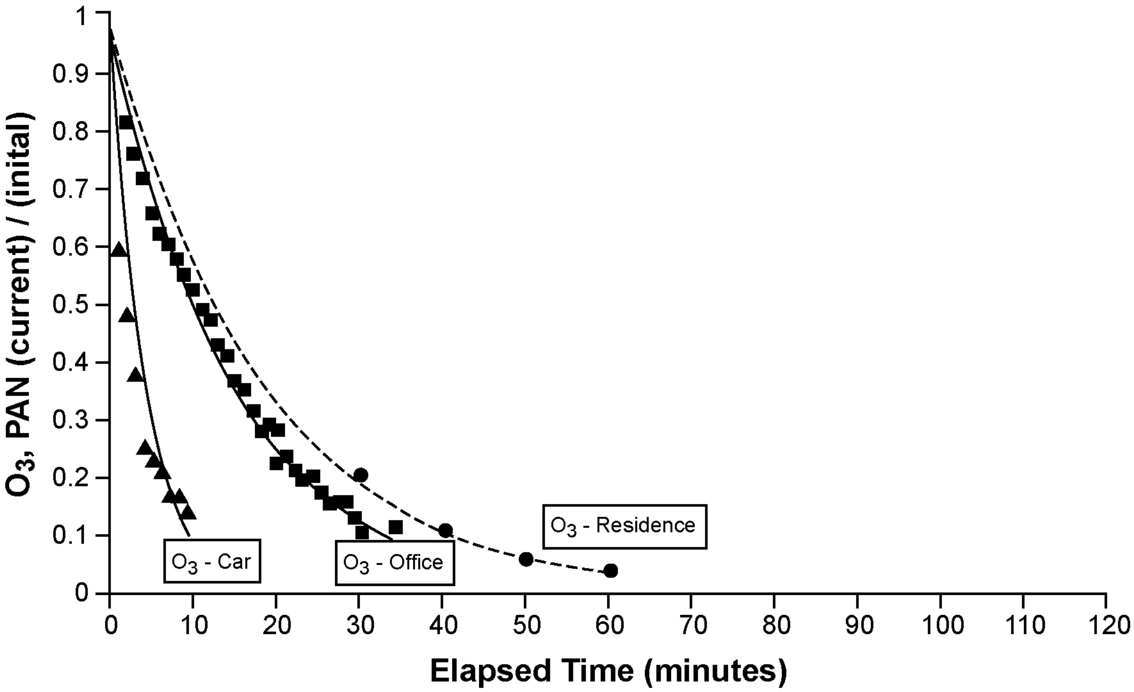

Figure AX3-88. Ozone decay processes versus time measured for several indoor rooms. Room temperature in all cases was ~27 °C and 29 °C in the car.

Adapted from: Jaboki and Fabian (1997).

indoor alkene emissions. Sarwar et al. (2002) suggested that the HO• reacts with terpenes to produce products with low vapor pressures that contribute to fine particle growth.

AX3.10.3 Ozone Concentrations in Microenvironments

Monitored Concentrations in Microenvironments

The 1996 O_3 AQCD for Ozone (U.S. Environmental Protection Agency, 1996a) reported O_3 I/O ratios for a variety of indoor environments including homes, office/laboratories, a hospital, museums, a school room, and automobiles and other vehicles. Ozone I/O ratios ranged from 0.09 to 1.0 for residences, 0.19 to 0.8 for offices/laboratories, hospital and school rooms, and 0.03 to 0.87 for museums and art galleries. The higher O_3 ratios were generally noted in indoor environments with high AERs or 100% outside air intake. Studies published since completion of the 1996 O_3 AQCD are discussed in this section. The findings of the more recent studies on O_3 I/O ratios are included in Table AX3-27.

Table AX3-27. Indoor/Outdoor Ozone Ratios

Location and Ventilation Conditions	Indoor/Outdoor Ratio Mean (range)	Comments	Reference
Toronto, Canada, Homes Winter – weekly (68) Summer – weekly (38) Summer – 12 h/day (128) – 12 h/night (36)	 0.07 ± 0.10 (ND - 0.63) 0.40 ± 0.29 (ND - 1.15) 0.30 ± 0.32 (ND - 1.42) 0.43 ± 0.54 (ND - 2.89)	Electrostatic air cleaners were present in about 50% of the homes. Air conditioners were present in about 80% of the homes, most were central units that used recycled air. Air conditioners used in only 13 of the 40 homes on a daily basis. Measurements were made both inside and outside of the homes for 5 consecutive 24-h periods. Homes with electrostatic air cleaners had higher I/O ratios during the winter months. The mean average weekly AER for all homes during the winter months was 0.69 ± 0.88 h^{-1} with 50% of the homes with an AER of less than 0.41 h^{-1}. For the summer months, the mean average AER was 1.04 ± 1.28 h^{-1} with 50% of the homes with an AER of less than 0.52 h.	Liu et al. (1995)
Boston, MA, Homes (26) Winter – continuously 24 h Summer – continuously 24 h	 0.30 ± 0.42 (ND - 1.31) 0.22 ± 0.25 (ND - 0.88)	Study examined the potential for O_3 to react with VOCs to form acid aerosols. Carbonyls were formed. No clear trend of O_3 with AERs. The average AER was 0.9 h^{-1} during the winter and 2.6 h^{-1} during the summer. Four residences in winter and nine in summer, with 24 h average concentrations. Air concentrations varied from 0-34.2 ppb indoors and 4.4-40.5 ppb outdoors.	Reiss et al. (1995)
Mexico City, School Windows/Doors Open (27) Windows/Doors Closed, cleaner off (41) Windows/Doors Closed, cleaner on (47)	 0.73 ± 0.04 0.17 ± 0.02 0.15 ± 0.02	Study conducted over 4-day period during winter months. Two-min averaged measurements were taken both inside and outside of the school every 30 min from 10 a.m. to 4 p.m. Estimated air exchange rates were 1.1, 2.1, and 2.5 h^{-1} for low, medium, and high flow rates. Ozone concentrations decreased with increasing relative humidity.	Gold et al. (1996)
Los Angeles, CA Homes (95) Other locations (57)	 0.28 0.18	Study conducted in September. Monitored O_3 concentrations consisted of twenty-one 24-h periods beginning at 7 p.m. and ending at 7 p.m. on the following day. Ozone concentrations were higher at the fixed monitoring sites, during the afternoon, the weather was sunny, and the temperature was high. I/O ratio was lower when windows were closed. The effect of air conditioning on the I/O was varied.	Johnson (1997)

Table AX3-27 (cont'd). Indoor/Outdoor Ozone Ratios

Location and Ventilation Conditions	Indoor/Outdoor Ratio Mean (range)	Comments	Reference
Mexico City	0.20 ± 0.18 (0.04 - 0.99)	Ozone monitoring occurred between September and July. Study included 3 schools and 145 homes. Most of the homes were large and did not have air conditioning. Ninety-two percent of the homes had carpeting, 13% used air filters, and 84% used humidifiers. Thirty-five percent opened windows frequently, 43% sometimes, and 22% never between 10 a.m. and 4 p.m. Ozone was monitored at the schools sites from 8 a.m. to 1 p.m. daily for 14 consecutive days. Homes were monitored for continuous 24-h periods for 14 consecutive days. I/O based on 1-h avg concentrations.	Romieu et al. (1998)
Homes (237)	0.1 - 0.3		
Schools (59)	0.3 - 0.4		
Los Angeles, Homes (239)	0.37 ± 0.25 (0.06 - 1.5)	Four hundred and eighty-one samples collected inside and immediately outside of home from February to December. Ratios based on 24-h avg O_3 concentrations indoors and outdoors. Low outdoor concentrations resulted in low indoor concentrations. However, high outdoor concentrations resulted in a range of indoor concentrations and ratios. I/O ratios were highest during the summer months.	Avol et al. (1998a)
Summer	0.43 ± 0.29		
Winter	0.32 ± 0.21		
California		I/O ratio was determined for 20 homes. Only 3 of the homes operated the air conditioning. I/O ratios based on 24-h continuous ambient concentrations and 0.5-1 h avg indoor concentrations.	Lee et al. (1999)
Homes			
no AC, window opened (20)	0.68 (n = 20)		
AC, windows closed (3)	0.09 (n = 3)		
Munich Germany		Indoor concentrations were dependent on the type of ventilation.	Jakobi and Fabian (1997)
Office	0.4 - 0.9		
Gymnasium	0.49 - 0.92		
Classroom	0.54 - 0.77		
Residence			
Bedroom	0.47 - 1.0		
Livingroom	0.74 - 1.0		
Hotel room	0.02		
Car	0.4 - 0.6		

Table AX3-27 (cont'd). Indoor/Outdoor Ozone Ratios

Location and Ventilation Conditions	Indoor/Outdoor Ratio Mean (range)	Comments	Reference
Montpellier, France, Homes (110)	0.41	Ozone measurements were made over 5-day periods in and outside of 21 homes during the summer and winter months. The winter I/O ratio was 0.31 compared to 0.46 during the summer months.	Bernard et al. (1999)
Southern CA, Homes Upland Mountains	0.68 ± 0.18 (windows open) 0.07 - 0.11 (AC used)	Ozone measurements were taken at 119 homes (57 in Upland and 62 in towns located in the mountains) during April and May. I/O ratios were based on average monthly outdoor concentrations and average weekly indoor concentrations. I/O ratio was associated with the home location, number of bedrooms, and the presence of an air conditioner. I/O ratios based on subset of the homes.	Geyh et al. (2000); Lee et al. (2002)
Krakow, Poland Museums (5)	0.13 - 0.42	Ozone continuously monitored at five museums and cultural centers. Monitoring conducted during the summer months for 21-46 h or 28-33 days at each of the sites. The I/O was found to be dependent on the ventilation rate, i.e., when the ventilation rate was high, the I/O ratio approached unity, while in rooms sequestered from the outdoor air or where air was predominantly recycled through charcoal filters, the O_3 levels indoors were greatly reduced resulting in low I/O ratios.	Salmon et al. (2000)
Buildings, Greece Thessaloniki Athens	0.24 ± 0.18 (0.01 to 0.75)	There was no heating/air conditioning system in the building at Thessaloniki. Windows were kept closed during the entire monitoring period. Complete air exchange took place every 3 h. I/O ratio ranged from 0.5-0.90, due to low deposition velocity on indoor surfaces. The air conditioning system in continuous use at the Athens site recirculated the air. Complete air exchange was estimated to be 1 h. Monitoring lasted for 30 days at each site, but only the 7 most representative days were used for calculation of the I/O ratio.	Drakou et al. (1998)

ND = not detectable.

Northeast States for Coordinated Air Use Management (NESCAUM, 2002) monitored levels of O_3 inside and outside of nine schools located in the New England states. The schools represented a variety of environmental conditions in terms of ambient O_3 concentration, sources, geographic location, population density, traffic patterns, and building types. Schools were monitored during the summer months to establish baseline O_3 concentrations and again during the fall after classes started. A monitor was placed directly outside of the school entrance and 50 feet away from the entrance in the hall. Where available, monitors were placed at locations identified as “problem” classrooms, classrooms with carpeting, or in rooms close to outdoor sources of O_3. As expected, outdoor concentrations of O_3 were higher than those found indoors. Averaged O_3 concentrations were low during the early morning hours (7:30 a.m.) but peaked to approximately 25 and 40 ppb around 1:30 p.m. indoors and outdoors, respectively.

Gold et al. (1996) compared indoor and outdoor O_3 concentrations in classrooms in Mexico City under three different ventilation conditions: windows/doors open, air cleaner off; windows/doors closed, air cleaner off; and windows/doors closed, air cleaner on. Two-min averaged outdoor O_3 levels varied between 64 and 361 ppb, while indoor O_3 concentrations ranged from 0 to 247 ppb. The highest indoor O_3 concentrations were noted when the windows/doors were open. The AERs were estimated to be 1.1, 2.1, and 2.5 h^{-1} for low, medium, and high air flow rates, respectively. The authors indicated that the indoor levels, and therefore O_3 exposure to students in schools, can be reduced to < 80 ppb by closing windows and doors even when ambient O_3 levels reach 300 ppb.

In a second Mexico City study, Romieu et al. (1998) measured O_3 concentrations inside and outside of 145 homes and three schools. Measurements were made between November and June. Most of the homes were large and did not have air conditioning. Ninety-five percent of the homes had carpeting, 13% used air filters, and 84% used humidifiers. Thirty-five percent of the homeowners reported that they opened windows frequently between the hours of 10 a.m. and 4 p.m., while 43% opened windows sometimes and 22% reported that they never opened windows during that time period. Homes were monitored for continuous 24-h periods for 14 consecutive days. Schools were monitored from 8 a.m. to 1 p.m. or continuously for 24 h. During the school monitoring periods the windows were frequently left open and the doors were constantly being opened and closed. The mean indoor and outdoor O_3 concentrations during 5-h measurements at the schools were 22 ppb and 56 to 73 ppb, respectively. The mean indoor and outdoor O_3 concentrations for measurements made over a 7- and 14-day period at the test homes were 5 and 27 ppb and 7 and 37 ppb, respectively. Ozone concentrations inside of homes were dependent on the presence of carpeting, the use of air filters, and whether the windows were open or closed. Air exchange rates were not reported.

Reiss et al. (1995) compared indoor and outdoor O_3 concentrations for residences in the Boston, MA area. Four residences were monitored during the winter months and nine residences during the summer months. Outside monitors were placed ~1 m away from the house. Monitoring was conducted over a continuous 24-h period. There were no indoor sources of O_3. Indoor O_3 concentrations were higher during the summer months, with concentrations reaching 34.2 ppb. Indoor O_3 concentrations reached as high as 3.3 ppb during the winter monitoring period. In one instance, O_3 concentrations were higher indoors than outdoors. The authors attributed that finding to analytical difficulties. Outdoor O_3 concentrations were generally higher during the summer monitoring period, with concentrations reaching 51.8 ppb. Indoor concentrations were dependent on the outdoor O_3 concentrations and AER. Indoor and outdoor O_3 concentrations, including the AERs at the times of the monitoring are included in Table AX3-28.

Avol et al. (1998a) monitored 126 home in the Los Angeles metropolitan area during February and December. Uniformly low ambient O_3 concentrations were present during the non-O_3 seasons. Indoor O_3 concentrations were always below outdoor O_3 concentrations. The mean indoor and outdoor O_3 concentrations over the sampling period were 13 ± 12 ppb and 37 ± 19 ppb, respectively. There was a correlation between indoor O_3 concentration and ambient temperatures. The effect was magnified when the windows were open. When a central refrigerant recirculating air conditioner was used, indoor O_3 concentrations declined. The authors were able to predict indoor O_3 levels with nearly the same accuracy using measurements made at regional stations coupled with window conditions as with measurements made directly outside the homes coupled with window conditions, suggesting that monitoring station data may be useful in helping to reduce errors associated with exposure misclassification. The authors cautioned that varying results may occur at different locations with different housing stock or at different times of the year.

Lee et al. (2002) reported indoor and outdoor O_3 concentrations in 119 homes of school children in two communities in southern California: Upland and San Bernadino county.

Table AX3-28. Indoor and Outdoor O_3 Concentrations in Boston, MA

				Indoor Data		Outdoor Data	
Residence	Indoor Ozone (ppb)	Outdoor Ozone (ppb)	AER (h^{-1})	Relative Humidity (%)	Temp. (°F)	Relative Humidity (%)	Temp. (°F)
Winter							
1 - Day 1	3.3	11.2	1	25-45	67-75	88	25
1 - Day 2	0	15	0.8	22-40	65-76	62	27
2 - Day 1	2.6	24.4	1	3-19	67-71	44	17
2 - Day 2	1.7	4.4	1	3-8	55-70	40	17
3 - Day 1	20.4	15.6	1	8-24	62-69	33	36
3 - Day 2	3.1	24.5	0.9	13-19	64-70	51	38
4 - Day 1	2.2	11.4	0.7	26-37	60-72	57	39
4 - Day 2	0.3	20.7	0.7	29-38	61-70	77	36
Summer							
1 - Day 1	5.6	32.4	3	28-44	71-74	44	65
1 - Day 2	0.6	13.4	2.3	37-44	70-74	59	60
2 - Day 1	0.8	14.3	2.4	48-54	73-79	54	70
2 - Day 2	5	24.1	2.1	46-60	72-78	64	73
3 - Day 1	34.2	38.9	4.6	48-63	64-80	52	71
3 - Day 2	6.9	14	3.1	45-53	65-69	52	62
4 - Day 1	4.3	30	1.4	37-60	66-75	51	67
4 - Day 2	4.9	40.5	1.8	38-68	67-79	64	67
5 - Day 1	1.4	17.5	5.1	30-50	69-74	54	58
5 - Day 2	1.9	19	3.5	39-63	N/A	40	64
6 - Day 1	0.8	8.2	0.5	59-73	74-77	76	72
6 - Day 2	1.7	18.6	0.7	43-66	76-78	47	76
7 - Day 1	3.9	40.1	1.1	57-70	70-77	51	75
7 - Day 2	0	33.9	1.1	58-73	72-75	64	72
8 - Day 1	22.9	51.8	3.2	66-81	71-77	75	75
8 - Day 2	23.5	31.6	6.3	43-67	66-79	48	72
9 - Day 1	1.6	20.9	2.1	N/A	N/A	37	70
9 - Day 2	1.2	25	1.7	33-52	75-79	70	66

N/A = not available
Adapted from: Reiss et al. (1995)

Measurements were made over one year. Outdoor and indoor O_3 concentrations were based on cautioned that varying results may occur at different locations with different housing stock or at different times of the year.

Lee et al. (2002) reported indoor and outdoor O_3 concentrations in 119 homes of school children in two communities in southern California: Upland and San Bernadino county. Measurements were made over one year. Outdoor and indoor O_3 concentrations were based on monthly and weekly averages, respectively. Housing characteristics were not found to affect indoor O_3 concentrations. Indoor O_3 concentrations were significantly lower than outdoor O_3 concentrations. Average indoor and outdoor O_3 concentrations were 14.9 and 56.5 ppb. Homes with air conditioning had lower O_3 concentrations, suggesting decreased ventilation or greater O_3 removal.

Chao (2001) evaluated the relationship between indoor and outdoor levels of various air pollutants, including O_3, in 10 apartments in Hong Kong during May to June. Air monitoring was conducted over a 48-h period. All participants had the habit of closing the windows during the evenings and using the air conditioner during the sleep hours. Windows were partially open during the morning. The air conditioners were off during the working hours. Indoor O_3 concentrations were low in all of the monitored apartments, ranging from 0 to 4.9 ppb with an average of 2.65 ppb. Outdoor O_3 concentrations ranged from 1.96 to 15.68 ppb. Table AX3-29 provides information on the indoor and outdoor O_3 concentrations and the apartment characteristics.

Drakou et al. (1995) demonstrated the complexity of the indoor environment. Measurements of several pollutants, including O_3, were made inside and outside of two nonresidential buildings in Thessaloniki and Athens, Greece. The building in Thessaloniki was a 58-m^3 metal structure. The ceiling and walls were covered with colored corrugated plastic sheeting, and the flooring was plastic tile. There was no heating/air conditioning system and the building was closed during the monitoring period. The AER ranged from 0.3 to 0.35 h^{-1}. The building in Athens was a 51-m^3 concrete structure. The air conditioning system (recirculated air) worked continuously during the monitoring period. A window was opened slightly to accommodate the monitors' sampling lines. The AER was approximately 1 h^{-1}. Monitoring lasted for 30 days at both locations, however, only data from the 7 most representative days were reported. Indoor O_3 concentrations closely followed the outdoor concentrations at the

Table AX3-29. Indoor and Outdoor O_3 Concentrations in Hong Kong

Apartment No.	Floor Area	Floor No.	Window Opening Frequency	AER (h^{-1})	Indoor O_3 Conc.	Outdoor O_3 Conc.
1	40	14	Seldom	1.44	0	1.96
2	47	13	Sometimes	1.97	4.96*	6.01*
3	140	2	Sometimes	0.83	1.0*	6.96*
4	67	5	Seldom	5.27	4.96*	8.76*
5	86	11	Sometimes	1.64	3.0*	7.80*
6	43	32	Sometimes	15.83	4.01*	8.76*
7	47	9	Always	15.91	0	3.0*
8	30	6	Seldom	3.25	2.05*	3.0*
9	26	35	Sometimes	2.1	4.9	15.68
10	20	15	Seldom	5.5	4.01*	4.96*

*Estimated Concentration.

Adapted from Chao (2001).

Thessaloniki building. The averaged 7-day indoor and outdoor O_3 concentrations were 9.39 and 15.48 ppb, respectively. The indoor O_3 concentrations at the Athens location were highly variable compared to the outdoor concentration. The authors suggested that a high hydrocarbon intrusion may be the reason for the variability in O_3 concentrations noted at this site. The averaged 7-day indoor and outdoor O_3 concentrations were 8.14 and 21.66 ppb, respectively.

Weschler et al. (1994) reported that indoor O_3 concentrations closely tracked outdoor O_3 concentrations at a telephone switching station in Burbank, CA. The switching building was flat-roofed, two-story (first floor and basement), uncarpeted, with unpainted brick walls. Each floor was 930 m^2 with a volume of 5095 m^3. Indoor O_3 concentrations were measured on the first floor using a perfluorocarbon tracer or an UV photometric analyzer. The AER were obtained by dividing the volumetric flow to the first floor by the volume of the first floor space or by perfluorocarbon tracer techniques. The AER ranged from 1.0 to 1.9 h^{-1}.

The major source of O_3 at the switching station was transport from outdoors. Indoor O_3 concentrations closely tracked outdoor concentrations, measuring from 30 to 70% of the outdoor concentrations. Indoor O_3 concentrations frequently exceed 50 ppb during the summer months, but seldom exceeded 25 ppb during the winter. During the early spring through late fall, indoor O_3 concentrations peaked during the early afternoon and approach zero after sunset. Ozone sinks included a surface removal rate between 0.8 and 1.0 h^{-1} and reactions with NO_x. Figures AX3-89 and AX3-90 compare the outdoor and indoor O_3 concentrations, including the AER, for two 1-week periods during the study.

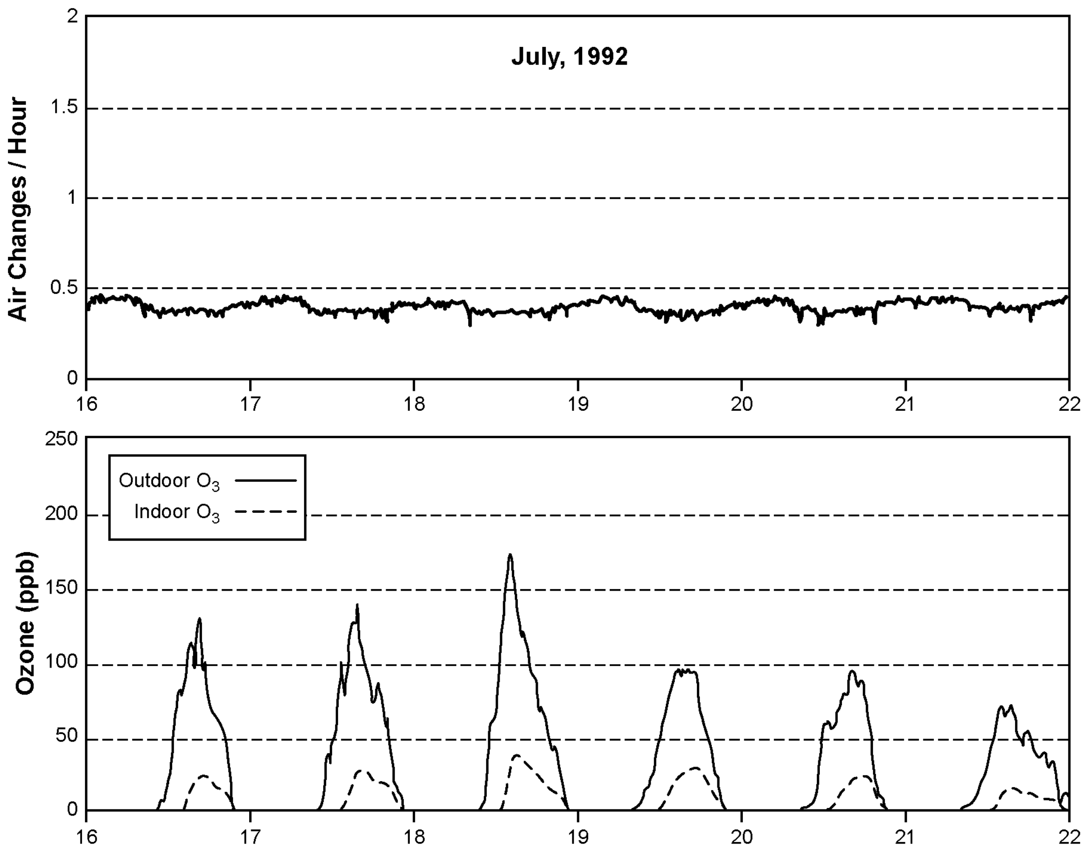

Figure AX3-89. Air exchange rates and outdoor and indoor O_3 concentrations during the summer at telephone switching station in Burbank, CA.

Source: Weschler et al. (1994).

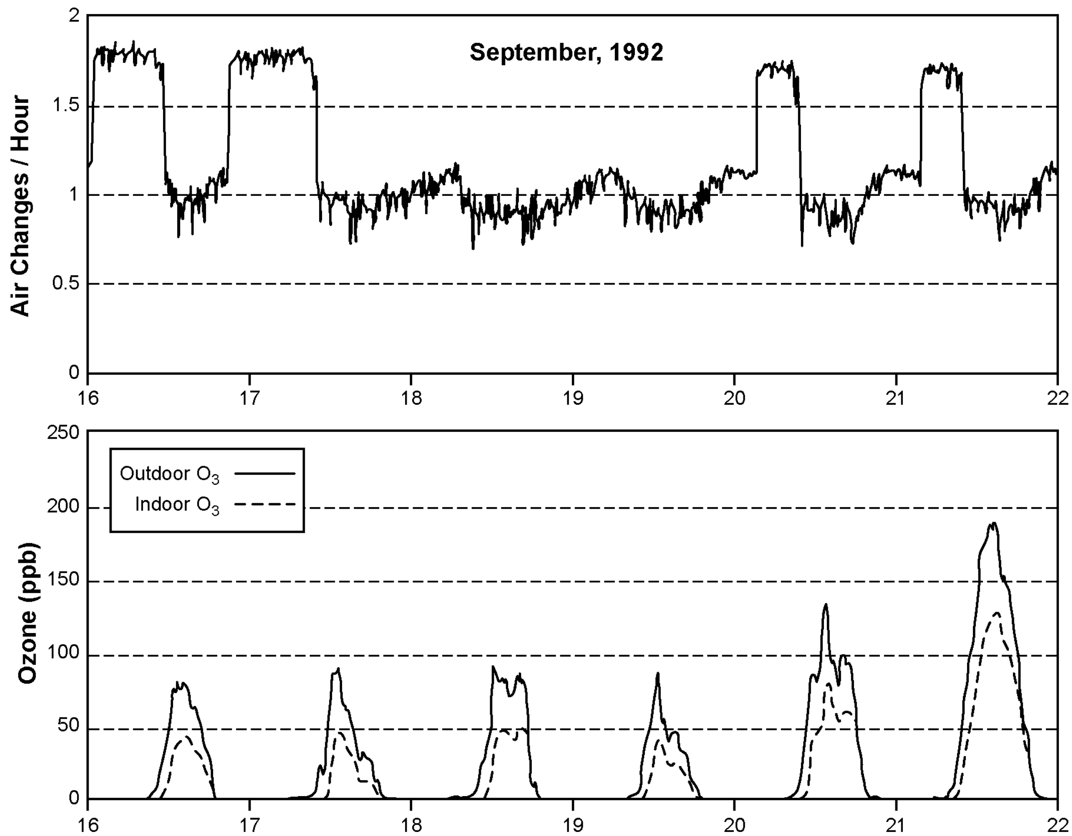

Figure AX3-90. Air exchange rates and outdoor and indoor O_3 concentrations during the fall at a telephone switching station in Burbank, CA.

Source: Weschler et al. (1994).

The relationships between indoor and outdoor O_3 concentrations in five museums and cultural centers (Wawel Castle, Matejko Museum, National Museum, Collegium Maius, and Cloth Hall) in Krakow, Poland were reported by Salmon et al. (2000). Measurements were made for up to 46 h and up to 33 days. Air exchange measurements were only made for the Matejko Museum and Wawel Castle. Both were naturally ventilated. However, the summertime AER for the Matejko Museum was more than twice that of the Wawel Castle site, 1.26 to 1.44 h^{-1} compared to 0.56 to 0.66 h^{-1}. The highest indoor O_3 concentrations were noted at the Matejko Museum during the summer. The findings are included in Table AX3-30 for those locations with reported AERs.

Table AX3-30. Indoor and Outdoor Ozone Concentrations

Location	Duration (hours)	AER	Average O_3 (ppb)
Matejko Museum	26		1988-2000
Outdoors (Town Hall Tower)			20
Indoors (third floor, west)		1.26	8.5
Wawel Castle	43		
Outdoors (Loggia)			14.7
Indoors (Senator's Hall)		0.63	2.5
Wawel Castle, outdoors	31.8		42[a]
Wawel Castle, Room 15	31		8
Wawel Castle, Senator's Hall	31.8		7
Matejko Museum, outdoors	26.9		21[b]
Matejko Museum, Indoor Gallery	26.9		9

[a]On Loggia of Piano Nobile Level, high above the street.
[b]At street level.

Adapted from Salmon et al. (2000).

Riediker et al. (2003) measured mobile source pollutants inside highway patrol vehicles in Wake County, NC. Measurements were made during the 3 p.m. to midnight shift between August 13 and October 11, 2001 in two patrol cars each day for a total of 50 shifts. All areas of rural and urban Wake County were patrolled. The prominent areas patrolled were major highways and interstates. Ozone concentrations inside the cars were compared with the O_3 measurements at the fixed station in northern Raleigh. The average O_3 concentration inside the cars was 11.7 ppb, approximately one-third of the ambient air concentration. Jakobi and Fabian (1997) found that O_3 concentrations in a moving car were independent of the type of ventilation (windows closed and ventilator operation/ventilator off and windows open). Ozone concentrations inside the car were found to closely follow the outdoor concentrations. When the car was parked, O_3 concentrations outdoors greatly exceeded concentrations inside the car (see Figure AX3-91).

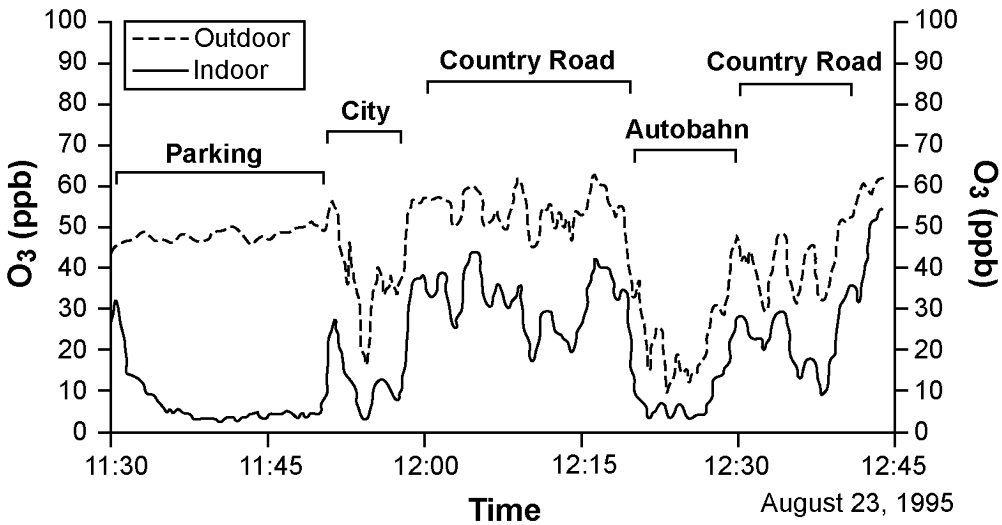

Figure AX3-91. Indoor and outdoor O_3 concentration in moving cars.

Source: Jaboki and Fabian (1997).

Few studies have been conducted in indoor environments containing O_3 sources. Black et al. (2000) measured O_3 concentrations in a photocopy room at the University of California during one business day. The room volume was 40 m^3. Ozone concentrations were generally below 20 ppb, but increased proportionately with increasing photocopier use. Ozone concentrations reached 40 ppb when the hourly average number of copies reached 45. Helaleh et al. (2002) reported daily average O_3 concentrations from 0.8 to 1.3 ppb and 0.9 to 1.0 ppb in a laboratory and photocopy room at a university in Japan. Outdoor O_3 concentrations ranged from 6 to 11 ppb. Because only limited information was available on the sampling system used in the study, the adequacy of the sampling system cannot be determined. Jakobi and Fabian (1997) measured O_3 concentrations in an office associated with the use of a photocopier and a laser printer. They noted a 3.0 ppb increase in O_3 from the use of a 3-year old printer run for 20 min at a copy rate of 8 pages/min. There was no detectable change in O_3 concentrations from the use of the laser printer.

The U.S. Environmental Protection Agency (Steiber, 1995) measured O_3 concentrations from the use of three home/office O_3 generators. The O_3 generators were placed in a 27 m^3 room with doors and windows closed and the heating, ventilating and air conditioning system off; the

AER was 0.3 h^{-1}. The units were operated for 90 min. Ozone concentrations at the low output setting ranged from nondetectable to 14 ppb (averaged output). At the high output setting, averaged output O_3 concentrations exceeded 200 ppb in several cases and had spike concentrations as high as 480 ppb.

Mass Balance Equations

Indoor concentrations of O_3 can be estimated using the mass balance model. The mass balance model is a general ventilation model that relates indoor pollutant concentrations to those outside. The mass balance model estimates the concentration of a pollutant over time. The simplest form of the model is represented by the following differential equation for a perfectly mixed microenvironment without an air cleaner:

$$\frac{dC_{IN}}{dt} = vC_{OUT} + \frac{S}{V} - vC_{IN} \qquad \text{(AX3-2)}$$

where dC_{IN} is the indoor pollutant concentration (mass/volume), t is time in hours, v is the air exchange rate, C_{OUT} is the outdoor pollutant concentration (mass/volume), V is the volume of the microenvironment, and S is the indoor source emission rate.

Nazaroff and Cass (1986) extended the mass balance model to include multiple compartments and interactions between different compounds. The extended model takes into account the effects of ventilation, filtration, heterogeneous removal, direct emission, and photolytic and thermal and chemical reactions. A more in-depth discussion of the mass balance model may be found in Shair and Heitner (1974) and in Nazaroff and Cass (1986).

Freijer and Bloemen (2000) used the one-compartment mass balance model to examine the relationship between O_3 I/O ratios as influenced by time patterns in outdoor concentrations, ventilation rate, and indoor emissions. The microenvironment was 250 m^3. Three different ventilation patterns with the same long-term average AER (0.64 h^{-1}) were used. A source pattern (direct emissions) of zero was used, because O_3 sources are not common. The time series for outdoor O_3 concentrations consisted of 100-day periods during the summer, with hourly measured concentrations. The following assumptions were made: (1) O_3 concentration in the air that enters the microenvironment is equal to the concentration of the outside air minus the fraction removed by filtration, (2) the O_3 concentration that leaves the microenvironment equals the O_3 concentration in the microenvironment, (3) the decay processes in the microenvironment are proportional to the mass of the pollutant, and (4) addition or removal of O_3 in the microenvironment also may occur through independent sources and sinks.

Figure AX3-92 represents the measured outdoor O_3 concentrations and modeled indoor O_3 concentrations. The indoor modeled O_3 concentrations were found to equal approximately 33% of the outdoor monitored concentrations.

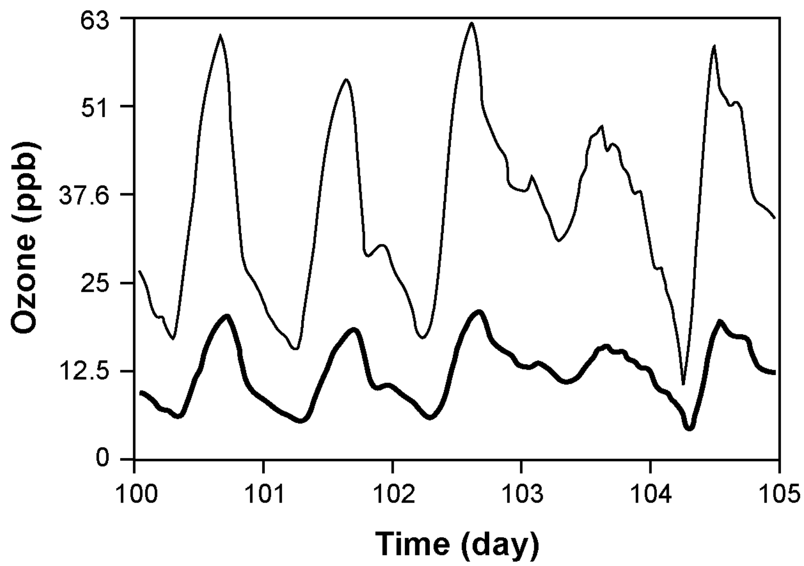

Figure AX3-92. Measured outdoor O_3 concentrations (thin line) and modeled indoor concentrations (bold line).

Source: Adapted from Freijer and Bloemen (2000).

AX3.11 HUMAN EXPOSURE TO OZONE AND RELATED PHOTOCHEMICAL OXIDANTS

AX3.11.1 Introduction

There are many definitions of exposure. Human exposure to O_3 and related photochemical oxidants are based on the measured O_3 concentrations in the individual's breathing zone as the individual moves through time and space. Epidemiological studies generally use the ambient concentrations as surrogates for exposure. Therefore, human exposure data and models provide the best link between ambient concentrations (from measurements at monitoring sites or estimated with atmospheric transport models), lung deposition and clearance and estimates of air concentration-exposure-dose relationships.

This section discusses the current information on the available human exposure data and exposure model development. This includes information on (a) the relationships between O_3 measured at ambient monitoring sites and personal exposures and (b) factors that affect these relationships. The information presented in this section is intended to provide critical links between ambient monitoring data and O_3 dosimetry as well as between the toxicological and epidemiologic studies presented in Annexes AX4, AX5, AX6, and AX7 of this document.

AX3.11.2 Summary of the Information Presented in the Exposure Discussion in the 1996 Ozone Criteria Document

The 1996 O_3 AQCD (U.S. Environmental Protection Agency, 1996a), based on then currently available information, indicated that less emphasis should be placed on O_3 concentrations measured at ambient monitoring stations. Fixed monitoring stations are generally used for monitoring associated with air quality standards and do not provide a realistic representation of individual exposures. Indoor/outdoor O_3 ratios reported in the literature were summarized for residences, hospitals, offices, art galleries, and museums. The differences in residential I/O were found to be a function of ventilation conditions. The I/O ratios were less than unity. In most cases, indoor and in-transit concentrations of O_3 were significantly different from ambient O_3 concentrations. Ambient O_3 varied from O_3 concentrations measured at fixed-site monitors. Very limited personal exposure measurements were available at the time the 1996 O_3 AQCD was published, so estimates of O_3 exposure or evaluated models were not provided. The two available personal exposure studies indicated that only 40% of the variability in personal exposures was explained by the exposure models using time-weighted indoor and outdoor concentrations. The discussion addressing O_3 exposure modeling primarily addressed work reported by McCurdy (1994) on population-based models (PBMs). Literature published since publication of the 1996 O_3 AQCD has also focused on PBMs. A discussion of individual-based models (IBMs) will be included in the description of exposure modeling in this document to improve our mechanistic understanding of O_3 source-to-exposure events and to evaluate their usefulness in providing population-based estimates.

AX3.11.3 Concepts of Human Exposure

Human exposure to O_3 and related photochemical oxidants occurs when individuals come in contact with the pollutant through "(a) the visible exterior of the person (skin and openings into the body such as mouth and nostrils) or (b) the so-called exchange boundaries where absorption takes place (skin, mouth, nostrils, lung, gastrointestinal tract)" (Federal Register, 1986). Consequently, exposure to a chemical, in this case O_3, is the contact of that chemical with the exchange boundary (U.S. Environmental Protection Agency, 1992). Therefore, inhalation exposure to O_3 is based on measurements of the O_3 concentration near the individual's breathing zone that is not affected by exhaled air.

AX3.11.4 Quantification of Exposure

Quantification of inhalation exposure to any air pollutant starts with the concept of the variation in the concentration of the air pollutant in the breathing zone, unperturbed by exhaled breath, as measured by a personal exposure monitor as a person moves through time and space.

Since the concentrations of O_3 and related photochemical oxidants vary with time and location and since people move among locations and activities, the exposure and dose received changes during the day. Furthermore, the amount of pollutant delivered to the lung is dependent upon the person's minute ventilation rate. Thus, the level of exertion is an important consideration in determining the potential exposure and dose. Inhalation exposure has been defined as the integral of the concentration as a function of time over the time period of interest for each individual (Ott, 1982, 1985; Lioy, 1990):

$$E = \int_{t_1}^{t_2} c(t)dt \qquad \text{(AX3-3)}$$

where E is inhalation exposure, $c(t)$ is the breathing zone concentration as a function of time and t_1 and t_2 the starting and ending time of the exposure, respectively.

AX3.11.5 Methods To Estimate Personal Exposure

There are two approaches for measuring personal exposure; direct and indirect methods (Ott, 1982, 1985). Direct approaches measure the contact of the person with the chemical concentration in the exposure media over an identified period of time. For the direct measurement method, a personal exposure monitor (PEM) is worn near the breathing zone for a specified time to either continually collect for subsequent analysis or directly measure the concentrations of the pollutant and the exposure levels.

The indirect method determines and measures the concentrations in all of the locations or "microenvironments" a person encounters or determines the exposure levels through the use of models or biomarkers. The concept of microenvironments is critical for understanding human exposure and aids in the development of procedures for exposure modeling using data from stationary monitors (indoor and outdoor). Microenvironments were initially defined as individual or aggregate locations (and sometimes even as activities taking place within a location) where a homogeneous concentration of the pollutant is encountered for a specified period of time. Thus, a microenvironment has often been identified with an "ideal" (i.e., perfectly mixed) compartment of classical compartmental modeling. More recent and general definitions view the microenvironment as a "control volume," indoors or outdoors, that can be fully characterized by a set of either mechanistic or phenomenological governing equations, when properly parameterized, given appropriate initial and boundary conditions. The boundary conditions typically reflect interactions with the ambient air and with other microenvironments. The parameterizations of the governing equations generally include the information on attributes of sources and sinks within each microenvironment. This type of general definition allows for the concentration within a microenvironment to be nonhomogeneous, provided its spatial profile and mixing properties can be fully predicted or characterized. By adopting this definition, the number of microenvironments used in a study is kept manageable, while existing variabilities in concentrations are still taken into account. The "control volume" variation could result in a series of microenvironments in the same location. If there are large spatial gradients within a location for the same time period, the space should be divided into the number of microenvironments needed to yield constant pollutant concentrations; the alternative offered by the control volume approach is to provide concentration as a function of location within it, so that the appropriate value is selected for calculating exposure. Thus, exposure to a person in a microenvironment is calculated using a formula analogous to equation AX3-2, but as the sum of the discrete products of measured or modeled concentrations (specific to the receptor and/or activity of concern) in each microenvironment by the time spent there. The equation is expressed as:

$$E = \sum_{i=1}^{n} c_i \Delta t_i \qquad \text{(AX3-4)}$$

where i specifies microenvironments from 1 to n, c_i is the concentration in the ith microenvironment, and Δt_i is the duration spent in the ith microenvironment. The total exposure for any time interval for an individual is the sum of the exposures in all microenvironments encountered within that time interval. This method should provide an accurate determination of exposure provided that all microenvironments that contribute significantly to the total exposures are included and the concentration assigned to the microenvironment is appropriate for the time period spent there.

Microenvironments typically used to determine O_3 exposures include indoor residences, other indoor locations, outdoors near roadways, other outdoor locations, and in-vehicles. Outdoor locations near roadways are segregated from other outdoor locations because N_2O emissions from automobiles alter O_3 and related photochemical oxidant concentrations compared to concurrent typical ambient levels. Indoor residences are typically separated from other indoor locations, because of the time spent there and potential differences between the residential environment and the work/public environment. A special concern for O_3 and related photochemical oxidants is their diurnal weekly (weekday-weekend) and seasonal variability. Few indoor O_3 sources exist, but include electronic equipment, O_3 generators, and copying machines. Some secondary reactions of O_3 take place indoors that produce related photochemical oxidants that could extend the exposures to those species above the estimates obtained from O_3 alone. (See discussion on O_3 atmospheric chemistry and indoor sources and concentrations earlier in this Annex.)

Measurement efforts to assess population exposures or exposures to large numbers of individuals over long time periods is labor intensive and costly, so exposure modeling is often done for large populations evaluated over time. Predicting (or reconstructing) human exposure to O_3 through mechanistic models is complicated by the fact that O_3 (and associated photochemical oxidants) is formed in the atmosphere through a series of chemical reactions that are nonlinear and have a wide range of characteristic reaction timescales. Furthermore, these reactions require the precursors VOCs and NO_x that are emitted by a wide variety of both anthropogenic and natural (biogenic) emission sources. This makes O_3 a secondary pollutant with complex nonlinear and multiscale dynamics in time and space. Concentration levels experienced by individuals and populations exposed to O_3 are therefore affected by (1) emission levels and spatiotemporal patterns of the gaseous precursors: VOCs and NO_x, that can be due to sources as diverse as a power plant in a different state, automobiles on a highway five miles away, and the gas stove in one's own kitchen; (2) ambient atmospheric as well as indoor microenvironmental transport, removal and mixing processes (convective, advective, dispersive and molecular/diffusional); and (3) chemical transformations that take place over a multitude of spatial scales, ranging from regional/sub-continental (100 to 1000 km), to urban (10 to 100 km), to local (1 to 10 km), to neighborhood (< 1 km), and to microenvironmental/personal. These transformations depend on the presence of co-occurring pollutants in gas and aerosol phases, both primary and secondary, and on the nature of surfaces interacting with the pollutants.

Further, the strong temporal variability of O_3, both diurnal and seasonal, makes it critical that definitions of integrated or time-averaged exposure employ appropriate averaging times in order to produce scientifically defensible analyses for either causes of O_3 production or health effects that result from O_3 exposure. An understanding of the effect of temporal profiles of concentrations and contacts with human receptors is essential. Short-term integrated metrics, such as hourly averages, 8-h running averages, etc., are needed to understand the relationship between O_3 exposure and observed health and other effects.

Health effects associated with O_3 have mostly been considered effects of acute exposures. Peak O_3 and related photochemical oxidants concentrations typically occur towards the latter portion of the day during the summer months. Elevated concentrations can last for several hours. Regional O_3 episodes often co-occur with high concentrations of airborne fine particles making it difficult to assess O_3 dynamics and exposure patterns. Furthermore, O_3 participates in multiphase (gas/aerosol) chemical reactions in various microenvironments. Several recent studies show that O_3 reacts indoors with VOCs and NO_x in an analogous fashion to that occurring in the ambient atmosphere (Lee and Hogsett, 1999; Wainman et al., 2000; Weschler and Shields, 1997). These reactions produce secondary oxidants and other air toxics that could play a significant role in cumulative human exposure and health-related effects within the microenvironment.

AX3.11.6 Exposures in Microenvironments

Ozone has been measured more extensively than the other photochemical oxidants. Ambient monitors have been established in most areas of the country, with extensive monitoring in regions that have been in noncompliance with the previous 1-h daily NAAQS. Monitoring station-measured hourly concentrations also have been used as surrogates of exposure in epidemiological studies and in evaluating exposure-related health effects. According to the Guideline on Ozone Monitoring Site Selection (U.S. Environmental Protection Agency, 1998), when designing an O_3 monitoring network, consideration should be given to (1) proximity to combustion emission sources, (2) distance from primary emission sources, and (3) the general wind direction and speed to determine the primary transport pathways of O_3 and its precursors. Finally, the 1-h daily maximum and 8-h average O_3 concentrations can have different spatial patterns with elevated daily 8-h O_3 concentrations typically being over a wider spatial area. Therefore, O_3 monitoring networks should determine the highest concentrations expected to occur in the area, representative concentrations for high population density areas, the impact of sources or source categories on air pollution levels, and general background concentration levels (U.S. Environmental Protection Agency, 1998).

The guideline also states that the monitor's O_3 inlet probe should be placed at a height and location that best approximates where people are usually found. However, complicating factors (e.g., security considerations, availability) sometimes result in the probe placement being elevated 3 to 15 m above ground level, a different location than the breathing zone (1 to 2 m) of the populace. Although there are some commonalities in the considerations for the sampling design for monitoring and for determining population exposures, differences also exist. These differences between the location and height of the monitor compared to the locations and breathing zone heights of people can result in different O_3 concentrations between what is measured at the monitor and exposure and, therefore, should be considered when using ambient air monitoring data as a surrogate for exposure in epidemiological studies and risk assessments.

AX3.11.7 Differences in Concentrations Among Microenvironments

Indoors

People spend the majority of their time indoors. In exposure analyses, I/O ratios may provide a reasonable estimate of indoor O_3 concentrations when outdoor O_3 concentrations are known. The reported I/O ratios vary greatly (see earlier discussion in this annex and U.S. Environmental Protection Agency, 1996a). A number of studies published since the completion of the 1996 O_3 AQCD (U.S. Environmental Protection Agency, 1996a) have examined the relationship between indoor and outdoor O_3 concentrations in several countries and varying building types and ventilation conditions. A description of the more recent studies appears in the discussion on indoor sources and concentrations earlier in this Annex.

Other Microenvironments

In addition to buildings and their associated outdoor microenvironments, two other microenvironments have been studied: within a vehicle and outdoors near a roadway. Johnson (1997) conducted a scripted study using four trained technicians to measure hourly average O_3 concentrations between 07:00 and 19:00 h in Los Angeles, CA during September and October 1995. The ratio of the microenvironmental concentrations to the fixed site monitor on days when the O_3 levels $\geq$ 20 ppb were as follows: indoor residence, 0.28; other locations indoors, 0.18; outdoor near roadways, 0.58; other locations outdoors, 0.59; and in-vehicle, 0.21. The concentrations indoors and within vehicles varied depending on whether the windows were opened (higher) or closed (lower) and the use of air conditioning. The lower outdoor concentrations, particularly near roadways, probably reflect the reaction of O_3 with NO emitted by automobiles.

A study of the effect of elevation on O_3 concentrations found that concentrations increased with increasing elevation. The ratio of O_3 concentrations at street level (3 m) compared to the rooftop (25 m) was between 0.12 and 0.16, though the actual concentrations were highly correlated (r = 0.63) (Väkevä et al., 1999). Differential O_3 exposures may, therefore, exist in apartments that are on different floors. Differences in elevation between the monitoring sites in Los Angeles and street level samples may have contributed to the lower levels measured by Johnson (1997). Furthermore, since O_3 monitors are frequently located on rooftops in urban settings, the concentrations measured there may overestimate the exposure to individuals outdoors in streets and parks, locations where people exercise and maximum O_3 exposure is likely to occur.

Chang et al. (2000) conducted a scripted exposure study in Baltimore during the summer of 1998 and winter of 1999, during which 1-h O_3 samples were collected by a technician who also changed his or her activity every hour. The activities chosen were selected to simulate older (> 65 years) adults, based on that reported in the National Human Activity Pattern Survey (NHAPS). Personal O_3 levels were significantly lower than the outdoor values, because more time was spent indoors. Mean summer concentrations were 15.0 ± 18.3 ppb, with a maximum of 76.3 ppb. The personal O_3 exposure levels within the outdoor and in-vehicle microenvironments were significantly correlated with ambient concentration, although the ratio of personal exposure to ambient levels was less than one, with only the top 5% of the ratios exceeding one, indicating that the ambient measurements lead to the maximum concentrations and exposures. The indoor concentrations did not correlate with outdoor measurements.

The scripted exposure studies show that the O_3 concentrations in the various microenvironments were typically lower than the ambient air concentrations measured at monitoring stations. Exposure models are useful for accounting for the reduced concentrations usually encountered in various microenvironments compared to ambient monitoring station concentrations (see discussion on exposure models later in this annex).

AX3.11.8 Activity Patterns/Time Spent in Microenvironments

The O_3 dose delivered to the lung is not only a function of the air concentration but also depends on the minute ventilation rate and the morphology of the respiratory tract. Estimates of the exercise level, which is related to minute ventilation rate and time spent outdoors, stratified by age, season, and gender have been compiled based on questionnaire data. Klepeis et al. (1996, 2001) reported in National Human Activity Pattern Survey (NHAPS) a probability-based telephone survey done in the early 1990s, that the highest levels of outdoor activity for yardwork/maintenance occur in the spring during morning to early afternoon and for sports/exercise in the summer (3 to 6% of respondents) during the middle of the day from noon to 3 p.m. The time period for sports/exercise in the spring (5% of respondents) was from 3:30 to 6 p.m. Outdoor activity time also vary between weekend/weekday with weekend activity being throughout the day (9 to 5 p.m.) and weekday outdoor activity shifts to latter in the day, with an initial rise at 3 p.m. that extends into the evening hours. These differences reflect the hours of more leisure activities. Since the highest outdoor O_3 concentrations occurs in the middle to the latter part of the day, which coincides with the time period of most physical activity, it is expected that individuals engaging in outdoor activities during this period will receive the maximum O_3 dose.

Klepeis et al. (1996, 2001) also reported differences in the amount of time that different age groups spend in various activities. School-age children were found to spend more time at sports/exercise than other age groups. Avol et al. (1998b) reported that the number of hours three groups of children (healthy, asthmatic, and wheezy randomly selected from a larger longitudinal health study) spent outdoors during the spring and summer on either high- or low-O_3 days were similar. However, the amount of time asthmatic children spent being physically active outdoors was smaller than the healthy or wheezy children, particularly during the summer on high-O_3 days. A small difference in the proportion of time spent being active during the summer was observed between wheezy children (lower) and healthy children. Thus, children with respiratory problems modified their behavior and received lower O_3 doses. Additionally, girls spent less time outdoors and were less physically active.

Adams (1993) determined population breathing averages by measuring heart rate, breathing frequency, and volume of air breathed in by children, adolescents, young/middle age adults, and seniors during a variety of activities. Adults of the same gender from adolescent through senior years breathed similar amounts of air during similar activities. Children were found to breathe more air than adults, relative to body surface area, breathing frequency, and heart rate. The time spent outdoors under medium- and high-activity levels has been reported to be 2% and 0.2% of the waking hours, respectively (Shamoo et al., 1994), which represents the time frame with the highest minute ventilation rate and, therefore, highest exposure to O_3. Alteration in the minute ventilation rate have been observed in asthmatic children when exposed to air pollutants (Linn et al., 1996). The children tested were fourth graders in public schools in three communities in southern California. Künzli et al. (1997) tested the reproducibility of the Activity Tables, a retrospective time-activity assessment questionnaire in 75 college freshmen. Students, ages 17 to 21 years, were asked to recall activities in which they had engaged. Four levels of activity were designated, based on the responses to the questions, to determine participation in specific activities along with estimates of the duration and frequency of participation. Internal consistency in the responses for activity level was found between and within two sets of the questionnaires administered at different times to the same individuals, although it appears that the reported number of hours devoted to physical activity was overestimated. Overall, having an estimate of the number of hours outdoors and how many of those hours were spent engaged in physical activity will improve the estimates for the high-end exposures.

AX3.11.9 Personal Exposure Monitors and Measurements

Modified passive samplers have been developed for use in determining O_3 exposure. The difficulty in developing a passive O_3 monitor is in identifying a chemical or trapping reagent that can react with O_3. Zhou and Smith (1997) evaluated the effectiveness of sodium nitrite, 3-methyl-2-benzothiazolinone acetone azine (MBTH), *p*-acetamidophenol (*p*-ATP), and indigo carmine as O_3-trapping reagents. Only sodium nitrite and MBTH gave sensitive, linear responses at environmentally relevant concentrations. However, MBTH overestimated the O_3 concentrations significantly, suggesting an interference effect. Sodium nitrite was found to be a valid reagent when an effective diffusion barrier was used. Scheeren and Adema (1996) used an indigo carmine-coated glass-fiber filter to collect spectrophotometrically measured O_3. The detection limit was 23 ppb for a 1-h exposure, with no interfering oxidants identified. The reagent was valid for a relative humidity range of 20 to 80%. The uptake rate was wind velocity dependent. However, wind velocity dependencies was compensated for by using a small battery-operated fan that continuously blew air across the face of the monitor at a speed of 1.3 m/s. The overall accuracy of the sampler, after correcting for samples collected under low-wind conditions, was 11 ± 9% in comparison to a continuous UV-photometric monitor. Sample stability was > 25 days in a freezer. Bernard et al. (1999) employed a passive sampler consisting of a glass-fiber filter coated with a 1,2-di(4-pyridyl)ethylene solution. The sample was analyzed spectrophotometrically after color development by the addition of 3-methyl-2-benzothiazolinone hydrazone hydrochloride. The sampler was used at 48 sites in Montpellier, France. The results from the passive sampler were highly correlated (0.9, $p < 0.0001$) with the results from the UV absorption analyzer of the regional air quality network. Detection limits were 17 ppb for 12-h and 8 ppb for 24-h samples with an overall variation coefficient of 5% for field-tested paired samples.

A series of studies have been conducted using a passive sampler developed by Koutrakis et al. (1993) at the Harvard School of Public Health. The sampler used sodium nitrate as the trapping reagent and included a small fan to assure sufficient movement of air across the face of the badge when sampling was done indoors. The passive sampler has been evaluated against the standard UV absorption technique used in studies in southern California (Avol et al., 1998a; Geyh et al., 1999, 2000; Delfino et al., 1996), Baltimore, MD (Sarnat et al., 2000), and Canada (Brauer and Brook, 1997).

Avol et al. (1998a) used nitrite-coated passive samplers to measure O_3 air concentrations indoors and outdoors of 126 homes between February and December 1994 in the Los Angeles metropolitan area. The detection limit of the method was near 5 ppb. Geyh et al. (1997, 1999) compared passive and active personal O_3 air samplers based on nitrite-coated glass-fiber filters. The active sampler was more sensitive allowing for the collection of short-term, 2.6-h samples. Comparison between the two samplers and UV photometric O_3 monitors demonstrated generally good agreement (bias for active personal sampler of ~6%). The personal sampler also had high precision (4% for duplicate analyses) and good compliance when used by children attending summer day camp in Riverside, CA.

Passive O_3 monitors have been used in several field studies to determine average daily O_3 exposure as well as in scripted studies to evaluate O_3 exposures over one to several-hour time periods. Delfino et al. (1996) measured 12-h personal daytime O_3 exposures in asthmatic patients in San Diego from September through October 1993. They found that the mean personal exposures were 27% of the mean outdoor concentrations. Individual exposure levels among the 12 asthmatic subjects aged 9 to 16 years varied greatly. Mean personal O_3 exposure levels were lower on Friday, Saturday, and Sunday than on other days of the week (10 versus 13 ppb), while the ambient air concentrations were higher Friday through Sunday. The authors suggested that the differences were due to higher weekday NO emissions from local traffic which titrated the ambient O_3 levels. The lower personal exposure levels on Friday, Saturday, and Sunday may have been an artifact of greater noncompliance, with the badges remaining indoors and, therefore, being exposed to lower O_3 concentrations. The overall correlation between the personal exposure concentrations between any two individuals and with the outdoor stationary site was only moderate (r = 0.45; range: 0.36 to 0.69). The O_3 concentrations at the stationary site exceeded the personal levels by an average of 31 ppb. Avol et al. (1998b) observed a poor correlation between personal exposure and fixed-site monitoring concentrations ($r = 0.28$, $n = 1336$ pairs) for a cohort of children (healthy, wheezy, and asthmatic). Sarnat et al. (2000) measured personal O_3 exposures during a 12-day longitudinal study of 20 older adults (> 64 years) in Baltimore, MD. Ten subjects participated in the summer and winter exposures and the remaining 10 participated in either the summer or winter exposure. No statistically significant overall correlations were identified between the personal and the ambient O_3 concentrations during either the winter or summer. Only a single individual ($n = 14$ summer and 13 winter) had a significant correlation with outdoor concentrations. Geyh et al. (2000) measured indoor and outdoor concentration and personal O_3 exposures in 169 elementary school children from 116 homes during a year-long sampling protocol in 2 communities in southern California. Samples were collected for 1 week per month. Boys had higher O_3 exposure than girls, probably reflecting the greater amount of time boys spent outdoors compared to girls (3.8 versus 3.2 h for the spring/summer and 2.9 versus 2.2 h for the fall/winter). The average personal O_3 exposures were lower than the levels measured at the nearest monitor stations retrieved from the AIRS. During the O_3 season, differences were found in indoor concentrations and personal O_3 exposures between the two communities participating in the study based on ambient air concentrations and differences in O_3 air exchange rates in the homes.

Brauer and Brook (1997) conducted personal exposure evaluations in three groups in Frazer Valley, Vancouver, Canada. The groups were divided by the amount of time spent outdoors: (1) the majority of the workday was spent indoors or commuting, (2) an intermediate amount of time was spent outdoors, and (3) the entire exposure monitoring period was outdoors. Time-activity data were collected for the first two groups to assess the proportion of time spent outdoors. For groups 1 and 2, the lowest quartile of participants based on the fraction of time spent outdoors had significantly lower O_3 exposure (mean personal exposure to outdoor concentration ratio = 0.18 and 0.35, respectively) compared to those in the upper quartile (mean ratio = 0.51 and 0.58, respectively; $p < 0.05$; Bonferroni multiple range test). The mean ratio was 0.96 with values ranging from near 0 to 2 for the group that spent the entire exposure-monitoring period outdoors. The authors attributed the extreme low ratios to random measurement error at low O_3 air concentrations (estimated at 35%), local variability in O_3

concentrations, and to differences between ground-level concentrations (where the personal samples were collected) 3-m above ground level (where the continuous monitors were located). The highest ratios may be due to either locale variability in O_3 concentrations or to an interference affecting the personal O_3 samplers, particularly at the lower concentration range, leading to a small positive error. Temporal plots of O_3 for the mean daily personal exposures and ambient concentrations showed the same general trend with general agreement between the personal exposures and ambient air concentrations for group 3. However, for groups 1 and 2, the day-to-day variability of the personal exposures and ambient O_3 concentrations had consistent patterns, suggesting that the ambient air was the primary source for O_3 exposure. The actual O_3 concentrations measured in the personal air space were always considerably lower than the ambient concentrations.

AX3.11.10 Trends in Concentrations Within Microenvironments

There have not been sufficient numbers of measurements of personal exposures or indoor O_3 concentrations to directly document trends over time or location. However, since O_3 concentrations in all microenvironments are primarily derived from ambient sources, trends in ambient air concentrations should reflect trends in personal exposure unless there are differences in activity patterns over time or locations. Overall, a significant downward trend in ambient O_3 concentrations has occurred from 1980 in most locations in the United States, although the trend in the latter part of the 1990s suggests that continued improvements in air quality may have leveled off. Greater declines in ambient O_3 concentrations appear to have occurred in urban centers than in rural regions. The decline in daily and weekly average O_3 concentrations from 1989 to 1995 in rural regions was 5% and 7%, respectively (Wolff et al., 2001; Lin et al., 2001; Holland et al., 1999). A detailed discussion of O_3 trends appears earlier in this annex.

AX3.11.11 Modeling Ozone Exposure

AX3.11.11.1 Issues of Terminology

Models of human exposure to O_3 can be characterized and differentiated based upon a variety of attributes. For example, exposure models can be classified as (1) potential exposure models, typically maximum outdoor concentration versus “actual” exposure, including locally modified microenvironmental outdoor and indoor exposures; (2) population versus “specific individual"-based exposure models; (3) deterministic versus probabilistic models; and (4) observation versus mechanistic air quality model-driven estimates of spatially and temporally varying O_3 concentration fields, etc.

Some points should be made regarding terminology and the directions of exposure modeling research (as related specifically to O_3 exposure assessments) before proceeding to discuss specific recent activities and developments. First, it must be understood that significant variation exists in the definitions for much of the terminology used in the published literature. The science of exposure modeling is an evolving field and the development of a "standard" and commonly accepted terminology is a process in evolution. Second, very often procedures/efforts listed in the scientific literature as "exposure models/exposure estimates," etc., may in fact refer to only a subset of the steps or components required for a complete exposure assessment. For example, some efforts focus solely on refining the subregional or local spatiotemporal dynamics of local O_3 concentrations starting from "raw" data representing monitor observations or regional grid-based model estimates. Nevertheless, such efforts are included in the discussion of the next subsection, as they can provide improved tools for the individual components that constitute a complete exposure assessment. On the other hand, formulations that are identified as exposure models, but focus only on ambient air quality predictions, are not included in the discussion that follows, as they do not provide true exposure estimates but, rather, ambient air estimates. These models are reviewed in an earlier section of this annex. It is recognized that ambient air concentrations are used as surrogates for exposure in some epidemiological studies. Third, O_3-exposure modeling is very often identified explicitly with population-based modeling, while models describing the specific mechanisms affecting the exposure of an individual to O_3, and possibly some of the co-occurring gas and/or aerosol phase pollutants, are usually associated with studies focusing on indoor chemistry modeling. Finally, in recent years, the focus of either individual- or population-based exposure modeling research has shifted from O_3 to other pollutants, mostly airborne toxics and particulate matter. However, many of the modeling components that have been developed in these efforts are directly applicable to O_3 exposure modeling and are, therefore, mentioned in the following discussion.

AX3.11.11.2 A General Framework for Assessing Exposure to Ozone

Once the individual and relevant activity locations for Individual Based Modeling (IBM), or the population and associated spatial (geographical) domain for Population Based Modeling (PBM) have been defined, along with the temporal framework of the analysis (period, resolution), the comprehensive modeling of individual/population exposure to O_3 (and related pollutants) will generally require several steps (or components, as some of them do not have to be performed in sequence). The steps represent a "composite" outline based on frameworks described in the literature over the last 20 years (Ott, 1982, 1985; Lioy, 1990; Georgopoulos and Lioy, 1994; U.S. Environmental Protection Agency, 1992, 1997) as well as on the structure of various existing inhalation exposure models (NEM/pNEM, HAPEM, SHEDS, REHEX, EDMAS, MENTOR-OPERAS, APEX, AIRPEX, AIRQUIS, etc.) (McCurdy, 1994; Johnson et al., 1992; Nagda et al., 1987; U.S. Environmental Protection Agency, 1996c; ICF Consulting, 2003; Burke et al., 2001; McCurdy et al., 2000; Georgopoulos et al., 2002a,b; Freijer et al., 1998; Clench-Aas et al., 1999; Kunzli et al., 1997). The conceptional frameworks of the models are similar. Figures AX3-93a,b provides a conceptual overview of the APEX as an example. The steps involved in defining exposure models include (1) estimation of the background or ambient levels of O_3 through geostatistical analysis of fixed monitor data, or emissions-based, photochemical, air quality modeling; (2) estimation of levels and temporal profiles of O_3 in various outdoor and indoor microenvironments such as street canyons, residences, offices, restaurants, vehicles, etc. through linear regression of available observational data sets, simple mass balance models, detailed (nonlinear) gas or gas/aerosol chemistry models, or detailed combined chemistry and computational fluid dynamics models; (3) characterization of relevant attributes of individuals or populations under study (age, gender, weight, occupation, etc.); (4) development of activity event (or exposure event) sequences for each member of the sample population or for each cohort for the exposure period; (5) calculation of appropriate inhalation (in general intake) rates for the individuals of concern, or the members of the sample population, reflecting/combining the physiological attributes of the study subjects and the activities pursued during the individual exposure events; (6) combination of intake rates and microenvironmental concentrations for each activity event to assess dose; (7) calculation of event-specific exposure and intake dose distributions for selected time periods (1-h and 8-h daily maximum, O_3 season averages, etc.); and (8) use of PBM to extrapolate population sample (or cohort) exposures and

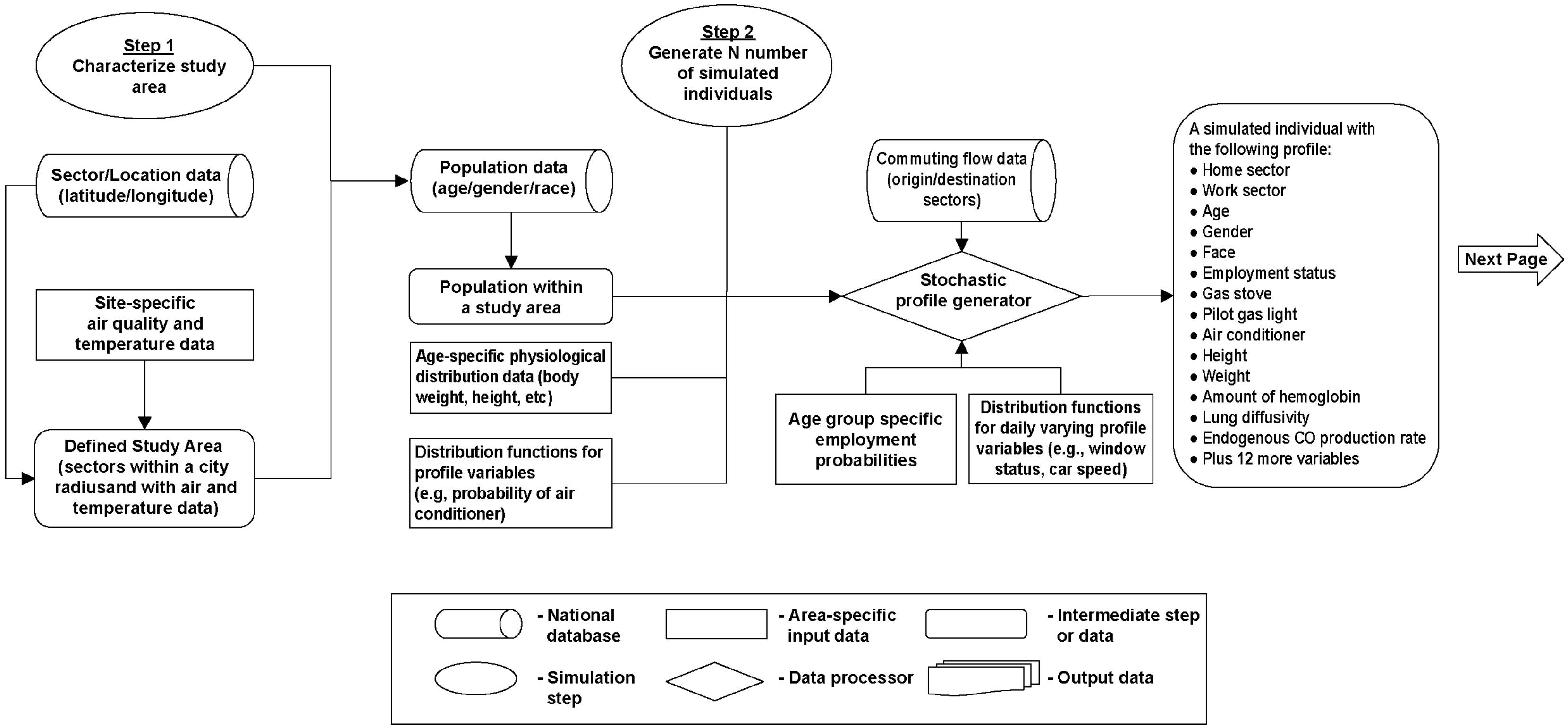

Figure AX3-93a. Detailed diagram illustrating components of APEX exposure model.

Source: www.epa.gov/ttn/fera/data/apex322/.

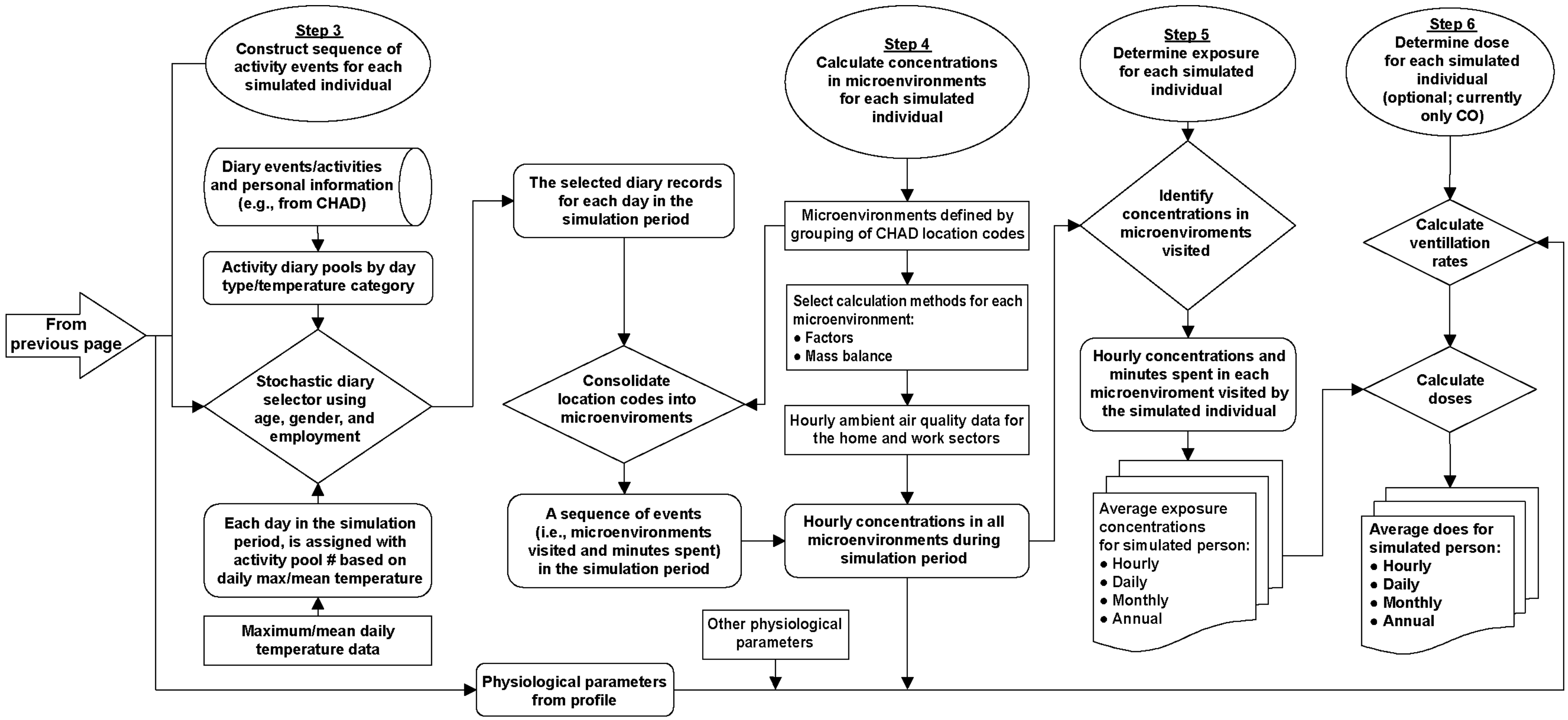

Figure AX3-93b. Detailed diagram illustrating components of APEX exposure model.

Source: www.epa.gov/ttn/fera/data/apex322/.

doses to the entire populations of interest. This process should aim to quantify, to the extent possible, variability and uncertainty in the various components, assessing their effects on the estimates of exposure.

Implementation of the above components of comprehensive exposure modeling has benefitted significantly from recent advances and expanded availability of computational technologies such as Relational Database Management Systems (RDBMS) and Geographic Information Systems (Purushothaman and Georgopoulos, 1997, 1999a,b).

AX3.11.11.3 Characterization of Ambient Concentrations of Ozone

As mentioned earlier, background and regional outdoor concentrations of pollutants over a study domain may be calculated either through emissions-based mechanistic modeling or through ambient-data-based modeling. Emissions-based models calculate the spatiotemporal fields of the pollutant concentrations using precursor emissions and meteorological conditions as inputs. The ambient-data-based models typically calculate spatial or spatiotemporal distributions of the pollutant through the use of interpolation schemes, based on either deterministic or stochastic models for allocating monitor station observations to the nodes of a virtual regular grid covering the region of interest. Kriging, a geostatistical technique, provides standard procedures for generating an interpolated O_3 spatial distribution for a given time period, using data from a set of observation points. The kriging approach, with parameters calculated specifically for each hour of the period of concern, was compared to the Urban Airshed Model (UAM-IV), a comprehensive photochemical grid-based model for deriving concentration fields. The concentration fields were then linked with corresponding population data to calculate potential outdoor population exposure. Higher exposure estimates were obtained with the photochemical grid-based model when O_3 concentrations were < 120 ppb, however, the situation was reversed when O_3 concentrations exceeded 120 ppb. The authors concluded that kriging O_3 values at the locations studied can reconstruct aspects of population exposure distributions (Georgopoulos et al., 1997a,b).

Carroll et al. (1997a,b) developed a spatial-temporal model, with a deterministic trend component, to model hourly O_3 levels with the capacity to predict O_3 concentrations at any location in Harris County, Texas during the time period between 1980 and 1993. A fast model-fitting method was developed to handle the large amount of available data and the substantial amount of missing data. Ozone concentration data used consisted of hourly measurements from 9 to 12 monitoring stations for the years 1980 to 1993. Using information from the census tract, the authors estimated that exposure of young children to O_3 declined by approximately 20% over the analysis period. The authors also suggested that the O_3 monitors are not sited in locations to adequately measure population exposures. Several researchers have questioned the suitability of the model for addressing spatial variations in O_3 (Guttorp et al., 1997; Cressie, 1997; Stein and Fang, 1997).

Spatiotemporal distributions of O_3 concentrations have alternatively been obtained using methods of the "Spatio-Temporal Random Field" (STRF) theory (Christakos and Vyas, 1998a,b). The STRF approach interpolates monitoring data in both space and time simultaneously. This method can analyze information on "temporal trends," which cannot be incorporated directly in purely spatial interpolation methods such as standard kriging. Further, the STRF method can optimize the use of data that are not uniformly sampled in either space or time. The STRF theory was further extended in the Bayesian Maximum Entropy (BME) framework and applied to O_3 interpolation studies (Christakos and Hristopulos, 1998; Christakos and Kolovos, 1999; Christakos, 2000). The BME framework can use prior information in the form of "hard data" (measurements), probability law descriptors (type of distribution, mean and variance), interval estimation (maximum and minimum values) and even constraint from physical laws. According to these researchers, both STRF and BME were found to successfully reproduce O_3 fields when adequate monitor data are available.

AX3.11.11.4 Calculation of Microenvironmental Concentrations

Once specific ambient/local spatiotemporal O_3 concentration patterns have been derived, microenvironments that can represent either outdoor or indoor settings must be characterized. This process can involve modeling of various local sources and sinks as well as interrelationships between ambient/local and microenvironmental concentration levels. Three approaches have been used in the past to model microenvironmental concentrations: empirical, mass balance, and detailed computational fluid dynamics (CFD).

The empirical fitting approach has been used to summarize the findings of recent field studies (Liu et al., 1995, 1997; Avol et al., 1998a). These empirical relationships could provide the basis for future, "prognostic" population exposure models.

Mass balance modeling has ranged from very simple formulations, assuming ideal (homogeneous) mixing and only linear physicochemical transformations with sources and sinks, to models that take into account complex multiphase chemical and physical interactions and nonidealities in mixing. Mass balance modeling is the most common approach used to model pollutant concentrations in enclosed microenvironments. As discussed earlier, the simplest microenvironmental setting is a homogeneously mixed compartment in contact with possibly both outdoor/local environments as well as with other microenvironments. The air quality of this idealized microenvironment is affected primarily by transport processes (including infiltration of outdoor air into indoor air compartments, advection between microenvironments, and convective transport); sources and sinks (local outdoor emissions, indoor emissions, surface deposition); and local outdoor and indoor gas and aerosol phase chemistry transformation processes (such as the formation of secondary organic and inorganic aerosols).

Numerous indoor air quality modeling studies have been reported in the literature; however, depending on the modeling scenario, only a limited number address physical and chemical processes that affect O_3 concentrations indoors (Nazaroff and Cass, 1986; Hayes, 1989, 1991). An example of a mass balance indoor air model for O_3 and benzene can be found in the work of Freijer and Bloemen (2000). They used outdoor O_3 measurements to parameterize a simplified linearized formulation of transport, transformation, and sources and sinks in the indoor microenvironment.

The pNEM/O_3 model includes a sophisticated mass balance model for enclosed (indoor and vehicle) microenvironments. The general form of this mass balance model is a differential equation that accounts for outdoor concentration, AER, penetration rate, decay rate, and indoor sources. Each of these parameters is represented by a probability distribution or by a dynamic relationship to other parameters that may change according to time of day, temperature, air conditioning status, window status, or other factors (Johnson, 2003).

Few indoor air models have considered detailed nonlinear chemistry, which, however, can have a significant effect on the indoor air quality, especially in the presence of strong indoor sources. Indeed, the need for more comprehensive models that can take into account the complex, multiphase processes that affect indoor concentrations of interacting gas phase pollutants and particulate matter has been recognized and a number of formulations have appeared in recent years. For example, the Exposure and Dose Modeling and Analysis System

(EDMAS) (Georgopoulos et al., 1997a) included an indoor model with detailed gas-phase atmospheric chemistry. This indoor model accounts for interactions of O_3 with indoor sinks and sources (surfaces, gas releases) and with entrained gas. The indoor model was dynamically coupled with the outdoor photochemical air quality models, UAM-IV and UAM-V (Urban Airshed Models), which provided the gas-phase composition of entrained air, and with a physiologically based O_3 uptake and dosimetry model. Subsequent work (Isukapalli and Georgopoulos, 2000; Isukapalli et al., 1999) expanded the framework and features of the EDMAS model to incorporate alternative representations of gas-phase chemistry as well as multiphase O_3 chemistry and gas/aerosol interactions. The new model is a component of the integrated Modeling Environment for Total Risk studies (MENTOR).

Sarwar et al. (2001, 2002) modeled estimates of indoor hydroxyl radical concentrations using a new indoor air quality model, Indoor Chemistry and Exposure Model (ICEM). The ICEM uses a modified SAPRC-99 atmospheric chemistry mechanism to simulate indoor hydroxyl radical production and consumption from reactions of alkenes with O_3. It also allows for the simulation of transport processes between indoor and outdoor environments, indoor emissions, chemical reactions, and deposition. Indoor hydroxyl radicals, produced from O_3 that penetrates indoors, can adversely impact indoor air quality through dark chemistry to produce photochemical oxidants.

Sørensen and Weschler (2002) used CFD modeling to examine the production of a hypothetical product from an O_3-terpene reaction under two different ventilation scenarios. The computational grid used in the model was nonuniform. There were significant variations in the concentrations of reactants between locations in the room, resulting in varying reaction rates. Because the “age of the air” differed at different locations in the room, the time available for reactions to occur also differed between locations.

Very few studies have focused on mechanistic modeling of outdoor microenvironments. Fraigneau et al. (1995) developed a simple model to account for fast NO-O_3 reaction/dispersion in the vicinity of a motorway. Proyou et al. (1998) applied a simple three-layer photochemical box model to an Athens street canyon. However, the adjustments of O_3 levels for sources, sinks, and mixing in outdoor microenvironments are done in a phenomenological manner in existing exposure models, driven by limited available observations. On-going research is evaluating approaches for quantifying local effects on outdoor O_3 chemistry in specific settings.

AX3.11.12 Population Exposure Models: Considerations of Activity Events and Population Demographics

Existing comprehensive inhalation exposure models treat human activity patterns as sequences of exposure events in which each event is defined by a geographic location and microenvironment. The EPA has supported the most comprehensive efforts in this area, leading to the development of the National Ambient Air Quality Standard Exposure Model and Probabilistic National Ambient Air Quality Standard Exposure Model (NEM and pNEM) (Johnson, 2003) and the Simulation of Human Exposure and Dose System (SHEDS) (Burke et al., 2001; McCurdy et al., 2000). The Air Pollutants Exposure model (APEX, version 3) [http://www.epa.gov/ttn/fera/data/apex322], a PC-based model, derived from the probabilistic NAAQS Exposure Model for carbon monoxide (pNEM/CO), will be used to help estimate human population exposure for criteria and air toxic pollutants as part of the EPA's overall Total Risk Integrated Methodology (TRIM) model framework. The model simulates the movement of individuals through time and space and their exposure to the given pollutant in indoor, outdoor, and in-vehicle microenvironments. Recent European efforts have produced some formulations that have similar general attributes as the above models but generally involve major simplifications in some of their components. Examples of recent European models addressing O_3 exposures include the AirPEx (Air Pollution Exposure) model (Freijer et al., 1998), which basically replicates the pNEM approach, and the AirQUIS (Air Quality Information System) model (Clench-Aas et al., 1999). A discussion of databases on time-activity data, and their influence on estimates of long-term ambient O_3 exposure, can be found in Kunzli et al. (1997), McCurdy (2000), and McCurdy et al. (2000).

The NEM/pNEM, APEX, and SHEDS families of models provide exposure estimates, defined by concentration and minute ventilation rate for each individual exposure event, and provide distributions of exposure and O_3 dose over any averaging period of concern from 1 h to an entire O_3 season. The above families of models also simulate certain aspects of the variability and uncertainty in the principal factors affecting exposure. pNEM divides the population of interest into representative cohorts based on the combinations of demographic characteristics (age, gender, employment), home/work district, residential cooking fuel, and then assigns activity diary records from CHAD (Consolidated Human Activities Database; www.epa.gov/chadnet1) (Glen et al., 1997) to each cohort according to demographic characteristic, season, day-type (weekday/weekend), and temperature. APEX and SHEDS generates a population demographic file containing a user-defined number of person-records for each census tract of the population based on proportions of characteristic variables (age, gender, employment, housing) obtained for the population of interest, and then assigns the matching activity information from CHAD to each individual record of the population, based on the characteristic variables.

The latest version of APEX allows for finer geographical units such as census tracts and automatically assigns population to the nearest monitor within a cutoff distance. Exposure district-specific temperatures can be specified and the user can select the variables that affect each parameter (e.g., the AER parameter in certain indoor microenvironments may depend on air conditioning status or window position). The mass balance algorithms have been enhanced to allow window position or vehicle speed to also be considered in determining AERs.

These models also allow for travel between census tracts for work. By specifying the commuting patterns, the variation of exposure concentrations due to commuting in different census tracts can be captured. The essential attributes of the pNEM, APEX, SHEDS, and MENTOR/SHEDS approaches are summarized in Table AX3-31.

From the above families of models only NEM/pNEM implementations have been extensively applied to O_3 studies. However, it is anticipated that APEX will be useful as an exposure modeling tool for assessing both criteria and hazardous air pollutants in the future. Recently, SHEDS has been modified and incorporated into MENTOR-OPERAS (Modeling ENvironment for TOtal Risk — Ozone and Particles Exposure and Risk Analysis System). This variant of SHEDS includes detailed indoor chemistry and other O_3-relevant microenvironmental processes, while providing interactive linking with CHAD for consistent definition of population characteristics and activity events. Nevertheless, the focus of the following will be on pNEM/O_3 implementations and applications, as they constitute the majority of the published O_3 exposure studies. The 1996 O_3 AQCD (U.S. Environmental Protection Agency, 1996a) also focused on the pNEM/O_3 family of models, referring to the review by McCurdy (1994) for the fundamental principles underlying its formulation and listing, in addition to the "standard" version, three pNEM/O_3-derived models (the Systems Applications International NEM [SAI/NEM]; the Regional Human Exposure Model [REHEX]; and the Event Probability Exposure Model [EPEM]).

Table AX3-31. Attributes of pNEM, SHEDS, APEX, and MENTOR/SHEDS Population Exposure Models

	pNEM	SHEDS	APEX	MENTOR/SHEDS
Exposure Estimate	Hourly averaged	Hourly averaged	Hourly averaged	Activity-event based
Characterization of the High-End Exposures	Yes	Yes	Yes	Yes
Spatial Scale/Resolution	Urban areas/Census tract level	Urban areas/Census tract level	Urban area/census tract level	Urban areas/Census tract level
Temporal Scale/Resolution	A year/one hour	A year/one hour	A year/one hour	A year/activity-event based time step
Population Activity Patterns Assembling	Top-down approach	Bottom-up approach	Bottom-up approach	Bottom-up approach
Microenvironment Concentration Estimation	Non-steady-state and steady-state mass balance equations (hard-coded)	Steady-state mass balance equation (residential) and linear relationship method (non-residential) (hard-coded)	Non-steady-state mass balance and linear relationship method (flexibility of selecting algorithms)	Non-steady-state mass balance equation with nonlinear indoor air chemistry module or regression methods (flexibility of selecting algorithms)
Microenvironmental (ME) Factors	Random samples from probability distributions	Random samples from probability distributions	Random samples from probability distributions	Random samples from probability distributions
Specification of Indoor Source Emissions	Yes (gas-stove, tobacco smoking)	Yes (gas-stove, tobacco smoking, other sources)	Yes (multiple sources defined by the user)	Yes (multiple sources defined by the users)

Rifai et al. (2000) compared applications of an updated version of REHEX, REHEX-II. The applications used NHAPS data for the southern states and the 48-state NHAPS or the Houston-specific time-activity pattern data. The results indicated a sensitivity to the specificity of the activity data: using Houston-specific data resulted in higher estimates of human exposure in some of the scenarios. For example, using NHAPS data lead to an estimated 275 thousand-exposure-hours between 120 to 130 ppb, while use of the Houston-specific activity data lead to an estimated 297 thousand-exposure-hours between 120 and 130 ppb (8% higher). Using the Houston-specific activity data in the model resulted in about 2,400 person-exposure-hours above 190 to 200 ppb O_3 while no exposure above this threshold was estimated when the NHAPS activity were used in the model.

The pNEM family of models used by the EPA has evolved considerably since the introduction of the first NEM model in the 1980s (Biller et al., 1981). The first such implementations of pNEM/O_3 in the 1980s used a reduced form of a mass balance equation to estimate indoor O_3 concentrations from outdoor concentrations. The second generation of pNEM/O_3 was developed in 1992 and used a simple mass balance model to estimate indoor O_3 concentrations. Subsequent enhancements to pNEM/O_3 and its input databases included revisions to the methods used to estimate equivalent ventilation rates (ventilation rate divided by body surface), to determine commuting patterns, and to adjust ambient O_3 levels to simulate attainment of proposed NAAQS. During the mid-1990s, the EPA applied updated versions of pNEM/O_3 to three different population groups in nine selected urban areas (Chicago, Denver, Houston, Los Angeles, Miami, New York, Philadelphia, St. Louis, and Washington): (1) the general population of urban residents, (2) outdoor workers, and (3) children who tended to spend more time outdoors than the average child. Reports by Johnson et al. (1996a,b,c) describe these versions of pNEM/O_3 and summarize the results of the application of the model to the nine urban areas. These versions of pNEM/O_3 used a revised probabilistic mass balance model to determine O_3 concentrations over 1-h periods in indoor and in-vehicle microenvironments (Johnson, 2003). The model assumed that there are no indoor sources of O_3, that the outdoor O_3 concentration and AER during the clock hour is constant at a specified value, and that O_3 decays at a rate proportional to the outdoor O_3 concentration and the indoor O_3 concentration.

The new pNEM-derived model, APEX, differs from earlier pNEM models in that the probabilistic features of the model are incorporated into a Monte Carlo framework. Instead of dividing the population of interest into a set of cohorts, APEX generates individuals as if they were being randomly sampled from the population. APEX provides each generated individual with a demographic profile that specifies values for all parameters required by the model. The values are selected from distributions and databases that are specific to the age, gender, and other specifications stated in the demographic profile. The EPA plans to develop future versions of APEX applicable to O_3 and other criteria pollutants. As mentioned earlier, the combined SHEDS/MENTOR-OPERAS system has also adopted this approach.

An important source of uncertainty in existing exposure modeling involves the creation of multiday, seasonal, or year long exposure activity sequences based on 1- to 3-day activity data for any given individual from CHAD. Currently, appropriate longitudinal data are not available and the existing models use various rules to derive longer-term activity sequences using 24-h activity data from CHAD.

AX3.11.13 Recent Developments: Activity Events and Inhalation Intake

An important development in inhalation exposure modeling, including O_3 exposure modeling, has been the consolidation of existing information on activity event sequences in CHAD (McCurdy, 2000; McCurdy et al., 2000). Indeed, most recent exposure models are designed (or have been redesigned) to obtain such information from CHAD. There are now about 22,600 person-days of sequential daily activity pattern data in CHAD. All ages of both genders are represented in CHAD. The data for each subject consist of one or more days of sequential activities, in which each activity is defined by start time, duration, activity type (140 categories), and microenvironment classification (110 categories). Activities vary from 1 min to 1 h in duration. Activities longer than 1 h are subdivided into clock-hour durations to facilitate exposure modeling. A distribution of values for the ratio of oxygen uptake rate to body mass (referred to as metabolic equivalents or METs) is provided for each activity type listed. The forms and parameters of these distributions were determined through an extensive review of the exercise and nutrition literature. The primary source of distributional data was Ainsworth et al. (1993), a compendium developed specifically to "facilitate the coding of physical activities and to promote comparability across studies."

Use of the information in CHAD provides a rational way for incorporating realistic intakes into exposure models by linking inhalation rates to activity information. As mentioned earlier, an exposure event sequence derived from activity-diary data is assigned to each population unit (cohort for pNEM- or REHEX-type models, or individual for APEX- or SHEDS-type models). Each exposure event is typically defined by a start and duration time, a geographic location and microenvironment, and activity level. The most recent pNEM, APEX, and SHEDS models have defined activity levels using the activity classification coding scheme incorporated into CHAD. A probabilistic module within the APEX- and SHEDS-type models converts the activity classification code of each exposure event to an energy expenditure rate, which in turn is converted into an estimate of oxygen uptake rate. The oxygen uptake rate is then converted into an estimate of ventilation rate ($\dot{V}_E$), expressed in L/min. Johnson (2001) reviewed the physiological principles incorporated into the algorithms used in pNEM and APEX to convert each activity classification code to an oxygen uptake rate and describes the additional steps required to convert oxygen uptake to $\dot{V}_E$.

McCurdy (1997a,b, 2000) recommended that ventilation rate be estimated as a function of energy expenditure rate. The energy expended by an individual during a particular activity can be expressed as:

$$EE = (MET)(RMR) \tag{AX3-5}$$

where EE is the average energy expenditure rate (kcal/min) during the activity, MET (metabolic equivalent of work) is a ratio specific to the activity and is dimensionless, and RMR is the resting metabolic rate of the individual expressed in terms of number of energy units expended per unit of time (kcal/min). If RMR is specified for an individual, then the above equation requires only an activity-specific estimate of MET to produce an estimate of the energy expenditure rate for a given activity. McCurdy et al. (2000) developed MET distributions for the activity classifications appearing in the CHAD database.

Finally, one issue that should be mentioned is that of evaluating comprehensive prognostic exposure modeling studies, for either individuals or populations, with field data. Attempts had been made to evaluate pNEM/O_3-type models using personal exposure measurements (Johnson et al., 1990). Although databases that would be adequate for performing a comprehensive evaluation are not expected to be available any time soon, a number of studies are building the necessary information base, as discussed previously. Some of these studies report field observations of personal, indoor, and outdoor O_3 concentrations and describe simple semiempirical personal exposure models that are parameterized using observational data and regression techniques.

AX3.11.14 Characterization of Exposure

AX3.11.14.1 Use of Ambient Ozone Concentrations

The use of ambient air monitoring stations is still the most common surrogate for assigning exposure in epidemiological studies. Since the primary source of O_3 exposure is the ambient air, monitoring concentration data would provide the exposure outdoors while exercising, a potential important exposure to evaluate in epidemiological studies as well as a relative assignment of exposure with time if the concentration were uniform across the region; the time-activity pattern were the same across the population; and the housing characteristics, such as ventilation rates and the O_3 sinks contributing to its indoor decay rates, were constant for the study area. Since these factors vary by population and location there will be errors in not only the magnitude of the total exposure, but also in the relative total exposure assignment based solely on ambient monitoring data. As discussed earlier in this section, spatial differences in O_3 concentrations within a city and between the height of the monitor and the breath zone (1 to 2 m) exist, increasing uncertainties. The potential exists to obtain more complete exposure assignments for both individuals and populations by modeling O_3 exposure based on ambient air concentration to account for spatial variations outdoors and for time spent indoors, provided housing characteristics and activity patterns can be obtained. For cohort studies, measurement of personal O_3 exposures using passive monitors is also possible.

The potential for error in determining pollutant exposure was also expressed by Krzyzanowki (1997), who indicated that while the typical estimate of exposure in epidemiological studies is “an average concentration of the pollutant calculated from the data routinely collected in the area of residence of the studied population. This method certainly lacks precision and, in most cases, the analyses that use it will underestimate the effect of specific concentrations of a pollutant on health.” It is further stated that when estimating exposure for epidemiological studies it is important to define: (1) representativeness of exposure or environmental data for the population at risk, (2) appropriateness of the averaging time for the health outcome being examined, and (3) the relationship between the exposure surrogate and the true exposure relative to the exposure-response function used in the risk assessment.

Numerous air pollutants can have common ambient air sources resulting in strong correlations among pollutant ambient air concentrations. As a result, some observed associations between an air pollutant and health effects may be due to confounding by other air pollutants. Sarnat et al. (2001) found that while ambient air concentrations of some air pollutants were correlated, personal $PM_{2.5}$ and several gaseous air pollutant (O_3, SO_2, NO_2, CO, and exhaust-related VOCs) exposures were not generally correlated. The findings were based on the results of a multipollutant exposure study of 56 children and elderly adults in Baltimore, MD conducted during both the summer and winter months. Ambient pollutant concentrations were not associated with corresponding personal exposures, except for $PM_{2.5}$. The gaseous pollutants were found to be surrogates of $PM_{2.5}$ and were generally not correlated. The authors concluded that multipollutant models in epidemiologic studies of $PM_{2.5}$ may not be suitable, and health effects attributed to the gaseous pollutants may be the result of $PM_{2.5}$ exposure. It should be noted that the 95th percentile O_3 concentrations in the study was lower than 60 ppb, an O_3 concentration at which respiratory effects are noted. It would be important to examine whether O_3 is a surrogate for personal $PM_{2.5}$ at high O_3 levels when attributing adverse health effects to O_3 or $PM_{2.5}$.

Kunzli et al. (1996) assessed potential lifetime exposure to O_3 based on the responses to a standardized questionnaire completed by 175 college freshmen in California. Questions addressed lifetime residential history, schools attended, general and outdoor activity patterns, driving habits and job history. The purpose was to determine what O_3 monitoring data to use for each time period of their lives, the potential correction factor for indoor levels and periods of high activity to account for differential doses to the lung due to physical activity. The reliability of the responses was checked by having each respondent complete the questionnaire twice, on different days, and the results compared. A lifetime O_3 exposure history was generated for each participant and a sensitivity analysis performed to evaluate which uncertainties would cause the greatest potential misclassification of exposure. Assigned lifetime O_3 concentrations from the nearest monitor yielded highly reliable cumulative values, although the reliability of residential location decreased with increasing residential locations. Individuals involved in moderate and heavy exercise could be reliably identified. Such an approach can be used to evaluate health outcomes associated with chronic exposures to O_3.

AX3.11.14.2 Exposure Selection in Controlled Exposure Studies

Ozone exposures in the environment are variable over time due to changes in the ambient concentrations during the day as the photochemical reactions proceed and also because people move between microenvironments that have different concentrations (Johnson, 1997). Exposures are repeated on sequential days since weather conditions that produce O_3 can move slowly through or become stagnant within a region. For simplicity, most controlled-exposure experiments are conducted at a single concentration for a fixed time period, with a limited number of studies being repeated on a single individual. Few studies have been conducted using multipollutants or photochemical agents other than O_3, to better represent "real-world" exposures with the exception of NO_2. Studies by Hazucha et al. (1992), Adams (2003), and Adams and Ollison (1997) examined the effect of varying O_3 exposure concentrations on pulmonary function. A description of, and findings in, the studies appears in Annex AX5 of this document.

AX3.11.14.3 Exposure to Related Photochemical Agents

Exposures to other related photochemical agents have not been measured using personal samplers nor are these agents routinely measured at O_3 monitoring stations. Photochemical agents produced in the ambient air can penetrate indoors and react with other pollutants to produce other potentially irritating compounds. Reiss et al. (1995) reported that organic acids, aldehydes and ketones were produced indoors by reactions of O_3 with VOCs. The produced compounds included oxidants that can be respiratory irritants. The indoor concentrations were dependent upon the O_3 concentrations indoors and the AER within the building. Weschler and Shields (1997) summarized indoor air chemical reactions that depend directly or indirectly on the presence of O_3. They indicated that O_3 concentrations are lower indoors than outdoors partly because of gas-phase reactions that produce other oxidants in an analogous fashion to photochemical smog in ambient air. The production of these species indoors is a function of the indoor O_3 concentration and the presence of the other necessary precursors, VOCs, and NO_2, along with an optimal AER. A variety of the photochemical oxidants related to O_3 that are produced outdoors, such as PAN and PPN, can penetrate indoors. These oxidants are thermally unstable and can decompose indoors to peroxacetyl radicals and NO_2 through thermal decay. PAN removal increases with increasing temperature, and at a given temperature, with increasing NO/NO_2 concentration ratio (Grosjean et al., 2001). Other free radicals that can form indoors include HO• and $HO_2^{\bullet}$. These free radicals can produce compounds that are known or suspected to be irritating. Little is known about exposure to some of these agents, as not all have been identified and collection and analytical methodologies have not be developed for their routine determination. Lee et al. (1999) reported that homogeneous (gas phase) and heterogenous (gas phase/solid surface) reactions occur between O_3 and common indoor air pollutants such as NO and VOCs to produce secondary products whose production rate depends on the AER and surface area within the home. Wainman et al. (2000) found that O_3 reacts indoors with *d*-limonene, emitted from air fresheners, to form fine particles in the range of 0.1 to 0.2 μm and 0.2 to 0.3 μm. The indoor process also produces compounds that have been identified in the ambient atmosphere. These species, plus others that may form indoors from other terpenes or unsaturated compounds can present an additional exposure to oxidants, other than O_3, at higher concentrations than present in ambient air, even as the O_3 concentration is being reduced indoors.

AX3.11.14.4 Exposure to Sensitive Populations

Personal O_3 concentrations have been measured for populations potentially susceptible to respiratory irritants including children, outdoor workers, the elderly, and individuals with chronic obstructive pulmonary disease (Table AX3-32). Children and outdoor workers have somewhat higher exposures than other individuals because they spend more time outdoors engaged in moderate and heavy exertion. Children are also more active outside and, therefore, have a higher minute ventilation rate than most adults (Klepeis et al., 1996, 2001). While the current data suggest trends in exposure magnitude for some populations, additional exposure studies are needed to generalize differences in exposure between the general population and potentially susceptible populations. Exposure modeling can be used to extend the current information available from measurement studies. Several states report days when high O_3 are occurring (O_3 alert days) to encourage sensitive individuals to modify their behavior to reduce their exposure to O_3. However, this change in behavior is not recorded in a database of time-activity patterns or used in exposure modeling as a discrete entity for sensitive populations.

Table AX3-32. Personal Exposure Concentrations

Location, Population, Sample Duration	n	Personal Exposure Mean[a] (range) (ppb)	Reference
San Diego, CA, Asthmatics ages 9-18 years, 12 hour	12	12 ± 12 (0-84) 10 weekend 12 weekday	Delfino et al. (1996)
Vancouver, Canada, Adult Workers, Daily	585		Brauer and Brook (1997)
High indoor time		(ND-9)	
Moderate indoor time		(ND-12)	
Only outdoor		(2-44)	
Southern California, Subjects 10-38 years	24		Liu et al. (1997)
Spring		13.6 ± 2.5 (- to 80)	
Fall		10.5 ± 2.5 (- to 50)	
Montpellier, France, Adults, Hourly	16	34.3 ± 17.6 (6.5-88)	Bernard et al. (1999)
Winter		15.4 ± 7.7 (6.5-40)	
Summer		44.1 ± 18.2(11-88)	
Souther California, Children 6-12 years, ≥ 6 days	169	6.2 ± 4.7 (0.5-41)	Geyh et al. (2000)
Upland - winter		19 ± 18 (0.5-63)	
- summer		5.7 ± 4.2 (0.5-31)	
Mountain - winter		25 ± 24 (0.5-72)	
- summer			
Baltimore, MD, Technician, Hourly[b]	1		Chang et al. (2000)
Winter		3.5 ± 7.5 (ND-49)	
Summer		15 ± 18 (ND-76)	
Baltimore, MD, Adults 75 ± 7 years, Daily	20		Sarnat et al. (2000)
Winter		3.5 ± 3.0 (ND-9.9)	
Summer		0. ± 1.8 (ND-2.8)	

[a]ND = not detected.
[b]Measurements made following scripted activities for 15 days.

Ozone exposure modeling has been conducted for the general population and sensitive subgroups. The pNEM/O_3 model takes into consideration the temporal and spatial distribution of people and O_3 throughout the area of consideration, variations in O_3 concentrations within microenvironments, and the effects of exertion/exercise (increased ventilation) on O_3 uptake. The pNEM/O_3 model consists of two principal parts: the cohort exposure program and the exposure extrapolation program. The methodology incorporated much of the general framework described earlier in this section on assessing O_3 exposure and consists of five steps: (1) define the study area, population of interest, subdivisions of the study area, and exposure period;

(2) divide population of interest into a set of cohorts; (3) develop exposure event sequence for each cohort for the exposure period; (4) estimate pollutant concentration and ventilation rate for each exposure event; and (5) extrapolate cohort exposures to population of interest (U.S. Environmental Protection Agency, 1996b).

There are three versions of the pNEM/O_3 model: general population (Johnson et al., 1996a), outdoor workers (Johnson et al., 1996b), and outdoor children (Johnson et al., 1996c, 1997). These three versions of the model have been applied to nine urban areas. The model also has been applied to a single summer camp (Johnson et al., 1996c). The general population version of the model uses activity data from the Cincinnati Activity Diary Study (CADS; Johnson, 1989). Time-activity studies (Wiley et al., 1991a; Johnson, 1984; Linn et al., 1993; Shamoo et al., 1991; Goldstein et al., 1992; Hartwell et al., 1984) were combined with the CADS data for the outdoor worker version of the model. Additional time-activity data (Goldstein et al., 1992; Hartwell et al., 1984; Wiley et al., 1991a,b; Linn et al., 1992; Spier et al., 1992) were also added to CADS for the outdoor children of the model (U.S. Environmental Protection Agency, 1996b). Home-work commuting patterns are based on information gathered by the U.S. Census Bureau. Ozone ambient air concentration data from monitoring stations were used to estimate the outdoor exposure concentrations associated with each exposure event. Indoor O_3 decay rate is assumed to be proportional to the indoor O_3 concentration. An algorithm assigns the equivalent ventilation rate (EVR) associated with each exposure event. The outdoor children model uses an EVR-generator module to generate an EVR value for each exposure event based on data on heart rate by Spier et al. (1992) and Linn et al. (1992). The models produce exposure estimates for a range of O_3 concentrations at specified exertion levels. The models were used to estimate exposure for nine air quality scenarios (U.S. Environmental Protection Agency, 1996b).

Korc (1996) used the REHEX-II model, a general purpose air pollution exposure model based on a microenvironmental approach modified to account for the influence of physical activity along and spatial and the temporal variability of outdoor air pollution. Ozone exposure was estimated by demographic groups across 126 geographic subregions for 1980 to 1982, and for 142 geographic subregions for 1990 to 1992. Simulation results were determined for population race, ethnicity, and per capita income and included indoor, in-transit, and outdoor microenvironments. Exposure modeling was stratified by age because of differences in time-activity patterns. Exposure distributions by regional activity pattern data were not considered, rather it was assumed that all individuals within a county had the same exposure distribution by race, ethnicity, and socioeconomic status. Model results for southern California indicated that the segment of the population with the highest exposures were children 6 to 11 years old. Individuals living in low income districts may have greater per capita hours of exposure to O_3 above the NAAQS than those living in higher income districts. The author indicated that O_3 exposure differences by race and ethnicity have declined over time. The noninclusion of details on activity patterns for different populations in the model limit the extrapolations that can be made from the model results.

Children appear to have higher exposures than adults and the elderly. Asthmatics appear to ventilate more than healthy individuals, but tend to protect themselves by decreasing their outdoor exercise (Linn et al., 1992). Additional data are still needed to identify and better define exposures to potentially susceptible populations and improve exposure models for the general population and subpopulation of concern.

REFERENCES

Adams, W. C. (1993) Measurement of breathing rate and volume in routinely performed daily activities [final report]. Sacramento, CA: California Environmental Protection Agency, Air Resources Board; contract no. A033-205.

Adams, W. C. (2003) Comparison of chamber and face mask 6.6-hour exposure to 0.08 ppm ozone via square-wave and triangular profiles on pulmonary responses. Inhalation Toxicol. 15: 265-281.

Adams, W. C.; Ollison, W. M. (1997) Effects of prolonged simulated ambient ozone dosing patterns on human pulmonary function and symptomatology. Presented at: 90th annual meeting of the Air & Waste Management Association; June; Toronto, Ontario, Canada. Pittsburgh, PA: Air & Waste Management Association; paper no. 97-MP9.02.

Adams, R. M.; Hamilton, S. A.; McCarl, B. A. (1985) An assessment of the economic effects of ozone on U.S. agriculture. J. Air Pollut. Control Assoc. 35: 938-943.

Adams, R. M.; Glyer, J. D.; Johnson, S. L.; McCarl, B. A. (1989) A reassessment of the economic effects of ozone on U.S. agriculture. JAPCA 39: 960-968.

Ainsworth; Haskell, W. L.; Leon, A. S.; Jacobs, D. R., Jr.; Montoye, H. J.; Sallis, J. F.; Paffenbarger, R. S., Jr. (1993) Compendium of physical activities: classification of energy costs of human physical activities. Med. Sci. Sports Exer. 25: 71-80.

Aldrich, F. D.; Brooks, B. O.; Davis, W. F.; DeBroy, J. A.; Li, S. T.; Schimke, R.; Utter, G. M. (1995) Health and productivity impact of organic volatiles from electronic office equipment. Presented at: Pacific Rim conference on occupational and environmental health; October; Sydney, Australia.

Allen, R. J.; Wadden, R. A.; Ross, E. D. (1978) Characterization of potential indoor sources of ozone. Am. Ind. Hyg. Assoc. J. 39: 466-471.

Aneja, V. P.; Li, Z. (1992) Characterization of ozone at high elevation in the eastern United States: trends, seasonal variations, and exposure. J. Geophys. Res. [Atmos.] 97: 9873-9888.

Avol, E. L.; Navidi, W. C.; Colome, S. D. (1998a) Modeling ozone levels in and around southern California homes. Environ. Sci. Technol. 32: 463-468.

Avol, E. L.; Navidi, W. C.; Rappaport, E. B.; Peters, J. M. (1998b) Acute effects of ambient ozone on asthmatic, wheezy, and healthy children. Cambridge, MA: Health Effects Institute; research report no. 82.

Beine, H. J.; Jaffe, D. A.; Herring, J. A.; Kelley, J. A.; Krognes, T.; Stordal, F. (1997) High-latitude springtime photochemistry. Part I: NO_x, PAN and ozone relationships. J. Atmos. Chem. 27: 127-153.

Bernard, N. L.; Gerber, M. J.; Astre, C. M.; Saintot, M. J. (1999) Ozone measurement with passive samplers: validation and use for ozone pollution assessment in Montpellier, France. Environ. Sci. Technol. 33: 217-222.

Berntsen, T. K.; Isaksen, I. S. A.; Myhre, G.; Fuglestvedt, J. S.; Stordal, F.; Larsen, T. A.; Freckleton, R. S.; Shine, K. P. (1997) Effects of anthropogenic emissions on tropospheric ozone and its radiative forcing. J. Geophys. Res. [Atmos.] 102: 28,101-28,126.

Berry, C. R. (1964) Differences in concentrations of surface oxidant between valley and mountaintop conditions in the southern Appalachians. J. Air Pollut. Control Assoc. 14: 238-239.

Bey, I.; Jacob, D. J.; Yantosca, R. M.; Logan, J. A.; Field, B.; Fiore, A. M.; Li, Q.; Liu, H.; Mickley, L. J.; Schultz, M. G. (2001a) Global modeling of tropospheric chemistry with assimilated meteorology: model description and evaluation. J. Geophys. Res. (Atmos.) 106: 23,073-23,095.

Bey, I.; Jacob, D. J.; Logan, J. A.; Yantosca, R. M. (2001b) Asian chemical outflow to the Pacific in spring: origins, pathways, and budgets. J. Geophys. Res. [Atmos.] 106: 23,097-23,113.

Biller, W. F.; Feagans, T. B.; Johnson, T. R.; Duggan, G. M.; Paul, R. A.; McCurdy, T.; Thomas, H. C. (1981) A general model for estimating exposure associated with alternative NAAQS. Presented at: 74th annual meeting of the Air Pollution Control Association; June; Philadelphia, PA. Pittsburgh, PA: Air Pollution Control Association; paper no. 81-18.4.

Black, M. S.; Worthan, A. W. (1999) Emissions from office equipment. In: Raw, G.; Aizlewood, C.; Warren, P., eds. Indoor Air '99, v. 2. London, England: Construction Research Communications Ltd.; pp. 454-459.

Black, D. R.; Harley, R. A.; Hering, S. V.; Stolzenburg, M. R. (2000) A new, portable, real-time monitor. Environ. Sci. Technol. 34: 3031-3040.

Blanchard, C. L.; Tanenbaum, S. J. (2003) Differences between weekday and weekend air pollutant levels in southern California. J. Air Waste Mange. Assoc. 53: 816-828.

Böhm, M.; McCune, B.; Vandetta, T. (1991) Diurnal curves of troposheric ozone in the western United States. Atmos. Environ. Part A 25: 1577-1590.

Bottenheim, J. W.; Barrie, L. A.; Atlas, E.; Heidt, L. E.; Niki, H.; Rasmussen, R. A.; Shepson, P. B. (1990) Depletion of lower tropospheric ozone during Arctic spring: The Polar Sunrise Experiment 1988. J. Geophys. Res. (Atmos.) 95: 18,555-18,568.

Bottenheim, J. W.; Barrie, L. A.; Atlas, E. (1993) The partitioning of nitrogen oxides in the lower Arctic troposphere during Spring 1988. J. Atmos. Chem. 17: 15-27.

Brauer, M.; Brook, J. R. (1997) Ozone personal exposures and health effects for selected groups residing in the Fraser Valley. In: Steyn, D. G.; Bottenheim, J. W., eds. The Lower Fraser Valley Oxidants/Pacific '93 Field Study. Atmos. Environ. 31: 2113-2121.

Bravo, H.; Echeverria, R. S.; Sanchez, P.; Palomera, M.; Lefohn, A. S. (2003) The "piston effect" observed in ozone concentrations in Mexico City. EM (August): 16-19.

Brice, K. A.; Penkett, S. A.; Atkins, D. H. F.; Sandalls, F. J.; Bamber, D. J.; Tuck, A. F.; Vaughan, G. (1984) Atmospheric measurements of peroxyacetylnitrate (PAN) in rural, south-east England: seasonal variations winter photochemistry and long-range transport. Atmos. Environ. 18: 2691-2702.

Browell, E. V.; Hair, J. W.; Butler, C. F.; Grant, W. B.; De Young, R. J.; Fenn, M. A.; Brackett, V. G.; Clayton, M. B.; Brasseur, L. A.; Harper, D. B.; Ridley, B. A.; Klonecki, A. A.; Hess, P. G.; Emmons, L. K.; Tie, X.; Atlas, E. L.; Cantrell, C. A.; Wimmers, A. J.; Blake, D. R.; Coffey, M. T.; Hannigan, J. W.; Dibb, J. E.; Talbot, R. W.; Flocke, F.; Weinheimer, A. J.; Fried, A.; Wert, B.; Snow, J. A.; Lefer, B. L. (2003) Ozone, aerosol, potential vorticity, and trace gas trends observed at high-latitudes over North America from February to May 2000. J. Geophys. Res. [Atmos.] 108(D4): 10.1029/2001JD001390.

Burke, J. M.; Zufall, M. J.; Özkaynak, H. (2001) A population exposure model for particulate matter: case study results for $PM_{2.5}$ in Philadelphia, PA. J. Exposure Anal. Environ. Epidemiol. 11: 470-489.

Carroll, R. J.; Chen, R.; George, E. I.; Li, T. H.; Newton, H. J.; Schmiediche, H.; Wang, N. (1997a) Ozone exposure and population density in Harris County, Texas. J. Am. Stat. Assoc. 92: 392-404.

Carroll, R. J.; Chen, R.; George, E. I.; Li, T. H.; Newton, H. J.; Schmiediche, H.; Wang, N. (1997b) Ozone exposure and population density in Harris County, Texas (rejoinder). J. Am. Stat. Assoc. 92: 414-415.

Chang, L.-T.; Koutrakis, P.; Catalano, P. J.; Suh, H. H. (2000) Hourly personal exposures to fine particles and gaseous pollutants—results from Baltimore, Maryland. J. Air Waste Manage. Assoc. 50: 1223-1235.

Chao, C. Y. (2001) Comparison between indoor and outdoor air contaminant levels in residential buildings from passive sampler study. Build. Environ. 36: 999-1007.

Chen, L.-W. A. (2002) Urban fine particulate matter: chemical composition and possible origins (dissertation). College Park, MD: University of Maryland, Department of Chemical Physics. Available from: University Microfilms, Ann Arbor, MI; AADAA-I3078297.

Chinkin, L. R.; Coe, D. L.; Funk, T. H.; Hafner, H. R.; Roberts, P. T.; Ryan, P. A. (2003) Weekday versus weekend activity patterns for ozone precursor emissions in California's South Coast Air Basin. J. Air Waste Manage. Assoc. 53: 829-843.

Christakos, G. (2000) Modern spatiotemporal geostatistics. New York, NY: Oxford University Press. (International Association for Mathematical Geology; studies in mathematical geology: 6).

Christakos, G.; Hristopulos, D. T. (1998) Spatiotemporal environmental health modelling. *A tractatus stochasticus*. Boston, MA: Kluwer Academic Publishers.

Christakos, G.; Kolovos, A. (1999) A study of the spatiotemporal health impacts of ozone exposure. J. Exposure Anal. Environ. Epidemiol. 9: 322-335.

Christakos, G.; Vyas, V. M. (1998a) A composite space/time approach to studying ozone distribution over eastern United States. Atmos. Environ. 32: 2845-2857.

Christakos, G.; Vyas, V. M. (1998b) A novel method for studying population health impacts of spatiotemporal ozone distribution. Soc. Sci. Med. 47: 1051-1066.

Clench-Aas, J.; Bartonova, A.; Bøhler, T.; Grønskei, K. E.; Sivertsen, B.; Larssen, S. (1999) Air pollution exposure monitoring and estimating. Part I. Integrated air quality monitoring system. J. Environ. Monit. 1: 313-319.

Cleveland, W. S.; Graedel, T. E.; Kleiner, B.; Warner, J. L. (1974) Sunday and workday variations in photochemical air pollutants in New Jersey and New York. Science (Washington, DC) 186: 1037-1038.

Code of Federal Regulations. (2000a) Appendix I to part 50—interpretation of the 8-hour primary and secondary national ambient air quality standards for ozone. C. F. R. 40: pt. 50, app. I.

Code of Federal Regulations. (2000b) Appendix D to part 58—Network design for state and local air monitoring stations (SLAMS), national air monitoring stations (NAMS), and photochemical assessment monitoring stations (PAMS). C. F. R. 40: pt. 58, app. D.

Coffey, P.; Stasiuk, W.; Mohnen, V. (1977) Ozone in rural and urban areas of New York State: part I. In: Dimitriades, B., ed. International conference on photochemical oxidant pollution and its control - proceedings: volume I; September 1976; Raleigh, NC. Research Triangle Park, NC: U.S. Environmental Protection Agency, Environmental Sciences Research Laboratory; pp. 89-96; report no. EPA-600/3-77-001a. Available from: NTIS, Springfield, VA; PB-264232.

Colome, S. D.; Wilson, A. L.; Tian, Y. (1994) California residential indoor air quality study. Volume 2. Carbon monoxide and air exchange rate: an univariate and multivariate analysis. Chicago, IL: Gas Research Institute; report no. GRI-93/0224.3.

Cooper, O. R.; Moody, J. L. (2000) Meteorological controls on ozone at an elevated eastern United States regional background monitoring site. J. Geophys. Res. [Atmos.] 105: 6855-6869.

Cressie, N. (1997) Ozone exposure and population density in Harris County, Texas [comment]. J. Am. Stat. Assoc. 92: 411-413.

Cristofanelli, P.; Bonasoni, P.; Collins, W.; Feichter, J.; Forster, C.; James, P.; Kentarchos, A.; Kubik, P. W.; Land, C.; Meloen, J.; Roelofs, G. J.; Siegmund, P.; Sprenger, M.; Schnabel, C.; Stohl, A.; Tobler, L.; Tositti, L.; Trickl, T.; Zanis, P. (2003) Stratosphere-troposphere exchange: a model and method evaluation. J. Geophys. Res. 108(D12): 10.1029/2002JD002600.

Daum, P. H.; Kleinman, L. I.; Newman, L.; Luke, W. T.; Weinstein-Lloyd, J.; Berkowitz, C. M.; Busness, K. M. (1996) Chemical and physical properties of plumes of anthropogenic pollutants transported over the North Atlantic during the North Atlantic Regional Experiment. J. Geophys. Res. [Atmos.] 101: 29,029-29,042.

Delfino, R. J.; Coate, B. D.; Zeiger, R. S.; Seltzer, J. M.; Street, D. H.; Koutrakis, P. (1996) Daily asthma severity in relation to personal ozone exposure and outdoor fungal spores. Am. J. Respir. Crit. Care Med. 154: 633-641.

Dickerson, R. R. (1985) Reactive nitrogen compounds in the Arctic. J. Geophys. Res. 90: 10,739-10,743.

Dickerson, R. R.; Huffman, G. J.; Luke, W. T.; Nunnermacker, L. J.; Pickering, K. E.; Leslie, A. C. D.; Lindsey, C. G.; Slinn, W. G. N.; Kelly, T. J.; Daum, P. H.; Delany, A. C.; Greenberg, J. P.; Zimmerman, P. R.; Boatman, J. F.; Ray, J. D.; Stedman, D. H. (1987) Thunderstorms: an important mechanism in the transport of air pollutants. Science (Washington, DC) 235: 460-465.

Drakou, G.; Zerefos, C.; Ziomas, I. (1995) A preliminary study on the relationship between outdoor and indoor air pollution levels. Fresenius' Environ. Bull. 4: 689-694.

Drakou, G.; Zerefos, C.; Ziomas, I.; Voyatzaki, M. (1998) Measurements and numerical simulations of indoor O_3 and NO_x in two different cases. Atmos. Environ. 32: 595-610.

Evans, G.; Finkelstein, P.; Martin, B.; Possiel, N.; Graves, M. (1983) Ozone measurements from a network of remote sites. J. Air Pollut. Control Assoc. 33: 291-296.

Evans, E. G.; Rhodes, R. C.; Mitchell, W. J.; Puzak, J. C. (1985) Summary of precision and accuracy assessments for the state and local air monitoring networks: 1982. Research Triangle Park, NC: U.S. Environmental Protection Agency, Environmental Monitoring Systems Laboratory; report no. EPA-600/4-85-031. Available from: NTIS, Springfield, VA; PB85-208171.

Faith, R.; Sheshinski, R. (1979) Misspecification of trend in spatial random-function interpolation with application to oxidant mapping. Philadelphia, PA: Siam Institute for Mathematics and Society; technical report no. 28.

Fan, S.-M.; Jacob, D. J.; Mauzerall, D. L.; Bradshaw, J. D.; Sandholm, S. T.; Blake, D. R.; Singh, H. B.; Talbot, R. W.; Gregory, G. L.; Sachse, G. W. (1994) Origin of tropospheric NO_x over subarctic eastern Canada in summer. J. Geophys. Res. [Atmos.] 99: 16,867-16,877.

Federal Register. (1986) Guidelines for estimating exposures. F. R. (September 24) 51: 34,042-34,054.

Fiore, A. M.; Jacob, D. J.; Bey, I.; Yantosca, R. M.; Field, B. D.; Fusco, A. C.; Wilkinson, J. G. (2002a) Background ozone over the United States in summer: origin, trend, and contribution to pollution episodes. J. Geophys. Res. (Atmos.) 107(D15): 10.1029/2001JD000982.

Fiore, A. M.; Jacob, D. J.; Field, B. D.; Streets, D. G.; Fernandes, S. D.; Jang, C. (2002b) Linking ozone pollution and climate change: the case for controlling methane. Geophys. Res. Lett. 29(19): 10.1029/2002GL015601.

Fiore, A.; Jacob, D. J.; Liu, H.; Yantosca, R. M.; Fairlie, T. D.; Li, Q. (2003a) Variability in surface ozone background over the United States: implications for air quality policy. J. Geophys. Res. (Atmos.) 108(D24): 10.1029/2003JD003855.

Fiore, A. M.; Jacob, D. J.; Mathur, R.; Martin, R. V. (2003b) Application of empirical orthogonal functions to evaluate ozone simulations with regional and global models. J. Geophys. Res. (Atmos.) 108(D14): 10.1029/2002JD003151.

Fowler, D.; Cape, J. N. (1982) Air pollutants in agriculture and horticulture. In: Unsworth, M. H.; Ormrod, D. P. Effects of gaseous air pollution in agriculture and horticulture. London, United Kingdom: Butterworth Scientific; pp. 3-26.

Fraigneau, Y. C.; Gonzalez, M.; Coppalle, A. (1995) Dispersion and chemical reaction of a pollutant near a motorway. Sci. Total Environ. 169: 83-91.
Freijer, J. I.; Bloemen, H. J. T. (2000) Modeling relationships between indoor and outdoor air quality. J. Air Waste Manage. Assoc. 50: 292-300.
Freijer, J. I.; Bloemen, H. J. T.; de Loos, S.; Marra, M.; Rombout, P. J. A.; Steentjes, G. M.; Van Veen, M. P. (1998) Modelling exposure of the Dutch population to air pollution. J. Haz. Mat. 61: 107-114.
Fujita, E. M.; Stockwell, W. R.; Campbell, D. E.; Keislar, R. E.; Lawson, D. R. (2003) Evolution of the magnitude and spatial extent of the weekend ozone effect in California's South Coast Air Basin, 1981-2000. J. Air Waste Manage. Assoc. 53: 802-815.
Fusco, A. C.; Logan, J. A. (2003) Analysis of 1970-1995 trends in tropospheric ozone at Northern Hemisphere midlatitudes with the GEOS-CHEM model. J. Geophys. Res. (Atmos.) 108: 10.1029/2002JD002742.
Georgopoulos, P. G.; Lioy, P. J. (1994) Conceptual and theoretical aspects of human exposure and dose assessment. J. Exposure Anal. Environ. Epidemiol. 4: 253-285.
Georgopoulos, P. G.; Arunachalam, S.; Wang, S. (1997a) Alternative metrics for assessing the relative effectiveness of NOx and VOC emission reductions in controlling ground-level ozone. J. Air Waste Manage. Assoc. 47: 838-850.
Georgopoulos, P. G.; Walia, A.; Roy, A.; Lioy, P. J. (1997b) Integrated exposure and dose modeling and analysis system. 1. Formulation and testing of microenvironmental and pharmacokinetic components. Environ. Sci. Technol. 31: 17-27.
Georgopoulos, P.; Yonone-Lioy, M. J.; Opeikum, R. E.; Lioy, P. (2002a) Environmental dynamics and human exposure to copper. Volume I: environmental dynamics and human exposure issues. New York, NY: International Copper Association.
Georgopoulos, P.; Wang, S. W.; Vyas, V. M.; Lioy, P. J.; Tan, H. C. (2002b) Environmental dynamics and human exposure to copper. Volume 2: framework and data sources for assessing human exposure to copper in the United States. New York, NY: International Copper Association.
Gettelman, A.; Holton, J. R.; Rosenlof, K. H. (1997) Mass fluxes of O_3, CH_4, N_2O, and CF_2Cl_2 in the lower stratosphere calculated from observational data. J. Geophys. Res. [Atmos.] 102: 19,149-19,159.
Geyh, A. S.; Wolfson, J. M.; Koutrakis, P.; Mulik, J. D.; Avol, E. L. (1997) Development and evaluation of a small active ozone sampler. Environ. Sci. Technol. 31: 2326-2330.
Geyh, A. S.; Roberts, P. T.; Lurmann, F. W.; Schoell, B. M.; Avol, E. L. (1999) Initial field evaluation of the Harvard active ozone sampler for personal ozone monitoring. J. Exposure Anal. Environ. Epidemiol. 9: 143-149.
Geyh, A. S.; Xue, J.; Ozkaynak, H.; Spengler, J. D. (2000) The Harvard Southern California chronic ozone exposure study: assessing ozone exposure of grade-school-age children in two southern California communities. Environ. Health Perspect. 108: 265-270.
Glen, G.; Lakkadi, Y.; Tippett, J. A.; del Valle-Torres, M. (1997) Development of NERL/CHAD: the National Exposure Research Laboratory consolidated human activity database. Research Triangle Park, NC: U.S. Environmental Protection Agency, Office of Research and Development; contract no. 68-D5-0049.
Gold, D. R.; Allen, G.; Damokosh, A.; Serrano, P.; Hayes, C.; Castillejos, M. (1996) Comparison of outdoor and classroom ozone exposures for school children in Mexico City. J. Air Waste Manage. Assoc. 46: 335-342.
Goldan, P. D.; Trainer, M.; Kuster, W. C.; Parrish, D. D.; Carpenter, J.; Roberts, J. M.; Yee, J. E.; Fehsenfeld, F. C. (1995) Measurements of hydrocarbons, oxygenated hydrocarbons, carbon monoxide, and nitrogen oxides in an urban basin in Colorado: implications for emission inventories. J. Geophys. Res. [Atmos.] 100: 22,771-22,783.
Goldstein, B. R.; Tardiff, G.; Hoffnagle, G.; Kester, R. (1992) Valdez health study: summary report. Anchorage, AK: Alyeska Pipeline Service Company.
Grivet, C. D. (1980) Modeling and analysis of air quality data [dissertation]. Palo Alto, CA: Stanford University. Available from: University Microfilms International; Ann Arbor, MI; publication no. 80-16,824.
Grosjean, E.; Grosjean, D. (1996) Carbonyl products of the gas phase reaction of ozone with symmetrical alkenes. Environ. Sci. Technol. 30: 2036-2044.
Grosjean, E.; Grosjean, D. (1998) The gas-phase reaction of alkenes with ozone: formation yields of carbonyls from biradicals in ozone-alkene-cyclohexane experiments. Atmos. Environ. 32: 3393-3402.
Grosjean, E.; Grosjean, D.; Woodhouse, L. F. (2001) Peroxyacetyl nitrate and peroxypropionyl nitrate during SCOS 97-NARSTO. Environ. Sci. Technol. 35: 4007-4014.
Guttorp, P.; Meiring, W.; Sampson, P. D. (1997) Ozone exposure and population density in Harris County, Texas [comment]. J. Am. Stat. Assoc. 92: 405-408.

Hartwell, T. D.; Clayton, C. A.; Ritchie, R. M.; Whitmore, R. W.; Zelon, H. S.; Jones, S. M.; Whitehurst, D. A. (1984) Study of carbon monoxide exposure of residents of Washington, DC and Denver, Colorado. Research Triangle Park, NC: U.S. Environmental Protection Agency, Office of Research and Development, Environmental Monitoring Systems Laboratory; report no. EPA-600/4-84-031.

Hayes, S. R. (1989) Estimating the effect of being indoors on total personal exposure to outdoor air pollution. JAPCA 39: 1453-1461.

Hayes, S. R. (1991) Use of an indoor air quality model (IAQM) to estimate indoor ozone levels. J. Air Waste Manage. Assoc. 41: 161-170.

Hazucha, M. J.; Folinsbee, L. J.; Seal, E., Jr. (1992) Effects of steady-state and variable ozone concentration profiles on pulmonary function. Am. Rev. Respir. Dis. 146: 1487-1493.

Heck, W. W.; Taylor, O. C.; Adams, R.; Bingham, G.; Miller, J.; Preston, E.; Weinstein, L. (1982) Assessment of crop loss from ozone. J. Air Pollut. Control Assoc. 32: 353-361.

Helaleh, M. I. H.; Ngudiwaluyo, S.; Korenaga, T.; Tanaka, K. (2002) Development of passive sampler technique for ozone monitoring. Estimation of indoor and outdoor ozone concentration. Talanta 58: 649-659.

Herring, J. A.; Jaffe, D. A.; Beine, H. J.; Madronich, S.; Blake, D. R. (1997) High-latitude springtime photochemistry. Part II: sensitivity studies of ozone production. J. Atmos. Chem. 27: 155-178.

Heuss, J. M.; Kahlbaum, D. F.; Wolff, G. T. (2003) Weekday/weekend ozone differences: what can we learn from them? J. Air Waste Manage. Assoc. 53: 772-788.

Holland, D. M.; Principe, P. P.; Vorburger, L. (1999) Rural ozone: trends and exceedances at CASTNet sites. Environ. Sci. Technol. 33: 43-48.

Holton, J. R.; Haynes, P. H.; McIntyre, M. E.; Douglass, A. R.; Rood, R. B.; Pfister, L. (1995) Stratosphere-troposphere exchange. Rev. Geophys. 33: 403-439.

Horowitz, L. W.; Walters, S.; Mauserall, D. L.; Emmons, L. K.; Rasch, P. J.; Granier, C.; Tie, X.; Lamarque, J.-F.; Schultz, M. G.; Tyndall, G. S.; Orlando, J. J.; Brasseur, G. P. (2003) A global simulation of tropospheric ozone and related tracers: description and evaluation of MOZART, version 2. J. Geophys. Res. [Atmos.] 108(D24): 10.1029/2002JD002853.

Howard-Reed, C.; Wallace, L. A.; Ott, W. R. (2002) The effect of opening windows on air change rates in two homes. J. Air Waste Manage Assoc. 52: 147-159.

ICF Consulting; ManTech Environmental Technology, Inc. (2003) Total Risk Integrated Methodology TRIM.Expo(Inhalation) user's document. Volume I: air pollutants exposure model (APEX, version 3) user's guide. Research Triangle Park, NC: U.S. Environmental Protection Agency, Office of Air Quality Planning and Standards. Available: http://www.epa.gov/ttn/fera/data/apex322/apexusersguidevoli4-24-03.pdf [7 September, 2004].

Intergovernmental Panel on Climate Change (IPCC). (2001) Climate change 2001: the scientific basis. Contribution of working group I to the third assessment report of the Intergovernmental Panel on Climate Change. Cambridge, United Kingdom: Cambridge University Press.

Isaksen, I. S. A.; Hov, O.; Hesstvedt, E. (1978) Ozone generation over rural areas. Environ. Sci. Technol. 12: 1279-1284.

Isukapalli, S. S.; Purushothaman, V.; Georgopoulos, P. G. (1999) Mechanistic modeling of the interrelationships between indoor/outdoor air quality and human exposure in a GIS framework. Presented at: 92nd Air & Waste Management Association Annual Meeting; June; St. Louis, MO. Pittsburgh, PA: Air & Waste Management Association.

Jacob, D. L.; Logan, J. A.; Murti, P. P. (1999) Effect of rising Asian emissions on surface ozone in the United States. Geophys. Res. Lett. 26: 2175-2178.

Jaffe, D. A. (1993) The relationship between anthropogenic nitrogen oxides and ozone trends in the Arctic troposphere. In: Niki, H.; Becker, K. H., eds. The tropospheric chemistry of ozone in the polar regions. New York, NY: Springer-Verlag. (NATO ASI series I: Global environmental change, vol. 7).

Jaffe, D. A.; Honrath, R. E.; Herring, J. A.; Li, S.-M.; Kahl, J. D. (1991) Measurements of nitrogen oxides at Barrow, Alaska during spring: evidence for regional and northern hemispheric sources of pollution. J. Geophys. Res. [Atmos.] 96: 7395-7405.

Jaffe, D.; Price, H.; Parrish, D.; Goldstein, A.; Harris, J. (2003) Increasing background ozone during spring on the west coast of North America. Geophys. Res. Lett. 30: 10.1029/2003GL017024.

Jakobi, G.; Fabian, P. (1997) Indoor/outdoor concentrations of ozone and peroxyacetyl nitrate (PAN). Int. J. Biometeorol. 40: 162-165.

James, P.; Stohl, A.; Forster, C.; Eckhardt, S.; Seibert, P.; Frank, A. (2003a) A 15-year climatology of stratosphere-troposphere exchange with a Lagrangian particle dispersion model: 1. Methodology and validation. J. Geophys. Res. 108(D12): 10.1029/2002JD002637.

James, P.; Stohl, A.; Forster, C.; Eckhardt, S.; Seibert, P.; Frank, A. (2003b) A 15-year climatology of stratosphere-troposphere exchange with a Lagrangian particle dispersion model. 2. Mean climate and seasonal variability. J. Geophys. Res. (Atmos.) 108(D12): 10.1029/2002JD002639.

Johnson, T. (1984) A study of personal exposure to carbon monoxide in Denver, Colorado. Research Triangle Park, NC: U.S. Environmental Protection Agency, Environmental Monitoring Systems Laboratory; report no. EPA-600/4-84-014.

Johnson, T. A. (1989) Human activity patterns in Cincinnati, Ohio. Palo Alto, CA: Electric Power Research Institute; report no. EPRI EN-6204.

Johnson, T. (1997) A pilot study in Los Angeles to measure personal ozone exposures during scripted activities. Washington, DC: American Petroleum Institute, Health and Environmental Sciences Department; API publication no. DR 218.

Johnson, T. (2001) A guide to selected algorithms, distributions, and databases used in exposure models developed by the Office of Air Quality Planning and Standards (DRAFT). Research Triangle Park, NC: U.S. Environmental Protection Agency, CERM report TR01.

Johnson, T. (2003) A guide to selected algorithms, distributions, and databases used in exposure models developed by the Office of Air Quality Planning and Standards. Research Triangle Park, NC: U.S. Environmental Protection Agency, Office of Research and Development; EPA grant no. CR827033. Available: http://www.epa.gov/ttn/fera/data/human/report052202.pdf [9 April, 2004].

Johnson, T.; Long, T. (2004) Determining the frequency of open windows in residences: a pilot study in Durham, North Carolina during varying temperature conditions. J. Exposure Anal. Environ. Epidemiol.: 10.1038/sj.jea.7500409.

Johnson, T. R.; Paul, R. A.; Capel, J. E.; McCurdy, T. (1990) Estimation of ozone exposure in Houston using a probabilistic version of NEM. Presented at: 83rd annual meeting and exhibition of the Air & Waste Management Association; June; Pittsburgh, PA. Pittsburgh, PA: Air & Waste Management Association; paper no. 90-150.1.

Johnson, T. R.; Wijnberg, L.; Capel, J. E.; Vostal, J. J. (1992) The use of activity diary data to estimate the probability of exposure to air pollution. In: Berglund, R. L., ed. Tropospheric ozone and the environment II: effects, modeling and control [papers from an international specialty conference]; November; Atlanta, GA. Pittsburgh, PA: Air & Waste Management Association; pp. 713-724. (A&WMA transactions series no. 20).

Johnson, T.; Capel, J.; McCoy, M. (1996a) Estimation of ozone exposures experienced by urban residents using a probabilistic version of NEM and 1990 population data. Research Triangle Park, NC: U.S. Environmental Protection Agency, Office of Air Quality Planning and Standards; contract no. 68-DO-0062.

Johnson, T.; Capel, J.; McCoy, M.; Mozier, J. W. (1996b) Estimation of ozone exposures experienced by outdoor workers in nine urban areas using a probabilistic version of NEM. Research Triangle Park, NC: U.S. Environmental Protection Agency, Office of Air Quality Planning and Standards; contract no. 63-D-30094, work assignment nos. 0-1 and 1-4.

Johnson, T.; Capel, J.; Mozier, J.; McCoy, M. (1996c) Estimation of ozone exposures experienced by outdoor children in nine urban areas using a probabilistic version of NEM. Research Triangle Park, NC: U.S. Environmental Protection Agency, Office of Air Quality Planning and Standards; contract no. 63-D-30094.

Johnson, T.; Mozier, J.; Capel, J. (1997) Supplement to "Estimation of ozone exposures experienced by outdoor children in nine urban areas using a probabilistic version of NEM (April 1996)". Research Triangle Park, NC: U.S. Environmental Protection Agency, Office of Air Quality Planning and Standards.

Johnson, T.; Myers, J.; Kelly, T.; Wisbith, A.; Ollison, W. (2004) A pilot study using scripted ventilation conditions to identify key factors affecting indoor pollutant concentrations and air exchange rate in a residence. J. Exposure Anal. Environ. Epidemiol. 14: 1-22.

Junge, C. E. (1963) Air chemistry and radioactivity. New York, NY: Academic Press. (Van Mieghem, J.; Hales, A. L., eds. International geophysics series: v. 4).

Kelly, N. A.; Wolff, G. T.; Ferman, M. A. (1984) Sources and sinks of ozone in rural areas. Atmos. Environ. 18: 1251-1266.

Klenø, J. G.; Clausen, P. A.; Weschler, C. J.; Wolkoff, P. (2001) Determination of ozone removal rates by selected building products using the FLEC emission cell. Environ. Sci. Technol. 35: 2548-2553.

Klepeis, N. E.; Tsang, A. M.; Behar, J. V. (1996) Analysis of the national human activity pattern survey (NHAPS) respondents from a standpoint of exposure assessment. Washington, DC: U.S. Environmental Protection Agency, Office of Research and Development; report no. EPA/600/R-96/074.

Klepeis, N. E.; Nelson, W. C.; Ott. W. R.; Robinson, J. P. Tsang, A. M.; Switzer, P.; Behar, J. V.; Hern, S. C.; Engelmann, W. H. (2001) The National Human Activity Pattern Survey (NHAPS): a resource for assessing exposure to environmental pollutants. J. Exposure Anal. Environ. Epidemiol. 11: 231-252.

Kley, D.; Volz, A.; Mulheims, F. (1988) Ozone measurements in historic perspective. In: Isaksen, I. S. A., ed. Tropospheric ozone - regional and global scale interactions: proceedings of the NATO advanced workshop on regional and global ozone interaction and its environmental consequences; June 1987; Lillehammer, Norway. Dordrecht, The Netherlands: D. Reidel Publishing Company; pp. 63-72. [NATO Advanced Science Institutes (ASI) studies: series C, mathematical and physical sciences v. 227].

Knudsen, H. P.; Lefohn, A. S. (1988) The use of geostatistics to characterize regional ozone exposures. In: Heck, W. W.; Taylor, O. C.; Tingey, D. T., eds. Assessment of crop loss from air pollutants: proceedings of an international conference; October 1987; Raleigh, NC. Essex, United Kingdom: Elsevier Science Publishers, Ltd.; pp. 91-105.

Korc, M. E. (1996) A socioeconomic assessment of human exposure to ozone in the South Coast Air Basin of California. J. Air Waste Manage. Assoc. 46: 547-557.

Koutrakis, P.; Sioutas, C.; Ferguson, S. T.; Wolfson, J. M.; Mulik, J. D.; Burton, R. M. (1993) Development and evaluation of a glass honeycomb denuder/filter pack system to collect atmospheric gases and particles. Environ. Sci. Technol. 27: 2497-2501.

Krzyzanowski, M. (1997) Methods for assessing the extent of exposure and effects of air pollution. Occup. Environ. Med. 54: 145-151.

Künzli, N.; Lurmann, F.; Segal, M.; Ngo, L.; Balmes, J.; Tager, I. B. (1996) Reliability of lifetime residential history and activity measures as elements of cumulative ambient ozone exposure assessment. J. Exposure Anal. Environ. Epidemiol. 6: 289-310.

Künzli, N.; Kelly, T.; Balmes, J.; Tager, I. B. (1997) Reproducibility of retrospective assessment of outdoor time-activity patterns as an individual determinant of long-term ambient ozone exposure. Int. J. Epidemiol. 26: 1258-1271.

Lagus Applied Technology, Inc. (1995) Air change rates in non-residential buildings in California. Sacramento, CA: California Energy Commission; contract no. 400-91-034; July.

Lavery, T. F.; Rogers, C. M.; Howell, H. K.; Burnett, M. C.; Wanta, C. A. (2002) Clean air status trends network (CASTNet) 2000 annual report. Available: http://www.epa.gov/castnet/library/annual00.html (9 September 2003).

Lebron, F. (1975) A comparison of weekend-weekday ozone and hydrocarbon concentrations in the Baltimore-Washington metropolitan area. Atmos. Environ. 9: 861-863.

Lee, K.; Vallarino, J.; Dumyahn, T. Ozkaynak, H.; Spengler, J. (1999) Ozone decay rates in residences. J. Air Waste Manage. Assoc. 49: 1238-1244.

Lee, K.; Xue, J.; Geyh, A. S.; Özkaynak, H.; Leaderer, B. P.; Weschler, C. J.; Spengler, J. D. (2002) Nitrous acid, nitrogen dioxide, and ozone concentrations in residential environments. Environ. Health Perspect. 110: 145-150.

Lefohn, A. S. (1984) A comparison of ambient ozone exposures for selected nonurban sites. Presented at: 77th annual meeting of the Air Pollution Control Association; June; San Francisco, CA. Pittsburgh, PA: Air Pollution Control Association; paper no. 84-104.1.

Lefohn, A. S. (1992) The characterization of ambient ozone exposures. In: Lefohn, A. S., ed. Surface level ozone exposures and their effects on vegetation. Chelsea, MI: Lewis Publishers, Inc.; pp. 31-92.

Lefohn, A. S.; Benedict, H. M. (1983) The potential for the interaction of acidic precipitation and ozone pollutant doses affecting agricultural crops. Presented at: 76th annual meeting of the Air Pollution Control Association; June; Atlanta, GA. Pittsburgh, PA: Air Pollution Control Association; paper no. 83-2.2.

Lefohn, A. S.; Jones, C. K. (1986) The characterization of ozone and sulfur dioxide air quality data for assessing possible vegetation effects. J. Air Pollut. Control Assoc. 36: 1123-1129.

Lefohn, A. S.; Mohnen, V. A. (1986) The characterization of ozone, sulfur dioxide, and nitrogen dioxide for selected monitoring sites in the Federal Republic of Germany. J. Air Pollut. Control Assoc. 36: 1329-1337.

Lefohn, A. S.; Runeckles, V. C. (1987) Establishing standards to protect vegetation - ozone exposure/dose considerations. Atmos. Environ. 21: 561-568.

Lefohn, A. S.; Shadwick, D. S. (1991) Ozone, sulfur dioxide, and nitrogen dioxide trends at rural sites located in the United States. Atmos. Environ. Part A 25: 491-501.

Lefohn, A. S.; Tingey, D. T. (1984) The co-occurrence of potentially phytotoxic concentrations of various gaseous air pollutants. Atmos. Environ. 18: 2521-2526.

Lefohn, A. S.; Davis, C. E.; Jones, C. K.; Tingey, D. T.; Hogsett, W. E. (1987) Co-occurrence patterns of gaseous air pollutant pairs at different minimum concentrations in the United States. Atmos. Environ. 21: 2435-2444.

Lefohn, A. S.; Knudsen, H. P.; McEvoy, L. R., Jr. (1988) The use of kriging to estimate monthly ozone exposure parameters for the southeastern United States. Environ. Pollut. 53: 27-42.

Lefohn, A. S.; Krupa, S. V.; Winstanley, D. (1990a) Surface ozone exposures measured at clean locations around the world. Environ. Pollut. 63: 189-224.
Lefohn, A. S.; Shadwick, D. S.; Mohnen, V. A. (1990b) The characterization of ozone concentrations at a select set of high-elevation sites in the eastern United States. Environ. Pollut. 67: 147-178.
Lefohn, A. S.; Benkovitz, C. M.; Tanner, R. L.; Smith, L. A.; Shadwick, D. S. (1991) Air quality measurements and characterizations for terrestrial effects research. In: Irving, P. M., ed. Acidic deposition: state of science and technology, volume I, emissions, atmospheric processes, and deposition. Washington, DC: The U.S. National Acid Precipitation Assessment Program. (State of science and technology report no. 7).
Lefohn, A. S.; Shadwick, D. S.; Ziman, S. D. (1998) The difficult challenge of attaining EPA's new ozone standard. Environ. Sci. Technol. 32: 276A-282A.
Lefohn, A. S.; Oltmans, S. J.; Dann, T.; Singh, H. B. (2001) Present-day variability of background ozone in the lower troposphere. J. Geophys. Res. [Atmos.] 106: 9945-9958.
Lelieveld, J.; Dentener, F. J. (2000) What controls tropospheric ozone? J. Geophys. Res. [Atmos.] 105: 3531-3551.
Leovic, K. W.; Sheldon, L. S.; Whitaker, D. A.; Hetes, R. G.; Calcagni, J. A.; Baskir, J. N. (1996) Measurement of indoor air emissions from dry-process photocopy machines. J. Air Waste Manage. Assoc. 46: 821-829.
Leovic, K. W.; Whitaker, D.; Brockmann, C.; Bayer, C. W.; Sojka, P. E. (1998) Evaluation of low-emitting products for use in the indoor environment. Presented at: 91st annual meeting of the Air & Waste Management Association; June; San Diego, CA. Pittsburgh, PA: Air & Waste Management Association; paper no. 98-TP48.02 (A292).
Li, Q.; Jacob, D. J.; Logan, J. A.; Bey, I.; Yantosca, R. M.; Liu, H.; Martin, R. V.; Fiore, A. M.; Field, B. D.; Duncan, B. N. (2001) A tropospheric ozone maximum over the Middle East. Geophys. Res. Lett. 28: 3235-3238.
Li, Q.; Jacob, D. J.; Fairlie, T. D.; Liu, H.; Martin, R. V.; Yantosca, R. M. (2002) Stratospheric versus pollution influences on ozone at Bermuda: reconciling past analyses. J. Geophys. Res. 107(D22): 10.1029/2002JD002138.
Lin, C.-Y.; Jacob, D. J.; Munger, J. W.; Fiore, A. M. (2000) Increasing background ozone in surface air over the United States. Geophys. Res. Lett. 27: 3465-3468.
Lin, C.-Y. C.; Jacob, D. J.; Fiore, A. M. (2001) Trends in exceedances of the ozone air quality standard in the continental United States, 1980-1998. Atmos. Environ. 35: 3217-3228.
Linn, W. S.; Shamoo, D. A.; Hackney, J. D. (1992) Documentation of activity patterns in 'high-risk' groups exposed to ozone in the Los Angeles area. In: Tropospheric ozone and the environment II: effects, modeling and control: papers from an Air & Waste Management Association international specialty conference; November, 1991; Atlanta, GA. Pittsburgh, PA: Air & Waste Management Association; pp. 701-712. (A&WMA publication TR-20).
Linn, W. S.; Spier, C. E.; Hackney, J. D. (1993) Activity patterns in ozone-exposed construction workers. J. Occup. Med. Toxicol. 2: 1-14.
Linn, W. S.; Shamoo, D. A.; Anderson, K. R.; Peng, R.-C.; Avol, E. L.; Hackney, J. D.; Gong, H., Jr. (1996) Short-term air pollution exposures and responses in Los Angeles area schoolchildren. J. Exposure Anal. Environ. Epidemiol. 6: 449-472.
Lioy, P. J. (1990) Assessing total human exposure to contaminants: a multidisciplinary approach. Environ. Sci. Technol. 24: 938-945.
Lisac, I.; Grubišić, V. (1991) An analysis of surface ozone data measured at the end of the 19th century in Zagreb, Yugoslavia. Atmos. Environ. Part A 25: 481-486.
Liu, D.-L.; Nazaroff, W. W. (2001) Modeling pollutant penetration across building envelopes. Atmos. Environ. 35: 4451-4462.
Liu, L.-J. S.; Koutrakis, P.; Leech, J.; Broder, I. (1995) Assessment of ozone exposures in the greater metropolitan Toronto area. J. Air Waste Manage. Assoc. 45: 223-234.
Liu, L.-J. S.; Delfino, R.; Koutrakis, P. (1997) Ozone exposure assessment in a southern California community. Environ. Health Perspect. 105: 58-65.
Liu, H.; Jacob, D. J.; Chan, L. Y.; Oltmans, S. J.; Bey, I.; Yantosca, R. M.; Harris, J. M.; Duncan, B. N.; Martin, R. V. (2002) Sources of tropospheric ozone along the Asian Pacific Rim: an analysis of ozonesonde observations. J. Geophys. Res. [Atmos.] 107(D21): 10.1029/2001JD002005.
Liu, H.; Jacob, D. J.; Bey, I.; Yantosca, R. M.; Duncan, B. N.; Sachse, G. W. (2003) Transport pathways for Asian pollution outflow over the Pacific: interannual and seasonal variations. J. Geophys. Res. (Atmos.) 108(D20): 10.1029/2002JD003102.
Liu, H.; Jacob, D. J.; Dibb, J. E.; Fiore, A. M.; Yantosca, R. M. (2004) Constraints on the sources of tropospheric ozone from ^{210}Pb-^{7}Be-O_3 correlations. J. Geophys. Res. (Atmos.) 109(D7): 10.1029/2003JD003988.

Logan, J. A. (1989) Ozone in rural areas of the United States. J. Geophys. Res. [Atmos.] 94: 8511-8532.
Logan, J. A. (1999) An analysis of ozonesonde data for the troposphere: recommendations for testing 3-D models and development of a gridded climatology for tropospheric ozone. J. Geophys. Res. 104: 16,115-16,149.
Ludwig, F. L.; Reiter, E.; Shelar, E.; Johnson, W. B. (1977) The relation of oxidant levels to precursor emissions and meteorological features: v. I, analysis and findings. Research Triangle Park, NC: U.S. Environmental Protection Agency, Office of Air Quality Planning and Standards; report no. EPA-450/3-77-022a. Available from: NTIS, Springfield, VA; PB-275 001.
Marr, L. C.; Morrison, G. C.; Nazaroff, W. W.; Harley, R. A. (1998) Reducing the risk of accidental death due to vehicle-related carbon monoxide poisoning. J. Air Waste Manage. Assoc. 48: 899-906.
Martin, R. V.; Jacob, D. J.; Yantosca, R. M.; Chin, M.; Ginoux, P. (2003) Global and regional decreases in tropospheric oxidants from photochemical effects of aerosols. J. Geophys. Res. [Atmos.] 108(D3): 10.1029/2002JD002622.
Matheron, G. (1963) Principles of geostatistics. Econ. Geol. 58: 1246-1266.
McCurdy, T. (1988) Relationships among ozone air quality indicators in urban areas. In: Wolff, G. T.; Hanisch, J. L.; Schere, K., eds. The scientific and technical issues facing post-1987 ozone control strategies: transactions of an APCA international specialty conference; November 1987; Hartford, CT. Pittsburgh, PA: Air & Waste Management Association; pp. 331-342. (APCA transactions series: no. 12).
McCurdy, T. R. (1994) Human exposure to ambient ozone. In: McKee, D. J., ed. Tropospheric ozone: human health and agricultural impacts. Boca Raton, FL: Lewis Publishers; pp. 85-127.
McCurdy, T. (1997a) Human activities that may lead to high inhaled intake doses in children aged 6-13. Environ. Toxicol. Pharmacol. 4: 251-260.
McCurdy, T. (1997b) Modeling the dose profile in human exposure assessments: ozone as an example. Rev. Toxicol. 1: 3-23.
McCurdy, T. (2000) Conceptual basis for multi-route intake dose modeling using an energy expenditure approach. J. Exposure Anal. Environ. Epidemiol. 10: 86-97.
McCurdy, T.; Glen, G.; Smith, L.; Lakkadi, Y. (2000) The National Exposure Research Laboratory's Consolidated Human Activity Database. J. Exposure Anal. Environ. Epidemiol. 10: 566-578.
Meagher, J. F.; Lee, N. T.; Valente, R. J.; Parkhurst, W. J. (1987) Rural ozone in the southeastern United States. Atmos. Environ. 21: 605-615.
Meloen, J.; Siegmund, P.; Van Velthoven, P.; Kelder, H.; Sprenger, M.; Wernli, H.; Kentarchos, A.; Roelofs, G.; Feichter, J.; Land, C.; Forster, C.; James, P.; Stohl, A.; Collins, W.; Cristofanelli, P. (2003) Stratosphere-troposphere exchange: a model and method intercomparison. J. Geophys. Res. 108(D12): 10.1029/2002JD002274.
Mohnen, V. A. (1989) Mountain cloud chemistry project: wet, dry and cloud water deposition. Research Triangle Park, NC: U.S. Environmental Protection Agency, Atmospheric Research and Exposure Assessment Laboratory; report no. EPA/600/3-89/009. Available from: NTIS, Springfield, VA; PB89-148597.
Mohnen, V. A.; Hogan, A.; Coffey, P. (1977) Ozone measurements in rural areas. J. Geophys. Res. 82: 5889-5895.
Monks, P. S. (2000) A review of the observations and origins of the spring ozone maximum. Atmos. Environ. 34: 3545-3561.
Morrison, G. C.; Nazaroff, W. W. (2000) The rate of ozone uptake on carpets: experimental studies. Environ. Sci. Technol. 34: 4963-4968.
Morrison, G. C.; Nazaroff, W. W. (2002) The rate of ozone uptake on carpet: mathematical modeling. Atmos. Environ. 36: 1749-1756.
Morrison, G. C.; Nazaroff, W. W.; Cano-Ruiz, J. A.; Hodgson, A. T.; Modera, M. P. (1998) Indoor air quality impacts of ventilation ducts: ozone removal and emissions of volatile organic compounds. J. Air Waste Manage. Assoc. 48: 941-952.
Mueller, F. X.; Loeb, L.; Mapes, W. H. (1973) Decomposition rates of ozone in living areas. Environ. Sci. Technol. 7: 342-346.
Murphy, D. M.; Fahey, D. W. (1994) An estimate of the flux of stratospheric reactive nitrogen and ozone into the troposphere. J. Geophys. Res. (Atmos.) 99: 5325-5332.
Murray, D. M.; Burmaster, D. E. (1995) Residential air exchange rates in the United States: empirical and estimated parametric distributions by season and climatic region. Risk Anal. 15: 459-465.
Nagda, N. L.; Rector, H. E.; Koontz, M. D. (1987) Guidelines for monitoring indoor air quality. Washington, DC: Hemisphere Publishing Corporation.
National Acid Precipitation Assessment Program. (1987) Interim assessment: the causes and effects of acidic deposition, volume I, executive summary. Washington, DC: Office of the Director of Research.

Nazaroff, W. W.; Cass, G. R. (1986) Mathematical modeling of chemically reactive pollutants in indoor air. Environ. Sci. Technol. 20: 924-934.
Newchurch, M. J.; Ayoub, M. A.; Oltmans, S.; Johnson, B.; Schmidlin, F. J. (2003) Vertical distribution of ozone at four sites in the United States. J. Geophys. Res. 108(D1): 10.1029/2002JD002059.
Niu, J.; Tung, T. C. W.; Burnett, J. (2001) Ozone emission rate testing and ranking method using environmental chamber. Atmos. Environ. 35: 2143-2151.
Northeast States for Coordinated Air Use Management (NESCAUM). (2002) Indoor/outdoor school air monitoring project. Boston, MA. Available: http://www.nescaum.org/pdf/schoolmonitoring.pdf [29 October, 2003].
O'Gara, P. J. (1922) Sulfur dioxide and fume problems and their solution. (presented at the 14th semiannual meeting of the American Institute of Chemical Engineers, Niagara Falls, Canada, June 19-22, 1922). Presented at: 14th semiannual meeting of the American Institute of Chemical Engineers; June; Niagara Falls, Canada. Proceedings and papers of the meeting summarized in J. Ind. Eng. Chem. 14: 744-745 by J. C. Olsen.
Odman, M. T.; Ingram, C. I. (1996) Multiscale air quality simulation platform (MAQSIP): source code documentation and validation. Research Triangle Park, NC: MCNC; technical report ENV-96TR002-v1.0. Available: http://www.ce.gatech.edu/~todman/maqsip.pdf (9 September 2003).
Olsen, M. A.; Douglass, A. R.; Schoeberl, M. R. (2002) Estimating downward cross-tropopause flux using column ozone and potential vorticity. J. Geophys. Res. 107(D22): 10.1029/2001JD002041.
Oltmans, S. J.; Lefohn, A. S.; Scheel, H. E.; Harris, J. M.; Levy, H., II; Galbally, I. E.; Brunke, E.-G.; Meyer, C. P.; Lathrop, J. A.; Johnson, B. J.; Shadwick, D. S.; Cuevas, E.; Schmidlin, F. J.; Tarasick, D. W.; Claude, H.; Kerr, J. B.; Uchino, O.; Mohnen, V. (1998) Trends of ozone in the troposphere. Geophys. Res. Lett. 25: 139-142.
Ott, W. R. (1982) Concepts of human exposure to air pollution. Environ. Int. 7: 179-196.
Ott, W. R. (1985) Total human exposure: an emerging science focuses on humans as receptors of environmental pollution. Environ. Sci. Technol. 19: 880-886.
Ott, W.; Langan, L.; Switzer, P. (1992) A time series model for cigarette smoking activity patterns: model validation for carbon monoxide and respirable particles in a chamber and an automobile. In: Measuring, understanding, and predicting exposures in the 21st century: proceedings of the conference; November 1991; Atlanta, GA. J. Exposure Anal. Environ. Epidemiol. 2(suppl. 2): 175-200.
Park, J.-H.; Spengler, J. D.; Yoon, D.-W.; Dumyahn, T.; Lee, K.; Ozkaynak, H. (1998) Measurement of air exchange rate of stationary vehicles and estimation of in-vehicle exposure. J. Exposure Anal. Environ. Epidemiol. 8: 65-78.
Park, R. J.; Pickering, K. E.; Allen, D. J.; Stenchikov, G. L.; Fox-Rabinovitz, M. S. (2004) Global simulation of tropospheric ozone using the University of Maryland Chemical Transport Model (UMD-CTM): 1. Model description and evaluation. J. Geophys. Res. [Atmos.] 109(D9): 10.1029/2003JD004266.
Pavelin, E. G.; Johnson, C. E.; Rughooputh, S.; Toumi, R. (1999) Evaluation of preindustrial surface ozone measurements made using Schönbein's method. Atmos. Environ. 33: 919-929.
Penkett, S. A. (1983) PAN in the natural atmosphere. Nature (London) 302: 293-294.
Penkett, S. A.; Brice, K. A. (1986) The spring maximum in photo-oxidants in the Northern Hemisphere troposphere. Nature (London) 319: 655-657.
Penkett, S. A.; Sandalls, F. J.; Lovelock, J. F. (1975) Observations of peroxyacetyl nitrate (PAN) in air in southern England. Atmos. Environ. 9: 139-140.
Piety, C. (2004) A review of the 2004 air quality season over the Mid Atlantic Region [presentation]. College Park, MD: University of Maryland, Department of Meteorology; November 5.
Pinto, J. P.; Lefohn, A. S.; Shadwick, D. S. (2004) Spatial variability of PM2.5 in urban areas in the United States. J. Air Waste Manage. Assoc. 54: 440-449.
Pippin, M. R.; Bertman, S.; Thornberry, T.; Town, M.; Carroll, M. A.; Sillman, S. (2001) Seasonal variation of PAN, PPN, and O3 at the upper Midwest PROPHET site. J. Geophys. Res. (Atmos.) 106: 24,451-24,463.
Prados, A. I. (2000) The export of ozone and other atmospheric trace species from North America: observations and numerical simulations [dissertation]. College Park, MD: The University of Maryland.
Prinz, B.; Krause, G. H. M. (1989) State of scientific discussion about the causes of the novel forest decline in the Federal Republic of Germany and surrounding countries. In: Bucher, J. B.; Bucher-Wallin, I., eds. Air pollution and forest decline, v. I: Proceedings of the 14th international meeting for specialists in air pollution effects on forest ecosystems; October 1988; Interlaken, Switzerland. Birmensdorf, Switzerland: Eidgenossische Anstalt fur das forstliche Versuchswesen (EAFV); pp. 27-34.

Prinz, B.; Krause, G. H. M.; Jung, K.-D. (1985) Untersuchungen der LIS Essen zur Problematik der Waldschäden [Investigations of the LIS Essen into the problem of forest damage]. In: Kortzfleisch, G., ed. Waldschäden: Theorie und Praxis auf der Suche nach Antworten [Forest damage: theory and practice in the search for answers]. München, Germany: R. Oldenbourg Verlag; pp. 143-194.
Proyou, A. G.; Ziomas, I. C.; Stathopoulos, A. (1998) Application of a three-layer photochemical box model in an Athens street canyon. J. Air Waste Manage. Assoc. 48: 427-433.
Pun, B. K.; Seigneur, C.; White, W. (2003) Day-of-week behavior of atmospheric ozone in three U.S. cities. J. Air Waste Manage. Assoc. 53: 789-801.
Purushothaman, V.; Georgopoulos, P. G. (1997) Computational tools to aid the estimation and visualization of potential human exposure to ozone. In: Proceedings of the Air & Waste Management Association Specialty Conference on Computing in Environmental Resource Management; December, 1996; Research Triangle Park, NC. Pittsburgh, PA: A&WMA; VIP-68.
Purushothaman, V.; Georgopoulos, P. G. (1999a) Evaluation of regional emissions control strategies for ozone utilizing population exposure metrics: a new GIS-based approach applied to the July 1995 episode over the OTAG domain. Piscataway, NJ: Environmental and Occupational Health Sciences Institute, Ozone Research Center; ORC technical report, ORC-TR99-02.
Purushothaman, V.; Georgopoulos, P. G. (1999b) Integrating photochemical modeling, geostatistical techniques and geographical information systems for ozone exposure assessment. Piscataway, NJ: Environmental and Occupational Health Sciences Institute, Ozone Research Center; ORC technical report, ORC-TR99-01.
Reagan, J. (1984) Air quality data interpretation. In: Heck, W. W.; Taylor, O. C.; Adams, R. M.; Bingham, G. E.; Miller, J. E.; Preston, E. M.; Weinstein, L. H., eds. National Crop Loss Assessment Network (NCLAN) 1982 annual report. Corvallis, OR: U.S. Environmental Protection Agency, Corvallis Environmental Research Laboratory; pp. 198-219; report no. EPA-600/4-84-049. Available from: NTIS, Springfield, VA; PB84-169358.
Regener, E. (1941) Ozonschicht und atmosphärische turbulenz. Ber. Dtsch. Wetterdienstes US-Zone No. 11: 45-57.
Reiss, R.; Ryan, P. B.; Koutrakis, P.; Tibbetts, S. J. (1995) Ozone reactive chemistry on interior latex paint. Environ. Sci. Technol. 29: 1906-1912.
Reiter, E. R. (1977a) Review and analysis. In: Mohnen, V. A.; Reiter, E. R., eds. International conference on oxidants, 1976 - analysis of evidence and viewpoints; part III. the issue of stratospheric ozone intrusion. Research Triangle Park, NC: U.S. Environmental Protection Agency, Environmental Sciences Research Laboratory; pp. 67-117; report no. EPA-600/3-77-115. Available from: NTIS, Springfield, VA; PB-279010.
Reiter, E. R. (1977b) The role of stratospheric import on tropospheric ozone concentrations. In: Dimitriades, B., ed. International conference on photochemical oxidant pollution and its control - proceedings: volume I; September 1976; Raleigh, NC. Research Triangle Park, NC: U.S. Environmental Protection Agency, Environmental Sciences Research Laboratory; pp. 393-410; report no. EPA-600/3-77-001a. Available from: NTIS, Springfield, VA; PB-264232.
Research Triangle Institute. (1990) An investigation of infiltration and indoor air quality. Albany, NY: New York State Energy Research and Development Authority; report no. NYERDA 90-11.
Reynolds, S. D.; Blanchard, C. L.; Ziman, S. D. (2003) Understanding the effectiveness of precursor reductions in lowering 8-hr ozone concentrations. J. Air Waste Manage. Assoc. 53: 195-205.
Reynolds, S.; Blanchard, C.; Zinman, S. (2004) Understanding the effectiveness of precursor reductions in lowering 8-hr ozone concentrations. Part II: the eastern United States. J. Air Waste Manage. Assoc. 53: 195-205.
Riediker, M.; Williams, R.; Devlin, R.; Griggs, T.; Bromberg, P. (2003) Exposure to particulate matter, volatile organic compounds, and other air pollutants inside patrol cars. Environ. Sci. Technol. 37: 2084-2093.
Rifai, H. S.; Hopkins, L.; Mehdizadeh, F. (2000) Developing human exposure estimates for indoor/outdoor air pollution in Houston. In: Environmental Institute of Houston - 1999 Annual Report. Houston, TX: Environmental Institute of Houston.
Roberts, J. M.; Williams, J.; Baumann, K.; Buhr, M. P.; Goldan, P. D.; Holloway, J.; Hübler, G.; Kuster, W. C.; McKeen, S. A.; Ryerson, T. B.; Trainer, M.; Williams, E. J.; Fehsenfeld, F. C.; Bertman, S. B.; Nouaime, G.; Seaver, C.; Grodzinsky, G.; Rodgers, M.; Young, V. L. (1998) Measurements of PAN, PPN, and MPAN made during the 1994 and 1995 Nashville Intensives of the Southern Oxidant Study: implications for regional ozone production from biogenic hydrocarbons. J. Geophys. Res. [Atmos.] 103: 22,473-22,490.
Roelofs, G. J.; Lelieveld, J.; Van Dorland, R. (1997) A three-dimensional chemistry/general circulation model simulation of anthropogenically derived ozone in the troposphere and its radiative climate forcing. J. Geophys. Res. [Atmos.] 102: 23,389-23,401.

Romieu, I.; Lugo, M. C.; Colome, S.; Garcia A. M.; Avila, M. H.; Geyh, A.; Velasco, S. R.; Rendon, E. P. (1998) Evaluation of indoor ozone concentration and predictors of indoor-outdoor ratio in Mexico City. J. Air Waste Manage. Assoc. 48: 327-335.

Roselle, S.J.; Schere, K. L. (1995) Modeled response of photochemical oxidants to systematic reductions in anthropogenic volatile organic compound and NO_x emissions. J. Geophys. Res. C: Oceans Atmos. 100: 22,929-22,941.

Rotman, D. A.; Atherton, C. S.; Bergmann, D. J.; Cameron-Smith, P. J.; Chuang, C. C.; Connell, P. S.; Dignon, J. E.; Franz, A.; Grant, K. E.; Kinnison, D. E.; Molenkamp, C. R.; Proctor, D. D.; Tannahill, J. R. (2004) IMPACT, the LLNL 3-D global atmospheric chemical transport model for the combined troposphere and stratosphere: model description and analysis of ozone and other trace gases. J. Geophys. Res. [Atmos.] 109(D4): 10.1029/2002JD003155.

Runeckles, V. C. (1974) Dosage of air pollutants and damage to vegetation. Environ. Conserv. 1: 305-308.

Ryerson, T. B.; Trainer, M.; Holloway, J. S.; Parrish, D. D.; Huey, L. G.; Sueper, D. T.; Frost, G. J.; Donnelly, S. G.; Schauffler, S.; Atlas, E. L.; Kuster, W. C.; Goldan, P. D.; Hübler, G.; Meagher, J. F.; Fehsenfeld, F. C. (2001) Observations of ozone formation in power plant plumes and implications for ozone control strategies. Science (Washington, DC) 292: 719-723.

Sabersky, R. H.; Sinema, D. A.; Shair, F. H. (1973) Concentrations, decay rates, and removal of ozone and their relation to establishing clean indoor air. Environ. Sci. Technol. 7: 347-353.

Sakugawa, H.; Kaplan, I. R. (1989) H2O2 and O3 in the atmosphere of Los Angeles and its vicinity: factors controlling their formation and their role as oxidants of SO2. J. Geophys. Res. [Atmos.] 94: 12,957-12,973.

Salmon, L. G.; Cass, G. R.; Bruckman, K.; Haber, J. (2000) Ozone exposure inside museums in the historic central district of Krakow, Poland. Atmos. Environ. 34: 3823-3832.

Sarnat, J. A.; Koutrakis, P.; Suh, H. H. (2000) Assessing the relationship between personal particulate and gaseous exposures of senior citizens living in Baltimore, MD. J. Air Waste Manage. Assoc. 50: 1184-1198.

Sarnat, J. A.; Schwartz, J.; Catalano, P. J.; Suh, H. H. (2001) Gaseous pollutants in particulate matter epidemiology: confounders or surrogates? Environ. Health Perspect. 109: 1053-1061.

Sarwar, M.; Corsi, R.; Kimura, Y.; Allen, D.; Weschler, C. (2001) Hydroxyl radicals in indoor environments. In: Proceedings of the Air & Waste Management Association's 94th Annual Conference & Exhibition; June; Orlando, FL. Pittsburgh, PA: Air & Waste Management Association.

Sarwar, G.; Corsi, R.; Kumura, Y.; Allen, D.; Weschler, C. J. (2002) Hydroxyl radicals in indoor environments. Atmos. Environ. 36: 3973-3988.

Saylor, R. D.; Chameides, W. L.; Chang, M. E. (1999) Demonstrating attainment in Atlanta using urban airshed model simulations: impact of boundary conditions and alternative forms of the NAAQS. Atmos. Environ. 33: 1057-1064.

Scheeren, B. A.; Adema, E. H. (1996) Monitoring ambient ozone with a passive measurement technique method, field results and strategy. Water Air Soil Pollut. 91: 335-350.

Seo, K.-H.; Bowman, K. P. (2002) Lagrangian estimate of global stratosphere-troposphere mass exchange. J. Geophys. Res. (Atmos.) 107(D21): 10.1029/2002JD002441.

Shair, F. H. (1981) Relating indoor pollutant concentrations of ozone and sulfur dioxide to those outside: economic reduction of indoor ozone through selective filtration of the make-up air. ASHRAE Trans. 87(pt. 1): 116-139.

Shair, F. H.; Heitner, K. L. (1974) Theoretical model for relating indoor pollutant concentrations to those outside. Environ. Sci. Technol. 8: 444-451.

Shamoo, D. A.; Johnson, T. R.; Trim, S. C.; Little, D. E.; Linn, W. S.; Hackney, J. D. (1991) Activity patterns in a panel of outdoor workers exposed to oxidant pollution. J. Exposure Anal. Environ. Epidemiol. 1: 423-438.

Shamoo, D. A.; Linn, W. S.; Peng, R.-C.; Solomon, J. C.; Webb, T. L.; Hackney, J. D.; Gong, H., Jr. (1994) Time-activity patterns and diurnal variation of respiratory status in a panel of asthmatics: implications for short-term air pollution effects. J. Exposure Anal. Environ. Epidemiol. 4: 133-148.

Shindell, D. T.; Faluvegi, G.; Bell, N. (2003) Preindustrial-to-present-day radiative forcing by tropospheric ozone from improved simulations with the GISS chemistry-climate GCM. Atmos. Chem. Phys. 3: 1675-1702.

Sillman, S.; Logan, J. A.; Wofsy, S. C. (1990) The sensitivity of ozone to nitrogen oxides and hydrocarbons in regional ozone episodes. J. Geophys. Res. [Atmos.] 95: 1837-1851.

Sillman, S.; He, D.; Pippin, M. R.; Daum, P. H.; Imre, D. G.; Kleinman, L. I.; Lee, J. H.; Weinstein-Lloyd, J. (1998) Model correlations for ozone, reactive nitrogen, and peroxides for Nashville in comparison with measurements: implications for O_3-NO_x-hydrocarbon chemistry. J. Geophys. Res. [Atmos.] 103: 22,629-22,644.

Singh, H. B.; Ludwig, F. L.; Johnson, W. B. (1977) Ozone in clean remote atmospheres: concentrations and variabilities. New York, NY: Coordinating Research Council, Inc.; report no. CRC-APRAC CAPA-15-76. Available from: NTIS, Springfield, VA; PB-272290.

Singh, H. B.; Ludwig, F. L.; Johnson, W. B. (1978) Tropospheric ozone: concentrations and variabilities in clean remote atmospheres. Atmos. Environ. 12: 2185-2196.

Singh, H. B.; Herlth, D.; O'Hara, D.; Zahnle, K.; Bradshaw, J. D.; Sandholm, S. T.; Talbot, R.; Crutzen, P. J.; Kanakidou, M. (1992) Relationship of peroxyacetyl nitrate to active and total odd nitrogen at northern high latitudes: influence of reservoir species on NO_x and O_3. J. Geophys. Res. 97: 16,523-16,530.

Smith, L. A.; Lefohn, A. S. (1991) Co-occurence of ozone and wet deposited hydrogen ion in the United States. Atmos. Environ. Part A 25: 2707-2716.

Solberg, S.; Krognes, T.; Stordal, F.; Hov, Ø.; Beine, H. J.; Jaffe, D. A.; Clemitshaw, K. C.; Penkett, S. A. (1997) Reactive nitrogen compounds at Spitsbergen in the Norwegian Arctic. J. Atmos. Chem. 28: 209-225.

Sørensen, D. N.; Weschler, C. J. (2002) Modeling-gas phase reactions in indoor environments using computational fluid dynamics. Atmos. Environ. 36: 9-18.

Spier, C. E.; Little, D. E.; Trim, S. C.; Johnson, T. R.; Linn, W. S.; Hackney, J. D. (1992) Activity patterns in elementary and high school students exposed to oxidant pollution. J. Exposure Anal. Environ. Epidemiol. 2: 277-293.

Sprenger, M.; Wernli, H. (2003) A northern hemispheric climatology of cross-tropopause exchange for the ERA 15 time period (1979-1993). J. Geophys. Res. 108(D12): 10.1029/2002JD002636.

Sprenger, M.; Maspoli, M. C.; Wernli, H. (2003) Tropopause folds and cross-tropopause exchange: a global investigation based upon ECMWF analyses for the time period March 2000 to February 2001. J. Geophys. Res. (Atmos.) 108(D12): 10.1029/2002JD002587.

Staehelin, J.; Thudium, J.; Buehler, R.; Volz-Thomas, A.; Graber, W. (1994) Trends in surface ozone concentrations at Arosa (Switzerland). Atmos. Environ. 28: 75-87.

Stasiuk, W. N., Jr.; Coffey, P. E. (1974) Rural and urban ozone relationships in New York State. J. Air Pollut. Control Assoc. 24: 564-568.

Steiber, R. S. (1995) Ozone generators in indoor air settings. Research Triangle Park, NC: U.S. Environmental Protection Agency, National Risk Management Research Laboratory; report no. EPA-600/R-95-154. Available from: NTIS, Springfield, VA; PB96-100201.

Stein, M. L.; Fang, D. (1997) Ozone exposure and population density in Harris County, Texas [comment]. J. Am. Stat. Assoc. 92: 408-411.

Stohl, A. (2001) A 1-year Lagrangian "climatology" of airstreams in the Northern Hemisphere troposphere and lowermost stratosphere. J. Geophys. Res. (Atmos.) 106: 7263-7279.

Taylor, G. E., Jr.; Hanson, P. J. (1992) Forest trees and tropospheric ozone: role of canopy deposition and leaf uptake in developing exposure-response relationships. Agric. Ecosyst. Environ. 42: 255-273.

Taylor, G. E., Jr.; Norby, R. J. (1985) The significance of elevated levels of ozone on natural ecosystems of North America. In: Lee, S. D., ed. Evaluation of the scientific basis for ozone/oxidants standards: proceedings of an APCA international specialty conference; November 1984; Houston, TX. Pittsburgh, PA: Air Pollution Control Association; pp. 152-175. (APCA transactions: TR-4).

Taylor, G. E., Jr.; McLaughlin, S. B.; Shriner, D. S. (1982) Effective pollutant dose. In: Unsworth, M. H.; Ormrod, D. P., eds. Effects of gaseous air pollution in agriculture and horticulture. London, United Kingdom: Butterworth Scientific; pp. 458-460.

Taylor, G. E., Jr.; Ross-Todd, B. M.; Allen, E.; Conklin, P.; Edmonds, R.; Joranger, E.; Miller, E.; Ragsdale, L.; Shepard, J.; Silsbee, D.; Swank, W. (1992) Patterns of tropospheric ozone in forested landscapes of the Integrated Forest Study. In: Johnson, D. W.; Lindberg, S. E., eds. Atmospheric deposition and forest nutrient cycling: a synthesis of the integrated forest study. New York, NY: Springer-Verlag; pp. 50-71. (Billings, W. D.; Golley, F.; Lange, O. L.; Olson, J. S.; Remmert, H., eds. Ecological studies: analysis and synthesis: v. 91).

Thompson, C. R.; Hensel, E. G.; Kats, G. (1973) Outdoor-indoor levels of six air pollutants. J. Air Pollut. Control Assoc. 23: 881-886.

Trainer, M.; Parrish, D. D.; Buhr, M. P.; Norton, R. B.; Fehsenfeld, F. C.; Anlauf, K. G.; Bottenheim, J. W.; Tang, Y. Z.; Wiebe, H. A.; Roberts, J. M.; Tanner, R. L.; Newman, L.; Bowersox, V. C.; Meagher, J. F.; Olszyna, K. J.; Rodgers, M. O.; Wang, T.; Berresheim, H.; Demerjian, K. L.; Roychowdhury, U. K. (1993) Correlation of ozone with NO_y in photochemically aged air. J. Geophys. Res. [Atmos.] 98: 2917-2925.

Turk, B. H.; Grimsrud, D. T.; Brown, J. T.; Geisling-Sobotka, K. L.; Harrison, J.; Prill, R. J. (1989) Commercial building ventilation rates and particle concentrations. ASHRAE Trans. 95(part 1): 422-433.

U.S. Environmental Protection Agency. (1978) Air quality criteria for ozone and other photochemical oxidants. Research Triangle Park, NC: Office of Health and Environmental Assessment, Environmental Criteria and Assessment Office; report no. EPA-600/8-78-004. Available from: NTIS, Springfield, VA; PB80-124753.
U.S. Environmental Protection Agency. (1985) Compilation of air pollutant emission factors. Volume I: stationary point and area sources. Volume II: mobile sources. 4th ed. Research Triangle Park, NC: Office of Air Qaulity Planning and Standards; Ann Arbor MI: Office of Mobile Sources; report nos. AP-42-ED-4-VOL-1 and AP-42-ED-4-VOL-2. Available from: NTIS, Springfield, VA; PB86-124906 and PB87-205266.
U.S. Environmental Protection Agency. (1986) Air quality criteria for ozone and other photochemical oxidants. Research Triangle Park, NC: Office of Health and Environmental Assessment, Environmental Criteria and Assessment Office; report nos. EPA-600/8-84-020aF-eF. 5v. Available from: NTIS, Springfield, VA; PB87-142949.
U.S. Environmental Protection Agency. (1992) National air quality and emissions trends report, 1991. Research Triangle Park, NC: U.S. Environmental Protection Agency,Office of Air Quality Planning and Standards; report no. EPA/450-R-92-001. Available from: NTIS, Springfield, VA; PB93-143998.
U.S. Environmental Protection Agency. (1996a) Air quality criteria for ozone and related photochemical oxidants. Research Triangle Park, NC: Office of Research and Development; report nos. EPA/600/AP-93/004aF-cF. 3v. Available from: NTIS, Springfield, VA; PB96-185582, PB96-185590, and PB96-185608. Available: http://cfpub2.epa.gov/ncea/.
U.S. Environmental Protection Agency. (1996b) Air quality criteria for particulate matter. Research Triangle Park, NC: National Center for Environmental Assessment-RTP Office; report nos. EPA/600/P-95/001aF-cF. 3v.
U.S. Environmental Protection Agency. (1996c) Review of national ambient air quality standards for ozone: assessment of scientific and technical information. OAQPS staff paper. Research Triangle Park, NC: Office of Air Quality Planning and Standards; report no. EPA/452/R-96/007. Available from: NTIS, Springfield, VA; PB96-203435. Available: http://www.epa.gov/ttn/naaqs/standards/ozone/s_o3_pr_sp.html (9 September 2003).
U.S. Environmental Protection Agency. (1997) Responses to significant comments on the 1996 proposed rule on the national ambient air quality standards for particulate matter (December 13, 1996; 61 FR 65638). Research Triangle Park, NC: National Center for Environmental Assessment; docket number A-95-54; July. ECAO-CD-92-0671; STD-081.
U.S. Environmental Protection Agency. (1998) Guideline on ozone monitoring site selection. Research Triangle Park, NC: U.S. Environmental Protection Agency, National Center for Environmental Assessment; EPA-454/R-98-002.
U.S. Environmental Protection Agency. (2002) Latest findings on national air quality: 2001 status and trends. Research Triangle Park, NC: Office of Air Quality Planning and Standards; report no. EPA-454/K-02-001. Available: http://www.epa.gov/air/aqtrnd01/ (22 July 2003).
U.S. Environmental Protection Agency. (2003a) Technology Transfer Network: Air Quality System (AQS). Washington, DC: Office of Air and Radiation. Available: http://www.epa.gov/ttn/airs/airsaqs/ [1 April, 2004].
U.S. Environmental Protection Agency. (2003b) Latest findings on national air quality: 2002 status and trends. Research Triangle Park, NC: Office of Air Quality Planning and Standards; report no. EPA/454/K-03-001. Available: http://www.epa.gov/airtrends/2002_airtrends_final.pdf [18 December, 2003]. Available: NTIS, Springfield, VA; PB2004-100183.
U.S. Environmental Protection Agency. (2004) Air quality criteria for particulate matter. Research Triangle Park, NC: National Center for Environmental Assessment; report no. EPA/600/P-99/002aF-bF. 2v. Available: http://cfpub.epa.gov/ncea/ [9 November, 2004].
Väkevä, M.; Hämeri, K.; Kulmala, M.; Lahdes, R.; Ruuskanen, J.; Laitinen, T. (1999) Street level versus rooftop concentrations of submicron aerosol particles and gaseous pollutants in an urban street canyon. Atmos. Environ. 33: 1385-1397.
Vingarzan, R. (2004) A review of surface ozone background levels and trends. Atmos. Environ. 38: 3431-3442.
Vingarzan, R.; Taylor, B. (2003) Trend analysis of ground level ozone in the greater Vancouver/Fraser Valley area of British Columbia. Atmos. Environ. 37: 2159-2171.
Volz, A.; Kley, D. (1988) Evaluation of the Montsouris series of ozone measurements made in the nineteenth century. Nature (London) 332: 240-242.
Vong, R. J.; Guttorp, P. (1991) Co-occurence of ozone and acidic cloudwater in high-elevation forests. Environ. Sci. Technol. 25: 1325-1329.
Von Kuhlmann, R.; Lawrence, M. G.; Crutzen, P. J.; Rasch, P. J. (2003) A model for studies of tropospheric ozone and nonmethane hydrocarbons: model description and ozone results. J. Geophys. Res. [Atmos.] 108(D9): 10.1029/2002JD002893.

Wainman, T.; Zhang, J.; Weschler, C. J.; Lioy, P. J. (2000) Ozone and limonene in indoor air: a source of submicron particle exposure. Environ. Health Perspect. 108: 1139-1145.

Wang, Y.; Logan, J. A.; Jacob, D. J. (1998) Global simulation of tropospheric O_3-NO_x-hydrocarbon chemistry 2. Model evaluation and global ozone budget. J. Geophys. Res. (Atmos.) 103: 10,727-10,755.

Wernli, H.; Bourqui, M. (2002) A Lagrangian "1-year climatology" of (deep) cross-tropopause exchange in the extratropical Northern Hemisphere. J. Geophys. Res. (Atmos.) 107(D2): 10.1029/2001JD000812.

Weschler, C. J. (2000) Ozone in indoor environments: concentration and chemistry. Indoor Air 10: 269-288.

Weschler, C. J.; Shields, H. C. (1997) Potential reactions among indoor pollutants. Atmos. Environ. 31: 3487-3495.

Weschler, C. J.; Shields, H. C. (1999) Indoor ozone/terpene reactions as a source of indoor particles. Atmos. Environ. 33: 2301-2312.

Weschler, C. J.; Shields, H. C. (2000) The influence of ventilation on reactions among indoor pollutants: modeling and experimental observations. Indoor Air. 10: 92-100.

Weschler, C. J.; Shields, H. C.; Naik, D. V. (1989) Indoor ozone exposures. JAPCA 39: 1562-1568.

Weschler, C. J.; Hodgson, A. T.; Wooley, J. D. (1992) Indoor chemistry: ozone, volatile organic compounds, and carpets. Environ. Sci. Technol. 26: 2371-2377.

Weschler, C. J.; Shields, H. C.; Naik, D. V. (1994) Indoor chemistry involving O_3, NO, and NO_2 as evidenced by 14 months of measurements at a site in southern California. Environ. Sci. Technol. 28: 2120-2132.

Wild, O.; Akimoto, H. (2001) Intercontinental transport of ozone and its precursors in a three-dimensional global CTM. J. Geophys. Res. [Atmos.] 106: 27,729-27,744.

Wiley, J. A.; Robinson, J. P.; Piazza, T.; Garrett, K.; Cirksena, K.; Cheng, Y.-T.; Martin, G. (1991a) Activity patterns of California residents. Final report. Sacramento, CA: California Air Resources Board; report no. ARB/R93/487. Available from: NTIS, Springfield, VA.; PB94-108719.

Wiley, J. A.; Robinson, J. P.; Cheng, Y.-T.; Piazza, T.; Stork, L.; Pladsen, K. (1991b) Study of children's activity patterns: final report. Sacramento, CA: California Air Resources Board; report no. ARB-R-93/489.

Wilson, A. L.; Colome, S. D.; Tian, Y.; Becker, E. W.; Baker, P. E.; Behrens, D. W.; Billick, I. H.; Garrison, C. A. (1996) California residential air exchange rates and residence volumes. J. Exposure Anal. Environ. Epidemiol. 6: 311-326.

Winner, D. A.; Cass, G. R. (2000) Effect of emissions control on the long-term frequency distribution of regional ozone concentrations. Environ. Sci. Technol. 34: 2612-2617.

Wolff, G. T.; Korsog, P. E. (1992) Ozone control strategies based on the ratio of volatile organic compounds to nitrogen oxides. J. Air Waste Manage. Assoc. 42: 1173-1177.

Wolff, G. T.; Lioy, P. J.; Wight, G. D.; Meyers, R. E.; Cederwall, R. T. (1977) An investigation of long-range transport of ozone across the midwestern and eastern United States. Atmos. Environ. 11: 797-802.

Wolff, G. T.; Lioy, P. J.; Taylor, R. S. (1987) The diurnal variations of ozone at different altitudes on a rural mountain in the eastern United States. JAPCA 37: 45-48.

Wolff, G. T.; Dunker, A. M.; Rao, S. T.; Porter, P. S.; Zurbenko, I. G. (2001) Ozone air quality over North America: part I—a review of reported trends. J. Air Waste Manage. Assoc. 51: 273-282.

Wong, S.; Wang, W.-C.; Isaksen, I. S. A.; Berntsen, T. K.; Sundet, J. K. (2004) A global climate-chemistry model study of present-day tropospheric chemistry and radiative forcing from changes in tropospheric O3 since the preindustrial period. J. Geophys. Res. [Atmos.] 109(D11): 10.1029/2003JD003998.

World Meteorological Organization. (1995) Scientific assessment of ozone depletion: 1994. Geneva, Switzerland: United Nations Environment Programme. (Global ozone research and monitoring project; no. 37).

World Meteorological Organization (WMO). (1999) Scientific assessment of ozone depletion: 1998. Geneva, Switzerland: World Meteorological Organization, Global Ozone and Monitoring Project; report no. 44.

Yeng, J.; Miller, D. R. (2002) Trends and variability of ground-level O_3 in Connecticut over the period 1981-1997. J. Air Waste Manage. Assoc. 52: 1354-1361.

Zhou, J.; Smith, S. (1997) Measurement of ozone concentrations in ambient air using a badge-type passive monitor. J. Air Waste Manage. Assoc. 47: 697-703.

EPA

United States
Environmental Protection
Agency

Please make all necessary changes in the below label, detach copy or copy, and return to the address in the upper left-hand corner.

If you do not wish to receive these reports CHECK HERE ☐; detach copy or copy, and return to the address in the upper left-hand corner.

PRESORTED STANDARD
POSTAGE & FEES PAID
EPA
PERMIT No. G-35

National Center for
Environmental Assessment
Research Triangle Park, NC 27711

EPA/600/R-05/004aA
January 2005